Methods in Molecular Biology 1733

Springer Protocols

Shao-Yao Ying *Editor*

MicroRNA Protocols

Third Edition

Humana Press

METHODS IN MOLECULAR BIOLOGY

Series Editor
John M. Walker
School of Life and Medical Sciences
University of Hertfordshire
Hatfield, Hertfordshire, AL10 9AB, UK

For further volumes:
http://www.springer.com/series/7651

MicroRNA Protocols

Third Edition

Edited by

Shao-Yao Ying

Department of Integrative Anatomical Sciences, USC, Keck School of Medicine, Los Angeles, CA, USA

Humana Press

Editor
Shao-Yao Ying
Department of Integrative Anatomical Sciences
USC, Keck School of Medicine
Los Angeles, CA, USA

ISSN 1064-3745 ISSN 1940-6029 (electronic)
Methods in Molecular Biology
ISBN 978-1-4939-7600-3 ISBN 978-1-4939-7601-0 (eBook)
https://doi.org/10.1007/978-1-4939-7601-0

Library of Congress Control Number: 2018931378

Printed on acid-free paper

This Humana Press imprint is published by Springer Nature
The registered company is Springer Science+Business Media, LLC
The registered company address is: 233 Spring Street, New York, NY 10013, U.S.A.

Preface

Since the first small noncoding RNA was identified, our knowledge about microRNAs (miRNAs) has grown exponentially. MiRNAs (endogenous, evolutionarily conserved small noncoding RNAs) participate in numerous aspects of development, differentiation, and homeostasis, consequently playing important roles in the pathogenesis, including their roles in the pathogenesis of cancer, diabetes, obesity, genetic and metabolic diseases, aging, and regenerative medicine. Profound progress has been made and the studies of miRNAs have been evolved from the analysis of miRNA, targets and expression profiling, and gain-or-loss of function to circulatory regulation and the post-transcriptional regulation of miRNAs. In addition, miRNAs have been shown to be stable in the biological fluid, can be easily isolated and measured, and closely associated with various diseases. There is a great potential of using miRNAs as novel diagnostic and prognostic biomarkers with high specificity and sensitivity. Even though miRNAs are increasingly popular drug targets, the direct use of mature miRNAs or their precursors for drugs, due to their stability and new in vivo delivery methodologi-es, has been much less explored. In addition, embryonic stem cell (ESC)-specific miRNAs have been shown to reprogram induced pluripotent stem (iPS) cells, which can be perpetually generated and produced the very ESC-miRNAs, providing a biogenic resource for potential drug production.

This book focuses on the analysis of miRNA, targets and expression profiling, various methods to determine its regulation of gene expression, the preparation and isolation of miRNAs in specific tissues, its detection in the biofluids as biomarkers, and potential application in cancer, wound healing, and miRNA-induced iPSCs. The first several chapters deal with the biogenesis, isolation, profiling, and analysis of exosomal miRNAs. Many chapters provide target validation, expression profiling, and regulation of gene expression by miRNAs; the emphasis here is to provide various methods that are readily reproducible for the analysis of the functional significance of miRNAs. Additional chapters describe techniques for studying exosomal miRNAs from iPSC-derived cardiomyocyte proliferation and regeneration. Several chapters deal with screening miRNAs in various conditions and miR-302/367-induced iPSCs. Finally, a chapter on glycylglycerins, recently discovered sugar-like RNA, in miRNA-mediated iPSCs was presented. The potential use of glycylglycerins in various biological processes, including wound healing, cardiovascular diseases, and cancer, may have immense practical benefit in developing miRNA-associated molecules as drugs.

Los Angeles, CA, USA *Shao-Yao Ying*

Contents

Contributors

Gabriella M. Andrade • *Faculty of Animal Sciences and Food Engineering, Department of Veterinary Medicine, University of Sao Paulo, Pirassununga, SP, Brazil*

Nuno Bastos • *Instituto de Investigação e Inovação em Saúde, Universidade do Porto, Porto, Portugal; Institute of Molecular Pathology and Immunology, University of Porto (IPATIMUP), Porto, Portugal*

Yihua Bei • *Cardiac Regeneration and Ageing Lab, School of Life Science, Shanghai University, Shanghai, China*

Suvendra N. Bhattacharyya • *RNA Biology Research Laboratory, Molecular Genetics Division, CSIR-Indian Institute of Chemical Biology, Kolkata, India*

Stephanie A. Booth • *Zoonotic Diseases and Special Pathogens, National Microbiology Laboratory, Public Health Agency of Canada, Winnipeg, MB, Canada; Department of Medical Microbiology and Infectious Diseases, Rady Faculty of Health Sciences, University of Manitoba, Winnipeg, MB, Canada*

Mainak Bose • *RNA Biology Research Laboratory, Molecular Genetics Division, CSIR-Indian Institute of Chemical Biology, Kolkata, India*

Gerrit J. Bouma • *College of Veterinary and Biomedical Sciences, Department of Biomedical Sciences, Animal Reproduction and Biotechnology Laboratory, Colorado State University, Fort Collins, CO, USA*

John A. Browne • *School of Agriculture and Food Science, University College Dublin, Dublin, Ireland*

Donald C. Chang • *WJWU & LYNN Institute for Stem Cell Research, Santa Fe Springs, CA, USA*

Shin-Ju E. Chang • *Division of Regenerative Medicine, WJWU & LYNN Institute for Stem Cell Research, Santa Fe Springs, CA, USA*

Lin Chen • *Center for Wound Healing & Tissue Regeneration, Department of Periodontics, College of Dentistry, University of Illinois at Chicago, Chicago, IL, USA*

Xuelian Chen • *Division of Periodontology, Diagnostic Sciences & Dental Hygiene, Herman Ostrow School of Dentistry, University of Southern California, Los Angeles, CA, USA; Division of Biomedical Sciences, Herman Ostrow School of Dentistry, University of Southern California, Los Angeles, CA, USA*

Zujian Chen • *Center for Molecular Biology of Oral Diseases, Department of Periodontics, College of Dentistry, University of Illinois at Chicago, Chicago, IL, USA*

Juliano Da Silveira • *Faculty of Animal Sciences and Food Engineering, Department of Veterinary Medicine, University of Sao Paulo, Pirassununga, SP, Brazil*

Luisa A. DiPietro • *Center for Wound Healing & Tissue Regeneration, Department of Periodontics, College of Dentistry, University of Illinois at Chicago, Chicago, IL, USA; Graduate College, University of Illinois at Chicago, Chicago, IL, USA*

F. Xavier Donadeu • *The Roslin Institute and Royal (Dick) School of Veterinary Studies, University of Edinburgh, Midlothian, Scotland, UK*

William Fang • *Department of Integrative Anatomical Sciences, Keck School of Medicine, University of Southern California, Los Angeles, CA, USA*

Gabriel R. Fries • *Translational Psychiatry Program, Department of Psychiatry and Behavioral Sciences, McGovern Medical School, University of Texas Health Science Center at Houston (UTHealth), Houston, TX, USA*
Yoichi Robertus Fujii • *Retroviral Genetics Group, Pharmaco-MicroRNA Genomics, Graduate School of Pharmaceutical Sciences, Nagoya City University, Nagoya, Aichi, Japan*
Masashi Fukuoka • *National Institute of Neuroscience, NCNP, Tokyo, Japan*
Pedro A.F. Galante • *Department of Anaesthesiology, Clinic of the University of Munich, Munich, Germany*
Bo Han • *Department of Surgery, Keck School of Medicine, University of Southern California, Los Angeles, CA, USA*
Ludwig Christian Hinske • *Department of Anaesthesiology, Clinic of the University of Munich, Munich, Germany*
Hirohiko Hohjoh • *National Institute of Neuroscience, NCNP, Tokyo, Japan*
Max Hübner • *Department of Anaesthesiology, Clinic of the University of Munich, Munich, Germany*
Jason Ioannidis • *The Roslin Institute and Royal (Dick) School of Veterinary Studies, University of Edinburgh, Midlothian, Scotland, UK*
Simone Kreth • *Department of Anaesthesiology, Clinic of the University of Munich, Munich, Germany*
Won Hee Lee • *Stanford Cardiovascular Institute, Stanford University School of Medicine, Stanford, CA, USA*
Yongqin Li • *Cardiac Regeneration and Ageing Lab, School of Life Science, Shanghai University, Shanghai, China*
Shi-Lung Lin • *Division of Regenerative Medicine, WJWU & LYNN Institute for Stem Cell Research, Santa Fe Springs, CA, USA*
Virgilia Macias • *Department of Pathology, College of Medicine, University of Illinois at Chicago, Chicago, IL, USA*
Anna Majer • *Viral Diseases Division, National Microbiology Laboratory, Public Health Agency of Canada, Winnipeg, MB, Canada*
Flávio Vieira Meireles • *Faculty of Animal Sciences and Food Engineering, Department of Veterinary Medicine, University of Sao Paulo, Pirassununga, SP, Brazil*
Sónia A. Melo • *Instituto de Investigação e Inovação em Saúde, Universidade do Porto, Porto, Portugal; Institute of Molecular Pathology and Immunology, University of Porto (IPATIMUP), Porto, Portugal; Medical Faculty, University of Porto, Porto, Portugal*
Sang-Ging Ong • *Stanford Cardiovascular Institute, Stanford University School of Medicine, Stanford, CA, USA*
Felipe Perecin • *Faculty of Animal Sciences and Food Engineering, Department of Veterinary Medicine, University of Sao Paulo, Pirassununga, SP, Brazil*
Joao Quevedo • *Translational Psychiatry Program, Department of Psychiatry and Behavioral Sciences, McGovern Medical School, University of Texas Health Science Center at Houston (UTHealth), Houston, TX, USA; Center for Excellence on Mood Disorders, Department of Psychiatry and Behavioral Sciences, McGovern Medical School, The University of Texas Health Science Center at Houston (UTHealth), Houston, TX, USA; Neuroscience Graduate Program, The University of Texas Graduate School of Biomedical Sciences at Houston, Houston, TX, USA; Laboratory of Neurosciences, Graduate Program in Health Sciences, Health Sciences Unit, University of Southern Santa Catarina (UNESC), Criciúma, SC, Brazil*

Judith Risse • *Edinburgh Genomics, University of Edinburgh, Edinburgh, UK; Bioinformatics Group, Wageningen University, Wageningen, NL, USA*

Alyne Simões • *Center for Wound Healing & Tissue Regeneration, Department of Periodontics, College of Dentistry, University of Illinois at Chicago, Chicago, IL, USA; Oral Biology Laboratory, Department of Biomaterials and Oral Biology, School of Dentistry, University of São Paulo, São Paulo, SP, Brazil*

Andres Stucky • *Division of Periodontology, Diagnostic Sciences & Dental Hygiene, Herman Ostrow School of Dentistry, University of Southern California, Los Angeles, CA, USA; Division of Biomedical Sciences, Herman Ostrow School of Dentistry, University of Southern California, Los Angeles, CA, USA*

Lichan Tao • *Department of Cardiology, The Third Affiliated Hospital of Soochow University, Changzhou, China*

Quinton A. Winger • *College of Veterinary and Biomedical Sciences, Department of Biomedical Sciences, Animal Reproduction and Biotechnology Laboratory, Colorado State University, Fort Collins, CO, USA*

Joseph C. Wu • *Stanford Cardiovascular Institute, Stanford University School of Medicine, Stanford, CA, USA*

Wen-Shu Wu • *Division of Hematology/Oncology, Department of Medicine and Cancer Center, University of Illinois at Chicago, Chicago, IL, USA*

Junjie Xiao • *Cardiac Regeneration and Ageing Lab, School of Life Science, Shanghai University, Shanghai, China*

Xuelian Xiao • *Department of Laboratory Medicine, The First Affiliated Hospital of Nanjing Medical University, Nanjing, China*

Jian Xu • *Department of Laboratory Medicine, The First Affiliated Hospital of Nanjing Medical University, Nanjing, China*

Daheng Yang • *Department of Laboratory Medicine, The First Affiliated Hospital of Nanjing Medical University, Nanjing, China*

Shao-Yao Ying • *Department of Integrative Anatomical Sciences, Keck School of Medicine, University of Southern California, Los Angeles, CA, USA*

Zhonghui Zhang • *School of Life Sciences, Shanghai University, Shanghai, China; Division of Hematology/Oncology, Department of Medicine and Cancer Center, University of Illinois at Chicago, Chicago, IL, USA*

Yan Zhao • *Center for Wound Healing & Tissue Regeneration, Department of Periodontics, College of Dentistry, University of Illinois at Chicago, Chicago, IL, USA*

Jiang F. Zhong • *Division of Periodontology, Diagnostic Sciences & Dental Hygiene, Herman Ostrow School of Dentistry, University of Southern California, Los Angeles, CA, USA; Division of Biomedical Sciences, Herman Ostrow School of Dentistry, University of Southern California, Los Angeles, CA, USA*

Xiaofeng Zhou • *Center for Wound Healing & Tissue Regeneration, Department of Periodontics, College of Dentistry, University of Illinois at Chicago, Chicago, IL, USA; Center for Molecular Biology of Oral Diseases, Department of Periodontics, College of Dentistry, University of Illinois at Chicago, Chicago, IL, USA; Graduate College, University of Illinois at Chicago, Chicago, IL, USA; UIC Cancer Center, University of Illinois at Chicago, Chicago, IL, USA*

Yang Zhou • *Stanford Cardiovascular Institute, Stanford University School of Medicine, Stanford, CA, USA*

Anna E. Zielak-Steciwko • *Institute of Animal Breeding, Wrocław University of Environmental and Life Sciences, Wrocław, Poland*

Chapter 1

The MicroRNA

Shao-Yao Ying, Donald C. Chang, and Shi-Lung Lin

Abstract

MicroRNAs (miRNAs), widely distributed, small regulatory RNA genes, target both messenger RNA (mRNA) degradation and suppression of protein translation based on sequence complementarity between the miRNA and its targeted mRNA. Different names have been used to describe various types of miRNA. During evolution, RNA retroviruses or transgenes invaded the eukaryotic genome and were inserted itself in the noncoding regions of DNA, conceivably acting as transposon-like jumping genes, providing defense from viral invasion and fine-tuning of gene expression as a secondary level of gene modulation in eukaryotes. When a transposon is inserted in the intron, it becomes an intronic miRNA, taking advantage of the protein synthesis machinery, i.e., mRNA transcription and splicing, as a means for processing and maturation. MiRNAs have been found to play an important, but not life-threatening, role in embryonic development. They might play a pivotal role in diverse biological systems in various organisms, facilitating a quick response and accurate plotting of body physiology and structures. Based on these unique properties, manufactured intronic miRNAs have been developed for in vitro evaluation of gene function, in vivo gene therapy, and generation of transgenic animal models. The biogenesis of miRNAs, circulating miRNAs, miRNAs and cancer, iPSCs, and heart disease are presented in this chapter, highlighting some recent studies on these topics.

Key words Small RNA, Noncoding RNAs, siRNA, miRNA, Intronic miRNA, Transposons, Biogenesis, Mechanism, Circulating miRNA, Cancer, iPSCs, Heart disease, Drug development

1 Introduction

The miRNA is a form of small, single-stranded RNA, 18- to 25-nucleotides (nt) long. It is transcribed from DNA, and instead of being translated into protein, it regulates the functions of other genes in protein synthesis. Therefore, miRNAs are genes that modulate other protein-coding genes. Even after considering the thousands of new putative genes identified from sequencing of the human genome, as well as the genes encoding transfer RNAs (tRNAs), ribosomal RNA (rRNAs), and small nucleolar RNA (snoRNAs), nearly 95% of the genome is noncoding DNA, a percentage that varies from species to species. Changes in these sequences are frequently associated with clinical and circumstantial

Shao-Yao Ying (ed.), *MicroRNA Protocols*, Methods in Molecular Biology, vol. 1733,
https://doi.org/10.1007/978-1-4939-7601-0_1,

malfunction. Some of these noncoding sequences are responsible for RNA-mediated gene silencing through an RNA interference (RNAi)-like mechanism. One potentially important class of genes corresponding to RNAs that lack significant open reading frames, and seem to encode RNA as their final product, is the miRNAs. These miRNAs can play critical roles in development, protein secretion, and gene regulation. Some of them are naturally occurring antisense RNAs, whereas others have structures that are more complex. To understand the diseases caused by dysregulation of these miRNAs, a tissue-specific expression system is needed to recreate the function and mechanism of individual miRNAs in vitro and in vivo.

This chapter provides a simple and general view of the concept that RNAs can directly regulate gene functions, with particular attention to a step-by-step approach to the study of miRNA. Hopefully, this information will help researchers who are new to this field to overcome problems encountered in the functional analysis of miRNA.

1.1 Small RNAs or Noncoding RNAs

A noncoding RNA (ncRNA) is any RNA molecule that functions without being translated into a protein. A ncRNA is also called a small RNA (sRNA). Less frequently, it is called nonmessenger RNA, small nonmessenger RNA, tiny noncoding RNA, small modulatory RNA, or small regulatory RNA. Broadly speaking, the DNA sequence from which an ncRNA is transcribed can be considered a RNA gene. In this chapter, we will confine our discussion to sRNAs; that is, transcripts of fewer than 300 nt that participate directly in RNA processing and degradation, but indirectly in protein synthesis and gene regulation. Because type II RNA polymerases (Pol-II) are inefficient in generating sRNAs of this size, the sRNAs are either directly transcribed by type III RNA polymerases or indirectly processed from a large transcript of Pol-II.

1.1.1 Transfer RNA

The most prominent example of ncRNA is tRNA, which is involved in the process of translation and is the first type of sRNA that was identified and characterized [1]. tRNA is RNA that transfers a specific amino acid to a growing polypeptide chain at the ribosomal site of protein synthesis during translation. The tRNA is a sRNA, 74- to 93-nt long, consisting of amino acid attachment and codon recognition sites, allowing translation of specific amino acids into a polypeptide. The secondary and tertiary structures of tRNAs are cloverleafs with four to five domains and an L-shaped three-dimensional structure, respectively.

1.1.2 Nucleolar RNA

Another example of ncRNA is rRNA. rRNA is the primary constituent of ribosomes. rRNA is transcribed from DNA and, in eukaryotes, it is processed in the nucleolus before being transported through the nuclear membrane. rRNA may produce snoRNAs, the second type of sRNA. Many of the newly discovered snoRNAs are

synthesized in an intron-processing pathway. Several snoRNAs and sno-ribonucleoproteins (RNPs) are known to be needed for processing of rRNA, but precise functions remain to be defined. In principle, snoRNAs could have several roles in ribosome synthesis including: folding of pre-rRNA, formation of rRNP substrates, catalyzing RNA cleavages, base modification, assembly of pre-ribosomal subunits, and export of product rRNP particles from the nucleus to the cytoplasm.

The snoRNA acts as a guide to direct pseudouridylation and 2′-*O*-ribose methylation of rRNA in the nucleolus. Consequently, the snoRNA guides the snoRNP complex to the modification site of the target rRNA via sequence hybridization. The proteins then catalyze the modification of bases in the rRNA. Therefore, this type of RNA is also called guided RNA.

The snoRNA is also associated with proteins forming part of the mammalian telomerase, as well as with proteins involved in imprinting on the paternal chromosomes. It is encoded in introns of genes transcribed by Pol-II, even when some of the host genes do not code for proteins. As a result, the intron, but not the exon, of these genes is evolutionarily conserved in vertebrates. In this way, some of the introns of the genes employed in plants or invertebrates are still functioning in vertebrates.

The structure of snoRNAs consists of conserved sequences base-paired to their target RNAs. Nearly all vertebrate guide snoRNAs originate from introns of either protein-coding or ncRNAs transcribed by Pol-II, whereas only a few yeast guide snoRNAs derive from introns, suggesting that introns accumulated during evolution reflect the conservation of transgenes incorporated into the introns, as mentioned above [2–4]. These introns are processed through pathways involving endonucleolytic cleavage by ribonuclease (RNase) III-related enzymes, exonucleolytic trimming, and possibly RNA-mediated cleavage, which occur in large complexes called exosomes [5, 6].

1.1.3 Nuclear RNA

Small nuclear RNA (snRNA) is a class of sRNA molecules that are found within the nuclei of eukaryotic cells. They are involved in a variety of important processes, such as RNA splicing (removal of introns from heteronuclear RNA) and maintaining the telomeres. snRNA are always associated with specific proteins, and the complexes are referred to as snRNP. Some examples of snRNA are U2 snRNAs, pre-5S rRNAs, and U6 snRNAs. U2 snRNAs in embryonic stem cells and pre-5S rRNAs in *Xenopus* oocytes facilitate cell survival after ultraviolet irradiation by binding to the conserved protein, R0. Eukaryotic U6 snRNAs are the five types of spliceosomal RNA involved in messenger RNA (mRNA) splicing (U1–U6). These snRNAs have a secondary structure consisting of a stem-loop, an internal loop, a stem-closing internal loop, and the conserved protein-binding site [7].

1.1.4 Phage and Viral RNA

Another form of small RNAs is 30 ribonucleotides in length and functions as a priming initiator for bacteriophage F1 DNA replication [8, 9]. This function is solely to initiate a given site on the phage DNA, suggesting a primitive defense against foreign pathogen invasion. The phage T4-derived intron is involved in a RNA–RNA interaction in the inhibition of protein synthesis [10].

1.1.5 Small Interfering RNA

The small interfering RNAs (siRNAs) are small double-stranded RNA (dsRNA) molecules, 20- to 25-nt in length, that interfere with the expression of genes via a part of RNAi involving the enzyme Dicer. The siRNA story began with the observation of pigment expression in the *Petunia* plant. van der Krol et al. [11] tried to intensify flower pigmentation by introducing additional genes, but unexpectedly observed reduced floral pigmentation in some plants, suggesting that gene silencing may be involved in naturally occurring regulation of gene function. This introduction of multiple transgenic copies of a gene into the Petunia plant resulted in gene silencing of not only the transgenic, but also the endogenous gene copy, as has been observed by others [12]. This suggests that cosuppression of homologous genes (the transfer gene and the endogenous gene) and possibly methylation are involved [12, 13]. This phenomenon is termed RNAi. Note that the transgene introduced to the Petunia plant is a dsRNA, which is perfectly complementary to the target gene.

When dsRNA was injected into Caenorhabditis elegans, Fire and his coworkers noticed gene silencing and RNAi [14]. RNAi is a mechanism by which small regulatory RNAs possessing a sequence complementary to that of a portion of a target gene interfere with the expression of that gene. It is thought that the dsRNA, once it enters the cells, is cut up by an RNase-III familial endonuclease, known as Dicer. Dicer consists of an amino-terminal helicase domain, a PAZ domain, two RNase III motifs, and a dsRNA-binding motif. Therefore, Dicer binds to the dsRNA and excises the dsRNA into siRNAs. These siRNAs locate other single-stranded RNA molecules that are completely complementary to either strand of the siRNA duplex. Then, the RNA-degrading enzymes (RNases) destroy the RNAs complementary to the siRNAs. This phenomenon is also called post-transcriptional gene silencing (PTGS) or transgene quelling. In other words, introducing transgenes, RNA viruses, or dsRNA sequences that are completely complementary to the targeted gene transcripts can silence gene expression.

In mammals, dsRNAs longer than 30 nt will activate an antiviral response, which will lead to the nonspecific degradation of RNA transcripts, the production of interferon, and the overall shutdown of host cell protein synthesis [15]. As a result, long dsRNA will not produce gene-specific RNAi activity in mammalian cells [16].

Several terms have been used to describe the same or similar phenomenon in different biological systems of different species, including siRNAs [17], small temporal Ranks [18], heterochromatic siRNAs [19], and small modulatory dsRNAs [20].

1.1.6 MicroRNA

miRNAs are small, single-stranded RNA genes possessing the reverse complement of the mRNA transcript of another protein-coding gene. These miRNAs can inhibit the expression of the target protein-coding gene. miRNA was first observed in C. elegans as RNA molecules of 18- to 23-nt that are complementary to the 3′ untranslated regions (UTR) of the target transcripts, including the lin-4 [21] and let-7 [22] genes. As a result, the development of the worm was regulated by these RNA genes. Subsequently, miRNAs were found to occur in diverse organisms, ranging from worms, to flies, to humans [23], suggesting that these molecules represent a gene family that has evolved from an ancient ancestral sRNA gene.

The miRNA is thought to be transcribed from DNA that is not translated, but regulates the expression of other genes. Primary transcripts of the miRNA genes (pri-miRNAs) are long RNA transcripts consisting of at least a hairpin-like miRNA precursor. PrimiRNAs are processed in the nucleus to precursor (pre)-miRNAs by the ribonuclease Drosha, with the help of microprocessor [24] and exported from the nucleus by Exportin-5 [25]. The 60- to 90-nt miRNA precursors form the stem and loop structures, and the cytoplasmic RNase III enzyme, Dicer, excises the miRNA from the pre-miRNA hairpin stem region. miRNAs and siRNAs seem to be closely related, especially taking the dsRNA and hairpin structures into account. The siRNA can be considered a duplex form of miRNA in which the RNA molecule contains both miRNA and its reverse complement. Therefore, one can consider siRNAs a type of miRNA precursor.

miRNAs suppress gene expression based on their complementarity to a part of one or more mRNAs, usually at a site in the 3′-UTR. The annealing of the miRNA to the target mRNA inhibits its protein translation. In some cases, the formation of dsRNA through the binding of miRNA triggers the degradation of the mRNA transcript through a process similar to RNAi, although, in other cases, it is thought that the miRNA complex blocks the protein translation machinery or otherwise prevents protein translation without causing the mRNA to be degraded.

Because most of the miRNA suppresses gene function based on partial complementarity, conceivably, one miRNA may target more than one mRNA, and many miRNAs may act on one mRNA, coordinately modulating the intensity of gene expression in various tissues and cells. Therefore, miRNAs may have a broad function in fine-tuning the protein-coding genes. Indeed, the discovery of miRNAs has revolutionized our understanding of gene regulation in the postgenome era.

1.1.7 Intronic miRNA

Some small regulatory RNAs are produced from intronic RNA fragments. For example, snoRNAs are produced from intronic segments from genes encoding ribosomal proteins and nucleolar proteins. In addition, some sRNAs are produced from genes in which exons no longer have the capacity to encode proteins. This type of intron processing involves RNase III-related enzymes, exonucleolytical trimming, and, possibly, RNA-mediated cleavage. Therefore, intronic miRNA is a new class of miRNA derived from the processing of introns of a protein-coding gene.

The major difference between the intronic miRNAs and the previously described intergenic miRNAs, such as *lin-4* and *let-7*, is the requirement of Pol-II and spliceosomal components for the biogenesis of intronic miRNAs [26]. Both intronic and intergenic miRNAs may share the same assembly process, namely the RNA-induced silencing complex (RISC), the effector of RNAi-related gene silencing. Although siRNA-associated RISC assembly has been used to predict miRISC assembly, the link between final miRNA maturation and RISC assembly remains to be determined. The characteristics of Dicer and RISC in siRNA vs miRNA mechanisms are distinctly different [27, 28].

The intronic miRNAs need to fulfill the following requirements. First, they share the same promoter with their encoding gene transcripts. Second, they are located in the non-protein-coding region of a primary gene transcript (the pre-mRNA). Third, they are coexpressed with the gene transcripts. Last, they are removed from the transcript of their coding genes by nuclear RNA splicing and excision processes to form mature miRNAs.

Certain of the currently identified miRNAs are encoded in the genomic intron region of a gene, but they are of an orientation opposite to that of the protein-coding gene transcript. Therefore, these miRNAs are not considered to be intronic miRNAs because they do not share the same promoter with the gene and they are not released from the protein-coding gene transcript by RNA splicing. The promoters of these miRNAs are located in the antisense direction to the gene, probably using the gene transcript as a potential target for the antisense miRNAs. A good example of this type of miRNA is *let-7c*, which is an intergenic miRNA located in the antisense region of the intron of a gene.

Transposon and Intronic miRNA

The intronic and other ncRNAs may have evolved to provide a second level of gene expression in eukaryotes, enabling fine-tuning of the complex network of gene activity. In bacterial and organellar genomes, group II introns contain both catalytic Ranks and retrotransposable elements. The retrotransposable elements make this type of intron mobile. Therefore, these introns are reversely spliced directly into a DNA target site and subsequently reverse transcribed by the intron-encoded gene. After insertion into the DNA, the introns are spliced out of the gene transcript to minimize the damage to the host.

There is a potential evolutionary relationship between group II introns and both eukaryotic spliceosomal introns and non-LTR-retrotransposons. Taking advantage of this feature, it is feasible to design mobile group II introns to be incorporated into gene-targeting vectors as "targetrons," to specifically target various genes [29]. There is evidence that introns in *Caenorhabditis* genes are recently gained and some of them are actually derived from "donor" introns present in the same genome. Further, a few of these new introns apparently derive from other introns in the same gene [30]. Perhaps the splicing machinery determines where introns are added to genes. On the other hand, some newly discovered brain-specific snoRNAs of unknown function are encoded in introns of tandem repeats, and the expression of these introns is paternally imprinted.

From an evolutionary vantage, transposons are probably very old and may exist in the common ancestor genome. They may enter the host multiple times for selfish parasitical reasons. This feature of transposons is similar to that of retroviruses. Too much transposon activity can destroy a genome. To counterattack the activity of transposons and viruses, some organisms developed a mechanism to remove and/or silence the activity of transposons and viruses. For example, bacteria frequently delete their genes so that transposons and retroviruses incorporated in the genome are removed. In eukaryotes, miRNA is a way of reducing transposon activity. Conceivably, miRNA may be involved in resistance against viruses, similar to the diversity of antibody production in an immune system, or in a to-be-identified mechanism for fighting disease.

Identical twins derived from the same zygote have the same genetic information in their nuclear DNA. Any differences between monozygotic twins later in life are mostly the result of environmental influences rather than genetic inheritance. However, monozygotic twins may not share all of their DNA sequences. Female monozygotic twins can differ because of differences in X-chromosome inactivation. Consequently, one female twin can have an X-linked condition, such as muscular dystrophy, and the other twin can be free of the condition. Monozygotic twins frequently demonstrate slightly different (but definitely distinguishing) disease susceptibility and, more generally, different physiology. For example, myotonic dystrophy is a dominantly inherited, multisystemic disease with a consistent constellation of seemingly unrelated and rare clinical features, including myotonia, muscular dystrophy, cardiac conduction defects, posterior iridescent cataracts, and endocrine disorders [31]. Type 2 myotonic dystrophy is caused by a CCTG expansion (mean, ~5000 repeats) located in intron 1 of the zinc finger protein 9 gene [32]. It is possible that monozygotic twins with this disorder display symptom heterogeneity because of miRNAs or different levels of insertion of intronic genes.

Class II transposons can cut and paste. The enzyme transposase binds to the ends of the transposon, which are repeats, and the

target site on the genome, which is cut to leave sticky ends. These two components are joined together by ligases. In this way, transposons increase the size of the genome because they leave multiple copies of themselves in the genome. It is highly possible that transposons are selectively advantageous for the genome to modulate gene regulation via miRNAs. It is not be too far-fetched to suggest that when transposons are inserted in the introns of the protein-coding gene, under appropriate conditions, they, a part of them, or their secondary structures, may become intronic miRNAs.

1.1.8 PIWI-Interacting RNA

PIWI Interacting RNAs, or piRNAs, are a class of small RNAs, first discovered in mammalian testes that are coupled with PIWI proteins, such as MILI, and control transposon activity [33]. piRNAs are predominantly expressed in the germlines of various species. PIWI proteins, germline-specific Argonaute proteins such as Argonaute 3, Aubergine, and PiWi, are a part of the Argonaute family of proteins which can bind to miRNA or siRNA to form RNA-induced silencing complexes (RISC) [34]. Loss of function of PIWI proteins and/or the piRNA loci on the genome leads to derepression of transposons and causes severe defects in gametogenesis and fertility (Citation piRNA). There are primary and secondary piRNAs that serve different purposes in the control of gametogenesis. The primary piRNA guides the PIWI proteins to possible transposon mRNA targets, and aids in the cleavage of the transposon, promoting the creation of a secondary piRNA from the cleaved mRNA which would target the antisense transposons [35]. A second cleavage event would lead to the original primary antisense piRNA that can target other transposons. This process is known as the Ping Pong cycle, which optimizes the existing piRNA to target active transposons [35].

1.1.9 Repeat Associated siRNA

Repeat Associated siRNA (rasiRNA) are a subcategory of piRNAs. Like piRNAs, it interacts with the Piwi-argonaute protein family and utilizes the Ping Pong cycle for its production [36]. It is longer than all the other small noncoding RNAs in RNA interference [37]. For its production RasiRNA does not require the dicer enzyme, which is essential in miRNA and siRNA production, but instead requires the argonaute proteins to direct the cleavage process. RasiRNA are produced from antisense strands of transposable elements (TE), and affects the antisense strands of TE and repeated sequences [37]. RasiRNAs hold an important role in transcriptional silencing and regulating cell structure. The loss of rasiRNAs may lead to the loss of germ cells or important developmental elements in organisms [37].

1.1.10 Trans-acting siRNA

Trans-acting siRNAs (tasiRNAs) are a subcategory of siRNAs in plants. Its production is guided by various plant miRNAs, for example miR-390, 160, and 167 targets tasiRNA precursors like TAS3 to cleave them with dicer-like proteins DCL4 and prepare them into tasiRNA [38]. Various miRNA pathways in tasiRNA production

have been found to be highly conserved between monocot and dicot plants, indication of a long history of tasiRNA production. TasiRNA has been shown to act, like other siRNA, in RNA interference. In experiments with Arabidopsis thaliana, TAS3 tasiRNAs and their corresponding miRNAs have been linked to various ARF genes, which are instrumental in the growth and development of the plant [39]. The precise signaling pathways of tasiRNAs are suggested to be similar to other siRNAs, though there have not been studies verifying it as such.

1.1.11 RNA Activation

Emerging evidence shows that small double-stranded RNAs targeting gene promoters are potent in inducing prolonged gene activation at the transcriptional level [40]. This phenomenon is termed RNA activation (RNAa) and is evolutionarily conservative. The small RNAs are referred to small activating RNAs (saRNA). Also, saRNAs induce epigenetic changes on the target promoter, resulting in alterations of gene expression [41]. Altogether, it is feasible that saRNAs with optimal properties can be used as therapeutic agents to induce de novo activation or re-expression of silenced tumor (or metastasis) suppressor genes.

1.1.12 lncRNA

Long noncoding RNAs (lncRNAs) are non-protein-coding transcripts longer than 200 nucleotides in length and are mostly transcribed by RNA polymerase II from different regions across the genome [42]. LncRNAs act at the interface of chromatin-modifying machinery and the genome, and regulate homeotic gene expression, epigenetic imprinting, and dosage compensation of entire chromosomes [43, 44]. The function of lncRNAs depends on their subcellular localization. Many lncRNAs are recognized as important modulators for nuclear functions [43, 45].

2 Biogenesis and Mechanism of miRNAs

2.1 Biogenesis of miRNAs

miRNA genes are distributed all throughout the genome. Many are localized in exonic or intronic regions, as well as intergenic locations [46]. The biogenesis of miRNAs starts with their transcription by RNA polymerase II [47], although some other miRNAs are transcribed by RNA polymerase III [47, 48].

Five steps are involved in miRNA biogenesis in vertebrates. First, miRNAs are transcribed from DNA by Type-II RNA polymerases [47, 49] to primary miRNAs (pri-miRNAs, 300–1000 nt). Second, the long pre-miRNAs is processed by Drosha-like endonucleases and DGCR8 (which compose the "Drosha microprocessor" complex) and/or spliceosomal components. The pre-miRNA have hairpin special secondary structure, including regions of imperfectly paired dsRNA, which are sequentially cleaved to one or more miRNAs. This step depends on the origin of the pri-miRNA,

whether located in an exon or an intron, respectively [24, 49]. This takes place because the Drosha microprocessor complex recognizes the base of the stem-loop hairpin structure, cleaves it, and releases in the nucleus to form miRNA precursors or pre-miRNAs (70–90 nt). Third, the pre-miRNA is exported out of the nucleus by Ran-GTP and a receptor, Exportin-5 [25, 50]. Fourth, in the cytoplasm, Dicer-like endonucleases further cleave the pre-miRNA by the RNase III enzyme Dicer and the cofactor transactivation-responsive RNA-binding protein (TRBP, also known as TARBP2) to generate a ~22-nt miRNA duplex. Only one of the two strands is the miRNA (the guide strand or leading strand); the other counterpart is named miRNA* (the passenger strand). The mature miRNA can block mRNA translation based on partial complementarity between the miRNA and the targeted mRNA, particularly via base pairing with the 3′ UTR of the mRNA. The strand with the weakest binding at its 5′-end, a U-bias at the 5′-end and an excess of purines is more likely to become the guide strand whereas the passenger strands have a perfect complementarity between the miRNA and the targeted mRNA, a C-bias at the 5′-end, and an excess of pyrimidines gets degraded [51]. Last, the mature miRNA is incorporated into a RNP to form the RISC, which executes RNAi-related gene silencing [45, 52]. Autoregulatory negative feedback via miRNAs regulates some genes, including those involved in the RNA silencing mechanism itself [53, 54].

Figure 1 shows a simplistic view of the four major parts of biogenesis of an miRNA such as miR-302 being transcribed from DNA by Type II RNA polymerase to primary miRNAs (pri-miRNAs, 300–1000 nt), processed by Drosha and DGCR8 (RNA endonucleases) in the nucleus to form miRNA precursors (70–90 nt), which have special hairpin secondary structure. Then, miRNA precursors such as miR-302 precursor (also called pre-miR-302), being exported to the cytoplasm by Exportin-5, are further processed by Dicer-like RNaseIII endoribonucleases in the cytoplasm to form mature miRNAs (20–22 nt) such as miR-302, which form RISC with other proteins to silence gene expression. Mir-302 precursor can be accumulated (in red oval) when the process of forming mature miR-302 and RISC complex is blocked by Dicer-negative, miR-302-expressing cells (in green square); Dicer is the enzyme responsible for the miRNA precursors into mature miRNA molecules.

In broad terms, both the 5′ UTR and the 3′ UTR of the intronic miRNA can be seen as a kind of intron extension; however, their processing during mRNA translation is different from that of the intron located between two protein-coding exons, termed the in-frame intron. The in-frame intron was originally thought to be a huge genetic wasteland in gene transcripts, but this stereotypical misconception was abandoned because of the finding of intronic miRNAs.

There are Drosha/DGCR8-independent pathways for generating pre-miRNA-like hairpins such as intronic miRNAs, which are

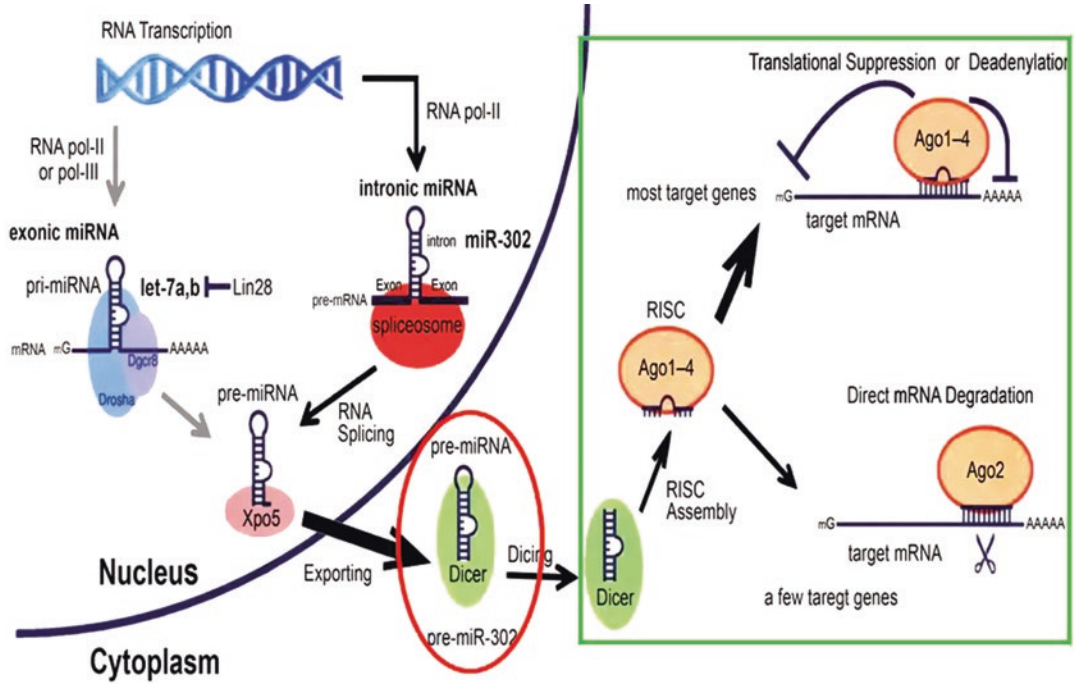

Fig. 1 Biogenesis of intronic microRNA miR-302. MiR-302 is a native intronic miRNA, encoded in the intronic region of the *La ribonucleoprotein domain family member 7* (*LARP7* or *PIP7S*) gene (host gene). During miR-302 biogenesis, primary miRNA precursors (pri-miRNA) are first transcribed by type-II RNA polymerases (RNA pol-II) along with the *LARP7* gene transcripts; then, the pri-miR-302 is spliced by cellular spliceosomes (**red**) to form hairpin-like miRNA precursors (pre-miRNA, in red oval). Next, the miRNA precursors are exported out of the nucleus by Exportin-5 (Xpo5) (pink) and further processed by Dicer-like RNaseIII endoribonucleases in cytoplasm to form mature miR-302s (21–23 nt). Consequently, mature miR-302s are assembled into RNA-induced silencing complexes (RISC) (orange) with argonaute proteins (Ago1–4) that carry out specific gene silencing (in green square)

excised by splicing and linearized by lariat debranching and further resection by nucleases. These non-canonical miRNAs, like canonical miRNAs, are incorporated to Ago1-4. Another example of non-canonical miRNAs is *Pri-mir-451* which is processed by Drosha/DGCR8, and the resulting ~18-bp *pre-mir-451* is directly incorporated to Ago2 [55]. Recently, agotrons, which escape both Drosha/DGCR8- and Dicer-processing, has been shown to form miRNA-like species by bypassing particular steps of the canonical miRNA biogenesis pathway [56].

2.2 Assembly of RISC

The RISC, or RNA-induced silencing complex, is a complex of many associated proteins. These proteins contain RNA so they are ribonucleoproteins, which combine an RNA and an RNA-binding protein together. In this way, a ribonucleoprotein incorporates one strand of a single-stranded RNA (ssRNA) fragment, such as microRNA (miRNA), or double-stranded small interfering RNA (siRNA). The single strand acts as a template for RISC to recognize complementary messenger

RNA (mRNA) transcript. Once found, one of the proteins in RISC, called Argonautes, select the strand with the less stable 5′ end and integrate it into RISC, then activate and cleave the mRNA (with the aid of RNase III Dicer), resulting in RNA interference (RNAi) and gene silencing [57].

The loading of Argonaute proteins with small RNAs is aided by a number of auxiliary factors as well as ATP hydrolysis [58]. The RISC-loading complex (RLC), the essential structure required to load dsRNA fragments into RISC in order to target mRNA, consists of dicer, TRBP (the human immunodeficiency virus transactivating response RNA-binding protein), and Argonaute 2. As described before, Dicer is an RNase III endonuclease, which generates the dsRNA fragments to be loaded that direct RNAi. TRBP is a protein with three double-stranded RNA-binding domains. Argonaute 2 is an RNase and is the catalytic center of RISC. Other members of Argonaute protein also load small RNAs [55].

The duplex of miRNAs are loaded into Argonaute (Ago) proteins, which preferentially retain the mature miRNA and eject the star strand. Ago proteins associate with cofactors of the GW182/TNRC6 family, and are guided by miRNAs to target transcripts and mediate their destabilization and/or translational suppression [59]. Animal miRNA/Ago complexes recognize targets via complements to their 5′ ends, preferentially nts 2–8 [60–63]. The posttranslational modifications of Argonaute proteins, such as prolyl-hydroxylation, phosphorylation, ubiquitination, and poly-ADP-ribosylation, alter miRNA activity at global or specific levels.

2.3 Some Other Molecules in RISC Assembly

Many factors can modify the biogenesis and mechanism of miRNAs. The multiple and sequential steps of the RISC assembly are aided by heat-shock organizing protein (Hsc70/Hsp90) chaperone machinery [64]. GW182 (so named because of its molecular weight and the presence of glycine and tryptophan repeats) interacts with Argonaute proteins and is required for miRNA-mediated gene silencing [65]. Similar to TRBP and the interface between Dicer and TRBP, PACT (kinase R–activating protein) also forms Dicer-PACT complexes, which contribute to proper miRNA length and strand selection in a subset of mammalian miRNAs [66]. ADAR1 (RNA-specific adenosine deaminase 1) catalyzes the hydrolytic deamination of adenosine to inosine in double-stranded RNA (dsRNA) referred to as A-to-I RNA editing. As a result, ADAR1 can edit miRNAs and affect RNA stability, splicing, and miRNA-target interactions [67]. On the other hand, some mRNAs can regulate ADAR1. Conceivably, overexpression of ADAR1 forms a reciprocal feedback loop with miRNA [68]. PARN [poly(A) specific ribonuclease] plays an important role in miRNA-dependent control of mRNA decay and into the mechanisms behind the regulation of p53 expression, thus facilitating the biogenesis of several important noncoding RNAs [69, 70]. The N-terminal helicase, a dynamically evolving Dicer domain, can be

dimerized itself mediated by ATPase activity as a mechanism for RNA length discrimination by a Dicer family protein, resulting in recognition of miRNA targets [71, 72]. eIF1A is a novel component of the Ago2-centered RNA-induced silencing complexes (RISCs) and augments Ago2-dependent RNAi and miRNA biogenesis [73].

2.4 Silencing of Gene Expression

miRNAs guide RISC to specifically recognize messenger RNA (mRNA) and when RISC binds to target mRNAs, a high degree of miRNA–mRNA complementarity (6–8 nt) through Watson–Crick base pairing, resulting in translational repression and mRNA cleavage [74]. Alternatively, central mismatches prevent degradation and facilitate translational repression by the possible mechanisms of RISCs bind to target mRNAs and repress initiation at the cap recognition stage, or at the 60S ribosomal recruitment stage. RISC can also prevent mRNA to circularize or RISC attachment to target mRNAs also facilitates premature separation from ribosomes, thus repressing translation at the post-initiation stage [75]. Further, some miRNAs can bind as ligands to receptors of the Toll-like receptor (TLR) and act as paracrine agonists of TLRs [76] or selectively activate innate immune effector cells via the TLR1-NF-κB signaling pathway [77].

3 Circulating miRNAs

miRNAs and their precursors have been thought to be unstable and frequently degradable, but now were found to be highly stable. Circulating miRNAs are found in the serum, saliva, urine, and other biological fluids. The levels of the circulating miRNAs have often been reported to be altered in patients. In addition, circulating miRNAs may be as effective as miRNAs. The stability of miRNAs in circulating fluids may be achieved by their association with Ago2 protein, multivesicular body, and incorporation into exosomes, microvesicles, or apoptotic bodies or into high-density lipoprotein particles [78], which could serve as useful clinical biomarkers [78, 79]. Indeed, the detection of blood miRNA levels as biomarkers for a variety of disease processes has been frequently reported and correlation between a positive therapy and specific changes in plasma miRNAs has been reported [80]. The miRNAs are stable to degradation and responsible for gene silencing in most eukaryotic cells that provide their potential usefulness as biomarkers for early detection in several diseases, including nearly many biological processes from development to oncogenesis.

Exosomes are tiny endosomal membrane vesicles (~40–150 nm in diameter). They are formed from the inward budding of endosomal members of the late endosomal compartment, subsequently become intracellular multi-vesicular endosomes (MVEs) [81, 82]. Many exosomes are packed in the MVEs and fused with the plasma

membrane, resulting in their release into the extracellular space and circulating miRNAs and may be as effective as miRNAs. Circulating miRNAs can be either bound to serum proteins and lipoproteins or be encircled in extracellular vesicles including exosomes, microvesicles, or apoptotic bodies [83, 84], making them one of the most promising biomarkers in various diseases for early diagnosis, prognosis, and therapeutic response prediction.

Despite their obvious potential as biomarkers, there are several problems that prevent the use of circulating miRNAs as diagnostic tools in clinical routine. Most importantly, despite years of intensive research no consensus on optimal protocols for standardization of sample collection, data normalization, and analysis was reached. The qPCR and microarray used for the measurements of circulating miRNAs depend on the design of miRNA-specific primers or microarray probes, similarities between different miRNAs might result in further difficulties comparing one study from another. The lack of known positive and negative miRNAs for human serum samples further contributes to a poor comparability between studies. Therefore, the validation of miRNA profiles by specific and selective methodologies to achieve accurate measurement as well as collecting overall numbers of a broad spectrum of different miRNAs are the steps for eventually implementing circulating miRNAs in the estimation of the clinical fate of patients with various diseases [85].

3.1 Direct Delivery of miRNA In Vivo

The advent of circulating miRNAs may considerably improve the delivery of miRNAs in vivo. Targeting miRNAs by gain or loss of function approaches have brought therapeutic effects in various disease models. However, delivery of miRNA mimics as drugs in vivo has not been established due to early perception that miRNAs are frequently degraded. Now, microRNAs are optimal biomarkers owing to high stability under storage and handling conditions and their presence in blood, urine, and other body fluids, it is possible that miRNA mimics can be directly delivered in vivo for treating diseases.

Conventional delivery systems for miRNAs include liposomal transfection, liposomes modified by adding long carbon chains and/or positively charged chemical group such as glycolipids, polyethylene glycol (PEG), glycerol esters, glycerol monooleate, aminated/amide polys, and sugar-encapsulation. These reagents usually fuse with the phospholipid bilayer of the cell membrane by passive diffusion. However, there are two major obstacles: low penetration and high degradation of miRNAs. Liposomes are minute spherical sacs of phospholipid molecules enclosing a water droplet to carry miRNAs into the tissues. Liposomes are often composed of phosphatidycholine-enriched phospholipid and may also contain mixed lipid chains with surfactant properties such as egg phosphatidylethanolamine. Polyethylenimines (PEIs) are positively charged,

linear, or branched polymers that are able to form nanoscale complexes with small RNAs, leading to a certain RNA protection, cellular delivery, and intracellular release.

Previously, we have used liposomes in vitro for miR-302 delivery [86]. MiR-302 mixed with polyethylenimine (PEI) were used for intratumoral injections based on jetPEI Delivery Reagent (Polyplus-transfection, Inc.) [87]. Both delivery methods resulted in efficient silencing of target genes. Tail vein injections of miR-302-367 were delivered by Neutral Lipid Emulsion (NLE, MaxSuppressor in vivo RNALancerII, BIOO Scientific) [88]. Recently, intravenous delivery of miR-let-7g mimics attenuated high-fat diet-induced neointima formation and atherosclerotic lesions, accompanied by the significant downregulation of LOX-1 [89]. These findings suggest that direct delivery of miRNA mimics in vivo is effective. Given that miRNA precursors are as effective as mature miRNAs.

A recent report showed that glycylglycerins, novel sugar alcohols, were tightly bounded with negatively charged miR-302 precursor via electro-affinity and subsequently formed sugar-like coats as microcapsules [90]. MiR-302 mixed with glycylglycerins protect the miRNA from degradation even at room temperature [90]. In addition, such a coating of glycylglycerins protected siR-302 from degradation and silenced the target genes of miR-302. An emulsion vehicle was developed, which contains only injectable pharmaceutical ingredients, i.e., excipients that have been used in FDA-approved intravenous injectable drug products or intravenous clinical trial materials with additional special ingredients. The emulsion consists of oil droplets with an average diameter of ≤200 nm, thus, it can be sterilized through a 0.2 μm filter. MiR-302 or miR-302 precursor mixed with the glycylglycerin emulsion was used for the delivery of glycylglycerin and miR-302/miR-302 precursor. Given that miRNA precursors may have longer half-life than that of the mature miRNA and miRNA precursors have been found to be as effective as the mature miRNAs [91], it is feasible to develop direct delivery of miRNA precursor as drugs for treating and/or managing diseases. Conceivably, a new strategy of direct delivery of miRNA precursors in vivo will expedite the incorporation of miRNAs and/or miRNA precursors as drugs for various diseases.

4 miRNAs and Cancer

The major explosion of interest and publications in the microRNA field has driven the rapid development of products and technologies, which address the potential application of miRNAs in cancer. Cancer is the leading cause of death in the United States. Development and metastasis of cancer is closely associated with cell proliferation, apoptosis, cell migration, cell invasion, and the epithelial-to mesenchymal

transition [92]. MiRNAs can act as tumor suppressors or oncogenes depending on their target genes [93]. A large body of evidence indicates that miRNAs regulate the expression of different genes that play an important role in cancer cell growth, apoptosis, cell invasion, migration, and metastasis [93–96, 165]. A search for miRNAs and cancer in PubMed has generated more than 26,000 articles. Even a search for review articles resulted in more than 5000 entries. Interested readers may refer to review articles on the topic [97–100]. Further, miRNA mimics and molecules targeted at miRNAs (anti-miRs) have shown promise in developing for therapeutics. Indeed, a few siRNA and miRNA have been approved for clinical trials against hepatitis, diabetes and fatty liver diseases, T cell lymphoma, scleroderma, mesothelioma, and multiple solid tumors [101].

Given that one miRNA frequently targets hundreds of mRNAs and miRNA regulatory pathways are complex, it is interesting to note that embryonic stem cell-specific miRNAs (ESC-specific miRNAs) have anti-tumor activities in various cancers. The ESC-specific miRNAs, imiR-302-367 and miR-371-373, are abundant in early embryonic cells but suddenly reduced to undetectable levels when differentiated [102]. In addition, ESC-specific miR-302 induced somatic cells or cancer cells to become pluripotent embryonic stem cells, which are tumor-free [86, 87, 103]. Subsequently, miR-302 has been reported in various types of cancer targeting different gene expressions [105–117, 124, 125]. Potentially, the miR-302 may be used to silence simultaneously the expression of several key genes essential for cancer progression and serve as a tumor suppressor in treating/managing cancer, including expression of key genes in cell cycle, global demethylation, apoptosis, and DNA repair as well as BMI-1, CXCR4, AKT1/2, Runx-1, and EGFR genes.

Long noncoding RNAs (lncRNAs) also play important roles in diverse biological processes, such as transcriptional regulation, cell growth, and tumorigenesis based on the gain-of-function and loss-of-function studies. For instance, overexpression of H19, MALAT1, HOTAIR, HULC, LINC00672, PANDAR, SPRY4-IT1, and BANCR, CASC11 promotes tumor development and these lncRNAs were biomarkers for diagnosis [118–123]. On the other hand, MEG3, GAS5, and its SNORD44 (a C/D box small nucleolar RNA in the host GAS5) and small nucleolar RNA host gene-growth arrest-specific 5 (GAS5) growth arrest specific and MEG3 are tumor suppressor in a range of human tumors [126–130]. The activity of lncRNAs, in some, is mediated by acting on miRNAs [126, 129, 130].

5 miRNAs and iPSCs

miRNAs enhance the classic reprogramming of iPSCs by ectopic expression of four transcription factors, Oct4, Sox2, Klf4, and cMyc [131]. MiRNAs alone, without any exogenous factors, can also

generate iPS cells more effectively than the classical 4 transcription factors. These special miRNAs are embryonic stem cell-specific (ESC-specific) miRNAs [132, 133]. Two miRNA clusters in mice, miR-290 and miR-302 and two in human, miR-371 and miR-302, are highly expressed in pluripotent stem cells [102, 132–134]. ESC-specific miR-302 is expressed at high levels at early stages of development and then declined [132, 133]. In hESCs and hiPSCs, miR-302 is the most predominant miRNAs and optimal levels of miR-302 are essential for cellular reprogramming [135]. Indeed, miR-302 family members are required for efficient reprogramming of somatic cells and are sufficient for iPSC generation in the absence of canonical reprogramming factors [133, 136]. By the same token, direct induction of pluripotent stem cells by miR-302 may convert one type of cells to another in vivo.

It is well known that some animals can regenerate large sections of the body, including amphibian limb regeneration; similar conversion of one type of tissue to another is metaplasia, which involves the transformation of one type of differentiated cells to another. Transformation of B lymphocytes to macrophages [137], or pancreatic exocrine cells to various types of endocrine cells [138], has been experimentally demonstrated by over-expressing specific transcription factors in these cells. As described above, induced embryonic-like puripotent stem cells from skin cancer cells by miR-302 formed no teratomas when injected in an undifferentiated form into the muscle of SCID mice, suggesting that they are tumor-free [86] and miR-302/367 or other ESC-specific miRNAs also induced iPSCs [131, 139]. Even a combinational approach of using mature microRNAs such as miR-200c, mi-302, and miR-369 induced mouse and human iPSCs [140]. The mechanism(s) underlying the miR-302-induced iPSCs are mediated through an epigenetic reprogramming similar to the natural zygotic reprogramming process in the two- to eight-cell-stage embryos, targeting epigenetic regulators such as AOF1/2, MECP1-p66, MECP2, and MBD2 [135]. In addition, cell cycle regulators such as Cyclin D1/D2, CDK2, BMI-1 [104] and PTEN [40], TGF-β regulators such as Lefty1/2 [141] and TGFBR2, and BMP inhibitors including DAZAP2, SLAIN1, and TOB2 [86, 87, 133, 142–144] are the targeted genes. Thus, miR-302 suppresses tumor growth in various types of cancer by targeting various types of genes, the ESC-specific miRNA may be ideal for regenerative medicine.

A reciprocal feedback between Oct4/Sox, Lefty, and miR-302 [133, 145–148] has been reported and miR-302-mediated iPSCs can produce miR-302 perpetually due to the miR-302/Oct 4 reciprocal feed-back mechanism [34, 50], providing a model for making miR-302 precursors. Judging by the recent observations that long noncoding RNAs (lncRNAs) and miR-302 precursor have a half-life longer than that of mature miRNAs [55], a miR-302 precursor with hairpin structure could be a better reagent for

treating and/or managing diseases. Indeed, miRNAs are more efficient in incorporating into the RNA-induced silencing complex [91, 149]. If a Pol-II-promoter-driven prokaryotic RNA transcription system can be developed, then, large amount, cost-effective miR-302 precursor can be generated for targeted treatment of various diseases. Conceivably, reprogramming cancer cells to form noncancerous/normal cells could pave the way for an innovative paradigm in treating/managing tumors in patients.

6 miRNAs and Heart Diseases

Cardiovascular diseases have a high-mortality rate. Several miRNAs have key roles in different aspects of the progression of cardiovascular diseases such as cardiac hypertrophy and fibrosis and myocardial infarction [150, 151]. Although human embryonic heart and heart of lower vertebrates has full capacity, the adult human heart has limited capacity to regenerate lost or damaged cardiomyocytes following cardiac insult because of the low proliferative rate of cardiomyocytes during adult life [152]. MiRNA are effective to stimulate cardiomyocyte proliferation and promote mammalian cardiac repair in vivo [152–156], including miR-15 family, miR-590, miR-199a [157]. Cardiac miRNAs such as miR-1, miR133a, miR-208a/b, and miR-499 are abundantly expressed in the myocardium. They also play a central role in cardiogenesis, heart function, and pathology [158, 159]. Other miR-302 modulate cardiovascular differentiation of cardiomyocyte progenitor cells and stem cells [160], differentiation of vascular smooth muscle cells (SMCs) [161, 162], and endothelial cells (ECs) [163]. Although a significant increase in miR-21 expression occurs in the failing myocardium, which is associated with fibrosis, a recent study stated that this miRNA is not essential for pathological cardiac remodeling [164].

It is intriguing to note that the microRNA cluster miR302-367 is important for cardiomyocyte proliferation during development and is sufficient to induce cardiomyocyte proliferation in the adult and promote cardiac regeneration [88]. Increased miR302-367 expression led to a profound increase in cardiomyocyte proliferation, in part through repression of the Hippo signal transduction pathway. Postnatal reexpression of miR302-367 and transient systemic application of mature miR-302-367 reactivated the cell cycle in cardiomyocytes, resulting in reduced scar formation after experimental myocardial infarction. But, long-term expression of miR302-367 induced cardiomyocyte dedifferentiation and dysfunction, suggesting that the optimal concentration of the miRNA is critical for the cardiomyocyte regeneration and repair, reduction of fibrosis, and restoration of cardiac function after experimental

cardiac infraction. These observations are consistent with the report that optimal levels of miR-302 are critical to the miR-302-induced iPSCs [135]. This study may lead to a single miRNA-mediated cardiomyocyte regeneration and repair for managing and/or treating heart failing in adults.

References

1. Holley RW (1965) Structure of an alanine transfer ribonucleic acid. JAMA 194:868–871
2. Maxwell ES, Fournier MJ (1995) The small nucleolar RNAs. Annu Rev Biochem 64: 897–934
3. Tycowski KT, Shu MD, Steitz JA (1996) A mammalian gene with introns instead of exons generating stable RNA products. Nature 379:464–466
4. Filipowicz W (2000) Imprinted expression of small nucleolar RNAs in brain: time for RNomics. Proc Natl Acad Sci U S A 97: 14035–14037
5. Allmang C, Kufel J, Chanfreau G, Mitchell P, Petfalski E, Tollervey D (1999) Functions of the exosome in rRNA, snoRNA and snRNA synthesis. EMBO J 18:5399–5410
6. van Hoof A, Parker R (1999) The exosome: a proteasome for RNA? Cell 99:347–350
7. Frank DN, Roiha H, Guthrie C (1994) Architecture of the U5 small nuclear RNA. Mol Cell Biol 14:2180–2190
8. Stavianopoulos JG, Karkus JD, Charguff E (1971) Nucleic acid polymerase of the developing chicken embryos: a DNA Polymerase preferring a hybrid template. Proc Natl Acad Sci U S A 68:2207–2211
9. Stavianopoulos JG, Karkus JD, Charguff E (1972) Mechanism of DNA replication by highly purified DNA polymerase of chicken embryos. Proc Natl Acad Sci U S A 69:2609–2613
10. Wank H, Schroeder R (1996) Antibiotic-induced oligomerisation of group I intron RNA. J Mol Biol 258:53–61
11. van der Krol AR, Mur LA, Beld M, Mol JN, Stuitje AR (1990) Flavonoid genes in petunia: addition of a limited number of gene copies may lead to a suppression of gene expression. Plant Cell 2:291–299
12. Napoli C, Lemieux C, Jorgensen RA (1990) Introduction of a chimeric chalcone synthase gene into Petunia results in reversible co-suppression of homologous genes in trans. Plant Cell 2:279–289
13. Matzke MA, Primig MJ, Trnovsky J, Matzke AJM (1989) Reversible methylation and inactivation of marker genes in sequentially transformed tobacco plants. EMBO J 8:643–649
14. Fire A, Xu S, Montgomery MK, Kostas SA, Driver SE, Mello CC (1998) Potent and specific genetic interference by double-stranded RNA in Caenorhabditis elegans. Nature 391:806–811
15. Shi Y (2003) Mammalian RNAi for the masses. Trends Genet 19:9–12
16. Sui G, Soohoo C, Affar el B, Gay F, Shi Y, Forrester WC, Shi Y (2002) A DNA vector-based RNAi technology to suppress gene expression in mammalian cells. Proc Natl Acad Sci U S A 99:5515–5520
17. Elbashir SM, Lendeckel W, Tuschl T (2001) RNA interference is mediated by 21- and 22-nucleotide RNAs. Genes Dev 15:188–200
18. Pasquinelli AE, Reinhart BJ, Slack F, Martindale MQ, Kuroda MI, Maller B, Hayward DC, Ball EE, Degnan B, Müller P, Spring J, Srinivasan A, Fishman M, Finnerty J, Corbo J, Levine M, Leahy P, Davidson E, Ruvkun G (2000) Conservation of the sequence and temporal expression of let-7 heterochronic regulatory RNA. Nature 408:86–89
19. Reinhart BJ, Bartel DP (2002) Small RNAs correspond to centromere heterochromatic repeats. Science 297:1831
20. Kuwabara T, Hsieh J, Nakashima K, Taira K, Gage FH (2004) A small modulatory dsRNA specifies the fate of adult neural stem cells. Cell 116:779–793
21. Lee RC, Feinbaum RL, Ambros V (1993) The C. elegans heterochronic gene lin-4 encodes small RNAs with antisense complementarity to lin-14. Cell 75:843–854
22. Lau NC, Lim LP, Weinstein EG, Bartel DP (2001) An abundant class of tiny RNAs with probable regulatory roles in Caenorhabditis elegans. Science 294:858–862
23. Lagos-Quintana M, Rauhut R, Meyer J, Borkhardt A, Tuschl T (2003) New microRNAs from mouse and human. RNA 9:175–179
24. Lee Y, Ahn C, Han J, Choi H, Kim J, Yim J, Lee J, Provost P, Rådmark O, Kim S, Kim VN (2003) The nuclear RNase III Drosha initiates microRNA processing. Nature 425:415–419
25. Lund E, Guttinger S, Calado A, Dahlberg JE, Kutay U (2003) Nuclear export of microRNA precursors. Science 303:95–98

26. Ying SY, Lin SL (2005) Intronic microRNAs (miRNAs). Biochem Biophys Res Commun 326:515–520
27. Lee YS, Nakahara K, Pham JW, Kim K, He Z, Sontheimer EJ, Carthew RW (2004) Distinct roles for Drosophila Dicer-1 and Dicer-2 in the siRNA/miRNA silencing pathways. Cell 117:69–81
28. Tang G (2005) siRNA and miRNA: an insight into RISCs. Trends Biochem Sci 30:106–114
29. Lambowitz AM, Zimmerly S (2004) Mobile group II introns. Annu Rev Genet 38:1–35
30. Coghlan A, Wolfe KH (2004) Origins of recently gained introns in Caenorhabditis. Proc Natl Acad Sci U S A 101:11362–11367
31. Harper PS (1989) Myotonic dystrophy, 2nd edn. Saunders, London
32. Liquori CL, Ricker K, Moseley ML, Jacobsen JF, Kress W, Naylor SL, Day JW, Ranum LP (2001) Myotonic dystrophy type 2 caused by a CCTG expansion in intron 1 of ZNF9. Science 293:864–867
33. Aravin AA, Sachidanadam R, Girard A, Fejes-Toth K, Hannon GJ (2007) Developmentally regulated piRNA clusters implicate MILI in transposon control. Science 316:744–747
34. Siomi MC, Miyoshi T, Siomi H (2010) piRNA-mediated silencing in Drosophila germlines. Semin Cell Dev Biol 21:754–749
35. Betel D, Sheridan R, Marks DS, Sander C (2007) Computational analysis of mouse piRNA sequence and biogenesis. PLoS Comput Biol 3:2219–2227
36. Shpiz S, Kwon D, Rozovsky Y, Kalmykova A (2009) rasiRNA pathway controls antisense expression of Drosophila telomeric transposons in the nucleus. Nucleic Acids Res 37:267–278
37. Pelisson A, Sarot E, Payen-Groschene G, Bucheton A (2007) A novel repeat-associated small interfering RNA -mediated silencing pathway downregulates complementary sense gypsy transcripts in somatic cells of the Drosophila ovary. J Virol 81:1951–1960
38. Gasciolli V, Mallory AC, Bartel DP, Vaucheret H (2005) Partially redundant functions of Arabidopsis DICER-like enzymes and a role for DCL4 in producing trans-acting siRNAs. Curr Biol 15:1–7
39. Allen E, Xie Z, Gustafson AM, Carrington JC (2005) MicroRNA-directed phasing during trans-acting siRNA biogenesis in plants. Cell 121:207–221
40. Li LC, Okino ST, Zhao H, Pookot D, Place RF, Urakami S, Enokida H, Dahiya R (2006) Small dsRNAs induce transcriptional activation in human cells. Proc Natl Acad Sci U S A 103:17337–17342
41. Place RF, Li LC, Pookot D, Noonan EJ, Dahiya R (2008) MicroRNA-373 induces expression of genes with complementary promoter sequences. Proc Natl Acad Sci U S A 105:1608–1613
42. Zhang H, Zhu JK (2014) Emerging roles of RNA processing factors in regulating long non-coding RNAs. RNA Biol 11:793–797
43. Batista PJ, Chang HY (2013) Long noncoding RNAs: cellular address codes in development and disease. Cell 152:1298–1307
44. Lee JT, Bartolomei MS (2013) X-Inactivation, imprinting, and long noncoding RNAs in health and disease. Cell 152:1308–1323
45. Chen LL, Carmichael GG (2010) Decoding the function of nuclear long non-coding RNAs. Curr Opin Cell Biol 22:357–364
46. Altuvia Y, Landgraf P, Lithwick G, Elefant N, Pfeffer S, Aravin A, Brownstein MJ, Tuschl T, Margalit H (2005) Clustering and conservation patterns of human microRNAs. Nucleic Acids Res 33:2697–2706
47. Lee Y, Kim M, Han J, Yeom KH, Lee S, Baek SH, Kim VN (2004) MicroRNA genes are transcribed by RNA polymerase II. EMBO J 23:4051–4060
48. Borchert GM, Lanier W, Davidson BL (2006) RNA polymerase III transcribes human microRNAs. Nat Struct Mol Biol 13:1097–1101
49. Lin SL, Chang D, DY W, Ying SY (2003) A novel RNA splicing-mediated gene silencing mechanism potential for genome evolution. Biochem Biophys Res Commun 310:754–760
50. Yi R, Qin Y, Macara IG, Cullen BR (2003) Exportin-5 mediates the nuclear export of pre-microRNAs and short hairpin RNAs. Genes Dev 17:3011–3016
51. Meijer HA, Smith EM, Bushell M (2014) Regulation of miRNA strand selection: follow the leader? Biochem Soc Trans 42:1135–1140
52. Khvorova A, Reynolds A, Jayasena SD (2003) Functional siRNAs and miRNAs exhibit strand bias. Cell 115:209–216
53. Hammond SM (2014) An overview of microRNAs. Nat Rev Mol Cell Biol 15:509–524
54. Ha M, Kim VN (2015) Regulation of microRNA biogenesis. Adv Drug Deliv Rev 87:3–14
55. Yang JS, Lai EC (2011) Alternative miRNA biogenesis pathways and the interpretation of core miRNA pathway mutants. Mol Cell 43:892–903
56. Daugaard I, Hansen TB (2017) Biogenesis and function of Ago-associated RNAs. Trends Genet 33:208–219

57. Watson JD (2008) Molecular biology of the gene. Cold Spring Harbor Laboratory Press, San Francisco, CA, pp 641–648
58. Dueck A, Meister G (2014) Assembly and function of small RNA - argonaute protein complexes. Biol Chem 395:611–629
59. Meister G (2013) Argonaute proteins: functional insights and emerging roles. Nat Rev Genet 14:447–459
60. Brennecke J et al (2005) Principles of microRNA-target recognition. PLoS Biol 3:e85
61. Doench JG, Sharp PA (2004) Specificity of microRNA target selection in translational repression. Genes Dev 18:504–511
62. Lai EC (2002) microRNAs are complementary to 3′ UTR sequence motifs that mediate negative post-transcriptional regulation. Nat Genet 30:363–364
63. Jee D, Lai EC (2014) Alteration of miRNA activity via context-specific modifications of Argonaute proteins. Trends Cell Biol 24: 546–553
64. Nakanishi K (2016) Anatomy of RISC: how do small RNAs and chaperones activate Argonaute proteins? Wiley Interdiscip Rev RNA 7:637–660
65. Ana Eulalio A, Felix Tritschler F, Regina Büttner R, Oliver Weichenrieder O, Elisa Izaurralde E, Vincent Truffault V (2009) The RRM domain in GW182 proteins contributes to miRNA-mediated gene silencing. Nucleic Acids Res 37:2974–2983
66. Wilson RC, Tambe A, Kidwell MA, Noland CL, Schneider CP, Doudna JA (2015) Dicer-TRBP complex formation ensures accurate mammalian microRNA biogenesis. Mol Cell 57:397–407
67. Grosshans H (2010) Regulation of MicroRNAs. Springer Science & Business Media, New York, NY
68. Cho CJ, Myung SJ, Chang S (2017) ADAR1 and microRNA; a hidden crosstalk in cancer. Int J Mol Sci 18(4):pii: E799. https://doi.org/10.3390/ijms18040799
69. Skeparnias I, Anastasakis D, Shaukat AN, Grafanaki K, Stathopoulos C (2015) Expanding the repertoire of deadenylases. RNA Biol 7:1–6
70. Zhang X, Devany E, Murphy MR, Glazman G, Persaud M, Kleiman FE (2015) PARN deadenylase is involved in miRNA-dependent degradation of TP53 mRNA in mammalian cells. Nucleic Acids Res 43:10925–10938
71. Svobodova E, Kubikova J, Svoboda P (2016) Production of small RNAs by mammalian Dicer. Pflugers Arch 468:1089–1102
72. Fitzgerald ME, Vela A, Pyle AM (2014) Dicer-related helicase 3 forms an obligate dimer for recognizing 22G-RNA. Nucleic Acids Res 42:3919–3930
73. Yi T, Arthanari H, Akabayov B, Song H, Papadopoulos E, Qi HH, Jedrychowski M, Güttler T, Guo C, Luna RE, Gygi SP, Huang SA, Wagner G (2015) eIF1A augments Ago2-mediated Dicer-independent miRNA biogenesis and RNA interference. Nat Commun 6:7194. https://doi.org/10.1038/ncomms8194
74. Pillai RS, Artus CG, Filipowicz W (2004) Tethering of human Ago proteins to mRNA mimics the miRNA-mediated repression of protein synthesis. RNA 10:1518–1525
75. Richard WC, Erik JS (2009) Origins and mechanisms of miRNAs and siRNAs. Cell 136:642–655
76. Fabbri M, Paone A, Calore F, Galli R, Gaudio E, Santhanam R, Lovat F, Fadda P, Mao C, Nuovo GJ, Zanesi N, Crawford M, Ozer GH, Wernicke D, Alder H, Caligiuri MA, Nana-Sinkam P, Perrotti D, Croce CM (2012) MicroRNAs bind to Toll-like receptors to induce prometastatic inflammatory response. Proc Natl Acad Sci U S A 109:E2110–E2116
77. He S, Chu J, Wu LC, Mao H, Peng Y, Alvarez-Breckenridge CA, Hughes T, Wei M, Zhang J, Yuan S, Sandhu S, Vasu S, Benson DM Jr, Hofmeister CC, He X, Ghoshal K, Devine SM, Caligiuri MA, Yu J (2013) MicroRNAs activate natural killer cells through Toll-like receptor signaling. Blood 121:4663–4671
78. Hessvik NP, Sandvig K, Llorente A (2013) Exosomal miRNAs as biomarkers for prostate cancer. Front Genet 1819:1154–1163
79. Phuyal S, Hessvik NP, Skotland T, Sandvig K, Llorente A (2014) Regulation of exosome release by glycosphingolipids and flotillins. FEBS J 281:2214–2227
80. Marfella R, Di Filippo C, Potenza N, Sardu C, Rizzo MR, Siniscalchi M, Musacchio E, Barbieri M, Mauro C, Mosca N, Solimene F, Mottola MT, Russo A, Rossi F, Paolisso G, D'Amico M (2013) Circulating microRNA changes in heart failure patients treated with cardiac resynchronization therapy: responders vs. non-responders. Eur J Heart Fail 15:1277–1288
81. Raposo G, Stoorvogel W (2013) Extracellular vesicles: exosomes, microvesicles, and friends. J Cell Biol 200:373–383
82. Harding CV, Heuser JE, Stahl PD (2013) Exosomes: looking back three decades and into the future. J Cell Niol 200:367–371
83. Cortez MA, Bueso-Ramos C, Ferdin J, Lopez-Berestein G, Sood AK, Calin GA (2011) MicroRNAs in body fluids--the mix of hormones and biomarkers. Nat Rev Clin Oncol 8:467–477

84. Creemers EE, Tijsen AJ, Pinto YM (2012) Circulating microRNAs: novel biomarkers and extracellular communicators in cardiovascular disease? Circ Res 110:483–495
85. Etheridge A, Lee I, Hood L, Galas D, Wang K (2017) Extracellular microRNA: a new source of biomarkers. Mutat Res 717:85–90
86. Lin SL, Chang DC, Chang-Lin S, Lin CH, DT W, Chen DT, Ying SY (2008) Mir-302 reprograms human skin cancer cells into a pluripotent ES-cell-like state. RNA 14:2115–2124
87. Lin SL, Chang DC, Ying SY, Leu D, Wu DT (2010) MicroRNA miR-302 inhibits the tumorigenecity of human pluripotent stem cells by coordinate suppression of the CDK2 and CDK4/6 cell cycle pathways. Cancer Res 70:9473–9482
88. Tian Y, Liu Y, Wang T, Zhou N, Kong J, Chen L, Snitow M, Morley M, Li D, Petrenko N, Zhou S, Lu M, Gao E, Koch WJ, Stewart KM, Morrisey EE (2015) A microRNA-Hippo pathway that promotes cardiomyocyte proliferation and cardiac regeneration in mice. Sci Transl Med 7(279):279ra38. https://doi.org/10.1126/scitranslmed.3010841
89. Liu M, Tao G, Liu Q, Liu K, Yang X (2017) MicroRNA let-7g alleviates atherosclerosis via the targeting of LOX-1 in vitro and in vivo. Int J Mol Med 40:57. https://doi.org/10.3892/ijmm.2017.2995
90. Chang-Lin S, Hung A, Chang DC, Lin YW, Ying SY, Lin SL (2016) Novel glycylated sugar alcohols protect ESC-specific microRNAs from degradation in iPS cells. Nucleic Acids Res 44:4894–4906
91. Huang X, Jia Z (2013) Construction of HCC-targeting artificial miRNAs using natural miRNA precursors. Exp Ther Med 6:209–215
92. Bartel D (2004) MicroRNAs: genomics, biogenesis, mechanism, and function. Cell 116:281–297
93. Zhang B, Pan X, Cobb GP, Anderson TA (2007) microRNAs as oncogenes and tumor suppressors. Dev Biol 302:1–12
94. Baranwal S, Alahari SK (2010) miRNA control of tumor cell invasion and metastasis. Int J Cancer 126:1283–1222
95. Palma Flores C, García-Vázquez R, Gallardo Rincón D, Ruiz-García E, Astudillo de la Vega H, Marchat LA, Salinas Vera YM, López-Camarillo C (2017) MicroRNAs driving invasion and metastasis in ovarian cancer: Opportunities for translational medicine. Int J Oncol 50:1461–1476
96. Yan J, Ma C, Gao Y (2017) MicroRNA-30a-5p suppresses epithelial-mesenchymal transition by targeting profilin-2 in high invasive non-small cell lung cancer cell lines. Oncol Rep 37:3146–3154
97. Jansson MD, Lund AH (2012) MicroRNA and cancer. Mol Oncol 6:590–610
98. Farazi TA, Hoell JI, Morozov P, Tuschl T (2013) MicroRNAs in human cancer. Adv Exp Med Biol 774:1–20
99. Acunzo M, Romano G, Wernicke D, Croce CM (2015) MicroRNA and **cancer**--a brief overview. Adv Biol Regul 57:1–9
100. Iorio MV, Croce CM (2017) MicroRNA dysregulation in cancer: diagnostics, monitoring and therapeutics. A comprehensive review. EMBO Mol Med 4:143. 10.15252/emmm.201707779
101. Rupaimoole R, Slack FJ (2017) MicroRNA therapeutics: towards a new era for the management of cancer and other diseases. Nat Rev Drug Discov 16:203–222
102. Suh MR, Lee Y, Kim JY, Kim SK, Moon SH, Lee JY, Cha KY, Chung HM, Yoon HS, Moon SY, Kim VN, Kim KS (2004) Human embryonic stem cells express a unique set of microRNAs. Dev Biol 270:488–498
103. Li HL, Wei JF, Fan LY, Wang SH, Zhu L, Li TP, Lin G, Sun Y, Sun ZJ, Ding J, Liang XL, Li J, Han Q, Zhao RC (2016) miR-302 regulates pluripotency, teratoma formation and differentiation in stem cells via an AKT1/OCT4-dependent manner. Cell Death Dis 7:e2078. https://doi.org/10.1038/cddis.2015.383
104. Liang Z, Ahn J, Guo D, Votaw JR, Shim H (2013) MicroRNA-302 replacement therapy sensitizes breast cancer cells to ionizing radiation. Pharm Res 30:1008–1016
105. Wang Y, Zhao L, Xiao Q, Jiang L, He M, Bai X, Ma M, Jiao X, Wei M (2016) miR-302a/b/c/d cooperatively inhibit BCRP expression to increase drug sensitivity in breast cancer cells. Gynecol Oncol 141:592–601
106. Zhao L, Wang Y, Jiang L, He M, Bai X, Yu L, Wei M (2016) MiR-302a/b/c/d cooperatively sensitizes breast cancer cells to adriamycin via suppressing P-glycoprotein (P-gp) by targeting MAP/ERK kinase kinase 1 (MEKK1). J Exp Clin Cancer Res 35:25. https://doi.org/10.1186/s13046-016-0300-8
107. Ge T, Yin M, Yang M, Liu T, Lou G (2014) MicroRNA-302b suppresses human epithelial ovarian cancer cell growth by targeting RUNX1. Cell Physiol Biochem 34:2209–2220
108. Yan GJ, Yu F, Wang B, Zhou HJ, Ge QY, Su J, YL H, Sun HX, Ding LJ (2014) MicroRNA miR-302 inhibits the tumorigenicity of endometrial cancer cells by suppression of Cyclin D1 and CDK1. Cancer Lett 345:39–47

109. Cai N, Wang YD, Zheng PS (2013) The microRNA-302-367 cluster suppresses the proliferation of cervical carcinoma cells through the novel target AKT1. RNA 19:85–95
110. Maadi H, Moshtaghian A, Taha MF, Mowla SJ, Kazeroonian A, Haass NK, Javeri A (2016) Multimodal tumor suppression by miR-302 cluster in melanoma and colon cancer. Int J Biochem Cell Biol 81(Pt A):121–132
111. Wang L, Yao J, Shi X, Hu L, Li Z, Song T, Huang C (2013) MicroRNA-302b suppresses cell proliferation by targeting EGFR in human hepatocellular carcinoma SMMC-7721 cells. BMC Cancer 13:448. https://doi.org/10.1186/1471-2407-13-448
112. Koga C, Kobayashi S, Nagano H, Tomimaru Y, Hama N, Wada H, Kawamoto K, Eguchi H, Konno M, Ishii H, Umeshita K, Doki Y, Mori M (2014) Reprogramming using microRNA-302 improves drug sensitivity in hepatocellular carcinoma cells. Ann Surg Oncol Suppl 4:S591–S600
113. Wang L, Yao J, Zhang X, Guo B, Le X, Cubberly M, Li Z, Nan K, Song T, Huang C (2014) miRNA-302b suppresses human hepatocellular carcinoma by targeting AKT2. Mol Cancer Res 12:190–202
114. Cai D, He K, Chang S, Tong D, Huang C (2015) MicroRNA-302b enhances the sensitivity of hepatocellular carcinoma cell lines to 5-FU via targeting Mcl-1 and DPYD. Int J Mol Sci 16:23668–23682
115. Bourguignon LY, Wong G, Earle C, Chen L (2012) Hyaluronan-CD44v3 interaction with Oct4-Sox2-Nanog promotes miR-302 expression leading to self-renewal, clonal formation, and cisplatin resistance in cancer stem cells from head and neck squamous cell carcinoma. J Biol Chem 287:32800–12824
116. Chen L, Min L, Wang X, Zhao J, Chen H, Qin J, Chen W, Shen Z, Tang Z, Gan Q, Ruan Y, Sun Y, Qin X, Gu J (2015) Loss of RACK1 promotes metastasis of gastric cancer by inducing a miR-302c/IL8 signaling loop. Cancer Res 75:3832–3841
117. Khodayari N, Mohammed KA, Lee H, Kaye F, Nasreen N (2016) MicroRNA-302b targets Mcl-1 and inhibits cell proliferation and induces apoptosis in malignant pleural mesothelioma cells. Am J Cancer Res 6:1996–2009
118. Hu Q, Wang YB, Zeng P, Yan GQ, Xin L, Hu XY (2017) Expression of long non-coding RNA (lncRNA) H19 in immunodeficient mice induced with human colon cancer cells. Eur Rev Med Pharmacol Sci 20:4880–4884
119. Ji Q, Liu X, Fu X, Zhang L, Sui H, Zhou L, Sun J, Cai J, Qin J, Ren J, Li Q (2014) Resveratrol inhibits invasion and metastasis of colorectal cancer cells via MALAT1 mediated Wnt/β-catenin signal pathway. PLoS One 8:e78700. https://doi.org/10.1371/journal.pone.0078700
120. Ma T, Wang RP, Zou X (2016) Dioscin inhibits gastric tumor growth through regulating the expression level of lncRNA HOTAIR. BMC Complement Altern Med 16(1):383
121. Li SP, HX X, Yu Y, He JD, Wang Z, YJ X, Wang CY, Zhang HM, Zhang RX, Zhang JJ, Yao Z, Shen ZY (2016) LncRNA HULC enhances epithelial-mesenchymal transition to promote tumorigenesis and metastasis of hepatocellular carcinoma via the miR-200a-3p/ZEB1 signaling pathway. Oncotarget 7:42431–42446
122. Li W, Li H, Zhang L, Hu M, Li F, Deng J, An M, Wu S, Ma R, Lu J, Zhou Y (2017) Long non-coding RNA LINC00672 contributes to p53 protein-mediated gene suppression and promotes endometrial cancer chemosensitivity. J Biol Chem 292:5801–5813
123. Zhang Z, Zhou C, Chang Y, Zhang Z, Hu Y, Zhang F, Lu Y, Zheng L, Zhang W, Li X, Li X (2016) Long non-coding RNA CASC11 interacts with hnRNP-K and activates the WNT/β-catenin pathway to promote growth and metastasis in colorectal cancer. Cancer Lett 376:62–73
124. Nagini S (2017) Breast cancer: current molecular therapeutic targets and new players. Anticancer Agents Med Chem 17:152–163
125. Li AX, Xin WQ, Ma CG (2015) Fentanyl inhibits the invasion and migration of colorectal cancer cells via inhibiting the negative regulation of Ets-1 on BANCR. Biochem Biophys Res Commun 465:594–600
126. Zhou X, Ji G, Ke X, Gu H, Jin W, Zhang G (2015) MiR-141 inhibits gastric cancer proliferation by interacting with long noncoding RNA MEG3 and down-regulating E2F3 expression. Dig Dis Sci 60:3271–3282
127. Guo Q, Cheng Y, Liang T, He Y, Ren C, Sun L, Zhang G (2015) Comprehensive analysis of lncRNA-mRNA co-expression patterns identifies immune-associated lncRNA biomarkers in ovarian cancer malignant progression. Sci Rep 5:17683. https://doi.org/10.1038/srep17683
128. Chang L, Li C, Lan T, Wu L, Yuan Y, Liu Q, Liu Z (2016) Decreased expression of long non-coding RNA GAS5 indicates a poor prognosis and promotes cell proliferation and invasion in hepatocellular carcinoma by regulating vimentin. Mol Med Rep 13:1541–1550
129. Xue Y, Ni T, Jiang Y, Li Y (2017) LncRNA GAS5 inhibits tumorigenesis and enhances radiosensitivity by suppressing miR-135b

expression in non-small cell lung cancer. Oncol Res 25:1305. https://doi.org/10.3727/096504017X14850182723737

130. Mei Y, Si J, Wang Y, Huang Z, Zhu H, Feng S, Wu X, Wu L (2017) Long noncoding RNA GAS5 suppresses tumorigenesis by inhibiting miR-23a 5 expression in non-small cell lung cancer. Oncol Res 25:1027. https://doi.org/10.3727/096504016X14822800040451
131. Judson RL, Babiarz JE, Venere M, Blelloch R (2009) Embryonic stem cell-specific microRNAs promote induced pluripotency. Nat Biotechnol 27:459–461
132. Li N, Long B, Han W, Yuan S, Wang K (2017) microRNAs: important regulators of stem cells. Stem Cell Res Ther 8:110. https://doi.org/10.1186/s13287-017-0551-0
133. Rosa A, Brivanlou AH (2013) Regulatory non-coding RNAs in pluripotent stem cells. Int J Mol Sci 14:14346–14373
134. Stadler B, Ivanovska I, Mehta K, Song S, Nelson A, Tan Y, Mathieu J, Darby C, Blau CA, Ware C, Peters G, Miller DG, Shen L, Cleary MA, Ruohola-Baker H (2010) Characterization of microRNAs involved in embryonic stem cell states. Stem Cells Dev 19:935–950
135. Lin SL, Chang DC, Lin CH, Ying SY, Leu D, Wu DT (2011) Regulation of somatic cell reprogramming through inducible mir-302 expression. Nucleic Acids Res 39:1054–1065, 2011
136. Kuo CH, Ying SY (2012) Advances in microRNA-mediated reprogramming technology. Stem Cells Int 2012:823709. https://doi.org/10.1155/2012/823709
137. Slack JM (2009) Metaplasia and somatic cell reprogramming. J Pathol 217:161–168
138. Li W, Nakanishi M, Zumsteg A, Shear M, Wright C, Melton DA, Zhou Q (2014) In vivo reprogramming of pancreatic acinar cells to three islet endocrine subtypes. Elife 3:e01846. https://doi.org/10.7554/eLife.01846
139. Anokye-Danso F, Trivedi CM, Juhr D, Gupta M, Cui Z, Tian Y, Zhang Y, Yang W, Gruber PJ, Epstein JA, Morrisey EE (2011) Highly efficient miRNA-mediated reprogramming of mouse and human somatic cells to pluripotency. Cell Stem Cell 8:376–388
140. Miyoshi N, Ishii H, Nagano H, Haraguchi N, Dewi DL, Kano Y, Nishikawa S, Tanemura M, Mimori K, Tanaka F, Saito T, Nishimura J, Takemasa I, Mizushima T, Ikeda M, Yamamoto H, Sekimoto M, Doki Y, Mori M (2011 Jun 3) (2011) Reprogramming of mouse and human cells to pluripotency using mature microRNAs. Cell Stem Cell 8(6):633–638. https://doi.org/10.1016/j.stem.2011.05.001
141. Barroso-delJesus A, Lucena-Aguilar G, Sanchez L, Ligero G, Gutierrez-Aranda I, Menendez P (2011) The Nodal inhibitor Lefty is negatively modulated by the microRNA miR-302 in human embryonic stem cells. FASEB J 25:1497–1508
142. Liao B, Bao X, Liu L, Feng S, Zovoilis A, Liu W, Xue Y, Cai J, Guo X, Qin B, Zhang R, Wu J, Lai L, Teng M, Niu L, Zhang B, Esteban MA, Pei D (2011) MicroRNA cluster 302–367 enhances somatic cell reprogramming by accelerating a mesenchymal-to-epithelial transition. J Biol Chem 286:17359–17364
143. Subramanyam D, Lamouille S, Judson RL, Liu JY, Bucay N, Derynck R, Blelloch R (2011) Multiple targets of miR-302 and miR-372 promote reprogramming of human fibroblasts to induced pluripotent stem cells. Nat Biotechnol 29:443–448
144. Lipchina I, Elkabetz Y, Hafner M, Sheridan R, Mihailovic A, Tuchil T, Sander C, Studer L, Betel D (2011) Genome-wide identification of microRNA targets human ES cells reveals a role for miR-302 in modulating BMP response. Genes Dev 25:2173–2186
145. Liu H, Deng S, Zhao Z, Zhang H, Xiao J, Song W, Gao F, Guan Y (2011) Oct4 regulates the miR-302 cluster in P19 mouse embryonic carcinoma cells. Mol Biol Rep 38:2155–2160
146. Card DA, Hebbar PB, Li L, Trotter KW, Komatsu Y, Mishina Y, Archer TK (2008) Oct4/Sox2-regulated miR-302 targets cyclin D1 in human embryonic stem cells. Mol Cell Biol 28:6426–6438
147. Hu S, Wilson KD, Ghosh Z, Han L, Wang Y, Lan F, Ransohoff KJ, Burridge P, Wu JC (2013) MicroRNA-302 increases reprogramming efficiency via repression of NR2F2. Stem Cells 31:259–268
148. Lin SL (2011) Concise review: deciphering the mechanism behind induced pluripotent stem cell generation. Stem Cells 29:1645–1649
149. Terasawa K, Shimizu K, Tsujimoto G (2011) Synthetic pre-miRNA-based shRNA as potent RNAi triggers. J Nucleic Acids 2011:131579
150. Gurha P (2016) MicroRNAs in cardiovascular disease. Curr Opin Cardiol 31:249–254
151. van Rooij E, Olson EN (2012) MicroRNA therapeutics for cardiovascular disease: opportunities and obstacles. Nat Rev Drug Discov 11:860–872
152. van Amerongen MJ, Felix B, Engel FB (2008) Features of cardiomyocyte proliferation and its potential for cardiac regeneration. J Cell Mol Med 12:2233–2244

153. Wu G, Huang ZP, Wang DZ (2013) MicroRNAs in cardiac regeneration and cardiovascular disease. Sci China Life Sci 56:907–913
154. Boon RA, Iekushi K, Lechner S, Seeger T, Fischer A, Heydt S, Kaluza D, Tréguer K, Carmona G, Bonauer A, Horrevoets AJ, Didier N, Girmatsion Z, Biliczki P, Ehrlich JR, Katus HA, Müller OJ, Potente M, Zeiher AM, Hermeking H, Dimmeler S (2013) MicroRNA-34a regulates cardiac ageing and function. Nature 495:107–110
155. Porrello ER, Johnson BA, Aurora AB, Simpson E, Nam YJ, Matkovich SJ, Dorn GW II, van Rooij E, Olson EN (2011) MiR-15 family regulates postnatal mitotic arrest of cardiomyocytes. Circ Res 109:670–679
156. Porrello ER, Mahmoud AI, Simpson E, Johnson BA, Grinsfelder D, Canseco D, Mammen PP, Rothermel BA, Olson EN, Sadek HA (2013) Regulation of neonatal and adult mammalian heart regeneration by the miR-15 family. Proc Natl Acad Sci U S A 110:187–192
157. Eulalio A, Mano M, Dal Ferro M, Zentilin L, Sinagra G, Zacchigna S, Giacca M (2012) Functional screening identifies miRNAs inducing cardiac regeneration. Nature 492:376–381
158. Ikeda S, He A, Kong SW, Lu J, Bejar R, Bodyak N, Lee KH, Ma Q, Kang PM, Golub TR, Pu WT (2009) MicroRNA-1 negatively regulates expression of the hypertrophy-associated calmodulin and Mef2a genes. Mol. Cell. Biol 29:2193–2204
159. Montgomery RL, Hullinger TG, Semus HM, Dickinson BA, Seto AG, Lynch JM, Stack C, Latimer PA, Olsen EN, van Rooij E (2011) Therapeutic inhibition of miR-208a improves cardiac function and survival during heart failure. Circulation 124:1537–1547
160. Sluijter JP, van Mil A, van Vliet P, Metz CH, Liu J, Doevendans PA, Goumans MJ (2010) MicroRNA-1 and -499 regulate differentiation and proliferation in human-derived cardiomyocyte progenitor cells. Arterioscler Thromb Vasc Biol 30:859–868
161. Yoo JK, Kim J, Choi SJ, Noh HM, Kwon YD, Yoo H, Yi HS, Chung HM, Kim JK (2012) Discovery and characterization of novel microRNAs during endothelial differentiation of human embryonic stem cells. Stem Cells Dev 21:2049–2057
162. Zhao W, Zhao SP, Zhao YH (2015) MicroRNA-143/-145 in cardiovascular diseases. Biomed Res Int 2015:531740
163. Chen T, Margariti A, Kelaini S, Cochrane A, Guha ST, Hu Y, Stitt AW, Zhang L, Xu Q (2015) MicroRNA-199b modulates vascular cell fate during iPS cell differentiation by targeting the Notch ligand Jagged1 and enhancing VEGF signaling. Stem Cells 33:1405–1418
164. Montgomery RL, Yu G, Latimer PA, Stack C, Robinson K, Dalby CM, Kaminski N, van Rooij E (2014) MicroRNA mimicry blocks pulmonary fibrosis. EMBO Mol Med 6:1347–1356
165. Cheng AM, Byrom MW, Jeffrey Shelton J, Lance P, Ford LP (2005) Antisense inhibition of human miRNAs and indications for an involvement of miRNA in cell growth and apoptosis. Nucleic Acids Res 33:1290–1297

Chapter 2

Target mRNA-Driven Biogenesis of Cognate MicroRNAs In Vitro

Mainak Bose and Suvendra N. Bhattacharyya

Abstract

miRNAs are 20–22 nucleotide long noncoding RNAs that act as post-transcriptional regulators of gene expression controlling more than half of protein coding genes in humans. Being the critical modulators of the mRNA translation process, biogenesis, function, and turnover of these small RNAs are tightly regulated in cells. We have reported that target mRNAs induce increased biogenesis of cognate miRNAs from pre-miRNAs by increased activity of Ago-associated Dicer endonuclease that processes precursor miRNAs to their mature form. In the current chapter, we discuss how target mRNA-driven RISC loading can be monitored in vitro using affinity-purified miRISC or recombinant AGO2 and DICER1 proteins and scoring the processivity of AGO2-associated DICER1 in vitro.

Key words miRNA, Precursor miRNA, Argonaute, Dicer processivity, RISC loading, Target mRNA

1 Introduction

Over the past one or two decades a plethora of small RNAs have been discovered that have different regulatory roles in eukaryotes [1–3]. The 20–22 nt long miRNAs comprise one of the most abundant classes of these small RNAs in somatic tissues. miRNAs are born as long primary transcripts (pri-miRNA) in the nucleus where they are processed by the Microprocessor complex (Drosha/DGCR8) into ~70 nt precursor miRNAs (pre-miRNA). Pre-miRNAs undergo processing in the cytoplasm by the DICER1/TRBP2 complex into double-stranded duplexes of which one strand is selected as guide strand and the other is degraded. Efficient miRNA functioning requires its assembly into miRNPs in which the miRNA guide/sense strand serves as the specificity determinant for target RNA recognition and the effector proteins in which miRNAs are assembled, primarily Argonaute, mediate translation repression and/or target RNA degradation. Animal miRNAs usually hybridize with imperfect complementarity to the 3′-untranslated region (UTR) of target mRNAs and promote translation repression [4, 5].

Shao-Yao Ying (ed.), *MicroRNA Protocols*, Methods in Molecular Biology, vol. 1733,
https://doi.org/10.1007/978-1-4939-7601-0_2,

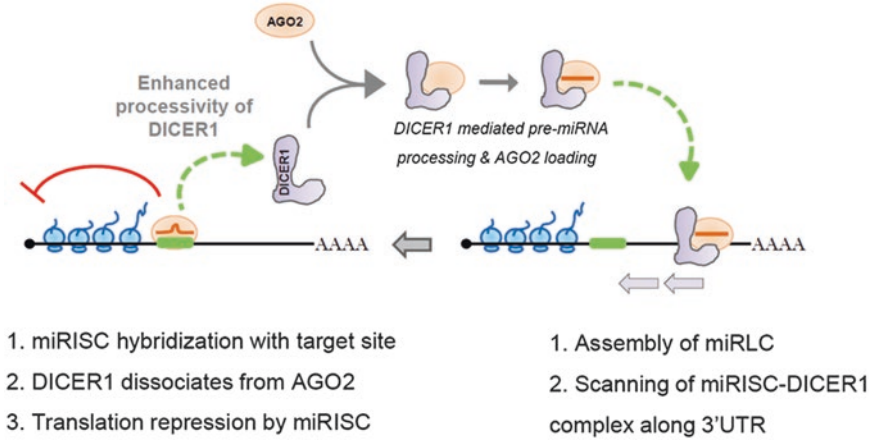

Fig. 1 A model of target-driven miRNA biogenesis. Schematic model of target mRNA-driven miRNA biogenesis (reproduced from ref. 7 with permission from *Nature Publishing Group*)

The exact mechanism of miRNA loading in humans needs further investigation. A human miRLC (miRNA Loading Complex) has been identified that primarily comprises a miRNA-free AGO2, DICER1, and TRBP2 [5, 6]. As per the canonical model of miRNA loading, within the miRLC RNase III endonuclease DICER1 processes the pre-miRNA followed by loading of the mature miRNA into AGO2. Furthermore, it has also been shown that once the AGO2 is loaded with the miRNA, the miRISC dissociates from the miRLC and the loaded miRISC can catalyze multiple rounds of target RNA repression [6].

We have shown that the presence of target mRNA increases pre-miRNA processing by AGO2-associated DICER1 leading to elevated biogenesis of cognate mature miRNA [7]. The processed miRNAs are loaded onto AGO2 to form functionally active miRISCs both in vivo and also in a cell-free system. Investigating the molecular mechanism of the event, we discovered that an increase in processivity of the enzyme DICER1 associated with the Ago proteins in the presence of target mRNA causes enhanced miRNA loading to Ago. However, after a successful miRNA loading, DICER1 remains associated with AGO2. The complex binds an mRNA and scans for a target site. Once the target site is found and a stable hybrid is formed, DICER1 dissociates from the miRLC and jumps to a fresh Argonaute for another round of miRNA loading. This step is accelerated when target mRNA is abundant, thereby contributing to increased processivity of DICER1, which leads to loading of a greater number of Argonaute molecules per unit of time (Fig. 1).

In this chapter we describe the in vitro RISC loading assay in the presence of target mRNAs, using affinity purified miRLC as well as miRLC reconstituted in vitro with recombinant AGO2 and DICER1. We also discuss the methodologies used to score the processivity of AGO2-associated DICER1 in the presence of target mRNA in an in vitro system.

2 Materials

All buffers and solutions are prepared using ultrapure water (GIBCO) and Molecular Biology grade reagents. All assays are carried out in RNase-free microcentrifuge tubes and pipette tips.

2.1 In Vitro RISC Loading Assay Using Affinity Purified miRLC

1. HEK293 cells stably expressing FLAG-HA-AGO2 (FH-AGO2) protein.
2. Dulbecco's Modified Eagle's Medium (DMEM) containing 2 mM glutamine and supplemented with 10% Fetal Calf Serum (FCS, GIBCO) and antibiotics (Penicillin and Streptomycin, GIBCO).
3. Anti-FLAG M2 affinity agarose (Sigma) beads.
4. Cell Lysis buffer: 10 mM HEPES pH 7.4, 200 mM KCl, 5 mM $MgCl_2$, 1 mM DTT, 1× EDTA-free protease inhibitor (Roche), 5 mM vanadyl ribonucleoside complex (Sigma), 1% Triton X-100.
5. Immunoprecipitation (IP) wash buffer: 20 mM Tris-HCl pH 7.4, 150 mM KCl, 5 mM $MgCl_2$, 1 mM DTT, 1× EDTA-free protease inhibitor (Roche).
6. Synthetic pre-miR-122 or pre-let-7a with radiolabeled or unlabeled phosphate at the 5′ end.
7. In vitro transcribed target mRNAs (RL-con and RL-3×bulge-miR-122/RL-3×bulge-let-7a) with m7G (7-methyl guanosine) cap and a polyA tail. Transcription carried out using mMESSAGE mMACHINE T7 transcription kit (Thermo Scientific) as per manufacturer's protocol. Poly adenylation of transcribed mRNAs done using Poly (A) tailing kit (Thermo Scientific; AM1350).
8. Reagents for synthetic pre-miRNA labeling: Synthetic pre-miR-122, T4 Polynucelotide Kinase (Thermo Scientific), 10× T4 PNK Buffer, γ^{32}P-ATP (Perkin Elmer) or ATP (Thermo Scientific), ultrapure water, G-50 RNA spin columns (Roche).
9. RISC loading assay buffer: 20 mM Tris-HCl pH 7.5, 200 mM KCl, 2 mM $MgCl_2$, 5% glycerol, 1 mM DTT, 40 U/ml RNase inhibitor (Fermentas).
10. Reagents for RNA isolation: TRIzol LS reagent (Thermo Scientific), chloroform, Acidic phenol pH 4.5, 2-propanol, 75% Ethanol, DEPC treated water (OmniPur).
11. Carrier tRNA (*E. coli* Glutamyl tRNA, Sigma) or Glycogen carrier (Thermo Scientific).
12. 8 M urea/12% polyacrylamide gel and midi-gel apparatus (Hoefer SE400 gel electrophoresis unit).

13. RNA loading dye (96% Formamide, Xylene Cyanol, Bromophenol blue).
14. Phosphorimager (Perkin Elmer).
15. Reagents for Reverse Transcriptase real-time (RT-PCR) for TaqMan miRNA assays (Thermo Scientific).
16. Standard reagents for western blotting including primary antibodies: anti-HA (Roche), anti-AGO2 (Novus Biologicals), and anti-DICER1 (Bethyl).

2.2 In Vitro Pre-miRNA Processing Assay Using Recombinant Proteins

1. Recombinant AGO2 (Sino Biologicals; *see* **Note 1**).
2. Recombinant Dicer (Recombinant Human Dicer Enzyme kit, Genlantis; *see* **Note 1**).
3. In vitro transcribed target mRNAs (RL-con and RL-3×bulge-miR-122) with m^7G (7-methyl guanosine) cap and a polyA tail.
4. Assay buffer: 20 mM Tris-HCl pH 7.5, 200 mM KCl, 2 mM $MgCl_2$, 5% glycerol, 1 mM DTT, 40 U/ml RNase inhibitor (Fermentas).
5. Standard reagents for western blotting including primary antibodies: anti-AGO2 (Novus Biologicals).
6. Silver Staining kit (Thermo Scientific).
7. 8 M urea/12% polyacrylamide gel and mini-gel apparatus (BioRad).
8. Reagents for Reverse Transcriptase real-time (RT-PCR) for TaqMan miRNA assays (Thermo Scientific).

2.3 Association of DICER1 and AGO2 Along the 3′ UTR After In Vitro Pre-miRNA Processing Assay

All reagents required for Subheading 2.1 are required here along with the following additional reagents.

1. HEK293 cells stably expressing FH-AGO2 protein.
2. N-HA-DICER1 plasmid.
3. Lipofectamine 2000 for transfection.
4. 3× FLAG peptide (Sigma).
5. ProteinG agarose beads (Thermo Scientific).
6. Protein G agarose bead Blocking buffer (5% BSA in Lysis buffer). Composition of Lysis buffer described in Subheading 2.1.
7. Primary antibodies: anti-AGO2 (Novus Biologicals), anti-DICER1 (Bethyl).

2.4 In Vitro Assay to Score the Processivity of DICER1

All reagents required for Subheadings 2.1 and 2.3 are required here along with the following additional reagents.

1. pre-let-7a (Pre-miR miRNA precursors, Thermo Scientific).
2. In vitro transcribed target mRNAs (RL-con and RL-3×bulge-let-7a) with m^7G (7-methyl guanosine) cap and a polyA tail.

3 Methods

We first describe the protocols used to carry out the in vitro RISC loading assays and subsequently discuss the in vitro systems used to prove target-driven miRNA biogenesis by increased processivity of AGO2-associated DICER1.

3.1 Preparation of Pre-miRNA for In Vitro RISC Loading Assay

1. Resuspend the lyophilized synthetic pre-miR122/pre-let-7a (Eurogentec) in DEPC-treated water and store aliquots at −80 °C.
2. For a single 20 μL labeling reaction, use 20 pmol of pre-miRNA and add the other reagents according to the table below (*see* **Note 2**):

Reagents	Volume (μL)
10× T4 PNK buffer	1.5
pre-miR-122/pre-miR-let-7a (50 μM)	0.4
γ^{32}P ATP (10 μCi/μL)	2.0
T4 PNK enzyme	1.5
Water	9.6
Total volume	15

3. Incubate the reaction at 37 °C for 30 min in a thermomixer, followed by quenching the reaction adding 85 μL Tris-EDTA (TE).
4. Remove the excess radioactivity by column-purifying the whole reaction using a standard G-50 RNA spin column using the manufacturer's instructions.
5. Isolate RNA from the column-purified 100 μL reaction using TRIzolLS (Thermo Scientific, *see* **Note 3**).
6. Resuspend RNA in 20 μL DEPC-treated water to generate a radiolabeled working stock of 1 pmol/μL (1 μM).

3.2 In Vitro RISC Loading Assay Using Affinity Purified miRLC

1. Culture HEK293 cells stably expressing FH-AGO2 in DMEM supplemented with 10% FCS in two 10 cm tissue culture dishes (*see* **Note 4**). Harvest the cells using a cell scraper after a wash with PBS and collect the cells in a microcentrifuge tube. Centrifuge the cell suspension at 600 × *g* for 5 min at 4 °C in a cold centrifuge. Re-wash with PBS and repeat the centrifugation step.
2. Add 500 μL of Cell Lysis Buffer to the cell pellet which has approximately 10^7 cells (*see* **Note 5**). Resuspend the cell pellet in the buffer and lyse the cells by rotating in a nutator at 4 °C.

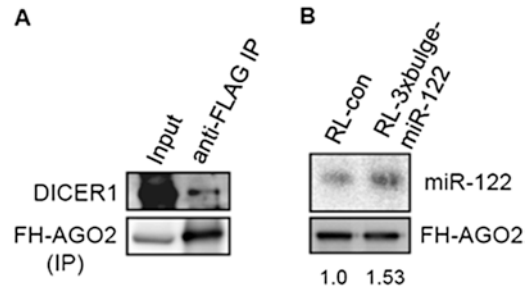

Fig. 2 In vitro RISC loading assay using affinity purified miRLC. Increased DICER1 activity in the presence of target mRNA contributes to enhanced miRNA production from pre-miRNA. (**a**) Immunoprecipitation of FH-AGO2 from FH-AGO2 stable HEK293 cells. Presence of associated endogenous DICER1 protein confirmed by western blotting. (**b**) in vitro RISC loading assay in the presence and absence of miR-122 target mRNA, RL-3×bulge-miR-122. RL-con serves as the target mRNA control. Autoradiography shows higher mature miR-122 produced in the presence of RL-3×bulge-miR-122 compared to RL-con (reproduced from ref. 7 with permission from *Nature Publishing Group*)

3. Post-lysis sonicate the cell lysate by three to four pulses of 60% amplitude (*see* **Note 6**). Centrifuge the sonicated lysate at 16,000 × *g* for 10 min at 4 °C. Take out the clear supernatant and re-spin the supernatant at 16,000 × *g* for 10 min at 4 °C to collect the final cell lysate cleared of cellular debris.
4. Meanwhile, pipette out approximately 40 μL of anti-FLAG M2 affinity agarose beads in a fresh 1.5 ml microcentrifuge tube (*see* **Note 7**) and wash the beads with IP wash buffer twice at 2000 × *g* for 2 min at 4 °C.
5. Add the clarified cell lysate on the washed beads and carry out the immunoprecipitation reaction overnight or approximately 16 h at 4 °C in a nutator.
6. The following day, spin the tubes at 2000 × *g* for 2 min at 4 °C to pellet the agarose beads. Discard the supernatant and wash the beads with IP wash buffer three times at 2000 × *g* for 2 min at 4 °C. Check the immunoprecipitation of FH-AGO2 and also verify association of endogenous DICER1 by western blotting (Fig. 2a). Prior to the final wash, separate the beads into four tubes and centrifuge as these beads can now be directly used for the assay (*see* **Note 7**).
7. Prepare a master mix with radiolabeled pre-miR-122/pre-let-7a (stock 1 pmol/μL) and the assay buffer. Distribute the mix equally into the assay tubes. Add target RNAs (working stock 200 ng/μL) at a final concentration of 25 ng/μL and make up volume of the reaction to 20 μL.

Master mix	
1 pmol/μL *pre-miR-122*	=0.2 μL
RISC Loading Assay buffer	=4.8 μL
Total	=5.0 μL

For each reaction

Components	Volume added (μL)
Master Mix	5
Target mRNA (200 ng/μL)	2.5
FH-AGO2 beads	5
Assay Buffer	7.5
Final volume	20

8. Carry out the reaction at 37 °C for 1 h in a thermomixer (shaking is optional).
9. Wash the reactions using 500 μL IP wash buffer per loading reaction, three times at 2000 × *g* for 2 min at 4 °C.
10. Add 50 μL of assay buffer to each tube along with 1 μL of carrier tRNA (10 μg/μL stock) and add equal volume of acidic phenol pH 4.5: chloroform (5:1). Mix well and isolate RNA using the standard RNA isolation protocol (*see* **Note 8**).
11. Dissolve RNA in 1× RNA Loading dye for electrophoresis (*see* **Note 9**).

3.3 Detection of Mature miRNA Product of In Vitro RISC Loading Assay by Gel Electrophoresis and Autoradiography

1. Cast the 8 M Urea/12% polyacrylamide gel using the Hoefer midi-gel electrophoresis apparatus (*see* **Note 10**). Pre-run the gel using 1× RNA loading dye for about 30 min before loading the samples.
2. Load the samples using a Hamilton syringe for accurate loading and run the gel at 180 V for around 4 h or until the bromophenol blue dye front has covered 90% of the gel length.
3. Fix the gel in a fixing solution (10% Methanol, 10% Acetic acid in water) for 45 min followed by vacuum-drying the gel for 30 min at 80 °C followed by another 1 h at room temperature.
4. Image the gel using phosphorimager (Fig. 2b).

3.4 In Vitro Pre-miRNA Processing Assay Using Recombinant Proteins

1. Recombinant human AGO2 (rAGO2; Sino Biologicals) and recombinant human DICER1 (rDICER1; Genlantis) were commercially obtained. Verify the purity of the rAGO2 by SDS-PAGE and silver staining (Fig. 3a).
2. In vitro pre-miR-122 processing assay was carried out using three different concentrations of rDICER1. For this assay,

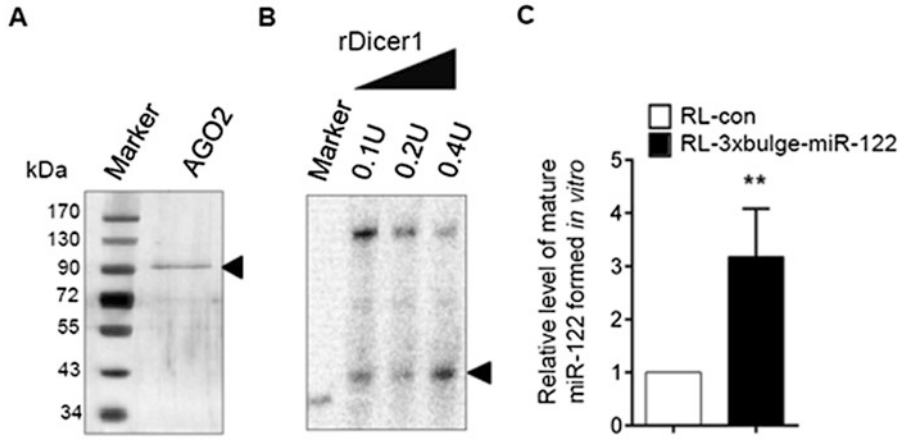

Fig. 3 In vitro RISC loading assay using recombinant proteins. (**a**) Silver staining of rAGO2 to confirm the absence of DICER1 protein contamination. (**b**) Pre-miRNA processing activity of rDICER1 using increasing amounts of the enzyme. Arrowheads mark the exact rAGO2 band in the silver-stained gel and the mature miR-122 formed in the autoradiogram (reproduced from ref. 7 with permission from *Nature Publishing Group*). (**c**) Real-time-based quantification of amount of mature miR-122 formed in vitro

incubate 0.1, 0.2 and 0.4 U of the rDICER1 enzyme with 10 nM synthetic 5′radiolabeled pre-miR-122 for 1 h at 37 °C (Fig. 3b). The components of a single reaction are given below (*see* **Note 11**).

Reagents	Amount
5′ radiolabeled pre-miR-122	0.2 µL
rDICER1	0.2 µL (0.1 U), 0.4 µL (0.2 U), 0.8 µL (0.4 U)
RISC Loading assay buffer	Make up volume to 20 µL
Total	20 µL

3. In a general in vitro pre-miRNA processing assay, add 50 ng of rAGO2 and 0.1 U of rDICER1 in a vial with 10 nM 5′ phosphorylated pre-miR-122/pre-let-7a, 500 ng target mRNA (RL-con, RL-3×bulge-miR-122/RL-3×bulge-let-7a), and RISC loading assay buffer in a 20 µL reaction. *See* table below.

Reagents	Amount
5′ phosphorylated pre-miRNA (1 µM)	0.2 µL (10 nM)
rDICER1	0.1 U (0.2 µL)
rAGO2 (10 ng/µL)	5 µL (50 ng)
Target mRNA	500 ng (add volume accordingly)
RISC Loading assay buffer	Volume to 20 µL
Total	20 µL

4. Mix properly, spin down the reaction, and incubate at 4 °C for 45 min to allow binding of proteins with each other and target mRNA.
5. After 45 min, shift the vials to 37 °C in a thermomixer and incubate for another 1 h for carrying out the DICER processing reaction.
6. Increase the reaction volume from 20 to 100 μL for the convenience of RNA isolation. Add 1 μL of carrier tRNA (10 μg/μL) and add equal volume of acidic phenol pH 4.5: chloroform (5:1). Mix well and isolate RNA using the standard RNA isolation protocol.
7. Detect the amount of mature miRNA formed by TaqMan-based real-time PCR as per the manufacturer's protocols (Fig. 3c).

3.5 Association of DICER1 and AGO2 Along the 3′ UTR After In Vitro Pre-miRNA Processing Assay

1. HEK293 cells stably expressing FH-AGO2 were transfected with N-HA-DICER1 plasmid. Transfect a 10 cm diameter tissue culture dish of 80% confluent HEK293 cells with 6 μg N-HA-DICER1. Split the cells after 24 h into two more 10 cm diameter dishes.
2. Harvest the cells after another 24 h; lyse the cells and immunoprecipitated FH-AGO2 using anti-FLAG agarose beads as described in Subheading 3.1.
3. Prepare 3× FLAG peptide solution in RISC Loading assay buffer by adding 3 μL of 3× FLAG Peptide (5 mg/ml stock) in 100 μL buffer. After three washes with Immunoprecipitation buffer, incubate the beads with 3× FLAG peptide solution (150 ng/μL final concentration) for 30 min on ice with intermittent tapping. Spin the beads at 6000 × *g* for 1 min and pipette out the supernatant, which is the eluted FH-AGO2 protein (*see* **Note 12**).
4. Perform an in vitro pre-miR-122 processing reaction of 100 μL volume using 10 nM 5′phoshorylated pre-miR-122, 25 ng/μL RL-3×bulge-miR-122 and eluted FH-AGO2 for 60 min at 37 °C.
5. Post-reaction, add 100 μL of assay buffer and divide the reaction into two equal halves. Move to the second immunoprecipitation reaction.
6. For the second immunoprecipitation, wash ProteinG agarose beads (20 μL bead volume per reaction) and block the beads for 1 h at 4 °C in Bead Blocking buffer. Re-wash the beads and for antibody binding, incubate the beads with anti-AGO2 and anti-DICER1 antibodies (1:50 v/v) in 100 μL lysis buffer. Let antibody binding proceed for at least 2–3 h.
7. Add one half of the reaction to anti-AGO2 containing vial and the other half to anti-DICER1 vial and immunoprecipitate for

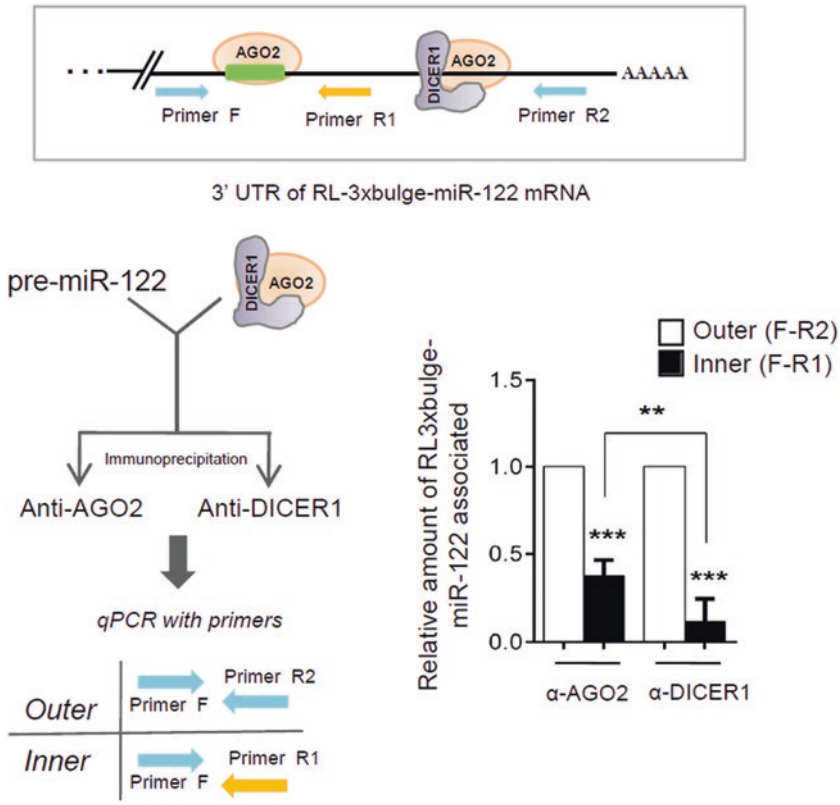

Fig. 4 Association of DICER1 and AGO2 with target site proximal and distal regions of the 3′UTR after in vitro pre-miRNA processing assay. The rationale behind the assay described in the top panel with a cartoon representation of the RL-3×bulge-miR-122 3′UTR. Scheme of the assay has been outlined in the left panel. In vitro RISC loading assay with FH-AGO2 immunoprecipitated from FH-AGO2 stable HEK293 cells transiently expressing N-HA-DICER1. Post reaction, AGO2 and DICER1 are immunoprecipitated using antibodies against the endogenous proteins. Real-time PCR-based quantification of the region of 3′UTR associated with AGO2 and DICER1 has been plotted (reproduced from ref. 7 with permission from *Nature Publishing Group*)

16 h at 4 °C. Wash the beads for three times with IP wash buffer and isolate RNA using Trizol LS and chloroform as discussed earlier.

8. Perform a real-time qRT-PCR using one common forward primer and two sets of reverse primers (Fig. 4). This is done to check the differential association of the two proteins, AGO2 and DICER1, along the 3′UTR. If DICER1 dissociates from AGO2 upon the recognition/hybridization with target site, then association of DICER1 in close vicinity of miRNA binding site should be lower compared to its association with the remaining half of the 3′UTR. Conversely, AGO2 should be associated equally with the target-proximal region as well as the rest of the 3′UTR.

3.6 In Vitro Assay to Score the Processivity of DICER1

1. HEK293 cells stably expressing FH-AGO2 were transfected with pre-let-7a miRNA precursor. Harvest the cells, lyse them, and perform immunoprecipitation as described in Subheading 3.1. Elute miRISC (FH-AGO2) enriched in let-7a, as described in Subheading 3.5. Approximately, elute miRISC immunoprecipitated from 10^7 cells in 10 μL of assay buffer.
2. Add miRISC, target mRNA (RL-con or RL-3×bulge-let-7a) and foreign precursor 5′ phosphorylated pre-miR-122 (10 nM) with RISC loading assay buffer in a 20 μL reaction.
3. Mix well and incubate at 37 °C for 30 min followed by RNA isolation as described earlier (Subheadings 3.1 and 3.4).

Reagents	Amount
miRISC (let-7a enriched)	10 μL
Target mRNA (RL-con/RL-3×bulge-let-7a)	500 ng (volume accordingly)
Pre-miR-122 (1 μM)	0.2 μL (10 nM)
RISC Loading assay buffer	Upto 20 μL
Total	20 μL

4. Measure the amount of mature miR-122 formed by TaqMan-based real-time PCR to score the processivity of the enzyme DICER1 (Fig. 5).

4 Notes

1. It is necessary to check the purity of the recombinant proteins. AGO2 should be free of any associated DICER1. Verify by running a SDS-PAGE and silver staining for AGO2. Enzymatic activity of DICER1 can be confirmed by a simple pre-miRNA processing assay (Subheading 3.4). The same assay using rAGO2 alone should not yield any mature miRNA species, reconfirming that rAGO2 is free of any associated functional DICER1 protein.
2. For the detection of mature miRNA product by qRT-PCR, 5′ end labeling is not required. However, the 5′ end of the synthetic pre-miRNA needs to be phosphorylated for recognition by DICER1. 5′ phosphorylation can be done using the same protocol using T4 PNK; only γ^{32}P ATP needs to be replaced by normal molecular biology grade ATP at a concentration of 0.2 mM in a 20 μL reaction.
3. For the isolation of the labeled RNA, it is advisable to use Glycogen as it is an inert carrier which significantly increases

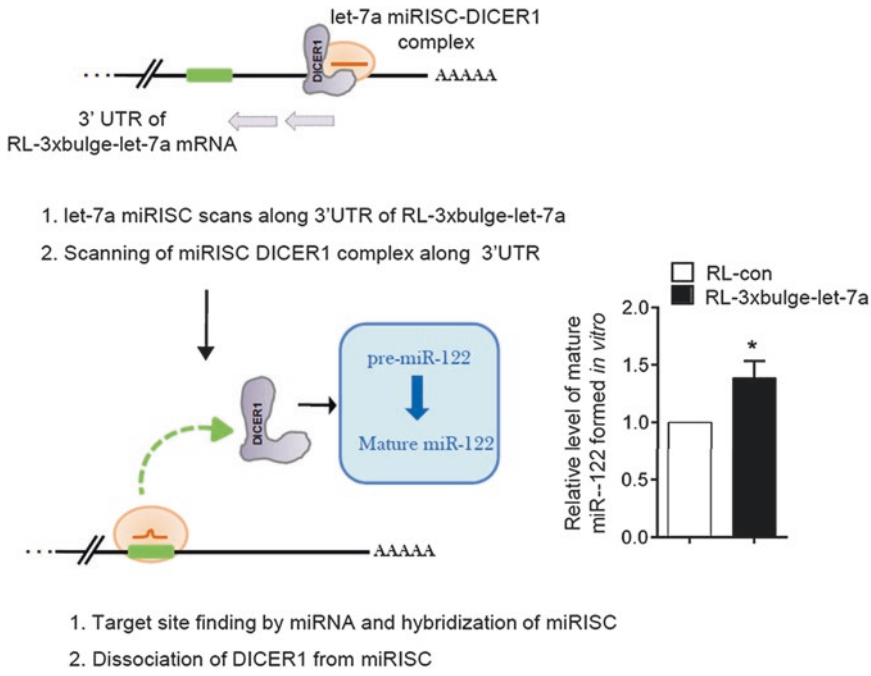

Fig. 5 In vitro assay to score the processivity of DICER1. Scheme of the assay has been outlined in the left panel. FH-AGO2 immunoprecipitated from FH-AGO2 stable HEK293 cells transiently expressing pre-let-7a was incubated with RL-3×ulge-let-7a target mRNA. Synthetic pre-miR-122 has been added to the assay so as to measure the processivity of DICER1. Real-time PCR-based quantification of the amount of mature miR-122 formed from the reaction in the presence and absence of let-7a target mRNA has been plotted (reproduced from ref. 7 with permission from *Nature Publishing Group*)

the recovery of nucleic acids by alcohol precipitation. Add 0.5–1 μL of Glycogen (20 mg/ml stock) during the isopropanol precipitation step and refrigerate at −20 °C overnight for best yields.

4. The cells should not be overgrown; 70–80% confluency is preferable during harvesting. Research from our laboratory has shown that over-confluent cells or cells from high density cultures differ in several physiological properties, including growth rate and miRNA metabolism [8].
5. The amount of lysis buffer used is important. For approximately 10^7 cells 500 μL is sufficient. Lowering or increasing the cell number should be taken note of and the amount of buffer used for lysis to be adjusted accordingly.
6. Note the rationale behind sonication of the cell lysate. Sonication is exclusively done for complete lysis of the cells and isolation of FH-AGO2 from all cellular compartments that might fail to lyse using 1% Triton X-100 alone. Experiments carried out in the absence of sonication yield less amount of FH-AGO2.

7. It is mandatory to pipette out anti-FLAG M2 beads or even normal Protein G-agarose beads using tips with widened mouth in order to avoid pipetting error. To achieve that we cut the mouth of the tips before use. Also, pipette out double the volume of beads needed, i.e., if 20 μL beads is needed pipette out 40 μL bead solution. Always autoclave cut tips before using.
8. The carrier tRNA should be added in the reaction after the completion of the assay, just before RNA isolation. Overnight precipitation at −20 °C is recommended here as well.
9. For real-time PCR-based detection of mature miRNA species from the assay, the RNA pellet should be dissolved in DEPC-treated water and not RNA loading dye.
10. Wash the lanes thoroughly before loading the samples as urea deposits in the lanes precluding accurate sample loading. To prevent sample loss during loading, wash lanes with TBE running buffer using a syringe needle.
11. Apart from purity checking, the pre-miRNA processing assay with increasing doses of rDICER1 is important to determine the amount of enzyme to be used for in vitro loading assays. For our experimental purpose, we required catalytic amounts of DICER1 with excess of AGO2 in order to detect the processivity of the DICER1 enzyme. Hence, the lowest unit of rDICER1 that yielded visible mature miRNA was fixed for subsequent assays.
12. Pipette out the eluted FH-AGO2 cautiously to avoid contamination with agarose beads. If necessary, re-spin the eluted protein to remove any extra contaminating beads.

References

1. Carthew RW, Sontheimer EJ (2009) Origins and Mechanisms of miRNAs and siRNAs. Cell 136:642–655
2. Ghildiyal M, Zamore PD (2009) Small silencing RNAs: an expanding universe. Nat Rev Genet 10:94–108
3. Kim VN, Han J, Siomi MC (2009) Biogenesis of small RNAs in animals. Nat Rev Mol Cell Biol 10:126–139
4. Bartel DP (2009) MicroRNAs: target recognition and regulatory functions. Cell 136:215–233
5. Ha M, Kim VN (2014) Regulation of microRNA biogenesis. Nat Rev Mol Cell Biol 15:509–524
6. Maniataki E, Mourelatos Z (2005) A human, ATP-independent, RISC assembly machine fueled by pre-miRNA. Genes Dev 19:2979–2990
7. Bose M, Bhattacharyya SN (2016) Target-dependent biogenesis of cognate microRNAs in human cells. Nat Commun 7:12200
8. Ghosh S, Bose M, Ray A, Bhattacharyya SN (2015) Polysome arrest restricts miRNA turnover by preventing exosomal export of miRNA in growth-retarded mammalian cells. Mol Biol Cell 26:1072–1083

Chapter 3

Isolation of Viral-Infected Brain Regions for miRNA Profiling from Formalin-Fixed Paraffin-Embedded Tissues by Laser Capture Microdissection

Anna Majer and Stephanie A. Booth

Abstract

Brain is a highly heterogeneous organ with numerous layers of specialized cells. Viral infection further adds complexity to downstream analysis because only a subpopulation of the brain is infected. In these instances, molecular changes that occur within infected cells are not truly reflected when whole tissue is used for downstream analysis. Laser capture microdissection (LCM) is a tool that allows for the selection and isolation of cells or regions of interest as determined by microscopic observation. It provides a platform for visually selecting the tissue that truly represents the material one wishes to study, such as viral infected cells. Formalin-fixed paraffin-embedded viral-infected tissue allows for safe handling and processing by LCM. Here, we describe a method whereby viral-infected regions of the brain were specifically isolated by LCM from the rest of the FFPE tissue. The isolated regions were then used to extract RNA for microRNA profiling. This approach can be applied to study microRNA changes from any viral infection in any given tissue.

Key words microRNA, Brain, Virus, Laser capture microdissection (LCM), Formalin-fixed paraffin-embedded (FFPE)

1 Introduction

A common problem when studying the host response to infection in complex tissues is untangling the molecular changes that occur in specific cell types, in infected cells, and in bystander cells. As a result, molecular changes that are identified in whole brain tissue represent an average response of all these effects. This effect is further compounded during a viral infection because only a subpopulation of cells undergoes active viral infection at any given time. In this case, changes in cellular constituents within virus-infected cells can be significantly diluted. Specific enrichment for cells or tissue areas that are highly infected by the virus can address these challenges and expose specific changes in cellular constituents that are related to viral infection. One such approach is the use of laser capture microdissection (LCM) which enables the physical separation of specific cells or regions of interest from the rest of the tissue.

Shao-Yao Ying (ed.), *MicroRNA Protocols*, Methods in Molecular Biology, vol. 1733,
https://doi.org/10.1007/978-1-4939-7601-0_3,

The LCM technology described in this protocol is performed on the Arcturus^{XT}™ (Nikon *Eclipe* Ti-E, Thermo Fisher Scientific) which employs an infrared (IR) laser for capture and an ultraviolet (UV) laser for cutting. The fundamental procedure for the Arcturus^{XT}™ LCM is to (1) visualize and select the cells or region of interest using a microscope, (2) melt a thermolabile polymer located on the bottom of a cap using the IR laser so that it adheres to the cell/tissue area, (3) activate the UV laser so that it precisely cuts around the region of interest (usually used to remove larger tissue areas without tearing), and (4) isolate the cells or region of interest by moving the cap from the tissue section. Once cells or tissue of interest is isolated from the section, extraction buffers are applied to the polymer allowing for the collection of molecules, such as microRNAs, for downstream analysis.

In this protocol, viral-infected mouse brain tissues that were formalin-fixed paraffin-embedded (FFPE) are used. The biological hazard that many viruses pose necessitates the need to inactivate the virus prior to handling the samples safely. This can be achieved by FFPE treatment of the tissue which results in cross-linking of proteins with each other and with nucleic acids [1, 2]. As a result, this process inactivates key enzymes that viruses require for replication and spread. However, FFPE processing of tissue also damages the DNA and RNA molecules [3–6], making it challenging to isolate nucleic acids from these samples for downstream applications such as quantitative real-time reverse-transcription PCR (qRT-PCR). For example, RNA extracted from FFPE tissue is fragmented to approximately 100 base pairs in length [7, 8] and only a small fraction of the mRNA population remains accessible for cDNA synthesis [9]. Although degraded RNA can still be processed by microarrays, the results are less reproducible than when using RNA from fresh or frozen samples [10]. Next-generation sequencing approaches show better correlation between FFPE versus frozen samples [11]; however, detection of viral genomes from FFPE samples for phylogenetic analysis was less successful [12]. In contrary, microRNAs (miRNAs) remain less prone to degradation and modification by the FFPE process because of their small size (~21 nucleotides in length) and association with protein complexes [13]. Indeed, miRNA expression profiles in FFPE tissues correlate well with expression profiles detected in frozen tissues [14].

In terms of function, miRNAs are predicted to post-transcriptionally regulate ~30% of all human genes [15] and many miRNAs are deregulated during diseases including viral infections [16]. In fact, many viruses actually encode their own miRNAs within their genomes [17, 18], further highlighting the important contribution miRNA have in terms of viral pathogenicity. Therefore, identifying miRNAs that are deregulated during viral infection will help enhance the understanding of the molecular pathways involved during disease.

Herein, we describe the method used to physically isolate a region of interest from the mouse brain tissue using LCM. We describe the procedure to stain and dehydrate the FFPE sections so that they will be suitable for LCM. We highlight the key considerations for successful LCM of viral-infected regions and describe the extraction of RNA from the isolated regions for downstream miRNA expression studies. The protocol described here can be followed to profile miRNA changes in any organ that is infected by any virus in order to illuminate molecular changes that occur during disease.

2 Materials

2.1 Staining of Tissue Sections

1. FFPE tissue section(s) on polyethylene naphthalate (PEN) membrane glass slides (Thermo Fisher Scientific).
2. RNAse Zap (Thermo Fisher Scientific).
3. DEPC-treated water (Thermo Fisher Scientific).
4. Arcturus® Paradise® Plus stain, slide jars and slides (Thermo Fisher Scientific).
5. Cresyl Violet acetate stain (Sigma-Aldrich).
6. 100% ACS grade ethanol alcohol (anhydrous) (Commercial Alcohols).
7. Xylene, histological grade (Fisher Chemical).
8. Nuclease-free water (Thermo Fisher Scientific).
9. 95% ethanol in nuclease-free water (prepare 25 mL per jar).
10. 75% ethanol in nuclease-free water (prepare 25 mL per jar).
11. Forceps.
12. Kimwipes® cleansing wipes or similar lint-free towels.

2.2 Laser Capture Microdissection

1. CapSure® Macro LCM Caps (Thermo Fisher Scientific).
2. Arcturus$^{XT™}$ Laser Capture Microdissection System (model: Nikon *Eclipse* Ti-E, Thermo Fisher Scientific).

2.3 RNA Extraction and qRT-PCR Profiling

1. RNAse Zap (Thermo Fisher Scientific).
2. Forceps (Sigma-Aldrich).
3. RNase-free 1.5 mL microcentrifuge tubes (Thermo Fisher Scientific).
4. RNase-free 0.2 mL microcentrifuge tube (Thermo Fisher Scientific).
5. Thermomixer or equivalent.
6. Arcturus® Paradise® Extraction and Isolation Kit (Thermo Fisher Scientific).
7. PureLink® DNase Set (Thermo Fisher Scientific).

8. TaqMan® MicroRNA Reverse Transcription Kit (Thermo Fisher Scientific).
9. TaqMan® Universal Master Mix II, no AmpErase UNG (catalog #4440040, Thermo Fisher Scientific).
10. TaqMan® miRNA Assays (specific miRNA requires assay ID as well, Thermo Fisher Scientific).
11. ViiA™ 7 System or equivalent.

3 Methods

Clean all the surfaces with RNAse Zap to remove possible RNA degrading enzymes and make sure to also clean the inside of the tissue flotation water bath.

3.1 Preparing Formalin-Fixed Paraffin-Embedded Sections

1. Fix mouse brain tissue in 10% Neutral Buffered Formalin for 14–24 h and prepare paraffin blocks following established protocols in your laboratory.
2. Using a rotary microtome, place block into the specimen holder and trim excess paraffin from the block surface. Cut and discard first 4–5 sections.
3. Cut two serial sections from the tissue block. One section (5–8 μm thick) will be used for immunohistochemistry (IHC) while the other section (8–30 μm thick) will be used for LCM.
4. Once cut, float sections with a brush onto heated water bath (~42 °C) containing DEPC-treated water. Make sure the sections are in the water bath for <2 min.
5. Float the thin section (5–8 μm thick) onto a glass slide and perform IHC following the protocols established in your laboratory. This section will serve as a roadmap for identifying the region(s) of interest, such as viral-infected cells. In our experiments, we performed IHC on an 8 μm thick section to identify viral-infected cells within mouse brain tissue [19].
6. Float the thicker section (8–30 μm) onto the surface of a PEN membrane slide that will be used for LCM (*see* **Note 1**). Air-dry the slide (1.5–3 h) at room temperature. Once dried, proceed to the next step or store the slide at −80 °C for up to 3 months.

3.2 Processing FFPE Brain Sections for Laser Capture Microdissection

1. Prepare 10 plastic slide jars containing ~25 mL of xylene, 100% ethanol, 95% ethanol, 75% ethanol, and nuclease-free water (Fig. 1) (*see* **Note 2**).
2. Only if the slide was previously frozen, remove it from the freezer and place in a 55 °C oven for 2 min (*see* **Note 3**). Otherwise, skip this step.

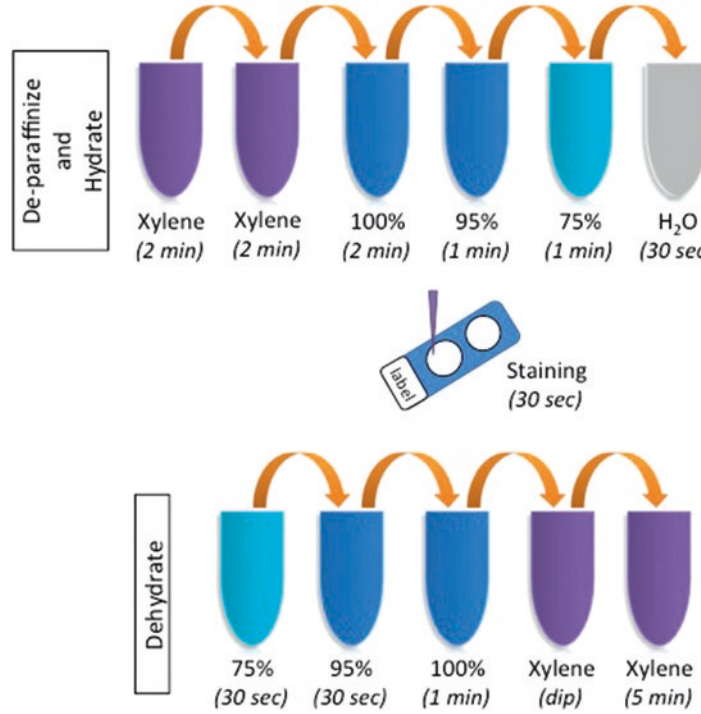

Fig. 1 Schematic diagram of de-paraffinization, staining, and dehydration of FFPE sections for LCM. Incubate the slide in two xylene washes followed by 100% ethanol to remove paraffin. Hydrate the section in 95% ethanol, 75% ethanol, and water followed by adding the stain onto the sectioned tissues. Subsequently wash off excess stain in 75% ethanol and dehydrate the slide in 95%, 100% ethanols followed by incubation in xylene to remove traces of water and ethanol

3. Place the slide gently in the first xylene wash for 2 min and then transfer to the second xylene jar for another 2 min.
4. Place the slide in 100% ethanol for 2 min followed by 95% ethanol for 1 min and then 75% ethanol for 1 min.
5. Place the slide in nuclease-free water for 30 s and then place flat on a Kimwipe (tissue side up). Add ~300 μL of Cresyl Violet stain directly to the tissue on the slide and incubate for 30 s (*see* **Note 4**).
6. Gently tip the slide perpendicular to the Kimwipe to wick away excess stain and place the slide in 75% ethanol for 30 s.
7. Transfer the slide to the 95% ethanol and incubate for 30 s. Place the slide in 100% ethanol for 1 min followed by gently dipping the slide in xylene until ethanol is washed off (*see* **Note 5**).
8. Place the slide in another xylene jar to incubate for 5–10 min.
9. Remove the slide from the last xylene wash, gently dab off excess liquid on a Kimwipe. Air-dry the slide in a fume hood

for 5–10 min by placing on a Kimwipe with the tissue facing up (*see* **Note 6**). Once dried, proceed to the next step.

3.3 Laser Capture Microdissection

We performed the cut and capture feature which uses the IR laser to melt the thermoplastic film onto the tissue followed by the UV laser cutting around the area of interest. This process allows for the removal of a large region of interest from the rest of the tissue without tearing.

1. Turn on the computer, the microscope, and the Arcturus^{XT} instrument. Start the software for the Arcturus^{XT} instrument.
2. In the "Setup tool" pane click "Present Stage." This will move the work surface so that the slides and caps can be loaded. Load the slides and LCM caps. Press the "i" icon on the top right corner of the "Setup tool" pane to open "Load Options." In the "Load Options" window, click on the "Slides" tab and select the position corresponding to where you loaded the slide. Slide(s) can also be named at this point. Select the "Caps" tab and select the type of caps and their positions (*see* **Note 7**). Click OK once complete.
3. "Inspect tools" pane allows you to view the slides by operating the microscope component of the instrument. The 2× magnification is selected as default. Each time you change the magnification you need to readjust the focus and brightness as necessary by selecting the up and down arrows. You can also select an autofocus and/or autobrightness option by clicking the icons located between the arrows for each respective setting.
4. The stage can be moved to view the area of interest by moving the trackball or by selecting the hand icon under the "Select tools" pane. Adjust the focus and brightness when necessary.
5. Select the 10× magnification and place a CapSure cap onto the slide by pressing the "Place cap" button in the "Microdissect tools" pane. Some of the cap should be positioned over a non-tissue area. This area will be used to optimize the IR laser settings. Move the field of view to this position.
6. In the "Microdissect tools" pane click the "i" button (top right corner) which will open the "Microdissect Options" pane. Go to the "UV Locate" tab and press the "Locate UV" button. This will fire the UV laser and a bright laser spot will appear in the main image window. Place the cursor in the center of the UV laser spot and click the spot. Then click OK in the "UV Locate" pane. A green circle will appear on the live image. This is the location of the UV laser (*see* **Note 8**).
7. In the "Microdissect Options" pane, click the "IR Locate" tab. Click "AutoLocate IR" and confirm that a blue plus sign appears on the live image corresponding to the location of the IR laser shot.

8. Confirm that you are at a non-tissue area to test the IR laser settings. Click the "IR Laser Test Fire" button in the "Microdissect tools" pane. Inspect the laser spot for the presence of a dark ring surrounding a clear center. This will indicate that the thermoplastic film is adequately melted and touches the tissue. Change these settings and click "Test IR shot" until you obtain the proper melting of the plastic (*see* **Note 9**). Once optimized, move the field of view back to the area of interest and fire the IR test spot near the area you wish to remove. This is to confirm that the IR settings remain adequate to melt the plastic film onto the tissue (*see* **Note 10**).
9. In the "Select tools" pane, use the Freehand Drawing tool to select the area for capture. Refer to the IHC stained section for relative coordinates for the area of interest. Once selected, go to the "Microdissect tools" pane and click the "Cut and Capture" button.
10. Once the cut and capture is complete, you can repeat the process by selecting another area for capture. When all the desired regions of interest are captured, in the "Microdissect tools" pane click the "Move cap to QC Caps station." This allows the inspection of captured material (*see* **Note 11**).
11. Unload the materials by clicking "Present Stage" in the "Setup tools" pane. Wearing gloves, carefully remove the cap from the QC Station area and continue to the next step.

3.4 RNA Extraction

Prior to isolation, clean all the surfaces with RNAse Zap to remove possible RNA degrading enzymes. Extract RNA using the Arcturus® Paradise® Extraction and Isolation reagents following the protocol recommended for the Macro LCM Caps.

1. Using forceps, carefully peel off the thermoplastic film polymer that is present on the cap and place it in a 1.5 mL microcentrifuge tube (*see* **Note 12**).
2. Prepare the Pro K Mix immediately before use by adding 300 μL of the Reconstitution buffer to 1 vial of dried Pro K Mix (600 μg). Gently vortex to dissolve completely and place on ice (1 vial can be used for 12 extractions).
3. Add 50 μL of the Pro K Mix, making sure that the tissue is immersed in the solution.
4. Incubate the sample at 37 °C for ~16 h without shaking (*see* **Note 13**).
5. Centrifuge the tube for 1 min at 800 × *g* and transfer the solution to a fresh tube provided in the kit, making sure to leave the thermoplastic film behind.
6. Thaw the DNase buffer (DNB) at room temperature and also pre-condition the MiraCol purification column (add 200 μL of

conditioning buffer to the filter, incubate for 5 min, and centrifuge at 16,000 × *g* for 1 min).

7. Add 53 µL of Binding buffer (BB) into the cell extract and mix well by gently pipetting up and down. Immediately add 103 µL of ethanol solution (EtOH) to the tube, mix and add to filter.
8. Centrifuge at 100 × *g* for 2 min, immediately followed by 16,000 × *g* for 1 min.
9. Wash the column by adding 100 µL of Wash Buffer 1 (W1) into the purification column and centrifuge at 8000 × *g* for 1 min.
10. To perform the on-column DNase digestion, mix 2 µL of DNase Mix with 18 µL of DNase buffer and add the entire amount to the column. Incubate for 20 min at room temperature.
11. Add 40 µL of W1 to the column and centrifuge at 8000 × *g* for 1 min.
12. Add 100 µL of Wash Buffer 2 (W2) to the column and centrifuge at 8000 × *g* for 1 min.
13. Add another 100 µL of W2 to the column and centrifuge at 8000 × *g* for 2 min. Typically, no wash buffer remains on the column, however, if any residual buffer remains then re-centrifuge at 16,000 × *g* for 1 min.
14. Transfer the column to a clean tube that is provided and add 14 µL of elution buffer directly to the membrane. Incubate for 1 min at room temperature and then centrifuge at 1000 × *g* for 1 min followed by 16,000 × *g* for 1 min.
15. Use immediately or store at −80 °C.

3.5 Profiling miRNAs by Real-Time PCR

We performed a two-step real-time PCR reaction using the TaqMan® miRNA Assays.

1. To profile several miRNAs from the same sample, we used a multiplex strategy at the cDNA step. Each cDNA reaction consisted of 2.5–4 µL of eluted RNA (*see* **Note 14**), 0.15 µL of dNTPs, 1 µL of MultiScribe Reverse Transcriptase, 1.5 µL of 10× Reverse Transcription Buffer, 0.19 µL of RNase Inhibitor, 4 µL of the primer mix (each primer was diluted 1:4), and nuclease-free water up to 15 µL (*see* **Note 15**). Each reaction was mixed well by pipetting, centrifuged for 2 min at 1000 × *g* and incubated in a thermocycler according to the manufacturer's instructions.
2. Each real-time PCR reaction consisted of 1.34 µL of cDNA, 1 µL of miRNA specific probe, 10 µL of TaqMan® Universal Master Mix II, no AmpErase UNG, and 7.66 µL of nuclease-free water. Mix well by pipetting and centrifuge for 2 min at 1000 × *g*. We followed the manufacturer's recommendations for the standard real-time PCR program on the ViiA™ 7 system (*see* **Note 16**).

3. Analyze the relative changes in miRNA expression between control and infected LCM cells/regions using the $2^{-\Delta\Delta CT}$ method [20] making sure to choose a reference miRNA as a normalizer that is not affected by the viral infection (*see* **Note 17**).

4 Notes

1. The thickness of the section depends on the amount of cells/regions intended for capture. We used 30 μm thick sections because we wanted to enrich the sample for viral infected cells.
2. Use fresh solutions and discard them according to standard procedures after processing eight slides or if not used for more than 1–2 weeks. If planning to leave the solution in a fume hood for 1 week, seal the cap with parafilm to prevent evaporation. When cleaning out the slide tubes, use 100% ethanol followed by wiping with RNAse Zap and then rinsing with nuclease-free water. This is especially important when processing infected and control tissue. Make sure that you clean out the containers when switching between the groups.
3. This step is important for the tissue to attach to the slide. If this is not performed the tissue has a much higher chance of being washed away during the rehydration and dehydration steps.
4. For proper staining, the tissue needs to be fully covered by Cresyl Violet to stain adequately. Therefore, the amount of stain added depends on the size of tissue sectioned. Other stains such as the Paradise stain can be substituted for Cresyl Violet.
5. Gently dunk the slide repeatedly in ethanol until there are no visible streaks of ethanol residue remaining. This is important to completely remove the water and ethanol from the slide, otherwise the LCM procedure will be less effective.
6. When tissue dries, you will notice that it becomes white. This is a good indication that the tissue is ready for LCM.
7. There are two sizes of caps, depending on the amount of material being captures select the appropriate caps. We used the Macro LCM Caps which have a larger area for capturing tissues because we were interested in capturing a larger area of interest. However, even if you plan to capture small areas but over numerous serial sections, we still recommend using a larger cap.
8. Make sure to confirm the location of the UV laser each time you place a new cap onto the slide, begin a new session or if the UV laser is not firing at the desired location.
9. If nothing is visible or if the inside of the spot is black, adjust the Power and Duration of the laser in the IR Spot Sizes tab. We found that a power of 50 mW and duration of 45 ms is a good

starting point for optimizing the IR laser settings. As a general rule, if the plastic is not melting, increase the IR laser power. If the cells cannot be detached, increase the duration of the IR.

10. We found that the IR settings may still need a slight adjustment when IR laser is fired over the tissue of interest.
11. If the area was not properly captured during microdissection, the same cap can be replaced in the area and the cut and capture procedure can be repeated. This can be done by right-clicking the cap that is in the QC station and selecting "Replace Cap on Slide" option. Click the "UV Cut" button to repeat all cuts and click the "IR Capture" button to repeat all captures.
12. We found that carefully removing the thermoplastic film from the cap resulted in no loss of tissue. However, care needs to be taken when performing this procedure as the tissue is very dry and can easily lift off the film. This is especially apparent when placing the sample into a microcentrifuge tube. Conversely, you can also use the Cap Insertion Tool available from Thermo Fisher Scientific to circumventing the need to peel off the thermoplastic film.
13. Parafilm the tubes to prevent evaporation and/or opening of the tubes during the long incubation period.
14. Depending on the type of sample and size of region of interest, the yield of RNA isolated may be too low to accurately detect by spectrophotometers such as Nanodrop or capillary electrophoresis system such as the Bioanalyzer. Furthermore, these do not directly measure the purity and integrity of the miRNAs within the sample. Therefore, we used a standard volumetric amount as input into the cDNA reaction to detect miRNAs from these samples. Specifically, we found that adding 2.5–4 μL of sample as a template was sufficient to detect medium to high abundant miRNAs.
15. This modification allowed detection of all miRNAs of interest from the same cDNA reaction. Furthermore, always include a non-template control at this step to validate that the primer mix does not amplify any nonspecific target.
16. When using probes for real-time PCR to detect miRNA targets, it is possible to extend the cycling beyond the 40 cycles set as the default for the program (i.e., can extend to 50 cycles). This will help detect lower abundant miRNAs from the sample, especially when only a small number of cells were collected. However, it is crucial to monitor any possible nonspecific amplification that occurs within the non-template controls and note the cycle that amplification takes place in comparison to your sample.
17. The reference miRNA chosen for normalization is particularly important. If screening only a small number of miRNAs, it is

recommended to test a number of potential reference miRNAs to determine which is the most stable and use that as a reference miRNA. This will change depending on the cell type under investigation. If performing a large-scale miRNA expression profiling study on these samples, mean expression value normalization is the best strategy for normalization [21].

References

1. Fox CH, Johnson FB, Whiting J et al (1985) Formaldehyde fixation. J Histochem Cytochem 33:845–853
2. Shi SR, Shi Y, Taylor CR (2011) Antigen retrieval immunohistochemistry: review and future prospects in research and diagnosis over two decades. J Histochem Cytochem 59:13–32
3. Tokuda Y, Nakamura T, Satonaka K et al (1990) Fundamental study on the mechanism of DNA degradation in tissues fixed in formaldehyde. J Clin Pathol 43:748–751
4. Williams C, Ponten F, Moberg C et al (1999) A high frequency of sequence alterations is due to formalin fixation of archival specimens. Am J Pathol 155:1467–1471
5. Srinivasan M, Sedmak D, Jewell S (2002) Effect of fixatives and tissue processing on the content and integrity of nucleic acids. Am J Pathol 161:1961–1971
6. von Ahlfen S, Missel A, Bendrat K et al (2007) Determinants of RNA quality from FFPE samples. PLoS One 2:e1261
7. Krafft AE, Duncan BW, Bijwaard KE et al (1997) Optimization of the isolation and amplification of RNA from formalin-fixed, paraffin-embedded tissue: the armed forces institute of pathology experience and literature review. Mol Diagn 2:217–230
8. Madabusi LV, Latham GJ, Andruss BF (2006) RNA extraction for arrays. Methods Enzymol 411:1–14
9. Godfrey TE, Kim SH, Chavira M et al (2000) Quantitative mRNA expression analysis from formalin-fixed, paraffin-embedded tissues using 5' nuclease quantitative reverse transcription-polymerase chain reaction. J Mol Diagn 2:84–91
10. Scicchitano MS, Dalmas DA, Bertiaux MA et al (2006) Preliminary comparison of quantity, quality, and microarray performance of RNA extracted from formalin-fixed, paraffin-embedded, and unfixed frozen tissue samples. J Histochem Cytochem 54:1229–1237
11. Hedegaard J, Thorsen K, Lund MK et al (2014) Next-generation sequencing of RNA and DNA isolated from paired fresh-frozen and formalin-fixed paraffin-embedded samples of human cancer and normal tissue. PLoS One 9:e98187
12. Mubemba B, Thompson PN, Odendaal L et al (2017) Evaluation of positive Rift Valley fever virus formalin-fixed paraffin embedded samples as a source of sequence data for retrospective phylogenetic analysis. J Virol Methods 243:10–14
13. Liu A, Tetzlaff MT, Vanbelle P et al (2009) MicroRNA expression profiling outperforms mRNA expression profiling in formalin-fixed paraffin-embedded tissues. Int J Clin Exp Pathol 2:519–527
14. Xi Y, Nakajima G, Gavin E et al (2007) Systematic analysis of microRNA expression of RNA extracted from fresh frozen and formalin-fixed paraffin-embedded samples. RNA 13:1668–1674
15. Lewis BP, Burge CB, Bartel DP (2005) Conserved seed pairing, often flanked by adenosines, indicates that thousands of human genes are microRNA targets. Cell 120:15–20
16. Trobaugh DW, Klimstra WB (2017) MicroRNA Regulation of RNA Virus Replication and Pathogenesis. Trends Mol Med 23:80–93
17. Skalsky RL, Cullen BR (2010) Viruses, microRNAs, and host interactions. Annu Rev Microbiol 64:123–141
18. Grundhoff A, Sullivan CS (2011) Virus-encoded microRNAs. Virology 411:325–343
19. Majer A, Caligiuri KA, Gale KK et al (2017) Induction of multiple miR-200/182 members in the brains of mice are associated with acute herpes simplex virus 1 encephalitis. PLoS One 12:e0169081
20. Schmittgen TD, Livak KJ (2008) Analyzing real-time PCR data by the comparative C(T) method. Nat Protoc 3:1101–1108
21. Mestdagh P, Van Vlierberghe P, De Weer A et al (2009) A novel and universal method for microRNA RT-qPCR data normalization. Genome Biol 10:R64

Chapter 4

Isolation and Analysis of Exosomal MicroRNAs from Ovarian Follicular Fluid

Juliano Da Silveira, Gabriella M. Andrade, Felipe Perecin, Flávio Vieira Meireles, Quinton A. Winger, and Gerrit J. Bouma

Abstract

Mammalian ovarian follicular growth is characterized by development of a large fluid filled antrum that separates mural granulosa cells and cumulus cells. Extensive communication between the different cell types is necessary for maturation of a developmentally competent oocyte. Here, we describe an approach for the isolation of cell-secreted exosomes from ovarian follicular fluid, identification of small RNAs (i.e., microRNAs) in exosomes, labeling of exosomes, and examining cell uptake of exosomes by follicular cells.

Key words Extracellular vesicles, microRNAs, Ovarian follicle

1 Introduction

This chapter describes the isolation and functional analysis of exosomal microRNAs isolated from ovarian follicular fluid. MicroRNAs are small, noncoding RNAs that bind 3′ untranslated regions of target mRNA directing them to the RNA-induced silencing complex resulting in mRNA degradation or posttranslational silencing [1]. Due to their relative small target recognition sequence (2–7 nt) they are able to bind and target potentially many different mRNAs, and numerous studies have highlighted their role in cell differentiation and function, including female reproductive physiology. For example, inhibition of microRNA maturation leads to abnormal development of the female reproductive tract [2]. In the ovary, absence of mature microRNAs leads to abnormal corpus luteum formation and disorganized spindle formation in oocytes leading to infertility [3].

Mammalian ovarian follicular development (folliculogenesis) is a highly coordinated process involving extensive signaling between somatic cells (granulosa and theca cells) and the oocyte. This bidirectional communication involves granulosa cells providing factors necessary for oocyte maturation, and oocyte secreting

Shao-Yao Ying (ed.), *MicroRNA Protocols*, Methods in Molecular Biology, vol. 1733,
https://doi.org/10.1007/978-1-4939-7601-0_4,

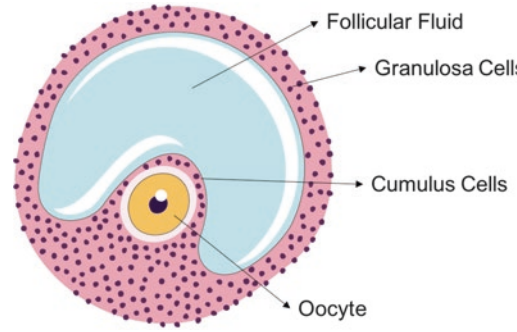

Fig. 1 Mature ovarian follicle. The ovarian follicle is composed by granulosa cells, cumulus cells, and oocyte. Within the mature follicle is a cavity called antrum filled with follicular fluid

signaling molecules to surrounding granulosa cells that dictate follicle growth and development [4]. Folliculogenesis is characterized by the development of dominant, mature follicles, which develop a large fluid filled antrum within the granulosa cell layers leading to outer mural granulosa cells and inner, oocyte-surrounding cumulus cells (Fig. 1). This follicular fluid (FF) contains hormones, growth factors, DNA, and RNAs (including microRNAs) and its contents often are used as indicators of oocyte quality and competence [5].

Initial experiments in our lab, using the mare as an animal model, focused on the idea that microRNAs are present in follicular fluid and could be used as a diagnostic marker of oocyte quality. A microRNA profiling PCR assay revealed the presence of the mature microRNA sequence for circulating miR-16 in ovarian follicular fluid. During this time the question arose whether microRNAs were simply present in ovarian follicular fluid due to cell turn-over, or if in fact these microRNAs somehow were shuttled between different cells and part of the bi-directional signaling program that exists between the somatic cells (granulosa and cumulus cells) or between the somatic cells and the oocyte. One way microRNAs could be shuttled from one cell to a different cell at some distance is if these microRNAs were packaged into cell-secreted vesicles. To that end studies were conducted to isolate, characterize, and examine cell-secreted vesicles within ovarian follicular fluid. Using in vitro and in vivo experiments we demonstrated for the first time that microvesicles and exosomes are present in ovarian follicular fluid, they contain proteins and microRNAs, and when isolated and labeled these vesicles can be taken up by surrounding granulosa cells in vivo. Subsequent studies demonstrated the presence of at least ~271 mature microRNA sequences in cell-secreted vesicles isolated from follicular fluid [6].

Microvesicles and exosomes are cell-secreted vesicles that differ in the way they are generated and secreted by cells, their contents,

and their size (e.g., 200–1000 nm vs. <200 nm, respectively). Both microvesicles and exosomes contain microRNAs, and although there is overlap, each contains their own unique microRNAs in follicular fluid [6]. Since our original finding of cell-secreted vesicles in ovarian follicular fluid, we primarily have focused on exosomes. Exosomes are likely to play a role in regulated and targeted cell-to-cell communication: (a) There is evidence that microRNAs are specifically targeted for exosome incorporation [7]. (b) Contrary to microvesicles, which are released through outward cell budding or fission, exosomes are formed as intraluminal vesicles inside late endosomes (i.e., multivesicular bodies). Following stimulation (e.g., intracellular calcium increase) multivesicular bodies fuse with the plasma membrane and intraluminal vesicles/exosomes are exocytosed and released into extracellular space [8]. (c) Exosome membranes contain transmembrane proteins and receptors that enable target cell-recognition leading to uptake and/or membrane fusion. Finally, studies from our lab and others have now described the presence of exosomes in ovarian follicular fluid, as well as oviductal [9, 10] and uterine fluid [11, 12] suggesting an important function for these cell-secreted vesicles and their cargo in cell communication within female reproductive physiology.

In this chapter, we will describe methods to isolate exosomes from ovarian follicular fluid, approaches to fluorescently label exosomes to monitor cell uptake, and isolate small RNAs (microRNAs, from here on referred to as miRNA) for RNAseq or real-time PCR analysis. Furthermore, bioinformatics approaches will be highlighted as a tool to discover potential pathways regulated by exosomal miRNAs.

2 Materials

2.1 Sample Collection and Processing Prior to Analysis

1. Follicular aspiration apparatus [13].
2. Conical collection tubes (50 mL) (Cornig®).
3. Centrifuge capable to speed between 300 × *g* and 20,000 × *g*.
4. Pipettes (Eppendorf®, Hamburgo, Germany) and filtered pipette tips (Axygen®).
5. Plastic plates (100 mm) (Cornig®).
6. Stereomicroscope.

2.2 Exosome Isolation

1. RNA/DNAse-free 1.5 ml tubes (Axygen®).
2. Pipettes (Eppendorf®) and filtered pipette tips (Axygen®).
3. Exoquick reagent (System Bioscience®).

2.3 RNA Isolation

1. Pipettes (Eppendorf®) and filtered pipette tips (Axygen®).
2. Centrifuge.

3. Tri reagent (Life Technologies®).
4. Polyacryl reagent.
5. DNAse (Thermo Fisher Scientific®).
6. Nanodrop spectrophotometer (Thermo Fisher Scientific®).

2.4 miRNA Profiling

1. Pipettes and filtered pipette tips.
2. miRNA cDNA synthesis kit.
3. Master mix reagents for miRNA analysis.
4. miRNA forward primers.
5. Real-Time PCR machine.

2.5 Bioinformatics and Pathway Discovery

1. Computer and internet access.
2. Pre-analyzed miRNA spreadsheet data.

2.6 Exosome Labeling and Cell Uptake

1. Pipettes.
2. Pipette tips.
3. Plastic tubes 1.5 mL.
4. Plastic plates.
5. PKH67 dye (Sigma Aldrich).
6. Nuclear stain DAPI.
7. Paraformaldehyde (PFA).
8. Bovine Serum Albumine (BSA).
9. Phosphate buffered saline (PBS).
10. DMEM/F12 medium.
11. Stereomicroscope.
12. Zeiss Axioplan 2 fluorescence microscope.

3 Methods

3.1 Sample Collection and Processing Prior to Analysis

Follicular fluid samples are obtained through ovarian follicle aspiration using an ultrasound-guided needle. The resulting follicular fluid is yellow and free of blood contaminants. After follicular fluid collection, the samples should be analyzed for the presence of a cumulus-oocyte-complex (COC). The follicular fluid sample can be stored at 37 °C until further processing. Samples should be processed after morphological evaluation of the recovered COC. This step should be performed to assess the quality and stage of follicular maturation associated with the isolated follicular fluid. Next the recovered follicular fluid can be processed prior to exosomes isolation.

1. Centrifuge follicular fluid at 300 × *g* for 10 min in order to remove live cells contained within the samples (*see* **Note 1**).
2. After centrifugation move the supernatant and place in a new 1.5 ml RNA/DNAse-free tube.
3. Centrifuge the supernatant at 2,000 × *g* for 10 min in order to remove dead cells.
4. After centrifugation move the supernatant and place in a new 1.5 ml RNA/DNAse-free tube.
5. Centrifuge the supernatant at 12,000 × *g* for 30 min in order to remove cell debris (*see* **Note 2**).
6. After centrifugation move the supernatant to a new RNA/DNAse-free tube and store in −80 °C until further use.

3.2 Exosome Isolation

1. Exosome isolation can be performed using ultracentrifugation or precipitation reagents such as Exoquick (*see* **Note 3**).
2. Prior to exosome isolation, place the samples at room temperature until completely thawed.
3. Exoquick isolation reagent works in a 1:5 ratio, thus a starting volume of 500 μL should be mixed with 100 μL of Exoquick reagent.
4. After mixing place the mixture at 4 °C overnight (*see* **Note 4**).
5. Following overnight incubation, centrifuge the sample at 1,500 × *g* for 30 min at room temperature.
6. After centrifugation, a white pellet will appear at the bottom of the tube.
7. Remove the supernatant and use 50–100 μL of 1× PBS to dilute the exosome pellet.
8. The diluted pellet can be used for exosome validation assays such as nanoparticle tracking analysis, transmission electron microscopy, and western blot. Additionally, the resuspended exosome pellet can be mixed with 200 μL of Tri reagent BD and stored at −80 °C or processed for RNA isolation (*see* **Note 5**).

3.3 RNA Isolation

1. After mixing 200 μL of Tri reagent to the 50 μL diluted exosome pellet, add 8 μL of Poly Acryl carrier to the mixture and homogenize it thoroughly.
2. Place the sample tube at room temperature for 5 min.
3. Add 128 μL of Chloroform and vortex the sample tube for 15 s (*see* **Note 6**).
4. Place the sample tube at room temperature for 5 min.
5. Centrifuge the sample at 12,000 × *g* for 15 min.
6. The resulting sample will have three separate phases (Fig. 2).

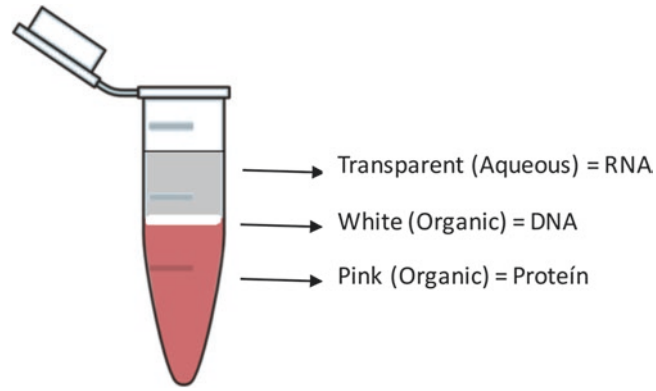

Fig. 2 Phase separation following chloroform and centrifugation. Aqueous phase is rich in RNA, while white and pink phases are rich in DNA and protein, respectively

7. Move the aqueous phase to a new RNA/DNAse-free tube.
8. Add 500 μL of isopropanol and store at room temperature for 5–10 min (*see* **Note 7**).
9. Centrifuge the samples at 20,000 × *g* for 30 min. RNA will form a white pellet in the bottom of the tube (*see* **Note 8**).
10. Remove the supernatant without disturbing the RNA pellet.
11. Add 1 ml of 75% ethanol to the pellet.
12. Wash the RNA pellet twice with freshly prepared 75% ethanol.
13. After the last wash, remove the ethanol and place the tube on a piece of paper to dry out leftover ethanol (~15 min).
14. The pellet will appear white and RNA/DNAse-free water can be added to the sample to dissolve the pellet.

3.4 MiRNA Profile in Extracellular Vesicles from Follicular Fluid

MiRNA expression profile can be performed using different techniques such as microarray, RNAseq, Taqman assays, or primer-based real-time PCR [14]. We will focus on the use of primer-based real-time PCR for miRNA analysis of 384 mature miRNA sequences in extracellular vesicles isolated from follicular fluid.

1. Prepare cDNA using miScript PCR System with 100–200 ng per sample, following the manufacturer's instructions (*see* **Note 9**).
2. Incubate total RNA, including the small RNA fraction, with 5× miScript HiSpec Buffer, 10× miScript Nucleic mix, RNase-free water, and miScript reverse transcriptase at 37 °C for 60 min, followed by 5 min at 95 °C.
3. Relative levels of 384 mature miRNAs can be examined using mature miRNA sequences downloaded from mirBase database [15].

4. Prepare the real-time PCR master mix in 10 μL reactions containing 2× Quantitec SYBR Green, 10 μM universal reverse primer, and miRNA-specific forward primer, and 0.024 μL of 1:4 diluted cDNA.

		×420
2× Quantitec SYBR Green	5 μL	2100 μL
10 μM universal reverse primer	1 μL	420 μL
cDNA		10 μL
RNAse-free water	2.98 μL	1250 μL
TOTAL:		9 μL per reaction

5. Add 1 μL of the forward primer to each well in the plate.
6. Place the real-time PCR plate in the PCR machine (*see* **Note 10**).
7. Add the PCR cycle conditions: 95 °C for 15 min, 45 cycles of 94 °C for 10 s, 55 °C for 30 s, and 70 °C for 30 s followed by a melt curve analysis to confirm amplification of single-cDNA products.
8. To identify the abundancy of miRNAs isolated from EVs, raw Ct values <37 and with a single suitable melting curve are normalized to the geometric mean of internal [16] controls. These can be miRNAs whose raw Cp values are (a) <37, (b) Cp values have a standard deviation <1.0 across all samples to be compared, and (c) are not significantly different between the comparison groups. In the case of exosomal miRNAs isolated from equine follicular fluid, miR-99b has been used as a reference control [17, 18].

3.5 Bioinformatics and Pathway Discovery

Identification of predicted mRNA targets or pathways can be performed using individual miRNAs or groups of miRNAs. Here, we will outline the approach using groups of miRNAs to identify pathways regulated by these exosomal miRNAs with similar expression profile.

1. When studying exosomal miRNAs isolated from non-rodent and non-primate species, compare identified exosomal miRNAs with human sequences in order to identify sequence similarities using mirBase (http://www.mirbase.org) [15] (*see* **Note 11**).
2. After the identification of sequence similarity (95–100%) with human miRNAs, perform bioinformatics analysis.
3. Submit miRNAs into DIANA-miRPath (http://diana.imis.athena-innovation.gr/DianaTools/index.php?r=mirpath), a miRNA pathway analysis web-server [19]. Perform miRNA analysis either single or as a group. Since exosomal miRNAs are present in "groups" this is our preferred approach, and

would yield potential pathways regulated by all identified exosomal miRNAs (*see* **Note 12**).

4. Identificate target genes using miRTarBase [20] and the similarity of miRNA-gene target 3'UTR interactions between species using TargetScan software [21] to confirm if your bioinformatics results are valid for the specie of interest (*see* **Note 13**).

3.6 Exosome Labeling and Uptake by Cells in Culture

Exosome labeling can be performed using different approaches. Here, we describe the use of PKH67 (Sigma Aldrich), a green fluorescent dye that labels lipid membranes, to label extracellular vesicles. After labeling, extracellular vesicles can be added to cell culture media, or can be injected into ovarian follicular fluid for in vivo analysis. Extracellular vesicles uptake by cells can be analyzed with fluorescence microscopy.

1. Isolate exosomes of interest according to protocol above.
2. Incubate exosomes in 2 μL of PKH67 (2 μM), for 30 min, at room temperature.
3. Incubate again in 1% of BSA, for 10 min, at room temperature.
4. Wash, four times, in FBS-free DMEM-F12 medium to remove dye excess (*see* **Note 14**).
5. Resuspend the labeled exosomes with cell culture medium (*see* **Note 15**).
6. Culture cells (granulosa cells a total of 5×10^5) in 4-well plates according to Portela et al. 2010 on the top of a coverslip.
7. After 24 h of treatment with the labeled exosomes, fix the cells attached at a coverslip with 4% PFA or 70% ethanol.
8. Perform nuclear staining using DAPI.
9. Use a fluorescence microscope to confirm the presence of fluorescent-labeled exosomes inside the cells (*see* **Note 16**).

4 Notes

1. Leftover cells can be used for RNA and protein isolation if needed.
2. It is important to perform these differential centrifugation steps prior to storage at −80 °C, since any contaminating cells could rupture during freezing.
3. Other precipitation reagents can also be utilized; however for the purpose of the present manuscript we will use Exoquick since it was the first described exosome precipitation solution.
4. It is important to make sure that the sample is well mixed. Do not use vortex, but pipette thoroughly.

5. If the exosome pellet is not completely dissolved it can react with Tri reagent and form a solid pellet that is hard to lyse which will affect RNA quality and yields.
6. Sample color should turn solid pink.
7. In order to store the aqueous phase plus the isopropanol place it in −80 °C. This sample can be stored overnight if necessary.
8. Depending on the sample type, RNA pellet can look white or have a gel-like appearance. RNA pellet can be attached to the bottom of the tube or float, be careful.
9. It is important to keep the final concentration of cDNA per well between 5 and 50 pg.
10. Before placing the plate in the thermocycler, centrifuge (2,000 × *g* for 3 min) it to allow contents to move to the bottom of the wells.
11. This is an important step prior to bioinformatics analysis.
12. MiRNA data processing can be used to identify exosomal miRNAs that are present or absent, as well as differentially expressed among experimental groups.
13. miRTarBase (http://mirtarbase.mbc.nctu.edu.tw/) provides information regarding miRNA-targets interactions, while Targetscan (http://www.targetscan.org/vert_71/) provides predict interactions. It is important to keep in mind the differences between species and tissues.
14. This washing step can be performed with the medium that will be used to culture cells.
15. For a negative control, use sterile PBS incubated with PKH67 in the same manner as described above.
16. Usually, the labeled exosomes are localized near the cell nucleus.

Acknowledgments

We are grateful for the funding supporting the research involving exosomal microRNAs from CSU CVMBS College Research Council, the Preservation of Equine Genetics, Cecil and Irene Hylton Foundation, and financial support from the Abney Foundation, Ed H. Honnen Award, the France Stone Scholarship, and the Assisted Reproduction Program at Colorado State University. Additional support came from grants funded by São Paulo Research Foundation-FAPESP (grant 2012/50533-2; grant 2013/08135-2; grant 2014/21034-3, grant 2013/10473-3; and grant 2014/22887-0).

References

1. Bartel DP (2009) MicroRNAs:target recognition and regulatory functions. Cell 136:215–233
2. Nagaraja AK, Andreu-vieyra C, Franco HL, Ma L, Chen R, Han DY, Zhu H, Agno JE, Gunaratne PH, Demayo FJ, Matzuk MM (2008) Deletion of Dicer in somatic cells of the female reproductive tract causes sterility. Mol Endocrinol 22:2336–2352
3. Luense LJ, Carletti MZ, Christenson LK (2009) Role of Dicer in female fertility. Trends Endocrinol Metab 20:265–272
4. Knight PG, Glister C (2006) TGF-β superfamily members and ovarian follicle development. Reproduction 132:191–206
5. Revelli A, Delle Piane L, Casano S, Molinari E, Massobrio M, Rinaudo P (2009) Follicular fluid content and oocyte quality: from single biochemical markers to mtabolomics. Reprod Biol Endocrinol 7:4330–4337
6. Da Silveira JC, Veeramachaneni DN, Winger QA, Carnevale EM, Bouma GJ (2012) Cell-secreted vesicles in equine ovarian follicular fluid contain miRNAs and proteins: a possible new form of cell communication within the ovarian follicle1. Biol Reprod 86:71
7. Villarroya-Beltri C, Gutiérrez-Vázquez C, Sánchez-Cabo F, Pérez-Hernández D, Vázquez J, Martin-Cofreces N, Martinez-Herrera DJ, Pascual-Montano A, Mittelbrunn M, Sánchez-Madrid F (2013) Sumoylated hnRNPA2B1 controls the sorting of miRNAs into exosomes through binding to specific motifs. Nature Commun 4:2980. https://doi.org/10.1038/ncomms3980
8. Arita S, Baba E, Shibata Y, Niiro H, Shimoda S, Isobe T, Kusaba H, Nakano S, Harada M (2008) B cell activation regulates exosomal HLA production. Eur J Immunol 38:1423–1434
9. Al-Dossary AA, Strehler EE, Martin-Deleon PA (2013) Expression and secretion of plasma membrane Ca2+-ATPase 4a (PMCA4a) during murine estrus: association with oviductal exosomes and uptake in sperm. PLoS One 8:e80181. https://doi.org/10.1371/journal.pone.0080181
10. Lopera-Vásquez R, Hamdi M, Fernandez-Fuertes B, Maillo V, Beltrán-Breña P, Calle A, Redruello A, López-Martín S, Gutierrez-Adán A, Yañez-Mó M, Ramirez MÁ, Rizos D (2016) Extracellular vesicles from BOEC in in vitro embryo development and quality. PLoS One 11:e0148083. https://doi.org/10.1371/journal.pone.0148083
11. Burns G, Brooks K, Wildung M, Navakanitworakul R, Christenson LK, Spencer TE (2014) Extracellular vesicles in luminal fluid of the ovine uterus. PLoS One 9:e90913. https://doi.org/10.1371/journal.pone.0090913
12. Campoy I, Lanau L, Altadill T, Sequeiros T, Cabrera S, Cubo-Abert P-BA, Garcia A, Borrós S, Santamaria A, Ponce J, Matias-Guiu X, Reventós J, Gil-Moreno A, Rigau M, Colas E (2016) Exosome-like vesicles in uterine aspirates: a comparison of ultracentrifugation-based isolation protocols. J Transl Med 14:180. https://doi.org/10.1186/s12967-016-0935-4
13. Carnevale EM, Ramirez RJ, Squires EL, Alvarenga MA, Vanderwall DK, McCue PM (2000) Factors affecting pregnancy rates and early embryonic death after equine embryo transfer. Theriogenology 54:965–979
14. Pritchard CC, Cheng HH, Tewari M (2012) MicroRNA profiling: approaches and considerations. Nat Rev Genet 13:358–369
15. Kozomara A, Griffiths-Jones S (2014) miRBase: annotating high confidence microRNAs using deep sequencing data. Nucleic Acids Res 42:D68–D73
16. Portela VM, Zamberlam G, Price CA (2010) Cell plating density alters the ratio of estrogenic to progestagenic enzyme gene expression in cultured granulosa cells. Fertil Steril 93:2050–2055
17. da Silveira JC, Carnevale EM, Winger QA, Bouma GJ (2014) Regulation of ACVR1 and ID2 by cell-secreted exosomes during follicle maturation in the mare. Reprod Biol Endocrinol 12:44
18. da Silveira JC, Winger QA, Bouma GJ, Carnevale EM (2015) Effects of age on follicular fluid exosomal microRNAs and granulosa cell transforming growth factor-β signalling during follicle development in the mare. Reprod Fertil Dev 27:897–905
19. Vlachos IS, Kostoulas N, Vergoulis T, Georgakilas G, Reczko M, Maragkakis M, Paraskevopoulou MD, Prionidis K, Dalamagas T, Hatzigeorgiou AG (2012) miRPath v. 2.0: investigating the combinatorial effect of microRNAs in pathways. Nucleic Acids Res 40:W498–W504
20. Chou CH, Chang NW, Shrestha S, Hsu SD, Lin YL, Lee WH, Yang CD, Hong HC, Wei TY, SJ T, Tsai TR, Ho SY, Jian TY, HY W, Chen PR, Lin NC, Huang HT, Yang TL, Pai CY, Tai CS, Chen WL, Huang CY, Liu CC, Weng SL, Liao

KW, Hsu WL, Huang HD (2016) miRTarBase 2016: updates to the experimentally validated miRNA-target interactions database. Nucleic Acids Res 44:D239–D247

21. Agarwal V, Bell GW, Nam JW, Bartel DP (2015) Predicting effective microRNA target sites in mammalian mRNAs. Elife 4:e05005. https://doi.org/10.7554/eLife.05005

Chapter 5

Profiling of MicroRNAs in the Biofluids of Livestock Species

Jason Ioannidis, Judith Risse, and F. Xavier Donadeu

Abstract

The value of circulating microRNAs (miRNAs) as noninvasive biomarkers of human disease has been extensively demonstrated. Significant potential also exists in other species, particularly in relation to control of veterinary diseases and selection/monitoring of production traits in livestock. Although robust protocols have been developed for miRNA profiling of human biofluids, significant optimization may be required before these can be applied to other species. In this chapter, we describe protocols for small-RNA sequencing and RT-qPCR analyses of plasma samples from livestock species. In addition, we provide brief data analysis protocols for small-RNA sequencing and RT-qPCR data. Finally, we highlight important considerations for these protocols such as low RNA yield, platform-specific biases, and optimal normalization approaches.

Key words Cow, miRNA, microRNA, Biomarker, Plasma, Follicular fluid, Sequencing

1 Introduction

MicroRNAs (miRNAs) are short noncoding RNAs with a generic role in post-transcriptional gene regulation during tissue development and homeostasis [1–3]. MiRNAs are released from cells and many can be detected in a relatively stable form in body fluids including serum, plasma, saliva, urine, and follicular fluid [4]. In recent years, many miRNAs in biofluids have been proposed as useful diagnostic/prognostic biomarkers of diseases including cancer [5], type II diabetes [6], liver disease [7], and many others. A distinct advantage of the use of extracellular miRNAs as biomarkers is that, in contrast to standard tissue biopsies, most biofluid compartments in the body can be sampled noninvasively.

High-throughput sequencing has now been established as a methodology of choice in miRNA research, as it allows comprehensive profiling of small RNA populations within tissues or developmental stages of interest. Analyses of small RNAs have been more challenging in biofluids than in solid tissues due to much lower RNA content and the abundance of enzymatic inhibitors in many

Shao-Yao Ying (ed.), *MicroRNA Protocols*, Methods in Molecular Biology, vol. 1733,
https://doi.org/10.1007/978-1-4939-7601-0_5,

biofluids; enzymatic inhibitors can affect PCR and thus the preparation of sequencing libraries. Despite continuous advances in this field, which is dominated by Illumina sequencing platforms, recent studies have highlighted the relatively low concordance (~50%) in miRNA detection across different platforms (sequencing, microarray, and RT-qPCR), reflecting platform-specific biases such as adaptor ligation bias [8, 9]. Because of this, it has become critical to cross-validate results from miRNA biomarker studies using different complementary approaches.

Small RNA biomarker discovery studies typically utilize a high-throughput profiling approach such as sequencing or PCR arrays to identify candidate sequences associated with a particular physiological or disease condition. Cell-free biofluid samples can be analyzed whole (e.g., plasma) or individual fractions containing small RNAs can be separated and analyzed in isolation (e.g., exosomal or lipoprotein fractions). Studies have shown that different fractions in plasma contain different miRNA sequences [10], and thus comprehensive screening of miRNA populations may be better achieved using unfractionated biofluid samples. Biomarkers identified by high-throughput approaches are validated in the same or a different cohort of samples using a different platform. In most cases validation is carried out using individual RT-qPCR assays which allow some control of enzymatic inhibition and sample contamination. The validated biomarkers can then be tested in wider subject cohorts and/or their function investigated in vitro or in vivo using, for example, luciferase reporter assays and gain-of-function or loss-of-function approaches.

In addition to their demonstrated value in human medicine, miRNAs have significant biomarker potential in agriculture, particularly for disease control and selection for desirable traits in livestock, with the aim of improving animal health and productivity. These are two main targets of food animal industries worldwide, which are faced with the challenge of sustainable food production for an ever-expanding human population. Limited studies in livestock species have already shown the potential of circulating miRNAs as biomarkers of stress and genetic background [11], infection [12], and grazing [13], as well as the potential of miRNAs in follicular fluid as reproductive biomarkers [14–16]. Continuous progress in this promising field will depend on the availability of robust protocols for screening and identification of small RNAs in a variety of biofluids, which can be used at both the individual and herd levels in a reproducible manner.

In this article, we describe protocols routinely used in our laboratory for the collection, preparation, and small-RNA profiling (using sequencing and RT-qPCR) of biofluid samples from livestock. The protocols we present have been validated for use in bovine plasma, however, we have also applied them successfully to bovine follicular fluid and to both equine plasma and follicular fluid, and should be useful for other biofluids, such as serum, urine, and saliva,

although they may have to be optimized for each specific application. Finally, we also provide a basic outline for the analysis of small-RNA sequencing using the Illumina platform and of RT-qPCR data.

2 Materials

2.1 Blood Sample Processing and Storage

1. 10 mL BD Vacutainer K2 EDTA Blood Collection Tubes (Becton Dickinson, USA).
2. 18 G Venepuncture Needles (Becton Dickinson).
3. BD Vacutainer Needle Holders (Becton Dickinson).
4. 1.5 mL RNase-free micro-centrifuge tubes.

2.2 RNA Extraction

All water solutions to be prepared using RNase-free water.

1. 1.5 mL RNase-free micro-centrifuge tubes.
2. TRIzol LS Lysis Buffer (Life Technologies, USA).
3. Syn-cel-miR-39-3p (Qiagen, NL); 1.8×10^8 copies/μL.
4. Chloroform; 99.9%.
5. RNA-Grade Glycogen (Sigma-Aldrich, USA); 20 mg/mL.
6. Isopropanol (analytical grade); 99.9%.
7. Ammonium acetate (Sigma-Aldrich); 5 M.
8. Ethanol (analytical grade); 70%.
9. RNase-free water (Qiagen).

2.3 RT-qPCR

We use Qiagen kits although several other companies, notably Exiqon (Denmark), provide a range of products for miRNA analyses.

1. RNase-free PCR tubes; 200 μL.
2. MiScript II RT kit (Qiagen); contains Reverse Transcriptase, Nucleic acid Mix, HiSpec Buffer, and RNase-free water.
3. MiScript SYBR Green PCR kit (Qiagen); contains Universal Primer, SYBR Green Mix and RNase-free water.
4. MiScript primer assays (Qiagen); reconstituted with 550 μL TE buffer.
5. 96-well, clear round-well PCR plates with flat caps.
6. A suitable platform for qPCR analyses (among the many different available we use Agilent Mx3005P qPCR system, Agilent Technologies, USA).

2.4 RT-qPCR Data Analysis

1. RT-qPCR analysis software (we use MxPro 4.1, Stratagene, USA).
2. Microsoft Excel (Microsoft, USA).
3. Statistics package (GraphPad, R, Minitab, or other).

2.5 Small RNA Sequencing Library Preparation

1. Illumina TruSeq Small-RNA Library Preparation Kit (Illumina, USA); contains 10 mM ATP, HML (Ligation Buffer), RA3 (RNA 3′ Adapter), RA5 (RNA 5′ Adapter), RNase Inhibitor, STP (Stop Solution), T4 RNA Ligase, Ultrapure water, 25 mM dNTP Mix, PML (PCR Mix), RP1 (RNA PCR Primer), RNA PCR Primer Index, RTP (RNA RT Primer), 5× Fist Strand Buffer, 100 mM DTT, CRL (Custom RNA Ladder), HRL (High Resolution Ladder).
2. T4 RNA Ligase 2 (Epicentre, USA); 200 U/μL.
3. Superscript II Reverse Transcriptase (Life Technologies).
4. Novex TBE gels; 6%, 10-well.
5. Novex TBE running buffer; 5×.
6. Ultrapure ethidium bromide (10 mg/mL).
7. Razor blade.
8. 5 μm filter tubes (IST Engineering).
9. High Sensitivity DNA Kit (Agilent).
10. High Sensitivity DNA Chip (Agilent).
11. DNA loading dye.

2.6 Sequencing Data Analysis Software

1. R programming language [17].
2. R studio 0.98 [18].
3. sRNAbench (part of sRNAtoolbox) [19].

3 Methods

3.1 Blood Sample Processing

This protocol describes steps involved in collection and processing of whole blood samples to obtain plasma with negligible cell content.

1. Collect whole blood in a 10 mL EDTA collection tube using appropriate 18G needles and needle holders, taking care not to induce hemolysis.
2. Invert each collection tube multiple times after sampling to ensure sufficient mixing of blood with anti-coagulant.
3. Proceed to **step 4** or store whole blood at 4 °C for as short a period as possible (*see* **Note 1**).
4. Centrifuge whole blood at 1900 × *g* for 10 min at 4 °C.
5. Aspirate the plasma supernatant (typically 40–60% of total blood volume) with a pipette, leaving a small volume to avoid disturbing the buffy coat. Aliquot the plasma into multiple micro-centrifuge tubes if required.
6. Centrifuge the aliquoted plasma for a second time at 16,000 × *g* for 10 min at 4 °C.

7. Aspirate the supernatant taking care not to disturb the cell pellet at the bottom of the tube.
8. Store plasma at −80 °C or proceed to RNA extraction. Avoid repeated freeze thawing of plasma samples (*see* **Note 2**).

3.2 RNA Extraction

This protocol uses TRIzol LS (Life Technologies) to extract RNA from bovine plasma, with some modifications aimed at improving RNA yield. We usually extract 350 μL of each sample which yields about 4 ng of RNA. To obtain larger yields, the samples can be split into multiple 350 μL aliquots which are extracted simultaneously. In our experience, extracting 350 μL of plasma provides sufficient RNA for downstream RT-qPCR profiling of miRNAs, whereas 1050 μL of plasma are sufficient for small-RNA sequencing.

1. Pipette the desired volume of plasma in a micro-centrifuge tube.
2. Add three volumes of TRIzol LS (1050 μL) to each tube containing plasma and homogenize by pipetting up and down several times.
3. Incubate the homogenate at room temperature for 5 min.
4. Spike each tube with 3.5 μL of syn-cel-miR-39-3p (total, 5.6×10^8 copies), prepared according to the manufacturer's instructions, and mix by vortexing.
5. Add 280 μL of chloroform to each tube and vortex for 15 s.
6. Incubate at room temperature for 10 min.
7. Centrifuge at 12,000 × *g* for 15 min at 4 °C.
8. Aspirate the top aqueous layer from each tube and place into a new micro-centrifuge tube (*see* **Note 3**).
9. Add 0.1 volumes of ammonium acetate salt and 20 μg of glycogen to assist with RNA precipitation. Add an equal volume of isopropanol and mix gently.
10. Incubate for 10 min at room temperature.
11. Centrifuge at 12,000 × *g* for 10 min at 4 °C. Aspirate and discard the supernatant (*see* **Note 4**).
12. Wash the resulting RNA pellet in at least 1 mL of 75% ethanol by vortexing.
13. Centrifuge at 8000 × *g* for 5 min at 4 °C. Remove the supernatant and all residual ethanol (*see* **Note 5**).
14. Dry the pellet by leaving the tube with the cap open for 10 min at room temperature.
15. Resuspend the pellet in 10 μL of RNase-free water by pipetting up and down (*see* **Note 6**).
16. Incubate the RNA solution in a heat block at 55 °C for 10 min.

17. As an optional step, an RNA quantification assay (e.g., RiboGreen by Thermo Fischer Scientific) can be used to determine RNA yield and exclude samples with exceptionally low yields. A significant amount of RNA extract may be used in this step.

3.3 RT-qPCR

This protocol uses the miScript PCR system (Qiagen) with some modifications to reduce the reaction volume and obtain the optimal amount of RNA for downstream applications. Note that results with at least the same quality can be generated using analysis platforms from other manufacturers, such as Exiqon. All the steps should be carried out on ice unless stated otherwise.

1. Set up a 10 μL reaction containing 2 μL of RNA, 1 μL of nucleics mix, 2 μL of HiSpec buffer, 1 μL of reverse transcriptase, and 4 μL of RNase-free water. Mix gently. No-RT (NRT) and no-template (NTC) controls should be included in each RT-qPCR assay in order to control for DNA contamination and primer-dimer formation, respectively. When preparing a master mix for multiple reactions prepare an excess 10% to allow for pipetting error (*see* **Note 7**).
2. Incubate the reaction in a PCR cycler for 60 min at 37 °C and then 5 min at 95 °C. Store cDNA at −20 °C until further use or proceed to qPCR.
3. Dilute each cDNA sample 40-fold in RNase-free water (*see* **Note 8**).
4. Prepare 10 μL qPCR reactions in a 96-well plate using 2 μL diluted cDNA, 1 μL universal primer, 1 μL miScript primer assay, 5 μL SYBR Green mix, and 1 μL RNase-free water.
5. Centrifuge the samples for 1 min at 1000 × *g* at room temperature to remove air bubbles.
6. Quantify the samples and controls (and standard curve if included) using technical replicates (duplicate or triplicate wells of a 96-well plate) on suitable qPCR equipment using the conditions outlined in Table 1.

Table 1
Conditions used for qPCR analysis of miRNAs in biofluid samples using the miScript PCR system (Qiagen)

Step	Duration	Temperature (°C)	Comments
Activation	15 min	95	–
Denaturation	15 s	94	Repeat for 40 cycles
Annealing	30 s	55	Repeat for 40 cycles
Extension	30 s	70	Repeat for 40 cycles

3.4 RT-qPCR Data Analysis

In this section, we briefly outline the steps required to analyze RT-qPCR data using a standard curve (*see* **Note 7**). If a standard curve is not used then data can be analyzed using the ΔΔCt method, information on which can be easily obtained online.

1. Perform quality control checks on RT-qPCR data:
   (a) Standard curve amplification efficiency should typically be 85–115% and R^2 should be >0.85.
   (b) Negative controls (NRT and NTC) should ideally be undetectable but in all the cases they should be detected at no less than 5 Cq values from the least abundant sample.
   (c) Dissociation curve should show a single well-defined peak.
2. Export sample Cq-values and copy number values (extrapolated from values obtained from the standard curve) to Microsoft Excel and calculate the mean expression value from all the technical replicates for each sample.
3. Normalize the mean expression level of the gene of interest to the mean expression level of the normalizer (or the mean expression of multiple normalizers; *see* **Note 9**) for each sample.
4. Plot normalized expression levels and analyze using suitable statistics package.

3.5 Small RNA Sequencing Library Preparation

In this section, we outline the steps for the preparation of small-RNA sequencing libraries from plasma RNA samples using the TruSeq small RNA library preparation kit. All the samples and reagents should be kept on ice unless otherwise specified. The protocol is for a single library; when using a master mix for multiple libraries, prepare 10% additional reagents to account for pipetting error.

1. Mix 1 μL of RA3 (3′ adapter) with 5 μL of RNA from each sample.
2. Incubate the mix for 2 min at 70 °C on a thermal cycler.
3. Prepare each 10 μL ligation reaction by combining the above mix with 2 μL HML (ligation buffer), 1 μL RNase inhibitor, and 1 μL T4 RNA ligase 2. Mix by pipetting.
4. Incubate the reaction for 1 h at 28 °C.
5. Add 1 μL of stopping mix (STP) and mix by pipetting.
6. Incubate for a further 15 min at 28 °C.
7. Preheat 1 μL of RA5 (5′ adapter) at 70 °C for 2 min on a thermal cycler.
8. Add 1 μL of 10 mM ATP to the 5′ adapter. Mix by pipetting.
9. Add 1 μL of T4 RNA ligase. Mix by pipetting.
10. Add 3 μL of the above mix to the product of the 3′ adaptor ligation reaction (**step 6**).

Table 2
PCR conditions for the amplification of small-RNA sequencing libraries, using the TruSeq Small-RNA Library Preparation Kit (Illumina)

Step	Duration	Temperature (°C)	Comments
Activation	30 s	98	–
Denaturation	10 s	98	Repeat for 11 cycles
Annealing	30 s	60	Repeat for 11 cycles
Extension	15 s	72	Repeat for 11 cycles
Termination	10 min	72	–

11. Incubate at 28 °C for 1 h.
12. Combine 6 μL of the resulting reaction from the above step with 1 μL RNA RT Primer and mix by pipetting.
13. Incubate the reaction for 2 min at 70 °C.
14. Prepare the following mix in a separate tube: 2 μL of 5× first strand buffer, 0.5 μL of 12.5 mM dNTP mix, 1 μL of 100 mM DTT, 1 μL of RNase inhibitor, and 1 μL of SuperScript II reverse transcriptase. Mix by pipetting.
15. Add the resulting mix (5.5 μL) to the mix from **step 13** and incubate for 1 h at 50 °C.
16. Prepare the following PCR master mix: 8.5 μL of ultrapure water, 25 μL of PML, 2 μL of RP1, 2 μL of RPIX. Mix by pipetting.
17. Add the PCR master mix to the product of the reaction from **step 15**.
18. Incubate following the conditions in Table 2.
19. The quality of the resulting DNA library can be assessed using a Bioanalyzer DNA chip.
20. Combine 2 μL CRL with 2 μL of DNA loading dye and mix by pipetting.
21. Combine 1 μL HRL with 1 μL of DNA loading dye and mix by pipetting.
22. Load 2 gel lanes with 2 μL CRL/loading dye mix.
23. Load 1 gel lane with 2 μL HRL/loading dye mix.
24. Load 2 gel lanes with 25 μL each of DNA / loading dye mix (total load volume, 50 μL).
25. Run the gel at 145 V for 60 min (*see* **Note 10**).
26. Stain the gel with ethidium bromide for 3 min and view in a UV trans-illuminator.

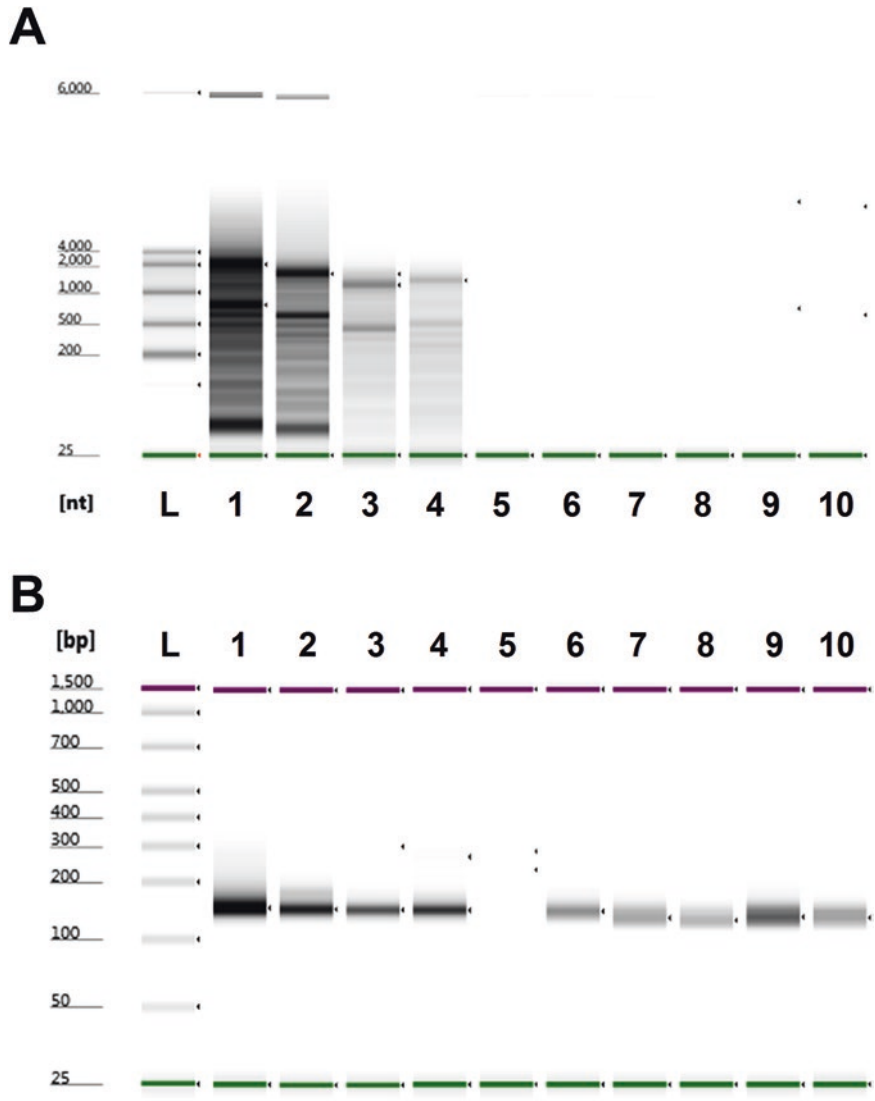

Fig. 1 (**a**) Electropherogram produced from RNA extracted from blood cell (lanes 1–4) and plasma samples (lanes 5–10) using TRIzol LS. (**b**) Electropherogram from cDNA libraries constructed from RNA samples in (**a**) using the TruSeq Small-RNA Library Preparation Kit (Illumina). Notice the difference in RNA profiles between lanes due to dramatically lower RNA content in plasma. Samples were analyzed using a Bioanalyzer RNA Pico Chip (**a**) and a High Sensitivity DNA Chip (**b**), both from Agilent

27. Carefully excise the gel bands at around 145–160 nucleotides (nt) and above in order to isolate the miRNA fragment of the library (*see* **Note 11** and Fig. 1).
28. Place the excised band in a gel breaker tube and centrifuge at 20,000 × *g* for 2 min.
29. Add 200 μL ultrapure water to the gel debris and rotate overnight to elute the DNA.

30. Transfer the eluted DNA to the top of a 5 μm filter and centrifuge at 600 × *g* for 10 s.
31. The resulting DNA library can be quality controlled on a Bioanalyzer DNA chip for the detection of a miRNA peak (*see* **Note 12**). The molarity of the resulting libraries can be adjusted to 2 nM using Tris–HCL 10 mM, pH 8.5 and stored at −20 °C.
32. Submit small RNA libraries for sequencing at 50-base single-end sequencing on the HiSeq 2500 Sequencing System (or a similar platform).

3.6 Small RNA Sequencing Data Analysis

Small RNA sequencing data in FASTQ format can be analyzed using sRNAbench software which performs preliminary processing and QC, mapping and differential expression analysis. Here, we briefly outline the steps involved. For detailed information please see the software manual.

1. The software can be run in genome mode using default settings, providing the desired genome as a reference and the latest version of miRBase (for the desired species) as the reference database in order to identify native as well as homologous miRNAs (*see* **Note 13**).
2. As an additional step, novel miRNAs as well as isomiRs (isomeric miRNAs) can be identified using sRNAbench's stepwise identification algorithm.
3. Prior to mapping, adapter sequences are trimmed from the reads and any reads with undetermined bases (N) and reads shorter than 15 nucleotides (a user-defined parameter) are automatically removed from the data set.
4. For mapping raw reads to the genome (or miRNA reference library) an alignment tool such as Bowtie can be used [20]. By default, this allows a single-nucleotide mismatch when mapping raw reads to the genome or to known miRNA sequences.
5. Following mapping, read counts per miRNA can be concatenated based on the mature miRNA sequence or individual miRNA loci (*see* **Note 14**).
6. sRNAbench can use edgeR internally for differential expression analysis in R language 3.2.1 [17, 21] (*see* **Note 15**).

4 Notes

1. If wet ice is used, avoid direct contact with collection tubes as rapid chilling could induce haemolysis and alter sample miRNA profiles.
2. Hemolysis typically alters miRNA profiles [22]. Hemolyzed plasma samples can be identified by visual inspection,

spectrophotometric measurements, and determination of miRNA expression ratios by RT-qPCR. The miR-451/miR-23a ratio was recently shown to be a very sensitive indicator of hemolysis [23]. It is good practice to systematically determine this parameter in all plasma samples before they are used for small RNA profiling.

3. Take care not to aspirate any of the colored layers as this will contaminate the RNA sample with phenol which will inhibit subsequent enzymatic reactions.
4. In some cases, the RNA pellet may be difficult to visualize after centrifugation. Prior marking of the position in the tube where the pellet is expected to sit after centrifugation may help localize the pellet.
5. Ensuring most of the residual ethanol is removed is important for quick drying of the RNA pellet. Use a pipette to remove all visible ethanol and then invert the tubes on absorbent paper and leave to dry.
6. The RNA solution will gradually turn cloudy during resuspension. Resuspending the RNA in less than 10 μL may be difficult.
7. We simultaneously prepare a standard curve containing dilutions (twofold increments) of pooled cDNA from several samples. Including a standard curve in each qPCR reaction allows for control of amplification efficiency (*see* section 3.4).
8. In our experience, freeze-thawing cDNA will have an impact on qPCR reaction efficiency and miRNA abundance; therefore, it is advisable to freeze multiple aliquots of cDNA and on the day of qPCR thaw a fresh aliquot for assaying.
9. No single housekeeping gene can be used as a universal normalizer for extracellular miRNA data. A small RNA should ideally be used. Several normalizers have been proposed [24, 25], however we recommend identifying potential normalizers from a high-throughput data set that is relevant to your experiment. Tools such as NormFinder can assist in identifying suitable normalizers [26].
10. For optimal separation of short-length sequences, stop the gel when the dye reaches the bottom of the gel.
11. The 147-nt band should primarily contain ~22-nt small RNA fragments consisting of mature miRNAs. The 157-nt band should contain ~30 nt RNA fragments of piwi-interacting RNAs, some miRNAs, and other regulatory small RNA molecules.
12. Due to the low yield of RNA from plasma samples, in our experience a miRNA peak is not always obvious; however, such libraries may still be of reasonable quality and produce more than 70% of mappable reads as miRNAs.

13. The quality of annotated miRNA data varies with each species. De novo identification of miRNAs is a better approach for poorly annotated species.
14. When mapping in genome mode it is important to use "counts per miRNA" as most mature miRNA reads will map to multiple genomic locations and sRNAbench counts are multi-mapping corrected. We found the mature_sense_singleA.grouped the most useful counts file to extract unique counts per miRNA.
15. Alternatively, read counts can be exported from sRNAbench and normalized to the total number of mapped reads per sample. These normalized values (reads per million mapped, RPMM) can be used for data presentation and statistical analysis independently of sRNAbench (e.g., using R packages).

Acknowledgments

We would like to thank Bushra Mohammed, Stephanie Schauer, and Sadanand Sontakke for assistance with developing protocols. This work was funded by Zoetis Inc. and BBSRC.

References

1. Donadeu FX, Schauer SN, Sontakke SD (2012) Involvement of miRNAs in ovarian follicular and luteal development. J Endocrinol 215(3):323–334. https://doi.org/10.1530/JOE-12-0252
2. Abernathy DG, Yoo AS (2015) MicroRNA-dependent genetic networks during neural development. Cell Tissue Res 359(1):179–185. https://doi.org/10.1007/s00441-014-1899-4
3. Vienberg S, Geiger J, Madsen S, Dalgaard LT (2016) MicroRNAs in metabolism. Acta Physiol (Oxf) 219:346. https://doi.org/10.1111/apha.12681
4. Weber JA, Baxter DH, Zhang S, Huang DY, Huang KH, Lee MJ et al (2010) The microRNA spectrum in 12 body fluids. Clin Chem 56(11):1733–1741. https://doi.org/10.1373/clinchem.2010.147405
5. Wang HY, Yan LX, Shao Q, Fu S, Zhang ZC, Ye W et al (2014) Profiling plasma MicroRNA in nasopharyngeal carcinoma with deep sequencing. Clin Chem 60:773. https://doi.org/10.1373/clinchem.2013.214213
6. Higuchi C, Nakatsuka A, Eguchi J, Teshigawara S, Kanzaki M, Katayama A et al (2015) Identification of circulating miR-101, miR-375 and miR-802 as biomarkers for type 2 diabetes. Metabolism 64(4):489–497. https://doi.org/10.1016/j.metabol.2014.12.003
7. Afonso MB, Rodrigues PM, Simao AL, Castro RE (2016) Circulating microRNAs as potential biomarkers in non-alcoholic fatty liver disease and hepatocellular carcinoma. J Clin Med 5(3):30. https://doi.org/10.3390/jcm5030030
8. Fuchs RT, Sun Z, Zhuang F, Robb GB (2015) Bias in ligation-based small RNA sequencing library construction is determined by adaptor and RNA structure. PLoS One 10(5):e0126049. https://doi.org/10.1371/journal.pone.0126049
9. Mestdagh P, Hartmann N, Baeriswyl L, Andreasen D, Bernard N, Chen C et al (2014) Evaluation of quantitative miRNA expression platforms in the microRNA quality control (miRQC) study. Nat Methods 11(8):809–815. https://doi.org/10.1038/nmeth.3014
10. Arroyo JD, Chevillet JR, Kroh EM, Ruf IK, Pritchard CC, Gibson DF et al (2011) Argonaute2 complexes carry a population of circulating microRNAs independent of vesicles in human plasma. Proc Natl Acad Sci U S A 108(12):5003–5008. https://doi.org/10.1073/pnas.1019055108
11. Ahanda ML, Zerjal T, Dhorne-Pollet S, Rau A, Cooksey A, Giuffra E (2014) Impact of the genetic background on the composition of the

chicken plasma MiRNome in response to a stress. PLoS One 9(12):e114598. https://doi.org/10.1371/journal.pone.0114598

12. Hansen EP, Kringel H, Thamsborg SM, Jex A, Nejsum P (2016) Profiling circulating miRNAs in serum from pigs infected with the porcine whipworm, Trichuris suis. Vet Parasitol 223:30–33. https://doi.org/10.1016/j.vetpar.2016.03.025
13. Muroya S, Ogasawara H, Hojito M (2015) Grazing affects Exosomal circulating MicroRNAs in cattle. PLoS One 10(8):e0136475. https://doi.org/10.1371/journal.pone.0136475
14. Donadeu FX, Sontakke SD, Ioannidis J MicroRNA indicators of follicular steroidogenesis. Reprod Fertil Dev 2016:906. https://doi.org/10.1071/RD15282
15. Noferesti SS, Sohel MM, Hoelker M, Salilew-Wondim D, Tholen E, Looft C et al (2015) Controlled ovarian hyperstimulation induced changes in the expression of circulatory miRNA in bovine follicular fluid and blood plasma. J Ovarian Res 8(1):81. https://doi.org/10.1186/s13048-015-0208-5.
16. da Silveira JC, Veeramachaneni DN, Winger QA, Carnevale EM, Bouma GJ (2012) Cell-secreted vesicles in equine ovarian follicular fluid contain miRNAs and proteins: a possible new form of cell communication within the ovarian follicle. Biol Reprod 86(3):71. https://doi.org/10.1095/biolreprod.111.093252.
17. R Core Team (2013) R: a language and environment for statistical computing. R Foundation for Statistical Computing, Vienna, Austria
18. RStudio Team (2015) RStudio: integrated development for R. RStudio Inc., Boston, MA
19. Rueda A, Barturen G, Lebron R, Gomez-Martin C, Alganza A, Oliver JL et al (2015) sRNAtoolbox: an integrated collection of small RNA research tools. Nucleic Acids Res 43(W1):W467–W473. https://doi.org/10.1093/nar/gkv555
20. Langmead B, Trapnell C, Pop M, Salzberg SL (2009) Ultrafast and memory-efficient alignment of short DNA sequences to the human genome. Genome Biol 10(3):R25. https://doi.org/10.1186/gb-2009-10-3-r25
21. Robinson MD, McCarthy DJ, Smyth GK (2010) edgeR: a bioconductor package for differential expression analysis of digital gene expression data. Bioinformatics 26(1):139–140. https://doi.org/10.1093/bioinformatics/btp616
22. Pritchard CC, Kroh E, Wood B, Arroyo JD, Dougherty KJ, Miyaji MM et al (2012) Blood cell origin of circulating microRNAs: a cautionary note for cancer biomarker studies. Cancer Prev Res (Phila) 5(3):492–497. https://doi.org/10.1158/1940-6207.CAPR-11-0370
23. Shah JS, Soon PS, Marsh DJ (2016) Comparison of methodologies to detect low levels of hemolysis in serum for accurate assessment of serum microRNAs. PLoS One 11(4):e0153200. https://doi.org/10.1371/journal.pone.0153200
24. Bae IS, Chung KY, Yi J, Kim TI, Choi HS, Cho YM et al (2015) Identification of reference genes for relative quantification of circulating MicroRNAs in bovine serum. PLoS One 10(3):e0122554. https://doi.org/10.1371/journal.pone.0122554
25. Schlosser K, McIntyre LA, White RJ, Stewart DJ (2015) Customized internal reference controls for improved assessment of circulating MicroRNAs in disease. PLoS One 10(5):e0127443. https://doi.org/10.1371/journal.pone.0127443
26. Andersen CL, Jensen JL, Orntoft TF (2004) Normalization of real-time quantitative reverse transcription-PCR data: a model-based variance estimation approach to identify genes suited for normalization, applied to bladder and colon cancer data sets. Cancer Res 64(15):5245–5250. https://doi.org/10.1158/0008-5472.CAN-04-0496

Chapter 6

Exosomal MicroRNAs as Potential Biomarkers in Neuropsychiatric Disorders

Gabriel R. Fries and Joao Quevedo

Abstract

This chapter will discuss the potential use of microRNAs, particularly those located in peripherally-isolated exosomes, as biomarkers in neuropsychiatric disorders. These extracellular vesicles are released as a form of cell-to-cell communication and may mediate the soma-to-germline transmission of brain-relevant information, thereby potentially contributing to the inter- or transgenerational transmission of behavioral traits. Recent novel methods allow for the enrichment of peripheral exosomes specifically released by neurons and astrocytes and may provide valuable brain-relevant biosignatures of disease.

Key words Biomarkers, Exosomes, MicroRNA, Neuropsychiatry, Periphery, Epigenetics

1 Introduction

A "biomarker" has been traditionally defined as a biological feature that can be used to detect the presence or progression of a disease or the effectiveness of a given treatment [1]. The use of biomarkers in medicine is a common and valuable approach in several clinical fields. However, no clinically relevant biomarker has been found for the field of neuropsychiatry, at least not of enough sensitivity and specificity to be actually used in the clinics. In particular, while several candidate biomarkers identified have shown high sensitivity, most of them are not specific to the particular disorder they were initially linked to.

While initial studies have focused on "candidate" markers, i.e., the investigation of specific proteins, genes, or metabolites hypothesized to be involved with the disorder based on previous evidence, the current gold standard approach relies on broad nonspecific screening methods ("omics"). By doing so, the analysis is not limited to known predefined markers and takes a systems biology perspective that better fits the extremely complex nature of psychiatric disorders, i.e., multifactorial disorders involving the interaction between several genes, proteins, and environmental stimuli [2].

Shao-Yao Ying (ed.), *MicroRNA Protocols*, Methods in Molecular Biology, vol. 1733,
https://doi.org/10.1007/978-1-4939-7601-0_6,

While proteomics and genomics have been traditionally the main focus of study in biomarkers research, epigenomic markers have been recently proposed as important players in the etiology, treatment, and progression of neuropsychiatric illness, suggesting them as valuable biomarkers worthy of investigation. Such markers depend both on the genotype and on the environment exposure, making them particularly relevant for such disorders.

Among the known epigenetic markers, of which DNA methylation is the most commonly investigated, microRNAs (miRNAs) represent an interesting target based on their widespread and global mechanisms of action. In particular, miRNAs have been shown to present important roles in neurobiological processes, such as neurogenesis, neural differentiation, and synaptic plasticity [3]. Moreover, they are active molecules with the ability to modulate gene expression and DNA methylation, and have been suggested to reflect altered physiology more directly than messenger RNAs, as well [3]. This chapter will briefly discuss the potential use and implications of miRNAs as biomarkers in neuropsychiatric disorders, with an emphasis on those located in peripheral exosomes.

2 Peripheral miRNAs as Biomarkers of Illness

Several different measures have been proposed as relevant biomarkers in medicine, including neuroimaging parameters, individual proteins, proteomic profiles in blood, plasma, serum, or cerebral spinal fluid (CSF), gene expression of particular genes and transcriptomic profiles in peripheral cells, among others [4]. Recently, biomarkers research has started to focus on miRNA as valuable measures with the potential to inform of pathophysiological mechanisms in disease.

In fact, miRNAs are particularly suitable as biomarkers since they can be found in several easily and noninvasively collected body fluids, such as saliva, urine, seminal plasma, tears, breast milk, and blood [5]. Moreover, miRNAs have also been detected in amniotic fluid, colostrum, bronchial lavage, cerebrospinal fluid, peritoneal fluid, and pleural fluid [3].

Accordingly, several studies have investigated differences in circulating miRNAs in neuropsychiatric diseases, including Alzheimer's disease (AD), Huntington's disease (HD), schizophrenia, bipolar disorder (BD), major depressive disorder (MDD), and autism spectrum disorder (ASD) [3], most of which point to important differences between patients and controls. Importantly, as for other types of biomarkers, the analysis of miRNAs as it is commonly performed 'suffers' from their tissue-specific properties and the heterogeneity of clinical populations under investigation [3]. In this context, comprehensive correlation studies between

periphery and the central nervous system are warranted, as well as novel approaches for the identification of the tissue of origin of the peripheral miRNAs being measured.

3 Circulating miRNAs

MicroRNAs can reach the peripheral circulation by either a passive release from cells (which typically occurs after cell death and is an energy-free process) or an active and selective secretion in response to a stimulus [3]. In general, these small RNA molecules can be found in different forms in the circulation: packaged inside microvesicles (MVs), exosomes, apoptotic bodies (ABs), or exist as a microvesicle-free miRNA associated with several multi-protein or lipoprotein complexes [3], such as the high-density lipoprotein (HDL) [5]. Of particular relevance for biomarkers research, circulating miRNAs are surprisingly stable and resistant to degradation from RNAse activity. Moreover, they have been shown to remain stable to severe conditions, as well, such as boiling, extreme pHs, extended storage, among others [3], which is likely due to the protection offered by their packaging into membrane-delimited vesicles.

Extracellular vesicles, such as those filled with miRNAs in the circulation, are thought to represent important vehicles in cell-to-cell communications in the body. These membrane-surrounded structures can be classified based on their sizes, components, and mechanisms of formation. While MVs are directly formed from the cell membrane, exosomes are released by exocytosis after the fusion of multivesicular bodies with the plasma membrane [5]. These multivesicular bodies are formed at endosomes by the inward budding of their delimiting membrane and can either fuse with lysosomes (resulting in the degradation of their content) or with the plasma membrane (resulting in the release of their context in the form of exosomes) (Fig. 1a) [6].

3.1 Exosomal miRNAs

Exosomes have typically between 40 and 100 nm in diameter and are secreted by most cell types, including neurons. These vesicles are known to be specially enriched in miRNAs, although their miRNA profiles do not necessarily reflect the profile of their cells of origin. This suggests an active sorting of the miRNAs to be packaged into the exosomes rather than a random and passive release. Accordingly, specific miRNAs have been shown to be preferentially sorted into exosomes, such as the miR-320 and miR-150 [5]. Of particular interest, exosomes have the ability to reach both neighboring and distant cells through circulation and deliver its content to these cells, ultimately transferring miRNAs and modulating the recipient cell's phenotype.

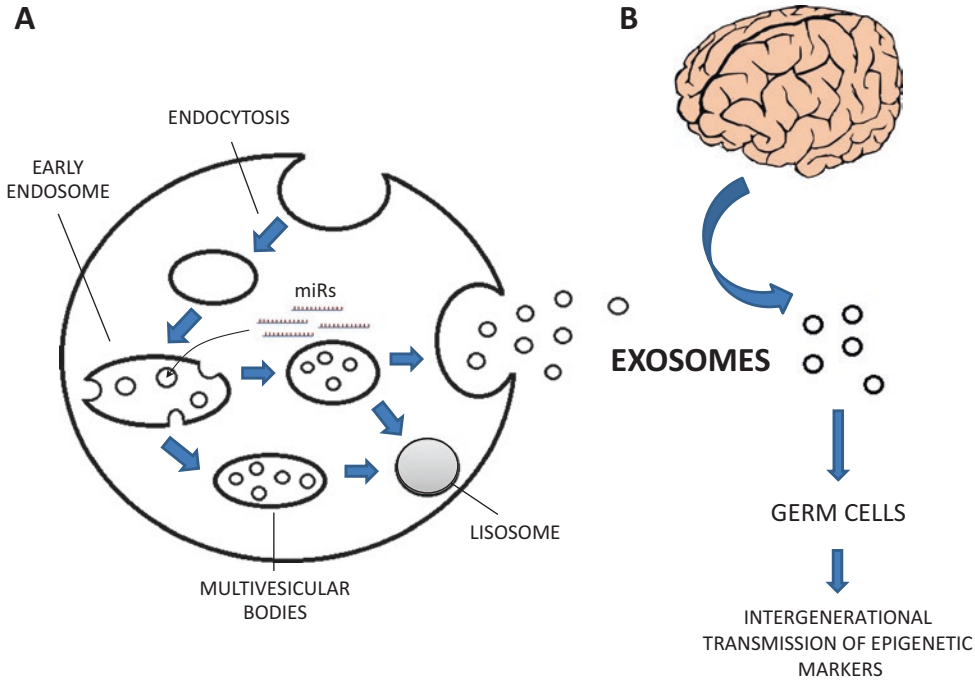

Fig. 1 (**a**) Formation and release of exosomes. Exosomes are generated by the inward budding of the surrounding membrane of the microvesicular bodies. These exosome-filled microvesicle bodies can be either fused with the lysosome (resulting in the degradation of the cargo) or with the plasma membrane for release of exosomes to the circulation. (**b**) Of particular relevance for neuropsychiatric disorders, exosomes released by brain cells can reach the peripheral circulation and deliver their context to germ cells. This soma-to-germline communication through exosomes has been hypothesized as one of the mechanisms underlying the non-genetic inter- and transgenerational transmission of epigenetic markers (such as DNA methylation), thereby potentially contributing to the transmission of behavioral traits over generations

Exosomal miRNAs have been proposed to act by two different mechanisms. One involves the typical action of miRNAs in negatively interfering with specific messenger RNAs (as any intracellular miRNA), while the other has been proposed to involve their ability to bind as ligands to toll-like receptors and trigger an inflammatory response (as reported for the exosomal miR-21 and miR-29a) [7]. Of note, the transfer of miRNAs by exosomes can have important implications for disease mechanisms, most notably tumor metastasis formation. In the context of neuropsychiatric illnesses, the implications have been proposed to include the transferring of epigenetic information from somatic to progenitor cells, thereby contributing to a non-genetic inter- and transgenerational transmission of behavioral traits [8–10] (Fig. 1b). This is quite interesting considering that a pool of circulating exosomes is thought to be released from neural tissues; neuronal exosomes can be released in response to synaptic activity [4] and might offer a valuable source of neuronal cell-specific information accessible in the periphery, as described in the next section.

3.2 Methodological Considerations

The analysis of peripheral exosomes, particularly their miRNA, is certainly a novel and particularly exciting approach in the field of neuropsychiatry. However, given its relatively recent start in the clinical context, exosome investigation still faces significant methodological challenges.

The study of exosomal miRNAs will typically require the initial isolation of exosome particles from the biological sample of interest, be it serum, plasma, cell culture supernatant, urine, or others (as discussed above). Currently available protocols for exosome enrichment differ in terms of the yield of isolated exosomes and may also lead to slight differences in their content [11, 12]. These include ultracentrifugation, density gradient separation, immunoaffinity capture, size exclusion chromatography, and commercial kits [5]. All of them might face the challenge of isolating very low quantities of exosomes, depending on the input sample. In these cases, high volumes of input sample might be required, depending on the downstream application. For the analysis of plasma-derived exosomal small RNA transcriptome by next-generation sequencing (NGS), for example, a study has shown that as little as 250 μL of human plasma might be sufficient for the isolation of an adequate quantity of exosomal miRNAs [13].

Once isolated, the enriched exosome fraction can be characterized by a plethora of different methods [14–17]. These include, among others, the use of transmission microscopy, scanning electron microscopy, dynamic light scattering, nanoparticle tracking analysis [18], and the analysis of specific proteins typically found in exosomes, such as CD63, CD9, and CD81 [5]. For the characterization of exosomal miRNAs, currently performed methods include miRNA microarrays, real-time quantitative PCR, and NGS. The main advantage of NGS compared to the other methods is that it is not limited to predefined known sequences, allowing for the potential discovery of novel RNA sequences and a deeper investigation of the sample.

Important for neuropsychiatric research, novel current methods have been proposed to specifically study immunochemically-isolated neuronally-derived circulating exosomes. Following total exosome isolation from human plasma samples, Goetzl and colleagues (2015) have used an antibody against the CD171 (L1 cell adhesion molecule [L1CAM] neural adhesion protein) to immune-enrich neural-derived exosomes from patients with AD [19]. Characterization of neurally-derived exosomes included the assessment of neuron-specific enolase and type 1 neural cell adhesion molecule (NCAM-1) along with the exosome marker CD81. A similar approach has been taken to enrich astrocyte-derived exosomes from peripheral plasma samples based on the immunolabeling of glutamine aspartate transporter (GLAST), as well [20]. Accordingly, miRNAs present in astrocyte-derived exosomes have been suggested to act as mediators of neuronal plasticity [21]. These innovative

approaches are quite interesting for neuropsychiatric research considering the possibility of peripherally measuring markers that originated specifically in the central nervous system, i.e., may represent a peripheral "window for the brain."

4 Conclusions

As briefly discussed in this chapter, exosomal miRNAs represent exciting potential biomarkers for neuropsychiatric disorder, particularly due to: (1) their availability in peripheral tissues; (2) their high stability against RNAses and other extreme conditions due to their location within membrane-surrounded structures; and (3) the possibility of specifically analyzing exosomes derived from the nervous system, which can ultimately inform of brain pathophysiological mechanisms. The latter is of particular relevance given that the tissue of origin of most peripherally-measured biomarkers so far is unknown.

Importantly, the study of exosomal miRNAs is still in its infancy in the field of Neuropsychiatry (particularly when compared to cancer research), and therefore the real clinical implications of their investigation are still quite hypothetical. Future longitudinal studies will need to be performed to investigate the potential use of exosomal miRNAs as biomarkers of risk, diagnosis/trait, state/acuity stage, treatment response, or prognosis [22]. Compared to other biomarkers currently under investigation, it is believed that the study of neural- or astrocyte-derived exosomal miRNAs is likely to provide brain-relevant disease-specific biosignatures that can overcome current limitations of biomarker research and significantly move the field forward.

References

1. Boksa P (2013) A way forward for research on biomarkers for psychiatric disorders. J Psychiatry Neurosci 38(2):75–77
2. Kobeissy F, Alawieh A, Mondello S et al (2012) Biomarkers in psychiatry: how close are we? Front Psych 3:114
3. Kichukova TM, Popov NT, Ivanov HY et al (2015) Circulating microRNAs as a novel class of potential diagnostic biomarkers in neuropsychiatric disorders. Folia Med (Plovdiv) 57(3–4):159–172
4. Lugli G, Cohen AM, Bennett DA et al (2015) Plasma Exosomal miRNAs in persons with and without Alzheimer disease: altered expression and prospects for biomarkers. PLoS One 10(10):e0139233
5. Zhang J, Li S, Li L et al (2015) Exosome and exosomal microRNA: trafficking, sorting, and function. Genomics Proteomics Bioinformatics 13(1):17–24
6. Stoorvogel W (2012) Functional transfer of microRNA by exosomes. Blood 119(3):646–648
7. Fabbri M, Paone A, Calore F et al (2012) MicroRNAs bind to toll-like receptors to induce prometastatic inflammatory response. Proc Natl Acad Sci U S A 109(31):E2110–E2116
8. Fries GR, Walss-Bass C, Quevedo J (2016) Non-genetic transgenerational transmission of bipolar disorder: targeting DNA methyltransferases. Mol Psychiatry 21(12):1653–1654
9. Sharma A (2014) Bioinformatic analysis revealing association of exosomal mRNAs and

proteins in epigenetic inheritance. J Theor Biol 357:143–149

10. Nagy C, Turecki G (2015) Transgenerational epigenetic inheritance: an open discussion. Epigenomics 7(5):781–790
11. Rekker K, Saare M, Roost AM et al (2014) Comparison of serum exosome isolation methods for microRNA profiling. Clin Biochem 47(1–2):135–138
12. Taylor DD, Zacharias W, Gercel-Taylor C (2011) Exosome isolation for proteomic analyses and RNA profiling. Methods Mol Biol 728:235–246
13. Huang X, Yuan T, Tschannen M et al (2013) Characterization of human plasma-derived exosomal RNAs by deep sequencing. BMC Genomics 14:319
14. Schageman J, Zeringer E, Li M et al (2013) The complete exosome workflow solution: from isolation to characterization of RNA cargo. Biomed Res Int 2013:253957
15. Gholizadeh S, Shehata Draz M, Zarghooni M et al (2017) Microfluidic approaches for isolation, detection, and characterization of extracellular vesicles: current status and future directions. Biosens Bioelectron 91:588–605
16. Rupert DL, Claudio V, Lässer C et al (2017) Methods for the physical characterization and quantification of extracellular vesicles in biological samples. Biochim Biophys Acta 1861(1 Pt A):3164–3179
17. Xu R, Greening DW, Zhu HJ et al (2016) Extracellular vesicle isolation and characterization: toward clinical application. J Clin Invest 126(4):1152–1162
18. Sokolova V, Ludwig AK, Hornung S et al (2011) Characterisation of exosomes derived from human cells by nanoparticle tracking analysis and scanning electron microscopy. Colloids Surf B Biointerfaces 87(1):146–150
19. Goetzl EJ, Boxer A, Schwartz JB et al (2015) Low neural exosomal levels of cellular survival factors in Alzheimer's disease. Ann Clin Transl Neurol 2(7):769–773
20. Goetzl EJ, Mustapic M, Kapogiannis D et al (2016) Cargo proteins of plasma astrocyte-derived exosomes in Alzheimer's disease. FASEB J 30(11):3853–3859
21. Lafourcade C, Ramírez JP, Luarte A et al (2016) MiRNAs in astrocyte-derived exosomes as possible mediators of neuronal plasticity. J Exp Neurosci 10(Suppl 1):1–9
22. Davis J, Maes M, Andreazza A et al (2015) Towards a classification of biomarkers of neuropsychiatric disease: from encompass to compass. Mol Psychiatry 20(2):152–153

Chapter 7

Identification and Validation of Potential Differential miRNA Regulation via Alternative Polyadenylation

Max Hübner, Pedro A.F. Galante, Simone Kreth, and Ludwig Christian Hinske

Abstract

MiRNAs control gene expression via recognition of specific sequences in the 3′ untranslated region of target genes, leading to mRNA degradation and consequently translational repression. The regulatory impact of miRNAs does not only depend on their expression levels, but also on their targets' mRNA configuration. Via alternative polyadenylation mRNA isoforms are created that may or may not contain the respective miRNA target sequence, turning the regulatory between these two on or off. In the following article, we describe our protocol on how to combine a bioinformatics evaluation of a potential miRNA–target gene interaction using the public web framework miRIAD with 5′ rapid amplification of cDNA ends (5′-RACE) in order to explore differential gene regulation by miRNAs through alternative polyadenylation.

Key words Differential miRNA targeting, 3′ RACE, Alternative polyadenylation, Intronic miRNAs, Tissue-specific regulation

1 Introduction

MiRNAs have established their role as potent regulators of the epigenome that are involved in a plethora of signaling pathways [1–4]. A significant fraction of miRNAs yield a relevant tissue specificity, leading to tissue-specific pathway regulation [5, 6]. However, apart from expression differences, gene-regulation through miRNAs can be modulated via another important mechanism: alternative polyadenylation [7, 8]. Since miRNA target identification relies on base-pair complementarity to the 3′-UTR of a gene, prolongation of shortening of such may turn miRNA for a certain gene on or off [9]. We recently found that this type of differential regulation appears to be a viable method to regulate host-targeting intronic miRNAs [7]. Moreover, recent publications show how alternative polyadenylation patterns are tissue specific [10–12]. It is therefore reasonable to assume that miRNAs may target certain

Shao-Yao Ying (ed.), *MicroRNA Protocols*, Methods in Molecular Biology, vol. 1733,
https://doi.org/10.1007/978-1-4939-7601-0_7,

genes in one tissue, but don't in another, an effect that is yet poorly investigated. Thus, we extended our previously published web resource miRIAD to incorporate alternative polyadenylation sites, distribution of site usage as well as miRNA and gene expression across tissues, protein interactions, and miRNA target predictions in order to allow the detection of differential miRNA targeting.

In the following article, we will show how to combine miRIAD with 3′ Rapid Amplification of cDNA Ends (RACE) to identify and validate differential miRNA targeting.

2 Materials

2.1 Reverse Transcription

1. RNA (*see* **Note 1**).
2. dNTP Mix (25 mM) of dATP, dCTP, dGTP, dTTP.
3. 3′ RACE Adapter.
4. 10× RT Buffer.
5. RNase Inhibitor.
6. M-MLV Reverse Transcriptase.
7. Nuclease-free water (ddH_2O).

2.2 Outer 3′ RLM-RACE PCR

1. RT reaction (from the previous step).
2. 10× PCR Buffer.
3. dNTP Mix (25 mM) of dATP, dCTP, dGTP, dTTP.
4. 3′ RACE gene-specific outer primer (10 μM) (*see* **Note 2**).
5. 3′ RACE Outer Primer.
6. Nuclease-free water (ddH_2O).
7. Thermostable DNA polymerase (0.25 μL of 5 U/μL) (*see* **Note 3**).

2.3 Inner 3′ RLM-RACE PCR

1. Outer 3′ RACE PCR (from the previous step).
2. 10× PCR Buffer.
3. dNTP Mix (25 mM) of dATP, dCTP, dGTP, dTTP.
4. 3′ RACE gene-specific inner primer (10 μM).
5. 3′ RACE Inner Primer to.
6. Nuclease-free water (ddH_2O).

3 Methods

3.1 Identification of Differential miRNA Targeting Using miRIAD

1. The webtool miRIAD is accessible at http://www.miriad-database.org.

2. On the main screen, select the species of interest (currently ten species available).
3. Type the name of the gene of interest, e.g., "ZFR."
4. In the representation of the 3′-UTR (Fig. 1), click on the little circles that represent poly(A)-sites. This will show tissue-specific usage of that site. In the case of ZFR, brain for example has equal expression of a ZFR variant with a 341 base pair 3′-UTR and a 1410 base pair 3′-UTR. Liver only presents with the 341 base pair variant.
5. Now, search for miRNAs that are predicted to target the 3′-UTR only in the longer variant: Move to the "miRNA binding sites" table, and use the filter fields below the table.
6. Select the UTR index (in case there are completely independent UTR regions) and the minimum poly(A) index (the count of alternating green colors in the UTR representation) to reduce the list of miRNAs to those that bind to the longer UTR isoform only.
7. If one is interested in specific tissues, the list can further be reduced by filtering for the tissue of maximum expression. In the given example, filtering might be applied to miRNAs that yield maximum expression in the brain.
8. Go through the list of miRNAs that remain in the table. Click on a miRNA of interest, little yellow boxes will show up in the UTR representation that represent potential target sites and verify that there are no additional target sites for that miRNA

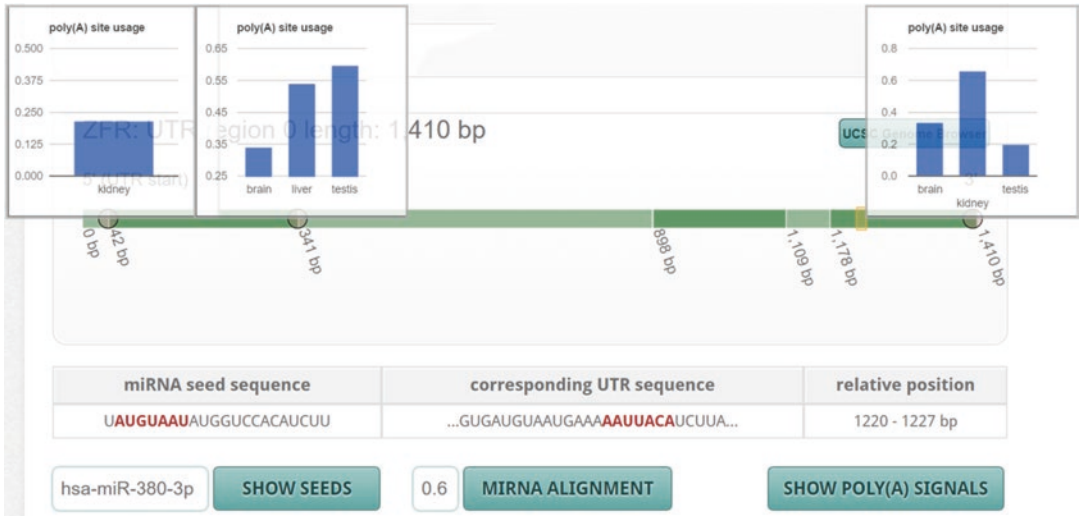

Fig. 1 Visual representation of the 3′-UTR of the gene *ZFR*. Alternative polyadenylation patterns are indicated by alternating shades of green. APA site usage across different tissues is shown for three polyadenylation sites. A potential target recognition site for miR-380-3p is indicated by a yellow box (position 1220–1227 bp after CDS)

close to the CDS. In the given example, hsa-miR-380-3p might be an interesting candidate.

9. An optional, additional step could be to check ZFR's interaction network for overrepresentation of miR-380-3p targets. This can be achieved via clicking on "[Load Network]" in the top left of the "Protein-protein interactions" table and then search for the respective miRNAs (e.g., miR-380-3p) in the miRNA table.

3.2 Validation of 3′-UTR Isoforms Using 3′-RACE

After the identification of a potential miRNA–target gene interaction, validate the existence of the UTR isoforms using Rapid Amplification of cDNA Ends.

3.3 Reverse Transcription

1. Gently mix RNA (1 μg total RNA or 50 ng poly(A) RNA), 4 μL dNTP mix, 2 μL RACE Adapter, 2 μL 10× RT Buffer, 1 μL RNAse inhibitor, 1 μL M-MLV Reverse transcriptase, and 8 μL nuclease-free water in a nuclease-free microcentrifuge tube on ice.
2. Spin the tube briefly.
3. Proceed to PCR or *see* **Note 4**.

3.4 Outer 3′ RLM RACE

1. Use 1 μL RT reaction (from the previous step), and add 5 μL 10× PCR Buffer(*see* **Note 5**), 4 μL dNTP, 2 μL 3′ RACE gene-specific outer primer (10 μM), 2 μL 3′ RACE Outer Primer, 1.25 U thermostable DNA polymerase (0.25 μL of 5 U/μL) and ddH_2O to a total reaction volume of 50 μL in a nuclease-free microcentrifuge tube on ice.
2. Spin the tube briefly.
3. Perform amplification by PCR with the following cycling conditions: 94 °C for 3 min denaturation, 35 cycles of 93 °C for 30 s, 60 °C for 30 s, 72 °C for 30 s and a final extension at 72 °C for 7 min (*see* **Note 5**) for targets longer than 1 kb, add 1 Min/kb to the extension time.
4. Separate PCR products on agarose gel (2%). If outer PCR yield is low or results in smear of bands, continue with inner 3′RLM RACE.

3.5 Inner 3′ RLM RACE

The Inner RACE further amplifies the PCR product of interest with a higher specificity. Here, the amplified PCR product(s) from the Outer RACE is selectively amplified by a specific primer.

1. Insert 1 μL Outer 3′ RACE PCR (from the previous step), 5 μL 10× PCR Buffer, 4 μL dNTP Mix, 2 μL 3′ RACE gene-

specific inner primer (10 μM), 2 μL 3′ RACE Inner Primer, 1.25 U thermostable DNA polymerase, and ddH_2O to a total reaction volume of 50 μL in a microcentrifuge on ice.

2. Spin the tube briefly.
3. Amplify the Outer RACE PCR products using the same PCR profile as in the Outer RACE PCR.
4. Separate PCR products on agarose gel (2%) containing Ethidium Bromide or another DNA visualizing agent. Visualize on an UV transilluminator. Run the samples from both PCRs to compare the products.

3.6 Verification of Correct Sequence

1. Excise and purify bands with a purification kit such as the Wizard® SV Gel and PCR Cleanup System (Promega).
2. Clone into a suitable vector such as the psc-B-amp/kan. This vector also contains restriction enzyme sites for subcloning procedures if needed.
3. Proceed to transformation and DNA plasmid preparation as described in [13].
4. Check insert size by restriction digestion.
5. Verify correct sequence by sequencing.

4 Notes

1. Use high-quality, freshly prepared total RNA. Use of poly(A) RNA as a template may increase amplification efficiency of low-expressed or difficult-to-amplify targets.
2. The self-provided forward primer for 3′RACE PCR should anneal to a nucleotide sequence within the coding sequence, preferably located approximately 200 bp upstream of the 3′UTR.
3. The type of DNA polymerase is highly dependent on multiple factors such as amplicon length and needs to be chosen carefully.
4. Reverse transcription reaction may be stored at −20 °C.
5. PCR cycling conditions are DNA polymerase-dependent and need to be adjusted individually. See reagent data sheet for further information.
6. An example blot of a 3′-RACE (outer and inner) for ZFR is shown in Fig. 2.

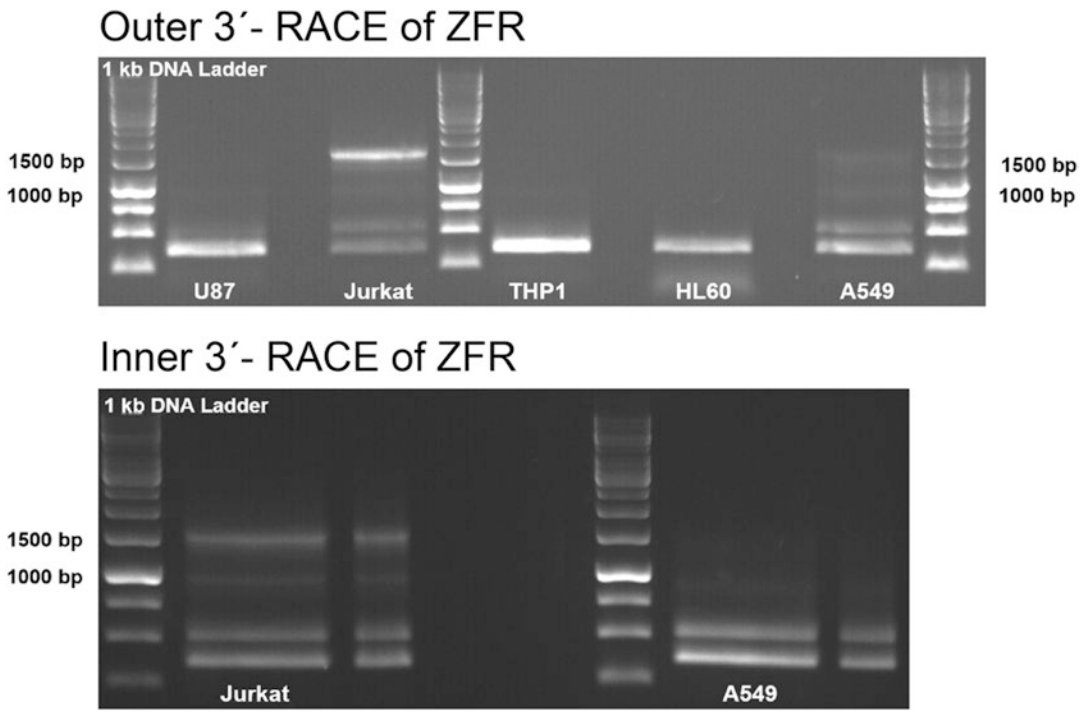

Fig. 2 Examples of 3′-RACE blots for ZFR

References

1. Schmitt DC, Madeira da Silva L, Zhang W, Liu Z, Arora R, Lim S et al (2015) ErbB2-intronic microRNA-4728: a novel tumor suppressor and antagonist of oncogenic MAPK signaling. Cell Death Dis 6:e1742
2. Yan L, Hao H, Elton TS, Liu Z, Ou H (2011) Intronic microRNA suppresses endothelial nitric oxide synthase expression and endothelial cell proliferation via inhibition of STAT3 signaling. Mol Cell Biochem 357:9–19
3. Goedeke L, Vales-Lara FM, Fenstermaker M, Cirera-Salinas D, Chamorro-Jorganes A, Ramírez CM et al (2013) A regulatory role for microRNA 33* in controlling lipid metabolism gene expression. Mol Cell Biol 33:2339–2352
4. Pang JC-S, Kwok WK, Chen Z, Ng H-K (2009) Oncogenic role of microRNAs in brain tumors. Acta Neuropathol 117:599–611
5. Hendrickson DG, Hogan DJ, McCullough HL, Myers JW, Herschlag D, Ferrell JE et al (2009) Concordant regulation of translation and mRNA abundance for hundreds of targets of a human microRNA. PLoS Biol 7:e1000238
6. Brawand D, Soumillon M, Necsulea A, Julien P, Csárdi G, Harrigan P et al (2011) The evolution of gene expression levels in mammalian organs. Nature 478:343–348
7. Hinske LC, Galante PAF, Limbeck E, Möhnle P, Parmigiani RB, Ohno-Machado L et al (2015) Alternative polyadenylation allows differential negative feedback of human miRNA miR-579 on its host gene ZFR. PLoS One 10:e0121507
8. Müller S, Rycak L, Afonso-Grunz F, Winter P, Zawada AM, Damrath E et al (2014) APADB: a database for alternative polyadenylation and microRNA regulation events. Database 2014. https://doi.org/10.1093/database/bau076
9. Kreth S, Limbeck E, Hinske LC, Schütz SV, Thon N, Hoefig K et al (2013) In human glioblastomas transcript elongation by alternative polyadenylation and miRNA targeting is a potent mechanism of MGMT silencing. Acta Neuropathol 125:671–681
10. Derti A, Garrett-Engele P, Macisaac KD, Stevens RC, Sriram S, Chen R et al (2012) A quantitative atlas of polyadenylation in five mammals. Genome Res 22:1173–1183
11. Zhou X, Li R, Michal JJ, X-L W, Liu Z, Zhao H et al (2016) Accurate profiling of gene expression and alternative Polyadenylation with whole Transcriptome termini site sequencing (WTTS-Seq). Genetics 203:683–697
12. Erson-Bensan AE, Can T (2016) Alternative polyadenylation: another foe in cancer. Mol Cancer Res 14:507–517
13. Heyn J, Hinske LC, Ledderose C, Limbeck E, Kreth S (2013) Experimental miRNA target validation. Methods Mol Biol 936:83–90

Chapter 8

How to Explore the Function and Importance of MicroRNAs: MicroRNAs Expression Profile and Their Target/Pathway Prediction in Bovine Ovarian Cells

Anna E. Zielak-Steciwko and John A. Browne

Abstract

Micro RNAs (miRNA) are integral components of genetic regulatory networks and act by binding to the transcripts of their corresponding target genes, leading to a decrease in protein production levels either by mRNA degradation or by translational repression. While the role of miRNAs is ubiquitous, they have a particular importance with regard to cell differentiation. The miRNA-target mRNA interaction has a significant impact on many signaling pathways and the cross-talk between them; playing a regulatory role in a variety of different physiological processes within the cells. Ovarian follicle development is a physiological process that is not fully understood with regard to miRNA regulation; there are many questions that remain with respect to the molecular regulation of this important process. Bovine follicular cells are a good experimental model for the investigation of these mechanisms, having direct implications on reproductive health in humans. This chapter describes how differentially expressed miRNAs are identified in the granulosa and theca cells of dominant and subordinate bovine ovarian follicles and the identification of their associated targets and pathways. This chapter systematically describes how the granulosa and theca cells are dissected from the ovarian follicles. Afterward, we present a detailed protocol for miRNA extraction, based on a combined TRI reagent/column clean-up method, and also miRNA expression profiling using both microarray and RT-qPCR. In addition, an outline is provided of the bioinformatic analysis which enables the prediction of miRNAs targets. Pathways associated with the differentially expressed miRNAs are also elucidated using DIANA-miRPath software.

Key words MicroRNAs expression, Target/pathway prediction, DIANA-miRPath, Ovarian follicles, Granulosa cells, Theca cells, Bovine

1 Introduction

Poor reproduction and fertility is a significant problem both for humans and other species including economically important livestock animals such as cattle and sheep. As a result of antagonistic pleiotropy, the use of artificial breeding programs to select for high milk yields in dairy cows has led to a significant reduction in their fertility [1]. Ultrasonography has firmly established that ovarian

Shao-Yao Ying (ed.), *MicroRNA Protocols*, Methods in Molecular Biology, vol. 1733,
https://doi.org/10.1007/978-1-4939-7601-0_8,

follicles develop in a wave-like pattern with two to three follicle waves of antral follicle growth occurring during human menstrual cycles [2] and bovine estrus cycles [3]. A wave is defined as the emergence of a cohort of small follicles, from which only one follicle is selected to become dominant and continue developing, while the rest undergo atresia via apoptosis at various stages of development [3]. The mechanism that regulates the selection of dominant follicle and the continuation of its growth is not clear. While much is known about ovarian follicle development, particularly the associated hormonal changes, many of the intracellular events remain unclear. Several studies, using a variety of molecular methods (e.g., microarray, RT-qPCR and RNA-Seq), have identified genes differentially expressed between dominant and subordinate follicles, broadening our understanding of the regulation of follicle development [4–8]. A lack of knowledge of the critical pathways and the key control points within them hinders our deeper understanding of the development of follicle.

MicroRNAs play an important regulatory function within the cell, directly affecting the abundance of messenger RNA molecules (mRNAs). Interpreting the biological role of miRNAs is a challenge as they can target multiple genes, and conversely genes can be targeted by multiple miRNAs. The interaction between miRNAs and their mRNA targets significantly influences signaling pathways, playing a regulatory role in a variety of different physiological processes. An online repository of miRNA sequences, miRBase, (www.mirbase.org), has been established, wherein each submitted miRNA molecule has a unique and fixed identifier, the mature microRNA identifier (MIMAT ID). The present annotation of miRBase (Release 21, June 2014) accommodates 28645 entries representing hairpin precursor miRNAs that express 35828 mature miRNA products in 223 species, including livestock animals [9]. To analyze miRNAs expression profiles a variety of commercial platforms are available, e.g., Exiqon (miRCURY LNA miroRNA array), Affymetrix (GeneChip miRNA array), or Agilent (miRNA Microarray) [10]. These array platforms, based on collections of miRNAs sequences, derived mainly from miRBase, profiles expression of numerous miRNAs. Our research group has been using the Exiqon platform to examine the expression of miRNAs between dominant and subordinate follicles in granulosa and theca cells. The Exiqon platform contains a total of 1488 human microRNAs, from miRBase version 18 [11]. The introduction of next-generation sequencing (NGS) platforms for the profiling of miRNAs (e.g., Illumina) has created new opportunities leading to the discovery of thousands of novel miRNA. Juxtaposition of different profiling technologies indicated that NGS is characterized by exceptional high dynamic range and sensitivity [12, 13]. These platforms require a high level of bioinformatic proficiency as data analysis is

demanding, also their high expense and labor requirement mean there is still a demand for miRNA microarray platforms.

A number of bioinformatic tools have been developed to analyze the interactions between miRNAs and their targets. These applications use a variety of algorithms, however, most of them were created based on experimental conclusions that assume that the 5′ end of the miRNA initially binds to the target mRNA by 2–7 nucleotides, called the "seed region." The seed match between the miRNAs and its target site must have perfect complementary. Additionally, the sequence conservation of the seed sequence can be used to verify the functionality of predicted target, which is usually higher than in non-seed region. This indicator is understood as preservation of a sequence across species. Furthermore, free energy can be used to assess binding energy/stability between the miRNA and its target mRNA; a higher stability indicates that the mRNA is the true potential target. The prediction of mRNA secondary structure and the availability of targets sites to interact with miRNAs can be further used to evaluate target predication. These four common features (seed match, conservation, free energy, and site accessibility) are used by most algorithms to predict miRNA targets [14]. Using these four criteria a score can be calculated for each target gene in which probability of interaction of the analyzed miRNA molecule with the gene can be estimated. Some of the more commonly used algorithms, based primarily on the criterion of conservatism, include: miRanda [15], TargetScan [16], and DIANA-microT [17]. For this study, we used the bioinformatic tools that are available on DIANA Lab (www.microrna.gr), which works on data accessible in the external databases such as: miRBase and Ensemble. Specifically, we worked with DIANA miRPath version 2 software, which evaluates the regulatory function of miRNAs and identifies molecular pathways associated with them. It should be noted that a version 3 is now available at www.microrna.gr/miRPathv3 [18]. This tool utilizes the results from microT-CDS and/or TargetScan v. 6.2 to predict targets using algorithms based on the conservation of miRNA-binding sites. The TarBase v. 7.0 option may also be used, restricting the analysis to experimentally validated miRNA:mRNA interactions. The identified potential targets can be map onto pathways using Kyoto Encyclopedia of Genes and Genomes (KEGG) pathways. This option enables the visualization of all the pathways in which targets of interest are involved, highlighting miRNAs that function in the same pathway.

This chapter describes the identification of miRNAs differentially expressed in the theca and granulosa cell of the bovine ovarian follicle and the use of in silico tools to explore their potential function.

2 Materials

Initially, disinfect the bench/laminar flow hood and all equipment with 70% ethanol and wipe with RNase Zap™, where possible procedures should be carried out on ice and biological samples should be snap frozen in liquid nitrogen (*see* **Note 1**). All the procedures should be performed in compliance with local health and safety guidelines.

2.1 Isolation of Granulosa and Theca Cells from Bovine Ovarian Follicles

1. Ice bucket.
2. Container with liquid nitrogen.
3. −80 °C freezer.
4. Waste container.
5. Sterile plastic containers (capacity of 120 mL).
6. Sterile petri dishes, one for each follicle.
7. Light microscope.
8. Sterile scalpel, # 11 blade.
9. Sterile 26-gauge needle.
10. Sterile syringe (1 mL).
11. Sterile forceps (*see* **Note 2**).
12. Sterile scraper (*see* **Note 2**).
13. Sterile scissors.
14. Sterile 2 mL tubes with screw cap (DNase/RNase free).
15. Centrifuge with cooling system (*see* **Note 3**).
16. Ice-cold phosphate-buffered saline (PBS), pH 7.4 (DNase/RNase free).

2.2 MicroRNA Extraction

1. TissueLyser (Qiagen).
2. Stainless steel beads (5 mm diameter, Qiagen) for use with the TissueLyser system.
3. Set of pipettes reserved for RNA work (P10, P200, P1000).
4. Sterile filter pipette tips (DNase/RNase free).
5. 1.5 mL micro-centrifuge tubes (DNase/RNase free).
6. Microcentrifuge with cooling system.
7. Vortex mixer.
8. Waste container.
9. TRI reagent (Sigma Aldrich).
10. 1-Bromo-3-chloropropane (Sigma Aldrich).
11. Ethanol (100%) (Sigma Aldrich).
12. RNeasy® Mini Kit (Qiagen).

13. NanoDrop (ND-1000 spectrophotometer, Technologies, Wilmington).
14. Agilent Bioanalyzer 2100.
15. RNA 6000 Nano Chip kit (Agilent Technologies).

2.3 miRNA Expression Profile

2.3.1 miRNAs Arrays

In our study the miRNA microarray analysis was performed by Exiqon (Vedbaek, Denmark). Their sixth generation miRNA array, miRCURY LNA™ microRNA Array, contained 1488 capture probes targeting mature human miRNA sequences based on miRBase version 18, in addition to several positive and negative controls. High-quality undegraded RNA is essential for optimum analysis, all the samples analyzed had RIN values greater than 7.5. The samples were labeled using the miRCURY LNA™ microRNA Hi-Power Labeling Kit, after which the samples were hybridized to the miRCURY microRNA Array. The slides were scanned using an Agilent G2565BA Microarray Scanner System (Agilent Technologies, Inc., USA) and analysis was performed using the ImaGene® 9 Analysis Software. Exiqon services supplied the final report containing the raw data, the QC analysis, and some preliminary differential miRNA expression analysis.

2.3.2 RT-qPCR

1. Set of accurate pipettes reserved for PCR work (P 2, P10, P20, P200).
2. Sterile filter pipette tips (DNase/RNase free).
3. 0.5 mL tubes (DNase/RNase free).
4. 1.5 mL micro-centrifuge tubes (DNase/RNase free).
5. Vortex mixer.
6. Standard PCR thermocycler.
7. Microcentrifuge.
8. Centrifuge for 96 wells PCR plates.
9. Optical 96-well reaction plates with optical cover (Applied Biosystems).
10. Real-time PCR cycler.
11. TE, pH 8.0 (Sigma-Aldrich).
12. miScript II Reverse Transcriptase (Qiagen).
13. miScript SYBER Green PCR Kit (Qiagen).
14. miScript Primer Assay (Qiagen) for selected miRNAs including internal control RNU6 (*see* **Note 4**).
15. qBase+ Software (Biogazelle, Ghent).

2.4 Target and Signaling Pathways Analysis

To carry out the bioinformatic analysis using DIANA-miRPath software a computer with access to Internet is required. This software allows users to create a personal account, which greatly facilitates analysis; however, registration is not mandatory and analysis

can be performed without it. In this program, we used the microT-CDS algorithm which predicts target genes based on the miRNA binding sites on the mRNA, the 3'UTR regions, and the coding sequences. Additionally, the software facilitates the identification and visualization of KEGG signaling pathways enriched in the specified predicted targets. The determination of targets/pathways can be conducted for one or multiple miRNAs, input lists are easily imported and results can be saved in several different formats (e.g., txt, xls, jpg, etc.) and directly downloaded.

3 Methods

3.1 Isolation of Granulosa and Theca Cells from Bovine Ovarian Follicles

Ovaries were collected from animals whose estrus cycle was synchronized. Prior to slaughter, estrus behavior was observed and the pattern of follicle development in the ovaries was monitored using transrectal ultrasonography (*see* **Note 5**). In the abattoir, ovaries from each animal were collected in ice-cold PBS and promptly returned to the laboratory for directly processing, all the subsequent procedures should be performed using the aseptic technique.

1. Dissect out each follicle from the ovary using a scissors and scalpel (Fig. 1).
2. Using a 1 mL syringe fitted with a 26-gauge needle, carefully withdraw the follicular fluid from each follicle. The follicular fluid can subsequently be used to determine the hormone concentration of each follicle (*see* **Note 6**).
3. Add 1 mL of cold PBS to each follicle and cut the follicle in half with a sterile scalpel. Granulosa cells appear as a white cloudy layer with extremely fine granularity. While observing the follicle under the microscope scrape the granulosa cells

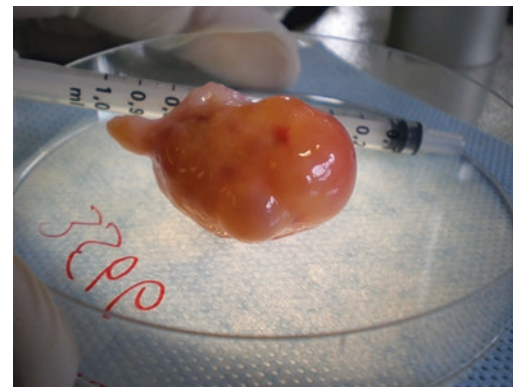

Fig. 1 Bovine ovary with follicles in different stages of development

away from the theca interna. Carefully place the collected granulosa cells along with the PBS into a sterile screw cap tube and centrifuge at 5000 × *g* for 5 min, remove the PBS from the pellet of cells using a pipette and snap freeze the samples in liquid nitrogen (*see* **Note 7**).

4. During the centrifugation of the granulosa cells add an additional 1 mL of cold PBS to the remaining follicle. Collect theca cells under the microscope; pull out the theca layer using a forceps and chop into small pieces, place the samples in a screw cap tube and snap freeze in liquid nitrogen (*see* **Note 7**).
5. The snap frozen isolated granulosa and theca cells should then be stored at −80 °C for miRNA or alternatively they can be processed immediately after dissection.

3.2 MicroRNA Extraction

Total RNA including the miRNA fraction is isolated using a combined TRI reagent/column clean-up protocol, standard precautions when handling RNA should be followed.

1. Thaw the samples on ice. Prior to homogenization add 1.0 mL of TRI reagent and a single 5 mm stainless steel bead to each sample. Place the tubes in TissueLyser™ (Qiagen) and homogenize at maximum speed for 2 min, alternative homogenization methods may be used (*see* **Note 8**).
2. Incubate the samples at room temperature for 5 min.
3. Add 200 μL of 1-Bromo-3-chloropropane to each sample (*see* **Note 9**). Shake vigorously for 15 s and then incubate at room temperature for 3 min.
4. Centrifuge the samples at 12,000 × *g* for 15 min at 4 °C. Three phases should be visible, an upper aqueous phase enriched for RNA, a white interphase enriched for DNA, and a lower red colored organic phase enriched for proteins.
5. Transfer the upper phase (approx. 450 μL) to a fresh labeled 1.5 mL tube; add 1.5 volumes of 100% ethanol (approx. 675 μL) and mix thoroughly by vortexing for 10 s.
6. Transfer the mixture directly into an RNeasy column (Qiagen) in two aliquots of approx. 600 μL and centrifuge at 8000 × *g* for 30 s between each addition. Discard the flow-through after each spin.
7. Wash the column with 700 μL of RW1 followed by two washes with RPE (500 μL) as per the manufacturer's instructions (Qiagen).
8. Spin column at maximum speed for 2 min to remove all residual wash buffers and to dry the column, place the column in a newly labeled 1.5 mL tube.
9. To elute the RNA, including the small RNAs, pipette 35 μL of RNase/DNase-free water directly onto the column, incubate

for 1 min at room temperature and centrifuge at 8000 × *g* for 60 s. The eluted RNA should be stored at −80 °C and kept on ice when in use.

10. Determine the RNA quantity using the NanoDrop™ and RNA quality using the RNA 6000 chip on the Agilent Bioanalyzer (*see* **Note 10**).

3.3 miRNA Expression Analysis

3.3.1 miRNAs Arrays Raw Data Analysis

1. Load the raw data file into limma R- package of Bioconductor ("https://bioconductor.org/biocLite.R").
2. After background correction (method = "subtract") and normalization of samples (normalizeWithinArrays—no offset) remove probes with no name, control probes and spike in probes from the analysis.
3. Use the lmFit and empirical Bayes functions within the Limma package to analyze differential expression between samples.
4. Use a Benjamini-Hochberg false discovery rate (FDR) correction set at 1% to control for type I errors (false positives).
5. The raw data from our experiment has been deposited in the Gene Expression Omnibus repository under accession number GSE55890.

3.3.2 RT-qPCR

1. Thaw the RNA samples on ice, reverse transcribe 1000 ng of RNA using miScript II RT in 20 μL of reaction volume, as per the manufacturer's instructions (Qiagen). It is important to choose the appropriate buffer, for mature miRNAs analysis the 5× miScript HiSpec buffer should be used.
2. Using a standard PCR thermocycler incubate the samples at 37 °C for 60 min followed by a 5 min incubation at 95 °C to inactivate the enzymes. Proceed directly to performing the RT-qPCR analysis, alternatively the cDNA can be stored at −20 °C.
3. Using a 96-well plate format prepare a 25 μL qPCR reaction for each sample as per the manufacturer's instructions; add 12.5 μL of 2× QuantiTec SYBER Green PCR Master Mix, 2.5 μL of 10× miScript Universal Primer, 2.5 μL of 10× miScript Primer Assay, 5 μL of RNase-free water, and 5 μL of the diluted template cDNA (*see* **Note 11**). Include RNU6 as a positive control. Perform each sample reaction in duplicates.
4. Suitable negative controls should be prepared including a "no RT control" to control for the presence of contaminating genomic DNA (*see* **Note 12**).
5. Seal the reaction plate with an optical cover and centrifuge it at 1000 × *g* for 2 min. Place the plate into the qPCR instrument and perform the reaction using the following cycling conditions; initial activation of 95 °C for 15 min and 45 cycles of

denaturation for 15 s at 94 °C, annealing for 30 s at 55 °C, followed by extension for 30 s at 70 °C, a melt curve analysis should be included (*see* **Note 13**).

6. After the run has completed export the Cq values using the Qiagen recommended default settings, examine the melt curves to confirm the presence of a single distinct peak corresponding to a single PCR product and assess the negative and positive controls.
7. Perform the data analysis using the qBASE+ analysis package (Biogazelle, Ghent), normalized relative expression values were calculated using a global mean normalization strategy and the data analyzed using unpaired T-tests.

3.4 Target and Signaling Pathway Analysis for Differentially Expressed miRNAs Using miRPath

1. To determine which miRNAs function in the same signaling pathways, highly significant ($p \leq 0.01$) differentially expressed miRNAs from the microarray data were selected for analysis. After opening the miRPath interface, select the species and either the microT-CDS/TargetScan algorithm or the TarBase option. Subsequently, enter the name of a specific miRNA sequence or the miRBase mature ID (MIMAT) from miRBase into the "Add miRNAs" window. For multiple miRNAs analysis, the list of selected miRNAs (name of sequences or MIMAT ID) can be uploaded by selecting the relevant text using the "Add miRNAs" option.
2. In the open panel, after uploading the data, decide which way the results will be merged. There are four options to choose: gene union, gene intersection, pathway union, and pathway intersection (*see* **Note 14**). Next, set the *p*-value threshold and MicroT threshold. To obtain sensitive and specific results of miRNA-mRNA interaction lower the threshold, it is suggested to begin with a value of 0.8 for MicroT. Additionally, you may apply a false discovery rate (FDR) with a significance threshold set at $p \leq 0.01$ or lower.
3. On the scoreboard pathways names are ranked by *p*-value, beside the *p*-value, the number of genes targeted in the particular pathway is given. Open "*see* genes" to find information about the targets (gene name, Ensembl ID, and their interactions in TarBase or microT-CDS). The number of miRNAs involved in the selected pathway out of all miRNAs used in the analysis is shown next. The last column, "details" displays information about which gene is regulated by which miRNA.
4. To visualize a KEGG map click on the name of a given signaling pathway. The map shows targets and their locations in the molecular pathway. Putative targets regulated by only one miRNA are highlighted in yellow, while putative targets

regulated by more miRNAs are highlighted in orange. To see the regulator miRNAs, move the cursor over the label with the gene's name. The function "Disable" hides genes, whereas "Enable" highlights the gene of interest with a red frame.

5. Save the results by pressing "download result" located on the top right side of the table. The output files contain a list of significantly enriched signaling pathways associated with the differentially expressed miRNAs ordered by *p*-value (from the most to least significant).

4 Notes

1. Due to the nature of the cells used here, RNAlater™ should not be used as a preservative as the protocol does not enable their effective recovery.
2. Forceps and scraper are essential elements of the granulosa and theca dissection. Therefore, we suggest having a variety of different types of forceps, e.g., normal, serrated, grooved, and toothed. We found the rigid "Lascod" scraper, a dental instrument (*see* Fig. 2), to be very useful for isolating the granulosa cells.
3. All centrifugations should be carried out at 4 °C.
4. miScript amplification kit contains only a miRNA-specific forward primer of investigated miRNA; before use centrifuge each vial and dissolve the content by adding 550 μL of TE, pH 8.0, aliquot out in smaller volumes for storage. Universal reverse primer and a universal reverse primer added to the target molecules during the RT-step.

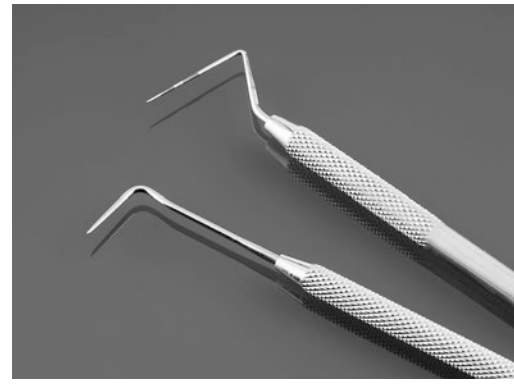

Fig. 2 Scraper "Lasod" for granulosa cells

5. Collecting follicles from synchronized animals facilitates the study of temporal gene expression associated with specific developmental stages.
6. Place the follicular fluid in a sterile screw cap tube, centrifuge at 500 × *g* for 10 min. Supernatant should be frozen in liquid nitrogen and stored at −80 °C until estradiol and progesterone analysis.
7. The isolated pellets of granulosa or theca cells may be snap frozen directly, alternative for RNA isolation add 1.0 mL of TRI reagent prior to freezing.
8. If a TissueLyser™ is not available, each sample of granulosa cells suspended in TRI reagent can be homogenized by passing it through a 20-gauge needle 5–10 times to disrupt clumps and cells. Each sample of theca suspended in TRI reagent can be homogenized using any suitable rotor-stator homogenizer such as the TissueRuptor (Qiagen) at maximum speed for 30 s, care should be taken to avoid heating of the sample. The homogenizer should be cleaned with ethanol and distilled water between each sample.
9. As chloroform is a suspected mutagen we recommended the use of 1-Bromo-3-chloropropane as an alternative, there is no discernible difference between the performances of the two reagents (*see* ref. 19).
10. Only samples with RIN values greater than 7.5 were used for further analysis (*see* Fig. 3a, b).
11. Prior to performing the RT-qPCR dilute each cDNA sample 1:40 using RNase/DNase-free water.
12. To prepare "no RT control" add to PCR reaction RNA template, instead of cDNA. Additionally, to exclude contamination or primer dimer formation for each primer on the plate run a "no template control" no template reaction.
13. Add the melt curve at the end of PCR cycling as per the instruments settings.
14. The "Genes Union" option finds all the genes that are targeted by at least one selected miRNA, whereas the "Genes Intersection" finds all the genes targeted by all the selected miRNAs or by the number of miRNAs defined by users; both the options are a priori methods. The "Pathways/Categories Union" option finds all the significantly targeted pathways by at least one selected miRNA, while "Pathways/Categories Intersection" finds all the significantly targeted pathways by all the selected miRNA; they are a posteriori methods.

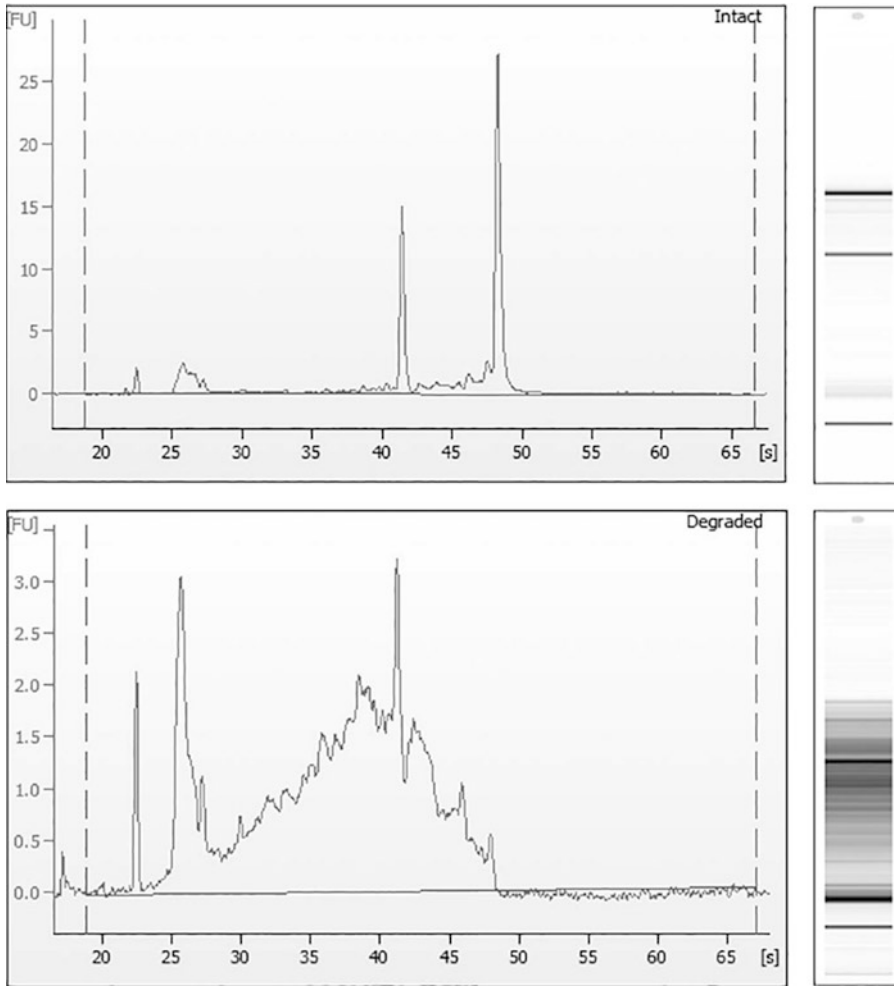

Fig. 3 Electropherograms presenting quality of total RNA, including miRNA, measure by Bioanalyzer (Agilent); **a**—intact total RNA, **b**—degraded total RNA

Acknowledgment

This work was supported by National Science Centre Poland (N N311 324136). We would like to thank S. Walsh for preparing the image presented in Fig. 1 and K. Smyk for preparing the image presented in Fig. 2.

References

1. Berry DP, Wall E, Pryce JE (2014) Genetics and genomics of reproductive performance in dairy and beef cattle. Animal 8:105–121
2. Baerwald AR, Adams GP, Pierson RA (2003) Characterization of ovarian follicular wave dynamics in women. Biol Reprod 69:1023–1031
3. Evans AC (2003) Characteristics of ovarian follicle development in domestic animals. Reprod Domest Anim 38:240–246

4. Evans AC, Ireland JL, Winn ME, Lonergan P, Smith GW, Coussens PM, Ireland JJ (2004) Identification of genes involved in apoptosis and dominant follicle development during follicular waves in cattle. Biol Reprod 70:1475–1484
5. Mihm M, Baker PJ, Ireland JL, Smith GW, Coussens PM, Evans AC, Ireland JJ (2006) Molecular evidence that growth of dominant follicles involves a reduction in follicle-stimulating hormone dependence and an increase in luteinizing hormone dependence in cattle. Biol Reprod 74:1051–1059
6. Zielak AE, Forde N, Park SD, Doohan F, Coussens PM, Smith GW, Ireland JJ, Lonergan P, Evans AC (2007) Identification of novel genes associated with dominant follicle development in cattle. Reprod Fertil Dev 19:967–975
7. Forde N, Mihm M, Canty MJ, Zielak AE, Baker PJ, Park S, Lonergan P, Smith GW, Coussens PM, Ireland JJ, Evans ACO (2008) Differential expression of signal transduction factors in ovarian follicle development: a functional role for betaglycan and FIBP in granulosa cells in cattle. Physiol Genomics 33:193–204
8. Walsh SW, Mehta JP, McGettigan PA, Browne JA, Forde N, Alibrahim RM, Mulligan FJ, Loftus B, Crowe MA, Matthews D, Diskin M, Mihm M, Evans AC (2012) Effect of the metabolic environment at key stages of follicle development in cattle: focus on steroid biosynthesis. Physiol Genomics 44:504–517
9. Kozomara A, Griffiths-Jones S (2014) miRBase: annotating high confidence microRNAs using deep sequencing data. Nucleic Acids Res 42(DI):D68–D73. https://doi.org/10.1093/nar/gkt1181
10. Dedeoğlu BG (2014) High-throughput approaches for microRNA expression analysis. In: miRNomics: microRNA biology and computational analysis, vol 1107. Springer, Berlin, pp 91–103
11. Zielak-Steciwko AE, Browne JA, McGettigan PA, Gajewska M, Dziecioł M, Szulc T, Evans ACO (2014) Expression of microRNAs and their target genes and pathways associated with ovarian follicle development in cattle. Physiol Genomics 46:735–745
12. Pritchard CC, Cheng HH, Tewari M (2012) MicroRNA profiling: approaches and considerations. Nat Rev Genet 13:358–369
13. Tam S, de Borja R, Tsao M, McPherson JD (2014) Robust global microRNA expression profiling using next-generation sequencing technologies. Lab Investig 94:350–358
14. Peterson SM, Thompson JA, Ufkin ML, Sathyanarayana P, Liaw L, Congdon CB (2014) Common features of microRNA target prediction tools. Front Genet 5:1–10
15. John B, Enright AJ, Aravin A, Tuschl T, Sander C, Marks DS (2004) Human MicroRNA targets. PLoS Biol 2:e363
16. Lewis BP, Burge CB, Bartel DP (2005) Conserved seed pairing, often flanked by adenosines, indicates that thousands of human genes are microRNA targets. Cell 120:15–20
17. Maragkakis M, Reczko M, Simossis VA, Alexiou P, Papadopoulos GL, Dalamagas T et al (2009) DIANA-microT web server: elucidating microRNA functions through target prediction. Nucleic Acids Res 37:W273–W276
18. Vlachos IS, Zagganas K, Paraskevopoulou MD, Georgakilas G, Karagkouni D, Vergoulis T, Dalamagas T, Hatzigeorgiou AG (2015) DIANA-miRPath v3.0: deciphering microRNA function with experimental support. Nucleic Acids Res 43:W460–W466. https://doi.org/10.1093/nar/gkv403
19. Chomczynski P, Mackey K (1995) Substitution of chloroform by bromo-chloropropane in the single-step method of RNA isolation. Anal Biochem 225:163–164

Chapter 9

Gene Silencing In Vitro and In Vivo Using Intronic MicroRNAs

Shi-Lung Lin and Shao-Yao Ying

Abstract

MicroRNAs (miRNAs), small single-stranded regulatory RNAs capable of interfering with intracellular messenger RNAs (mRNAs) that contain either complete or partial complementarity, are useful for the design of new therapies against cancer polymorphism and viral mutation. Numerous miRNAs have been reported to induce RNA interference (RNAi), a post-transcriptional gene-silencing mechanism. Recent evidence also indicates that they are involved in the transcriptional regulation of genome activities. They were first discovered in *Caenorhabditis elegans* as native RNA fragments that modulate a wide range of genetic regulatory pathways during embryonic development, and are now recognized as small gene silencers transcribed from the noncoding regions of a genome. In humans, nearly 97% of the genome is noncoding DNA, which varies from one individual to another, and changes in these sequences are frequently noted to manifest in clinical and circumstantial malfunction; for example, type 2 myotonic dystrophy and fragile X syndrome were found to be associated with miRNAs derived from introns. Intronic miRNA is a new class of miRNAs derived from the processing of non-protein-coding regions of gene transcripts. The intronic miRNAs differ uniquely from previously described intergenic miRNAs in the requirement of RNA polymerase (Pol)-II and spliceosomal components for its biogenesis. Several kinds of intronic miRNAs have been identified in *C. elegans*, mouse, and human cells; however, their functions and applications have not been reported. Here, we show for the first time that intron-derived miRNA is not only able to induce RNAi in mammalian cells but also in fish, chicken embryos, and adult mice cells, demonstrating the evolutionary preservation of this gene regulation system in vivo. These miRNA-mediated animal models provide artificial means to reproduce the mechanisms of miRNA-induced disease in vivo and will shed further light on miRNA-related therapies.

Key words MicroRNA (miRNA), RNA interference (RNAi), RNA polymerase type II (Pol II), RNA splicing, Intron, RNA-induced gene-silencing complex (RISC), Gene silencing in vivo

1 Introduction

Nearly 97% of the human genome is noncoding DNA, which varies from one species to another, and changes in these sequences are frequently noted to manifest in clinical and circumstantial malfunction. Numerous non-protein-coding genes are recently found to encode miRNAs, which are responsible for RNA-mediated gene silencing through RNAilike pathways [1–3]. RNAi is a post-transcriptional

Shao-Yao Ying (ed.), *MicroRNA Protocols*, Methods in Molecular Biology, vol. 1733,
https://doi.org/10.1007/978-1-4939-7601-0_9,

gene-silencing mechanism that can be triggered by small regulatory RNA molecules, such as miRNA and small interfering RNA (siRNA). miRNAs, which are small single-stranded regulatory RNAs, can interfere with intracellular mRNAs that contain either complete or partial complementarity; a trait useful for the design of new therapies against cancer polymorphism and viral mutation [4, 5]. A much more rigid complementarity is required for double-stranded siRNA-induced RNAi gene silencing.

miRNAs were first discovered in *C. elegans* as native RNA fragments that modulate a wide range of genetic regulatory pathways during embryonic development [6]. Currently, varieties of natural miRNAs have been found to be derived from hairpin-like RNA precursors in almost all eukaryotes, including yeast (*Schizosaccharomyces pombe*), plant (*Arabidopsis* spp.), nematodes (*C. elegans*), flies (*Drosophila melanogaster*), fishes, mice, and humans; they have been found to provide intracellular defense against viral infections and regulation of certain gene expressions during development [7–17]. In contrast, natural siRNAs were abundantly discovered in plants and low-level animals (worms and flies), but rarely in mammals [18, 19]. The intronic miRNA is a new class of miRNAs derived from the processing of gene introns. As shown in Fig. 1, the intronic miRNAs differ uniquely from previously described intergenic miRNAs in the requirement of Pol II and spliceosomal components for their biogenesis [20, 21]. We have shown, for the first time, that these intron-derived miRNAs are able to induce RNA interference in not only human and mouse cells, but also in zebrafish, chicken embryos, and adult mice, demonstrating the evolutionary preservation of the intron-mediated gene regulation through miRNA-associated mechanisms in vertebrates in vitro and in vivo. These findings suggest the existence of an intracellular miRNA-mediated gene regulatory system for fine-tuning the degradation of protein-coding mRNAs [22].

The introns occupy the largest proportion of noncoding sequences in the protein-coding DNA of a genome. The transcription of the genomic protein-coding DNA generates precursor (pre)-mRNA with four major parts: a 5′-untranslated region (UTR), a protein-coding exon, a noncoding intron, and a 3′-UTR [23]. In a broad definition, both 5′- and 3′-UTRs can be seen as a kind of intron extension; however, their processing during mRNA translation is different from the intron located between two protein-coding exons, termed the in-frame intron. The in-frame intron can be up to several tens of kilobase nucleotides long and was thought to be a huge genetic waste in gene transcripts. Recently, this stereotypical misunderstanding was changed with the discovery of intronic miRNAs. Approximately 10–30% of some spliced introns are found in the cytoplasm, with moderate half-lives [24, 25].

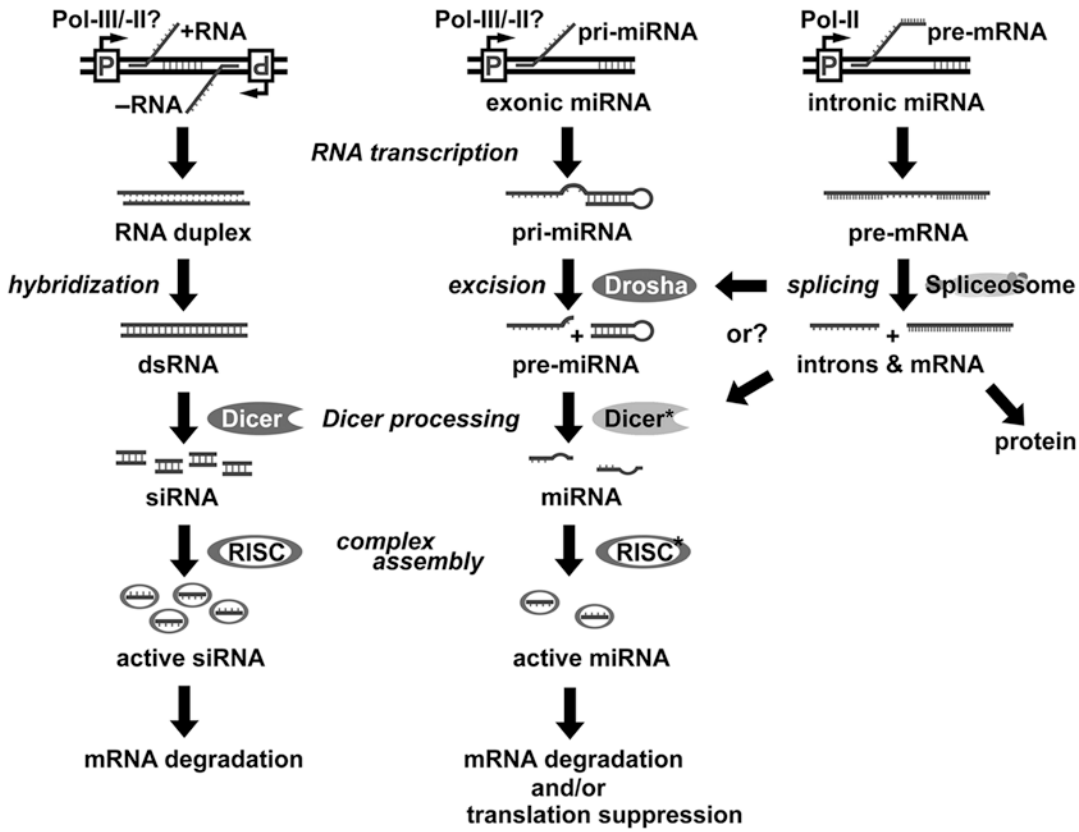

Fig. 1 Comparison of biogenesis and RNA interference (RNAi) mechanisms among small interfering RNA (siRNA); intergenic (exonic) microRNA (miRNA) and intronic miRNA. siRNA is likely formed by two perfectly complementary RNAs transcribed from two different promoters (remains to be determined) and further processing into 19- to 22-bp duplexes by the ribonuclease (RNase) III familial endonuclease, Dicer. The biogenesis of intergenic miRNAs, e.g., lin-4 and let-7, involves a long transcript primary precursor (pri-miRNA), which is probably generated by RNA polymerase (Pol) II or III RNA promoters, whereas intronic miRNAs are transcribed by the Pol II promoters of its encoded genes and coexpressed in the intronic regions of the gene transcripts (pre-messenger RNA [mRNA]). After RNA splicing and further processing, the spliced intron may function as a pri-miRNA for intronic miRNA generation. In the nucleus, the pri-miRNA is excised by Drosha RNase to form a hairpin-like pre-miRNA template and then exported to the cytoplasm for further processing by Dicer* to form mature miRNAs. siRNA and miRNA pathways are processed by different Dicers. All three small regulatory RNAs are finally incorporated into a RNA-induced-silencing complex, which contains either a strand of siRNA or a single-strand of miRNA. The effect of miRNA is considered more specific with fewer adverse consequences than that of siRNA because only one strand is involved. However, siRNAs primarily trigger mRNA degradation, whereas miRNAs can induce either mRNA degradation or suppression of protein synthesis depending on the sequence complementarity to the target gene transcripts

The biogenic process of intronic miRNA presumably involves five steps (Fig. 1). First, miRNA is generated as a long primary precursor miRNA (pri-miRNA) encoded within a gene transcript (pre-mRNA) by Pol II [20, 26]. Second, the pre-mRNA is excised by spliceosomal components and/or Drosha-like ribonuclease (RNase)

III endonucleases to release hairpin-like intronic structures and form pre-miRNA [20, 27]. Third, the pre-miRNA is exported out of the nucleus, probably by Ran–guanosine triphosphate and a receptor Exportin-5 [28, 29]. In the cytoplasm, Dicer-like nucleases cleave the pre-miRNA to form mature miRNA. Lastly, the mature miRNA is incorporated into a ribonuclear particle (RNP), which becomes the RNA-induced gene-silencing complex (RISC), capable of executing RNAi-associated gene-silencing effects [30, 31]. Although the in vitro model of siRNA-associated RISC assembly has been studied, the link between the final miRNA maturation processes and RISC assembly remains to be determined.

The characteristics of Dicer and RISC have been reported to be distinct between the siRNA and miRNA mechanisms [32, 33]. In zebrafish, we have recently observed that the stem-loop structure of pre-miRNAs is involved in the strand selection for mature miRNA during RISC assembly [21]. These findings suggest that the duplex structure of siRNA may be not essential for the assembly of miRNA-associated RISC. Conceivably, a method to distinguish the individual properties and differences between miRNA and siRNA biogenesis would facilitate our understanding of the evolutional and functional relationship between these two RNA-mediated gene-silencing pathways. In addition, the differences may provide an explanation for the prevalence of native siRNAs in invertebrates and their rarity in mammals.

The intronic miRNA must fulfill the following conditions: first, they must share the same promoter with their encoded genes, and second, they are spliced out of the transcript of their encoded genes and further processed into mature miRNAs. Although some of the currently identified miRNAs are encoded in the genomic intron region of a gene but in the opposite orientation to the gene transcript, those miRNAs are not intronic miRNAs because they neither share the same promoter with the gene nor need to be released from the gene transcript by RNA splicing. The promoters of those miRNAs are located in the antisense direction to the gene, likely using the gene transcript as a potential target for the antisense miRNAs. For example, let-7c was found to be an intergenic miRNA located in the antisense region of a gene intron.

More than 90 intronic miRNAs have been identified using bioinformatics approaches [34, 35], but the functions of the vast majority of these intronic molecules remain undetermined. According to the strictly expressive correlation of intronic miRNAs to their encoded genes, one may speculate that the levels of condition-specific, time-specific, and individual-specific gene expressions are determined by interactions of different miRNAs on single or multiple genes. This interpretation accounts for a more accurate genetic expression of various traits, and any deregulation of the interactions, thus, will result in genetic diseases. For instance, monozygotic twins frequently demonstrate slightly, but definitely

distinguishing, disease susceptibility and physiological behaviors. For instance, a long CCTG expansion in intron 1 of the zinc finger protein-9 gene has been correlated to type 2 myotonic dystrophy in one twin with a higher susceptibility [36]. Although the expansion motif confers high affinity to certain RNA-binding proteins, the interfering role of intron-derived expansion fragments remains to be elucidated.

Another more-established example, involving intronic expansion fragments in its pathogenesis, is fragile X syndrome, which represents approx 30% of human-inherited mental retardation. An intronic CGG repeat (rCGG) expansion in the 5′-UTR of the FMR1 gene causes mutation in 99% of individuals with fragile X syndrome [37]. FMR1 encodes an RNA-binding protein, fragile X mental retardation protein, which is associated with polyribosome assembly in an RNP-dependent manner, and is capable of suppressing translation through an RNAi-like pathway. Fragile X mental retardation protein also contains a nuclear localization signal and a nuclear export signal for shuttling certain mRNAs between the nucleus and cytoplasm [38]. Jin et al. proposed an RNAi-mediated methylation model in the CpG region of the FMR1 rCGG expansion, which is targeted by a hairpin RNA derived from the 3′-UTR of the FMR1 expanded allele transcript [37]. The Dicer-processed hairpin RNA triggers the formation of RNA-induced initiator of transcriptional gene silencing on the homologous rCGG sequences and leads to heterochromatin repression of the FMR1 locus. These examples suggest that natural evolution gives rise to more complexity and more variety of introns in higher animals and plants for coordinating their vast gene expression volumes and interactions; therefore, any deregulation of miRNAs derived from introns may lead to genetic diseases involving intronic expansion or deletion, such as myotonic dystrophy and fragile X mental retardation.

To understand diseases caused by the deregulation of intronic miRNAs, an artificial expression system is needed to recreate the function and mechanism of the miRNA in vitro and in vivo. The same approach may be used to design and develop therapies for various intronic miRNA-related diseases. Using artificial introns carrying hairpin-like pre-miRNA, we successfully generated mature miRNA molecules with a full capacity to trigger RNAi-like gene silencing in human prostate cancer (LNCaP), human cervical cancer (HeLa), and rat neuronal stem (HCN-A94-2) cells [20, 39].

The artificial intron of Fig. 2a was located in a mutated HcRed1 red fluorescent membrane protein (rGFP) gene to form a recombined SpRNAi–rGFP gene, in which the functional fluorescent structure was disrupted by the splicing-competent RNA intron (SpRNAi) insertion. Thus, we were able to determine the occurrence of intron splicing and rGFP–mRNA maturation through the appearance of red fluorescent emission on the membranes of transfected cells. There is

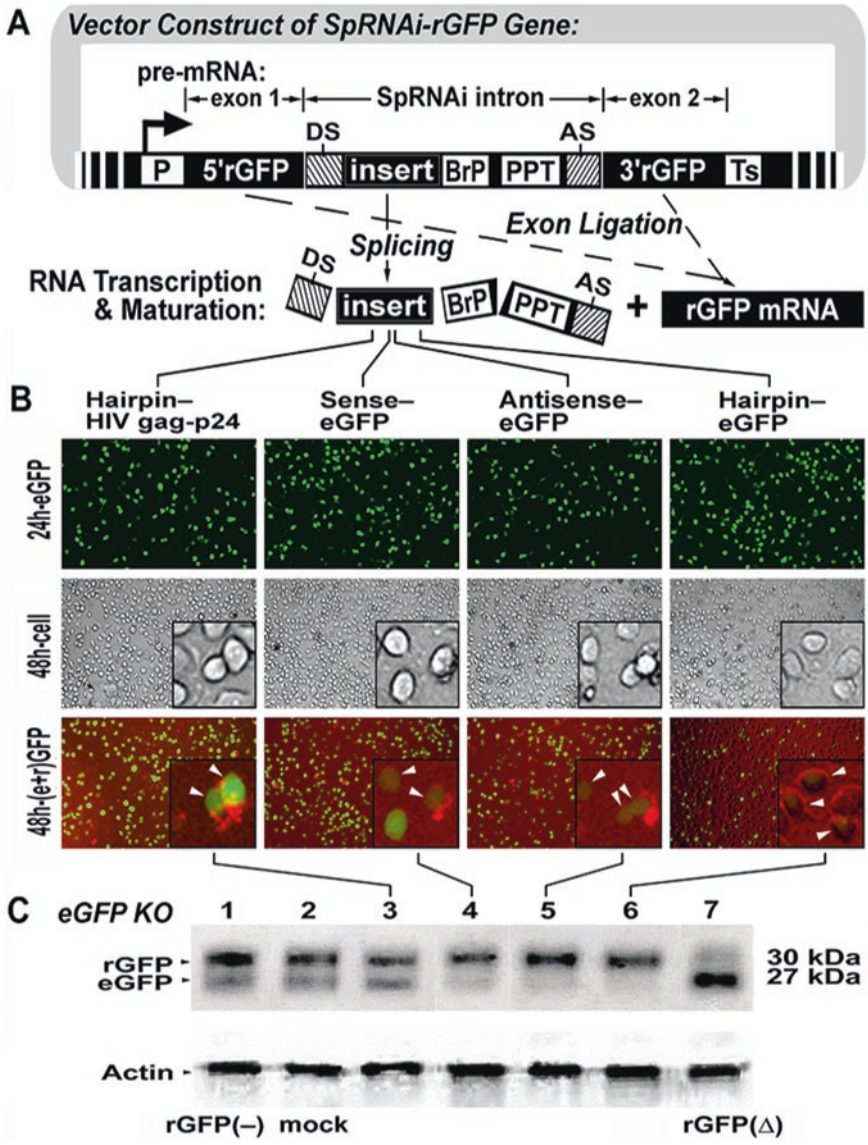

Fig. 2 Strategy for analysis of intronic microRNA (miRNA) mechanisms using artificial *SpRNAi–rGFP* gene vectors. (**a**) The *SpRNAi–rGFP* gene consists of a 5′-RNA promoter (P), an artificial intron (SpRNAi) flanked with two red fluorescent proteins (rGFP) exon fragments, and a 3′-proximity of transcription and translation termination codons (Ts). The construction of SpRNAi includes a 5′-splice donor site (DS), a 3′-splice acceptor site (AS), a poly-pyrimidine tract (PPT), a branch-point domain (BrP), and an inserted pre-miRNA oligonucleotide (insert) in the 5′-proximity of SpRNAi between the DS and BrP sites. During messenger RNA (mRNA) maturation, the SpRNAi is spliced out of the *SpRNAi–rGFP* pre-mRNA and further processed into miRNAs for gene silencing, whereas the mature rGFP mRNA is translated into rGFP for the target identification. (**b**) Simultaneous expression of rGFP and silencing of *Aequorea victoria* green fluorescent protein (eGFP) by various *SpRNAi–rGFP* transfections. At 24 h after transfection, approximate total cell numbers and eGFP-positive cell populations were observed with very few apoptotic or differentiated cells, whereas no detectable silencing of eGFP occurred. The RNA interference (RNAi) effect was detected 42 h after transfection, showing that the gene knock-down potency of the *SpRNAi–rGFP* genes containing inserts homologous to hairpin-eGFP was much greater than the sense-eGFP, which was approximately equal to the antisense-eGFP, which was

no homology or complementarity between the SpRNAi–rGFP gene and its expression vectors. After transfection of SpRNAi–rGFP genes containing synthetic inserts homologous to a targeted gene exon, we found that a hairpin insert comprising both sense and antisense exon strands resulted in maximal effects of gene silencing.

As shown in Fig. 2, the transfection of various SpRNAi–rGFP genes targeting the nucleotides 279–303 open-reading frame region of the enhanced *Aequorea victoria* green fluorescent protein (eGFP) was found to be highly significant ($n = 4$; $p < 0.01$) in silencing eGFP protein expression. The use of eGFP-positive HCN-A94-2 rat neuronal stem cells offered an excellent visual aid to observe the decreased green fluorescent emission of eGFP in the red fluorescent rGFP reporter gene-expressing cells. Silencing of eGFP was detected 42–48 h after transfection, indicating a potential requirement for precise timing of the production of sufficient small interfering intron inserts from the SpRNAi–rGFP gene.

Quantitative knock-down levels of eGFP protein were significantly altered (Fig. 2b), and there were modest reduction rates of 56 ± 6% for the transfection of inserts homologous to the sense strand of the eGFP target, of 50 ± 4% for the antisense strand of the GFP target, and a significant rate of 81 ± 2% for the hairpin inserts containing both strands of the eGFP target. No knockdown specificity to eGFP was detected by the transfection of intron-free rGFP gene, or for the SpRNAi–rGFP gene containing hairpin inserts homologous to either integrin-β1 exon 1 or the human immunodeficiency virus (HIV)-1 gag-p24 gene. The Western blot results shown in Fig. 2c confirmed the knock-down regulation observed and demonstrated that such a gene-silencing effect is determined by the hairpin structures of the pre-miRNA inserts.

The intron-derived miRNA system is able to be activated in a specific cell type under the control of a Pol II-directed transcriptional machinery. Our research group was the first to discover the biogenesis of miRNA-like precursors from the 5′-proximal intron regions of gene transcripts (pre-mRNAs) produced by the mammalian Pol II. Depending on the promoter of the miRNA-encoded gene transcript, intronic miRNA is coexpressed with its encoding gene in the specific cell population, which activates the promoter and expresses the gene. This type of miRNA generation relies on the coupled interaction of nascent Pol II-mediated pre-mRNA transcription and intron excision, occurring within certain nuclear regions proximal to genomic perichromatin fibrils [4, 20, 40, 41].

Fig. 2 (continued) much greater than the hairpin-human immunodeficiency virus (HIV) p24 (negative controls). (**c**) Western blot analyses confirmed the knock-down potency of (**b**). The lanes from left to right indicate the *SpRNAi–rGFP* transfection with genes containing various inserts homologous to the open-reading frame of eGFP, namely: (1) rGFP(–) (blank controls); (2) hairpin-integrin-β1 exon 1 (negative controls); (3) hairpin-HIV gag-p24; (4) sense-eGFP; (5) antisense-eGFP; (6) hairpin-eGFP; and (7) rGFPΔ (DS-defective controls)

After Pol II RNA processing and splicing excision, some of the intron-derived miRNA fragments can form mature miRNAs and effectively silence the target genes through the RNAi mechanism, whereas the exons of pre-mRNA are ligated together to form a mature mRNA for protein synthesis [4, 20]. Because miRNAs are single-stranded molecules insensitive to double-stranded RNA-dependent protein kinase R (PKR) and 2′,5′-oligoadenylate synthetase (2-5A)-induced interferon systems, the use of this Pol II-mediated miRNA generation can be safe in vitro and in vivo, preventing the cytotoxic effects of double-stranded RNAs (dsRNAs) and siRNAs. Interferon-induced protein kinase PKR can trigger cell apoptosis, whereas activation of the interferon-induced 2-5A system leads to extensive cleavage of single-stranded RNAs (i.e., mRNAs) [42, 43]. Although both the PKR and the 2-5A systems contain dsRNA-binding motifs that are highly conserved for binding to dsRNAs, these motifs do not bind to either single-stranded RNAs or RNA–DNA hybrids. These findings indicate a new function for mammalian introns in intracellular miRNA generation and gene regulation, which can be used as a tool for analysis of gene functions, improvement of current RNAi technology, and development of gene-specific therapeutics against cancers and viral infections.

The components of the Pol II-mediated SpRNAi system include several consensual nucleotide elements: a 5′-splice site, a branch-point domain, a poly-pyrimidine tract, and a 3′-splice site (Fig. 2a). Additionally, a pre-miRNA insert-sequence is placed within the artificial intron between the 5′-splice site and the branch-point domain. This portion of the intron would normally form a lariat structure during RNA splicing and processing. We currently know that spliceosomal U2 and U6 small nuclear RNPs, both helicases, may be involved in the unwinding and excision of the lariat RNA fragment into pre-miRNA; however, the detailed processing remains to be elucidated. Further, the SpRNAi contains translation stop codon domains in its 3′-proximal region to facilitate the accuracy of RNA splicing, which, if present in a cytoplasmic mRNA, would signal the diversion of a splicing-defective pre-mRNA to the nonsense-mediated decay pathway and, thus, cause the elimination of any unspliced pre-mRNA in the cell.

For intracellular expression of the SpRNAi, we need to insert the SpRNAi construct into the DraII cleavage site of a rGFP gene from mutated chromoproteins of coral reef *Heteractis crispa*. The cleavage of rGFP at its 208th nucleotide site by the restriction enzyme, DraII, generates an AG–GN nucleotide break, with three recessing nucleotides in each end, which forms 5′ and 3′ splice sites, respectively, after the SpRNAi insertion. Because this intronic insertion disrupts the expression of functional rGFP, it becomes possible to determine the occurrence of intron splicing and rGFP–mRNA maturation via the appearance of red fluorescent emission

around the membrane surface of the transfected cells. The rGFP also provides multiple exonic splicing enhancers to increase RNA-splicing efficiency.

To test the requirement of a siRNA-like duplex construct in a miRNA-associated RISC (miRISC) assembly, the pre-miRNAs were designed to contain perfectly matched stem arm domains. Although most of the native pre-miRNAs contain a mismatched area in their stem arms, it is not necessary for us to construct an imperfectly paired stem arm to trigger RNAi-related gene silencing. Previous studies have demonstrated that a mature miRNA can be generated by placing a perfectly matched siRNA duplex in the miR-30 pre-miRNA structure [27, 44]. Further, there are many genes not subjected to the regulation of native miRNAs, in particular, eGFP, which can be otherwise silenced by intracellular transfection of a pre-miRNA containing a perfectly matched stem arm construct. Therefore, we define a mature miRNA based on its biogenetic function and mechanism, rather than the structural complementarity of its precursor. In this view, any small hairpin RNA can be a pre-miRNA, if a mature miRNA is successfully processed from the small hairpin RNA and further assembled into miRISC for target gene silencing.

This designed miRNA system has been tested in zebrafish, establishing the fact that intronic miRNAs can be used as an effective strategy to silence specific target genes in vivo. We first tried to resolve the structural design of pre-miRNA inserts for the best gene-silencing effect and found that a strong structural bias exists in the selection of a mature miRNA strand during the assembly of the RNAi effector, RISC. RISC is a protein–RNA complex that directs either target gene transcript degradation or translational repression through the RNAi mechanism. Formation of siRNA duplexes has been reported to play a key role in the assembly of the siRNA-associated RISC. The two strands of the siRNA duplex are functionally asymmetric, but assembly into the RISC complex is preferential for only one strand. Such preference is determined by the thermodynamic stability of each 5′-end base pairing in the strand.

Based on this siRNA model, the formation of miRNA and its complementary miRNA (miRNA*) duplexes was thought to be an essential step for the assembly of miRISC. If this were true, no functional bias would be observed in the stem-loop of a pre-miRNA. Nevertheless, we observed that the stem-loop of the intronic pre-miRNA was involved in the strand selection of a mature miRNA for the RISC assembly in zebrafish. In these experiments, we constructed miRNA-expressing SpRNAi–rGFP vectors, as previously described [4, 20]; and two symmetric pre-miRNAs, miRNA–stem-loop–miRNA* (0) and miRNA* –stem-loop–miRNA (8), were synthesized and inserted into the vectors, respectively. Both pre-miRNAs contained the same double-stranded stem arm region, which was directed against the eGFP nucleotide 280–302 sequence.

Because the intronic insert region of the SpRNAi–rGFP recombined gene is flanked with a PvuI and an MluI restriction site at the 5′- and 3′-ends, respectively, the primary insert can be easily removed and replaced by various gene-specific inserts (e.g., anti-eGFP) possessing cohesive ends. By changing the pre-miRNA inserts directed against different gene transcripts, this intronic miRNA generation system provides a valuable tool for genetic and miRNA-associated research in vivo.

To determine the structural preference of the designed pre-miRNAs, we isolated the zebrafish small RNAs by mirVana® miRNA isolation columns (Ambion, Austin, TX) and precipitated all potential miRNAs complementary to the target eGFP region by latex beads containing the target RNA sequence. One effective miRNA identity, miR-eGFP (280/302), was verified in the transfections of the 5′-miRNA–stem-loop–miRNA*-3′ construct, as shown in Fig. 3a (gray-shading sequences). Because the effective mature miRNA was detected only in the zebrafish when transfected by the 5′-miRNA–stem-loop–miRNA*-3′ construct, the miRISC seems to prefer interacting with the 8 construct rather than the 0 pre-miRNA. The eGFP expression was constitutively driven by the β-actin promoter located in almost all zebrafish cells, whereas Fig. 3b shows that transfection of the SpRNAi–rGFP vector into the transgenic (UAS:gfp) zebrafish coexpressed rGFP, serving as a positive indicator for the miRNA generation in the transfected cells. This approach has been successfully used in several mouse and human cell lines to demonstrate RNAi effects [20, 39].

We applied the liposome-capsulated vector (total 60 μg) to the fish and found that the vector easily penetrated almost all tissues of the 2-week-old zebrafish larvae within 24 h, achieving fully systemic delivery of the miRNA effect. The indicator rGFP was detected in all of the fishes transfected by either 5′-miRNA*–stem-loop–miRNA-3′ or 5′-miRNA–stem-loop–miRNA*-3′ premiRNA, whereas the silencing of target eGFP expression (green) was observed only in the fishes transfected by the 5′-miRNA–stem-loop–miRNA*-3′ pre-miRNA (Fig. 3b, c).

The suppression level of eGFP in the gastrointestinal tract was found to be less effective, probably because of the high RNase activity in this region. Switching the stem-loop position has changed the thermostability of the 5′-end of the siRNA-like stem

Fig. 3 (continued) Because the color combination of EGFP and RGFP displayed more red than green (as shown in deep orange), the expression level of target EGFP (green) was significantly reduced in ✂, while miRNA indicator RGFP (red) was evenly present in all vector transfections. (**c**) Western blot analysis of the EGFP protein levels confirmed the specific silencing result of (**b**). No detectable gene silencing was observed in fishes without (Ctl) and with liposome only (Lipo) treatments. The transfection of either a U6-driven siRNA vector (siR) or an empty vector (Vctr) without the designed pre-miRNA insert resulted in no gene silencing significance

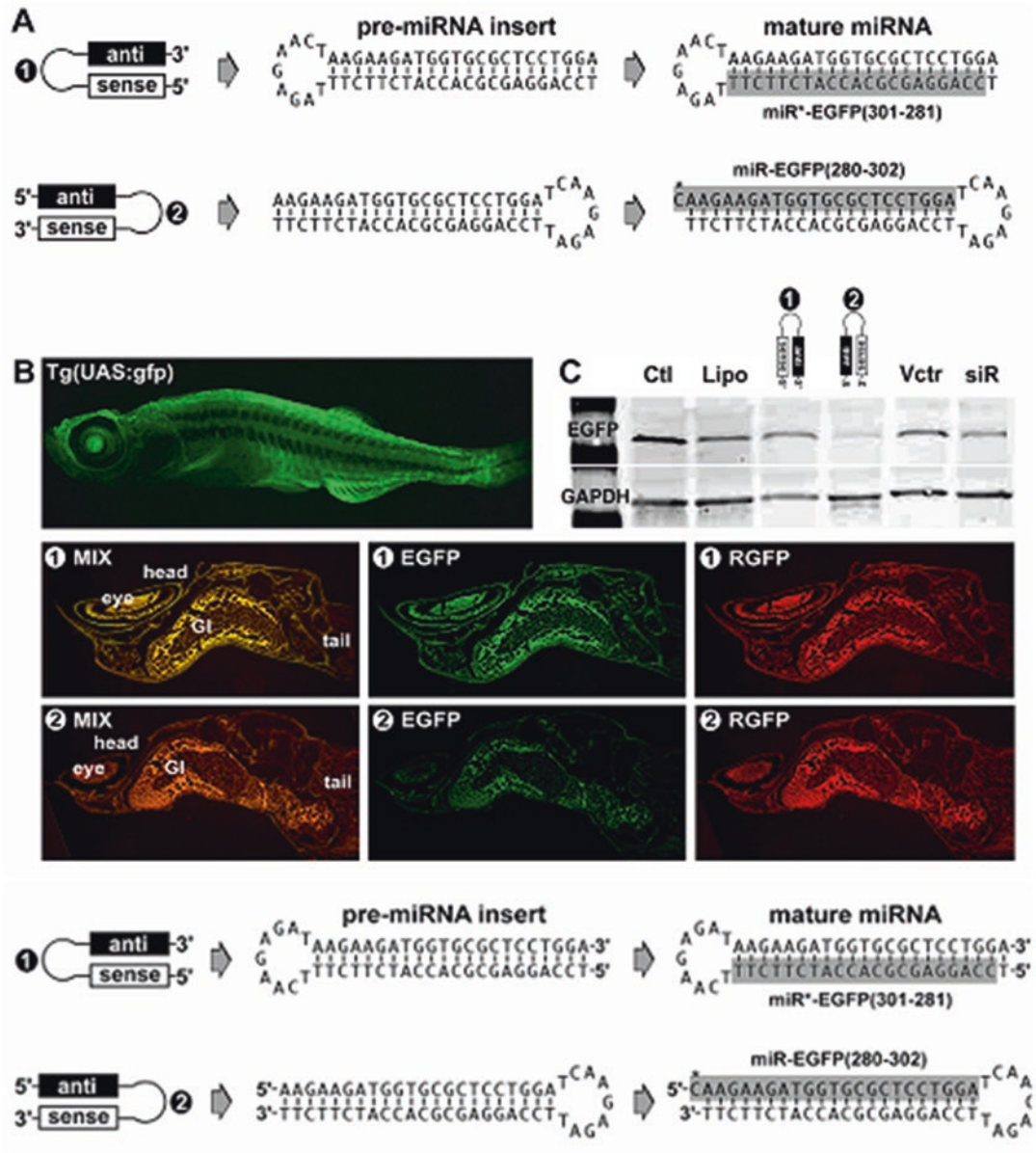

Fig. 3 Structural preference of miRNA–miRNA* asymmetry in miRNA-induced gene silencing complex (RISC) in vivo. Different preferences of RISC assembly were observed by transfection of 5′-miRNA*-stemloop-miRNA-3′ (✂) and 5′-miRNA-stemloop-miRNA*-3′ (✂) pre-miRNA constructs in zebrafish, respectively. (**a**) Based on the RISC assembly rule of siRNA, the processing of both ✂ and ✂ should result in the same siRNA duplex for RISC assembly; however, the experiments demonstrate that only the ✂ construct was used in the RISC assembly for silencing target EGFR. Due to the fact that miRNA is predicted to be complementary to its target messenger RNA, the "antisense" (black bar) refers to the miRNA and the "sense" (white bar) refers to its complementarity, miRNA*. One mature miRNA, namely miR-*Aequoreq victoria* green fluorescent protein (eGFP)-(280/302), was detected in the ✂-transfected zebrafishes, whereas the ✂ transfection produced different miRNA: miR*-EGFR(301–281), which was partially complementary to the miR-eGFP(280/320). (**b**) In vivo gene silencing efficacy was only observed in the transfection of the ✂ pre-miRNA construct, but not the ✂ construct.

arm, resulting in different miRNA maturation patterns; thus, we suggest that the stem-loop of a premiRNA may be involved in Dicer recognition and strand selection of a mature miRNA for effective RISC assembly and the resultant gene silencing. Given that the cleavage site of Dicer in the stem arm determines the strand selection of mature miRNA [27], the stem-loop may function as a determinant for the recognition of specific cleavage sites. Therefore, different from the dual open-ends of siRNA, a hairpin-like pre-miRNA has the advantage of using its stemloop structure to control the asymmetry of miRNA maturation for a more efficient RISC assembly.

Consistent evidence of miRNA-induced gene-silencing effects in mammalian cell lines and zebrafish demonstrates the preservation of an ancient intron-mediated gene regulation system in eukaryotes. In these in vitro and in vivo models, the intron-derived miRNAs determine the activation of RNAi-associated gene-silencing pathways. We herein provide the first evidence for the biogenesis and function of intronic miRNAs, both in vitro and in vivo. Evolution gives rise to more complexity and more variety of introns in higher animal and plant species for coordinating their vast gene expression volumes and interactions. Deregulation of these miRNAs due to intronic expansion or deletion could be the likely cause of various genetic diseases, such as myotonic dystrophy and fragile X mental retardation. Gene expression produces not only a gene transcript for its own protein synthesis but also for intronic miRNAs, capable of interfering with the expression of other genes. Thus, the expression of a particular gene may result in the gain of function of that particular gene but the consequent loss of function of other genes that are complementary to the mature intronic miRNAs. In volatile environments, an array of genes can swiftly and accurately coordinate their expression patterns with each other through the mediation of their intronic miRNAs, bypassing time-consuming translation processes.

Conceivably, intron-mediated gene regulation may be as important as the mechanisms by which transcription factors regulate the gene expression. It is likely that intronic miRNA is able to trigger cell transitions quickly in response to external stimuli without tedious protein synthesis. Undesired gene products are reduced by both transcriptional inhibition and/or translational suppression via miRNA regulation. This could enable a rapid switch to a new gene expression pattern without the need to produce various transcription factors. This regulatory property of miRNAs may serve as one of the most ancient gene modulation systems before the emergence of proteins. With the vast variety of miRNAs and the complexity of genomic introns, a thorough investigation of miRNA variants in the human genome will markedly improve the understanding of genetic diseases and improve the design of miRNA-based drugs. Learning how to exploit such a novel gene regulation system for future therapies will be a forthcoming challenge.

2 Materials

2.1 Synthetic Oligonucleotides Used for SpRNAi–rGFP Gene Construction

1. Sense SpRNAi sequence: 5′-dephosphorylated GTAAGTGGTC CGATCGTCGC GACG CGTCAT TACTAACACTAT CATACTTATC CTGTCCCTTT TTTTTCCACA GCTAG GACCT TCGTGCA-3′ (100 pmol/μL in autoclaved ddH_2O).
2. Antisense SpRNAi sequence: 5′-phosphorylated TGCACGAAGG TCCTAGCTGT GGA AAAAAAA GGGACAGGAT AAGTATGATA GTTAGTAATG ACGCGTCGCG ACG ATCGGAC CACTTAC-3′ (100 pmol/μL in autoclaved ddH_2O).
3. 2× Hybridization buffer: 200 mM KOAc, 60 mM HEPES-KOH, 4 mM MgOAc, pH 7.4 at 25 °C.
4. 0.5 μg/μL pHcRed1-N1/1 plasmid vector (BD Biosciences, Palo Alto, CA).
5. Incubation chambers at 94, 65, and 4 °C.

2.2 Restriction Enzyme Digestion and Sequential Ligation with Cohesive Ends

1. 10× L buffer: 100 mM Tris–HCl, pH 7.5 at 37 °C; 100 mM $MgCl^2$; and 10 mM dithiothreitol (DTT).
2. Restriction enzymes, including DraII, BfrI, NheI, and BsmI.
3. DraII digestion reaction mix: 14 μL autoclaved ddH_2O, 4 μL of 10× L buffer, and 2 μL DraII; prepare the reaction mix just before use.
4. DraII/BfrI digestion reaction mix: 2 μL autoclaved ddH_2O, 4 μL of 10× L buffer, 2 μL DraII, and 2 μL BfrI; prepare the reaction mix just before use.
5. 10× Ligation buffer: 660 mM Tris–HCl, pH 7.5 at 20 °C; 50 mM $MgCl_2$; 50 mM DTT; and 10 mM adenosine triphosphate (ATP).
6. 5 U/μL T4 DNA ligase.
7. Ligation reaction mix: 4 μL autoclaved ddH_2O, 4 μL of 10× ligation buffer, and 2 μL T4 ligase; prepare the reaction mix just before use.
8. 10× M buffer: 100 mM Tris–HCl, pH 7.5 at 37 °C; 500 mM NaCl; 100 mM $MgCl_2$; and 10 mM DTT.
9. NheI digestion reaction mix: 4 μL autoclaved ddH_2O, 4 μL of 10× M buffer, and 2 μL.
   NheI; prepare the reaction mix just before use.
10. 10× H buffer: 500 mM Tris–HCl, pH 7.5 at 37 °C; 1 M NaCl; 100 mM $MgCl_2$; and 10 mM DTT.
11. BsmI digestion reaction mix: 4 μL autoclaved ddH_2O, 4 μL of 10× H buffer and 2 μL BsmI; prepare the reaction mix just before use.

12. 10 U/μL T4 polynucleotide kinase.
13. Ligation/phosphorylation reaction mix: 2 μL autoclaved ddH_2O, 4 μL of 10× ligation buffer, 2 μL T4 ligase, and 2 μL T4 polynucleotide kinase; prepare the reaction mix just before use.
14. Incubation chambers at 65, 37, 16, and 4 °C.
15. 1% agarose gel electrophoresis.
16. Gel extraction kit (Qiagen, Valencia, CA).
17. Microcentrifuge: 17,900 × *g*.

2.3 Cloning of the SpRNAi–rGFP Gene Construct

1. 10× H buffer: 500 mM Tris–HCl, pH 7.5 at 37 °C; 1 M NaCl; 100 mM $MgCl_2$; and 10 mM DTT.
2. Restriction enzymes, including XhoI and XbaI.
3. XhoI/XbaI digestion reaction mix: 2 μL autoclaved ddH_2O, 4 μL of 10× H buffer, 2 μL XhoI, and 2 μL XbaI; prepare the reaction mix just before use.
4. 10× Ligation buffer: 660 mM Tris–HCl, pH 7.5 at 20 °C; 50 mM $MgCl_2$; 50 mM DTT; and 10 mM ATP.
5. 5 U/μL T4 DNA ligase.
6. Ligation reaction mix: 4 μL autoclaved ddH_2O, 4 μL of 10× ligation buffer, and 2 μL T4 ligase; prepare the reaction mix just before use.
7. Low salt Luria-Bertani culture broth.
8. Expand cloning kit (Roche Diagnostics, Indianapolis, IN).
9. DH5α transformation-competent *E. coli* cells (Roche).
10. 10× $MgSO_4$ solution: 1 M $MgSO_4$.
11. 1× $CaCl_2$ solution: 0.1 M $CaCl_2$.
12. 10× Glucose solution: 1 M glucose.
13. Incubation shaker: 37 °C; 285 rpm vortex.
14. Incubation chambers: 37, 16, and 4 °C.
15. Luria-Bertani agar plate containing 50 mg/mL kanamycin.
16. Spin Miniprep kit (Qiagen).
17. Microcentrifuge: 17,900 × *g*.

2.4 Insertion of Pre-miRNA Into the SpRNAi–rGFP Gene Construct

1. Sense pre-miRNA sequence: 5′-GTCCGATCGT CAAGAAGATG GTGCGCTCCT GGA TCAAGAG ATTCCAGGAG CGCACCATCT TCTTCGACGC GTCAT-3′ (100 pmol/μL in autoclaved ddH_2O).
2. Antisense pre-miRNA sequence: 5′-ATGACGCGTC GAAGAAGATG GTGCGCTCCT GGAATCTCTT GATCCAGGAG CGCACCATCT TCTTGACGAT CGGAC-3′ (100 pmol/μL in autoclaved ddH_2O).

3. 2× Hybridization buffer: 200 mM KOAc, 60 mM HEPES-KOH, and 4 mM MgOAc, pH 7.4 at 25 °C.
4. 10× H buffer: 500 mM Tris–HCl, pH 7.5 at 37 °C; 1 M NaCl; 100 mM $MgCl_2$; and 10 mM DTT.
5. Restriction enzymes, including PuvI and MluI.
6. PuvI/MluI digestion reaction mix: 2 μL autoclaved ddH_2O, 4 μL of 10× H buffer, 2 μL PuvI, and 2 μL MluI; prepare the reaction mix just before use.
7. 10× Ligation buffer: 660 mM Tris–HCl, pH 7.5 at 20 °C; 50 mM $MgCl_2$; 50 mM DTT; and 10 mM ATP.
8. 5 U/μL T4 DNA ligase.
9. Ligation reaction mix: 4 μL autoclaved ddH_2O, 4 μL of 10× ligation buffer, and 2 μL T4 ligase; prepare the reaction mix just before use.
10. Incubation chambers: 65, 37, and 16 °C.
11. 1% agarose gel electrophoresis.
12. Gel extraction kit (Qiagen).
13. Microcentrifuge: 17,900 × *g*.

2.5 Liposomal Transfection of the SpRNAi–rGFP Gene Construct

1. RPMI-1640 cell culture medium, serum-free.
2. FuGENE transfection reagent (Roche).
3. Cell culture incubator.

3 Methods

3.1 Synthetic Oligonucleotides Used for SpRNAi–rGFP Gene Construction

The SpRNAi artificial intron is formed by hybridization of the sense and antisense SpRNAi sequences, which are synthesized to be perfectly complementary to each other. Both of the SpRNAi sequences must be purified by polyacrylamide gel electrophoresis (PAGE) before use and stored at −20 °C.

1. Hybridization: mix the sense and antisense SpRNAi sequences (5 μL for each sequence) in 10 μL of 2× hybridization buffer, heat to 94 °C for 3 min, and cool to 65 °C for 10 min. Stop the reaction on ice.

3.2 Restriction Enzyme Digestion and Sequential Ligation With Cohesive Ends

Two rGFP exons are provided by DraII cleavage of the pHcRed1-N1/1 plasmid vector between the 881st and 882nd nucleotide sites, forming an AG–GN nucleotide break with 5′-G(T/A)C protruding nucleotides in the cleaved ends. The 5′-GTC protruding nucleotides need to be removed from the end of the first exon for blunt-end ligation, whereas the 5′-GAC protruding end of the second exon is used to ligate with the 3′-DraII-restricted end of the SpRNAi intron. After the ligation

of the SpRNAi intron and the second rGFP exon, add the first rGFP exon to the 5′ end of the ligated sequence by blunt-end ligation, so as to form a complete SpRNAi–rGFP gene cassette (*see* **Note 1**).

1. DraII cleavage: add the DraII digestion reaction mix to the SpRNAi hybrid. Add the DraII/ BfrI digestion reaction mix to 30 μL of the pHcRed1-N1/1 plasmid vector. Incubate both the reactions at 37 °C for 4 h and stop the reaction on ice.
2. Purification of the DraII- and DraII/BfrI-digested sequences: load and run the above reactions from **step 1** in 1% agarose gel electrophoresis and cut out of the DraII-digested SpRNAi hybrid sequence and two other oligonucleotide fragments (one 1760 bp and another 715 bp), which are derived from the DraII/BfrI-cleaved pHcRed1-N1/1 plasmid vector. Separately recover these three oligonucleotide sequences into different tubes in 30 μL autoclaved ddH_2O, using the gel extraction columns and following the manufacturer's suggestions. Store the 1760-bp pHcRed1-N1/1 fragment at 4 °C for 2 week before use (*see* **Note 2**).
3. Ligation: mix 15 μL of the DraII-digested SpRNAi hybrid sequence with 15 μL of the 715 bp pHcRed1-N1/1 fragment and add the ligation reaction mix. Incubate the reaction at 16 °C for 16 h and stop the reaction on ice.
4. Purification of the ligation product: load and run the ligation in 1% agarose gel electrophoresis and cut out the ligated sequence (~800 bp) using a clean surgical blade. Recover the sequence in one tube of 30 μL autoclaved ddH_2O, using the gel extraction column and following the manufacturer's suggestions.
5. Cleavage by NheI and BsmI: add the BsmI digestion reaction mix to the ligation product. Add the NheI digestion reaction mix to the 1760-bp pHcRed1-N1/1 fragment. Incubate both the reactions at 37 °C for 4 h and stop the reaction on ice.
6. Purification of the NheI and BsmI-digested sequences: load and run the reactions in 1% agarose gel electrophoresis and cut out the NheI- and BsmI-digested sequences, respectively, using a clean surgical blade. Recover the two oligonucleotide sequences in one tube of 30 μL autoclaved ddH_2O, using the gel extraction columns and following the manufacturer's suggestions.
7. Ligation: add the ligation/phosphorylation reaction mix to the extraction. Incubate the reaction at 16 °C for 16 h and stop the reaction on ice.
8. Purification of the ligation product: load and run the ligation in 1% agarose gel electrophoresis and cut out the ligated sequences using a clean surgical blade. Recover the sequence

in one tube of 30 μL autoclaved ddH_2O, using the gel extraction column and following the manufacturer's suggestions. The final ligation product forms the SpRNAi–rGFP gene cassette (*see* **Note 1**).

3.3 Cloning of the SpRNAi–rGFP Gene Construct

To express the SpRNAi–rGFP gene in transfected cells, clone the SpRNAi–rGFP gene cassette into the pHcRed1-N1/1 plasmid vector, replacing the original HcRed protein sequence. Because the functional fluorescent structure of HcRed is disrupted by the SpRNAi intron insertion, one can determine the occurrence of intron splicing and miRNA maturation through the appearance of red fluorescent emission on the cell membranes. The red rGFP serves as a visual indicator for the generation of intronic miRNAs. This intron-derived miRNA system is activated under the control of cytomegalovirus-IE promoter.

1. Cleavage by XhoI and XbaI: add the XhoI/XbaI digestion reaction mix to the SpRNAi– rGFP gene cassette and the pHcRed1-N1/1 plasmid vector, respectively. Incubate both the reactions at 37 °C for 4 h and stop the reactions on ice.
2. Purification of the XhoI/XbaI-digested sequences: load and run the reactions in 1% agarose gel electrophoresis and cut out the XhoI/XbaI-digested SpRNAi–rGFP sequence and the 4000-bp pHcRed1-N1/1 fragment, respectively, using a clean surgical blade. Recover the two oligonucleotide sequences in one tube of 30 μL autoclaved ddH_2O, using the gel extraction column and following the manufacturer's suggestions.
3. Ligation: add the ligation reaction mix to the extraction. Incubate the reaction at 16 °C for 16 h and stop the reaction on ice.
4. Plasmid amplification: transfect the ligation product into the DH5α transformation-competent *E. coli* cells using the expanded cloning kit and following the manufacturer's suggestions.
5. Plasmid recovery: isolate and collect the amplified SpRNAi–rGFP plasmid in one tube of 30 μL autoclaved ddH_2O, using a spin Miniprep filter and following the manufacturer's suggestions.

3.4 Insertion of Pre-miRNA into the SpRNAi–rGFP Gene Construct

The SpRNAi–rGFP vector does not contain any intronic pre-miRNA structure. Because the intronic insert region of the SpRNAi–rGFP vector is flanked with a PvuI and an MluI restriction site at the 5′ and 3′ ends, respectively, the primary insert can be easily removed and replaced by various gene-specific inserts (e.g., anti-eGFP) possessing cohesive ends (*see* **Note 3**).

1. Hybridization: mix the sense and antisense pre-miRNA sequences (5 μL for each sequence) in 10 μL of 2× hybridization buffer, heat to 94 °C for 3 min, and cool to 65 °C for 10 min. Stop the reaction on ice.

2. Cleavage by MluI and PvuI: add the MluI/PvuI digestion reaction mix to the SpRNAi–rGFP vector and the pre-miRNA hybrid construct, respectively. Incubate the reaction at 37 °C for 4 h and stop the reaction on ice.
3. Purification of the MluI/PvuI-digested sequences: load and run the reactions in 1% agarose gel electrophoresis and cut out the MluI/PvuI-digested SpRNAi–rGFP sequence and the pre-miRNA fragment, respectively, using a clean surgical blade. Recover the two oligonucleotide sequences in one tube of 30 μL autoclaved ddH_2O, using the gel extraction column and following the manufacturer's suggestions.
4. Ligation: add the ligation reaction mix to the extraction. Incubate the reaction at 16 °C for 16 h and stop the reaction on ice.
5. Plasmid amplification: transfect the ligation product into the DH5α transformation-competent *E. coli* cells using the expanded cloning kit and following the manufacturer's suggestions.
6. Plasmid recovery: isolate and collect the amplified SpRNAi–rGFP plasmid in one tube of 30 μL autoclaved ddH_2O, using a spin Miniprep filter and following the manufacturer's suggestions (*see* **Note 4**).

3.5 Liposomal Transfection of the SpRNAi–rGFP Gene Construct

To increase transfection efficiency, we use liposomal reagents to facilitate the delivery of the *SpRNAi–rGFP* vector into target cells.

1. Preparation of FuGENE: add 6 μL of the FuGENE reagent into 100 μL of RPMI-1640 medium in a clean tube and gently mix the solution, following the manufacturer's suggestions. Add 20 μg (in less than 50 μL) of the *SpRNAi–rGFP* vector into the liposomal dilution from Subheading 3.4, **step 6**, and gently mix the solution following the manufacturer's suggestions. Store the mixture at 4 °C for 30 min.
2. Transfection: add the mixture into the center of the cell culture and gently mix the cell culture medium.
3. Cell culture: culture the treated cells in a cell culture incubator under the condition essential for the cell type.

4 Notes

1. Because of the low efficiency of blunt-end ligation and 5′-nucleotide hydrolysis of the first *rGFP* exon, the chance to obtain a correct *SpRNAi–rGFP* gene sequence is approx. 1 in 50 (2%). The final *SpRNAi–rGFP* gene sequence must be confirmed by DNA sequencing.

2. Because there is no enzymatic method to remove the 5′-protruding trinucleotide of the first *rGFP* exon, we need to use hydrolysis, which takes approx 2–3 weeks to remove three nucleotides from the end of an oligonucleotide sequence.
3. The synthetic pre-miRNA sequences that we present here are directed against the 279- to 303-nt region of enhanced eGFP. The principle for designing an intronic pre-miRNA insert is to synthesize two mutually complementary oligonucleotides, including one 5′-GTCCG ATCGTC, 19- to 27-nt antisense target gene sequence—TCAAGAGAT (stem-loop)—19- to 27-nt sense target gene sequence, CGACGCGTCAT-3′; and another 5′-ATGA CGGTCG, 19- to 27-nt antisense target gene sequence—ATCTCTTGA (stem-loop)—19- to 27-nt sense target gene sequence, GACGATCGGAC-3′. The hybridization of these two oligonucleotide sequences forms the intronic pre-miRNA insert, which contains a 5′-PuvI and a 3′Mlu1 restriction site for further ligation into the intron region of an *SpRNAi–rGFP* gene cassette. All synthetic oligonucleotides must be purified by PAGE to ensure their highest purity and integrity.
4. The sequence of the final *SpRNAi–rGFP* gene cassette and its pre-miRNA insert must be confirmed by DNA sequencing.

References

1. Ambros V (2004) The functions of animal microRNAs. Nature 350:431–355
2. Nelson P, Kiriakidou M, Sharma A, Maniataki E, Mourelatos Z (2003) The microRNA world: small is mighty. Trends Biochem Sci 28:534–539
3. Ying SY, Lin SL (2005) Intronic microRNA (miRNA). Biochem Biophys Res Commun 326:515–520
4. Lin SL, Ying SY (2004) Novel RNAi therapy – intron-derived microRNA drugs. Drug Design Rev 1:247–255
5. Tuschl T, Borkhardt A (2002) Small interfering RNAs: a revolutionary tool for the analysis of gene function and gene therapy. Mol Interv 2:158–167
6. Ambros V (1989) A hierarchy of regulatory genes controls a larva regulatory specificity, the notion that target-site recogni- to-adult developmental switch in *C. elegans*. Cell 57:49–57
7. Hall IM, Shankaranarayana GD, Noma K, Ayoub N, Cohen A, Grewal SI (2002) Establishment and maintenance of a heterochromatin domain. Science 297:2232–2237
8. Llave C, Xie Z, Kasschau KD, Carrington JC (2002) Cleavage of Scarecrow-like mRNA targets directed by a class of Arabidopsis miRNA. Science 297:2053–2056
9. Rhoades MW, Reinhart BJ, Lim LP, Burge CB, Bartel B, Bartel DP (2002) Prediction of plant microRNA targets. Cell 110:513–520
10. Lee RC, Feibaum RL, Ambros V (1993) The C. elegans heterochromic gene *lin-4* encodes small RNAs with antisense complementarity to *lin-14*. Cell 75:843–854
11. Reinhart BJ, Slack FJ, Basson M, Pasquinelli AE, Bettinger JC, Rougvie AE, Horvitz HR, Ruvkun G (2000) The 21-nucleotide let-7 RNA regulates developmental timing in *Caenorhabditis elegans*. Nature 403:901–906
12. Lau NC, Lim LP, Weinstein EG, Bartel DP (2001) An abundant class of tiny RNAs with probable regulatory roles in *Caenorhabditis* elegans. Science 294:858–862
13. Brennecke J, Hipfner DR, Stark A, Russell RB, Cohen SM (2003) Bantam encodes a developmentally regulated microRNA that controls cell proliferation and regulates the proapoptotic gene hid in *Drosophila*. Cell 113: 25–36
14. Xu P, Vernooy SY, Guo M, Hay BA (2003) The Drosophila microRNA Mir-14 suppresses cell death and is required for normal fat metabolism. Curr Biol 13:790–795

15. Lagos-Quintana M, Rauhut R, Meyer J, Borkhardt A, Tuschl T (2003) New microRNAs from mouse and human. RNA 9:175–179
16. Mourelatos Z, Dostie J, Paushkin S, Sharma A, Charroux B, Abel L, Rappsilber J, Mann M, Dreyfuss G (2002) miRNPs: a novel class of ribonucleoproteins containing numerous microRNAs. Genes Dev 16:720–728
17. Zeng Y, Wagner EJ, Cullen BR (2002) Both natural and designed micro RNAs can inhibit the expression of cognate mRNAs when expressed in human cells. Mol Cell 9:1327–1333
18. Zeng Y, Yi R, Cullen BR (2003) MicroRNAs and small interfering RNAs can inhibit mRNA expression by similar mechanisms. Proc Natl Acad Sci U S A 100:9779–9784
19. Carthew RW (2001) Gene silencing by double-stranded RNA. Curr Opin Cell Biol 13:244–248
20. Lin SL, Chang D, Wu DY, Ying SY (2003) A novel RNA splicing-mediated gene silencing mechanism potential for genome evolution. Biochem Biophys Res Commun 310:754–760
21. Lin SL, Chang D, Ying SY (2005) Asymmetry of intronic pre-miRNA structures in functional RISC assembly. Gene 356:32–38
22. Ying SY, Lin SL (2004) Intron-derived microRNAs–fine tuning of gene functions. Gene 342:25–28
23. Kramer A (1996) The structure and function of proteins involved in mammalian pre-mRNA splicing. Annu Rev Biochem 65:367–409
24. Clement JQ, Qian L, Kaplinsky N, Wilkinson MF (1999) The stability and fate of a spliced intron from vertebrate cells. RNA 5:206–220
25. Nott A, Meislin SH, Moore MJ (2003) A quantitative analysis of intron effects on mammalian gene expression. RNA 9:607–617
26. Lee Y, Kim M, Han J, Yeom KH, Lee S, Baek SH, Kim VN (2004) MicroRNA genes are transcribed by RNA polymerase II. EMBO J 23:4051–4060
27. Lee Y, Ahn C, Han J, Choi H, Kim J, Yim J, Lee J, Provost P, Radmark O, Kim S, Kim VN (2003) The nuclear RNase III Drosha initiates microRNA processing. Nature 425:415–419
28. Lund E, Guttinger S, Calado A, Dahlberg JE, Kutay U (2004) Nuclear export of microRNA precursors. Science 303:95–98
29. Yi R, Qin Y, Macara IG, Cullen BR (2003) Exportin-5 mediates the nuclear export of pre-microRNAs and short hairpin RNAs. Genes Dev 17:3011–3016
30. Schwarz DS, Hutvagner G, Du T, Xu Z, Aronin N, Zamore PD (2003) Asymmetry in the assembly of the RNAi enzyme complex. Cell 115:199–208
31. Khvorova A, Reynolds A, Jayasena SD (2003) Functional siRNAs and miRNAs exhibit strand bias. Cell 115:209–216
32. Lee YS, Nakahara K, Pham JW, Kim K, He Z, Sontheimer EJ, Carthew RW (2004) Distinct roles for Drosophila Dicer-1 and Dicer-2 in the siRNA/miRNA silencing pathways. Cell 117:69–81
33. Tang G (2005) siRNA and miRNA: an insight into RISCs. Trends Biochem Sci 30:106–114
34. Rodriguez A, Griffiths-Jones S, Ashurst JL, Bradley A (2004) Identification of mammalian microRNA host genes and transcription units. Genome Res 14:1902–1910
35. Ambros V, Lee RC, Lavanway A, Williams PT, Jewell D (2003) MicroRNAs and other tiny endogenous RNAs in *C. elegans*. Curr Biol 13:807–818
36. Liquori CL, Ricker K, Moseley ML, Jacobsen JF, Kress W, Naylor SL, Day JW, Ranum LPW (2001) Myotinic dystrophy type 2 caused by a CCTG expansion in intron 1 of ZNF9. Science 293:864–867
37. Jin P, Alisch RS, Warren ST (2004) RNA and microRNAs in fragile X mental retardation. Nat Cell Biol 6:1048–1053
38. Eberhart DE, Malter HE, Feng Y, Warren ST (1996) The fragile X mental retardation protein is a ribonucleoprotein containing both nuclear localization and nuclear export signals. Hum Mol Genet 5:1083–1091
39. Lin SL, Ying SY (2004) New drug design for gene therapy – taking advantage of Introns. Lett Drug Design Discov 1:256–262
40. Zhang G, Taneja KL, Singer RH, Green MR (1994) Localization of pre-mRNA splicing in mammalian nuclei. Nature 372:809–812
41. Ghosh S, Garcia-Blanco MA (2000) Coupled in vitro synthesis and splicing of RNA polymerase II transcripts. RNA 6:1325–1334
42. Stark GR, Kerr IM, Williams BR, Silverman RH, Schreiber RD (1998) How cells respond to interferons. Annu Rev Biochem 67:227–264
43. Sledz CA, Holko M, de Veer MJ, Silverman RH, Williams BR (2003) Activation of the interferon system by short-interfering RNAs. Nat Cell Biol 5:834–839
44. Boden D, Pusch O, Silbermann R, Lee F, Tucker L, Ramratnam B (2004) Enhanced gene silencing of HIV-1 specific siRNA using microRNA designed hairpins. Nucleic Acid Res 32:1154–1158

Chapter 10

Mining Exosomal MicroRNAs from Human-Induced Pluripotent Stem Cells-Derived Cardiomyocytes for Cardiac Regeneration

Sang-Ging Ong, Won Hee Lee, Yang Zhou, and Joseph C. Wu

Abstract

Myocardial infarction is the leading cause of morbidity and mortality worldwide. Recent advances in cardiac regenerative therapy have allowed for novel modalities in replenishing the damaged myocardium. However, poor long-term engraftment and survival of transplanted cells have largely precluded effective cell replacement. As an alternative to direct cell replacement, the release of paracrine protective factors may be a more plausible effector for cardioprotection which may partially be mediated through secretion of microvesicles, or exosomes, that contribute to cell-cell communication. In this chapter, we describe the isolation of exosomes from induced pluripotent stem cells-derived cardiomyocytes for subsequent microRNA profiling for a better understanding of the biological cargo contained within exosomes.

Key words Exosomes, iPSC-CMs, microRNA, Stem cell, Heart

1 Introduction

Cardiovascular diseases (CVDs) are the primary cause of morbidity and mortality worldwide [1]. Following myocardial infarction, there is a major loss of cardiomyocytes due to necrosis, and replacement of damaged myocardium is an intense area of research in the field of cardiac regenerative medicine [2]. Various cell types, including mesenchymal stem cells (MSCs), cardiac progenitor cells (CPCs), embryonic stem cells-derived cardiomyocytes (ESC-CMs), and induced pluripotent stem cells-derived cardiomyocytes (iPSC-CMs), have been investigated in both preclinical and clinical studies with mixed results, with a common issue being the poor survival of transplanted cells [3–7]. Positive outcomes of such studies are being associated with the secretion of paracrine factors in the absence of adequate cell survival, which may be mediated by the release of a novel class of small vesicles termed exosomes [7, 8].

Exosomes are endosomal membrane vesicles with diameters of ~40–150 nm that originate in the late endosomal compartment

Shao-Yao Ying (ed.), *MicroRNA Protocols*, Methods in Molecular Biology, vol. 1733,
https://doi.org/10.1007/978-1-4939-7601-0_10,

from the inward budding of endosomal membranes, leading to the formation of intracellular multi-vesicular endosomes (MVEs) [9, 10]. Groups of exosomes are packed in the MVEs and upon their fusion with the plasma membrane, these exosomes are released into the extracellular space. Various studies have reported the role of exosomes in mediating intercellular communication by serving as vehicles for transferring various biological molecules, including DNA, RNA, proteins, and lipids between cells [11–14]. Consistent with these studies, the roles of exosomes isolated from various types of stem cells such as MSCs, CPCs, ESCs, iPSCs, and $CD34^+$ have been investigated in mediating cardiac regeneration. These exosomes are known to possess anti-apoptotic effects in both host and transplanted cells, and they also stimulate angiogenesis, reduce infarct size, and improve cardiac recovery [15–19]. Importantly, enrichment of protective microRNAs appears to be responsible for the beneficial effects of exosomes in cardiac regeneration [11, 15, 20, 21].

In the following text, we have outlined a protocol for differentiating human iPSCs into cardiomyocytes, and described the methods required for isolating exosomes secreted by iPSC-CMs for subsequent microRNA analysis, which will help advance our understanding of exosomes and how they can be used for mediating cardiac regeneration moving forward.

2 Materials

2.1 Cultivation and Passaging of Human iPSCs

1. Essential 8 medium (ThermoFisher).
2. BD Matrigel.
3. ROCK Inhibitor, Y-27632.
4. DMEM/F12 media.
5. 0.5 M EDTA.
6. Dulbecco's phosphate-buffered saline (DPBS) 1×, without Ca^{2+}/Mg^{2+}.
7. Tissue culture plates, 6-well.
8. Humidified 5% CO_2 incubator.

2.2 Cardiac Differentiation of Human iPSCs

1. RPMI 1640 medium (ThermoFisher).
2. RPMI 1640 medium, no glucose (ThermoFisher).
3. B27 Supplement (50×), serum free (ThermoFisher).
4. B27 Supplement (50×), minus insulin (ThermoFisher).
5. CHIR99021.
6. IWR-1.
7. Tissue culture plates, 6-well.
8. Humidified 5% CO_2 incubator.

2.3 Hydration and Saturation of Filter Units for Concentration

1. Amicon Ultra-15 centrifugal units, 100 kDa (Millipore).
2. Dulbecco's phosphate-buffered saline (DPBS) 1×, without Ca^{2+}/Mg^{2+}.
3. Bovine serum albumin.
4. Centrifuge.

2.4 Preparation and Concentration of iPSC-CMs Conditioned Medium

1. Conical tubes, 50 mL.
2. Refrigerated centrifuge.
3. Optional: exosome-depleted FBS.
4. 0.22 μM filter units.
5. Hydrated 100 kDa centrifugal units.

2.5 Isolation of Exosomes

1. Total exosome isolation reagent from cell culture media (ThermoFisher).
2. Fridge.
3. Refrigerated centrifuge.
4. Dulbecco's phosphate-buffered saline (DPBS) 1×, without Ca^{2+}/Mg^{2+}.
5. Eppendorf tubes.

2.6 RNA Isolation from Exosomes

1. miRCURY™ RNA isolation kit—cell & plant (Exiqon).
2. Centrifuge.
3. 96–100% ethanol.
4. β-mercaptoethanol (add 10 μL per 1 mL lysis buffer).
5. RNase-free water.

3 Methods

3.1 Cultivation and Passaging of Human iPSCs

1. Thaw an aliquot of Matrigel at 4 °C, and dilute it at 200–300 times in DMEM/F12 media. Mix well and add 1 mL of Matrigel solution per well into 6-well plates.
2. Incubate the Matrigel-coated plates in a 37 °C cell culture incubator for at least 30 min prior to use, plates can be kept for several days before use.
3. Prepare essential 8 (E8) medium by adding 10 mL of supplement into 500 mL of basal medium, and keep it at 4 °C for up to 2 weeks. Allow the medium to reach room temperature prior to use.
4. Thaw a vial of frozen iPSCs, and add the thawed cell suspension into 4 mL of E8 medium in a sterile 15 mL conical tube.

5. Centrifuge the tube at 300 × *g* for 3 min at room temperature.
6. Aspirate the supernatant and gently resuspend cells into 2 mL of E8 medium supplemented with 10 μM of Rho-associated protein kinase (ROCK) inhibitor (S1049, Selleck Chemicals).
7. Plate cells in 1 well of 6-well plate and incubate the cells in a 37 °C 5% CO_2 incubator.
8. Replace with fresh medium without ROCK inhibitor the next day, and continue maintaining the cells with daily medium exchange until ~85% confluency (typically 4 days after plating).
9. Cells can then be passaged at split ratios between 1:6 and 1:12. For passaging, aspirate the media from cells to be passaged and wash briefly with 1 mL of PBS (without Ca^{2+} and Mg^{2+}). Aspirate the PBS wash.
10. Add 1 mL of room temperature 0.5 mM EDTA solution to the cells and incubate at room temperature for 5–6 min. During the wait, prepare 24 mL of E8 medium with 10 μM of ROCK inhibitor.
11. Carefully aspirate the EDTA solution from the well without rinsing the cells.
12. Take 1 mL out of the 24 mL of E8 medium with 10 μM of ROCK inhibitor and add gently into the well to dislodge the cells, resuspend 1 to 2 more times if needed.
13. Recover the 1 mL cell suspension and add it back to the remaining 23 mL of E8 medium with 10 μM of ROCK inhibitor.
14. Resuspend gently once, and pipet 2 mL of cell suspension into each well of two 6-well plates for a 1:12 split ratio.
15. Replace cell culture media daily as mentioned in **step 8** and passage as needed.

3.2 Cardiac Differentiation of Human iPSCs

1. Cardiac differentiation is initiated when iPSCs are between 70% and 85% confluency. Aspirate the spent E8 medium, and replace with 2 mL of RPMI/B27-Ins medium supplemented with 8 μM of CHIR99021 (day 0) (S2924, Selleck Chemicals). Return the cells to the 37 °C 5% CO_2 incubator for 48 h.
2. On day 2, aspirate the spent medium and replace with 2 mL of RPMI/B27-Ins medium. Return the cells to the incubator.
3. On day 3, aspirate the spent medium and replace with 2 mL of RPMI/B27-Ins medium supplemented with 5 μM of IWR-1 (S7086, Selleck Chemicals). Return the cells to the incubator for 48 h.
4. On day 5, aspirate the spent medium and replace with 2 mL of RPMI/B27-Ins medium. Return the cells to the incubator for 48 h.

5. On day 7, aspirate the spent medium and replace with 2 mL of RPMI/B27+Ins medium. Return the cells to the incubator for 48 h.
6. On day 9, aspirate the spent medium and replace with 2 mL of RPMI/B27+Ins medium. Return the cells to the incubator for 24 h.
7. On day 10, aspirate the spent medium, and glucose starvation (for eliminating contaminating cells) is started by the addition of 2 mL of RPMI no glucose/B27+Ins medium. Return the cells to the incubator and repeat this step every 2 days.
8. On day 15 (end of glucose starvation), aspirate the spent medium and replace with 2 mL of RPMI/B27+Ins medium. Return the cells to the incubator and repeat this step every 2 days. Spontaneously contracting troponin T cardiac type 2 positive cardiomyocytes will be present and ready for use, or can be further cultured as desired (*see* **Note 1**).

3.3 Hydration and Saturation of Filter Units for Concentration

Amicon columns of 50 kDa or 100 kDa from Millipore or Vivaspin columns from Sartorius are recommended, with polyethersulfone (PES) as membranes.

1. Columns are washed with 10 mL of PBS (1×) at 3000 × *g* for 20 min at room temperature.
2. Membrane is then saturated with 10 mL of 1% BSA diluted in PBS (1×). Incubate the columns overnight to decrease nonspecific binding of proteins and thus exosomes to the column.
3. On the following day, remove the 1% BSA and wash manually with 2 mL of PBS (1×). Decant the liquid.
4. Wash the membrane with 10 mL of PBS (1×) with a 10 min centrifugation at 3000 × *g* at room temperature.
5. Conditioned medium (see the next section) can be loaded on the membrane at this point.

3.4 Preparation and Concentration of iPSC-CMs Conditioned Medium

1. iPSC-CMs are allowed to grow in RPMI/B27+Ins medium for 24–48 h (*see* **Note 2**). Conditioned medium is then collected and can be stored at 4 °C for short-term storage. Alternatively, the conditioned medium can be frozen at −80 °C for long-term storage.
2. Centrifuge the conditioned medium at 500 × *g* for 5 min at 4 °C. Collect the supernatant and discard the pellet.
3. Centrifuge the supernatant at 3000 × *g* for 10 min at 4 °C. Collect the supernatant and discard the pellet.
4. Filter the supernatant through a 0.22 μM filter.
5. The filtrated conditioned medium can then be loaded into filter units (see the previous section) for concentration.

6. Upon loading of filtrate into filter units, the columns can be concentrated by centrifugation at 3000 × *g* at room temperature. Length of centrifugation and sample volume input will need to be optimized to obtain a desired concentration factor, a 20×-fold concentration is recommended to avoid exosome aggregation, vesicle damage, or loss.
7. The concentrate can then be recovered manually by pipetting and stored at 4 °C. It is recommended to continue subsequent processing steps within the next few hours to prevent degradation of exosomal sample (*see* **Note 3**).

3.5 Isolation of Exosomes

There are various methods for isolation of exosomes, including ultracentrifugation, precipitation-based methods, and immunobeads. Here, we describe a method (Total exosome isolation reagent from cell culture media, ThermoFisher) that only requires general laboratory equipment and hence is broadly applicable to most laboratories.

1. 0.5 volumes of total exosome isolation reagent is added to the concentrated conditioned medium (e.g., 500 μL of reagent to 1 mL of concentrate) (*see* **Note 4**). Mix well by vortexing until the solution is homogenous.
2. Incubate the samples at 4 °C overnight.
3. On the following day, centrifuge the samples at 13,000 × *g* for 1 h at 4 °C.
4. Aspirate and discard the supernatant. Care should be taken to prevent accidental dislodging of the pellet (may be invisible at times).
5. Resuspend the pellet in a desired volume of 1× PBS, and the exosomes are now ready for subsequent analysis and can be stored at 4 °C for short-term storage or −20 °C for long-term storage. A representative image of iPSC-CMs-derived exosomes as characterized by transmission electron microscopy is shown in Fig. 1.
6. Alternatively, the pellet can be used immediately for RNA isolation by resuspension in lysis buffer.

3.6 RNA Isolation from Exosomes

The authors have routinely used miRCURY™ RNA isolation kit–cell & plant from Exiqon to isolate exosomal RNA.

1. Add 350 μL of lysis solution with β-mercaptoethanol directly to the exosome pellet and resuspend well.
2. Add 200 μL of 100% ethanol to the lysate and mix well by vortexing.
3. Assemble a column with provided collection tubes. Apply all the lysate with ethanol onto the column and centrifuge for 1 min at 13,000 × *g*.

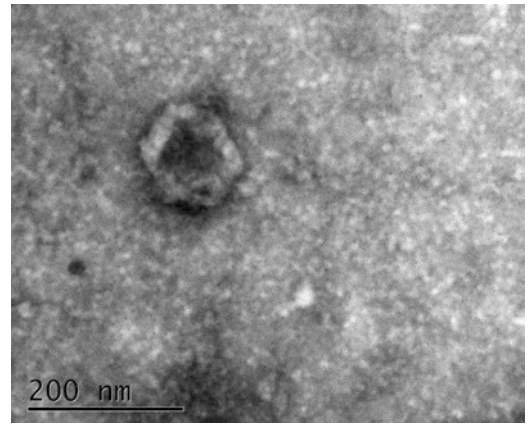

Fig. 1 Characterization of iPSC-CMs-derived exosomes by transmission electron microscopy. A round (~120 nm diameter) exosome containing a lipid bilayer is shown (arrowhead). It has an electron-dense content

4. Discard the flow-through and reassemble the spin column with its collection tube.
5. Add 400 μL of wash solution to the column and centrifuge for 1 min at 13,000 × *g*.
6. Discard the flow-through and reassemble the spin column with its collection tube.
7. Repeat washing the column two more times by adding another 400 μL of wash solution and centrifuge for 1 min at 13,000 × *g*.
8. Discard the flow-through and reassemble the spin column with its collection tube.
9. Spin the column for 2 min at 13,000 × *g* to thoroughly dry the resin. Discard the collection tube.
10. Place the column into a new elution tube. Add 35 μL of RNase-free water to the column.
11. Centrifuge for 2 min at 200 × *g*, followed by 1 min at 13,000 × *g*.
12. The purified RNA sample can now be stored at −80 °C for subsequent processing including microRNA analysis and sequencing.

Using this isolation method, the authors have detected microRNAs based on several platforms, including TaqMan assays, SYBR-Green-based microRNA qPCR arrays, and Illumina HiSeq 2000. An electropherogram of exosomal microRNA extracted using the methods above, and analyzed by Bioanalyzer 2100 on a small RNA chip, is shown in Fig. 2.

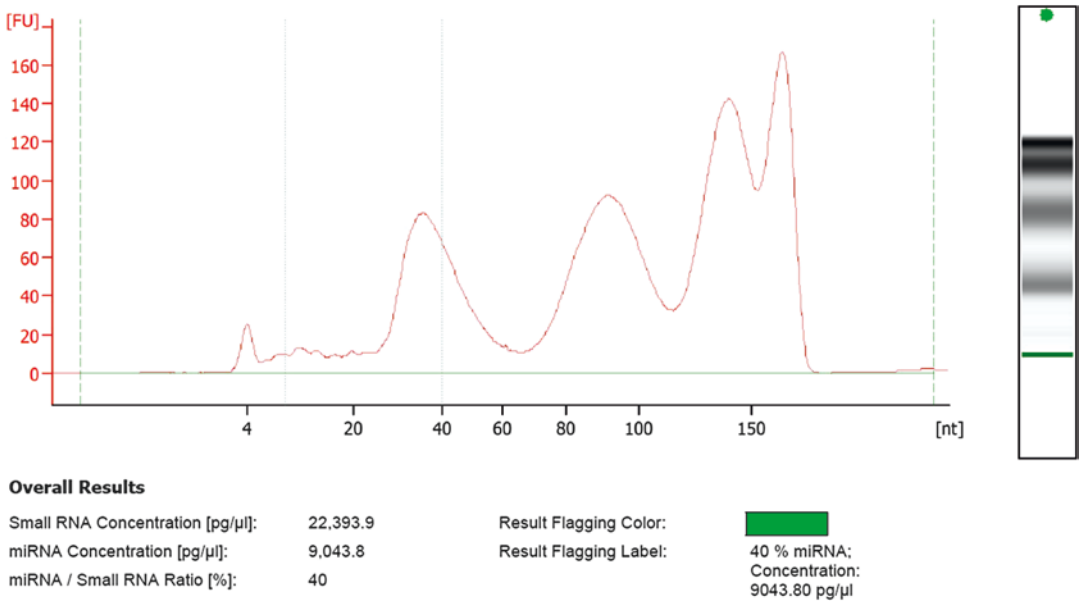

Fig. 2 Electropherogram of exosomal small RNAs isolated from iPSC-CMs conditioned medium measured by Bioanalyzer 2100 with the Small RNA assay. The electropherogram is plotted as fluorescence intensity (*Y*-axis) versus size (*X*-axis). Two distinct regions are defined with the Small RNA assay including small RNA region from 0 to 150 nt (delineated by dashed green lines) and the microRNA region from 10 to 40 nt (delineated by dotted gray lines). Nearly 40% of miRNAs were detected for this particular sample. The data can also be displayed as a densitometry plot as shown on the right

4 Notes

1. iPSC-CMs should be at a high purity before being used for exosome production and isolation to reduce the presence of contaminating exosomes from non-cardiac cells such as fibroblasts or endothelial cells.
2. FBS should not be used as it contains a high abundance of cow-derived exosome vesicles. If absolutely required, exosome-depleted FBS growth supplement which is commercially available (e.g., System Biosciences) should be used instead of regular FBS. Users may also consider an alternate chemically defined media for growth of human iPSC-CMs [22].
3. Handling and isolation of exosomes can be performed in a non-sterile condition for downstream applications such as immunoblotting, RNA analysis, or proteomic studies.
4. We recommend concentrating cell culture medium by ultrafiltration prior to isolation of exosome for ease of handling (e.g., reduced volume, visible pellet).

Acknowledgments

We are grateful for the funding support from National Institutes of Health (NIH) Pathway to Independence Award K99 HL130416, Stanford Child Health Research Institute and the Stanford NIH-NCATS-CTSA grant UL1 TR001085 (S.G.O.), American Heart Association (AHA) 16SDG27560003 (W.H.L.), AHA 17MERIT33610009, NIH R01 HL133272, NIH R01 113006, NIH R01 HL123968, NIH R01 HL132875, California Institute of Regenerative Medicine (CIRM) DR2A-05394 and CIRM RT3-07798 (J.C.W.).

References

1. Benjamin EJ, Blaha MJ, Chiuve SE, Cushman M, Das SR, Deo R, de Ferranti SD, Floyd J, Fornage M, Gillespie C, Isasi CR, Jimenez MC, Jordan LC, Judd SE, Lackland D, Lichtman JH, Lisabeth L, Liu S, Longenecker CT, Mackey RH, Matsushita K, Mozaffarian D, Mussolino ME, Nasir K, Neumar RW, Palaniappan L, Pandey DK, Thiagarajan RR, Reeves MJ, Ritchey M, Rodriguez CJ, Roth GA, Rosamond WD, Sasson C, Towfighi A, Tsao CW, Turner MB, Virani SS, Voeks JH, Willey JZ, Wilkins JT, Wu JH, Alger HM, Wong SS, Muntner P, American Heart Association Statistics C, Stroke Statistics S (2017) Heart disease and stroke statistics-2017 update: a report from the American Heart Association. Circulation 135(10):e146–e603. https://doi.org/10.1161/CIR.0000000000000485
2. Matsa E, Sallam K, Wu JC (2014) Cardiac stem cell biology: glimpse of the past, present, and future. Circ Res 114(1):21–27. https://doi.org/10.1161/CIRCRESAHA.113.302895
3. Noiseux N, Gnecchi M, Lopez-Ilasaca M, Zhang L, Solomon SD, Deb A, Dzau VJ, Pratt RE (2006) Mesenchymal stem cells overexpressing Akt dramatically repair infarcted myocardium and improve cardiac function despite infrequent cellular fusion or differentiation. Mol Ther 14(6):840–850. https://doi.org/10.1016/j.ymthe.2006.05.016
4. Bolli R, Chugh AR, D'Amario D, Loughran JH, Stoddard MF, Ikram S, Beache GM, Wagner SG, Leri A, Hosoda T, Sanada F, Elmore JB, Goichberg P, Cappetta D, Solankhi NK, Fahsah I, Rokosh DG, Slaughter MS, Kajstura J, Anversa P (2011) Cardiac stem cells in patients with ischaemic cardiomyopathy (SCIPIO): initial results of a randomised phase 1 trial. Lancet 378(9806):1847–1857. https://doi.org/10.1016/S0140-6736(11)61590-0
5. Laflamme MA, Chen KY, Naumova AV, Muskheli V, Fugate JA, Dupras SK, Reinecke H, Xu C, Hassanipour M, Police S, O'Sullivan C, Collins L, Chen Y, Minami E, Gill EA, Ueno S, Yuan C, Gold J, Murry CE (2007) Cardiomyocytes derived from human embryonic stem cells in pro-survival factors enhance function of infarcted rat hearts. Nat Biotechnol 25(9):1015–1024. https://doi.org/10.1038/nbt1327
6. Shiba Y, Fernandes S, Zhu WZ, Filice D, Muskheli V, Kim J, Palpant NJ, Gantz J, Moyes KW, Reinecke H, Van Biber B, Dardas T, Mignone JL, Izawa A, Hanna R, Viswanathan M, Gold JD, Kotlikoff MI, Sarvazyan N, Kay MW, Murry CE, Laflamme MA (2012) Human ES-cell-derived cardiomyocytes electrically couple and suppress arrhythmias in injured hearts. Nature 489(7415):322–325. https://doi.org/10.1038/nature11317
7. Ong SG, Huber BC, Lee WH, Kodo K, Ebert AD, Ma Y, Nguyen PK, Diecke S, Chen WY, Wu JC (2015) Microfluidic single-cell analysis of transplanted human induced pluripotent stem cell-derived cardiomyocytes after acute myocardial infarction. Circulation 132(8):762–771. https://doi.org/10.1161/CIRCULATIONAHA.114.015231
8. Ong SG, Wu JC (2015) Exosomes as potential alternatives to stem cell therapy in mediating cardiac regeneration. Circ Res 117(1):7–9.https://doi.org/10.1161/CIRCRESAHA.115.306593
9. Raposo G, Stoorvogel W (2013) Extracellular vesicles: exosomes, microvesicles, and friends. J Cell Biol 200(4):373–383. https://doi.org/10.1083/jcb.201211138
10. Harding CV, Heuser JE, Stahl PD (2013) Exosomes: looking back three decades and

into the future. J Cell Biol 200(4):367–371. https://doi.org/10.1083/jcb.201212113

11. Ong SG, Lee WH, Huang M, Dey D, Kodo K, Sanchez-Freire V, Gold JD, Wu JC (2014) Cross talk of combined gene and cell therapy in ischemic heart disease: role of exosomal microRNA transfer. Circulation 130(11 Suppl 1):S60–S69. https://doi.org/10.1161/CIRCULATIONAHA.113.007917
12. Valadi H, Ekstrom K, Bossios A, Sjostrand M, Lee JJ, Lotvall JO (2007) Exosome-mediated transfer of mRNAs and microRNAs is a novel mechanism of genetic exchange between cells. Nat Cell Biol 9(6):654–659. https://doi.org/10.1038/ncb1596
13. Costa-Silva B, Aiello NM, Ocean AJ, Singh S, Zhang H, Thakur BK, Becker A, Hoshino A, Mark MT, Molina H, Xiang J, Zhang T, Theilen TM, Garcia-Santos G, Williams C, Ararso Y, Huang Y, Rodrigues G, Shen TL, Labori KJ, Lothe IM, Kure EH, Hernandez J, Doussot A, Ebbesen SH, Grandgenett PM, Hollingsworth MA, Jain M, Mallya K, Batra SK, Jarnagin WR, Schwartz RE, Matei I, Peinado H, Stanger BZ, Bromberg J, Lyden D (2015) Pancreatic cancer exosomes initiate pre-metastatic niche formation in the liver. Nat Cell Biol 17(6):816–826. https://doi.org/10.1038/ncb3169
14. Hoshino A, Costa-Silva B, Shen TL, Rodrigues G, Hashimoto A, Tesic Mark M, Molina H, Kohsaka S, Di Giannatale A, Ceder S, Singh S, Williams C, Soplop N, Uryu K, Pharmer L, King T, Bojmar L, Davies AE, Ararso Y, Zhang T, Zhang H, Hernandez J, Weiss JM, Dumont-Cole VD, Kramer K, Wexler LH, Narendran A, Schwartz GK, Healey JH, Sandstrom P, Labori KJ, Kure EH, Grandgenett PM, Hollingsworth MA, de Sousa M, Kaur S, Jain M, Mallya K, Batra SK, Jarnagin WR, Brady MS, Fodstad O, Muller V, Pantel K, Minn AJ, Bissell MJ, Garcia BA, Kang Y, Rajasekhar VK, Ghajar CM, Matei I, Peinado H, Bromberg J, Lyden D (2015) Tumour exosome integrins determine organotropic metastasis. Nature 527(7578):329–335. https://doi.org/10.1038/nature15756
15. Feng Y, Huang W, Wani M, Yu X, Ashraf M (2014) Ischemic preconditioning potentiates the protective effect of stem cells through secretion of exosomes by targeting Mecp2 via miR-22. PLoS One 9(2):e88685. https://doi.org/10.1371/journal.pone.0088685
16. Ibrahim AG, Cheng K, Marban E (2014) Exosomes as critical agents of cardiac regeneration triggered by cell therapy. Stem Cell Rep 2(5):606–619. https://doi.org/10.1016/j.stemcr.2014.04.006
17. Chen L, Wang Y, Pan Y, Zhang L, Shen C, Qin G, Ashraf M, Weintraub N, Ma G, Tang Y (2013) Cardiac progenitor-derived exosomes protect ischemic myocardium from acute ischemia/reperfusion injury. Biochem Biophys Res Commun 431(3):566–571. https://doi.org/10.1016/j.bbrc.2013.01.015
18. Barile L, Lionetti V, Cervio E, Matteucci M, Gherghiceanu M, Popescu LM, Torre T, Siclari F, Moccetti T, Vassalli G (2014) Extracellular vesicles from human cardiac progenitor cells inhibit cardiomyocyte apoptosis and improve cardiac function after myocardial infarction. Cardiovasc Res 103(4):530–541. https://doi.org/10.1093/cvr/cvu167
19. Sahoo S, Klychko E, Thorne T, Misener S, Schultz KM, Millay M, Ito A, Liu T, Kamide C, Agrawal H, Perlman H, Qin G, Kishore R, Losordo DW (2011) Exosomes from human CD34(+) stem cells mediate their proangiogenic paracrine activity. Circ Res 109(7):724–728. https://doi.org/10.1161/CIRCRESAHA.111.253286
20. Yu B, Kim HW, Gong M, Wang J, Millard RW, Wang Y, Ashraf M, Xu M (2015) Exosomes secreted from GATA-4 overexpressing mesenchymal stem cells serve as a reservoir of anti-apoptotic microRNAs for cardioprotection. Int J Cardiol 182:349–360. https://doi.org/10.1016/j.ijcard.2014.12.043
21. Khan M, Nickoloff E, Abramova T, Johnson J, Verma SK, Krishnamurthy P, Mackie AR, Vaughan E, Garikipati VN, Benedict C, Ramirez V, Lambers E, Ito A, Gao E, Misener S, Luongo T, Elrod J, Qin G, Houser SR, Koch WJ, Kishore R (2015) Embryonic stem cell-derived exosomes promote endogenous repair mechanisms and enhance cardiac function following myocardial infarction. Circ Res 117(1):52–64. https://doi.org/10.1161/CIRCRESAHA.117.305990
22. Burridge PW, Matsa E, Shukla P, Lin ZC, Churko JM, Ebert AD, Lan F, Diecke S, Huber B, Mordwinkin NM, Plews JR, Abilez OJ, Cui B, Gold JD, Wu JC (2014) Chemically defined generation of human cardiomyocytes. Nat Methods 11(8):855–860. https://doi.org/10.1038/nmeth.2999

Chapter 11

Quantitative Analysis of Precursors MicroRNAs and Their Respective Mature MicroRNAs in Cancer Exosomes Overtime

Nuno Bastos and Sónia A. Melo

Abstract

Exosomes are a cell-to-cell communication system that transports information to neighbor and/or distant cells. Their content is composed of lipids, proteins, RNAs, and DNA. The role of exosomes released by cancer cells in disease progression has been widely studied. Here, we report a detailed protocol to quantify precursor microRNAs and mature microRNAs overtime in exosomes of cancer cells. Those precursor microRNAs that are packaged together with RISC proteins will get further processed in the exosomes overtime and an accumulation of the mature form of the microRNAs will occur.

Key words Exosomes, Exosomes isolation, Pre-microRNAs, MicroRNAs, qPCR

1 Introduction

Exosomes, extracellular vesicles of 40–150 nm in diameter, are important mediators of intercellular communication with neighbor/distant cells [1]. For the past years, extensive research in cancer brought new insights into the pivotal role of exosomes-mediated communication in several biological processes such as proliferation, angiogenesis, and migration/metastasis [2–6]. Exosomes are able to modulate recipient cells through transfer of their cargo, which consists of proteins, DNA, and RNAs (mRNAs, microRNAs, and other noncoding RNAs) [7, 8]. Exosomal RNAs have been described as key mediators of exosomes role in cancer [9]. We have shown that specific microRNAs in cancer exosomes become enriched overtime in these extracelular vesicles while in culture. At the same time, their respective precursor microRNAs (pre-microRNAs) are downregulated. The presence of RISC-loading complex proteins in exosomes concludes that specific pre-microRNAs get packaged in exosomes while engaged with RISC proteins and finish their biogenesis process while in these

Shao-Yao Ying (ed.), *MicroRNA Protocols*, Methods in Molecular Biology, vol. 1733,
https://doi.org/10.1007/978-1-4939-7601-0_11,

extracelular vesicles. Here, we demonstrate how to perform the analysis of microRNA maturation in cancer exosomes, highlighting the do's and dont's to efficiently measure this process.

2 Materials

2.1 Cell Culture

T75cm^2 flasks.

T25cm^2 flasks.

RPMI Complete Medium: RPMI medium, 10% FBS, 1% penicylin-streptomycin.

Exosomes-depleted RPMI Complete Medium: RPMI medium, 10% Exosomes-depleted FBS, 1% penicylin-streptomycin.

Trypsin 1×.

PBS 1×.

2.2 Exosomes Isolation and Purification

10 mL syringe.

Whatman™ 0,2 μm filtre.

PBS 1×.

11 and 30 mL ultracentrifuge tubes.

2.3 Exosomes RNA Extraction

Protease-free Rnase.

10× RNase inhibitor.

Trizol.

Chloroform.

Isopropanol.

Ethanol 75%.

RNase/Dnase-free H_2O.

2.4 RNA Quantification

q-PCR plate.

Invitrogen™ SuperScript® III RT/ Platinum® *Taq* Mix (including RNaseOUT™).

2× SYBR® Green Reaction Mix.

Target pre-microRNA forward primer.

Target pre-microRNA reverse primer.

ROX reference dye.

RNase/Dnase-free H_2O.

dNTPs.

Reverse Transcriptase enzyme.

10× Reverse Transcription buffer.

RNase inhibitor.

TaqMan microRNA primer.

TaqMan 2× Universal PCR Master Mix.

3 Methods

3.1 Cell Culture

1. Plate the cells in a T75cm^2 flask to obtain an inicial confluence of 50%.
2. Wash the cells with PBS 1× on the next day and add 11 mL of exosomes-depleted RPMI medium.
3. After 24 h, cell culture medium is collected for exosomes isolation and purification.

3.2 Exosomes Isolation and Purification

1. Cell culture media collected to a 50 mL falcon tube is centrifuged for 10 min at 800 × *g* to remove cell debris.
2. Perform an additional centrifugation of 5 min at 2000 × *g*.
3. Filter the supernatant using a Whatman™ 0.2 μm filter directly into an ultracentrifuge tube.
4. After calibrating the tubes, perform an ultracentrifugation at 100,000 × *g* for 2 h for exosomes isolation.
5. Remove the supernatant and add PBS 1× to the exosomes pellet. Do not ressuspend the pellet at this stage.
6. Perform an ultracentrifugation at 100,000 × *g* for 2 h—washing step.
7. After the washing step, remove the supernatant and slowly ressuspend exosomes pellet in 5 mL RPMI media with FBS depleted of exosomes.
   (a) An exact duplicate sample is ressupended in a saline solution (0.9%) and analyzed on the NanoSight.

3.3 Exosomes Culture

1. The same number of exosomes (for samples to be compared overtime) in culture media should be placed in a T25 cm^2 flask.
2. After 72 h, remove cell culture medium and isolate exosomes as stated previously. Exosomes are also cultured for only 24 h to act as control.

3.4 Exosomes RNA Extraction

1. Prior to RNA extraction, treat exosomes with 500 mg/mL proteinase K dissolved in RNase-free water for 60 min at 37 °C followed by heat inactivation of the protease for 10 min at 60 °C.
2. Next, incubate exosomes with 2 mg/mL protease-free RNase for 15 min at 37 °C followed by adding 10× concentrated RNase inhibitor.

3. Resuspend exosomes in 500 μL of Trizol LS and store at −80 °C or initiate RNA extraction.
4. Add 100 μL of chloroform and vortex strongly.
5. Centrifuge at 12,000 × *g* for 15 min at 4 °C.
6. Transfer the upper phase (aqueous phase) to an RNase-free tube.
7. Add 250 μL of isopropanol and vortex.
8. Incubate overnight at −20 °C for efficient RNA precipitation.
9. On the next day, centrifuge at 12,000 × *g* for 10 min.
10. Remove the supernatant and wash with 1 mL of ethanol 75% diluted in RNase and Dnase-Free H_2O.
11. Centrifuge at 7500 × *g* for 5 min at 4 °C.
12. Remove the supernatant and briefly dry the RNA for 5–10 min (Note: do not use speed vacuum).
13. Add 30 μL of RNase and Dnase-Free H_2O to the pellet.
14. Treat RNA with DNase for 20 min at 37 °C.
15. Add 1 μL of 0.5 M EDTA (to a final concentration of 5 mM).
16. Heat inactivate at 75 °C for 10 min.
17. Store the RNA at −80 °C.

3.5 Real-Time PCR Quantification

3.5.1 Precursor MicroRNAs

Pre-microRNAs are quantified using the SuperScript III Platinum One-Step RT-qPCR kit (Invitrogen) in a Real-Time PCR Thermocycler. Set up reactions in a qPCR plate on ice. Volumes used for a single run are described below.

Invitrogen™ SuperScript® III RT/ Platinum® *Taq* Mix (including RNaseOUT™)	0.4 μL
2× SYBR® green reaction	10 μL
Forward primer (10 μM)	1 μL
Reverse primer (10 μM)	1 μL
Rox reference dye	0.4 μL
RNA (150 ng)	≤10 μL
RNase/DNase free H_2O	to 20 μL

Cycling program used is listed below:

- 50 °C for 3 min hold.
- 95 °C for 5 min hold.
- 40 cycles of
  - 95 °C for 15 s.
  - 60 °C for 30 s.

- 40 °C for 1 min.

Melting curve:

- 95 °C for 15 s.
- 60 °C for 1 min.
- 95 °C for 30 s.
- 60 °C for 15 s.

3.5.2 MicroRNAs

MicroRNA expression analysis is performed using reverse transcription followed by real-time PCR analysis.

Reverse Transcription
Mix (single run):

dNTPs	0.05 μL
Reverse transcriptase enzyme	0.33 μL
10× RT buffer	0.5 μL
RNase inhibitor	0.068 μL
Primer	1 μL
RNA (10 ng/μL)	1 μL
RNase/DNase free H_2O	2.06 μL

Incubate reaction mix at 16 °C for 30 min, 42 °C for 30 min, and 85 °C for 5 min to obtain cDNA for each specific microRNA and the respective loading control.

3.6 Real-Time PCR

Perform a qPCR analysis in a Real-Time PCR Thermocycler for each target microRNA.
Mix (single run):

TaqMan 2× universal PCR master mix	5 μL
RNase/Dnase-free H_2O	2.5 μL
TaqMan MicroRNA primer	0.5 μL
Reverse transcriptase product	2 μL

Cycling program used is listed below.

- 50 °C for 2 min hold.
- 95 °C for 10 min hold.
- 40 cycles of
  - 95 °C for 15 s.
  - 60 °C for 1 min.

Expression of microRNAs is normalized to the expression of 18S rRNA that serves as loading control. Each measurement should be performed in triplicate (experimental) and three independent experiments (biological). MicroRNA fold change is determined using the $2^{-\Delta\Delta Ct}$ formula, as previously reported [10]. Comparisons should only be made between the samples which were isolated together and divided for different culture times (one isolation divided in as many fractions needed for overtime quantification).

4 Notes

1. The number of T75 flasks platted will depend on the number of exosomes produced by a cell line. Cell lines with low rates of production of exosomes (like the MCF10A), plate more cells in more flasks, so that after exosomes isolation you have comparable amount with cancer cells-derived exosomes. Numbers can be normalized after measuring the concentration of exosomes by nanoparticle tracking analysis (NanoSight).
2. When doing the ultracentrifugations, if the volume from different media tubes is not equal, calibrate the tubes by adding to the media the required volume of PBS 1×.
3. After exosomes isolation from cell culture supernatants, add PBS 1× to wash the pellet, but do not ressupend it. This can compromise the integrity of the exosomes in the preparation.
4. After the washing step of the exosomes, pellets in different tubes can be pulled together so the final yield of exosomes is better.
5. In Subheading 3.3, **step 2**, the exosomes for 72 and for 24 h culture should be taken from the same isolated pool. Isolate exosomes, calculate their concentration on NanoSight and, from the same isolated sample/tube, take the exact same volume for 24 and 72 h culture. In this way you guarantee that the same sample is being looked at, at different time points, and not that different isolated samples are being looked at different time points.

Acknowledgments

Our laboratory is primarily supported by the project NORTE-01-0145-FEDER-000029, supported by Norte Portugal Regional Programme (NORTE 2020) under the PORTUGAL 2020 Partnership Agreement, through the European Regional Development Fund (ERDF) and FEDER funds through the COMPETE Program (POCI-01/0145-FEDER-016618), as well as national

funds through Foundation for Science and Technology (FCT) PTDC/BIM-ONC/2754/2014. SAM is supported by FCT IF/00543/2013.

References

1. Mathivanan S, Ji H, Simpson RJ (2010) Exosomes: extracellular organelles important in intercellular communication. J Proteomics 73(10): 1907–1920
2. Costa-Silva B et al (2015) Pancreatic cancer exosomes initiate pre-metastatic niche formation in the liver. Nat Cell Biol 17(6):816–826
3. Hoshino A et al (2015) Tumour exosome integrins determine organotropic metastasis. Nature 527(7578):329–335
4. Peinado H et al (2012) Melanoma exosomes educate bone marrow progenitor cells toward a pro-metastatic phenotype through MET. Nat Med 18(6):883–891
5. Ekström EJ et al (2014) WNT5A induces release of exosomes containing pro-angiogenic and immunosuppressive factors from malignant melanoma cells. Mol Cancer 13(1):88
6. Baglio SR et al (2017) Blocking tumor-educated MSC paracrine activity halts osteosarcoma progression. Clin Cancer Res 23(14):3721–3733
7. Kahlert C, Kalluri R (2013) Exosomes in tumor microenvironment influence cancer progression and metastasis. J Mol Med (Berl) 91(4):431–437
8. Kahlert C et al (2014) Identification of double-stranded genomic DNA spanning all chromosomes with mutated KRAS and p53 DNA in the serum exosomes of patients with pancreatic cancer. J Biol Chem 289(7):3869–3875
9. Melo SA et al (2014) Cancer exosomes perform cell-independent MicroRNA biogenesis and promote tumorigenesis. Cancer Cell 26(5):707–721
10. Livak KJ, Schmittgen TD (2001) Analysis of relative gene expression data using real-time quantitative PCR and the 2(−Delta Delta C(T)) method. Methods 25(4):402–408

Chapter 12

Quantum Language of MicroRNA: Application for New Cancer Therapeutic Targets

Yoichi Robertus Fujii

Abstract

MicroRNA (miRNA) is the noncoding gene: therefore, the miRNA gene inheritably controls protein gene expression through transcriptional and post-transcriptional levels. Aberrant expression of miRNA genes causes various human diseases, especially cancers. Although cancer is a complex disease, cancer/miRNA implication has yet been grasped from the perspective of miRNA profile in bed side. Since miRNA is the mobile genetic element, the clinical verification of miRNA in microvesicle of blood is too much straggle to predict potential cancer/miRNA associations without bioinformatical computing. Further, experimental investigation of miRNA/cancer pathways is expensive and time-consuming. While the accumulated data (big data) of miRNA profiles has been on line as the databases in cancers, using the database algorithms for miRNA target prediction have reduced required time for conventional experiments and have cut the cost. Computational prediction of miRNA/target mRNA has shown numerous significant outcomes that are unobtainable only by experimental approaches. However, ID of miRNA in the annotation is an arbitrary number and the ID is not related with miRNA its functions. Therefore, it has not been physicochemically shown why multiple miRNAs in blood or tissues are useful for diagnosis and porgnosis of human diseases or why function of single miRNA in cancer is rendered to oncomir or tumopr suppressor. In addition, it is less cleared why environmental factors, such as temperature, radiation, therapeutic anticancer immune or chemical agents can alter the expression of miRNAs in the cell. The ceRNA theory would not be enough for the investigation of such subjects. Given miRNA/target prediction tools, to elucidate such issues with computer simulation we have previously introduced the quantum miRNA/miRNA interaction as a new scoring using big database. The quantum score was implicated in miRNA synergisms in cancer and participated in the miRNA/target interaction on human diseases. On the other hand, ribosomal RNA (rRNA) is the dominant RNA species of the cells. It is well known that ribosomopathies, such as Diamond-Blackfan anemia, dyskeratiosis congenital, Shwachman-Diamond syndrome, 5q-myelodysplastic syndrome, Treacher Collins syndrome, cartilage-hair hypoplasia, North American Indian childhood cirrhosis, isolated congenital asplenia, Bowen-Conradi syndrome and cancer are caused by altered expression of ribosomal proteins or rRNA genes. We have proposed the hypothesis that the interaction among miRNAs from rRNA and/or other cellular miRNAs would be involved into cancer as the ribosomopathy. Subsequently, we found rRNA-derived miRNAs (rmiRNAs) by using the sequence homology search (miPS) with miRNA database (miRBase). Further, the pathway related with cancer between rmiRNA/target protein gene was predicted by miRNA entangling target sorting (METS) algorithm. In this chapter, we describe about the usage of in silico miRNA identification program, miRNA/target prediction search through the database and quantum language of miRNA by the METS, and the

Shao-Yao Ying (ed.), *MicroRNA Protocols*, Methods in Molecular Biology, vol. 1733,
https://doi.org/10.1007/978-1-4939-7601-0_12,

ontology analysis. In particular, the METS algorithm according to the quantum value would be useful simulator to discover a new therapeutic target aganist cancer. It may also partly contribute to the elucidation of complex mechanisms and development of agents of anti-cancer.

Key words AluRNA, Big data, Biomarker, Cancer, microRNA, Quantum, Ribosomal RNA

1 Introduction

MicroRNAs (miRNAs) are single-stranded, noncoding, and small RNAs. A function of them is fine-tuning by suppression or augmentation of protein gene expression by targeting the messenger RNAs (mRNAs) 3′-UTR with incomplementary paring of bases of the nucleotide [1]. A miRNA regulates hundreds of messenger RNAs (mRNAs) and vice versa, therefore, most of all protein-coding genes would be controlled by cellular miRNAs. Although cellular miRNAs modulate biological pathways, aberrant expression of the miRNA genes could induce carcinogenesis. Since environmental carcinogens, such as viruses, chemicals, and hormones, induce tumor and it is associated with dysregulation of miRNAs, miRNAs can be applied for biomarkers of cancers [2].

RNA wave 2000 is the theory about characteristic of miRNAs [3, 4], and it consists of four critical pillars: (1) the miRNA gene is a mobile genetic element inducing transcriptional and post-transcriptional regulation via networking processes; (2) the miRNA information expands to intracellular, intercellular, intraorgan, interorgan, intraspecies, and interspecies under a lifecycle of the global environment; (3) mobile miRNAs self-proliferate; (4) cells contain two types of information as the resident and genomic miRNAs. Mechanisms of tumorigenesis and metastasis are involved in the RNA wave 2000 theory [5]. Further, resident miRNAs are localized in the cytoplasm as the non-DNA form, for instance, erythrocytes are anucleated; however, miRNAs in the red blood cells control their metabolisms without de novo miRNA production. As such evidences, we have been interested in miRNA biogeneration from ribosomal RNA (rRNA) in cancer.

rRNA is an essential RNA for the structure and the function of ribosomes. rRNA is consistently transcribed in the nucleus and is the dominant species of RNAs. In the human genome, the rRNA gene (rDNA) organizes tandem repeat on the short arms of acrocentric chromosomes (Chr), such as Chr 13, 14, 15, 21, and 22 [6]. The repeating unit is composed of non-transcribed spacer (NTS) and RNA45S. The RNA45S contains seven components as 5′-exterminal transcribed spacer (5′-ETS), 18S rRNA, internal transcribed spacer 1 (ITS1), 5.8S rRNA, ITS2, 28S rRNA, and 3′-ETS. In the nucleus, rDNA region forms a large structure known as the nucleolus, in which the multiple and massive transcripts of rRNA under rRNA processing and biogenesis are

observed [7]. The RNA45S gene is initially transcribed as 47S pre-rRNA through multiple processing. Mature rRNAs are transported into the cytoplasm and construct the mature ribosomal complex with ribosomal protein complexes (RPs) [8]. Defects of RPs or the rRNA genes cause functional insufficiency of ribosome, called ribosomopathy [9]. This kind of ribosomal dysfunction is observed in cancer [10]. While increasing ribosome synthesis enhances protein production to rapidly proliferate tumor cells, inhibition of ribosome upregulation would have been available for anti-cancer therapy [11]. Further, ribosome dysfunctions may be implicated in aberration of miRNA expression. Intriguingly, miRNA biogeneration-related proteins, Drosha, Dicer, and Ago, have an important role for rRNA processing [12]. Human Alu, a member of short interspersed element (SINE), has been related to rRNA biogenesis and Alu RNA interacts with miRNAs in the nucleolar [13]. We have hypothesized that the resident miRNAs from rRNA would be a factor in a necessary-sufficient condition of cancer.

The interaction between miRNA and target mRNA is important to investigate the molecular pathways in cancer cells; however, as described above, multiple interactions among miRNAs and targets are too complicated to confirm tumorigenesis pathway. To solve this problem, development of computing tools has been necessary. Algorithms for miRNA target prediction have been developed with sequence complementally, seed region-based complementary, thermodynamic stability, conservation and flanking sequence searches, etc. [1]. For instance, TargetScan and miRTarBase identify candidates of the miRNA target protein gene as the web tools based on the strength of interaction between the seed region and target site of miRNAs [14]. However, miRNA/target network pathway prediction is complex because all predicted miRNA/target interactions are numerous in a disease. Therefore, novel ideas are necessary for miRNA/target computation and the layer analysis of miRNA/target associations to develop novel therapeutic agents of cancers. We have shown in the previous MicroRNA Protocols that miRNA sequences can be transformed into the quantum ket alignments under the RNA wave 2000 theory [4]. Synergies of miRNA/miRNA have been implicated in the regulation of miRNA/target [15]. Although we have proposed to score the quantum miRNA/miRNA interaction as dynamic nexus score (DNS) (Fig. 1) [16], the values of DNS were correlated with miRNA synergistic effects, and the changing values between DNSs and the context scores of miRNA/target SNPs and target mutations were deeply implicated in the relation of miRNA/disease. In recent advanced computation by the integration of miRNA/miRNA functional similarity, human-disease association has been shown with high levels (AUC in ROC; approximate 0.9) [17, 18]. As the implementations of the previous ket alignments upon miRNAs, the quantum language of miRNA has been integrated

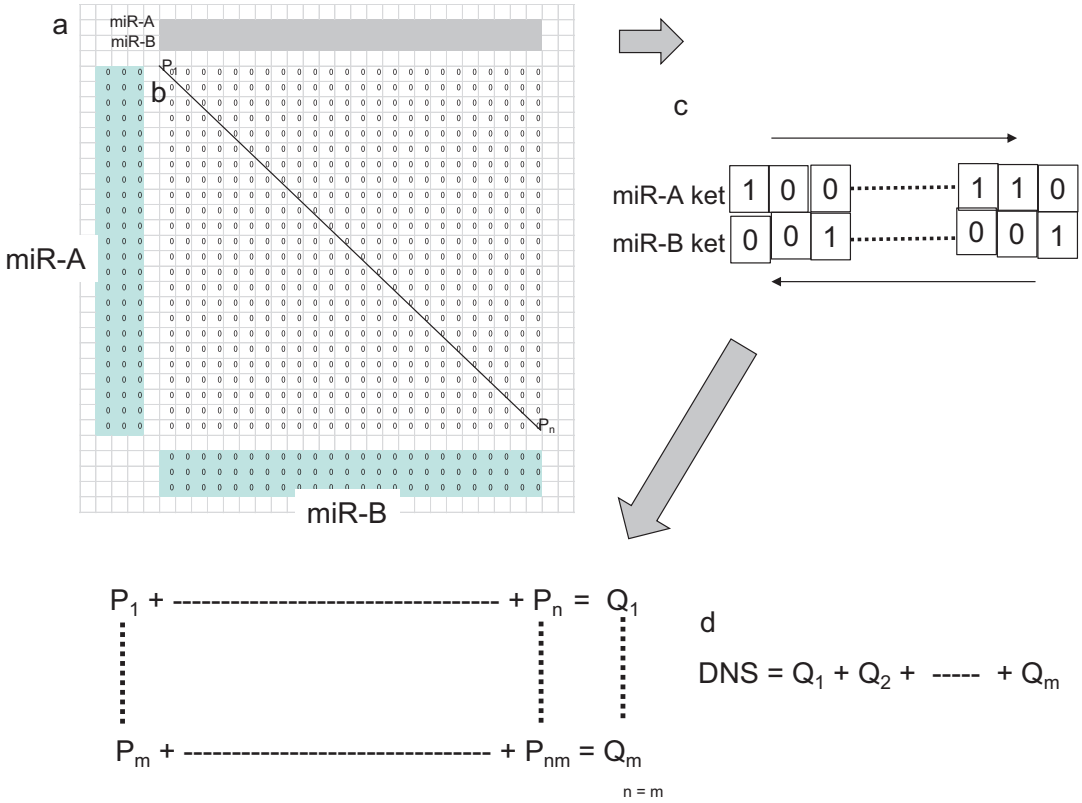

Fig. 1 MESer1 calculation. The kets of miR-A and miR-B are loaded into the upper gray panel (panel a) (window; 3). The decreasing diagonal (solid line b) in the matrix is SNS (P_1 + ---- + P_n). Rotation between ket A and ket B (panel c) makes DNS (Q_1 + ---- + Q_m, n = m) (panel d)

into the pipeline of comprehensive computer-based miRNA/target analysis [19]. Subsequently, we found 17 of human ribosomal RNA-derived resident miRNAs (rmiRNAs) and the top 5 of high DNS were in rmiRNAs, rmiR-4466 in 5′ETS, rmiR-3656 in 28S, rmiR-1268a and rmiR-1268b in 3′ETS, and rmiR-6729. These high DNS rmiRNAs were predicted to be associated with cancer in GO and KEGG pathway analysis. miR-3656 has been associated with breast cancer as a biomarker [20]. It is strongly suggested that rmiRNA would have a function in cancer stress. The processing protocol could be applied for other diseases, such as Alzheimer disease and HIV-1 infection [1]. In this chapter, we show the processes of our miRNA gene analysis with three programs, miPS, MESer, and METS. The quantum language of miRNA would virtualize as a novel strategy for the prediction of novel cancer targets.

2 Materials

2.1 Preparation of RNA Sequence Data

1. miRNA sequence data (mature.fa and hairpin.fa) was downloaded from miRBase release 21 (http://www.mirbase.org). Human genome coordinate data (hsa.gff3) was also obtained from miRbase.
2. Human rRNA sequence data was downloaded from European Nucleotide Archive release 127 (ENA) (http://www.ebi.ac.uk/ena) and National Center for Biotechnology Information (NCBI) (http://www.ncbi.nim.nih.gov). rRNA data, RNA45S5 (NR_046235), and human rRNA complete repeating unit (U13361.1) were used (*see* **Note 1**). Human tRNA sequence data was downloaded from Genomic tRNA database, GtRNAdb (http://gtmadb.ucsc.edu).
3. tRF data was obtained from tRFdb (http://genome.bioch.verginia.edu/trfdb).
4. Alu sequence data was downloaded from SINE Base (http://sine.eimb.ru) (*see* **Note 2**).

3 Methods

3.1 Detection of miRNA Sequences in miPS Program

1. miPS program is prepared for the detection of miRNA sequences by using C++ computing language. The miPS can search the sequence of query RNAs (miRNAs) from the target RNA sequence (rRNA or Alu) in sense and antisense (*see* **Note 3**). The conventional homology analysis tools could also be available for the detection of miRNA sequences, such as Genetyx-Win (Software development Co. Ltd., Tokyo, Japan). In the case of rRNA, the miPS program is run to detect the sequences of 1881 human precursor miRNAs and 2588 mature miRNAs against RNA45S5 (NR_046235).
2. To examine a hairpin-shaped precursor of the pre-miRNAs, the secondary structure of annotated pre-miRNAs is investigated in miRBase. The passenger strands of detected pre-miRNA are defined (*see* **Note 4**). The miPS is run to detect the defined passenger strands in rRNA or Alu.
3. High or low similarity group of pre-miRNAs is prepared and high groups were selected from the obtained pre-miRNAs.

3.2 Prediction of Secondary Structures

1. The precursor sequences of high similarity groups are presumed and listed comparing with the original pre-miRNA sequences in miRbase.

2. In the case of rRNA, rRNA-hosted miRNA analogs (rmiRNAs) are presumed (*see* **Note 5**).
3. The secondary structure of the listed pre-miRNAs is checked by using Mfold web server (http://unafold.ma.albany.edu/?q=mfold/ma-folding-form) (*see* **Note 6**).

3.3 Quantum Score for MESer Program

1. The quantum state of miRNA has been the physicochemical equivalent of the binary ket information in the quantum computing. Quantum ket interaction of miRNA/miRNA or miRNA/target RNA is set up in the matrix to simply understand (Fig. 1, panel a). The superposed state between *a* and *b* miRNAs is represented as,

$$f = \sum_{i,j=1}^{n} \left(a_{ij} \otimes b_{ij} \right)$$

The 5′ ends of two miRNAs are i=1 and j=1.

The whole static quantum interaction between miRNA A and B can be calculated into an intersecting points (P) as static nexus score (SNS)(Fig. 1, solid line b).

$$\mathrm{SNS} = \sum_{i=1}^{n} P_i$$

Back to the Schrödinger equation,

$$i\hbar\psi' = H\psi \qquad (1)$$

ψ is the wave function.

$$\psi = a_0 \,|0> + b_1 \,|1>$$

As a_0 and b_1 are the amplitudes corresponding to *a* and *b* miRNA kets respectively,

$$|a_0|^2 + |b_1|^2 = 1$$

Hamiltonian $\boldsymbol{H}$ is given by

$$H = -\gamma \hbar \mathrm{B}\, \mathrm{I}^z = -\hbar\omega_0 \mathrm{I}^z$$

γ is a gyromagnetic ratio and B is a magnetic field. ω_0 is a natural frequency of the rotator.

$$\omega_0 = -\gamma B$$

Since energy of ground state |0> (the bases of nucleic acids A, U and C) and excite state |1> (the base of nucleic acid G),

$$|0\rangle = -\frac{1}{2}\hbar\omega_0$$

$$|1\rangle = \frac{1}{2}\hbar\omega_0$$

ψ on time t is,

$$\psi(t) = a_0(t)\,|0> + b_1(t)\,|1> \tag{2}$$

Substitute (2) into (1)

$$H(a_0(t)\,|0> + b_1(t)\,|1>) = -\hbar\omega_0 \mathrm{I}^z(a_0(t)\,|0> + b_1(t)\,|1>)$$

I^z is an operator for z-directional component of spin.

$$\mathrm{I}^z = \frac{1}{2}\left(|0><0| - |1><1|\right)$$

From (1),

$$\begin{aligned} i\hbar(\dot{a}_0\,|0> + \dot{b}_1\,|1>) = -\frac{1}{2}\hbar\omega_0\left(|0><0| - |1><1|\right) \\ \times(a_0(t)\,|0> + b_1(t)\,|1>) \end{aligned} \tag{3}$$

In the form of determinant as follows,

$$\begin{aligned} &\left(|0><0| - |1><1|\right)(a_0(t)\,|0> + b_1(t)\,|1>) \\ &= \begin{pmatrix} 1 & 0 \\ 0 & -1 \end{pmatrix}\left\{a_0(t)\begin{pmatrix} 1 \\ 0 \end{pmatrix} + b_1(t)\begin{pmatrix} 0 \\ 1 \end{pmatrix}\right\} \\ &= a_0(t)\begin{pmatrix} 1 \\ 0 \end{pmatrix} + b_1(t)\begin{pmatrix} 0 \\ -1 \end{pmatrix} \end{aligned}$$

Ordinary differential of (3) is performed as follows,

$$i\frac{\mathrm{d}a_0}{\mathrm{d}t} = \dot{a}_0 = -\frac{1}{2}\omega_0\,\dot{a}_0$$

$$i\frac{\mathrm{d}b_1}{\mathrm{d}t} = i\,\dot{b}_1 = \frac{1}{2}\omega_0\,\dot{b}_1$$

$$a_0(t) = a_0 \mathrm{e}^{\mathrm{t}\omega_0 i/2}$$

$$b_1(t) = b_1 \mathrm{e}^{-\mathrm{t}\omega_0 i/2}$$

Along to (2) and when $t = 0$,

$$\begin{aligned} \psi(t) &= a_0(0)\mathrm{e}^{\mathrm{t}\omega_0 i/2}\,|0> + b_1(0)\mathrm{e}^{-\mathrm{t}\omega_0 i/2}\,|1> \\ &= a_0\,|0> + b_1\,|1> \end{aligned}$$

Therefore, the whole static quantum interaction between miRNA a and b can be rotated (Fig. 1, panel c). Since kets of

```
00 Sub meser1 ()
01  ,
02  ,  meser1 Macro
03  ,
04
05  ,
06
07 Dim i, j, k As Integer
08
09 Range(Columns(1), Columns(100)).ColumnWidth = 3
10 Range(Rows(1), Rows(100)).RowHeight = 21
11
12 Range(Cells(2, 6), Cells(3, 29)).Interior.ColorIndex = 15
13 Range(Cells(5, 2), Cells(28, 4)).Interior.ColorIndex = 20
14 Range(Cells(30, 6), Cells(32, 29)).Interior.ColorIndex = 20
15
16 For i = 2 To 4
17 For j = 5 To 28
18 k = i + j - 1
19 If k > 29 Then k = k - 24
20 Cells(j, i).FormulaR1C1 = "=R2C" & k
21 Next
22 Next
23
24 For i = 30 To 32
25 For j = 6 To 29
26 k = i + j - 30
27 If k > 29 Then k = k - 24
28 Cells(i, j).FormulaR1C1 = "=R3C" & k
29 Next
30 Next
31
32 Cells(5, 6).FormulaR1C1 = "=RC2*R30C+RC3*R31C+RC4*R32C"
33 Cells(5, 6).AutoFill Destination:=Range(Cells(5, 6), Cells(5, 29)), Type:=xlFillDefault
34 Range(Cells(5, 6),Cells(5, 29)).AutoFill Destination:=Range("F5:AC28"), Type:=xlFillDefault
35
36 End Sub
```

Fig. 2 VBA macro. The macro program for Excel is represented

two miRNAs revolve in the matrix, SNS between two kets of miRNAs (A_i and B_j) shows different values in each relative location shifting. Subsequently, the different values (Q) are summed up as dynamic nexus score (DNS) (Fig. 1, panel d).

$$\mathrm{DNS} = \sum_{i=1}^{n} Q_i \tag{4}$$

When kets of two miRNAs are different length, the surplus space of 3′ end region of miRNA is filled up with zeros.

2. Matrix for DNS values is calculated by Excel Visual Basic (VAB) for the application macro program of MESer1 (Fig. 2). After MESer1 executed the program in a sheet of Excel, the area of the matrix (Fig. 1, panel a) could copy and paste into another Excel sheet. In the MESer, the DNS are computed between miRNA/miRNA, or miRNA/rmiRNA, or miRNA/Alu. Algorithm MESer is depicted in Fig. 1 according to formula (4).

3. Load miR-A ket and miR-B ket (5′ → 3′) in (panel a) lines of the upper panel. Each intersection points (solid line b) in the matrix are summed up from P_1 to P_n in the lower panel. Q_1 is the total value.
4. One by one, move the kets each other on the counter clock direction (panel c). Collect from Q_1 to Q_m (n = m).
5. Sum up from Q_1 to Q_m (panel d). It is DNS between miR-A and miR-B. MESer tool computes the processing.

3.4 METS Algorithm to Detect Multi-miRNA Interaction

miRNA entangling target sorting (METS) algorithm is aimed to simplify the complex of miRNA/target networks by DNS. Since multi-miRNA interaction is correlated with synergy of miRNA/miRNA and with human diseases, DNS could be used as a filter.

1. Predicted targets of miRNAs are searched by TargetScanHuman (http://www.targetscan.org/). Two series of miRNA/target network data are extracted from completely predicted miRNA/target (A) and experimentally validated miRNA/target (B).
2. miRNAs from completely predicted and experimentally validated targets are reversely searched by miRTarBase (http://mirtarbase.mbc.nctu.edu.tw/). And then DNS of miRNA/miRNA is calculated between original miRNAs and the sorted miRNAs. Select top 5–10 of DNSs between the miRNA first choice in (1) and miRNA. Targets in top 5–10 DNSs of miRNAs are selected as well in completely predicted data (C) and experimentally validated data (D). Targets validated with at least one strong evidence or more than three less strong evidence are extracted top 10 targets in conserved sites that are selected.
3. The same predicted or validated targets are matched from data A and data C or data B and data D. Partially predicted targets (E) and completely validated targets (F) are obtained. Simultaneously, miRNA/miRNA interactions are predicted from the selected target data D and E.
4. miRNA/target networks are extracted. miRNA/ validated target networks (probably ready-made pathway) and miRNA/predicted target networks (possible new pathway) are combined under multi-miRNA interaction. The processes of algorithm are shown in Fig. 3. The results of miR-17/92 cluster and miR-21 are shown in Fig. 4a and b, respectively (*see* **Note 7**).

3.5 Prediction of Biological Function of Protein Genes

1. Biological function analysis is performed from obtained target data with Gene Ontology (GO) (http://www.geneontology.org/) and Kyoto Encyclopedia of Genes and Genomes (KEGG) (http://www.genome.jp/kegg/) through GeneCodis3 web tool (http://genecodis.cnb.csic.es/).
2. Network of miRNA target/miRNA target is searched by STRING (string-db.org) [1].

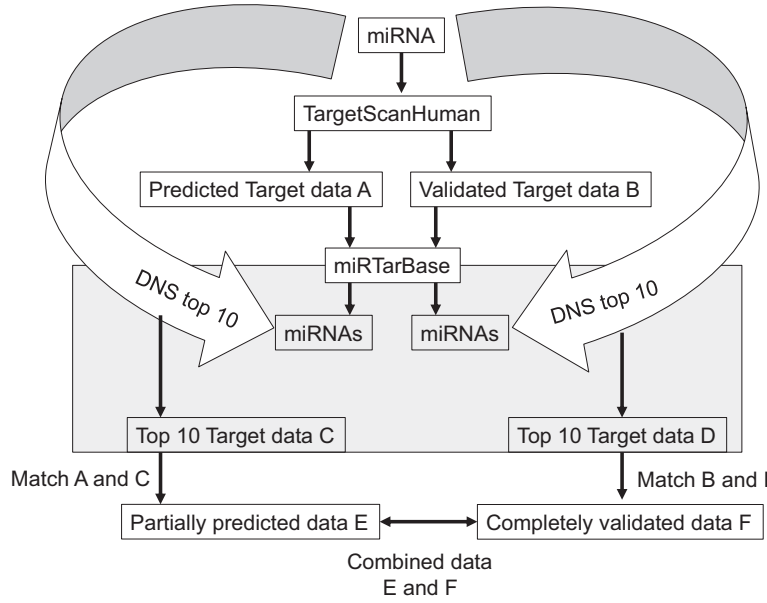

Fig. 3 METS analysis. The process of METS is shown

4 Notes

1. The sequence polymorphisms are presented in rDNA.
2. The branch of Alu family is constructed in big nodes; therefore, Alu sequence data should be selected according to the purpose of the investigation.
3. The miRNA sequence has to be detected by in sense and antisense.
4. Since the passenger strand of a detected miRNA is not listed in the data of mature miRNA sequence in some cases, the passenger strand has to be defined. For instance, miR-663a is only recorded as the guide strand. The 5p sequences of miR-663a as precursor pre-miRNA are CCUUCCGGCGUCCCAGGC GGGGCGCCGCGGGACCGCCCUCGUGUCUGUGGC GGUGGGAUCCCGCGGCCGUGUUUUCCUGGUGG CCCGGCCAUG and the mature of it is AGGCGGGGCGCC GCGGGACCGC. Therefore, the miRNA-3p is defined by the secondary structure, such as GUGGGAUCCCGCGGCCGU GUUUUCCU.
5. Although rDNA locates in Chr 13, 14, 15, 21, and 22, hsa-miR-663a locates in 26208186–26208278 [-] in Chr 20. Therefore, miR-663a is classified into the rmiRNA gene.
6. Mfold parameters; 37 °C; 1M NaCl; linear RNA; percent suboptimality 5; upper bound on the number of computed

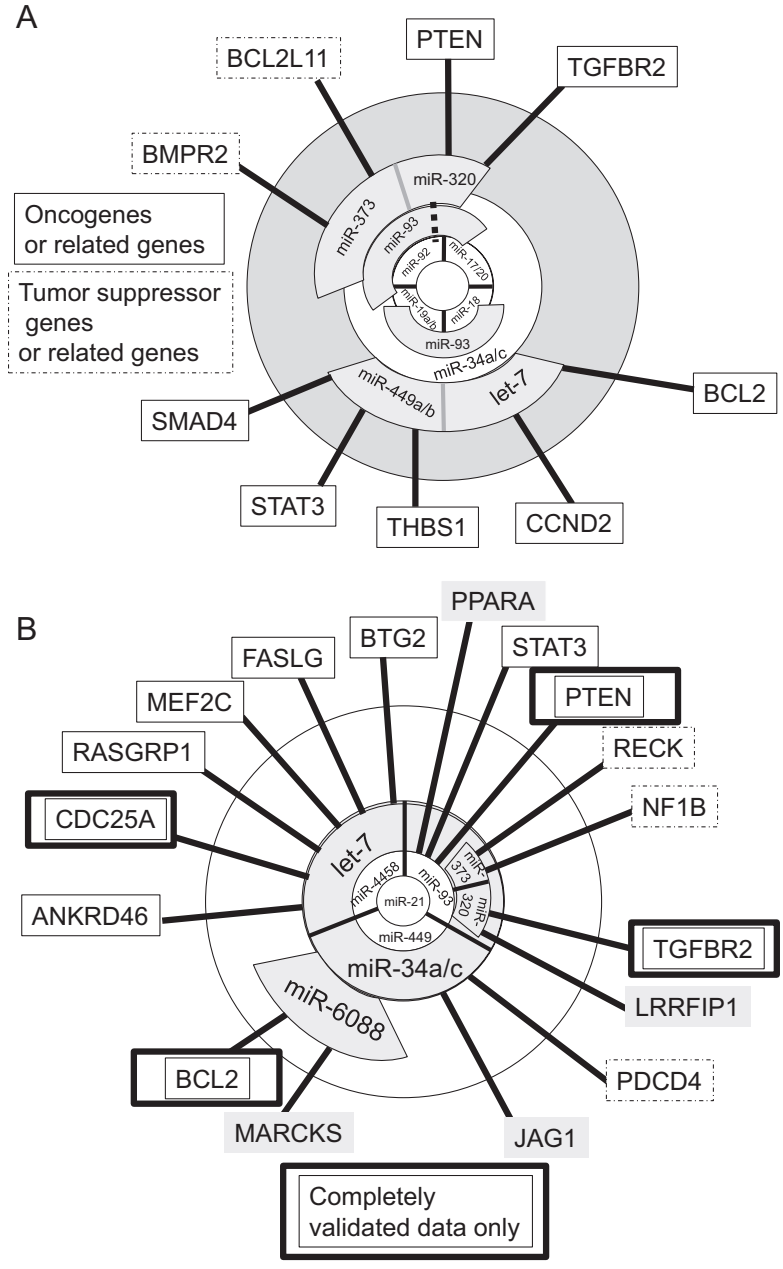

Fig. 4 The miRNA/target pathways and miRNA/miRNA interactions. miR-17/92 cluster/target (**A**) and miR-21/target (**B**) pathways and miRNA/miRNA association are depicted. miR-17/92 and miR-21 are bifunctional. For example, miR-17/92 is oncomir in lung cancer and is tumor suppressor in B-cell leukemia. miR-21 is oncomir in brain cancer and is tumor suppressor in breast cancer. Therefore, after this analysis, pathway analysis in each cell or organ is needed

foldings 50; window parameter default; the maximum interior/buldge loop size 30; the maximum asymmetry of an interior/buldge loop 30; the maximum distance No limit.

7. In the case of miR-21-5p, prediction data only shows the area under the curve (AUC) 0.53 in receiver operating characteristic (ROC) but by combined with validated data, AUC is increased up to 0.78. However, too much high AUC would prevent discovery of neo-network between miRNA/target. By using the top 5 of DNS, sensitivity is increased up to 0.961 and accuracy is increased up to 0.866. As the same that above AUC, high accuracy by high levels of limitation on Top category would kill the new putative target of miRNA which is no one isolates. In Fig. 4B, only four targets are predicted with high top score of DNS and validated data (bold squares).

References

1. Fujii YR (2017) The microRNA 2000: from HIV-1 to healthcare. Scientific Research Publishing, Paseo Segovia Irvine, CA
2. Tang S, WK W, Li X, Wong SH, Wong N, Chan MT, Sung JJ, Yu J (2016) Stratification of digestive cancers with different pathological features and survival outcomes by microRNA expression. Sci Rep 6:24466
3. Fujii YR (2010) RNA genes: retroelements and virally retroposable microRNAs in human embryonic stem cells. Open Virol J 4:63–75
4. Fujii YR (2013) The RNA gene information: retroelement-microRNA entangling as the RNA quantum code. Methods Mol Biol 936:47–67
5. Fujii YR (2009) Oncoviruses and pathogenic microRNAs in humans. Open Virol J 3:37–51
6. Stults DM, Killen MW, Pierce HH, Pierce AJ (2008) Genomic architecture and inheritance of human ribosome RNA gene clusters. Genome Res 18:13–18
7. Henras AK, Plisson-Chastang C, O'Donohue MF, Chakraborty A, Gleizes PE (2015) An overview of pre-ribosomal RNA processing in eukaryotes. RNA 6:225–242
8. Lafontaine DLJ, Tollervey D (2001) The function and synthesis of ribosomes. Nat Rev Mol Cell Biol 2:514–520
9. Luft F (2010) The rise of a ribosomopathy and increased cancer risk. J Mol Med 88:1–3
10. Montanaro L, Trere D, Derenzini M (2008) Nucleolus, ribosomes, and cancer. Am J Pathol 173:301–310
11. Brighenti E, Tere D, Derenzini M (2015) Targeted cancer therapy with ribosome biogenesis inhibitors: a real possibility? Oncotarget 6:38617–38627
12. Liang XH, Crooke ST (2011) Depletion of key protein components of the RISC pathway impairs pre-ribosomal RNA processing. Nucleic Acids Res 39:4875–4889
13. Caudron-Herger M, Pankert T, Seiler J, Nemeth A, Voit R, Grummt I, Rippe K (2015) Alu element-containing RNAs maintain nucleolar structure and function. EMBO J 34:2758–2774
14. Riffo-Campos A, Riquelme I, Brebi-Mieville P (2016) Tools for sequence-based miRNA target prediction: what to choose? Int J Mol Sci 17:E1987
15. Yoshikawa M, Osone T, Fujii YR (2016) MicroRNA memory I: the positive correlation between synergistic effects of microRNAs in cancer and a novel quantum scoring system. J Adv Med Phar Sci 5(4):1–16
16. Osone T, Yoshikawa M, Fujii YR (2016) MicroRNA memoryII: a novel scoring integration model for prediction of human disease by microRNA/microRNA quantum multi-interaction. J Adv Med Pharm Sci 5(4): 1–18
17. Yu H, Chen X, Lu L (2017) Large-scale prediction of microRNA-disease associations by combinatorial prioritization algorithm. Sci Rep 7:43792
18. You ZH, Huang ZA, Zhu Z, Yan GY, Li ZW, Wen Z, Chen X (2017) PBMDA: a novel and

effective path-based computational model for miRNA-disease association prediction. PLoS Comput Biol 13:e1005455

19. Yoshikawa M, Fujii YR (2016) Human ribosomal RNA-derived resident microRNAs as the transmitter of information upon the cytoplasmic cancer stress. Biomed Res Int 2016:7562085
20. Matamala N, Vargas MT, Gonzalez-Campora R, Minambres R, Anas JI, Menendez P, Andres-Leon E, Gomez-Lopez G, Yanowsky K, Calvete-Candenas J, Inglada-Perez L, Martinez-Delgado B, Benitez J (2015) Tumor microRNA expression profiling identifies circulating microRNAs for early breast cancer detection. Clin Chem 61:1098–1106

Chapter 13

In Vitro Methods for Analyzing miRNA Roles in Cancer Cell Proliferation, Invasion, and Metastasis

Jian Xu, Xuelian Xiao, and Daheng Yang

Abstract

MicroRNAs (miRNAs) are small noncoding, single-stranded RNAs consisting of 20–24 nucleotides (Bartel, Cell 116:281–297, 2004), which regulate target genes expression by interacting with 3′-untranslated regions (3′-UTRs) of target mRNAs, leading to translation repression or mRNA degradation (Filipowicz et al., Nat Rev Genet 9:102–114, 2008; Nilsen, Trends Genet 23:243–249, 2007). Accumulating evidence has elucidated them as oncogenes or tumor suppressors in cancers such as hepatocellular carcinoma, breast cancer, and lung cancer (Liu et al., Gastroenterology 136:683–693, 2009; Yu et al., Cell 131:1109–1123, 2007; Zhou et al., Sci Rep 7:42680, 2017; Iorio and Croce, Carcinogenesis 33:1126–1133, 2012). MiRNAs are involved in various biological processes, including cell proliferation (Liu et al., Mol Cancer Res 11:1314–1325, 2013), differentiation (Liu et al., Mol Cancer Res 11:1314–1325, 2013), apoptosis (Pan et al., Oncol Res 24:429–435, 2016), invasion and metastasis (Liu et al., Nat Commun 8:14270, 2017). Understanding the role of miRNAs in tumor gives new perspective on cancer diagnosis and therapy (Rupaimoole and Slack, Nat Rev Drug Discov 16:203–222, 2017; Berindan-Neagoe et al., CA Cancer J Clin 64:311–336, 2014). This chapter will focus on the in vitro methods for identifying miRNAs roles in cell proliferation, invasion, and metastasis in tumor development, which includes CCK-8 assay, Wound Healing assay, and Transwell assay.

Key words MiRNA, Proliferation, Invasion, Metastasis

1 Introduction

This chapter presents biochemical approaches for exploring effect of miRNA on tumor cell proliferation, invasion, and metastasis. We will take miR-145 as an example and the tumor cell line investigated here is lung adenocarcinoma cell line A549 [1], the methods are applicable to other miRNAs and tumor cell lines in general.

1.1 Up/Downregulate miR-145 Level by Transfection

A549 cells were maintained in DMEM media with 10% (v/v) fetal bovine serum (FBS). We plated A549 cells (3×10^5/well) in 2 mL complete media without antibiotics into a 6-well cell culture plate. You should adjust cell number seeded per well according to cell volume and cell growth rate. Gently rock the dish so that the cells

Shao-Yao Ying (ed.), *MicroRNA Protocols*, Methods in Molecular Biology, vol. 1733,
https://doi.org/10.1007/978-1-4939-7601-0_13,

are dispersed evenly. Incubate the cells at 37 °C in a 5% CO_2 incubator for 24 h.

Transfection should be performed when the cells grow to 70–80% confluence. Too high or too low cell density may reduce transfection efficiency. The transfection reagent we used was Lipofectamine 2000(Invitrogen), which is a proprietary formulation for transfecting nucleic acids into a wide range of eukaryotic cells. Positively charged liposomes form complexes with negatively charged phosphate group of nucleic acids, which are endocytosed by cells afterward.We used cy3 labeled miR-145 mimic or inhibitor (Ribobio) to upregulate or downregulate miR-145 level in A549. MiR-145 mimic/negative control (NC) or inhibitor/negative control (NC) as well as Lipofectamine 2000 were diluted in Opti-MEM (Gibco) media respectively. We optimized the final concentration of miR-145 mimic/NC for 100 nM and inhibitor/NC for 200 nM. Then gently mix the two prepared solutions above in 5 min, incubate for about 20 min at room temperature to ensure adequate adsorption of nucleic acids by liposomes. The complex keeps stable in 6 h. Media contains no FBS and antibiotics can be a replacement of Opti-MEM media in general. A great deal of negatively charged protein in serum may interfere with the adsorption of nucleic acids by cationic liposomes, thus affecting the efficiency of transfection. Moreover, antibiotics should not be added to the media since that liposomes increase permeability of cell membrane, otherwise it will increase cytotoxicity and decrease transfection efficiency as well. Then we added prepared solutions into the wells after cell washing. Five hours later, we changed the solutions into DMEM media with 10% FBS.

1.2 Detect miR-145 Expression Level by qRT-PCR

We observed the fluorescence in A549 cells at 48 h after transfection to assess the transfection efficiency (Fig. 1a). Then we harvested A549 cells and extracted total RNA using miRcute miRNA isolation kit (TIANGEN). Similar to conventional RNA extraction techniques, the cells are lysed and nucleic acid-protein is disassociated. Then RNA is absorbed by spin column which has stronger affinity for RNA especially for small RNA (<200 nt). We typically retrieve 5–15 μg RNA from 10^6 cells. The A260/A280 ratio was measured by protein nucleic acid spectrometer to detect the purity and concentration of the extracted RNA. cDNA was obtained by reverse transcriptionusing TaqMan microRNA reverse transcription kit (Applied Biosystems). The MiR-145 expression level was detected by qRT-PCR (Fig. 1b).

1.3 Detect Cell Proliferation by CCK-8 Assay

Cell viability was detected by CCK-8 assay. Compared with MTT assay, CCK-8 assay is more sensitive and less toxicity to cells. We collected A549 cells at 48 h after transfection, and seeded in quintuplicate at a density of 2000 cells/well in the 96-well plate.

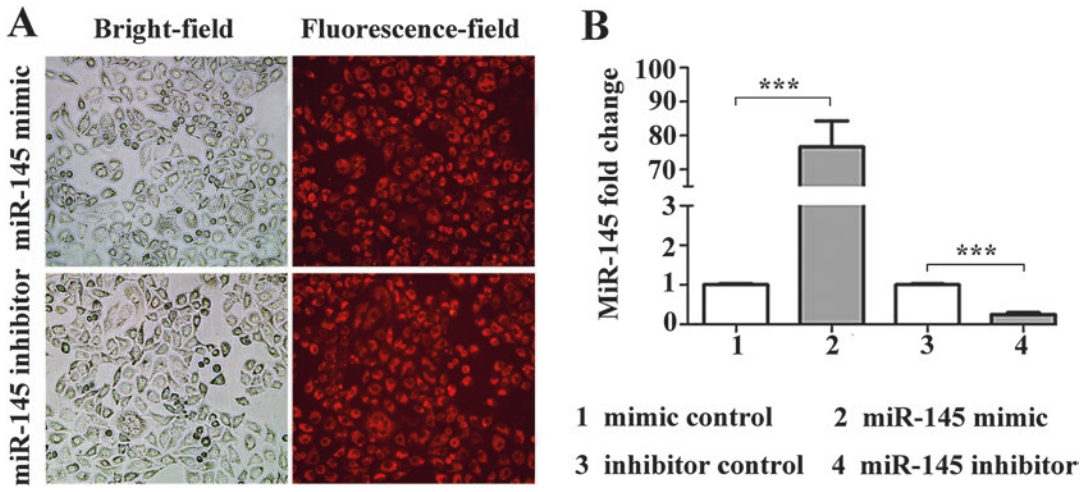

Fig. 1 MiR-145 expression levels in A549 cells transfected with miR-145 mimic/NC or inhibitor/NC labeled by cy3 fluorescent dye. (**a**) Images of A549 cells under light and fluorescence scope at 48 h after transfection. Red fluorescence was observed in vast majority of cells. (**b**) MiR-145 expression levels in A549 cells at 48 h after transfection were detected by qRT-PCR. Data is presented as mean ± SD. Each assay is repeated for tree times. MiR-145 level was significantly upregulated or downregulated by miR-145 mimic or inhibitor. ***$P < 0.001$, statistically significant

The number of cells seeded per well varies between different cell lines to keep cell growing in monolayer, which is favor of drug entering into cells. PBS or water would better be added into the wells on the edge of the plate rather than solutions in case of sample evaporating. 100 μL DMEM media diluted CCK-8 (Beyotime) (v/v = 10:1) solutions were added into the wells at regular intervals when the cells were well adherent. OD values were measured at detection wavelength of 450 nm after incubation for 0.5–4 h (Fig. 2). We set up blank control without A549 cells in parallel with experimental group.

1.4 Detect Cell Migration by Wound Healing Assay

Wound healing assay is a simple method imitating cell migration in vivo to some extent. It is based on observation of cells migration into a gap namely "wound" that is created on a cell monolayer. This assay is commonly used in combined with transfection to evaluate the effect of a certain gene on cell migration [2, 3]. We plated A549 cells (3×10^5/well) in the 6-well plate, then transfected with miR-145 mimic/NC or inhibitor/NC at second day. The 100% confluent cell monolayer formed at 48 h after transfection and we scraped it using a p200 pipet tip, then changed into FBS-free media for that obvious cell proliferation induced by FBS will give bias to assess cell migration. The image of initial (0 h) gap and residual width (48 h) after wounding were acquired and then the average distance was calculated by Image J software (Fig. 3).

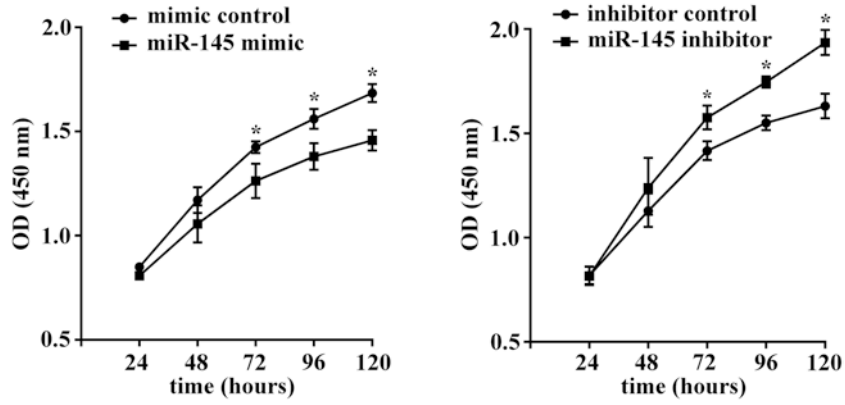

Fig. 2 The effect of miR-145 on A549 cells proliferation detected by CCK-8 assay. A549 cells were transfected with miR-145 mimic/NC or inhibitor/NC for 48 h, then the cells were seeded into a 96-well plate, CCK-8 was added into the cells at 24, 48, 72, 96 and 120 h, and OD values were measured accordingly. Data is presented as mean ± SD. Cells transfected with miR-145 mimic proliferated slower significantly than the control, while miR-145 inhibitor promoted cell proliferation. *$P < 0.05$, statistically significant

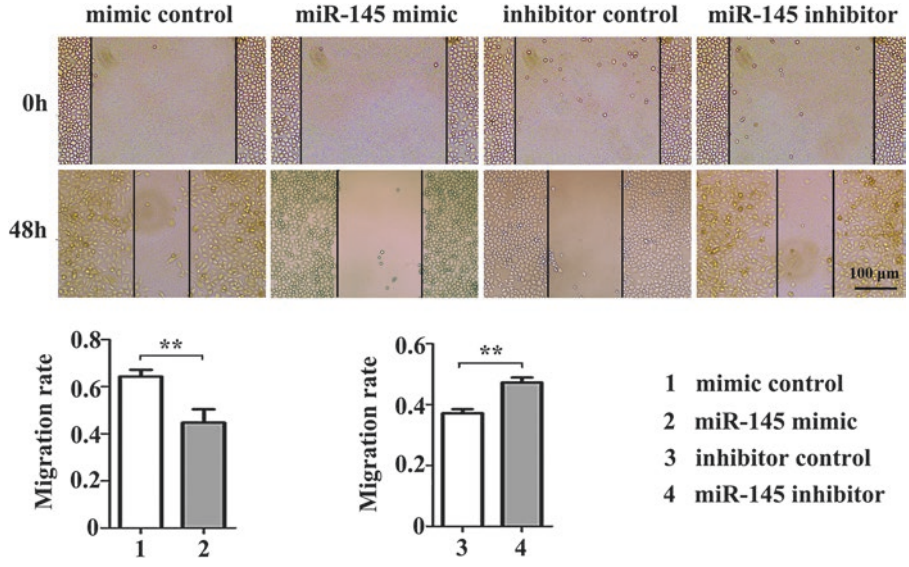

Fig. 3 The effect of miR-145 on A549 cells migration detected by wound healing assay. A549 cells were transfected with miR-145 mimic/NC or inhibitor/NC for 48 h, and images were acquired at 0 h and 48 h after wounding. Migration rate was calculated based on the average distance analyzed by Image J, take miR-145 mimic/NC group as an example, migration rate = $(Width_{0\,h} - Width_{48\,h})/Width_{0\,h}$. Data is presented as mean ± SD. Each assay is repeated for three times. Cells overexpressing miR-145 migrated slower than the control, on the contrary, cells transfected with miR-145 inhibitor had a higher migration rate compared with control. **$P < 0.01$, statistically significant

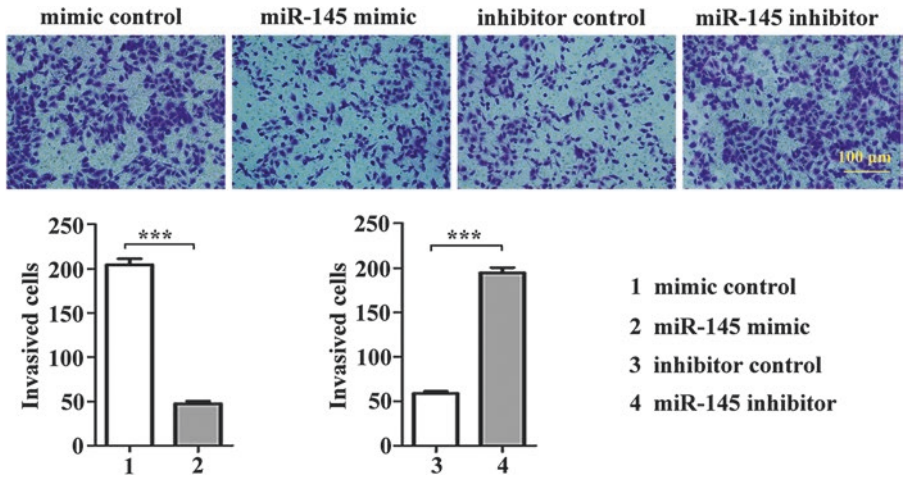

Fig. 4 The effect of miR-145 on A549 cells invasion detected by transwell assay. A549 cells were transfected with miR-145 mimic/NC or inhibitor/NC for 48 h, and images were acquired at 24 h after transfected cell seeding into inserts. Data is presented as mean ± SD. Each assay is repeated for three times. The ability of invasion in cells transfected with miR-145 mimic was stronger than the control, while transfection of miR-145 inhibitor contributed to the opposite. ***$P < 0.001$, statistically significant

1.5 Detect Cell Invasion by Transwell Assay

The device used in transwell assay mainly consists of a transwell chamber at bottom and a transwell insert inside a chamber. The bottom of the insert is a kind of membrane filters, polycarbonate membrane, for example, which is matrigel-coated manually to simulate the extracellular matrix (ECM) in vivo. Cells must secret matrix metalloproteinase (MMP) to go through the matrigel [4, 5]. 1×10^5 transfected A549 cells resuspended in FBS-free DMEM media were seeded into each insert, and 500 μL complete media was added into the lower chamber. Make the inoculated cell number similar between experiment group and control group as far as possible. Bubbles must be removed once it emerges between polycarbonate membrane and liquid level of the lower chamber. Cell number on the migrated side of membrane was counted at multiple views after cell washing and staining at 24 h (Fig. 4).

2 Materials

2.1 Up/Downregulate miR-145 Expression Level by Transfection

1. A549 cell line from the Cell Bank of the Chinese Academy of Sciences.
2. Fetal bovine serum (GibcoBRL, Gaithersburg, MD) and DMEM media (Hyclone, USA).
3. Antibiotics solution: 1,000,000 U Penicillin and 1,000,000 U Streptomycin diluted in 100 mL sterile ddH_2O.

4. PBS, pH 7.3 (Hyclone, USA).
5. Trypsin-EDTA Solution (Beyotime, China).
6. Cy3 labled miR-145 mimic/negetive control and miR-145 inhibitor/negetive control (Ribobio, China).
7. Lipofectamine® 2000 reagent (Invitrogen, USA).
8. Opti-MEM media (Gibco, USA).
9. Improved Neubauer Hemocytometer (CANY, China).
10. 6-well cell culture plate (Greiner, Germany).
11. Fluorescence microscope (Olympus, Japan).

2.2 Detect miR-145 Expression Level by qRT-PCR

2.2.1 Total RNA Extraction

1. MiRcute miRNA Isolation Kit(TIANGEN, China): lysate MZ, Buffer RW, Buffer MRD, RNase-Free ddH_2O, RNase-Free SpinColumns miRelute, RNase-Free Spin Columns miRspin, RNase-Free Centrifuge Tubes, RNase-Free Collection Tubes.
2. Chloroform.
3. Isopropyl alcohol.
4. Ethanol (95–100%).
5. Nucleic acid spectrometer (Pharmacia, USA).

2.2.2 Quantification of miRNA Expression Level by Real-Time PCR

1. TaqMan MicroRNA Reverse Transcription Kit (Applied Biosystems, USA): 10× RT buffer (10×), dNTPs (100 mM), RNase inhibitor (20 U/μL), Reverse transcriptase (50 U/μL) (Applied Biosystems, USA).
2. TaqMan MicroRNA Primers and Probes (Applied Biosystems, USA): 5× RT miR-145, 20× TM miR-145; TaqMan U6 snRNA Primers and Probes (Applied Biosystems, USA): 5× RT U6 snRNA, 20× TM U6 snRNA.
3. TaqMan Gene Expression Master Mix (20×) (Applied Biosystems, USA).
4. PCR amplification system 2720 (Applied Biosystems, USA), PCR amplification system 7500 (Applied Biosystems, USA).
5. 96-well reaction plate (AXYGENE, USA).

2.3 Detect Cell Proliferation by CCK-8 Assay

1. 96-well cell culture plate (Greiner, Germany).
2. Fetal bovine serum (GibcoBRL, Gaithersburg, MD) and DMEM media (Hyclone, USA).
3. PBS, pH 7.3 (Hyclone, USA).
4. Cell Counting Kit-8 reagent (Beyotime, China).
5. iMark Microplate Reader (Bio-Rad, USA).

2.4 Detect Cell Migration by Wound Healing Assay

1. 6-well cell culture plate or culture plates in other size (Greiner, Germany).
2. Ruler, marker pen.

3. P200 pipet tip.
4. PBS, pH 7.3 (Hyclone, USA).
5. DMEM media (Hyclone, USA).
6. Inverted microscope (Olympus, Japan).

2.5 Detect Cell Invasion by Transwell Assay

1. Transwell Permeable Supports (CORNING, USA): 6.5 mm Insert, 24-Well Plate, 8.0 μm Ploycarbonate Membrane.
2. MaxGel™ ECM mixture (Sigma, USA).
3. Fetal bovine serum (GibcoBRL, Gaithersburg, MD) and DMEM media (Hyclone, USA).
4. Cotton swabs.
5. PBS, pH 7.3 (Hyclone, USA).
6. 95% (v/v) ethanol.
7. 1% crystal violet: dilute 0.4 g crystal violet in 40 mL PBS.
8. Glass slides.
9. Inverted microscope (Olympus, Japan).

3 Methods

3.1 Up/Downregulate miRNA Expression Level by Transfection

1. Harvest cells in logarithmic growth phase and resuspend in media (*see* **Note 1**), count cell number with improved Neubauer hemocytometer under an optical microscope.
2. Plate A549 cells (3×10^5/well) in 2 mL complete media without antibiotics into the 6-well cell culture plate (*see* **Note 2**), gently rock the dish to make cells dispersed as evenly as possible instead of getting into a huddle. Adjust cell number seeded per well according to different cell volumes and cell growth rates or different size dishes.
3. Incubate at 37 °C in a 5% CO_2 incubator for 24 h so that the cells reach 70–90% confluence on the day of transfection.
4. Transfection reagents preparation:
   (a) Dilute miRNA mimic/control or inhibitor/control in 250 μL Opti-MEM media (*see* **Note 3**), pipet gently, then incubateat room temperature for 5 min.
   (b) Dilute Lipofectamine 2000 in 250 μL Opti-MEM media, pipet gently, then incubate at room temperature for 5 min.
   (c) Mix diluted miRNA mimic/control or inhibitor/control with diluted Lipofectamine 2000 respectively, pipet gently, then incubate at room temperature for 20 min.
5. Remove media from the wells and wash the cells with PBS twice, add 1.5 mL Opti-MEM media into each well.

6. Add the 500 μL prepared solutions into each well respectively, rock the dish back and forth gently to mix.
7. Change the media into complete media without antibiotics after 4–6 h.
8. Incubate at 37 °C in a 5% CO_2 incubator for 24–72 h.

3.2 Detect miRNA Expression Level by qRT-PCR

3.2.1 Total RNA Extraction

1. RNA extraction can be performed at 24–48 h after transfection referred to the manufacturer's instructions (*see* **Notes 4** and **5**).
   (a) For monolayer cells: discard the media and add 1 mL lysis MZ directly into the well per unit (10 cm^2) without washing and digestion, pipet to mix and ensure that no cell clumps are visible, then collect lysate in a RNA-free tube.
   (b) For cell suspension: centrifuge at 2100 rpm (400 × *g*) for 5 min, carefully remove all supernatant by aspiration, then disrupt cell clumps by adding 1 mL MZ per (1–5) × 10^6 cells, vortex vigorously for ~30 s to mix. Do not wash cells before adding Buffer MZ, otherwise mRNA will be degraded.
2. Place the tube containing the homogenate on the benchtop at room temperature for 5 min, to fully separate nucleic acids and protein.
3. Optional: centrifuge the lysate at 12,000 rpm (~13,400 × *g*) for 5 min at 4 °C to remove any particulate material when preparing samples with high content of fat, proteins, polysaccharides, or extracellular material. Then transfer the supernatant to a new tube.
4. Add 200 μL chloroform per 1 mL MZ into the tube and close the lid securely, vortex vigorously for 15 s, put it at room temperature for 5 min.
5. Centrifuge at 12,000 rpm (~13,400 × *g*) at 4 °C for 15 min. The sample is divided into three phases: an upper colorless, aqueous phase containing RNA; a white interphase; a lower organic phase. The volume of aqueous phase is around 50% of Buffer MZ added.
6. Transfer the supernatant to a new tube and be careful not to touch the interphase, measure the total volume of the supernatant during the process.
7. Add ethanol (95–100%) 1.5 times that of the supernatant volume into the tube, pipet or rotate to mix thoroughly (precipitate may form after addition of ethanol, but this will not affect the procedure).
8. Transfer the solution into a Spin Column miRspin (the volume transfered should be less than 700 μL each time), centrifuge at

12,000 rpm (~13,400 × *g*) at room temperature for 30 s, discard the flow-through in a collection tube. MiRspin can be used again until transfer of all the solution.

9. Add 500 μL Buffer MRD into the miRspin (ensure that alcohol has been added), close the lid, and incubate at room temperature for 2 min, centrifuge at 12,000 rpm (~13,400 × *g*) at room temperature for 30 s to remove residual protein, discard the flow-through.
10. Add 600 μL Buffer RW into the miRspin (ensure that alcohol has been added), close the lid, and incubate at room temperature for 2 min, centrifuge at 12,000 rpm (~13,400 × *g*) at room temperature for 30 s to wash the column, discard the flow-through.
11. Repeat **step 8**.
12. Centrifuge at 12,000 rpm (~13,400 × *g*) at room temperature for 1 min, discard the flow-through, put the miRspin at room temperature for ~2 min to dry it in case of residual buffer RW influencing on RT-PCR.
13. Transfer the miRspin into a new RNase-free centrifuge tube, add 30 ~100 μL RNase-free ddH_2O into the miRspin, close the lid and incubate at room temperature for 2 min, centrifuge at 12,000 rpm (~13,400 × *g*) at room temperature for 2 min to elute the RNA. Repeat it if you want to obtain more RNA.
14. Measure the concentration of RNA by a nucleic acid spectrometer and dilute RNA concentration into ~2 ng/μL. RNA solution should be stored at −70 °C avoiding repeated freeze-thaw cycles for ~1 year.

3.2.2 Quantification of miRNA by qRT-PCR

Reverse Transcription

1. Prepare RT master mix on ice. The components and volumes for each 15 μL reaction are listed below, which can be scaled up to the desired number of RT reactions.

Component	Volume
10× RT buffer	1.5 μL
dNTPs, 100 mM	0.15 μL
RNase inhibitor, 20 U/μL	0.19 μL
Reverse transcriptase, 50 U/μL	1 μL
Total RNA	10 ng
RNA-free ddH_2O	Add to 12 μL
Total volume	12 μL

2. Cap the tube, vortex gently, and centrifuge for 3–5 s to bring the solution to the bottom of the tube, then place on ice.

3. Take out RT primers, then vortex gently and centrifuge for 3–5 s.
4. Add 12 μL RT master mix above into a well of 96-well reaction plate for each 15 μL reaction, set up 2 replicates for each group.
5. Add 3 μL 5× RT primer which includes 1.5 μL 5× RT miR-145 and 1.5 μL 5× RT U6 snRNA into corresponding well, cap the wells securely.
6. Vortex gently, then centrifuge for 3–5 s, and make sure to get rid of bubbles by flipping gently, then place on ice.
7. Perform reverse transcription subjected to the following program of heating: 16 °C 30 min, 42 °C 30 min, 85 °C 5 min and hold at 4 °C.
8. Set the reaction volume to 15 μL.
9. Load the plate wells into the thermal cycler, then start the RT run.

Quantitative Real-Time PCR (qRT-PCR)

1. Prepare qPCR reaction mix. Pipet the following components into each well of 96-well reaction plate and set up 2 replicates for each group.

Component	Volume
TaqMan gene expression master mix (20×)	10 μL
Specific probe (miRNA or U6) (20×)	1 μL
cDNA	1.33 μL
Nuclease-free H_2O	7.67 μL
Total volume	20 μL

2. Cap the wells securely, vortex gently and centrifuge briefly, make sure to get rid of bubbles by flipping gently.
3. Perform qPCR subjected to the following program of heating: 50 °C 2 min for 1 cycle, 95 °C 10 min for 1 cycle, 95 °C 15 s, 60 °C 1 min for 45 cycle.
4. Load the plate wells into the thermal cycler, then start the qPCR run.
5. Data analysis: relative quantification is applied for calculating miRNA expression level using U6 as internal control. $\triangle Ct = Ct_{\text{miRNA}} - Ct_{\text{U6}}$, $\triangle\triangle Ct = \triangle Ct_{\text{miR-145}} - \triangle Ct_{\text{miR-NC,}}$ $2^{-\triangle\triangle Ct}$ represents the fold change of miRNA level.

3.3 Detect Cell Proliferation by CCK-8 Assay

1. Harvest cells at 48 h after transfection and plate 2000/well A549 cells in 100 μL complete median to 96-well cell culture plate (*see* **Note 6**), set up 5 × 5 repeats for each group and set up blank control without cells in parallel with experimental

group. Adjust the number of cells depending on different cell types.

2. Incubate at 37 °C in a 5% CO_2 incubator.
3. Add 10 μL CCK-8 reagent into each group which contains five repeats at 24 h (*see* **Note 7**), gently make it to avoid the occurrence of bubbles to prevent effect on OD value detection. Change fresh media for residual cells every 2 days.
4. Incubate at 37 °C in a 5% CO_2 incubator.
5. Detect the OD values at detection wavelength of 450 nm after incubation for 0.5–4 h using iMarkMicroplate Reader.
6. Repeat **steps 3–5** at 48, 72, 96, and 120 h.
7. Draw growth curves of cells based on OD values by software, GraphPad prism 6.

3.4 Detect Cell Migration by Wound Healing Assay

1. Mark the 6-well cell culture plate on the outer bottom of the dish as reference lines of the image capture, draw at least 5 lines in parallel every 0.5–1 cm.
2. Plate A549 cells (3×10^5/well) in a 6-well plate the day before transfection. Transfect the cells at second day according to the instructions presented in Subheading 3.1.
3. Incubate at 37 °C in a 5% CO_2 incubator for 24–48 h until the formation of 100% confluent cell monolayer.
4. Scratch the cell monolayer with the help of a ruler to create a "wound" vertical to reference lines using a p200 pipettip.
5. Wash the cells with PBS three times, rock the dish back and forth carefully to remove the cells scratched.
6. Capture the first image of the wound, refer to the marks on the dish.
7. Add FBS-free media into the well along the edge of it carefully, then incubate at 37 °C in a 5% CO_2 incubator for 6–72 h.
8. Capture a second image of the wound in the same field based on the reference lines in **step 5** at 6 h, 12 h, 24 h, 48 h, 72 h. Incubation time should be determined empirically based on different cell types, but time longer than 72 h is not recommended for that different rate of cell proliferation may contribute to bias of migration analysis.
9. Analyze the first and second images with software Image Jto calculate the average distance between cells and the migration rate.

3.5 Detect Cell Invasion by Transwell Assay

1. Matrigel preparation.
   (a) Dilute ECM mixture in media containing no FBS and antibiotics at a proportion of 1/9 (v/v), rotate to mix.

(b) Add 70 μL prepared solution into the bottom of insert attached to 24-well plate, gently make it to avoid producing bubbles.

(c) Incubate at 37 °C in a CO_2 incubator for 2–4 h until matrigel concretion.

2. Harvest cells at 48 h after transfection, add A549 cells (1×10^5/well) in 100–200 μL FBS-free media into the insert, set up 2 repeats for each group. Adjust the number of cells depending on invasion ability of different cell types or different size dishes.
3. Add 500 μL complete media into the lower chamber, put the insert in the chamber. Make sure the media touches the bottom of membrane and get rid of bubbles.
4. Incubate at 37 °C in a 5% CO_2 incubator for 12–48 h. Time for incubation various from different cell types.
5. Staining.

(a) Take the insert out of the chamber, remove matrigel and cells from the unmigrated side with cotton swabs gently (*see* **Note 8**), wash with PBS twice gently.

(b) Discard media in the lower chamber, then wash with PBS twice to remove unattached cells.

(c) Fix cells on the migrated side by steeping insert in 95% ethanol for 10–15 min, wash with PBS once, allow it to dry.

(d) Stain cells by soaking insert in 1% crystal violet solution for 15–20 min, allow the membrane to dry.

(e) Wash with PBS twice to remove excess stain, turn the insert upside-down and allow it to dry.

6. Put the insert on a glass slide, capture images under high power (×10) at 5–15 regular fields and calculate average number of invasive cells per HPF.

4 Notes

1. Tare care to keep cell culture in sterile conditions to avoid contamination.
2. To weaken cell toxic in transfection, antibiotics should not be added into media during the proceed of cell seeding to cell harvest.
3. As for transfection, one needs to optimize the final concentration of miRNA mimic or inhibitor and Lipofectamine 2000 referred to the manufacturer's instructions and continuing exploration as well.

4. Change your gloves regularly during RNA extraction, because bacteria carried by your skin may result in RNase contamination.
5. Use RNase-free materials including tubes and tips to isolate RNA.
6. Add PBS or water into the wells on the edge of 96-well plate instead of solutions in case of sample evaporating, when you detect cell proliferation by CCK-8 assay.
7. CCK-8 reagent can be added into media directly in general, but one needs to change fresh media after cell washing if the sample under test owns oxidizability and reducibility.
8. As for transwell assay, the cells on the unmigrated side of the membrane must be completely removed with cotton swabs.

Acknowledgment

This study was supported by the Key Laboratory of Laboratory Medicine of Jiangsu Province of China and a project funded by the Priority Academic Program Development of Jiangsu Higher Education Institutions. We are grateful to the technical support from the National Key Clinical Department of Laboratory Medicine of Jiangsu Province Hospital.

References

1. Mo D, Yang D, Xiao X, Sun R, Huang L, Xu J (2017) MiRNA-145 suppresses lung adenocarcinoma cell invasion and migration by targeting N-cadherin. Biotechnol Lett 39(5):701–710
2. Liu K, Xie F, Gao A, Zhang R, Zhang L, Xiao Z, Hu Q, Huang W, Huang Q, Lin B et al (2017) SOX2 regulates multiple malignant processes of breast cancer development through the SOX2/miR-181a-5p, miR-30e-5p/TUSC3 axis. Mol Cancer 16(1):62
3. Zhou R, Zhou X, Yin Z, Guo J, Hu T, Jiang S, Liu L, Dong X, Zhang S, Wu G (2016) MicroRNA-574-5p promotes metastasis of non-small cell lung cancer by targeting PTPRU. Sci Rep 6:35714
4. Jablonska-Trypuc A, Matejczyk M, Rosochacki S (2016) Matrix metalloproteinases (MMPs), the main extracellular matrix (ECM) enzymes in collagen degradation, as a target for anticancer drugs. J Enzyme Inhib Med Chem 31(sup1):177–183
5. Shields SE, Ogilvie DJ, McKinnell RG, Tarin D (1984) Degradation of basement membrane collagens by metalloproteases released by human, murine and amphibian tumours. J Pathol 143(3):193–197

Chapter 14

Isolation and Identification of Gene-Specific MicroRNAs

Shi-Lung Lin, Donald C. Chang, and Shao-Yao Ying

Abstract

Computer programming has identified hundreds of genomic hairpin sequences, many with functions yet to be determined. Because transfection of hairpin-like microRNA precursors (pre-miRNAs) into mammalian cells is not always sufficient to trigger RNA-induced gene silencing complex (RISC) assembly, a key step for inducing RNA interference (RNAi)-related gene silencing, we have developed an intronic miRNA expression system to overcome this problem by inserting a hairpin-like pre-miRNA structure into the intron region of a gene, and hence successfully increase the efficiency and effectiveness of miRNA-associated RNAi induction in vitro and in vivo. This intronic miRNA biogenesis mechanism has been found to depend on a coupled interaction of nascent messenger RNA transcription and intron excision within a specific nuclear region proximal to genomic perichromatin fibrils. The intronic miRNA so obtained is transcribed by type-II RNA polymerases, coexpressed within a primary gene transcript, and then excised out of the gene transcript by intracellular RNA splicing and processing machineries. After that, ribonuclease III (RNaseIII) endonucleases further process the spliced introns into mature miRNAs. Using this intronic miRNA expression system, we have shown for the first time that the intron-derived miRNAs are able to elicit strong RNAi effects in not only human and mouse cells in vitro but also in zebrafishes, chicken embryos, and adult mice in vivo. We have also developed a miRNA isolation protocol, based on the complementarity between the designed miRNA and its targeted gene sequence, to purify and identify the mature miRNAs generated. As a result, several intronic miRNA identities and structures have been confirmed. According to this proof-of-principle methodology, we now have full knowledge to design various intronic pre-miRNA inserts that are more efficient and effective for inducing specific gene silencing effects in vitro and in vivo.

Key words MicroRNA (miRNA) biogenesis, Gene cloning, RNA interference (RNAi), RNA-induced gene silencing complex (RISC), Asymmetric assembly, Zebrafish

1 Introduction

More than 90 intronic microRNAs (miRNA) have been identified using the bioinformatic approaches to date [1], but the functions of the vast majority of these intronic miRNAs remain unclear. According to the strictly expressive correlation of intronic miRNAs to their encoded genes, one may speculate that the levels of condition-specific, time-specific, and individual-specific gene expression are determined by interactions of distinctive miRNAs on single or

Shao-Yao Ying (ed.), *MicroRNA Protocols*, Methods in Molecular Biology, vol. 1733,
https://doi.org/10.1007/978-1-4939-7601-0_14,

multiple gene modulation. This interpretation accounts for more accurate expression of various genetic traits and any dysregulation of the interactions will thus result in genetic disorders. For instance, monozygotic twins frequently demonstrate slightly, but definitely distinguishing, disease susceptibility and physiological behavior. Such as, a long CCTG expansion in the intron 1 of a zinc finger protein ZNF9 gene has been correlated to type 2 myotonic dystrophy in either one of the twins with higher susceptibility [2]. Since the expansion motif often obtains high affinity to certain RNA-binding proteins, the resulting intron-derived expansion fragments may play an important role in this disease. Another more established example involving intronic expansion fragments in its pathogenesis is fragile X syndrome, which represents about 30% of human-inherited mental retardation. Intronic CGG repeat (rCGG) expansion in the 5′-UTR of *FMR1* gene is the causative mutation in 99% of individuals with fragile X syndrome [3]. *FMR1* encodes an RNA-binding protein, FMRP, which is associated with polyribosome assembly in an RNP-dependent manner and capable of suppressing translation through an RNAi-like pathway. FMRP also contains a nuclear localization signal (NLS) and a nuclear export signal (NES) for shuttling certain mRNAs between the nucleus and cytoplasm [4]. Jin et al. proposed an RNAi-mediated methylation model in the CpG region of *FMR1* rCGG expansion, which is targeted by a hairpin RNA derived from the 3′-UTR of the *FMR1* expanded allele transcript [3]. The Dicer-processed hairpin RNA triggers the formation of RNA-induced initiator of transcriptional gene silencing (RITS) on the homologous rCGG sequences and leads to heterochromatin repression of the *FMR1* locus. These examples suggest that natural evolution gives raise to more complexity and more variety of introns in higher animals and plants for coordinating their vast gene expression volumes and interactions; therefore, any dysregulation of miRNAs derivation from introns may thus lead to genetic diseases involving intronic expansion or deletion, such as myotonic dystrophy and fragile X mental retardation.

To understand the diseases caused by dysregulation of intronic miRNAs, an artificial expression system is needed to recreate the functions and mechanisms of the miRNAs involved in vivo. The same approach may be used to develop and test potential therapies for the diseases. Using artificial introns carrying hairpin-like miRNA precursors (pre-miRNA), we have successfully generated mature miRNAs with full function in triggering RNAi-like gene silencing in zebrafish [5]. We introduced hairpin-like pre-miRNAs into 2-week-old zebrafish larvae and successfully tested the processing mechanism and functional significance of different miRNA–miRNA* structures, using an intronic miRNA expression system reported previously [6, 7]. The pre-miRNA expression was driven by a cytomegalovirus (CMV) IE promoter, which has been established as a viable approach for manipulating RNA expression in

zebrafish [8]. Based on conventional reasoning, the stem-loop structure located in either end of the miRNA-miRNA* duplex should be equally cleaved by Dicer in order to form siRNA and hence functional bias would not be seen in pre-miRNAs with different stem-loop locations. However, we observed different gene silencing responses when comparing the transfection results from a pair of symmetric hairpin pre-miRNA constructs, as shown in Fig. 1a between 5′-miRNA*-stem-loop-miRNA-3′ (construct **#1**) and 5′-miRNA-stem-loop-miRNA*-3′ (construct **#2**). Although both pre-miRNAs contained the same perfectly matched siRNA-like duplex in the stem-arm region, different kinds of mature miRNAs were identified, suggesting that the stem-loop structures of pre-miRNAs can affect Dicer recognition and result in different siRNA products. Therefore, this type of stem-loop asymmetry leads to more preferential strand selection of the mature miRNA for more effective RISC assembly.

To determine the structural preference of the hairpin pre-miRNAs, we have isolated the small RNAs in zebrafish using *mir*Vana miRNA isolation columns (Ambion, Austin, TX) and then precipitated all potential miRNAs complementary to the target *EGFP* region, using latex beads containing the target RNA sequence. The designed pre-miRNA constructs were directed against the target green fluorescent protein (*EGFP*) mRNA sequence nucleotides 280–302 in the transgenic (*UAS:gfp*) zebrafish, of which the *EGFP* expression was constitutively driven by the β-actin promoter in almost all cells. As shown in Fig. 1b, two major miRNA identities were verified to be active (gray-shading sequences). Because of the fast turn-over rate of small RNAs in vivo [9, 10], the shorter miR-EGFP(282/300) may be a degraded form of the miR-EGFP(280–302). The first 5′-cytosine (labeled by an asterisk *) of the miR-EGFP(280–302) was not included in the designed target region and probably provided by the original intron sequence because the cytosine (C*) is the most adjacent nucleotide close to the 5′-end of the designed pre-miRNA in the intron. Because the miR-EGFP(280–302) miRNA was detected only in the zebrafish transfected with the 5′-miRNA-stem-loop-miRNA*-3′ construct (**#2**), the stem-loop of the #2, rather than the #1, pre-miRNA is able to determine the correct anti-sense *EGFP* sequence for effective miRNA-associated RISC (miRISC) assembly. Given that Dicer cleavage resulted in different mature miRNAs generated from two symmetric pre-miRNA constructs with the same siRNA stem arm (Fig. 2), switching the pre-miRNA stem-loop location may change the cleavage orientation in Dicer, so as to make different siRNAs. One possibility for this preference is that the structure and/or sequence of the stem-loop preferably facilitate miRNA maturation from one orientation than the other. Alternatively, the stem-loop may change the Dicer recognition and, thus, may generate differently asymmetric profiles to the

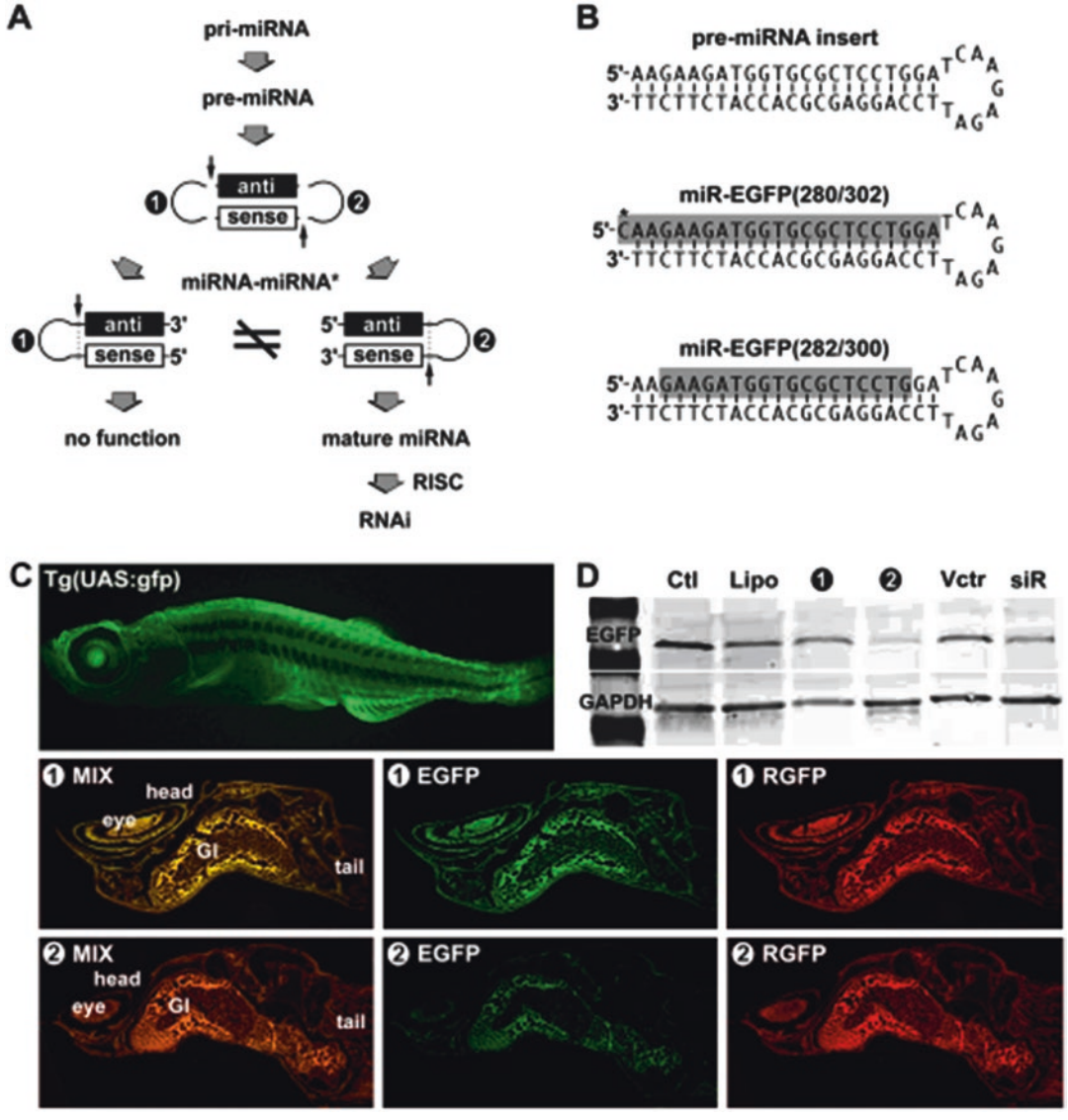

Fig. 1 Structural preference of miRNA–miRNA* asymmetry in miRISC in vivo. (**a**) We have demonstrated that only the **#2** construct was used in effective miRISC assembly. Because a mature miRNA is defined to be complementary to its targeted messenger RNA, the label "anti" (anti-sense; black bar) refers to the miRNA and the "sense" (white bar) refers to its complementarity, miRNA*. (**b**) Two designed mature miRNA identities were found only in the **#2**-transfected zebrafishes, namely miR-EGFP(280/302) and miR-EGFP(282/300). (**c**) In vivo gene silencing efficacy was only observed in the transfection of the **#2** pre-miRNA, but not the **#1** construct. Since the mixture color of EGFP and RGFP displayed more red than green (as shown in deep orange), the expression level of target EGFP (green) was significantly reduced in #2-transfected fishes, while miRNA indicator RGFP (red) was evenly present in all transfections. A strong strand selection was observed in favor of the 5′-stem strand of the designed pre-miRNAs in RISC. (**d**) Western blot analysis of protein expression levels confirmed the specific EGFP silencing result of (**c**). No detectable gene silencing was observed in fishes without (Ctl) and with liposome only (Lipo) treatments. The transfection of either a U6-driven siRNA vector (siR) or an empty vector (Vctr) without the designed pre-miRNA insert resulted in no gene silencing significance

Fig. 2 Bias of miRNA–miRNA* asymmetry in miRISC assembly in vivo. Different preferences of RISC assembly were observed in the transfections of 5′-miRNA*-stem-loop-miRNA-3′ (**#1**) and 5′-miRNA-stem-loop-miRNA*-3′ (**#2**) pre-miRNA constructs in zebrafish, respectively. Based on the assembly rule of siRISC, the processing of both **#1** and **#2** pre-miRNAs should result in the same siRNA duplex for RISC assembly; however, the present experiments demonstrated that only the **#2** construct was able to silence target *EGFP*. An effective mature miRNA, namely miR-EGFP(280/302), was detected in the **#2**-transfected zebrafishes directed against target *EGFP mRNA*, whereas transfection of the **#1** construct produced another different miRNA, miR*-EGFR(301–281), which was partially complementary to the miR-EGFP(280/302) and possessed no gene silencing effects on *EGFP* expression

pre-miRNA stem-arm. In either way, the cleavage site of Dicer in the pre-miRNA stem arm determines the strand selection of a mature miRNA, and the pre-miRNA stem-loop likely functions as a determinant for the recognition of the special cleavage site. Based on this proven principle of the intronic pre-miRNA structures, we are now able to design correct and effective pre-miRNA inserts for the intronic miRNA expression systems.

2 Materials

2.1 Small RNA Isolation

1. *mir*Vana miRNA isolation kit (Ambion, Austin, TX).
2. Incubation chamber: 65 and 4 °C.
3. 1× nuclease-free hybridization buffer: 100 mM KOAc, 30 mM HEPES KOH, 2 mM MgOAc, pH 7.4 at 25°C (*see* **Note 1**).
4. Microcentrifuge: 17,900 × *g* (*see* **Note 2**).

2.2 Complementary Affinity Precipitation and Poly(A) Tailing

1. Synthetic 5′-fluorescein-linked oligonucleotides homologous to the targeted gene sequence (Sigma-Genosys), e.g., as shown here a synthetic anti-EGFP oligonucleotide 5′-fluorescein-AGAAGATGGT GCGCTCCTGG A-3′ (100 pmol/μL in DEPC-treated ddH_2O).
2. Anti-fluorescein monoclonal antibody, biotin-conjugated (Invitrogen, Carlsbad, CA).
3. Streptavidin bead suspension (Invitrogen).
4. Incubation shaker: 25°C, 120 rpm.
5. Incubation chamber: 65 and 4 °C.

6. Microcentrifuge: 17,900 × *g*.
7. DEPC-treated H_2O: Stir double distilled water with 0.1% DEPC for longer than 12 h and autoclave twice at 120 °C under approx 1.2 kgf/cm^2 for 20 min twice.
8. RNA tailing: Poly(A) tailing kit (Ambion, Austin, TX).

2.3 Complementary DNA Generation and Polyacrylamide Gel Purification

1. Oligo$(dT)_{20}$ primer: 5′-dephosphorylated TTTTTTTTTT TTTTTTTTTT-3′ (100 pmol/μL in DEPC -treated ddH_2O).
2. 100 U/μL SuperScript II MMLV reverse transcriptase and 5× reverse transcription buffer (250 mM Tris–HCl, pH 8.3, 250 mM KCl, 15 mM $MgCl_2$, and 10 mM dithiothreitol).
3. Reverse transcription mix: 8 μL DEPC-treated ddH_2O, 6 μL of 5× reverse transcription buffer, 2 μL of 10 mM deoxyribonucleoside triphosphate mix (10 mM each for deoxyadenosine triphosphate, deoxyguanosine triphosphate, deoxycytosine triphosphate, and deoxythymidine triphosphate), 1 μL of 25 U/μL RNase Inhibitor, 2 μL SuperScript II MMLV reverse transcriptase; prepare the reaction mix just before use.
4. Incubation chamber: 94, 65, 42, and 4 °C.
5. Electrophoresis system for polyacrylamide gel (Bio-Rad, Hercules, CA).
6. 15% Tris-borate-ethylenediaminetetraacetic acid/urea polyacrylamide gel for oligonucleotides (Bio-Rad).
7. Mini whole gel eluter (Bio-Rad).

3 Methods

3.1 Small RNA Isolation

The small intracellular RNAs (fewer than 200 nucleotides) are isolated and collected on a glass-fiber filter using the *mir*Vana miRNA isolation kit. These small RNAs include 5S ribosomal RNA, transfer RNA, small nucleolar RNA (snoRNA), small nuclear RNA, small mitochondrial noncoding RNA (smnRNA), miRNA, and probably siRNA.

1. Small RNA isolation: apply 100 to 10^7 cells to a *mir*Vana miRNA isolation reaction, following the manufacturer's protocol. Collect the final RNAs in 30 μL of 1× nuclease-free hybridization buffer.

3.2 Complementary Affinity Precipitation and Poly(A) Tailing

Small RNAs complementary to the target sequence are recovered by binding to fluorescein-linked target oligonucleotides and then precipitated by further binding to biotin-conjugated anti-fluorescein monoclonal antibodies and streptavidin beads. The resulting small RNAs are protected by adding poly(A) tails in their 3′-termini using *E coli* poly(A) polymerase I.

1. Complementary annealing: Add 2 μL of synthetic 5′-fluorescein-linked oligonucleotides to the isolated small RNAs and mix well. Incubate the mixture in an incubation chamber at 65 °C for 5 min, and then switch the mixture to an incubation shaker at 25 °C for 30 min.
2. Precipitation: Add 10 μL of the biotin-conjugated anti-fluorescein monoclonal antibodies to the mixture and incubate the mixture in an incubation shaker at 25 °C for 30 min. Add 10 μL of streptavidin bead suspension to the mixture and continue to incubate the mixture in an incubation shaker at 25 °C for 30 min. Precipitate the bound RNAs by centrifugation at 17,900 × *g* for 10 min and discard the supernatant. Dissolve the pellet in 10 μL of DEPC-treated ddH_2O.
3. Poly(A) RNA tailing: Add poly(A) tails to the 3′-termini of the purified RNAs using *E. coli* poly(A) polymerase I, following the manufacturer's suggestions.
4. Reaction stop: Heat the reaction at 94 °C for 2 min and then cool on ice immediately. Remove the beads by centrifugation at 17,900 × *g* for 10 min and transfer the supernatant to a clean new tube.

3.3 Complementary DNA Generation and Polyacrylamide Gel Purification

The starting material is approx. 1 μg of the poly(A)-tailed small RNAs. The complementary DNAs are synthesized by reverse transcription from the poly(A)-tailed small RNAs with the oligo$(dT)_{20}$ primer. The use of MMLV reverse transcriptase also adds a short poly(dC) tail in the 3′-end of each cDNA sequence, which is used for DNA sequencing in conjunction with a poly$(dG)_{10}$ primer.

1. Primer annealing: Mix 10 μL of the RNA supernatant with 1 μL oligo$(dT)_{20}$ primer, heat to 65 °C for 5 min to minimize secondary structures, and then cool on ice.
2. Complementary DNA (cDNA) synthesis: Add 14 μL of the reverse transcriptase mix to the above hybrids, heat to 42 °C for 20 min, and then cool on ice.
3. Denaturation of RNA-cDNA hybrids: Heat the reaction at 94 °C for 2 min and then cool on ice immediately.
4. Polyacrylamide gel electrophoresis: Load and run the denatured cDNAs on a 15% Tris-borate-thylenediaminetetraaetic acid/urea gel and recover each cDNA band using the mini whole gel eluter system, following the manufacturer's suggestions. The cDNAs so obtained are ready for DNA sequencing using the poly$(dG)_{10}$ primer. The resulting cDNA sequences are perfectly complementary to the miRNAs, from which the cDNAs are reverse-transcribed (*see* **Note 3**).

4 Notes

1. Autoclave the 1× hybridization buffer twice at 120 °C under about 1.2 kgf/cm^2 for 20 min.
2. Relative centrifugal force (RCF) (g) = $(1.12 \times 10^{-6}) \times (\text{rpm})^2 \times r$, where r is the radius in centimeters measured from the center of the rotor to the middle of the spin column, and rpm is the speed of the rotor in revolutions per minute.
3. Although most of the native pre-miRNAs contain mismatched area in their stem-arms, it is not necessary for us to construct an imperfect paired stem-arm in order to trigger RNAi-related gene silencing. Previous studies have demonstrated that a mature miRNA can be generated by placing a perfectly matched siRNA duplex in the miR-30 pre-miRNA structure [11, 12]. Furthermore, there are many genes not subjected to the regulation of native miRNAs, in particular, *EGFP*, which can be otherwise silenced by intracellular transfection of the pre-miRNA containing a perfectly matched stem-arm construct. Therefore, we define a mature miRNA based on its biogenetic function and mechanism, rather than the structural complementarity of its precursor. In this view, any small hairpin RNA can be seen as a pre-miRNA if a mature miRNA is successfully processed from the small hairpin RNA and further assembled into miRISC for target gene silencing.

References

1. Rodriguez A, Griffiths-Jones S, Ashurst JL, Bradley A (2004) Identification of mammalian microRNA host genes and transcription units. Genome Res 14:1902–1910
2. Liquori CL, Ricker K, Moseley ML, Jacobsen JF, Kress W, Naylor SL, Day JW, Ranum LPW (2001) Myotinic dystrophy type 2 caused by a CCTG expansion in intron 1 of ZNF9. Science 293:864–867
3. Jin P, Alisch RS, Warren ST (2004) RNA and microRNAs in fragile X mental retardation. Nat Cell Biol 6:1048–1053
4. Eberhart DE, Malter HE, Feng Y, Warren ST (1996) The fragile X mental retardation protein is a ribonucleoprotein containing both nuclear localization and nuclear export signals. Hum Mol Genet 5:1083–1091
5. Lin SL, Chang D, Ying SY (2005) Asymmetry of intronic pre-miRNA structures in functional RISC assembly. Gene 365:32–38
6. Lin SL, Chang D, Wu DY, Ying SY (2003) A novel RNA splicing-mediated gene silencing mechanism potential for genome evolution. Biochem Biophys Res Commun 310:754–760
7. Lin SL, Ying SY (2004) Novel RNAi therapy – intron-derived microRNA drugs. Drug Des Rev 1:247–255
8. Verri T, Argenton F, Tomanin R, Scarpa M, Storelli C, Costa R, Colombo L, Bortolussi M (1997) The bacteriophage T7 binary system activates transient transgene expression in zebrafish (Danio Rerio) embryos. Biochem Biophys Res Commun 237:492–495
9. Tourriere H, Chebli K, Tazi J (2002) mRNA degradation machines in eukaryotic cells. Biochimie 84:821–837
10. Wilusz CJ, Wilusz J (2004) Bringing the role of mRNA decay in the control of gene expression into focus. Trends Genet 20:491–497
11. Lee Y, Ahn C, Han J, Choi H, Kim J, Yim J, Lee J, Provost P, Radmark O, Kim S, Kim VN (2003) The nuclear RNase III Drosha initiates microRNA processing. Nature 425:415–419
12. Boden D, Pusch O, Silbermann R, Lee F, Tucker L, Ramratnam B (2004) Enhanced gene silencing of HIV-1 specific siRNA using microRNA designed hairpins. Nucleic Acids Res 32:1154–1158

Chapter 15

Comprehensive Measurement of Gene Silencing Involving Endogenous MicroRNAs in Mammalian Cells

Masashi Fukuoka and Hirohiko Hohjoh

Abstract

MicroRNAs (miRNAs) are functional small noncoding RNAs that work as mediators in gene silencing and that play important roles in gene regulation. A number of miRNAs have been found and their expression profiles have been examined by means of various microarray systems and real-time polymerase chain reaction (PCR) systems. Conventional microarrays as well as real-time PCR are able to detect existing miRNAs, in which inactive miRNAs that hardly contribute to gene silencing may be also contained. Here, we describe a comprehensive miRNA bioassay system with reporter genes for the detection of active miRNAs that are present in the RNA-induced silencing complexes, and actually working as mediators in gene silencing.

Key words Active miRNAs, Comprehensive bioassay, Luciferase reporter gene, psiCHECK2 vector, Heat shock

1 Introduction

MicroRNAs (miRNAs) are 21~23-nucleotide-long small noncoding RNAs that are processed from longer (initial) transcripts by digestion with RNase III enzymes, Drosha in the nucleus, and Dicer in the cytoplasm. The processed, or matured, miRNA is incorporated into the RNA-induced silencing complex (RISC) and functions as a mediator in gene silencing (review articles [1–3]). MicroRNAs play important roles in gene regulation by inhibiting translation of messenger RNAs (mRNAs) that are partially complementary to the miRNAs, and by digestion of mRNAs that are nearly complementary to the miRNAs, or RNA interference (RNAi); and such a gene regulation involving miRNAs appears to contribute to various vital functions and phenomena such as cell proliferation, differentiation, development, and senescence [1–6].

A number of miRNA genes have been found in animals and plants [see the microRNA database (miRBase): http://www.mirbase.org/

Shao-Yao Ying (ed.), *MicroRNA Protocols*, Methods in Molecular Biology, vol. 1733,
https://doi.org/10.1007/978-1-4939-7601-0_15,

index.shtml]. Most of miRNA genes are expressed by RNA polymerase II [7], and expression profiles of miRNAs have been examined by using a conventional array system with capture probes for miRNAs and by reverse transcription quantitative polymerase chain reaction (RT-qPCR) with specific primers and probes. Many studies exhibited tissue- and stage-specific miRNA expression patterns [8–14], and such a specific expression of miRNAs suggests that they may be capable of becoming useful biomarkers.

Conventional microarrays and RT-qPCR are capable of detecting miRNAs that exist on-site, but not capable of discriminating inactive miRNAs from active miRNAs that are indeed working as mediators in gene silencing. It may be of importance to see the real nature of active miRNAs associated with various vital functions. In this chapter, we describe a comprehensive miRNA bioassay using reporter genes for the detection of active miRNAs that are functioning as mediators in cells, and provide an example of investigation of active miRNAs under heat-shock conditions by using the assay system [15].

2 Materials

2.1 Construction of Reporter Genes

1. psiCHECK™-2 Vector (Promega, Fitchburg, WI, USA).
2. Chemically synthesized oligonucleotide DNAs directed against miRNAs (Sigma-Aldrich, St. Lois, MO, USA).
3. 10× annealing buffer [100 mM Tris–HCl (pH 8.0), 10 mM EDTA, 1 M NaCl].
4. Restriction enzymes: *Xho*I (Nippon gene, Tokyo, Japan), *Spe*I (Nippon gene), *Nhe*I (Nippon gene), and *Pme*I (New England Biolabs, Ipswich, MA, USA).
5. 2× Ligation Mix (Nippon gene).
6. JM109 Competent Cells, >10^8cfu/μg (Promega).
7. S.O.C. Medium (Thermo Fisher Scientific, Waltham, MA, USA).
8. LB-agar plates containing 100 μg/mL ampicillin.
9. LB media containing 60 μg/mL ampicillin.
10. Wizard® SV Gel and PCR Clean-Up System (Promega).
11. PureYield™ Plasmid Miniprep System (Promega).
12. Agarose [Agarose ME (Iwaikagaku, Tokyo, Japan) was used in our experiment.].
13. 1× Tris-Acetate EDTA (TAE) buffer [50× TAE (Bio-Rad, Hercules, CA, USA) was diluted and used in our experiment.].
14. Ethidium bromide.

15. λ-Hind III digest (TAKARA BIO, Kusatsu, Shiga, Japan) as a DNA marker.
16. T7 EEV promoter primer (Promega).

2.2 Cell Culture

1. HeLa cells.
2. T75 cell culture flasks (Greiner bio-one, Kremsmünster, Austria).
3. Nunc™ Edge 96-Well Plate, sterile (Thermo Fisher scientific) (*see* **Note1**).
4. D-MEM(High Glucose) with L-Glutamine, Phenol Red and Sodium Pyruvate (Wako, Osaka, Japan) supplemented with 10% fetal bovine serum (Thermo Fisher scientific), 100 units/mL penicillin, and 100 μg/mL streptomycin (Wako).
5. 0.25% Trypsin-EDTA solution (Sigma-Aldrich).
6. D-PBS (−) (Wako).

2.3 Transfection of Reporter Plasmids

1. Lipofectamine® 2000 Transfection Reagent (Thermo Fisher scientific).
2. Opti-MEM® I Reduced Serum Medium (Thermo Fisher scientific).
3. UltraPure™ DNase/RNase-Free Distilled Water (Thermo Fisher scientific).
4. 96-well PCR plates [BMPCR-96-C PCR plates (BM-Bio, Tokyo, Japan) were used in our experiment.].
5. 8-strip PCR tube cap [PCR-8C (BM-Bio) caps were used in our experiment].
6. Reagent reservoirs.

2.4 Dual Luciferase Reporter Assay

1. Dual-Luciferase® Reporter Assay System (Promega).
2. Plate shaker [A MS3 digital shaker (IKA, Staufen im Breisgau, Germany) was used in our experiment.].
3. White 96-well plates [Nunc™ F96 MicroWell™ Black and White Polystyrene Plates (Thermo Fisher scientific) were used in our experiment].
4. Luminomer [A Fusion Universal Microplate Analyzer (Perkin Elmer, Waltham, MA, USA) was used in our experiment].

3 Methods

3.1 Construction of Reporter Plasmids

We used the psiCHECK™-2 vector (promega) carrying the *Renilla* and *Photinus luciferase* genes for the construction of reporter plasmids in our assay for miRNAs (Fig. 1). The target sequences of miRNAs of interest were chemically synthesized and inserted into

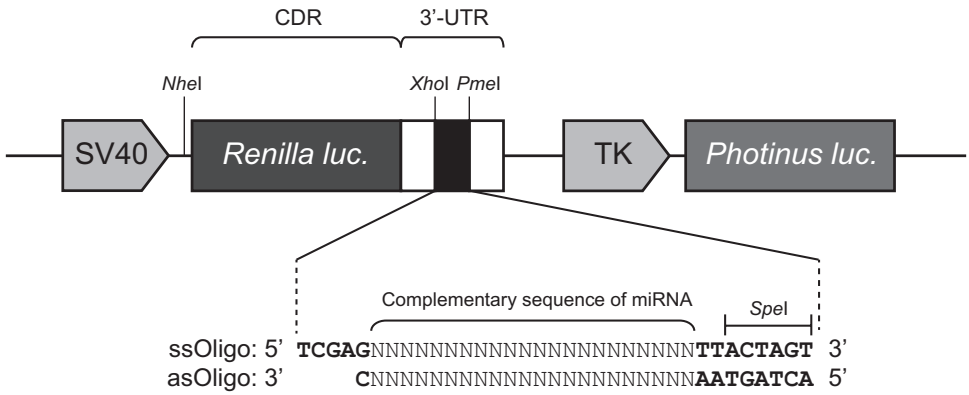

Fig. 1 Schematic drawing of constructed reporter plasmid. Reporter plasmids were constructed with the psi-CHECK™-2 vector by inserting synthetic oligonucleotide duplexes directed to miRNAs of interest into the 3′-UTR of the *Renilla luciferase* gene. Target sequences of miRNA are indicated by N, and the sequence in the sense-strand (indicated by N in ssOligo) is corresponding to the complementary sequence of a miRNA of interest. The inserted oligoDNA duplexes carry the *Spe*I restriction enzyme site for judgment of proper clones, and possess a cohesive and a blunt ends matched to the *Xho*I and *Pme*I digested ends, respectively. The SV40 and TK promoters and the *Photinus luciferase* gene as a control reporter gene are indicated. CDR: coding region. When the reporter plasmids are introduced into mammalian cells, both the reporter genes in the plasmids are expressed. If miRNAs function in cells, the *Renilla luciferase* transcripts carrying the target sequences of the miRNAs should be degraded by a strong gene silencing, or RNAi. The *Photinus luciferase* transcripts that are simultaneously expressed would be free from such a gene silencing and become a control for normalization of the target *Renilla luciferase*

the 3′-untranslated region (UTR) of the *Renilla luciferase* gene. The *Renilla luciferase* mRNAs carrying the target sequences of miRNAs as well as the *Photinus luciferase* mRNAs (as a control) were expressed in cells after transfection of the reporter plasmids. When miRNAs of interest were present in the cells and working as mediators in gene silencing, the *Renilla luciferase* mRNAs carrying the targets of the miRNAs should be degraded by a strong gene silencing, or RNA interference (RNAi), thereby resulting in a decrease in the level of the *Renilla* luciferase activity equal to its protein level. The *Photinus luciferase* mRNAs and proteins, on the other hand, would be expressed without suppression, and used as a control for normalization of the *Renilla luciferase* expression. We constructed such reporter plasmids for the detection of 143 miRNAs [15].

3.1.1 Design of Target Sequences of miRNAs

1. Based on the miRbase (http://www.mirbase.org/), a miRNA database, target sequences for miRNAs of interest are designed. The designed sequences are as follows:

   Sense-strand: 5′-**TCGAG**NNNNNNNNNNNNNNNNNNNN**TTACTAGT**-3′.

   Antisense-strand: 5′-**ACTAGTAA**NNNNNNNNNNNNNNNNNNNN**C**-3′.

Note that the sequence indicated by N in the sense-strand is the complementary sequence of miRNA of interest.

2. Chemically synthesize sense and antisense oligonucleotide DNAs of the designed target sequences (*see* **Note 2**).

3.1.2 Annealing

1. Mix the following reagents in a 0.5 mL tube:
   (a) 1 μL of 10× annealing buffer.
   (b) 1 μL of 100 μM sense-strand oligoDNA.
   (c) 1 μL of 100 μM antisense-strand oligoDNA.
   (d) 7 μL of distilled water (10 μL in total).
2. Heat-denature at 80 °C for 5 min, and anneal at room temperature over 30 min. Store at 4 °C.
3. The resultant (annealed) double-strand oligoDNAs have a cohesive *Xho*I end and a blunt end, and also generate the *Spe*I site that is absent in the psiCHECK™-2 vector (Fig. 1).

3.1.3 Preparation of Reporter Plasmids

1. Prepare 50 μL of reaction mix as follows:
   (a) 5 μL of 10× Restriction enzyme buffer.
   (b) 1 μL of the psiCHECK™-2 vector (1 μg/μL).
   (c) 42 μL of distilled water.
   (d) 1 μL of *Xho*I (5–20 units/μL).
   (e) 1 μL of *Pme*I (10 units/μL).
2. Incubate at 37 °C for 6 h~overnight.
3. Electrophoretically separate digested vectors on 1% agarose gels in 1× TAE buffer (*see* **Note 3**).
4. Cut a band containing the vector DNA fragment out of the gels after ethidium bromide staining.
5. Purify the DNA fragment by a Wizard® SV Gel and PCR Clean-Up System according to the manufacturer's instructions (Promega).
6. Measure the concentration of the purified vector fragment. Store at 4 °C or −20 °C.

3.1.4 Ligation, Transformation, Isolation Plasmids and Check of Insertion

1. Prepare 6 μL of ligation mix in a 0.5 mL tube as follows:
   (a) 2 μL of the purified vector DNA fragment (≈10 ng/μL).
   (b) 1 μL of the annealed (double-stranded) target oligoDNAs.
   (c) 3 μL of 2× Ligation Mix (Nippon gene).
2. Incubate at 16 °C for 30 min.
3. Add the whole reaction (6 μL) into 20 μL of JM109 competent cells (*see* **Note 4**) on ice.
4. Incubate the cells for 30 min on ice.

5. Heat shock at 42 °C for 1 min, and immediately chill on ice.
6. Incubate on ice for 2 min.
7. Add 100 μL of S.O.C. Medium (Thermo Fisher Scientific) and incubate at 37 °C for 1 h.
8. Seed the cells onto LB-agar plates containing 100 μg/mL ampicillin.
9. Incubate at 37 °C overnight.
10. Pick up about ten transformants (bacteria colonies) and culture them in 3 mL of LB medium containing 60 μg/mL ampicillin at 37 °C overnight with vigorous shaking.
11. Isolate and purify plasmid DNAs by a PureYield™ Plasmid Miniprep System (Promega) according to the manufacturer's instructions.
12. Prepare 15 μL of restriction enzyme reaction mix as follows:
    (a) 1.5 μL of 10× restriction enzyme buffer.
    (b) 3 μL of plasmid solution.
    (c) 10 μL of distilled water.
    (d) 0.25 μL of *Spe*I (5–20 units/μL).
    (e) 0.25 μL of *Nhe*I (5–20 units/μL).
13. Incubate the reaction at 37 °C for 5 h.
14. Examine the reaction by gel electrophoresis with 1% agarose gels in 1× TAE buffer, followed by ethidium bromide (0.5 μg/mL) staining.
15. Positive plasmids are expected to have one original *Nhe*I site and one newly generated *Spe*I site after ligation (*see* Subheading 3.1.2). Therefore, plasmids that can exhibit two digested bands as positive clones (Fig. 2).
16. Confirm the plasmids by means of sequence determination with the T7 EEV promoter primer.
17. Prepare 100 ng/μL reporter plasmid solution after confirmation.

3.2 Transfection of Reporter Plasmids into HeLa Cells and Heat-Shock

Transfection of many reporter plasmids at the same time into cells would be of particular importance for obtaining reproducible data, but is quite difficult. We used 96-well PCR plates for handling such many reporter plasmids for their transfection.

3.2.1 Preparation of 96-Well PCR Plates Containing Density-Controlled Plasmid Solution

1. Add 90 μL of UltraPure DNase/RNase-Free Distilled Water (Thermo Fisher Scientific) into each well of 96-well PCR plates.
2. Dispense 10 μL of purified reporter plasmids (100 ng/μL) into the wells one by one (*see* **Note 5**).

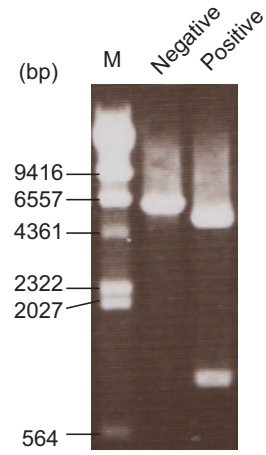

Fig. 2 Check of constructed reporter plasmids with restriction enzymes. Constructed reporter plasmids were digested with *Nhe*I and *Spe*I, and examined by agarose-gel electrophoresis followed by ethidium bromide staining. Positive clones exhibit two digested DNA bands, whereas empty psiCHECH-2 vectors (negative) show just a single DNA band. M: λ-*Hind*III marker

3. Cover the wells with 8-strip PCR caps tightly, and then vortex the plates followed by centrifugation at 1200 × *g* for 3 min at room temperature.
4. Use the diluted reporter plasmids (10 ng/μL) as working materials thereafter. Store them at 4°C (*see* **Note 6**).

3.2.2 Transfection

When miRNA activity is examined using 143 reporter plasmids, 12 control wells containing empty psiCHECK™-2 vectors and 4 blank wells together with 143 test wells containing the reporter plasmids should be prepared (159 wells in total) (*see* Fig. 3). Therefore, in case of using 96-well culture plates for assay, the examinations must be divided into two groups and carried out, i.e., two 96-well culture plates are needed for one assay. The protocol below describes a case of duplicate examinations (transfections).

1. The day before transfection, seed 5×10^3 HeLa cells onto each well of 96-well culture plates (4 plates) in growth medium without antibiotics.
2. Incubate the cells at 37 °C in a 5% CO_2 humidified chamber overnight.
3. Take 4 μL (2 μL/assay) of each reporter plasmid solution from the working 96-well PCR plates using a multichannel pipette, and transfer it to new 96-well PCR plates.

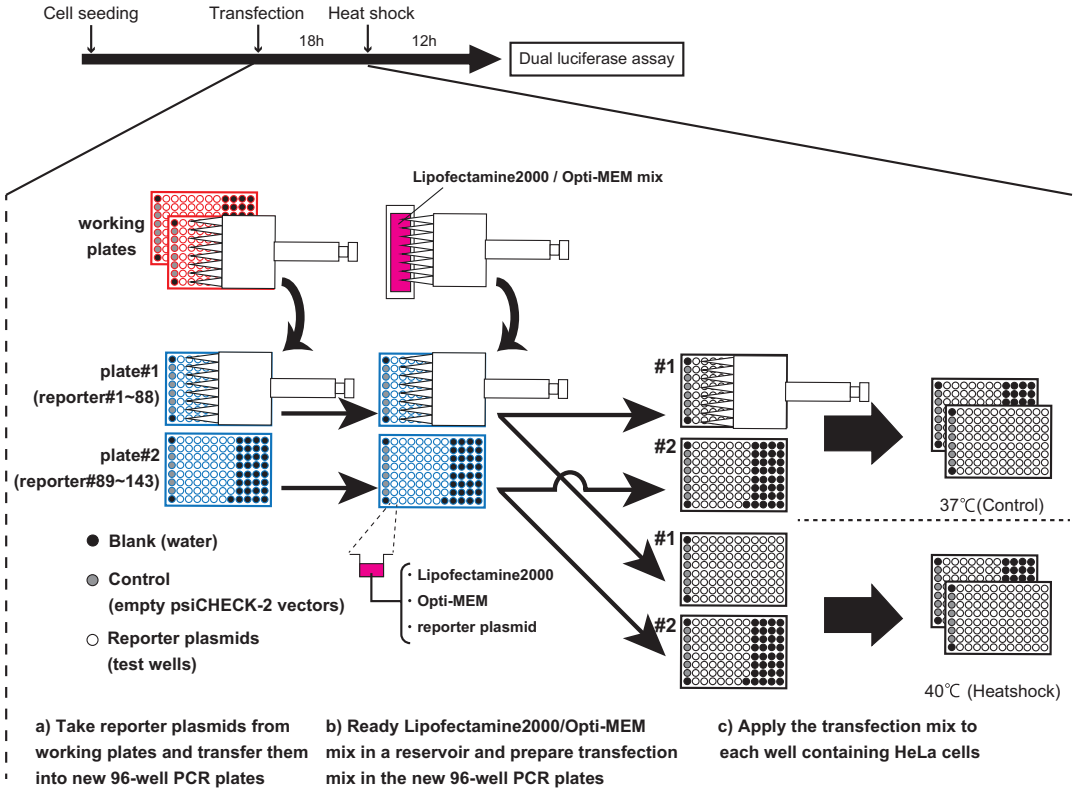

Fig. 3 Schematic transfection procedure and heat-shock treatment. HeLa cells are seeded onto 96-well culture plates. The next day, transfection of reporter plasmids is carried out as follows: (**a**) take a necessary amount of reporter plasmids from working 96-well plates and transfer them to new 96-well PCR plates; (**b**) mix the reporter plasmids with Lipofectamine2000/Opti-MEM mix; (**c**) add the transfection mix into 96-well culture plates containing HeLa cells. A half group of the culture plates are subjected to a heat-shock treatment at 40 °C, and luciferase activities were analyzed by a dual luciferase assay

4. Prepare a transfection mix enough for transfection to 350 wells [(159 wells and 16 extra wells) × 2 (duplication)]:
   (a) 70 μL (0.2 μL × 350wells) of Lipofectamine® 2000 Transfection Reagent.
   (b) 7 mL (20 μL × 350wells) of Opti-MEM® I Reduced Serum Medium (*see* **Note 7**).
5. Incubate at room temperature for 5 min.
6. Transfer the Lipofectamine2000/Opti-MEM mix into a reagent reservoir.
7. Add 40 μL (20 μL/assay) of the Lipofectamine2000/Opti-MEM mix into each well of the 96-well PCR plates containing reporter plasmids using a multichannel pipette, and mix them by pipetting several times.
8. Incubate at room temperature for 20 min.

9. If necessary, centrifuge the plates at 1200 × *g* for 3 min.
10. Add 20 μL of each Lipofectamine2000/Opti-MEM/plasmid mix into a culture well containing HeLa cells using a multichannel pipette, and duplicate the operation.
11. Incubate at 37 °C in a 5% CO_2 humidified chamber.

3.2.3 Heat-Shock

1. Ready a 5% CO_2 humidified chamber the temperature of which is at 40 °C.
2. After 18 h–incubation following the transfection described above (3-2-2-10, 11), a half group of transfected cells are subjected to a heat shock at 40 °C.
3. Incubate the cells at 40 and 37 °C (as a control) for further 12 h (*see* **Note 8**).

3.3 Luciferase Assay

1. Remove growth media from wells of 96-well culture plates and wash cells with D-PBS.
2. Add 35 μL of 1× Passive Lysis Buffer (Promega) into each well.
3. Shake the culture plates by a plate shaker at 1000 rpm for 15 min at room temperature.
4. Determine the *Photinus* and *Renilla* luciferase activities by a Dual-Luciferase reporter assay system (Promega) with 20 μL of each cell lysate according to the manufacturer's instructions. Details are as follows:
   (a) While shaking (3-3-3), dispense 20 μL of LARII into white 96-well plates (Thermo scientific) (*see* **Note 9**).
   (b) Add 20 μL of each cell lysate into LARII and mix them (*see* **Note 10**).
   (c) Measure the *Photinus* luciferase activity.
   (d) Add 20 μL of the Stop&Glo reagent to each well, and shake the plates by a plate shaker at 1000 rpm for 1 min (*see* **Note 11**).
   (e) Measure the *Renilla* luciferase activity.
5. Calculate the expression level of target reporter genes for miRNAs.
   (a) Subtract a background signal (obtained from blank wells) from the data.
   (b) Normalize the *Renilla* luciferase activity to the *Photinus* luciferase activity.
   (c) Further normalize the data to the data obtained from the empty psiCHECK-2 vector as a control. Figure 4 indicates the data of gene silencing that were obtained using 143 reporter plasmids (*see* **Notes 12** and **13**).

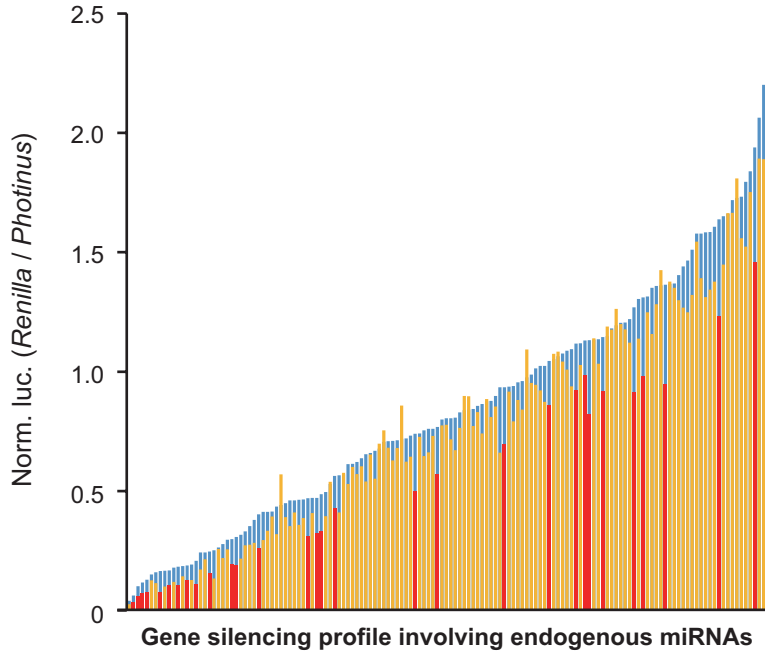

Fig. 4 Gene silencing profile involving endogenous miRNAs. The data of gene silencing that were obtained with 143 constructed reporter plasmids were arranged in increasing order of the normalized luciferase expression ratios at 37 °C, and aligned from the lowest value (left) to the highest one (right). Each bar graph indicates Mean ± SD ($n = 4$). The data obtained at 37 °C (blue bars) were overlapped with the data that were obtained at 40 °C (yellow bars), in which the data showing a statistically significant decrease (Student's t-test, two-tailed, $P < 0.05$) were indicated by red bars

4 Notes

1. We recommend using 96-well plates that are designed to reduce the edge effect, which occurs when culture medium evaporates from the plate (mostly around the edge) during incubation, and which may alter cell viability.
2. The sense oligonucleotide DNA sequences we designed are available at https://doi.org/10.1371/journal.pone.0103130.
3. Isolation and purification of digested vector DNAs by agarose-gel electrophoresis would produce a better ligation and a better yield of proper reporter plasmids.
4. JM109 competent cells (Promega) are divided into 20 μL aliquots into 1.5 mL tubes in advance and stored at −80 °C. During ligation, divided competent cells are put on ice for gradually thawing.

5. In addition to the wells containing reporter plasmids, blank and control wells containing distilled water and empty psiCHECK-2 vectors, respectively, should be prepared. We recommend preparing at least three control wells for the calculation of an average and normalization thereafter.
6. Before using the working plates, the plates should be centrifuged to reduce contamination.
7. Prepare a little more transfection mix than you need, because of a loss of the transfection mix during transfection operation.
8. To confirm a heat-shock response in cells treated at 40 °C, we examined the activation of *HSF1* in the cells by means of a reporter assay using the pGL4.41[luc2P/HSE/Hygro] Vector (Promega) carrying a heat shock element (HSE) in the promoter region of the *Photinus luciferase* reporter gene. We also examined the phosphorylation state of HSF1 protein by western blotting [15].
9. We recommend using white microplates such as Nunc™ F96 MicroWell™ Black and White Polystyrene Plates (Thermo scientific) in luminescence measurement for minimizing autoluminescence and maximizing true reflection.
10. Make sure that the bottom of wells is filled with LARII and that cell lysate is mixed well with LARII. Insufficient reaction causes false result.
11. If necessary, reduce the "rpm" of the plate shaker used not to spill out of the LARII/cell lysate mix from the wells.
12. The luciferase activity may be influenced by different temperatures. We recommend performing a pilot experiment using empty psiCHECK-2 vectors to see what degree of temperature would be influenced to the expression of reporter genes.
13. When mammalian cells other than HeLa cells are used, we recommend performing a pilot experiment to see a suitable amount of reporter plasmids for cells you would like to use, for obtaining reproducible results.

References

1. He L, Hannon GJ (2004) MicroRNAs: small RNAs with a big role in gene regulation. Nat Rev Genet 5:522–531
2. Ambros V (2004) The functions of animal microRNAs. Nature 431:350–355
3. Filipowicz W, Bhattacharyya SN, Sonenberg N (2008) Mechanisms of post-transcriptional regulation by microRNAs: are the answers in sight? Nat Rev Genet 9:102–114
4. Stefani G, Slack FJ (2008) Small non-coding RNAs in animal development. Nat Rev Mol Cell Biol 9:219–230
5. Gorospe M, Abdelmohsen K (2011) MicroRegulators come of age in senescence. Trends Genet 27:233–241
6. Takahashi M, Eda A, Fukushima T, Hohjoh H (2012) Reduction of type IV collagen by upregulated miR-29 in normal elderly mouse and klotho-deficient, senescence-model mouse. PLoS One 7:e48974
7. Lee Y, Kim M, Han J, Yeom KH, Lee S et al (2004) MicroRNA genes are transcribed by RNA polymerase II. EMBO J 23: 4051–4060

8. Lagos-Quintana M, Rauhut R, Yalcin A, Meyer J, Lendeckel W et al (2002) Identification of tissue-specific microRNAs from mouse. Curr Biol 12:735–739
9. Liu CG, Calin GA, Meloon B, Gamliel N, Sevignani C et al (2004) An oligonucleotide microchip for genome-wide microRNA profiling in human and mouse tissues. Proc Natl Acad Sci U S A 101:9740–9744
10. Babak T, Zhang W, Morris Q, Blencowe BJ, Hughes TR (2004) Probing microRNAs with microarrays: tissue specificity and functional inference. RNA 10:1813–1819
11. Hohjoh H, Fukushima T (2007) Expression profile analysis of microRNA (miRNA) in mouse central nervous system using a new miRNA detection system that examines hybridization signals at every step of washing. Gene 391:39–44
12. Hohjoh H, Fukushima T (2007) Marked change in microRNA expression during neuronal differentiation of human teratocarcinoma NTera2D1 and mouse embryonal carcinoma P19 cells. Biochem Biophys Res Commun 362:360–367
13. Eda A, Tamura Y, Yoshida M, Hohjoh H (2009) Systematic gene regulation involving miRNAs during neuronal differentiation of mouse P19 embryonic carcinoma cell. Biochem Biophys Res Commun 388:648–653
14. Eda A, Takahashi M, Fukushima T, Hohjoh H (2011) Alteration of microRNA expression in the process of mouse brain growth. Gene 485:46–52
15. Fukuoka M, Yoshida M, Eda A, Takahashi M, Hohjoh H (2014) Gene silencing mediated by endogenous microRNAs under heat stress conditions in mammalian cells. PLoS One 9:e103130

Chapter 16

Screening miRNA for Functional Significance by 3D Cell Culture System

Bo Han

Abstract

Cell-based assays play important roles in cell biology and drug discovery. 3D cell culture, which allows cells to grow or interact with their surrounding in all three dimensions, provides more physiological information for the in vivo tests. Here, we describe a tunable collagen-based 3D cell culture system based on collagen material crosslinked with transgluminase, to study the function of miR. Methods including gel handling, proliferation assays, gene, and protein expressions in a 3D setting are described.

Key words 3D culture, Col-Tgel, Gelatin, Transglutaminase, miRNA, Proliferation assay, Gene expression, Immunohistochemical staining

1 Introduction

MicroRNAs (miRNAs) are short (20–26 nucleotides), noncoding RNAs that are important regulators of gene expression and cellular functions [1]. They are generated from genomic DNA and positively or negatively regulate gene expression through translational repression, mRNA destabilization, and/or mRNA cleavage [2–4]. miRNAs need as few as 7 nucleotides to complementarily bind to their targets; therefore, a wide range of genes can be subject to regulation. miRNAs regulate many aspects of the cellular processes, and provide new therapeutic targets for drug development. In general, miRNA therapy could be categorized into two mechanisms: miRNA replacement therapy that restores the miRNA expression and miRNA inhibition therapy that inhibits the miRNA expression [5, 6].

miRNA biology has been extensively studied, but the function of many miRNAs is still unknown. A critical limitation has been the lack of high-throughput yet biological relevant in vitro models. The function of miRNA has usually been studied in two dimensional

Shao-Yao Ying (ed.), *MicroRNA Protocols*, Methods in Molecular Biology, vol. 1733,
https://doi.org/10.1007/978-1-4939-7601-0_16,

(2D) cell culture models. However, 2D culture systems do not accurately reflect the situation in vivo, where cells grow within a complex three-dimensional (3D) microenvironment and cells are surrounded by extracellular matrices (ECM). Characterizations of miRNA stability in biological fluids, penetration efficiency in tissue, uptake rate by the target cells, and their functions under hypoxic or normoxic environment are beyond the capability of the 2D model. Thus 3D cultures were introduced to improve the simulation of such conditions in the living organism to study the function of miRNA.

Design criteria for 3D scaffolds include biomaterial selection, degradation rate and mode, physical properties, and cell-matrix interactions [7]. Here are example protocols to study miRNA functions using collagen-based transglutaminase crosslinked 3D culture models [8].

2 Materials

Prepare all the solutions using ultrapure water.

2.1 Transglutamiase Purification

Dissolve 3 g microbial transglutaminase (ACTIVA TI Ajinomoto, Japan) from *Streptomyces mobaraense* in buffer A (20 mM phosphate and 2 mM EDTA, pH 6.0). Mix dissolved TGase with 3 mL of pre-equilibrated S Sepharose FF beads (Sigma) and incubate at 4 °C overnight with occasional vortexing. Load protein solution and beads mixture into a column. Wash beads with 4 volumes of bead with buffer A. Elute TGase with buffer B (Buffer A with 800 mM NaCl) with a fraction collector. Aliquot 10 μL of solution from each vial and monitor protein concentration with Bradford (Bio-Rad), utilizing BSA as a standard. Change three 1 mL vials of peak elations and dilute proteins with eluting buffer to 20 μg/mL TGasse. Aliquot 100 μL of TGase in each vial and store TGase at −80 °C until use [9].

2.2 Gelatin Gel Preparation

Prepare 10% gelatin water solution by adding 10 g of gelatin powder (bovine skin type B, 225 bloom, Sigma) into 100 mL of d-H_2O. Sterilize the gelatin solution with autoclave liquid cycle and store at 4 °C until use. To prepare cell embedding gel, warm the gelatin solution in 37 °C water bath for at least 30 min. The final gel concentration used in the experiment is cell type and study purpose decides (*see* **Note 1**).

2.3 SDS Sample Buffer

250 mM Tris pH 6.8, 10% SDS, 50% glycerol, 2.5 mg/mL of bromophenol blue.

2.4 Zymograft Developing Buffer 50 mM Tris, 5 mM $CaCl_2$, and 200 mM NaCl, pH 7.5.

2.5 Coomassie Blue Solution 62.5% ethanol, 25% acetic acid, and 0.125% Coommasie blue R250 (Bio-Rad, CA).

3 Methods

Carry out all the procedures at room temperature unless otherwise specified.

3.1 Tumor Cell Subculture Culture human breast carcinoma cell MDA MB-231, pancreatic cancer cell line CFPAC-1, and colorectal carcinoma cell line HCT-116 cells (ATCC, American Type Cell Collection, VA) with high glucose Dulbecco's modified Eagle medium, Iscove's Modified Dulbecco's Medium, or McCoy5a modified medium (DMEM, IMDM, and McCoy5a, Corning, VA) with 10% (v/v) fetal bovine serum (FBS, Hyclone, ThermoScientific) and 1% (v/v) penicillin-streptomycin (PS, Corning, VA) supplement respectively in a humidified atmosphere of 5% CO_2 and 37 °C. Change culture medium every 2–3 days.

3.2 3D Culture Preparation and Drug Treatment

1. Detach 80% confluent monolayer cultured cells with 0.25% trypsin in HBSS (Corning, VA). Neutralize digestive enzyme with complete medium and perform cell count with 10 μL of cell aliquot with hemacytometer. Aliquot 2×10^6 cells into a micro-centrifugal tube and centrifuge for 5 min at $1000 \times g$ to pellet cells (*see* **Note 2**). Add 0.5 mL of culture medium without serum to suspend cell pellet. Add 0.5 mL of 10% gelatin solution into 0.5 mL of cell suspension, and then add 50 μL of pre-thawed TGase, mix with gentle pipetting (*see* **Note 3**). The final gel concentration is 5% and cell density is 1×10^6 cells/mL.
2. Pipette 20 μL of cell-gel mixture and cast on the surface of each well of a 48-well suspension cell culture plate. Incubate the plate at 37 °C for 1 h to solidify gel on the surface of non-treated tissue culture plate. Add 500 μL of corresponding culture medium to submerge a half-dome-shaped 3D construct for cell culture and drug treatment (*see* **Note 4**).
3. Add miR-302 preparations to the culture medium with serial dilutions; incubate the plate for an appropriate length of time in the incubator depending on the assay purpose. For example, add miR-302 reagent at day 0 to study cancer cell tumoid formation in 3D culture. Or, add miR-302 reagent at day 7 to study miR-302 effects on the disruption of tumoroid or on the inhibition of cell proliferation.

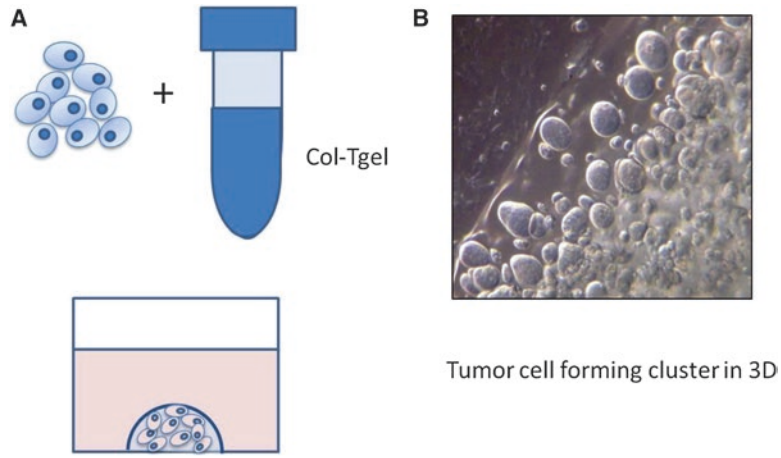

Fig. 1 (**a**) Schematic illustration of 3D culture. (**b**) HCT116 cells form tumoroids after 10 days in 3D culture

3.3 Cell Proliferation and Viability Assay

1. *Cell number counts:* At the end of the experiments (Fig. 1) (*see* **Note 5**), release the cells from the constructs with 200 μL of 0.1% collagenase in HBSS for 1 h at 37 °C with rocking. Neutralize the digested constructs with 200 μL culture medium and further dilute to 10 mL with PBS. Count cells using the Z™ Series COULTER COUNTER® Cell and Particle Counter (Beckman Coulter, CA). Gate the particle size at 9.49 μm to exclude cell debris and average triplet well counting.
2. *Cell viability:* At determined time points, add 200 μL of CCK-8 working solution (CCK-8, Dojindo Molecular Technologies, MD) directly to the culture medium and incubate at 37 °C for an appropriate length of time (e.g., 2, 4, 6, 12, 24 h depending on cell metabolism rate) in the incubator. Transfer 100 μL of medium into each well of a flat-bottom 96 well-plate. Read absorbance at 450 nm with multiplate reader (Molecular Device, CA), subtracting solution control of CCK-8 working solution (*see* **Note 6**).
3. *Qualitative and imaging of cell viability:* Prepare 5 mg/mL MTT (3-(4, 5-dimethylthiazol-2-yl)-2, 5-diphenyltetrazolium bromide, Sigma-Aldrich, MO) solution with culture medium and filter with 0.22 μm syringe filter to sterilize. Replace the medium with fresh MTT containing medium (MTT: medium ratio 1:10) and incubate cell constructs for 2–8 h at 37 °C depending on the cell metabolism rate (Fig. 2). Record image under light microscope with digital camera (Nikon, Japan). Remove the medium, wash construct with PBS for three times, and add 200 μL of DMSO into each well and incubate at room temperature for 2 h. Read colored solution at 570 nm and subtract the background absorbance at 690 nm (*see* **Note 7**).

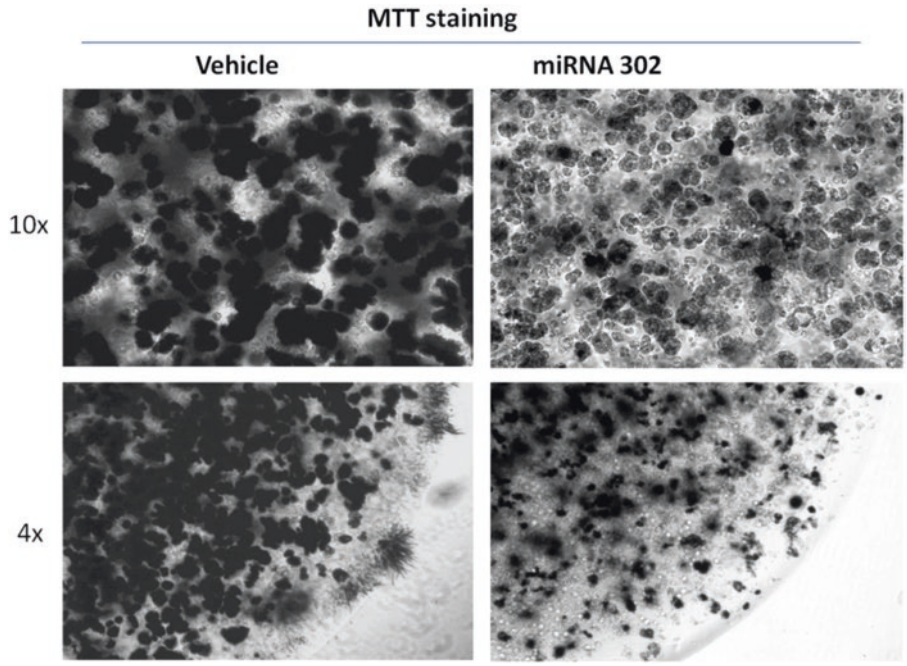

Fig. 2 MTT staining of CFPAC cells treated with miR-302 for 48 h in 3D model

3.4 Immunocytochemistry

1. *Visualize cell morphology change by F-actin staining:* Fix cell/gel constructs at predetermined time points with 10% phosphate-buffered formalin for 10 min at room temperature. Wash with Tris-buffered saline and tween-20 (TBST) for three times, each 15 min. Stain with 30 nM rhodamine phalloidin and 30 nM DAPI dihydrochloride in the dark at room temperature (Life Technologies, NY). The Col-Tgel-Cell construct was rinsed with Tris-buffered saline with 0.05% Tween 20 (TBST, pH 7.4), fixed in 10% neutral formalin solution (VWR International, PA) for 10 min, and incubated in blocking buffer (5% BSA in TBST) for 30 min. Then, 50 μL of Rhodamine 110 Phalloidin (Biotium, CA) was diluted in each 2 mL blocking buffer, and 500 μL of the solution was used to stain each sample. After 2 h of incubation at 4 °C, the Col-Tgel-Cell construct was counterstained with DAPI (Biotium, CA) for 5 min and visualized under an EVOS fluorescence microscope (Advanced Microscopy Group, WA).
2. *Live and dead cells staining:* At the test time point, aspirate cell culture medium and wash cell gel construct with PBS three times, 10 min each. Prepare test solution of LIVE/DEAD Viability/Cytotoxicity kit (Life Technologies, NY) following manufacture protocol. Add 200 μL of the combined LIVE/DEAD® assay reagents into each well to cover 3D construct.

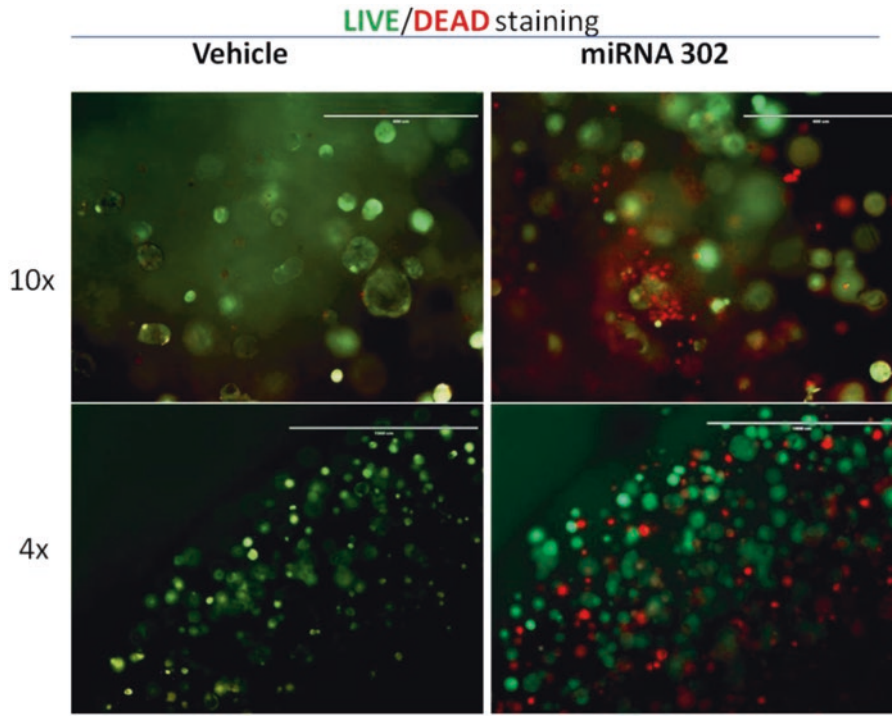

Fig. 3 Live/dead staining of CFPAC cells treated with miR-302 or vehicle for 48 h in Col-Tgel 3D model

Incubate the 3D cells for 60 min at room temperature. View and record labeled cells under a fluorescence microscope (Fig. 3) (*see* **Note 8**).

3.5 Gelatinolytic Zymograph Assay

1. *Detect matrix metalloproteinases* activity in the 3D cell layer by gelatin-based zymography. Culture 3D cells with miRNA for different lengths of time. Aspirate culture medium and wash 3D constructs with PBS for three times. Add 50 μL of PBS in each well and use scraper to de-attach gel 3D gel from surface. Transfer gel debris and solution into a microtube and homogenize (manual or electronic) with 0.25% Triton X-100. Perform three cycles of freeze-thaw in a −80 °C freezer. Centrifuge at 16,000 × *g* for 10 min and collect the supernatant for zymograph assay. Add SDS sample buffer to the collected supernatant at a 1:1 ratio. Apply samples to Ready Gel Zymogram Gel (Bio-Rad, CA) at 90 V for 3 h. Rinse gel 2.5% (v/v) Triton X-100 and incubate gel with developing at 37 °C for 24 h. Stain gel with Coomassie blue solution and de-staining gel with (30% methanol and 1% formic acid). Record results with digital camera (*see* **Note 9**).

3.6 Study Cell-Matrix Interaction by Immunostaining of β1-Integrin

1. Remove the cell culture medium, wash the sample twice with TBST.
2. Fix cell gel construct with a 10% neutral formalin solution for 10 min.
3. Incubate in a peroxidase suppressor solution (Thermo Scientific, NH) for 30 min. Incubate in the blocking buffer (5% BSA in TBST) for 30 min.
4. Incubate the sample with the primary antibody working solution (anti-β1-Integrin polyclonal antibody in blocking buffer, 1:400, Thermo Scientific, NH) overnight.
5. Incubate in the secondary antibody working solution (biotinylated anti-rabbit produced in goat in blocking buffer, 1:800, Sigma, MO) for 1 h.
6. Incubate in the SPPU working solution (ultrasensitive streptavidin-peroxidase polymer in blocking buffer, 1:800, Sigma, MO) for 30 min to amplify detection signals.
7. Incubate the sample in the DAB working solution (metal-enhanced substrate solution diluted with stable peroxide buffer, 1:10, Thermo Scientific, NH) to develop color.
8. Stop the reaction by washing the sample with TBST when the desired color developed (~5 min). Examine the anchored cells with a microscope (*see* **Note 10**).

3.7 Total RNA Extraction and RT-PCR Analysis of the Gene Expression

1. Extract total RNA of cells grown in the 3D Col-Tgel using Trizol reagent (Invitrogen, CA) according to the single-step acid-phenol guanidinium extraction method [10].
2. Collect gel constructs with scrapper in 1.5 mL tubes containing 1 mL Trizol reagent (*see* **Note 11**). Homogenize thoroughly and removal of insoluble substances by centrifugation at 13,000 × *g* for 5 min. Treat sample with 1-bromo-3-chloropropane. Precipitate total RNA using chilled ethanol, and dissolve acquired RNA with RNase-free water.
3. Quantify RNA concentration spectrometrically at 260 and 280 nm and determine the purity at 230 and 260 nm. Perform real-time PCR with one-step SYBR green reagents according to the manufacturer's protocol (Bio-Rad, CA). Normalize the expression of target gene according to the GAPDH gene reference by using the ΔΔCt method.

4 Notes

1. Gel stiffness can be adjusted by gel concentration when using Col-Tgel. For example, 9% gelatin exhibits a yield strength about 32.32 ± 1.9 kPa, 6% is about 13.51 ± 2.13 kPa, and 3% is about 1.58 ± 0.42 kPa [11].

2. Tilt centrifuge tube and aspirate medium as much as possible from cell pellet to prevent disturbing cell pellets.
3. Very gently pipette to mix cells and gel well without introducing air bubble. If need more time to prepare other samples, leave cell and gel mixture at room temperature in the capped tubes. After adding TGase, there is 10–30 min working window before gels solidify.
4. Keep the cell-gel mixing tube to check on the gelling status. Stick a pipet tip into the tube to make sure gel solidified. Add culture medium carefully on the top of the gel.
5. The biocompatibility and transparency of the Col-Tgel allows for direct observation under a light microscope, and direct staining to avoid tedious steps like sectioning and antigen retrieval.
6. Cells sense extracellular matrix rigidity through bidirectional interaction with the surrounding ECM and respond accordingly. 3D matrix composition and rigidity affects cell proliferation and metabolism rate [8, 11].
7. In 2D culture, cell proliferation rate sometimes could be represented by indirect metabolism markers such as MTT assay or CCK-8 assay. However, in 3D culture, either the matrix itself or matrix-created microenvironment exerts a big impact on the cell metabolism rate. For example, MTT negative cells may only be slow or dormant metabolism cells instead of dead cells. Multiple assays such as live/dead staining, thymidine incorporation, BrdU staining should be used to define cell proliferation status.
8. The gel provides a stable and durable platform for long-term studies. Tumor cells and stromal are cultured in 3D gel for 28 days and beyond [12]. Cells not only respond to chemical stimuli such as growth factors, cytokines, and hormones or miRs [13–15], but also the mechanical properties of the extracellular matrix, such as elastic modulus or rigidity, pore size, porosity, and dynamic mechanical vibration [16–18]. Thus, select correct controls are critical for performing 3D culture assays.
9. Since 3D gel forms a barrier for MMP diffusion, the MMPs released in culture medium, in the gel, and cell associated MMPs can be separated and analyzed.
10. Compared to 2D culture, extra steps and longer washing time are needed to remove nonspecific bindings and gel-trapped dye.
11. Make sure the samples are homogenized with sufficient Trizol reagent since gel construct contains water.

References

1. Ling H, Fabbri M, Calin GA (2013) MicroRNAs and other non-coding RNAs as targets for anticancer drug development. Nat Rev Drug Discov 12(11):847
2. Doench JG, Sharp PA (2004) Specificity of microRNA target selection in translational repression. Genes Dev 18(5):504–511
3. Nilsen TW (2007) Mechanisms of microRNA-mediated gene regulation in animal cells. Trends Genet 23(5):243–249
4. Guo H-S et al (2005) MicroRNA directs mRNA cleavage of the transcription factor NAC1 to downregulate auxin signals for Arabidopsis lateral root development. Plant Cell 17(5):1376–1386
5. Iorio MV, Croce CM (2012) MicroRNA dysregulation in cancer: diagnostics, monitoring and therapeutics. A comprehensive review. EMBO Mol Med 4(3):143–159
6. Esquela-Kerscher A, Slack FJ (2006) Oncomirs--microRNAs with a role in cancer. Nat Rev Cancer 6(4):259
7. Baker BM, Chen CS (2012) Deconstructing the third dimension–how 3D culture microenvironments alter cellular cues. J Cell Sci 125(13):3015–3024
8. Fang JY et al (2014) Tumor bioengineering using a transglutaminase crosslinked hydrogel. PLoS One 9(8):e105616
9. Kuwahara K et al (2009) Cell delivery using an injectable and adhesive transglutaminase–gelatin gel. Tissue Eng Part C Methods 16(4):609–618
10. Chomczynski P, Sacchi N (1987) Single-step method of RNA isolation by acid guanidinium thiocyanate-phenol-chloroform extraction. Anal Biochem 162(1):156–159
11. Tan S et al (2014) The synergetic effect of hydrogel stiffness and growth factor on osteogenic differentiation. Biomaterials 35(20):5294–5306
12. Fang JY et al (2016) From competency to dormancy: a 3D model to study cancer cells and drug responsiveness. J Transl Med 14(1):38
13. Bax DV et al (2009) Cell adhesion to tropoelastin is mediated via the C-terminal GRKRK motif and integrin αVβ3. J Biol Chem 284(42):28616–28623
14. Phillips JE et al (2010) Human mesenchymal stem cell differentiation on self-assembled monolayers presenting different surface chemistries. Acta Biomater 6(1):12–20
15. Bartel DP (2009) MicroRNAs: target recognition and regulatory functions. Cell 136(2):215–233
16. Engler AJ et al (2006) Matrix elasticity directs stem cell lineage specification. Cell 126(4):677–689
17. Nemir S, West JL (2010) Synthetic materials in the study of cell response to substrate rigidity. Ann Biomed Eng 38(1):2–20
18. Rowlands AS, George PA, Cooper-White JJ (2008) Directing osteogenic and myogenic differentiation of MSCs: interplay of stiffness and adhesive ligand presentation. Am J Phys Cell Phys 295(4):C1037–C1044

Chapter 17

Neonatal Rat Cardiomyocytes Isolation, Culture, and Determination of MicroRNAs' Effects in Proliferation

Lichan Tao, Yihua Bei, Yongqin Li, and Junjie Xiao

Abstract

Cardiomyocytes loss is a major contributor for many cardiovascular diseases including heart failure and myocardial infarction. Although extremely limited, adult cardiomyocytes are able to proliferate. Understanding the molecular mechanisms controlling cardiomyocytes proliferation is extremely important for enhancing cardiomyocyte proliferation to promote cardiac regeneration and repair. MicroRNAs (miRNAs, miRs) are powerful controllers of many essential biological processes including cell proliferation. Here, we described in detail a protocol for isolation and culture of neonatal rat cardiomyocytes and the determination of miRNAs' effects in proliferation based on two well-established methods including EdU and Ki67 immunofluorescent stainings.

Key words Cardiomyocyte, MicroRNA, Proliferation, Ki67, EdU

1 Introduction

The loss of cardiomyocytes or its insufficient capability to proliferation is a major cause for many cardiovascular diseases including myocardial infarction and heart failure [1]. However, unlike amphibians and fish, which retain a strong capacity of cardiac regeneration throughout the whole life [2], the heart in mammals has been considered to be a post-mitotic organ without any proliferative capacity fostered by the notion that cardiomyocytes in mammals withdraw from cell cycle and terminally differentiate after birth [3, 4]. Recently, accumulating evidence has indicated that cardiomyocytes could proliferate albeit at extremely low frequencies (<1%) in adult mammalian hearts, including in human [3, 5–8]. In physiological conditions, cardiomyocyte turnover mainly originates from activation of resident cardiomyocytes at a rate of 1.4–4% per year in a normal mouse heart [9]. In pathological conditions, especially in ischemic hearts, the rate of cardiomyocyte renewal may increase significantly [10]. Many signaling pathways have been associated with cardiomyocytes proliferation [1]. Thus,

Shao-Yao Ying (ed.), *MicroRNA Protocols*, Methods in Molecular Biology, vol. 1733,
https://doi.org/10.1007/978-1-4939-7601-0_17,

it is highly needed to provide a common protocol to measure cardiomyocytes proliferation.

To determine cardiomyocytes proliferation, the standardized method for neonatal rat cardiomyocytes isolation should be provided. Following mechanical and enzymatic dissociation of the heart tissue [11], some protocols for neonatal rat cardiomyocytes isolation frequently have two important issues: First, low cell yield and viability. Due to mechanical damage and operational problems, the cardiomyocyte yield is frequently extremely low and even failed to support one single experiment [11]. Second, insufficient depletion of non-contractile cardiac stromal cells, especially fibroblasts, would affect the phenotype and function of cardiomyocytes [12–14]. In light of this, extraordinary efforts are needed to improve the protocol characterizing primary isolation of cardiomyocytes.

5-ethynyl-2-deoxyuridine (EdU) incorporated into cellular DNA during DNA replication is a common strategy to detect DNA synthesis in proliferating cells [15, 16]. Besides that, the assessment of the expression of nuclear protein Ki67 is also a classic experiment to detect cell proliferation [17]. MicroRNAs (miRNAs, miRs) are powerful controllers of many essential biological processes including cell proliferation [18–20]. Here, we provided a detailed protocol for using them as the determination of miRNAs' effects in neonatal rat cardiomyocytes proliferation.

Taken together, in this chapter, we will in detail describe the protocol for isolation and culture of neonatal rat cardiomyocytes and the determination of miRNAs' effects in proliferation based on two well-established methods including EdU and Ki67 immunofluorescent stainings. Although karyokinesis, cytokinesis, and direct cell number counting should be measured to fully prove neonatal rat cardiomyocytes proliferation, this protocol is extremely useful to rapidly screen miRNAs that might be able to promote neonatal rat cardiomyocytes proliferation, providing the promise for development of novel therapeutics for the treatment of many cardiovascular diseases based on enhancing cardiomyocytes proliferation.

2 Materials

Tissue samples: heart tissues were derived from neonatal rats (from 0–3-day old Sprague-Dawley rats). Animals were first anesthetized with carbon dioxide and sacrificed by cervical dislocation, then cardiac ventricular tissues were removed and washed in ice-cold ADS (*see* **Note 1**). Heart tissues were washed again with cold ADS and finally minced into pieces of approximately 1 mm^3.

Prepare all solutions with ultrapure water (prepared by purifying deionized water) and analytical grade reagents. During the process of cardiomyocytes isolation and culture, all the items strictly follow sterilization principles.

2.1 Cardiomyocytes Isolation and Culture

1. 10× ADS (100 mL) solution: 6.8 g NaCl, 4.76 g HEPES, 0.138 g Na_2HPO_4, 0.6 g glucose, 0.4 g KCl and 0.051 g $MgSO_4$ (containing 7 H_2O). Make up to 100 mL with ultrapure water, adjust pH value to 7.35–7.45, and finally filtrate with 0.22 μm filter. 1× ADS (1 L) solution: dissolve 100 mL 10× ADS in 900 mL sterile water. Store at 4 °C.
2. Trypsin-collagenase 2 buffer (100 mL): 60 mg trypsin and 40 mg collagenase 2. Make up to 100 mL with 1× ADS solution. Incubate at 37 °C for 1–2 h before use.
3. Horse serum (HS). Incubate at 37 °C for 30 min before use.
4. Culture medium for neonatal rat cardiomyocytes: 500 mL DMEM-F12, 25 mL fetal calf serum (FBS), 50 mL HS and 6 mL penicillin-Streptomycin solution (P/S). Incubate at 37 °C for 30 min before use.
5. Percoll solution: Percoll stock solution (100 mL): 90 mL Percoll solution and 10 mL 10× ADS solution. Top Percoll solution (20 mL): 9 mL Percoll stock solution and 11 mL 1× ADS solution. Bottom Percoll solution (20 mL): 13 mL Percoll stock solution and 7 mL 1× ADS solution (*see* **Note 2**). All Percoll solutions were stored at 4 °C.
6. Coating buffer: 1% gelatin: 0.2 g gelatin and 20 mL PBS. Store at 4 °C.

2.2 miRNA Mimic and Inhibitor Transfection

1. Mimic/Inhibitor/negative control (NC) stock (20 nmol): 5 nmol mimic/Inhibitor (Ribobio) and 250 mL sterile water. Store at −20 °C.
2. Opti-MEM: store at 4 °C.
3. Transfection reagent: Lipofectamine ™ 2000 reagent (lipo 2000, Invitrogen), store at 4 °C.

2.3 EdU and Ki67 Immunostaining

1. Click-iT® EdU imaging kit with alexa fluor® 488/594 (Invitrogen, C10086), including: 5 mg material EdU powder (A), 4 mL Alexa Fluor azide (B), 4 mL DMSO (C), 4 mL Click-iT® EdU reaction buffer (D), 400 mg Click-iT® EdU additive powder (F), 4 mL $CuSO_4$ (E), and 35 μL hoechst (G). Store at 4 °C.
2. Monoclonal anti-α-actinin antibody (Sigma, A7811). Store at −20 °C.
3. Monoclonal anti-Ki67 antibody (Abcam, ab16667). Store at −20 °C.
4. Fixing solution: 4% PFA: 4 mL PFA and 96 mL PBS. Store at room temperature.
5. Permeabilized buffer: 0.5% PBST (100 mL): 100 mL PBS and 500 μL Triton-x-100. Store at room temperature.

6. Blocking solution: 10% goat serum (100 mL): 10 mL goat serum and 90 mL PBST. Store at 4 °C.
7. Secondary antibody conjuncted with 488/594 (Jackson ImmunoResearch Laboratories). Store at −20 °C.
8. DAPI (Invitrogen). Store at −20 °C.

3 Methods

All the procedures were carried out at room temperature unless otherwise specified.

3.1 Cardiomyocyte Isolation and Culture

1. Minced cardiac ventricular tissues were transferred to a 200 mL glass bottle and resuspended in 30 mL (*see* **Note 3**) trypsin-collagenase 2 buffer for 30 min in the preheated cell vibrator at 100 rpm, 37 °C.
2. The cell suspensions (trypsin-collagenase 2 buffer containing isolated cells) were collected, transferred to a fresh 50 mL centrifuge tube (collecting tube) (*see* **Note 4**) and enzyme activity was terminated by the addition of 6 mL horse serum.
3. Cell suspensions from a collecting tube were centrifuged for 5 min at 1000 rpm and the resulting cell pellet was resuspended in a 2 mL warmed neonatal cardiomyocytes culture medium.
4. Fresh 30 mL trypsin-collagenase 2 buffer was added to the remaining tissue pieces for 20 min in the preheated cell vibrator at 100 rpm, 37 °C.
5. Repeat **steps 2–4** until ventricular tissues fragments were completely dissolved (*see* **Note 5**).
6. Coating 3–4 pieces of 24-well cell culture plate, each well added 500 μL coating buffer. Incubate at 37 °C for over 2 h before use.
7. Prepare percoll buffer: 4 mL top percoll solution and 3 mL bottom percoll solution in a 15 mL centrifuge tube (*see* **Note 6**).
8. Cell suspensions from all collecting tubes were pooled, filtered (*see* **Note 7**), and centrifuged for 5 min at 1000 rpm and the resulting cell pellet was resuspended in 8 mL cold 1× ADS.
9. The cell suspension was layered on the top of the percoll solution, each percoll solution added 2 mL cell suspension (*see* **Note 8**).
10. 15 mL tubes were centrifuged at 3000 rpm, 4 °C for 30 min using standard protocols of acceleration and deceleration speed 0.
11. Cardiomyocytes could be removed from the newly formed layer between the percoll solutions (band 2). Stromal cells

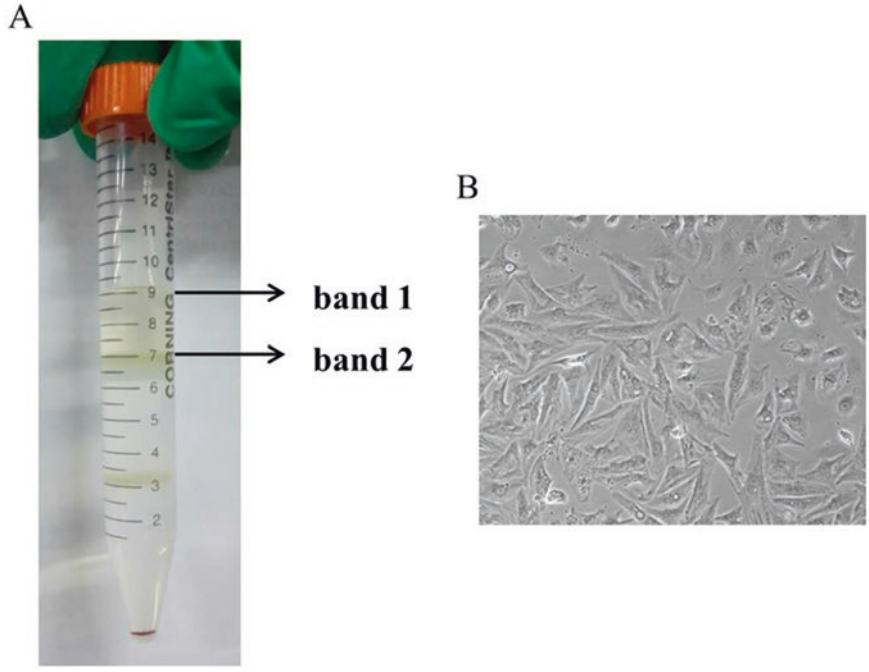

Fig. 1 Primary isolation of cardiomyocytes from neonatal rats. (**a**) Morphological characterization of cells after percoll gradient centrifugation. Band 1 referred to cardiac stromal cells including fibroblasts. Band 2 referred to cardiomyocytes. (**b**) Purity of cardiomyocytes in culture. Bright field image taken after 2 days of cardiomyocytes isolation. Scale bar represented 100 μm

including fibroblasts on the top of the transparent percoll solution (band 1) were harvested separately (Fig. 1).

12. Cardiomyocytes were pooled, diluted in 1:4 warmed neonatal cardiomyocytes culture medium, and centrifuged at 1000 rpm for 5 min. The cell pellet was resuspended in a 10 mL neonatal cardiomyocytes culture medium.
13. Add 10 μL cell suspension to count total number of isolated cells. After acquiring the quantity of cardiomyocytes, cell suspension was diluted in corresponding volume of neonatal cardiomyocytes culture medium according to experimental needs.
14. Cardiomyocytes were seeded at a density of 2×10^5/mL on gelatin-coated multiwell plates and placed in a humidified incubator at 37 °C and 5% CO_2 (*see* **Note 9**) (Fig. 1).

3.2 miRNA Mimic and Inhibitor Transfection

1. Cardiomyocytes were prepared 6–8 h in antibiotic and serum-free culture medium (DMEM-F12) before transfection (*see* **Note 10**).
2. Prepare mimic/inhibitor or their respective negative control reaction mixture (24-well cell culture plate):
   (a) Solution 1: 1.25 μL mimic/2.5 μL Inhibitor and 50 μL Opti-MEM (*see* **Note 11**).

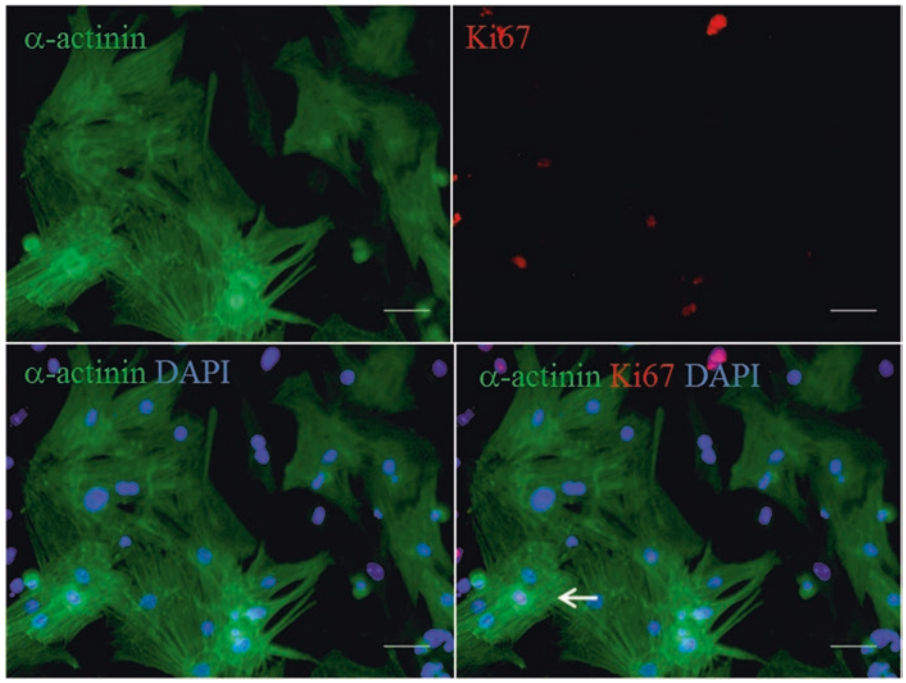

Fig. 2 Cell proliferation was measured by Ki67 (red)/α-actinin (green)/DAPI (blue) immunofluorescent staining. Scale bar represented 50 μm

(b) Solution 2: 2 μL lipo 2000 and 50 μL Opti-MEM.

(c) Solution 3: add solution 2 to solution 1 with sufficient mixing and stand at room temperature for 15 min.

(d) Transfection mixture: add 150 μL DMEM-F12 to solution 3 with sufficient mixing.

3. Remove half of the culture medium from each cell plate and add transfection mixture (*see* **Note 12**).
4. After 6–8 h, remove the culture medium and change to fresh DMEM-F12 Medium.

3.3 Ki67/α-Actinin Immunofluorescent Staining (Fig. 2)

Immunofluorescent staining was performed after 4 days in culture (*see* **Note 13**).

1. Remove the culture medium, rinse cardiomyocytes gently with PBS 3 times, 5 min each time.
2. Cardiomyocytes were fixed with 4% PFA for 20 min (*see* **Note 14**), then remove 4% PFA.
3. Wash cardiomyocytes with PBS 3×, 5 min each time.
4. Cardiomyocytes were permeabilized with PBST for 20 min, then remove PBST.
5. Wash as in **step 3**.

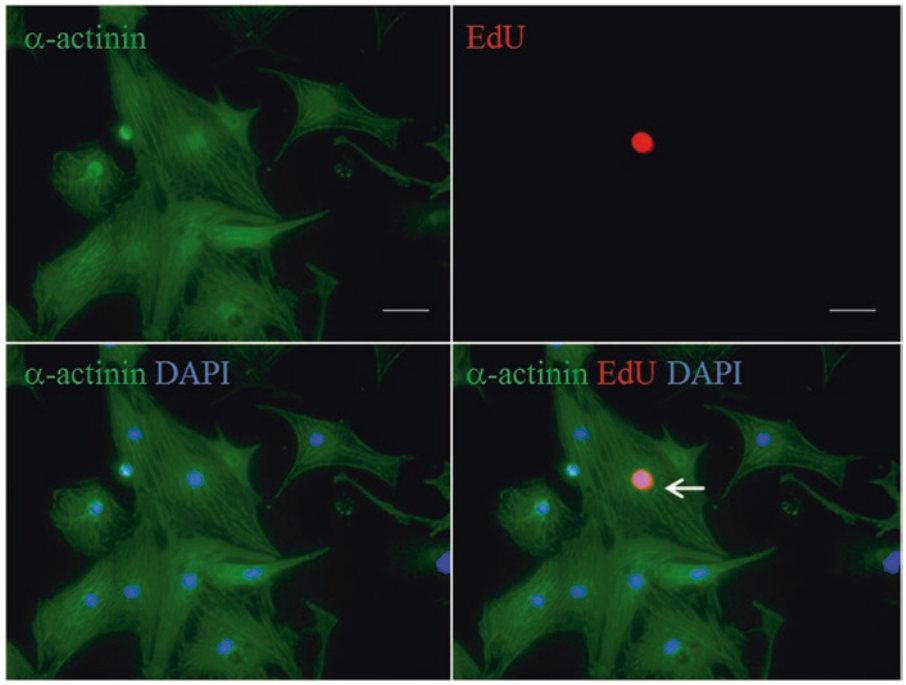

Fig. 3 Cell proliferation was measured by EdU (red)/α-actinin (green)/DAPI (blue) immunofluorescent staining. Scale bar represented 50 μm

6. Add 10% goat serum and block for 1 h, then remove blocking solution.
7. Diluted primary antibodies (Ki67/α-actinin) were added and placed at 4 °C overnight (*see* **Note 15**).
8. Remove diluted primary antibodies, wash as **step 3**.
9. Diluted second antibodies were added and placed in a cassette at room temperature for 2 h (*see* **Note 16**).
10. Wash as in **step 3**.
11. Diluted DAPI (1:1000 dilution, diluted in blocking solution) was added to mark cell nuclei for 20 min.
12. Wash as in **step 3**.
13. Analysis was performed at a confocal microscope (Carl Zeiss). 15-20 fields (200× magnification) were taken from every sample and the rate of Ki67-α-actinin double positive cells to α-actinin positive cells was calculated.

3.4 Edu/α-Actinin Immunofluorescent Staining (Fig. 3)

1. Immunofluorescent staining of α-actinin was demonstrated as in Ki67/α-actinin immunofluorescent staining step (*see* **Note 17**).
2. Prepare EdU stock solutions (*see* **Note 18**):
   (a) 10 mM material EdU stock solutions (A): 2 mL DMSO and 5 mg material EdU powder, mixed and stored at 4 °C.

10 μM material EdU working solution: 10 mL culture medium and 10 μL EdU stock solution (*see* **Note 19**).

(b) Alexa Fluor azide (B) working solution: 70 μL DMSO and 4 mL Alexa Fluor azide. Mixed and stored at 4 °C.

(c) 1× Click-iT® EdU reaction buffer (D): 4 mL Click-iT® EdU reaction buffer and 36 mL ultrapure water. Mixed and stored at 4 °C.

(d) 10× Click-iT® EdU additive buffer (D): 2 mL ultrapure water and 400 mg Click-iT® EdU additive powder. Mixed and store at −20 °C.

3. EdU labeling

(a) Prepare material EdU working solution (10 μM): 10 mL culture medium and 10 μL EdU stock solution.

(b) Remove half of the culture medium and add same volume of material EdU working solution (10 μM) 24 h before immunofluorescent staining (*see* **Note 20**).

4. EdU detection

(a) 1× Click-iT® EdU additive buffer: 9 mL ultrapure water and 1 mL 10× Click-iT® EdU additive buffer (D) (*see* **Note 21**).

(b) Prepare reaction mixture (1 mL): 860 μL 1× Click-iT® EdU reaction buffer, 40 μL $CuSO_4$, 2.5 μL Alexa Fluor azide, and 100 μL 1× Click-iT® EdU additive buffer (*see* **Note 22**).

(c) Add EdU reaction mixture and place in a cassette at room temperature for 30 min.

(d) Wash cardiomyocytes with PBS 3×, 5 min each time.

(e) Diluted DAPI (1:1000 dilution, diluted in blocking solution) was added to mark cell nuclei for 20 min.

(f) Wash as in **step 4**.

5. Analysis was performed at a confocal microscope (Carl Zeiss). 15-20 fields (200× magnification) were taken from every sample and the rate of EdU-α-actinin double positive cells to α-actinin positive cells was calculated.

4 Notes

1. When taking the ventricular tissue away from the rat body, remove irrelevant substances such as lung, blood vessels, and atria. Before mincing into pieces, ventricular tissues are needed to be washed with ice-cold 1× ADS for several times to remove blood cells.

2. The Percoll stock solution can be stored at 4 °C for 1 week. Also top percoll solution and bottom percoll solution need to be freshly prepared before use.
3. Following enzymatic dissociation of the heart tissue, a certain number of heart tissues correspond to a certain volume of trypsin-collagenase 2 buffer. In our lab, 15 rats correspond to 30 mL trypsin-collagenase2 buffer each time.
4. Before transferring cell suspension, stand the glass bottle for 3–5 min after taking out from cell vibrator, which will help in obtaining maximized amount of cardiomyocytes.
5. During the process of dissolution, slightly reduce the amount of trypsin-collagenase 2 buffer and dissolved time according to the remaining tissue fragments.
6. To acquire maximized amount of cardiomyocytes, 7 rats correspond to 1 piece of percoll solution. Percoll solution is a two-layer density gradient consisting of 4 mL top percoll solution and 3 mL bottom percoll solution. When preparing percoll solution, add top percoll solution first, then slowly add bottom percoll solution with 2 mL injector from the bottom of centrifuge tube.
7. The purpose of the filter of pooled cell suspensions is to remove the collagen.
8. To avoid destroying the two-layer structure of percoll solution, slowly add cell suspension to the top of percoll solution.
9. Cardiomyocytes cultures are left undisturbed for 36 h and subsequent media changes performed every 48 h.
10. Before transfection, the density of cardiomyocytes needs to achieve >70% confluence.
11. The working concentrations of mimic and Inhibitor are different. For mimic: working concentration is 50 nmol, while for Inhibitor: the working concentration is 100 nmol.
12. To reduce the damage of transfection on cardiomyocytes, the half-changing method is used: remove half of the culture medium and add another half volume of fresh culture medium with transfection mixture.
13. To avoid affecting proliferative detection, culture medium for cardiomyocytes needs to change to DMEM-F12 without FBS or HS after culturing for 36 h.
14. For a 24-well cell culture plate, 200 μL fixing solution/permeabilized buffer/blocking solution/diluted primary antibody/diluted second antibody per well is enough for immunofluorescent staining.
15. Different antibodies have different dilution ratios. For primary antibodies, anti α-actinin monoclonal mouse IgM: 1:100

dilution, dilute in blocking solution, anti Ki67 monoclonal rabbit IgG: 1:50–1:100 dilution. For second antibodies, Alexa Fluor 488-conjugated polyclonal donkey anti-mouse IgM: 1:100 dilution, Alexa Fluor 594-conjugated polyclonal donkey anti-rabbit IgG: 1:100 dilution.

16. After adding fluorophore-conjugated secondary antibodies, all the procedures need to be shielded from light.
17. When performing EdU/α-actinin co-immunofluorescent staining, α-actinin is stained first and all the procedures of EdU staining need to be shielded from light.
18. Before preparing stock solutions, all the materials of EdU kit except Hoechst needed to be placed at room temperature for 3–5 min.
19. EdU stock solutions can be stored at 4 °C or −20 °C for 1 year. The material EdU (A) working solution needs to be freshly prepared before use.
20. In order to reduce the stimulation of cardiomyocytes, half of culture medium is removed and add the same volume of EdU working solution (10 μM).
21. 1× Click-iT® EdU additive buffer needs to be freshly prepared before use.
22. When preparing EdU reaction mixture, strictly follow the order and finish within 15 min.

Acknowledgments

This work was supported by the grants from National Natural Science Foundation of China (81570362, 91639101, and 81200169 to J.J. Xiao and 81400647 to Y. Bei), Innovation Program of Shanghai Municipal Education Commission (2017-01-07-00-09-E00042), the grant from Science and Technology Commission of Shanghai Municipality (17010500100), and the development fund for Shanghai talents (to J.J. Xiao).

References

1. Yutzey KE (2017) Cardiomyocyte proliferation: teaching an old dogma new tricks. Circ Res 120:627–629
2. Foglia MJ, Poss KD (2016) Building and rebuilding the heart by cardiomyocyte proliferation. Development 143:729–740
3. Walsh S, Ponten A, Fleischmann BK, Jovinge S (2010) Cardiomyocyte cell cycle control and growth estimation in vivo – an analysis based on cardiomyocyte nuclei. Cardiovasc Res 86:365–373
4. Porrello ER, Mahmoud AI, Simpson E, Hill JA, Richardson JA, Olson EN, Sadek HA (2011) Transient regenerative potential of the neonatal mouse heart. Science 331:1078–1080
5. van Berlo JH, Molkentin JD (2014) An emerging consensus on cardiac regeneration. Nat Med 20:1386–1393

6. Liu X, Xiao J, Zhu H, Wei X, Platt C, Damilano F, Xiao C, Bezzerides V, Bostrom P, Che L, Zhang C, Spiegelman BM, Rosenzweig A (2015) miR-222 is necessary for exercise-induced cardiac growth and protects against pathological cardiac remodeling. Cell Metab 21:584–595
7. Bergmann O, Bhardwaj RD, Bernard S, Zdunek S, Barnabé-Heider F, Walsh S, Zupicich J, Alkass K, Buchholz BA, Druid H, Jovinge S, Frisén J (2009) Evidence for cardiomyocyte renewal in humans. Science 324:98–102
8. Senyo SE, Steinhauser ML, Pizzimenti CL, Yang VK, Cai L, Wang M, Wu TD, Guerquin-Kern JL, Lechene CP, Lee RT (2013) Mammalian heart renewal by pre-existing cardiomyocytes. Nature 493:433–436
9. Malliaras K, Zhang Y, Seinfeld J, Galang G, Tseliou E, Cheng K, Sun B, Aminzadeh M, Marban E (2013) Cardiomyocyte proliferation and progenitor cell recruitment underlie therapeutic regeneration after myocardial infarction in the adult mouse heart. EMBO Mol Med 5:191–209
10. Koitabashi N, Kass DA (2011) Reverse remodeling in heart failure – mechanisms and therapeutic opportunities. Nat Rev Cardiol 9:147–157
11. Louch WE, Sheehan KA, Wolska BM (2011) Methods in cardiomyocyte isolation, culture, and gene transfer. J Mol Cell Cardiol 51:288–298
12. LaFramboise WA, Scalise D, Stoodley P, Graner SR, Guthrie RD, Magovern JA, Becich MJ (2007) Cardiac fibroblasts influence cardiomyocyte phenotype in vitro. Am J Physiol Cell Physiol 292:C1799–C1808
13. Dispersyn GD, Geuens E, Ver Donck L, Ramaekers FC, Borgers M (2001) Adult rabbit cardiomyocytes undergo hibernation-like dedifferentiation when co-cultured with cardiac fibroblasts. Cardiovasc Res 51:230–240
14. Miragoli M, Salvarani N, Rohr S (2007) Myofibroblasts induce ectopic activity in cardiac tissue. Circ Res 101:755–758
15. Salic A, Mitchison TJ (2008) A chemical method for fast and sensitive detection of DNA synthesis in vivo. Proc Natl Acad Sci U S A 105:2415–2420
16. Tao L, Bei Y, Chen P, Lei Z, Fu S, Zhang H, Xu J, Che L, Chen X, Sluijter JP, Das S, Cretoiu D, Xu B, Zhong J, Xiao J, Li X (2016) Crucial role of miR-433 in regulating cardiac fibrosis. Theranostics 6:2068–2083
17. Pathmanathan N, Balleine RL (2013) Ki67 and proliferation in breast cancer. J Clin Pathol 66(6):512
18. Eulalio A, Mano M, Dal Ferro M, Zentilin L, Sinagra G, Zacchigna S, Giacca M (2012) Functional screening identifies miRNAs inducing cardiac regeneration. Nature 492: 376–381
19. Shi J, Bei Y, Kong X, Liu X, Lei Z, Xu T, Wang H, Xuan Q, Chen P, Xu J, Che L, Liu H, Zhong J, Sluijter JP, Li X, Rosenzweig A, Xiao J (2017) miR-17-3p contributes to exercise-induced cardiac growth and protects against myocardial ischemia-reperfusion injury. Theranostics 7:664–676
20. Piccoli MT, Gupta SK, Thum T (2015) Noncoding RNAs as regulators of cardiomyocyte proliferation and death. J Mol Cell Cardiol 89:59–67

Chapter 18

Gene Manipulation with Micro RNAs at Single-Human Cancer Cell

Andres Stucky, Xuelian Chen, and Jiang F. Zhong

Abstract

Micro RNAs (miRNAs) are small RNAs processed from longer precursor RNA transcripts that can fold back on themselves to form Watson-Crick paired hairpin structures. Once processed from the longer molecule, the small RNA is much too short to code for proteins but can play other very important roles, like gene regulation. The phenomenon of RNA interference was initially observed by Napoli and Jorgensen in transgenic petunia flowers, where gene suppression was observed after introducing a transgene of chalcone synthase (CHS) belonging to the flavonoid biosynthesis pathway. miRNAs were first discovered for their roles in development but it has quickly become evident that they have causal roles in cancer as well. miRNA can also be used to manipulate genes for the investigation of carcinogenesis. Single-cell transcriptome profiling studies in our laboratory suggest that carcinogenesis often is the result of the malfunction of multiple members of a molecular pathway. Here, we describe a protocol to manipulate multiple cancer-related genes in a single human cell to investigate how multiple genes interact during carcinogenesis.

Key words Gene manipulation, Cancer, Single-cell

1 Introduction

In 2006, the Nobel Prize in Medicine was jointly awarded to Craig Mello and Andrew Fire for the discovery of RNA interference or gene silencing by double-stranded RNA in *Caenorhabditis elegans*. Since then, a variety of miRNA families have been discovered in almost all metazoan organisms and have been well studied in a variety of model organisms including *C. elegans* and *Arabidopsis thaliana*.

The phenomenon of RNA interference was initially observed by Napoli and Jorgensen in transgenic petunia flowers, where gene suppression was observed after introducing a chalcone synthase (CHS) transgene belonging to the flavonoid biosynthesis pathway [1]. This resulted in white petunia petals, instead of the expected dark blue coloration. Later in 1992, a similar phenomenon known as "quelling" was observed in *Neurospora crassa* while attempting to enhance orange pigmentation by the al1 gene of this fungus [2].

Shao-Yao Ying (ed.), *MicroRNA Protocols*, Methods in Molecular Biology, vol. 1733,
https://doi.org/10.1007/978-1-4939-7601-0_18,

Micro RNAs (miRNAs) are small RNAs processed from longer precursor RNA transcripts that can fold back on themselves to form Watson-Crick paired hairpin structures. Once processed from the longer molecule, the small RNAs are too short to code for proteins but they play other important roles, like gene regulation.

Much like other genes, miRNAs can be highly conserved among various species with very similar orthologs in humans, flies, and worms. There can also be several miRNA homologs within a single species that can produce highly similar, if not identical copies, of the same miRNA. In humans, there are 277 miRNA-coding genes constituting 153 families of miRNAs conserved in mammalian species. Of the 153 families conserved in mammals, 87 of them are shared with zebrafish and up to 33 are shared with flies and worms. Scientists rapidly recognized the potential uses of miRNAs in the treatment of disease and the silencing of any gene of interest upon demand. Moreover, the discovery of RNA interference added another layer of complexity to our understanding of gene regulatory networks.

RNA interference is a process inside eukaryotic and prokaryotic cells by which mRNA sequences are selected and targeted for destruction so that no protein is produced from the message. Interfering RNAs can come in three different flavors: small interfering RNAs (siRNAs), short hairpin RNAs (shRNAs), and micro RNAs (miRNAs). All three types perform similar gene silencing functions, but they vary with respect to the way they are produced, the extent of gene silencing they accomplish, and the process through which they achieve it.

In eukaryotes, the three key proteins required for the manufacture of miRNAs are Argonaut (AGO) and two endonucleases, Drosha and Dicer. The first step in the process is the initial transcription of a larger 100–120 nt primary RNA (pri-miRNA) transcript by Pol2 polymerase. While still in the nucleus, pri-miRNAs are bound by a Drosha/Pasha (DGCR8) binding complex that recognizes a specific motif in the hairpin molecule, which is then cleaved about one helical turn from the base of the hairpin. This releases a 70 nt pre-miRNA hairpin which exits the cell nucleus with the aid of the exportin 5 complex [3]. Once in the cytoplasm, the miRNA encounters Dicer, which then cleaves off the miRNA loop, leaving only a 15–21 nt pre-miRNA duplex with a 2 nt overhang at the 3′ region and a 5′ monophosphate. Following cleavage, the miRNA:miRNA*duplex strand is loaded onto the RNA binding pocket in the Argonaut (AGO) protein, the major component of the RNA-Interfering Silencing Complex (RISC). It is not yet clear which strand of the miRNA duplex is loaded, but there are indications that it is the strand with the least stable pairing at its 5′ end which has a higher binding probability. The passenger strand is then released and the active miRNA complex migrates to the targeted mRNA and forms a nuclear hybrid

structure with the target structure. Once nucleated, Argonaut recognizes the dsRNA and cleaves the mRNA, leaving the bound miRNA intact.

In humans, the Argonaut family is composed of four distinct proteins, human Argonaut 1-4 (hAgo1-hAgo4), all of which share similar architectural domains. The Mid, N, and PIWI domains form a base upon which the PAZ domain rests. This structure is critical for the binding and slicing of interfering RNAs. Consistent with the biochemistry of the slicer function, the PIWI domain of Argonaut has been shown to resemble a RNase H enzyme. A binding site in the Mid domain anchors the phosphate backbone of the guide strand at the 5′ end [4], whereas the 3′ end attaches to the PAZ domain [5]. A highly conserved DEDH catalytic tetramer in the PIWI active site is the critical slicing component in Argonaut [6, 7]. The remaining components needed for targeted mRNA cleavage are the RNA guide strand and a Mg^{2+} molecule [8].

In most cases, miRNA-mRNA pairing is not fully complementary; thus, the key target site of miRNA is a set of 6 nt, called the seed of the miRNA, that extends from nucleotides 2 through 7 at the 5′ end. This sequence can be often complemented by a pair in nucleotide 8 or an A in the position 1 complementary site, so either or both of these complementary sites would form a seed of 8 pairing nucleotides which are most frequently conserved in the untranslated regions (UTRs) [9]. Interestingly, pairing at the 3′ end in the center of the miRNA appears to play very little role in target recognition or binding, though occasionally some pairing at the 3′ end will supplement the seed pairing, even compensating at times for a certain teeter due to mismatch in the seed region, but these events are very rare and only account for about 1–5% of functional miRNA [10]. The length of the actual seed pairing site ensures that a single miRNA can have numerous mRNA targets and indicates that mammalian mRNAs are under powerful selective pressure to preserve their pairing to miRNA in their UTRs. It has even been observed that on average there are a roughly 400 conserved targets per miRNA family and up to 4 or 5 conserved miRNA binding sites per conserved target. Therefore, a single target can be monitored by several different miRNAs, depending on the cellular context, and often multiple miRNAs are working together to orchestrate the magnitude and timing of gene silencing [9]. A single miRNA can have multiple targets. Conversely, a single miRNA might not be sufficient to silence a single target, so genetic engineering kits for gene silencing provide a set of up to three miRNAs to ensure strong silencing and target specificity. For these reasons, miRNAs are ideal tools to manipulate multiple genes in a molecular pathway, such as those responsible for carcinogenesis.

Here, we describe a protocol for gene manipulation with miRNA. These techniques hold potential for the development of miRNA cancer therapy. For instance, loss of the miR-34 tumor

suppressor leads to faulty regulation of its downstream mytotic (MET, WNT, MYC) [11–13] and anti-apoptotic (BCL-2, SIRT-1 and Survivin) targets and cell cycle regulators (CyclinD, CDK6, and CDK4) [14]. Pathway inhibition can be restored by miR-34 supplementation, or with the addition of a CDK4-targeting siRNA, thereby repressing the associated pathway [15]. Although miRNA therapeutics have been found to suppress gene expression effectively compared to anti-sense oligonucleotides, they are still limited by their high biological instability and off-target effects, and the difficulty of delivering them to the desired cell system. To a certain extent, some of these hurdles have been overcome by using chemically synthesized molecules with special modifications such as cholesterol conjugates, morpholinos, cationic lipids, and nanoparticles [16]. Current progress in developing miRNA-based anticancer therapies has been most promising in the modulation of cancer cell miRNA by various chemoprophylactic agents.

2 Materials and Methods

All the solutions should be prepared beforehand, with buffers using ultrapure RNase-free water and molecular-grade reagents. Follow proper sterile and safe laboratory techniques, as well as all chemical and biological waste disposal regulations.

2.1 Selection of siRNA Sequences

1. Select a DNA sequence, preferably more than 50–100 nt downstream of the start codon within the open reading frame of your cDNA of choice. 5′ or 3′ untranslated regions (UTRs) as UTR-binding proteins could restrict RISC binding to the target RNA [17].
2. Search for a sequence 19–21 nt between a 5′ AA and a 3′ UU (5′-AA(N19-21)UU), in an mRNA sequence that shows an approximate 50% G/C content. High-G-content sequences should be avoided as they are likely to form G-quartet structures. Synthesize the sense siRNA as 5′-(N19)TT, and the sequence of the antisense siRNA as 5′-(N′19)TT, where N′19 denotes the reverse complement sequence of N19. N19 and N′19 indicate ribonucleotides; T indicates 2′-deoxythymidine.
3. Perform a basic local alignment search (BLAST) of the selected siRNA sequences against expression sequence tags (EST) mRNA libraries for your organism of interest to confirm that only a single gene is targeted. Preferred sites for BLAST are NCBI (www.ncbi.nlm.nih.gov/BLAST)and Ensembl (www.ensembl.org).
4. Synthesis of several siRNA duplexes might be required to control for knock-down target specificity; effective siRNA duplexes should produce the same phenotype. A scrambled nonspecific

siRNA duplex should be designed as a negative control. Most RNAI kits will provide this control duplex. The use of an unrelated target gene that is absent from the selected model can be used as a positive RNAI control. If the siRNA does not work, make sure that the mRNA sequence used for the selection of the siRNA duplexes is reliable; it could contain sequencing errors, mutations, or polymorphisms.

5. Most predesigned DNA oligos purchased from a vendor will come already annealed. Otherwise, dsDNA should be incubated for 1 min at 90 °C, followed by 1 h at 37 °C in annealing buffer (4 mM magnesium acetate, 200 mM potassium acetate, 60 mM Hepes–KOH, pH 7.4). To prepare 100 μL of a 20 μM siRNA duplex solution, combine 50 μL 2× annealing buffer, sense siRNA to a 20 μM final concentration, antisense oligonucleotide to a 20 μM final concentration, and sterile RNase-free water.
6. Store the RNA suspension solution at −20 °C. The solution may be frozen and thawed several times without requiring any further heat-shock treatments. During use, it is recommended that the RNA solutions be thawed over ice and kept on ice as much as possible to minimize the hydrolysis of RNA.
7. The MW of the siRNA may be assessed by loading 0.5 μL 20 μM of sense, antisense, and duplex siRNA onto 4% agarose gels for loading of the samples. First, dilute the samples with a few microliters of 0.5× TBE buffer (45 mM Tris base, 45 mM boric acid, 1 mM Na2 EDTA) and sucrose loading buffer. Run the gel in 0.5× TBE buffer at 80 V for 1 h. The RNA bands can be visualized under UV light after ethidium bromide staining. Preferably, the ethidium bromide should be added to the 4% gel/0.5× TBE solution at a concentration of 0.04% mg/L prior to casting of the gel.
8. Culture the cell line of interest in a humidified incubator with 5% CO_2 and 95% humidity at 37 °C in Dulbecco's modified Eagle's medium (DMEM) supplemented with 10% fetal bovine serum (FBS), 100 units/mL penicillin, and 100 μg/mL streptomycin (in the case of embryonic or progenitor stem cells, use the cell type-specific medium). Passage cells when they reach 90% confluency to maintain exponential growth. For a general reference for cell culture, please see Freshney 2016 [18]. The number of passages could affect DNA and siRNA transfection efficiencies as well as the experimental outcome. As a rule, do not exceed 30 passages for transformed cells or the 3rd or 4th passage in the case of embryonic or progenitor stem cells. Freeze and store low-passage number cells in liquid nitrogen, so they can be thawed and used when convenient.

9. To prepare for the experiment, passage cells 24 h before siRNA transfection. Trypsinize 90% confluent cells with enough trypsin–EDTA to cover the bottom of the culture plate for 5 min or until the cells have detached completely. Dilute the cell suspension 1:5 with fresh DMEM medium, transfer to a 15 or 50 ml tube and spin at 600 × *g* to pellet the cells. Wash and spin the cells twice with PBS, then add enough medium to transfer 500 µL aliquots of 5×10^3 cells/cm^2 into each well of a 24-well plate.
10. If an immunofluorescent reporter is used to visualize transfection efficiency [19], cells should be plated on round coverslips and placed at the bottom of the 24-well plates prior to addition of cell suspension. Transfection should be performed according to cell confluence indicated by the manufacturer of the transfection reagent that will be used.
11. Transfection of duplex RNAs into tissue culture cells can usually be achieved using cationic lipids. Testing a variety of lipid agents with each cell type might be necessary to identify the optimal reagent to introduce the RNA duplex into the cells with the highest efficiency and least toxicity. A fluorescently labeled transfection control duplex may be added to the transfection mix (10 nm) to visually assess the transfection efficiency. The cells should show both fluorescent puncta and cytoplasmic diffusion while still appearing healthy. In cases where the cells are resistant to cationic lipid transfection, introduction of the siRNA can be achieved by electroporation.
12. On the day of transfection, replace old medium with 0.5 mL of fresh DMEM. To prepare the transfection mixture, add 2 µL Lipofectamine (or preferred transfection reagent, according to the manufacturer's recommendation) to 50 µL serum-free medium. Mix by gently inverting the tube and incubate the suspension for 5 min at room temperature without movement.
13. In a separate tube, add 2 nM of your siRNA duplex and 10 nM fluorescent probe to 50 µL serum-free medium and vortex, then spin down briefly on a tabletop centrifuge. Allow incubating at room temperature for 5 min.
14. Combine the transfection mixture with the siRNA suspension, gently mix, and allow the formation of liposome complexes by incubating for 20–25 min at room temperature. Be careful not to exceed a 30 min incubation time.
15. Add the 100 µL liposome complexes to the well containing 0.5 mL of DMEM, mix gently for 30 s, and incubate the plate for 20–48 h at 37 °C. Cytoplasmic fluorescent diffusion should be visible 48 h following the transfection.

Fig. 1 Fluorescent visualization of TYE563-tagged RNA inside cells. RNA tagged with red fluorescent dye TYE563 is inside the majority of cells

2.2 Fluorescent Visualization

1. Fix and permeabilize the cells by removing the medium and incubating the cells in a 10% formalin solution for 30 min. Wash the formalin-fixed cells with phosphate-buffered saline (PBS: 137 mM NaCl, 7 mM Na_2HPO_4, 1.5 mM KH_2PO_4, 2.7 mM KCl, pH 7.1) remove excess PBS. If no further staining is required, mount cover slips on microscope slides using a mounting solution and seal the edges of the coverslip with a small amount of clear nail polish.
2. If further staining is required, place the coverslips in a covered chamber prepared by soaking filter paper in water and placing on the bottom of the chamber. It is important that the prepared cells do not dry out during the staining process. Spread 1 mL of primary antibody appropriately diluted in PBS and 10% FBS evenly over the entire surface of the coverslip and incubate at room temperature for 60 min. Wash the cells with PBS 3× and add an appropriately diluted fluorescent-tagged secondary antibody. Incubate for 30 min, wash three times and coverslip as before. Visualize the cells under a fluorescent microscope (Fig. 1).

2.3 Detection of Protein by Western Blotting

1. Remove the tissue culture medium from the siRNA-treated cells. Rinse the cells twice with 200 µL PBS and add 200 µL trypsin–EDTA. Incubate for 5 min at room temperature and resuspend the cells in 800 µL DMEM medium to quench trypsin.
2. Transfer the cells to a 1.5 mL tube. Collect the cells by centrifugation at 3000 rpm (600 × *g*) for 4 min at 4 °C to pellet the cells. Resuspend the pellet in ice-cold PBS and centrifuge again. Remove the supernatant and add 25 µL of 2× concentrated Laemmli buffer with 10% concentration of sodium dodecyl sulfate (SDS) to the cell pellet obtained from one well of a 24-well plate. Incubate the sample for 10 min in a boiling water bath and vortex.

3. Load the samples onto minigels with an appropriate acrylamide concentration to resolve the corresponding molecular weight of the targeted protein [20]. Perform SDS–PAGE electrophoresis using a constant 20 mA current. Transfer proteins from the acrylamide minigels onto nitrocellulose membrane using transfer buffer (25 mM Tris, 192 mM glycine, 0.01% SDS, 20% methanol), with a constant 333 mA current for 2 h in a cold room. Incubate the membrane in blocking solution (5% milk powder in TBST (0.2% Tween 20, 20 mM Tris–HCl, 150 mM NaCl, pH 7.4)) for 1 h at 37 °C.
4. Add the appropriate dilution of primary antibody and incubate for 2 h at room temperature or at 4 °C overnight. Wash the blot three times with TBST for 10 min. Incubate the blot with horseradish peroxidase (HRP)-conjugated secondary antibody at a dilution of 1:2000. Proceed to ECL detection according to the vendor's instructions. Details of the Western blotting procedure were published previously [20].

3 Note

Unlike messenger RNAs, the precursor RNAs for interfering RNAs are double-strand. Primary or precursor miRNAs can be produced in several different ways. In the case of miRNA, a single miRNA stem loop transcript is produced from a gene. For shRNA, three individual hairpins are produced from the same transcript; each hairpin is a 20–25 nt sequence that fold backs onto itself to form a short hairpin structure. The hairpin is exported from the nucleus and Dicer cleaves both RNA strands to form two complementary sequences. Finally, in the case of siRNA, a large double-stranded mRNA transcript is synthesized from the same locus after Dicer processing. This system can produce a large amount of smaller RNA duplexes called small interfering RNAs (siRNAs). Other differences between miRNA and siRNA include the fact that miRNAs are single-stranded and come from endogenous noncoding RNA found within the introns of long RNA molecules, whereas siRNAs are usually found as exogenous double-stranded RNA. These siRNAs then guide the siRNA-AGO complex to silence the same loci from which they were produced, ensuring a very efficient feedback loop to silence transgenes, transposons, and viruses. This stands in contrast to miRNAs, which can inhibit many different mRNAs because their pairing is imperfect. siRNAs typically show perfect pairing with their mRNA target. Given the major roles that siRNA and miRNA play in the control of gene expression, it is not surprising they have both been extensively studied for therapeutic application in RNA-induced transcriptional silencing (RITS) [21].

Acknowledgments

This work was supported by grants R01CA197903 and R01CA1645093 from the National Institutes of Health, USA (J.F.Z.), and CHE1213161 from the National Science Foundation USA (J.F.Z.), and an internal grant from the University of Southern California (J.F.Z. and P.P.S.).

References

1. Napoli C, Lemieux C, Jorgensen R (1990) Introduction of a chimeric chalcone synthase gene into petunia results in reversible co-supression of homologous genes in trans. Plant Cell 2:279–289
2. Romano N, Macino G (1992) Quelling: transient inactivation of gene expression in Neurospora crassa by transformation with homologous sequences. Mol Microbiol 6(22):3343–3353
3. Kim VN (2005) MicroRNA biogenesis: coordinated cropping and dicing. Nat Rev Mol Cell Biol 6(5):376–385
4. Parmar R, Willoughby JL, Liu J, Foster DJ, Brigham B, Theile CS, Charisse K, Akinc A, Guidry E, Pei Y, Strapps W, Cancilla M, Stanton MG, Rajeev KG, Sepp-Lorenzino L, Manoharan M, Meyers R, Maier MA, Jadhav V (2016) 5'-(E)-Vinylphosphonate: a stable phosphate mimic can improve the RNAi activity of siRNA-GalNAc conjugates. Chembiochem 17:985–989
5. Lingel A, Simon B, Izaurralde E, Sattler M (2004) Nucleic acid 3'-end recognition by the Argonaute2 PAZ domain. Nat Struct Mol Biol 11:576–577
6. Liu J, Carmell MA, Rivas FV, Marsden CG, Thomson JM, Song JJ, Hammond SM, Joshua-Tor L, Hannon GJ (2004) Argonaute2 is the catalytic engine of mammalian RNAi. Science 305:1437–1441
7. Rivas FV, Tolia NH, Song JJ, Aragon JP, Liu J, Hannon GJ, Joshua-Tor L (2005) Purified Argonaute2 and an siRNA form recombinant human RISC. Nat Struct Mol Biol 12:340–349
8. MacRae IJ, Ma E, Zhou M, Robinson CV, Doudna JA (2008) In vitro reconstitution of the human RISC-loading complex. Proc Natl Acad Sci U S A 105:512–517
9. Bartel DP (2004) MicroRNAs: genomics, biogenesis, mechanism, and function. Cell 116:281–297
10. Macfarlane LA, Murphy PR (2010) MicroRNA: biogenesis, function and role in cancer. Curr Genomics 11:537–561
11. Cheng CY, Hwang CI, Corney DC, Flesken-Nikitin A, Jiang L, Oner GM, Munroe RJ, Schimenti JC, Hermeking H, Nikitin AY (2014) miR-34 cooperates with p53 in suppression of prostate cancer by joint regulation of stem cell compartment. Cell Rep 6:1000–1007
12. Kim NH, Kim HS, Kim NG, Lee I, Choi HS, Li XY, Kang SE, Cha SY, Ryu JK, Na JM, Park C, Kim K, Lee S, Gumbiner BM, Yook JI, Weiss SJ (2011) p53 and microRNA-34 are suppressors of canonical Wnt signaling. Sci Signal 4:ra71
13. Zhang DG, Zheng JN, Pei DS (2014) P53/microRNA-34-induced metabolic regulation: new opportunities in anticancer therapy. Mol Cancer 13:115
14. Achari C, Winslow S, Ceder Y, Larsson C (2014) Expression of miR-34c induces G2/M cell cycle arrest in breast cancer cells. BMC Cancer 14:538
15. Zhang YH, Wang QQ, Li H, Ye T, Gao F, Liu YC (2016) miR-124 radiosensitizes human esophageal cancer cell TE-1 by targeting CDK4. Genet Mol Res 15:2–10
16. Jain CK, Gupta A, Dogra N, Kumar VS, Wadhwa G, Sharma SK (2014) MicroRNA therapeutics: the emerging anticancer strategies. Recent Pat Anticancer Drug Discov 9:286–296
17. Peek AS, Behlke MA (2007) Design of active small interfering RNAs. Curr Opin Mol Ther 9:110–118
18. Freshney RI (2016) Culture of animal cells: a manual of basic technique and specialized applications. Wiley-Blackwell, Hoboken, NJ
19. Landen CN, Chavez-Reyes A, Bucana C, Schmandt R, Deavers MT, Lopez-Berestein G, Sood AK (2005) Therapeutic Eph A2 gene targeting in vivo using neutral liposomal small interfering RNA delivery. Cancer Res 65:6910–6918
20. Mahmood T, Yang PC (2012) Western blot: technique, theory, and trouble shooting. N Am J Med Sci 4:429–434
21. Rao DD, Vorhies JS, Senzer N, Nemunaitis J (2009) siRNA vs. shRNA: similarities and differences. Adv Drug Deliv Rev 61:746–759

Chapter 19

Laser Capture Microdissection of Epithelium from a Wound Healing Model for MicroRNA Analysis

Alyne Simões, Zujian Chen, Yan Zhao, Lin Chen, Virgilia Macias, Luisa A. DiPietro, and Xiaofeng Zhou

Abstract

MicroRNAs are ~22 nucleotide-long noncoding RNAs influencing many cellular processes (including wound healing) by their regulatory functions on gene expression. The ability to analyze microRNA in different cells at the wound site is essential for understanding the critical role(s) of microRNA during various phases of wound healing. Laser capture micro-dissection (LCM) is an effective method to distinguish between relevant and non-relevant cells or tissues and enables the researcher to obtain homogeneous, ultra-pure samples from heterogeneous starting material. We present here our protocol for procuring epithelial cells from a mouse wound healing model using a Leica LMD7000 Laser Microdissection system, as well as the RNA isolation and downstream microRNA analysis. Using this method, researchers can selectively and routinely analyze regions of interest down to single cells to obtain results that are relevant, reproducible, and specific.

Key words LCM, MicroRNA, Wound healing, RNA isolation, Epithelial cells, Mouse, Frozen sample

1 Introduction

Laser Capture Microdissection (LCM) was developed in 1996 at the National Cancer Institute [1]. It is an automated sample preparation technique that enables isolation of specific cells from a mixed population under microscopic visualization. This technique is characterized by the use of a laser coupled to an inverted light microscope to selectively extract a pure cell population of interest from a heterogeneous mixture of cells in a typical tissue section [2]. There are two general classes of LCM: The infrared (IR) laser capture system and the ultraviolet (UV) laser-cutting system. In the IR system, while viewing the target cells, an IR, low power laser is pulsed through the top of the cap, hitting the transfer film, which then melts and bonds to the identified cells. Cells are then removed selectively from the tissue section when the cap is lifted [3]. In the UV-system, the tissue sections are attached to a specific membrane

Shao-Yao Ying (ed.), *MicroRNA Protocols*, Methods in Molecular Biology, vol. 1733,
https://doi.org/10.1007/978-1-4939-7601-0_19,

slide. The laser energy melts the demarked membrane area, allowing the selected cells to fall into a collection device by gravity [3].

LCM allows for more efficient and accurate results with downstream applications, including microgenomic analysis of microRNAs using next-generation sequencing, microarrays, and quantitative PCR (qPCR) techniques. However, common challenges observed during LCM collection are related to low yield and suboptimal RNA quality. The quantity and quality of LCM-derived RNA are affected by many factors, including the quality of starting material, tissue fixation procedure, time to preservation before microdissection, type of preservation, tissue handling during sectioning, efficiency of microdissection, and the post-LCM RNA isolation procedure [4, 5]. Proper optimization of these procedures will substantially improve the effectiveness of LCM and provide greater utility for investigating critical questions in complex biological systems, such as the role of microRNA in would healing. In this chapter, we demonstrate LCM-epithelial cell collection from tissue harvested from a wound healing model; these samples were collected for future analysis of microRNAs.

MicroRNAs, non-protein-coding small endogenous RNAs, have been shown to regulate many developmental, physiological, and disease processes, including wound healing [6, 7]. The mechanism underlying epithelial tissue healing and pathologies, such as failure to repair, are not fully understood. This is an important topic in basic biomedical research since it involves a fundamental principle of survival [8]. An oral mucosal wound healing model was chosen because it nearly always shows superior wound healing when compared with other tissues. Thus oral mucosa wound healing is an optimal model for investigating the mechanism underlying the highly orchestrated healing process.

2 Materials and Equipment

An RNase-free environment is essential when working with RNA samples. It is important to designate a special area for RNA work only. All the surfaces and the tools (including glassware and plastic ware) that will be in contact with the samples need to be cleaned with RNaseZap (ThermoFisher Scientific) or another RNase decontamination solution and then rinsed with DEPC-treated nuclease-free water. Prepare all the solutions using DEPC-treated nuclease-free water and analytical grade reagents. If not indicated, the reagents are prepared and stored at room temperature. Always wear sterile disposable gloves when handling reagents and RNA samples and discard all biohazard material in appropriate containers. Change gloves frequently as the protocol progresses from crude extract to more purified material.

2.1 Sample Harvest and Section

1. Surgical instruments, such as incisors, forceps, scalpel, etc.
2. Disposable base molds (15 × 15 × 5 mm).
3. Optimal Cutting Temperature (OCT) Compound (Fisher HealthCare). OCT is a ready-to-use embedding medium for embedding tissue samples prior to frozen sectioning on a microtome-cryostat.
4. Permanent marker to label samples.
5. Dry ice (avoid direct skin contact).
6. −80 °C freezer.
7. Cryostat for the preparation of frozen tissue sections. The cryochamber temperature should be at −20 °C.
8. Glass slides.
9. Microscope.
10. Polyethylene naphthalate (PEN) membrane glass slides (ThermoScientific, catalog #: LCM0522). For LCM, special membrane mounted slides should be used to facilitate the photo ablation and sample collection. PEN membrane slides are suitable for both the IR laser capture system and the UV laser-cutting system.
11. 50 mL centrifuge sterile tubes to store individual slides.

2.2 Staining and LCM

1. 100% ethanol (ethyl alcohol, absolute, 200 proof for molecular biology).
2. Freshly prepared 50% (vol/vol) ethanol in DEPC-treated Nuclease-free water. Add 250 mL of ACS grade 100% ethanol and 250 mL of DEPC-treated Nuclease-free water to a bottle labeled "50% Ethanol." Mix well.
3. Freshly prepared 75% (vol/vol) ethanol in DEPC-treated Nuclease-free water. Add 375 mL of ACS grade 100% ethanol and 125 mL of DEPC-treated Nuclease-free water to a bottle labeled "75% Ethanol." Mix well.
4. Freshly prepared 95% (vol/vol) ethanol in DEPC-treated Nuclease-free water. Add 475 mL of ACS grade 100% ethanol and 25 mL of DEPC-treated Nuclease-free water to a bottle labeled "95% Ethanol." Mix well.
5. Cresyl violet stain (contained in LCM Staining Kit, Ambion; stored at 4 °C).
6. Absorbent paper, timer, pipette, and tips.
7. Xylene.
8. Slide chambers, slide tubes, and slide holder.
9. Hydrophobic barrier pen (Thermo Fisher Scientific), designed for use with frozen or paraffin-embedded tissue sections mounted on glass slides.

10. Forceps to insert and remove slides from solutions.
11. Collection tubes with caps (0.5 mL).
12. Special collection devices for caps and microcentrifugation tubes.
13. QIAzol Lysis reagent, included in miRNeasy Mini Kit (Qiagen).
14. Mini centrifuge.

2.3 RNA Isolation

1. QIAzol Lysis reagent, included in miRNeasy Mini Kit (Qiagen).
2. Chloroform.
3. Collection tubes (1.5 and 2 mL), included in miRNeasy Mini Kit (Qiagen).
4. 100% ethanol (ethyl alcohol, absolute, 200 proof for molecular biology).
5. RNeasy Mini Spin Columns, included in miRNeasy Mini Kit (Qiagen).
6. RNase-free water.
7. RNase-free DNase Set (Qiagen). This kit contains DNase I (lyophilized), RNase free water (to dissolve the DNase), and Buffer RDD.
8. Buffer RWT, included in miRNeasy Mini Kit (Qiagen). This buffer is supplied as a concentrate. Before using for the first time, add 2 volumes of ethanol (96–100%) to prepare a working solution.
9. Buffer RPE, included in miRNeasy Mini Kit (Qiagen). This buffer is supplied as a concentrate. Before using for the first time, add 4 volumes of ethanol (96–100%) to prepare a working solution.

3 Methods

3.1 Sample Harvest and Section

The mouse oral mucosal wound healing protocol was followed and the tissue specimens were harvested as previously described [9, 10]. In brief, 8-week-old female Balb/c mice were anesthetized with ketamine (100 mg/kg) and xylazine (5 mg/kg) and a palate incision was made (1.0 mm width and 4 mm length, approximately) using a scalpel blade surgical #15. At 24 h post-wounding, the animals were sacrificed and specimens were harvested. The animal study was approved by the Institutional Animal Care and Use Committee at University of Illinois at Chicago.

The quality of starting material is essential for the RNA yield and quality. For best results, use either fresh samples or samples that have been quickly frozen in liquid nitrogen and stored at

−80 °C. This will minimize degradation of crude RNA by limiting the activity of endogenous RNases.

1. Clean all contacting surface with RNaseZap.
2. Add OCT Compound to the cryomold (about 2/3 full).
3. Immediately after tissue collection, embed tissue directly in the OCT Compound. Use forceps to orient the tissue (if necessary) and add more OCT Compound until the tissue is completed covered (Fig. 1a, b). Place OCT-embedded tissue upon a flat surface of dry ice (*see* notes regarding the specimen orientation inside the embedded medium).
4. Once frozen, store the samples at −80 °C until the sections will be prepared.
5. Precool the cryostat to −20 °C.
6. Clean the knife holder with 100% ethanol and treat the brushes with RNaseZap to eliminate RNase contamination.
7. Mark the base of the sample with a permanent marker for correct orientation. Next, remove the block from the cryomold and attach it to the stainless-steel tissue holder usingOCT compound. Place the tissue holder on the metal grid of the cryochamber.
8. Trim the excess frozen OCT until you start to see the wound tissue on the microscope (use a glass slide to collect the sections until the wound is observed).
9. Set the cutting thickness to 10 μm (Fig. 1c).
10. Cut at least eight frozen sections per slide, avoiding the top and bottom thirds of the slide (Fig. 1d). Sections should be placed upon a labeled PEN membrane slide.
11. Place the slide inside a sterile slide tube previously cooled at −20 °C. Keep all the slides at −20 °C until they can be stored at −80 °C. (Frozen sections for RNA isolation can be stored at −80 °C for up to 1 month [5]).

3.2 Staining of the LCM Slides

This step is required to visualize the cells of interest under the microscope for the LCM procedure. The steps described below are modified from a LCM Staining Kit protocol (Ambion). Other commercially available kits such as the Arcturus HistoGene LCM Frozen Section Staining Kit or a simple Toluidine Blue Staining can also be used.

1. Remove the slides from −80 °C (using dry ice) and place them at −20 °C.
2. Dip the slide in a tube with 95% ethanol solution for 35 s.
3. Dip the slide in a tube with 75% ethanol solution for 35 s.
4. Dip the slide in a tube with 50% ethanol solution for 30 s. Cap and invert the tube gently during this step to help dissolve the OCT.

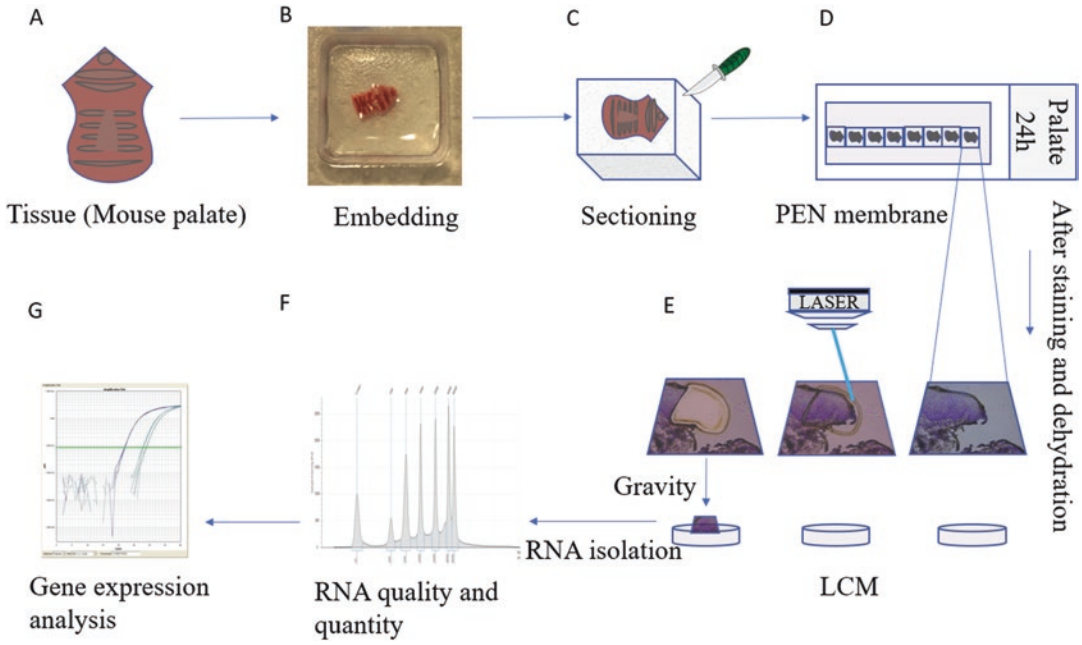

Fig. 1 Overall procedure. This cartoon demonstrates an approach regarding LCM-mediated epithelial cell collection from a mouse oral mucosa wound healing model. (**a**) Mouse oral mucosa tissue obtained from wound healing model. (**b**) Tissue specimen is embedded in Optimal Cutting Temperature (OCT) Compound. (**c**) Specimen is sectioned and (**d**) placed on PEN membrane glass slide. (**e**) After staining and dehydration, LCM was performed and the cells of interest were selectively harvested and fall into a collection device by gravity. (**f**) RNA isolated and RNA quality and quantity analyses. (**g**) MicroRNA expression analysis using the RNA samples isolated from LCM-captured epithelial cells from the wound healing model

5. Lay the slide on a flat surface. Mark the location of the tissue section on the edges of the slide with a hydrophobic barrier pen.
6. Add 300 μL of Cresyl Violet to the tissue section using a pipette and wait 40 s (Note: The exact time of each step of the staining procedure may be different depending on the tissue type).
7. Drain off stain in a plastic tube and dip the slide in a tube with 50% ethanol solution for 30 s.
8. Transfer the slide to a tube with 75% ethanol solution for 30 s.
9. Transfer the slide to a tube with 95% ethanol solution for 35 s.
10. Place the slide in the first 100% ethanol solution for 35 s.
11. Transfer the slide to a tube with the second 100% ethanol solution for 35 s.
12. Rinse the slide in a tube with a solution of Xylene (under fume hood)
13. Place the slide in a tube with a second Xylene solution for 5 min (under fume hood).
14. Immediately after the final Xylene step, place the slide on ice. The samples are now ready for the LCM procedure. (The slides

can be kept in −80 °C for short-term storage. For best RNA quality and yields, perform LCM procedure on the same day).

3.3 Laser Capture Microdissection (LCM)

The LCM procedure described here is based on a Leica LMD7000 Laser Microdissection system.

1. Clean the LCM staging area and contacting surface with RNaseZap. Turn on the microscope, laser, and computer.
2. Access the LCM software program and load the collection tubes and LCM slides on their respective holder assembles. The cap of the collection tube is used for collecting the LCM-captured cells, and it is secured in the holder. The LCM slide is clamped in the specimen holder with the membrane to the bottom.
3. The collection tube holder and the LCM slide holder can be selected through LCM software. Movement and focusing, for example, can be adjusted with a joystick controller.
4. Calibrate the laser in a region far away of the specimen ("Laser", "Calibrate").
5. Use a 1.25× objective to localize the section.
6. Change to objective 10×.
7. Select the respective cap (the location of the collector to receive the LCM harvested cells).
8. Select "Line," "Close Lines" (Draw shapes), and "Draw + Cut" (Cut shapes) to draw a line around the interested area. Several pieces can be marked and cut consecutively ("Multiple Shapes").
9. After the selection, set the power, aperture, and speed of laser to 50, 20, and 10, respectively.
10. Select "Start Cut" to start laser cut (Fig. 1e, f). The laser cutting can be monitored on the computer screen in real time, and the selectively dissected tissue pieces should drop to the cap of the collection tube by gravity.
11. If the sample does not drop, click "Move + Cut" on the "Cut Shape" toolbar and move the laser manually to cut the bridges of tissues (Figs. 1g and 2a–d).
12. Move to another section and repeat the procedure.
13. To remove the slide and the collection tube, click "Unload." Detach the collection tube carefully and put the tube onto the cap to close.
14. Immediately after LCM collection the samples will be centrifuged (10,000 × *g* for 1 min).
15. Add 700 µL QIAzol Lysis Reagent to the samples. Homogenize the samples by vortexing for 1 min. Homogenized cell lysate can be stored at −80 °C for several months.

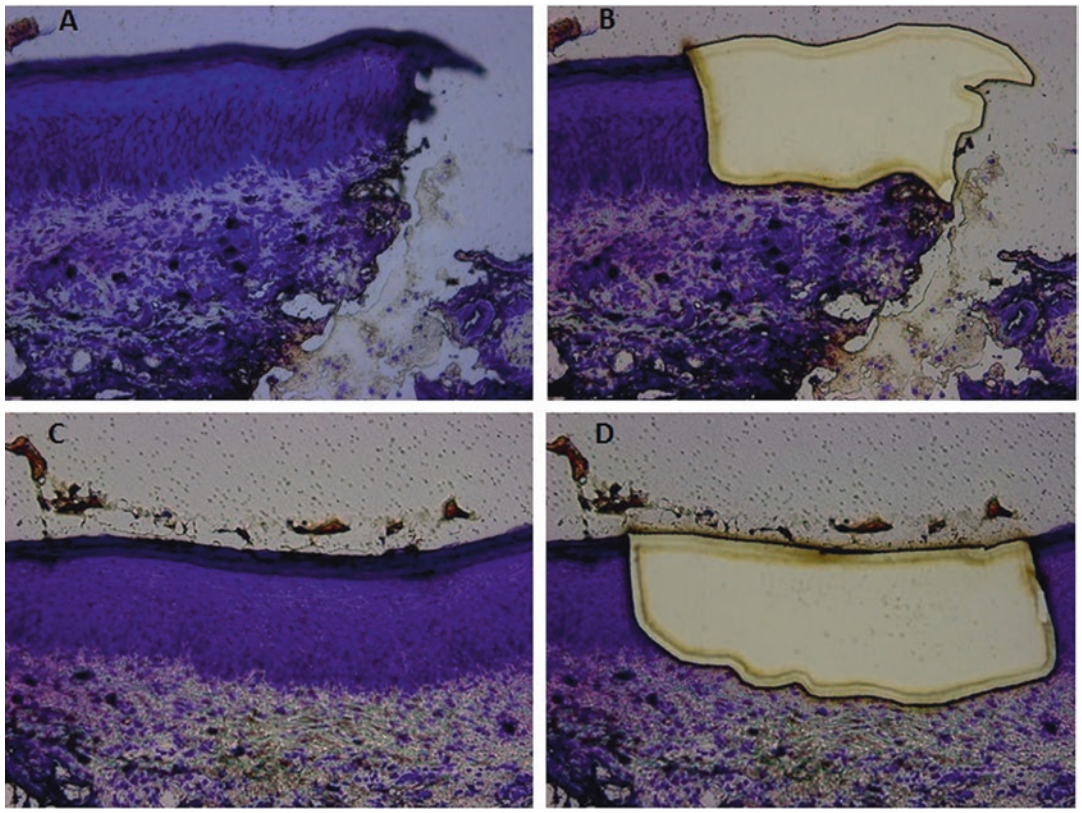

Fig. 2 LCM-mediated epithelial cell collection from a wound healing model. Representative images of LCM mediated isolation of epithelial cells from the wound edge (**a** and **b**) and unwounded (**c** and **d**) areas from a mouse oral mucosal wound healing model. **a** and **c**: before LCM. **b** and **d**: after laser ablation. Magnification 200×

3.4 RNA Isolation and Downstream MicroRNA Analysis

The total RNA (including small RNA) isolation protocol presented here is based on a miRNeasy Mini Kit from Qiagen. A number of other commercially available kits can be used for this step (with proper modification), including the mirVana miRNA Isolation Kit (Ambion) and the Direct-zol RNA MiniPrep (Zymo Research). RecoverAll Total Nucleic Acid Isolation Kit (Ambion) can be used for extracting total nucleic acids (RNA, miRNA, and DNA) from LCM captured cells from formalin-fixed paraffin-embedded (FFPE) tissues.

1. Incubate the homogenate at Room Temperature (RT) for 5 min.
2. Add 140 μL chloroform to samples and cap the tube securely. Shake vigorously for 20 s.
3. Incubate at RT for 2–3 min.
4. Centrifuge for 15 min at 12,000 × *g* at 4 °C.
5. Transfer the upper aqueous phase to a new collection tube. Avoid transferring any interphase.

6. Add 1.5 volume (usually 525 μL) of 100% ethanol and mix thoroughly by pipetting.
7. Pipet up to 700 μL of the sample, including any precipitate, into a RNeasy Mini column in a 2 mL collection tube. Close the lid and centrifuge at 10,000 × *g* for 30 s at RT. Discard the flow-through.
8. Repeat **step 7** for the remainder of the samples.
9. Pipet 350 μL Buffer RWT into the RNeasy Mini Spin Column and centrifuge for 30 s at 10,000 × *g* to wash. Discard the flow-through.
10. Add 10 μL DNase I stock solution to 70 μL Buffer RDD. Mix by gently inverting the tube. Do not vortex.
11. Pipet the DNase I incubation mix (80 μL) directly onto the RNeasy Mini Spin Column membrane and place on the bench-top at 20–30 °C for 15 min (make sure to pipet the DNase I incubation mix directly onto the RNeasy membrane).
12. Pipet 500 μL Buffer RWT into the RNeasy Mini Spin Column and centrifuge for 30 s at 10,000 × *g*. Keep the flow-through.
13. Apply the flow-through to the same RNeasy Mini Spin Column and centrifuge for 30 s at 10,000 × *g*. Discard the flow-through.
14. Add 500 μL Buffer RPE to the same RNeasy Mini Column. Close the lid and centrifuge for 2 min at 10,000 × *g*.
15. Place the RNeasy Mini column into a new 2 mL collection tube. Centrifuge at full speed for 1 min to further dry the membrane.
16. Transfer the RNeasy Mini column to a new 1.5 mL collection tube. Pipette 30 μL RNase-free water directly onto the RNeasy Mini column membrane. Close the lid, and centrifuge for 1 min at 10,000 × *g* to elute the RNA.
17. Use the flow-through to analyze the RNA quantity and quality (Fig. 1f). RNA concentration is typically quantified based on OD absorbance using a spectrophotometer (e.g., NanoDrop from Thermo Fisher Scientific). However, due to the relatively low RNA yield from the LCM-captured cells, an alternative quantification method may be used in addition to (or instead of) the OD method, such as the Qubit RNA HS Assay Kit from ThermoFisher Scientific. Typical RNA quality control methods include electrophoresis-based analysis using instruments such as TapeStation System from Agilent Technologies. The TapeStation System offers the RIN algorithm (RNA Integrity Number) to determine RNA quality using a numerical system which represents the integrity of RNA. With high-quality starting material, optimized procedure, and proper technique, an RIN value as

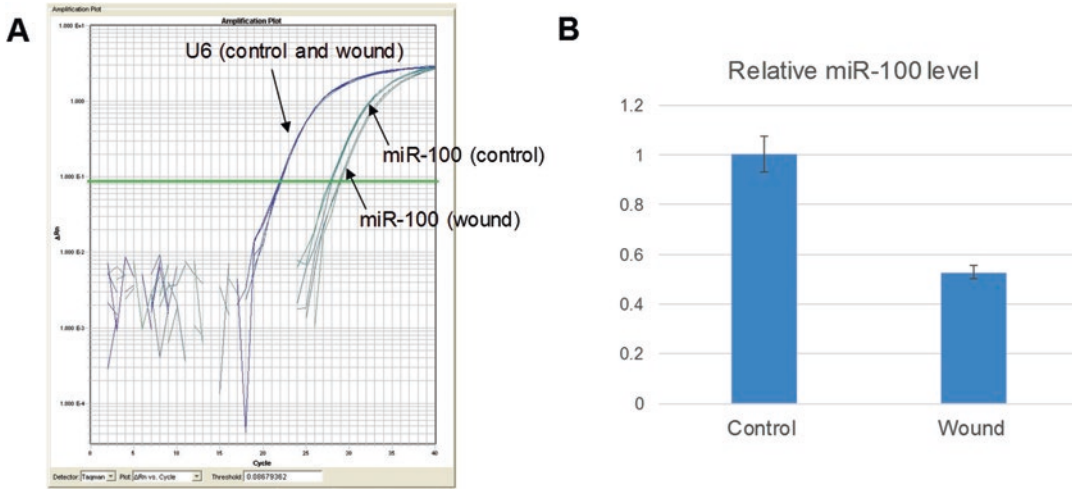

Fig. 3 QPCR-based microRNA analysis on LCM-captured epithelial cells from a wound healing model. Representative qPCR analysis of RNA samples isolated from LCM-captured epithelial cells from wounded and unwounded (control) areas. TaqMan microRNA assays for miR-100 and U6 small nuclear RNA (Applied Biosystems) were used for the qPCR analysis using a 7900HT Fast Real-Time PCR system (Applied Biosystems). The qPCR amplification curves were shown in (**a**). The relative miR-100 levels were computed using the $2^{-\text{delta delta Ct}}$ method, where U6 was used as an internal reference (**b**)

high as 7.0 can be achieved for RNA isolated from LCM-captured cells.

18. If sufficient RNA quality and quantity are achieved, downstream microgenomic analysis based on next-generation sequencing, microarray, and qPCR technologies can be performed to assess the levels of specific microRNAs (Figs. 1g and 3). A representative result from TaqMan-based qPCR analysis is shown in Fig. 3, demonstrating a decrease in the miR-100 level in epithelial cells harvested from a wounded area as compared to epithelial cells from an unwounded area (control sample). This is in agreement with our previously published findings [11, 12].

4 Notes

1. Pay attention to the orientation of the sample when embedding it. The wound should be perpendicular to the blade. Mark the direction of the cut that should be performed on the disposable base mold (cryomold).
2. Avoid bubbles in the OCT Compound when embedding the sample.
3. The staining process is crucial for the tissue layer visualization as it permits accurate selection of the desired areas of the tissue.

4. To preserve RNA integrity during sample fixation, storage, and staining, as well as during the LCM procedure and isolation process, perform all the procedures as quickly as possible and avoid storing the sections for too long between the procedures.
5. During the sectioning process, the microscope slide should be kept in the cryochamber while the sections are placed onto it to avoid RNA degradation.
6. If you are cutting different tissues, you should use a different blade area for each one to avoid contamination between them.
7. Use a new blade to perform the sections.
8. Do not allow the slides to thaw before starting the staining steps.
9. During the staining steps, in between transferring the slides from one solution to another, blot the slides gently on absorbent paper to remove access solution.
10. For best staining results, change the wash solutions (the four solutions after using Cresyl Violet dye) every four slides and the Xylene solutions every six slides.
11. Some of the stained tissue mounted LCM slides (especially those retrieved from −80 °C storage) may be too wet to proceed to LCM immediately. These slides can be dried on a 42 °C hot plate for short time. However, this drying step should be kept to a minimum because long-term exposure to elevated temperature will lead to RNA degradation.
12. When performing LCM, be sure that you insert the slide in the specimen holder with the tissue facing downward. Otherwise, the desired area will be dissected but not dropped on the cap.
13. PEN Membrane Glass Slides (ThermoFisher Scientific) can be used for both IR laser capture and UV laser cutting. PEN Membrane Frame Slides (ThermoFisher Scientific) provide additional flexibility by allowing microdissection of non-dehydrated samples.
14. Depending on the cells of interest, pooling LCM-captured samples from multiple slides may be necessary to obtain sufficient amounts of RNA. For example, to obtain sufficient RNA for microRNA analysis on epithelial cells from the wound edges of our oral mucosa wound healing model, we typically pool samples from six slides (with at least eight sections on each slide).
15. During LCM, the sections must be sufficiently dehydrated to drop into the cap of the collection tube after laser ablation.
16. After the initial LCM cut, occasionally some target tissues (especially large pieces) may not fall into the collection cap. Further cutting these tissue pieces in half may help them to fall by the force of gravity.

17. When removing the collection tube with the microdissected samples, you should detach the tube very carefully because if the cap hits the holder, the samples may be lost.
18. The homogenization step before the RNA isolation is critical for disrupting the cell membranes. Incomplete homogenization may lead to significantly reduced RNA yields.
19. The On-Column DNase Digestion step with the RNase-Free DNase Set (Qiagen) is optional based on the downstream application. For example, removal of genomic DNA contamination is highly recommended for qPCR and small-RNA-seq analysis. An additional DNA removal procedure can be carried out after the RNA isolation using kits such as RNA Clean-up & Concentration from Zymo Research.

Acknowledgment

This work was supported in part by NIH PHS grants (R21DE025926, R03CA171436, R01GM50875, and S10RR026493) and a Lilly USA Research Award in Cancer Prevention and Early Detection. Dr. Alyne Simões was supported by a scholarship from São Paulo Research Foundation (2016/16332-0). We thank Dr. Wendy Cerny for editorial assistance.

References

1. Emmert-Buck MR, Bonner RF, Smith PD, Chuaqui RF, Zhuang Z, Goldstein SR, Weiss RA, Liotta LA (1996) Laser capture microdissection. Science 274(5289):998–1001
2. Best CJ, Emmert-Buck MR (2001) Molecular profiling of tissue samples using laser capture microdissection. Expert Rev Mol Diagn 1(1):53–60. https://doi.org/10.1586/14737159.1.1.53
3. Liu A (2010) Laser capture microdissection in the tissue biorepository. J Biomol Tech 21(3):120–125
4. Gautam V, Singh A, Singh S, Sarkar AK (2016) An efficient LCM-based method for tissue specific expression analysis of genes and miRNAs. Sci Rep 6:21577. https://doi.org/10.1038/srep21577
5. Espina V, Wulfkuhle JD, Calvert VS, VanMeter A, Zhou W, Coukos G, Geho DH, Petricoin EF III, Liotta LA (2006) Laser-capture microdissection. Nat Protoc 1(2):586–603. https://doi.org/10.1038/nprot.2006.85
6. Fahs F, Bi X, Yu FS, Zhou L, Mi QS (2015) New insights into microRNAs in skin wound healing. IUBMB Life 67(12):889–896. https://doi.org/10.1002/iub.1449
7. Pastar I, Khan AA, Stojadinovic O, Lebrun EA, Medina MC, Brem H, Kirsner RS, Jimenez JJ, Leslie C, Tomic-Canic M (2012) Induction of specific microRNAs inhibits cutaneous wound healing. J Biol Chem 287(35):29324–29335. https://doi.org/10.1074/jbc.M112.382135
8. Eming SA, Tomic-Canic M (2017) Updates in wound healing: mechanisms and translation. Exp Dermatol 26(2):97–98. https://doi.org/10.1111/exd.13281
9. Chen L, Arbieva ZH, Guo S, Marucha PT, Mustoe TA, DiPietro LA (2010) Positional differences in the wound transcriptome of skin and oral mucosa. BMC Genomics 11:471. https://doi.org/10.1186/1471-2164-11-471
10. Turabelidze A, Guo S, Chung AY, Chen L, Dai Y, Marucha PT, DiPietro LA (2014) Intrinsic differences between oral and skin keratinocytes. PLoS One 9(9):e101480. https://doi.org/10.1371/journal.pone.0101480

11. Jin Y, Tymen SD, Chen D, Fang ZJ, Zhao Y, Dragas D, Dai Y, Marucha PT, Zhou X (2013) MicroRNA-99 family targets AKT/mTOR signaling pathway in dermal wound healing. PLoS One 8(5):e64434. https://doi.org/10.1371/journal.pone.0064434

12. Chen D, Chen Z, Jin Y, Dragas D, Zhang L, Adjei BS, Wang A, Dai Y, Zhou X (2013) MicroRNA-99 family members suppress Homeobox A1 expression in epithelial cells. PLoS One 8(12):e80625. https://doi.org/10.1371/journal.pone.0080625

Chapter 20

Transgene-Like Animal Models Using Intronic MicroRNAs

Shi-Lung Lin, Shin-Ju E. Chang, and Shao-Yao Ying

Abstract

Transgenic animal models are valuable tools for testing gene functions and drug mechanisms in vivo. They are also the best similitude for a human body for etiological and pathological research of diseases. All pharmaceutically developed medicines must be proven to be safe and effective in animals before approval by the Food and Drug Administration (FDA) to be used in clinical trials. To this end, the transgenic animal models of diseases serve as the front line of drug evaluation. However, there is currently no transgenic animal model for microRNA (miRNA)-related research. MiRNAs, small single-stranded regulatory RNAs capable of silencing intracellular gene transcripts (mRNAs) that contain either complete or partial complementarity to the miRNA, are useful for the design of new therapies against cancer polymorphism and viral mutation. Recently, varieties of natural miRNAs have been found to be derived from hairpin-like RNA precursors in almost all eukaryotes, including yeast (*Schizosaccharomyces pombe*), plant (*Arabidopsis* spp.), nematode (*Caenorhabditis elegans*), fly (*Drosophila melanogaster*), fish, mouse and human, involving intracellular defense against viral infections and regulation of certain gene expressions during development. To facilitate the miRNA research in vivo, we have developed a state-of-the-art transgenic strategy for silencing specific genes in zebrafish, chicken, and mouse, using intronic miRNAs. By the insertion of a hairpin-like pre-miRNA structure into the intron region of a gene, we have found that mature miRNAs were successfully transcribed by RNA polymerases type II (Pol-II), coexpressed with the encoding gene transcripts, and excised out of the encoding gene transcripts by intracellular RNA splicing and processing mechanisms. In conjunction with retroviral transfection, the designed hairpin-like pre-miRNA construct has also been placed in the intron regions of a cellular gene for tissue-specific expression, specifically regulated by the gene promoter of interest. Because the retroviral vectors are integrated into the genome of its host cells, we can select and propagate the most effective transgenic animals to form a stable model line for further research. Here, we have shown for the first time that transgene-like animal models were generated using the intronic miRNA expression system reported previously, which has been proven to be useful for studying miRNA function as well as the related gene regulation in vivo.

Key words MicroRNA (miRNA), RNA interference (RNAi), Transgenic animal, Type II RNA polymerases type (Pol-II), RNA splicing, Intron, Embryonic development

1 Introduction

Conventional transgenic animal models rely on the utilization of antisense oligonucleotide and dominant-negative technologies to generate loss-of-function mutants in vivo. Antisense

Shao-Yao Ying (ed.), *MicroRNA Protocols*, Methods in Molecular Biology, vol. 1733,
https://doi.org/10.1007/978-1-4939-7601-0_20,

oligonucleotides complementary to a gene transcript [messenger RNA (mRNA)] directly bind to the mRNA and then either to degrade the target mRNA or to suppress the translation of the gene; while dominant-negative methods generate defective proteins to negatively compete with a targeted normal protein for reducing the protein function. Both of the methods contain problems for transgenic animal research. Single-stranded antisense DNA or RNA, including phosphothio-, methylthio-, and morpholino-oligonucleotides, are relatively inefficient for gene silencing in vivo because its effect only lasts for a short time and is often required for pharmacological (nearly toxic) dosage to be effective. Nevertheless, dominant-negative methods are not better because defective proteins cannot completely eliminate normal protein function and frequently generate inconsistent results due to variable gene knockdown conditions.

To circumvent these problems, recent approaches using RNA interference (RNAi) mechanisms provide a stable, effective, and highly specific alternative [1, 2]. RNAi is a post-transcriptional gene-silencing phenomenon triggered by small regulatory RNAs, such as small interfering RNA (siRNA) and miRNA [3, 4]. These small RNA molecules usually function as a gene silencer, interfering with intracellular expression of genes complementary to the small RNAs. miRNAs, small single-stranded regulatory RNAs capable of interfering with intracellular mRNAs that contain either complete or partial complementarity, are useful for designing new therapies directed against cancer polymorphism and viral mutation [1, 4]. This flexible characteristic is different from double-stranded siRNAs because a much more rigid complementarity is required for triggering siRNA-induced RNAi effects. Currently, varieties of natural miRNAs have been found to be derived from hairpin-like RNA precursors in almost all eukaryotes, including yeast (*Schizosaccharomyces pombe*), plant (*Arabidopsis* spp.), nematode (*Caenorhabditis elegans*), fly (*Drosophila melanogaster*), fish (*Danio rerio*), avian, mouse and human, and have been found to be involved in intracellular defense against viral infections and regulation of life-essential gene expressions during development [5–15]. Because of these advantages, we used miRNA as a tool for establishing transgenic animal models for research.

Most of protein-coding genes are transcribed by Pol-II, which are very inefficient in generating short RNA sequences fewer than 100 nucleotides; thus, the minimal mRNA size in eukaryotes is usually greater than 300 nucleotides [16, 17]. To generate the short transcripts of siRNA (19–23 bp), current vector-based RNAi systems used Pol-III promoters to transcribe the siRNA. The application of Pol-III-directed siRNA-expressing vectors has been found to offer better efficacy and stability for RNAi induction in many cell lines in vitro [2, 18–20]; however, several in-vivo studies [21, 22] using the Pol-III-mediated siRNA expression systems

have failed to provide tissue-specific effectiveness in the targeted cell population because of the ubiquitous existence of Pol-III activities in almost all cell types. Moreover, because the read-through effect of Pol-III frequently occurs on a short transcription template, long siRNAs can be synthesized and thus cause interferon-mediated cytotoxicity [23, 24]. Such a problem can also result from the competitive conflict between the Pol-III promoter and another viral promoter of the vector (i.e., long terminal repeat and cytomegalovirus promoters).

Furthermore, Sledz et al. and we have noted that high-dose siRNA (e.g., >250 nM in human T cells) can trigger interferon-induced toxicity similar to that of long double-stranded RNA (dsRNA) [25, 26]. It is known that interferon-induced double-stranded RNA-dependent protein kinase (PKR) can trigger cell apoptosis, while activation of interferon-induced 2′,5′-oligoadenylate synthetase leads to extensively non-specific cleavage of single-stranded RNAs (i.e., mRNAs) [27]. Both PKR and 2′,5′-oligoadenylate synthetase contain dsRNA-binding motifs that are highly conserved for binding to dsRNAs, but these motifs are insensitive to single-strand RNAs. Because miRNAs are single-stranded RNA molecules, a Pol-II-mediated miRNA generation system provides a much safer and less cytotoxic means for both in-vitro and in-vivo gene silencing applications [28]. These findings indicate the advantages of Pol-II-mediated intronic miRNA expression and its related gene regulation, which can be used as a tool for testing gene functions, improving current RNAi technologies, and developing gene-specific transgenic animal models for studying disease mechanisms and the possible therapies.

We are the first research group who discovered the biogenesis of miRNA precursors (pre-miRNAs) derived from the 5′-proximal intron regions of primary gene transcripts (pre-mRNAs) produced by the mammalian Pol-II [29] (Fig. 1a). Depending on the promoter of the miRNA-encoding gene, intronic miRNA is co-expressed with its encoding gene transcripts in a specific cell population or under a special condition, in which the gene promoter can be properly activated. Using artificial introns carrying pre-miRNA structures, we have successfully generated mature miRNA molecules with full function in triggering RNAi-related gene silencing in human prostate cancer (LNCaP), human cervical cancer (HeLa), and rat neuronal stem cell lines in vitro and zebrafish in vivo [29, 30].

We have designed an artificial intron (SpRNAi) for expressig intronic miRNAs. The artificial intron was placed in a mutated HcRed1 red fluorescent protein (RGFP) gene to form a recombined SpRNAi-rGFP gene cassette, in which the functional fluorescent protein structure was disrupted by the intron insertion. Therefore, we were able to determine the occurrence of intron splicing and miRNA generation through the appearance of red

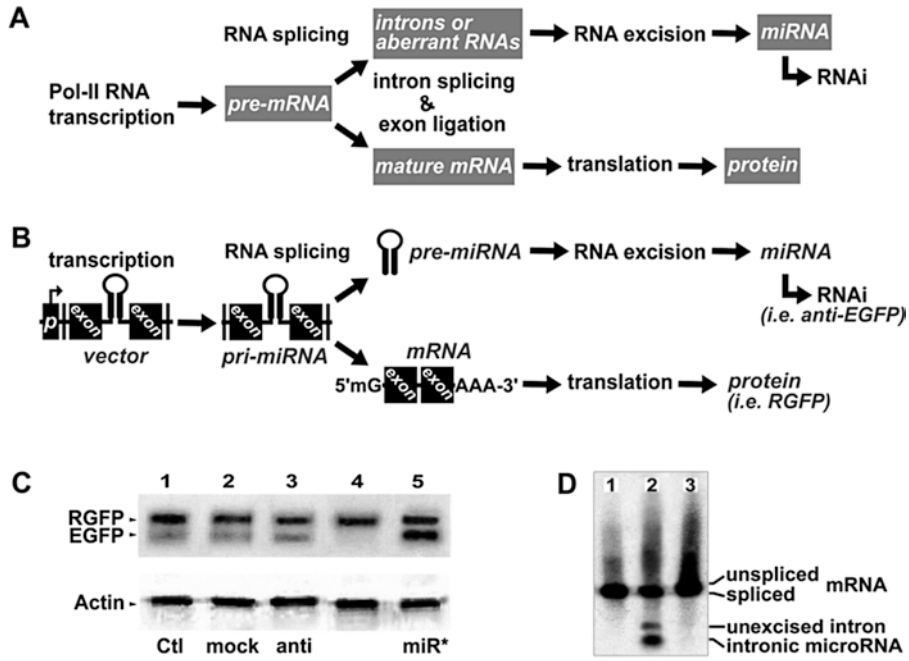

Fig. 1 Biogenesis and function of intronic miRNAs. (**a**) The native intronic miRNA is co-transcribed with a long primary messenger RNA (pre-mRNA) by Pol-II and cleaved out of the pre-mRNA by an intracellular RNA splicing machinery, spliceosome. The spliced intron with one or more hairpin-like secondary structures is further processed into mature miRNAs capable of triggering RNA interference (RNAi) effects, whereas the ligated exons become a mature mRNA for protein synthesis. (**b**) We designed an artificial intron containing miRNA precursor (pre-miRNA), namely SpRNAi, to mimic the biogenesis processes of the native intronic miRNAs. (**c**) When a designed intronic miR-EGFP(280–302)–stem-loop construct was tested in the EGFP-expressing transgenic (UAS:gfp) zebrafishes, we detected a strong RNAi effect only on the target EGFP (lane 4). No detectable gene silencing effect was observed in other lanes. From left to right: 1, blank vector control (Ctl); 2, miRNA–stem-loop targeting human immunodeficiency virus-p24 (mock); 3, miRNA without stem-loop (anti); and 5, stem-loop–miRNA* complementary to the miR-EGFP(280–302) sequence (miR*). The off-target genes, such as the vector red fluorescent protein (RGFP) and fish actin, were not affected, indicating the high target specificity of miRNA-mediated gene silencing. (**d**) Three different miR-EGFP(280–302) expression systems were tested for miRNA biogenesis. From left to right: 1, vector expressing intron-free RGFP, no pre-miRNA insert; 2, vector expressing RGFP with an intronic 5′-miRNA-stem-loop-miRNA*-3′ insert; and 3, vector similar to the construct in lane 2, but with a defected 5′-splice site in the intron. Northern bolt analysis probing the miR-EGFP(280–302) sequence showed that the mature miRNA was released only from the spliced intron of the lane 2 construct

fluorescent emission in the transfected cells. The red RGFP here serves as a visual indicator for the generation of intronic miRNAs. This intron-derived miRNA system can be activated under the control of a specific Pol-II promoter of interest.

As shown in Fig. 1b, after Pol-II RNA processing and splicing excision, some of the intron-derived miRNA fragments form mature miRNAs and can effectively silence the target genes via the RNAi mechanism, while the exons of the encoding gene transcripts

are ligated together to form mature mRNAs for protein synthesis (e.g., RGFP). Based on this miRNA generation model, we have tested various pre-miRNA constructs, and observed that the production of intron-derived miRNA fragments was originated from the 5′-proximity of the intron sequence between the 5′-splice site and the branching point. These miRNAs were able to trigger strong suppression of genes possessing more than 70% of complementarity to the miRNA sequences, whereas non-homologous miRNAs, i.e., an empty intron without the pre-miRNA insert, an intron with an off-target miRNA insert (negative control), and a splicing-defective intron, showed no silencing effects on the targeted genes. Similar gene silencing results can be recreated in the zebrafish directed against enhanced green fluorescent protein (EGFP) expression (Fig. 1c), indicating the consistent preservation of the intronic miRNA biogenesis system in vertebrates. Further, no effect was detected on off-target genes, such as RGFP and β-actin, suggesting the high specificity of miRNA-directed RNA interference (RNAi). We have confirmed the identity of the intron-derived miRNAs, which were sized approx 18–25-nt, similar to the intronic miRNAs in *C. elegans* [31]. Moreover, the intronic small RNAs isolated by guanidinium-chloride ultracentrifugation can elicit strong, but short-term gene-silencing effects on the homologous genes in the transfected cells, indicating their temporary RNAi effects [1]. Thus, the long-term (>1 month) gene-silencing effect that we observed in vivo, using the Pol-II-mediated intronic miRNA expression system, is likely maintained by constitutive miRNA generation from the vector rather than by the stability of the miRNAs.

We have successfully tested the feasibility of localized gene silencing in chicken embryos in vivo using the intronic miRNA approach and discovered that the interaction between pre-mRNA and genomic DNA may be essential for the miRNA biogenesis. The in-vivo model of chicken embryos has been widely used in the research of developmental biology, signal transduction, and flu vaccine development. As an example, the β-catenin gene was selected because it plays a critical role in the biological development and ontogenesis [32]. β-catenin is known to be involved in the growth control of skin and liver tissues in chicken embryos. The loss-of-function of β-catenin is lethal in many transgenic animals.

As shown in Fig. 2, experimental results demonstrated that the miRNAs derived from a designed intronic pre-miRNA construct transfected into the cell nucleus were capable of inhibiting β-catenin gene expression in the liver and skin of developing chicken embryos. In this animal model, we found that the intronic miRNA generation relies on a coupled interaction of nascent Pol-II-directed pre-mRNA transcription and intron excision occurring proximal to genomic perichromatin fibrils. This observation also indicates that

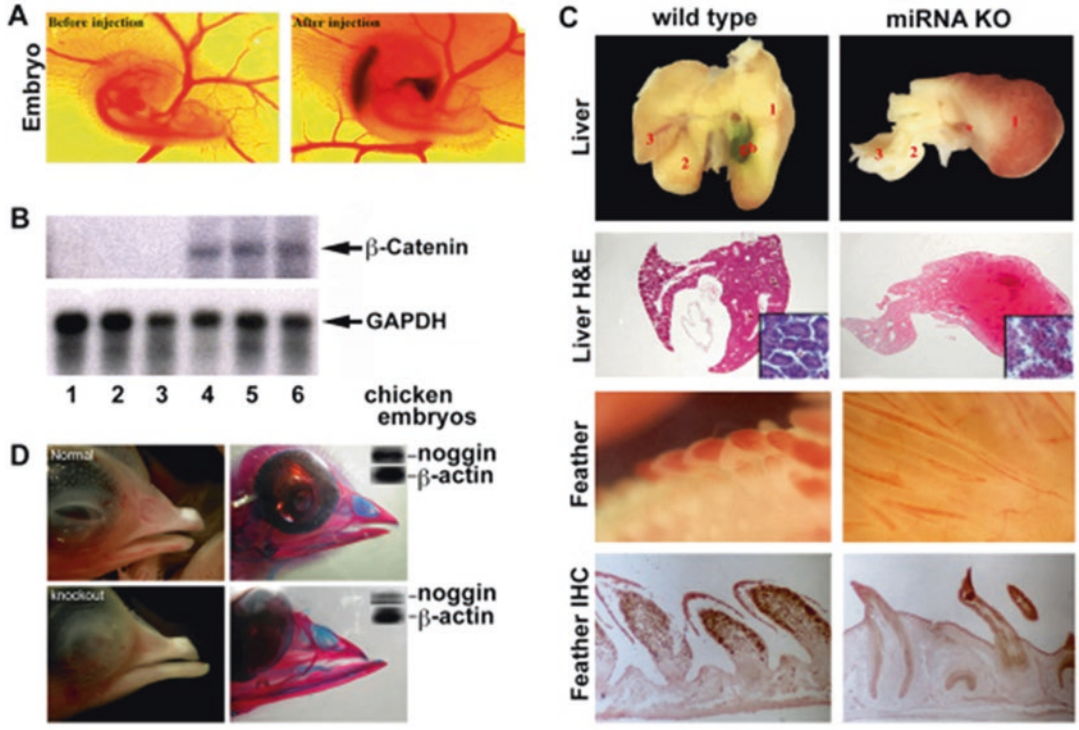

Fig. 2 In vivo gene silencing effects of man-made anti-β-catenin (**a**-**c**) and anti-noggin miRNA (**d**) on special organ development in chicken embryos. (**a**) The mixtures of an intronic miRNA expression construct and fast green dye were injected into the chicken embryos near the liver primordia area below the heart. (**b**) Northern blots of extracted RNAs from chicken embryonic livers with (lanes 1–3) and without (lanes 4–6) anti-β-catenin miRNA treatments were shown. All three knockouts (KO) showed a >98% specific silencing effect on β-catenin expression but not that of house-keeping genes, such as *glyceraldehyde phosphate dehydrogenase*. (**c**) Liver formation of the β-catenin KOs was significantly hindered (upper right 2 panels). Microscopic examination revealed a loose structure of hepatocytes, indicating the loss of cell-cell adhesion particularly in adherens junctions formed between β-catenin and cell membrane E-cadherin during early liver development. In most affected regions, feather growth in the skin close to the injection area was also inhibited (lower right two panels). Immunohistochemistry staining for β-catenin protein expression (brown) showed a significant decrease in the feather follicle sheaths. H&E, hematoxyline and eosin staining. (**d**) The lower beak development was increased by the mandible injection of the anti-noggin pre-miRNA construct (lower panel) in comparison with the wild type (upper panel). Right panels showed bone (alizarin red) and cartilage (alcian blue) staining to demonstrate the outgrowth of bone tissues in the lower beak of the *noggin* KO. Further Northern blot analysis (inserts) confirmed a 60–65% decrease of *noggin* mRNA expression in the lower beak area

the pre-mRNA–genomic DNA interaction may facilitate new miRNA generation by Pol-II-mediated RNA excision for relatively long-term gene silencing. Alternatively, Pol-II may function as an RNA-dependent RNA polymerase for producing more miRNAs because mammalian Pol-II has been reported to possess RNA-dependent RNA polymerase activities [33, 34]. Taken together, the data suggest that Pol-II-mediated RNA generation and excision is involved in intronic miRNA biogenesis, resulting

in single-stranded small RNAs of approx 20 nt comparable to the general sizes of Dicer-processed miRNAs frequently observed in the regulations of numerous developmental events.

To generate loss-of-function animal models using intronic miRNAs, we transfected chicken embryos with the *SpRNAi-rGFP* construct containing an intronic hairpin anti-β-catenin pre-miRNA, which was directed against the protein-coding region of the chicken β-catenin gene sequence (NM205081) with perfect complementarity. A perfectly complementary miRNA theoretically triggers targeted mRNA degradation more efficient than translational repression. Using embryonic day 3 chicken embryos, a dose of 25 nM of the *SpRNAi-rGFP* construct was injected into the body region close to where the liver primordia would form (Fig. 2a). For efficient delivery into target tissues, the construct was mixed with the FuGENE liposomal transfection reagent (Roche Biomedicals, Indianapolis, IN). A 10% (v/v) fast green solution was also added during the injection as a dye indicator. The mixtures were injected into the ventral side, near the liver primordia area, below the heart, using heat-pulled capillary needles. After injection, the embryonic eggs were sealed with sterilized scotch tapes and incubated in a humidified incubator at 39–40 °C until day 12, when the embryos were examined and photographed under a dissection microscope. Several malformations were observed, however the embryos still survived and there was no visible overt toxicity or overall perturbation of embryo development. The liver was the closest organ to the injection site and, thus, was most dramatically affected in its phenotypes. Other regions, particularly the skin close to the injection site, were also affected by the diffused miRNA effects. As shown in Fig. 2b, Northern blot analysis detecting the target β-catenin mRNA expression in the dissected livers showed that β-catenin expression in the wild-type livers remained normal (lanes 1–3), whereas those of the miRNA-treated samples were decreased dramatically (lanes 4–6). The miRNA-mediated silencing effect markedly down-regulated more than 98% of β-catenin mRNA expression in the embryonic chicken, but had no influence in the housekeeping gene, glyceraldehydes phosphate dehydrogenase (GAPDH) expression, indicating its high target specificity and very limited interferon-related cytotoxicity in vivo.

Ten days after the primordial injection with the anti-β-catenin pre-miRNA construct, the embryonic chicken livers showed an enlarged and engorged first lobe, but the size of the second and third lobes of the livers were dramatically decreased (Fig. 2c). Histological sections of normal livers showed hepatic cords and sinusoidal spaces with few blood cells. In the anti-β-catenin miRNA-treated embryos, the general architecture of the hepatic cells in lobes 2 and 3 remained unchanged; however, there were islands of abnormal regions in lobe 1. The endothelium development

seemed to be defective, and blood was leaked outside of the blood vessels. Abnormal types of hematopoietic cells were also observed between the spaces of hepatocytes, particularly dominated by a population of small cells with round nuclei and scanty cytoplasm. In severely affected regions, hepatocyte connections were disrupted (Fig. 2c, inserts) and the diffused miRNA effect further inhibited the feather growth in the skin area close to the injection site. The results showed that the anti-β-catenin miRNA was very effective in knocking down the targeted gene expression at a very low dose and was effective over a long period of time (≥10 days). Furthermore, the miRNA-mediated gene silencing effect seemed to be very specific and safe because off-targeted organs were normal, indicating that the small, single-stranded composition of miRNA possessed no overt toxicity.

In another attempt to silencing *noggin* expression in the mandible beak area using the same approach (Fig. 2d), it was observed that an enlarged lower beak morphology is reminiscent of the previously reported bone morphogenetic protein (BMP4)-overexpressing chicken embryos [35, 36]. Skeleton staining showed the outgrowth of bones and cartilage tissues in the injected mandible area (Fig. 2d, right panels), and Northern blot analysis further confirmed that approx 60% of *noggin* mRNA expression was knocked out in this region (inserts). Because BMP4, a member of transforming growth factor-β superfamily, is known to promote bone development and the *noggin* is an antagonist of *BMP2/4/7* genes, it is not surprised to discover that our miRNA-mediated *noggin* knockouts created a morphological change resemble to the *BMP4*-overexpressing results as previously reported in chicken and other avian models. Thus, our finding of the intronic miRNA-mediated gene silencing pathway presents a great potential of using this localized transgene-like approach in creating animal models for developmental biology research.

To further test the intronic miRNA effects on adult mammals (Fig. 3), we used the same intronic miRNA expression approach as previously reported in zebrafish for silencing mouse skin pigments. Patched albino (white) skins of melanin-knockout mice (W-9 black) were created by a succession of intracutaneous transduction of 50 μg of anti-tyrosinase (Tyr) pre-miRNA construct for 4 days (total 200 μg). The Tyr, a type I membrane protein and copper-containing enzyme, catalyzes the critical and rate-limiting step of tyrosine hydroxylation in the biosynthesis of melanin (black pigment) in skins and hairs. After 13-day incubation, the expression of melanin was blocked due to a great loss of its intermediates resulted from the anti-Tyr miRNA silencing effect. On the contrary, the blank control and the U6-directed siRNA-transfected mice presented normal skin color (black), indicating that the loss of melanin is specifically effective in the miRNA transfections. Moreover, Northern blot analysis using RNA-polymerase chain reaction-amplified

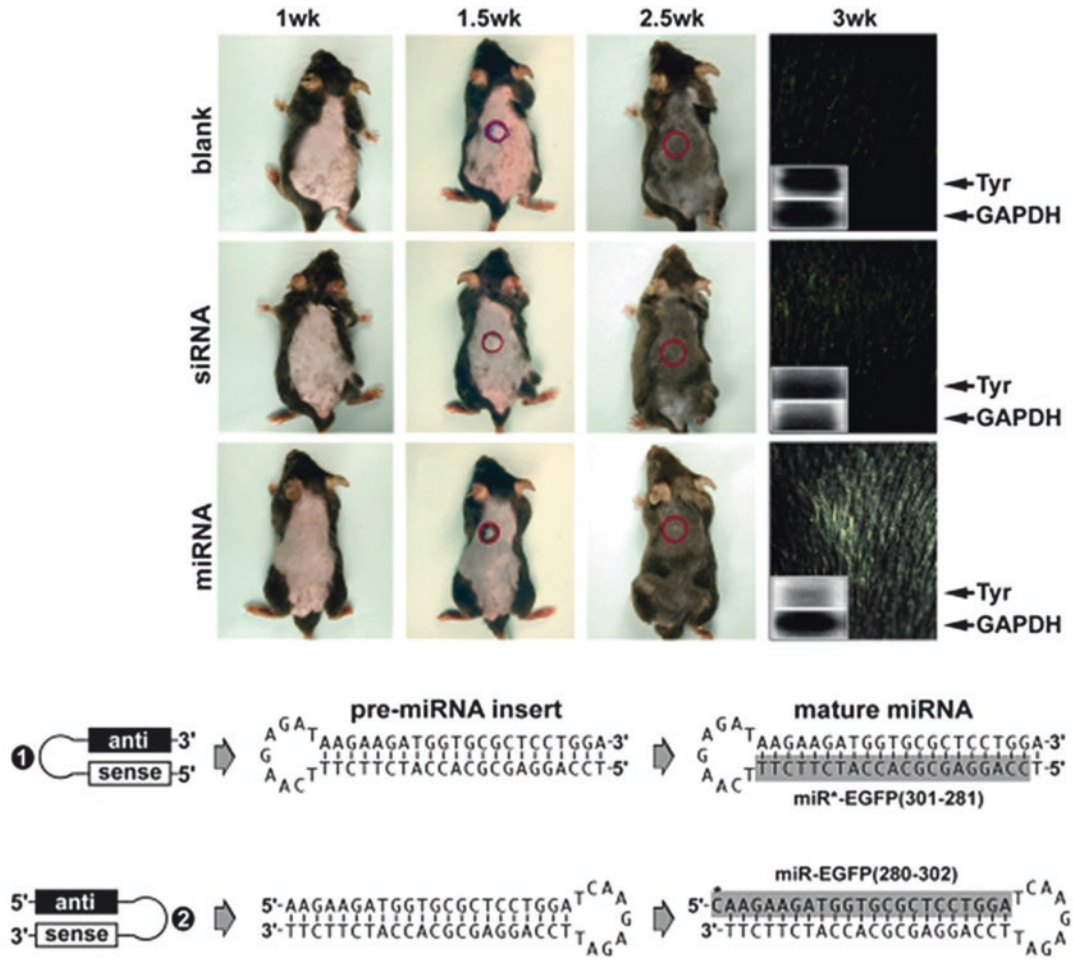

Fig. 3 In vivo effects of anti-tyrosinase (*Tyr*) miRNA on the mouse pigment production in local skins. Transfection of the designed anti-*Tyr* miRNA induced a strong gene silencing effect on tyrosinase (*Tyr*) expression but not house-keeping glyceraldehyde phosphate dehydrogenase (GAPDH) expression, whereas transfection of U6-directed small interfering RNA (siRNA) triggered mild non-specific RNA degradation of both *Tyr* and *GAPDH* gene transcripts. Because Tyr is an essential enzyme for black pigment melanin production, the success of *Tyr* silencing can be observed by a significant loss of the black color in mouse hairs. The red circles indicate the location of intracutaneous injections. Northern blot analysis of *Tyr* mRNA expression in local hair follicles confirmed the effectiveness and specificity of the intronic miRNA-mediated gene silencing effect (inserts)

mRNAs from hair follicles showed a 76.1 ± 5.3% decrease of Tyr expression 2-days after the miRNA transfection, whereas mild degradation of off-target gene transcripts was detected in the siRNA-transfected skins (seen from smearing patterns of both housekeeping control GAPDH and target Tyr mRNAs). Thus, these results suggest that the use of intronic miRNA expression provides a powerful new strategy for developing in vivo applications, particularly for localized tissue treatments. Under the same dosage, the miRNA transfections did not cause detectable

cytotoxicity effect, whereas the siRNA transfections showed non-specific mRNA degradation, as previously reported [25, 26]. This finding demonstrates the fact that intronic miRNA is safe and effective even under in vivo conditions, without the side effects of dsRNA. The results also indicate that this miRNA-mediated gene-silencing effect is stable and efficient in knocking down the target gene expression for a relatively long period of time, because the hair regrowth requires at least 10-day recovery. Therefore, the intronic miRNA approach offers relatively long-term, effective, and safe gene manipulation in specific animal tissues or organs, preventing the lethal effects of global gene knockouts in the conventional transgenic animal model.

To date, more than 135 miRNAs have been identified to be highly conserved between mammals and other animals [37]. This may be an underestimate because the information based on non-coding regions of a variety of genome species remains largely unknown and new ortholog annotation of miRNAs, such as intronic miRNAs, are not considered. Approximately 10–30% of a spliced intron is exported into cytoplasm, with a moderate half-life [38]. Also, several types of intronic miRNAs have been identified in *C. elegans*, mouse and human genomes [29, 31, 37]. Hence, it is understandable that the current miRNA computing programs do not fully predict the number of potential miRNA-like molecules. The finding of intronic miRNAs has opened up a new avenue for predicting miRNA varieties. Although there may be more than one type of new miRNAs to be found and many new parameters needed to be defined for different miRNAs, the similarities and differences among these different types of miRNAs will provide better understanding of the small regulatory RNA world. Indeed, the new miRNA species identified in a variety of plants and animals have gradually and greatly broadened our difinition of "small regulatory RNA" in the recent years.

2 Materials

2.1 Preparation of Pre-miRNA Inserts

1. Sense pre-miRNA sequence: 5′-GTCCGATCGTC ATCAAG TCAGCTTGGGTTGCCA TCAAGAGAT TGGCAACCCA AGCTGACTTGAT CGACGCGTCAT-3′ (100 pmol/μL in autoclaved ddH_2O).
2. Antisense pre-miRNA sequence: 5′-ATGACGCGTCG ATCA AGTCAGCTTGGGTTGCCA ATCTCTTGA TGGCAAC CCAAGCTGACTTGAT ACGATCGGAC-3′ (100 pmol/μL in autoclaved ddH_2O).
3. 2× hybridization buffer: 200 mM KOAc, 60 mM HEPES KOH, 4 mM MgOAc, pH 7.4 at 25 °C.
4. Incubation chamber: 94, 65 and 4 °C.

2.2 Change of Pre-miRNA Inserts Located in the SpRNAi-rGFP Gene Cassette

1. SpRNAi-rGFP gene vector (University of Southern California File #3443).
2. 10× H buffer: 500 mM Tris–HCl, pH 7.5 at 37 °C, 1 M NaCl, 100 mM $MgCl_2$, 10 mM dithioerythritol DTT).
3. Restriction enzymes, including *PuvI* and *MluI* (5 U/μL for each enzyme).
4. *PuvI/MluI* digestion reaction mix: 12 μL autoclaved ddH_2O, 4 μL 10× H buffer, 2 μL *PuvI* and 2 μL *MluI*; prepare the reaction mix just before use.
5. 10× ligation buffer:660 mM Tris–HCl, pH 7.5 at 20 °C, 50 mM $MgCl_2$, 50 mM dithioerythritol, 10 mM ATP.
6. T4 DNA ligase (5 U/μL).
7. Ligation reaction mix: 4 μL autoclaved ddH_2O, 4 μL 10× ligation buffer and 2 μL T4 ligase; prepare the reaction mix just before use.
8. Incubation chamber: 65, 37, and 16 °C.
9. 1% agarose gel electrophoresis.
10. Gel extraction kit (Qiagen, Valencia, CA).
11. Low salt Luria-Bertani (LB) culture broth.
12. Expand cloning kit (Roche Diagnostics, Indianapolis, IN).
13. DH5α transformation competent *E. coli* cells (Roche).
14. 10× $MgSO_4$ solution: 1 M $MgSO_4$.
15. 1× $CaCl_2$ solution: 0.1 M $CaCl_2$.
16. 10× Glucose solution: 1 M Glucose.
17. Incubation chamber: 42 and 4 °C.
18. Incubation shaker: 37 °C, 285 rpm vortex.
19. Luria-Bertani agar plate containing 50 μg/mL kanamycin.
20. Spin miniprep kit (Qiagen).
21. Microcentrifuge: 17,900 × *g*.

2.3 Cloning of the SpRNAi-rGFP Gene Cassette into a Viral Vector

1. Retroiral vector: e.g., eplication-competent avian sarcoma virus (RCAS) vector.
2. 10× H buffer: 500 mM Tris–HCl, pH 7.5 at 37 °C, 1 M NaCl, 100 mM $MgCl_2$, 10 mM DTT.
3. Restriction enzymes, including *XhoI* and *XbaI*.
4. *XhoI/XbaI* digestion reaction mix: 2 μL autoclaved ddH_2O, 4 μL 10× H buffer, 2 μL *XhoI* and 2 μL *XbaI*; prepare the reaction mix just before use.
5. 10× ligation buffer:660 mM Tris–HCl, pH 7.5 at 20 °C, 50 mM $MgCl_2$, 50 mM dithioerythritol, 10 mM ATP.
6. 5 U/μL T4 DNA ligase.

7. Ligation reaction mix: 4 μL autoclaved ddH_2O, 4 μL 10× ligation buffer, and 2 μL T4 ligase; prepare the reaction mix just before use.

2.4 Viral Packaging and Titer Quantitation

1. Serum-free RPMI 1640 cell culture medium.
2. FuGENE transfection reagent (Roche).
3. Chicken embryonic fibroblast (CEF) cell culture.
4. Cell culture incubator.
5. Lentivirus purification kit (Cell Biolabs).
6. Microcentrifuge: 17,900 × *g*.

3 Methods

3.1 Preparation of Pre-miRNA Inserts

The intronic pre-miRNA insert is formed by hybridization of the sense and antisense pre-miRNA sequences, which are synthesized to be perfectly complementary to each other. Both of the SpRNAi sequences must be purified by polyacrylamide gel electrophoresis (PAGE) before use and stored at −20 °C.

1. Hybridization: Mix the sense and antisense pre-miRNA sequences (5 μL for each sequence) in 10 μL of 2× hybridization buffer, heat to 94 °C for 3 min, and cool to 65 °C for 10 min. Stop the reaction on ice.

3.2 Change of Pre-miRNA Inserts Located in the SpRNAi-rGFP Gene Cassette

Because the intronic insert region of the SpRNAi-RGFP vector is flanked with a *PvuI* and an *MluI* restriction site at its 5′- and 3′-end, respectively, the primary pre-miRNA insert can be easily removed and replaced by various gene-specific inserts (e.g., anti-EGFP) possessing matched cohesive ends (*see* **Note 1**).

1. Cleavage by *MluI* and *PvuI*: Add the *PvuI*/*MluI* digestion reaction mix to the 20 μL of SpRNAi-rGFP vector and the above pre-miRNA hybrid, respectively. Incubate the reaction at 37 °C for 4 h and stop the reaction on ice.
2. Purification of *MluI* and *PvuI*-digested sequences: Load and run the above reactions in 1% agarose gel electrophoresis and cut out the *MluI* and *PvuI*-digested SpRNAi-rGFP sequence and the pre-miRNA fragment, respectively, using a clean surgical blade. Recover the two oligonucleotide sequences in one tube of 30 μL autoclaved ddH_2O using the gel extraction column and following the manufacturer's suggestions.
3. Ligation: Add the ligation reaction mix to the above extraction. Incubate the reaction at 16 °C for 16 h and stop the reaction on ice.
4. Plasmid amplification: Transfect the above ligation product into the DH5α transformation competent *E. coli* cells using

the expand cloning kit and following the manufacturer's suggestions.

5. Plasmid recovery: Isolate and collect the amplified SpRNAi-rGFP plasmid from the DH5α transformation competent *E. coli* cells into a tube of 30 μL autoclaved ddH_2O using a spin Miniprep filter following the manufacturer's suggestions (*see* **Note 2**).

3.3 Cloning of the SpRNAi-rGFP Gene Cassette into a Viral Vector

To express the SpRNAi-rGFP gene in chicken embryos, transfer the SpRNAi-rGFP gene cassette from the pHcRed1-N1/1 plasmid vector to the RCAS vector. Because the functional fluorescent structure of HcRed is disrupted by the SpRNAi intron insertion, one can determine the occurrence of intron splicing and miRNA maturation through the appearance of red fluorescent rGFP emission on the cell membranes. The RGFP protein also serves as a quantitative marker for measuring the titer activity of the pre-miRNA-expressing RCAS virus using flow cytometry. This intron-derived miRNA system is activated under the control of the *Xenopus* elongation factor 1-α enhancer-promoter located in the RCAS vector.

1. Cleavage by *XhoI* and *XbaI*: Add the *XhoI/XbaI* digestion reaction mix to the pHcRed1-N1/1 plasmid vector containing an SpRNAi-rGFP gene cassette and the RCAS retroviral vector, respectively. Incubate both the reactions at 37°C for 4 h and stop the reaction on ice.
2. Purification of *XhoI/XbaI*-digested sequences: Load and run the above reactions in 1% agarose gel electrophoresis and cut out of the *XhoI/XbaI*-digested SpRNAi-rGFP sequence and the big RCAS fragment, respectively, using a clean surgical blade. Recover the two oligonucleotide sequences in one tube of 30 μL autoclaved ddH_2O using the gel extraction column and following the manufacturer's suggestions.
3. Ligation: Add the ligation reaction mix to the above extraction. Incubate the reaction at 16 °C for 16 h and stop the reaction on ice.

3.4 Viral Packaging and Titer Quantitation

To increase transfection efficiency, we use liposomal reagents to facilitate the delivery of the SpRNAi-rGFP vector into the packaging cells.

1. Preparation of FuGENE: Add 6 μL of the FuGENE reagent into 100 μL of RPMI 1640 medium in a clean tube and gently mix the solution, following the manufacturer's suggestions. And add 20 μg (in less than 50 μL) of the SpRNAi-rGFP vector into the liposomal dilution and gently mix the solution, following the manufacturer's suggestions. Store the mixture at 4 °C for 30 min.

2. Transfection: Add the above mixture into the center of the chicken embryonic fibroblast cell culture and gently mix the cell-culture medium. Grow the transfected cells in a cell culture incubator at 37 °C, 5% CO_2 for 48–72 h.
3. Purification of viral particles: Harvest and concentrate the viral particles from the medium suspension using a lentivirus purification filter, following the manufacturer's protocol (*see* **Note 3**).

4 Notes

1. The synthetic pre-miRNA sequences that we show here are directed against the 5′-coding region of the chicken β-catenin gene sequence (NM205081, sense 110–131 nts) with perfect complementarity. The principal rule for designing an intronic pre-miRNA insert is to synthesize two mutually complementary oligonucleotides, including one 5′-GTCCGATCGTC—19- to 27-nt antisense target gene sequence—TCAAGAGAT (stemloop)—19- to 27-nt sense target gene sequence—CGACGCGTCAT-3′ and another 5′-ATGACGGTCG—19- to 27-nt antisense target gene sequence—ATCTCTTGA (stem-loop)—19- to 27-nt sense target gene sequence—GACGATCGGAC-3′. The hybridization of these two oligonucleotide sequences forms the intronic pre-miRNA insert, which contains a 5′-*PvuI* and a 3′-*Mlu1* restriction site for further ligation into the intron region of an *SpRNAi-rGFP* gene cassette. All synthetic oligonucleotides must be purified by PAGE to ensure their highest purity and integrity.
2. The sequence of the final *SpRNAi-rGFP* gene cassette and its pre-miRNA insert must be confirmed by DNA sequencing.
3. The RGFP protein can serve as a quantitative marker for measuring the titer levels of the pre-miRNA-expressing RCAS virus using either flow cytometry or the lentivirus quantitation kit (Cell Biolabs). The RGFP-specific monoclonal antibody can be purchased from BD Biosciences (Palo Alto, CA).

References

1. Lin SL, Ying SY (2004) Novel RNAi therapy – intron-derived microRNA drugs. Drug Des Rev 1:247–255
2. Tuschl T, Borkhardt A (2002) Small interfering RNAs: a revolutionary tool for the analysis of gene function and gene therapy. Mol Interv 2:158–167
3. Nelson P, Kiriakidou M, Sharma A, Maniataki E, Mourelatos Z (2003) The microRNA world: small is mighty. Trends Biochem Sci 28:534–539
4. Ying SY, Lin SL (2005) Intronic microRNA (miRNA). Biochem Biophys Res Commun 326:515–520
5. Hall IM, Shankaranarayana GD, Noma K, Ayoub N, Cohen A, Grewal SI (2002) Establishment and maintenance of a heterochromatin domain. Science 297:2232–2237

6. Llave C, Xie Z, Kasschau KD, Carrington JC (2002) Cleavage of Scarecrow-like mRNA targets directed by a class of Arabidopsis miRNA. Science 297:2053–2056
7. Rhoades MW, Reinhart BJ, Lim LP, Burge CB, Bartel B, Bartel DP (2002) Prediction of plant microRNA targets. Cell 110:513–520
8. Lee RC, Feibaum RL, Ambros V (1993) The C. elegans heterochromic gene *lin-4* encodes small RNAs with antisense complementarity to *lin-14*. Cell 75:843–854
9. Reinhart BJ, Slack FJ, Basson M, Pasquinelli AE, Bettinger JC, Rougvie AE, Horvitz HR, Ruvkun G (2000) The 21-nucleotide let-7 RNA regulates developmental timing in *Caenorhabditis elegans*. Nature 403:901–906
10. Lau NC, Lim LP, Weinstein EG, Bartel DP (2001) An abundant class of tiny RNAs with probable regulatory roles in *Caenorhabditis* elegans. Science 294:858–862
11. Brennecke J, Hipfner DR, Stark A, Russell RB, Cohen SM (2003) Bantam encodes a developmentally regulated microRNA that controls cell proliferation and regulates the proapoptotic gene hid in *Drosophila*. Cell 113:25–36
12. Xu P, Vernooy SY, Guo M, Hay BA (2003) The Drosophila microRNA Mir-14 suppresses cell death and is required for normal fat metabolism. Curr Biol 13:790–795
13. Lagos-Quintana M, Rauhut R, Meyer J, Borkhardt A, Tuschl T (2003) New microRNAs from mouse and human. RNA 9:175–179
14. Mourelatos Z, Dostie J, Paushkin S, Sharma A, Charroux B, Abel L, Rappsilber J, Mann M, Dreyfuss G (2002) miRNPs: a novel class of ribonucleoproteins containing numerous microRNAs. Genes Dev 16:720–728
15. Zeng Y, Wagner EJ, Cullen BR (2002) Both natural and designed micro RNAs can inhibit the expression of cognate mRNAs when expressed in human cells. Mol Cell 9:1327–1333
16. Hirose Y, Manley JL (2000) RNA polymerase II and the integration of nuclear events. Genes Dev 14:1415–1429
17. Kramer A (1996) The structure and function of proteins involved in mammalian pre-mRNA splicing. Annu Rev Biochem 65:367–409
18. Miyagishi M, Taira K (2002) U6 promoter-driven siRNAs with four uridine 3′ overhangs efficiently suppress targeted gene expression in mammalian cells. Nat Biotechnol 20:497–500
19. Lee NS, Dohjima T, Bauer G, Li H, Li MJ, Ehsani A, Salvaterra P, Rossi J (2002) Expression of small interfering RNAs targeted against HIV-1 rev transcripts in human cells. Nat Biotechnol 20:500–505
20. Paul CP, Good PD, Winer I, Engelke DR (2002) Effective expression of small interfering RNA in human cells. Nat Biotechnol 20:505–508
21. Xia H, Mao Q, Paulson HL, Davidson BL (2002) siRNA-mediated gene silencing in vitro and in vivo. Nat Biotechnol 20:1006–1010
22. McCaffrey AP, Meuse L, Pham TT, Conklin DS, Hannon GJ, Kay MA (2002) RNA interference in adult mice. Nature 418:38–39
23. Gunnery S, Ma Y, Mathews MB (1999) Termination sequence requirements vary among genes transcribed by RNA polymerase III. J Mol Biol 286:745–757
24. Schramm L, Hernandez N (2002) Recruitment of RNA polymerase III to its target promoters. Genes Dev 16:2593–2620
25. Sledz CA, Holko M, de Veer MJ, Silverman RH, Williams BR (2003) Activation of the interferon system by short-interfering RNAs. Nat Cell Biol 5:834–839
26. Lin SL, Ying SY (2004) Combinational therapy for HIV-1 eradication and vaccination. Int J Oncol 24:81–88
27. Stark GR, Kerr IM, Williams BR, Silverman RH, Schreiber RD (1998) How cells respond to interferons. Annu Rev Biochem 67:227–264
28. Lin SL, Ying SY (2004) New drug design for gene therapy – taking advantage of introns. Lett Drug Des Discov 1:256–262
29. Lin SL, Chang D, Wu DY, Ying SY (2003) A novel RNA splicing-mediated gene silencing mechanism potential for genome evolution. Biochem Biophys Res Commun 310:754–760
30. Lin SL, Chang D, Ying SY (2005) Asymmetry of intronic pre-miRNA structures in functional RISC assembly. Gene 356:32–38
31. Ambros V, Lee RC, Lavanway A, Williams PT, Jewell D (2003) MicroRNAs and other tiny endogenous RNAs in *C. elegans*. Curr Biol 13:807–818
32. Butz S, Larue L (1995) Expression of catenins during mouse embryonic development and in adult tissues. Cell Adhes Commun 3:337–352
33. Filipovska J, Konarska MM (2000) Specific HDV RNA-templated transcription by pol II in vitro. RNA 6:41–54
34. Modahl LE, Macnaughton TB, Zhu N, Johnson DL, Lai MM (2000) RNA-dependent replication and transcription of hepatitis delta virus RNA involve distinct cellular RNA polymerases. Mol Cell Biol 20:6030–6039
35. Abzhanov A, Protas M, Grant BR, Grant PR, Tabin CJ (2004) Bmp4 and morphological

variation of beaks in Darwin's finches. Science 305:1462–1465

36. Wu P, Jiang TX, Suksaweang S, Widelitz RB, Chuong CM (2004) Molecular shaping of the beak. Science 305:1465–1466
37. Rodriguez A, Griffiths-Jones S, Ashurst JL, Bradley A (2004) Identification of mammalian microRNA host genes and transcription units. Genome Res 14:1902–1910
38. Clement JQ, Qian L, Kaplinsky N, Wilkinson MF (1999) The stability and fate of a spliced intron from vertebrate cells. RNA 5:206–220

Chapter 21

Application of TALE-Based Approach for Dissecting Functional MicroRNA-302/367 in Cellular Reprogramming

Zhonghui Zhang and Wen-Shu Wu

Abstract

MicroRNAs are small 18–24 nt single-stranded noncoding RNA molecules involved in many biological processes, including stemness maintenance and cellular reprogramming. Current methods used in loss-of-function studies of microRNAs have several limitations. Here, we describe a new approach for dissecting miR-302/367 functions by transcription activator-like effectors (TALEs), which are natural effector proteins secreted by *Xanthomonas* and *Ralstonia* bacteria. Knockdown of the miR-302/367 cluster uses the Kruppel-associated box repressor domain fused with specific TALEs designed to bind the miR-302/367 cluster promoter. Knockout of the miR-302/367 cluster uses two pairs of TALE nucleases (TALENs) to delete the miR-302/367 cluster in human primary cells. Together, both TALE-based transcriptional repressor and TALENs are two promising approaches for loss-of-function studies of microRNA cluster in human primary cells.

Key words TALE, TALEN, Transcriptional repressor, MicroRNA, Cellular reprogramming, Human cells

1 Introduction

MicroRNAs (miRNAs) are important gene regulators that bind to partially complementary target sites in messenger RNAs (mRNAs) and result in degradation of target mRNAs or translational repression of encoded proteins [1]. To date, there are 1281 and 2042 mature miRNAs in mouse and human genomes, respectively. These miRNAs are implicated in many biological processes, diseases, development, and cellular reprogramming [1, 2]. Several approaches for knockdown of miRNAs have been extensively used, such as locked nucleic acid (LNA) oligonucleotides, antagomirs, and miRZip inhibitors [3–5]. Unfortunately, LNA and antagomirs can only transiently inhibit miRNA function. In contrast, miRZips are stably expressed RNAi hairpins and can permanently inhibit miRNA function; however, their inhibitor efficiency, similar to that

Shao-Yao Ying (ed.), *MicroRNA Protocols*, Methods in Molecular Biology, vol. 1733,
https://doi.org/10.1007/978-1-4939-7601-0_21,

of LNA and antagomir, is dependent on their dosage in each cell. In addition, the specificity of these three miRNA inhibitors is inversely proportional to their dosage delivered in cells. Therefore, there are significant concerns regarding the specificity and potency of these miRNA inhibitors [4].

To overcome these obstacles, we describe two approaches for studying miRNA functions: (1) TALE-based transcriptional repressor for knockdown of miRNA cluster, and (2) TALENs for knockout of miRNA clusters. TALE is protein consisting of multiple repeated, highly conserved 33–34 amino acid sequences [6], which can be quickly engineered to bind virtually and desired DNA sequence. Thus, TALE can regulate expression of endogenous genes when tethered with transcription activator or repressor domains and edit the genome when fused with the Fok I cleavage domain. TALEN is an emerging technology for genome editing [7].

Here, we applied these two approaches to study roles of the endogenous-specific miR-302/367 cluster in cellular reprogramming, which is polycistronic miRNA consisting of five mature miRNAs. In this study, we efficiently knocked down the expression of mature miR-302/367 miRNAs using the TALE-based transcriptional repressor and deleted the entire miRNA cluster by TALENs to investigate the roles of this cluster in cellular reprogramming.

2 Materials

2.1 Cell Culture

1. 293T cells were maintained by our lab. Primary human foreskin fibroblasts were purchased from Millipore Company. Human primary hepatocytes were obtained from ScienCell Research Laboratories. Human iPSCs were generated from human primary cells.
2. 293T cells were cultured in Dulbecco's Modified Eagle's Medium (DMEM) (high glucose) containing 10% fetal bovine serum (FBS) and 1% penicillin/streptomycin. Human hepatocytes were cultured in DMEM/F12 supplemented with 10% FBS and 1% penicillin/streptomycin. Human foreskin fibroblasts were cultured in FibroGRO™-LS complete media (Millipore). Human iPSCs were cultured in conventional hESC culture medium containing DMEM/F12, 20% knockout serum replacement, 1% Glutamine, 1% nonessential amino acids, 1% penicillin/streptomycin, 0.1 mM β-mercaptoethanol, and 20 ng/ml human FGF-2. For long-term use, all medium is stored at 4 °C and warmed prior to every use.
3. 6-well and 12-well plates.
4. 0.025% Trypsin-EDTA solution, 1× PBS buffer.

2.2 Preparation of Retrovirus and Lentivirus

1. pCL-Ampho (IMGENEX) is a retroviral packaging vector.
2. Lenti-Pac HIV Expression Packaging Kit containing packaging vectors for lentivirus generation is purchased from Genecopoeia.
3. Fugene HD transfection reagent (Roche) for transfection of DNA into 293T cells.

2.3 Plasmid Construction

1. Primers to amplify ~1 kb of miR-302/367 promoter region: 5′-CTGACGGGCCCCAAATCCATCCATTC-3′ and 5′-CTGACAAGCTTGGAGCCCACCCAACA-3′.
2. Specific sequences to target the promoter region of human miR-302/367 cluster: TALE1: 5′-TACATTCCCTGAGAGCT-3′ and TALE2: 5′-TGTTAACATTGACATCT-3′.
3. Specific sequences to delete the human miR-302/367 cluster: TALEN-a: 5′-ttctaaagttatgccatt-3′; TALEN-b: 5′-tcagagtatttagagctg-3′; TALEN-c: 5′-tctattttccttggaagc-3′; TALEN-d: 5′-attcagaaagacatcat-3′.
4. Primers for the construction of miR-302/367 donor vector to target the miR-302/367 cluster:
   (a) Primers for amplifying the left arm:
   Forward primer: 5′-gttgtaaaacgacggccagtgaattcgagctcctccactgtctgtttccatttctgactc-3′
   Reverse primer: 5′-CTCAAGCATGCTCTTCTCCACaacaaaatggcat aactttagaagaa-3′
   (b) Primers for amplifying GFP-puro expression cassette:
   Forward primer: 5′-ttgttGTGGAGAAGAGCATGCTTGAG-3′
   Reverse primer: 5′-ggaagTCAGGCACCGGGCTTGCGGGTC-3′
   (c) Primers for amplifying the right arm:
   Forward primer: 5′- GACCCGCAAGCCCGGTGCCTGActtccttaatgatgtctt tctgaataa-3′
   Reverse primer: 5′-GGAAACAGCTATGACCATGATTACGCCAAGCTTGTAGAGGTAAGAATCAAGAATAACTA-3′

   The left arm, GFP-puro expression cassette, and right arm were fused together by overlapping PCR and cloned into SacI and HindIII sites of pUC19.

2.4 Luciferase Reporter Assay

1. Passive cell lysis buffer and luciferase assay kit were purchased from Promega and used for luciferase reporter assay according to the manufacturer's instructions.
2. Luciferase reporter plasmid for miR-302/367 promoter (pGL3-basic vector) (Promega) containing an insert from

~1 kb promoter region of the miR-302/367 cluster at a concentration of 100 ng/μl, and pCMV-LacZ for normalization at a concentration of 50 ng/μl.

3. Z buffer with 4 mg/ml *o*-nitrophenyl-β-D-galactopyranoside (ONPG): 60 mM Na_2HPO_4, 40 mM NaH_2PO_4, 10 mM KCl, 1 mM $MgSO_4$, 40 mM 2-mercaptoethanol (2-ME), 4 mg/ml ONPG. Store the solutions at 4 °C.
4. White-walled 96-well plates for measurement of luciferase activities and clear-walled 96-well plates for measurement of galactosidase activities in cell lysates.

2.5 Extraction of Genomic DNA, RNA, and RT-PCR

1. QIAamp DNA Mini Kit (Qiagen) for genomic DNA preparation.
2. Quick-RNA™ MicroPrep Kit (Zymo Research) for total RNA preparation.
3. ZymoPURE™ Plasmid Midiprep Kit (Zymo Research) for plasmid DNA preparation (*see* **Note 1**).
4. The CFX96 Touch™ Real-Time PCR Detection System (Bio-Rad) is used to perform qPCR.
5. TaqMan MicroRNA Reverse Transcription Kit (Applied Biosystems) for mature microRNA reverse-transcription.
6. Superscript III Fist-Strand Synthesis System (Invitrogen) for total RNA reverse-transcription.

2.6 Human iPSC Generation

1. Sodium butyrate (500 mM), Y27632 (ROCK inhibitor, 10 mM) is purchased from Sigma and dissolved in ultrapure water, store at −20 °C. SB431542, and PD0325901 is purchased from Sigma and dissolved in DMSO and stored at −20 °C.
2. 6-well or 48-well cell culture plates coated with 2 ml Matrigel (hESC-qualified).

2.7 Alkaline Phosphatase Staining

1. Alkaline Phosphatase Detection Kit (Stemgent) for alkaline phosphatase staining.
2. Paraformaldehyde: 4% solution in phosphate-buffered saline (PBS). Store the solutions at 4 °C.
3. 1× PBS solution. Store at room temperature.

3 Methods

3.1 Luciferase Reporter Assay

1. 293T cells were cultured in 24-well plate overnight and then co-transfected with 100 ng of luciferase reporter, 50 ng of pCMV-LacZ (used for normalization of transfection efficiency), and 350 ng of plenti-EF1α-TALE1-KRAB or plenti-EF1α-TALE2-KRAB or plenti-EF1α-TALE-control by using Fugene HD.

2. After 48 h post-transfection, remove cell culture media, rinse the wells carefully with 1 ml of PBS, and remove PBS.
3. Add 250 μl of 1× passive lysis buffer to each well of the 24-well plate that contains cells.
4. Transfer the cells into new 1.5 ml Eppendorf tubes and centrifuging at top speed at 4 °C for 5 min.
5. Take 5 μl of supernatant to a 0.5 ml Eppendorf tube prior to luciferase activity reading.
6. Turn on the luminometer. Add 50 μl of luciferase assay reagent into the tube. A 2-s premeasurement delay should be followed by a 10 s measurement period for each reporter assay.
7. Place 5 μl of supernatant to a clear-walled 96-well plate, add 100 μl of 4 mg/ml Z buffer ONPG, mix well by pipetting, and incubate until the sample becomes yellow. Stop the reaction by adding 100 μl of 1 M sodium carbonate. Mix well. Measure A_{420nm} by plate reader.
8. Process raw data by dividing each luciferase measurement by its corresponding β-galactosidase measurement, giving corrected/normalized luciferase activity. Statistical analysis of the data should also be performed using Microsoft Excel.

3.2 Retrovirus and Lentivirus Preparation

1. To produce the retrovirus and lentivirus, 8 × 10^5 293T cells were cultured in 60 mm dish the day before transfection.
2. For OKSM retrovirus generation, 1.5 μg of pCL-Ampho (IMGENEX) plus 2.5 μg of pMig-OKSM, by Fugene HD (Roche), according to the manufacturer's instruction.
3. For lentivirus production, 293T cells were transfected with a mixture of DNA containing 2.5 μg of plenti-EF1α-KRAB-TALE1 or plenti-EF1α-TALE-control and 2.5 μg packaging mixture (Genecopoeia) by Fugene HD.
4. After 48 h of transfection, the virus-containing media were collected and filtered with 0.45 μm filter. For each construct, three dishes of cells are transfected and the virus-containing media were mixed together (*see* **Note 2**).

3.3 Design and Construction of TALE-KRAB Specific for the Promoter Region of Human miR-302/367 Cluster

1. Replace the DNA fragment containing the NLS sequence and VP16 activation domain in the pLenti-EF1α-Backbone vector [8] with a 339 bp of DNA fragment covering a NLS sequence and the KRAB domain by Nhe I and Xba I double digestion, the resultant plasmid was named plenti-EF1α-TALE-KRAB (Fig. 1).
2. The target sequences for TALE and TALEN were selected by online TAL effector design tools (https://tale-nt.cac.cornell.edu/node/add/single-tale). TALE1 and TALE2 were designed to target the specific sequences (TACATTCCCTGAGAGCT

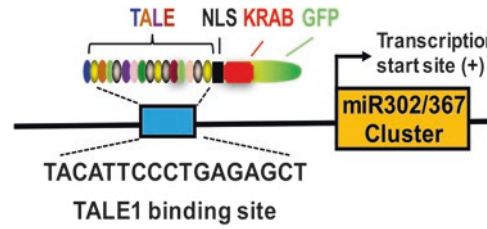

Fig. 1 Design of a miR-302/367-specific TALE1-KRAB transcriptional repressor for knockdown of the miR-302/367 cluster. A DNA-binding domain was designed to bind the indicated sequence within the proximal region upstream of the transcription start of the miR-302/367 cluster and fused to the N terminus of the KRAB transcriptional repressor domain, which is fused in-frame with GFP gene via 2A sequence. *NLS* nuclear localization signal

and TGTTAACATTGACATCT), respectively, at upstream of the transcription start of the miR-302/367 promoter. Assemble TALE1 and TALE2 using the first generation of PCR assemble approach [8] and then inserted into the BsmB I site of pLenti-EF1α-KRAB vector.

3.4 Design and Construction of TALENs and Donor Plasmid for Deletion of Human miR-302/367 Cluster

1. The target sequences for TALEN were selected by online TALEN design tools (https://talent.cac.cornell.edu/node/add/talen and http://zifit.partners.org/ZiFiT/TALZiFiTNuclease.aspx) and were assembled and cloned into corresponding pTAELN_v2 vectors provided in the TALE toolbox kit (Addgene, Cambridge, MA), using the second generation of PCR assembly approach recently developed by Zhang's group [9]. To facilitate deletion of the miR-302/367 cluster, we designed two pairs of TALENs with following target sequences: (1) ttctaaagttatgccatt (TALEN-a), (2) tcagagtatttagagctg (TALEN-b), (3) tctattttccttggaagc (TALEN-c), and (4) tattcagaaagacatcat (TALEN-d).
2. To construct the donor DNA plasmid for replacing the miR-302/367 cluster, 1 kb of homologous arms corresponding to the miR-302/367 cluster were amplified, cloned into pUC19 and a CMV-eGFP-2A-puromycin (GFP-puro) expression cassette was then inserted between the two arms (Fig. 2).
3. All inserts were confirmed by DNA sequencing. A total of five constructs were ready for further functional studies.

3.5 Viral Infection

1. Seed the human cells into 6-well plates the day before infection.
2. Add the fresh filtered supernatant containing viral particles and 1 μg/ml polybrene into the wells. Spin the plates at 1000 × *g* (*see* **Note 3**).

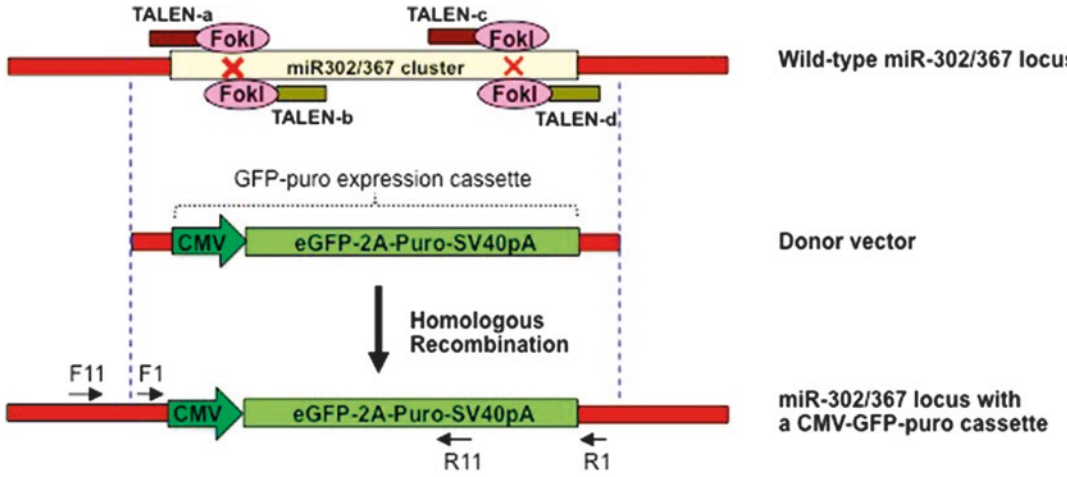

Fig. 2 Diagram of strategy for TALENs-mediated knockout of the miR-302/367 cluster. Two pairs of TALENs (TALEN-a/b and TALEN-c/d) targeted their specific binding sites in the 5′ and 3′ ends of the miR-302/367 cluster, respectively. In the donor vector, the CMV-eGFP-2A-Puro expression cassette was flanked by the two homology arms (red font color) at the 5′ and 3′ ends, respectively. Homologous recombination (HR) was mediated by the expression of the TALENs in the presence of the donor vector. Targeting leads to site-specific integration of the CMV-eGFP-2A-Puro expression cassette (green font color). Primers F1 and R1 were located in the 50 and 30 homology arms and near the CMV promoter and SV40pA, respectively. Forward primer F11 was located upstream of the 5′ arm and reverse primer R11 was located in GFP

3. After centrifugation, place the plate in the CO_2 incubator for 2 h.
4. Remove all media and add fresh culture media.

3.6 Generation of Human iPSCs

1. 1×10^4 human fibroblasts are seeded in a 6-well plate at 1 day before transduction.
2. Add fresh OKSM retroviral particles containing 4 μg/ml polybrene, followed by centrifugation (1000 × *g* for 30 min).
3. Four days post-infection, the cells were split by using 0.025% trypsin-EDTA and plate on 1× MEF feeder cultured in fibroblast medium.
4. After 24 h, the medium was switched to the hESC culture medium with 0.5 mM sodium butyrate, 2 μM SB431542, and 0.5 μM PD0325901.
5. The media were changed every other day.
6. Colonies will appear around day 15 and should be picked onto 1 well of a fresh Matrigel-coated 48-well plate into hESC culture medium containing 10 μM Y27632. Total protocol time for hiPSCs generation should be approximately 1 month (*see* **Note 4**).
7. Perform alkaline phosphatase staining. Count the positive colonies (Fig. 3).

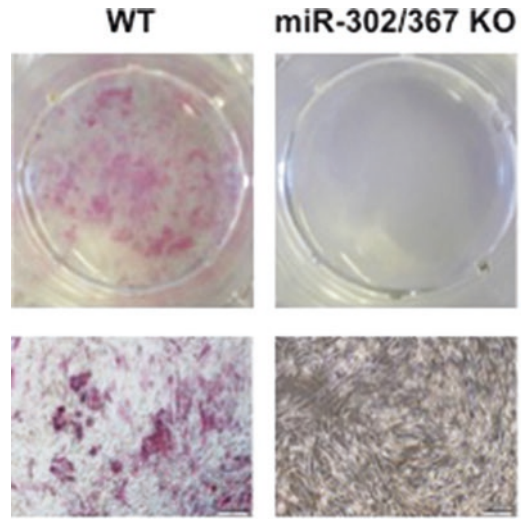

Fig. 3 Alkaline phosphatase staining of wild-type and miR-302/367 KO HFFs during reprogramming. Wild-type and miR-302/367 KO HFFs were transduced with OKSM-expressing retroviruses and then were seeded on feeder cells in 12-well plates at a density of 10,000 transduced cells per well 4 days after infection. Infected cells were cultured in hESC culture medium for 3 weeks. iPS-like colonies were then stained by alkaline phosphatase staining

3.7 TaqMan qPCR Assay of the miRNAs

1. Prepare total RNA by using Quick-RNA™ MicroPrep Kit. Dilute RNA to 5 ng/μl with RNase/DNase-free water.
2. Use 10 ng of total RNA per the reverse transcription. Prepare 12 μl of RT reaction mixer with 0.15 μl of 100 mM dNTPs with dTTP, 1 μl of MultiScribe™ Reverse Transcriptase (50 U/μl), 1.5 μl of 10× Reverse Transcription Buffer, 0.19 μl of RNase Inhibitor (20 U/μl), 5 μl of RNA (2 ng/μl), and 4.16 μl of Nuclease-free water. Add 3 μl of 5× RT primer. The RT PCR conditions are: 16 °C for 30 min, 42 °C for 30 min, 85 °C for 5 min.
3. Prepare qPCR reaction with 1 μl of TaqMan MicroRNA Assay (20×), 1.33 μl of product from RT reaction, 10 μl of TaqMan Universal PCR Master Mix II, 7.67 μl of Nuclease-free water. The qPCR condition are: 95 °C for 10 min and then 15 s at 95 °C and 1 min at 60 °C for 40 cycles. GADPH is used as endogenous control.

4 Notes

1. All plasmid DNAs are prepared by Zymo Research Kit without endotoxin.
2. Retroviral and lentiviral particles can be collected from 24 to 96 h after transfection.

3. Viral infection should be performed at 35–37 °C for 30 min.
4. For human iPSC generation, Matrigel-coated plates are essential for the adherence and reprogramming stage. Keep everything cold. After the diluted Matrigel is added to each plate, these plates can also be wrapped and stored at 4 °C for 1 week. During reprogramming process the media should be changed every 2 days.

References

1. Bartel DP (2004) MicroRNAs: genomics, biogenesis, mechanism, and function. Cell 116(2): 281–297
2. Johnston RJ, Hobert O (2003) A microRNA controlling left/right neuronal asymmetry in Caenorhabditis elegans. Nature 426(6968): 845–849
3. Liao B et al (2011) MicroRNA cluster 302–367 enhances somatic cell reprogramming by accelerating a mesenchymal-to-epithelial transition. J Biol Chem 286(19):17359–17364
4. Robertson B et al (2010) Specificity and functionality of microRNA inhibitors. Silence 1(1):10
5. Xia H, Ooi LL, Hui KM (2012) MiR-214 targets beta-catenin pathway to suppress invasion, stem-like traits and recurrence of human hepatocellular carcinoma. PLoS One 7(9):e44206
6. Moscou MJ, Bogdanove AJ (2009) A simple cipher governs DNA recognition by TAL effectors. Science 326(5959):1501
7. Hockemeyer D et al (2011) Genetic engineering of human pluripotent cells using TALE nucleases. Nat Biotechnol 29(8):731–734
8. Zhang F et al (2011) Efficient construction of sequence-specific TAL effectors for modulating mammalian transcription. Nat Biotechnol 29(2):149–153
9. Sanjana NE et al (2012) A transcription activator-like effector toolbox for genome engineering. Nat Protoc 7(1):171–192

Chapter 22

Mechanism and Method for Generating Tumor-Free iPS Cells Using Intronic MicroRNA miR-302 Induction

Shi-Lung Lin and Shao-Yao Ying

Abstract

Today's researchers generating induced pluripotent stem cells (iPS cells or iPSCs) usually consider their pluripotency rather than potential tumorigenicity. Oncogenic factors such as c-Myc and Klf4 are frequently used to boost the survival and proliferative rates of iPSCs, creating an inevitable problem of tumorigenicity that hinders the therapeutic usefulness of these iPSCs. To prevent stem cell tumorigenicity, we have examined mechanisms by which the cell cycle genes are regulated in embryonic stem cells (ESCs). Naturally, ESCs possess two unique stemness properties: pluripotent differentiation into almost all cell types and unlimited self-renewal without the risk of tumor formation. These two features are also important for the use of ESCs or iPSCs in therapy. Currently, despite overwhelming reports describing iPSC pluripotency, there is no report of any tumor prevention mechanism in either ESCs or iPSCs. To this, our studies have revealed for the first time that an ESC-specific microRNA (miRNA), miR-302, regulates human iPSC tumorigenicity through cosuppression of both cyclin E-CDK2 and cyclin D-CDK4/6 cell cycle pathways during G1-S phase transition. Moreover, miR-302 also silences BMI-1, a cancer stem cell gene marker, to promote the expression of two senescence-associated tumor suppressor genes, p16Ink4a and p14/p19Arf. Together, the combinatory effects of inhibiting G1-S cell cycle transition and increasing p16/p14(p19) expression result in an attenuated cell cycle rate similar to that of 2-to-8-cell-stage embryonic cells in early zygotes (20–24 h/cycle), which is however slower than the fast proliferation rate of iPSCs induced by the four defined factors Oct4-Sox2-Klf4-c-Myc (12–16 h/cycle). These findings provide a means to control iPSC tumorigenicity and improve the safety of iPSCs for the therapeutic use. In this chapter, we review the mechanism underlying miR-302-mediated tumor suppression and then demonstrate how to apply this mechanism to generate tumor-free iPSCs. The same strategy may also be used to prevent ESC tumorigenicity.

Key words miR-302, MicroRNA (miRNA), Tumor suppressor, iPSC, ESC, Stem cell, Cell cycle, CDK2, CDK4/6, Cyclin D, BMI-1, p16Ink4a, p14/p19Arf, p21Cip1/Waf1, CDKN1A, RNAi

1 Introduction

Somatic cell reprogramming (SCR) is an epigenetic mechanism required for the generation of induced pluripotent stem cells (iPSCs). The process of SCR is initiated by global DNA demethylation, which erases most of genomic methylation sites and resets all kinds of different somatic gene expression patterns to a unique

Shao-Yao Ying (ed.), *MicroRNA Protocols*, Methods in Molecular Biology, vol. 1733,
https://doi.org/10.1007/978-1-4939-7601-0_22,

embryonic stem cell (ESC)-like transcriptome profile. In human iPSCs, we have identified the functional roles of miR-302 in SCR [1, 2]. MiR-302, the most abundant microRNA (miRNA) in human ESCs (hESCs), not only silences the expression of lysine-specific histone demethylase 1/2 (LSD1/2, AOF2/1 or KDM1/1B) and DNA (cytosine-5-)-methyltransferase 1 (DNMT1) to induce global DNA demethylation but also stimulates cellular Oct4-Sox2-Nanog coexpression to promote the full reprogramming of somatic cells into ESC-like iPSCs [2]. Hence, miR-302 can replace all four previously defined factors (either Oct4-Sox2-Klf4-c-Myc or Oct4-Sox2-Nanog-Lin28) for iPSC induction. Accompanying this miR-302-induced SCR mechanism, we further identified a parallel tumor suppression mechanism, in which miR-302 attenuates both cyclin E-cyclin-dependent kinase 2 (CDK2) and cyclin D-CDK4/6 cell cycle pathways to inhibit iPSC tumorigenicity [3]. This tumor suppression mechanism provides a breakthrough advantage in the preparation of tumor-free iPSCs, which are useful for clinical trials and therapies. Based on the dual function of miR-302 in SCR induction and tumor suppression, we have successfully developed and tested an inducible miR-302 expression system for generating various tumor-free iPSCs derived from normal and cancerous human cells [1–3]. To distinguish the miRNA-induced pluripotent stem cells from other four-factor-induced iPSCs, we herein refer to these miR-302-induced tumor-free iPSCs as mirPSCs.

Each individual mirPSC can grow into a single colony or embryoid body with a relatively slow cell cycle rate (20–24 h/cycle). Due to miR-302-mediated cell cycle attenuation, mirPSCs often present a quiescent cell-like morphology and form three-dimensional sphere colonies similar to that of a morula stage zygote (Fig. 1a). These mirPSCs strongly express Oct4, Sox2, Nanog, Lin28, and many other major hESC markers (Fig. 1b, c), resembling the gene expression pattern of hESCs, determined by immunocytochemical staining and western blotting analyses. The transcriptome of mirPSCs also contains an average of >92% similarity to that of hESCs, determined by microarray analysis of global gene expression [1, 2]. Further, genomic DNA demethylation, the first sign of SCR, has been well established in the mirPSCs [1, 2]. Particularly, we noted that mirPSCs are pluripotent but not tumorigenic because they form teratoma-like tissue cysts only in the uterus or peritoneal cavity of pseudopregnant immunocompromised SCID-beige mice, but not elsewhere [1, 2]. These tissue cysts, not like teratomas, contain various but relatively organized tissue regions derived from all three embryonic germ layers. Notably, the presence of partial homeobox (HOX) gradient expression was also frequently observed in these tissue cysts (Lin et al. unpublished). Furthermore, when xenografted into normal male mice, the mirPSCs can be differentiated and assimilated into

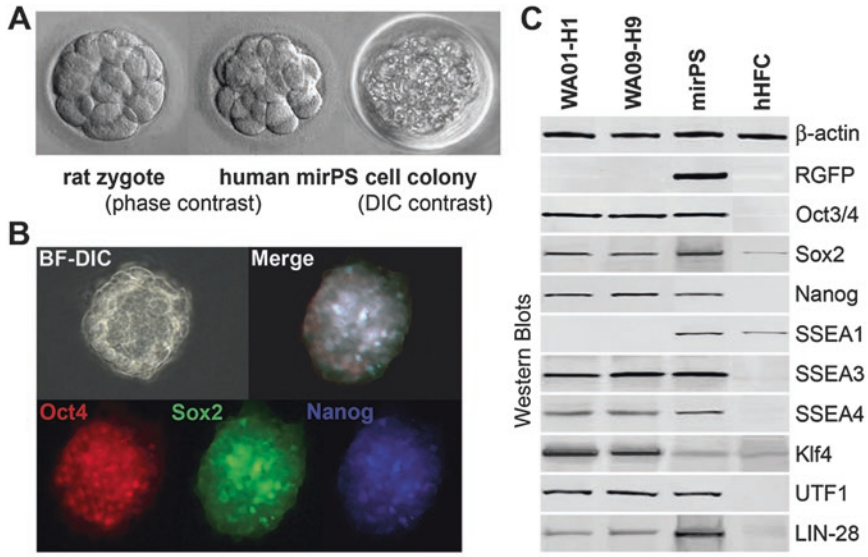

Fig. 1 Morphological and genetic properties of mirPSCs. (**a**) A morphological comparison between a morula-stage rat embryo and a mirPSC colony at 16–32-cell stage. *BF-DIC* refers to bright field with differential interference contrast. (**b**) Fluorescent microscope examination showing the homogeneous expression of the core reprogramming factors Oct3/4, Sox2 and Nanog in a mirPSC-derived embryoid body. (**c**) Western blots confirming the expression patterns of major hESC-specific markers in mirPSCs, of which the results are comparable to those found in hESCs H1 and H9 ($n = 4$, $p < 0.01$)

surrounding tissues, indicating a potential in-vivo application for regenerative medicine [3]. Taken together, our findings have demonstrated that miR-302 functions to reprogram somatic cells into hESC-like iPSCs with a high level of pluripotency but less or no tumorigenicity.

MiR-302-mediated gene silencing is dose-dependent. The tumor suppression function of miR-302 only occurs when its cellular concentration reaches over 1.1–1.3-folds of the miR-302 level in hESC H1 or H9 cells, which is also the optimal miR-302 level for inducing iPSC formation [2, 3]. As shown in Fig. 2, when the miR-302 level is equal to or lower than that in hESCs, only large tumor suppressor homolog 2 (LATS2), but not CDK2, is silenced. Yet, when the miR-302 level is higher than that in hESCs, both CDK2 and LATS2 are silenced and hence cell cycle is attenuated at the G1-phase check point [3]. Given that LATS2 inhibits the cyclin E-CDK2 pathway to block G1-S cell cycle transition [4], the co-suppression of CDK2 by miR-302 can further ensure this LATS2 function even in the absence of LATS2. Moreover, the CDK2 silencing effect also counteracts the suppressive effect of miR-367 on CDKN1C (p57, Kip2), a cell cycle inhibitor against both CDK2 and CDK4, subsequently leading to a reduced cell cycle rate (Lin et al. unpublished). Through this dose-dependent gene silencing mechanism, miR-302 fine-tunes the functions of its

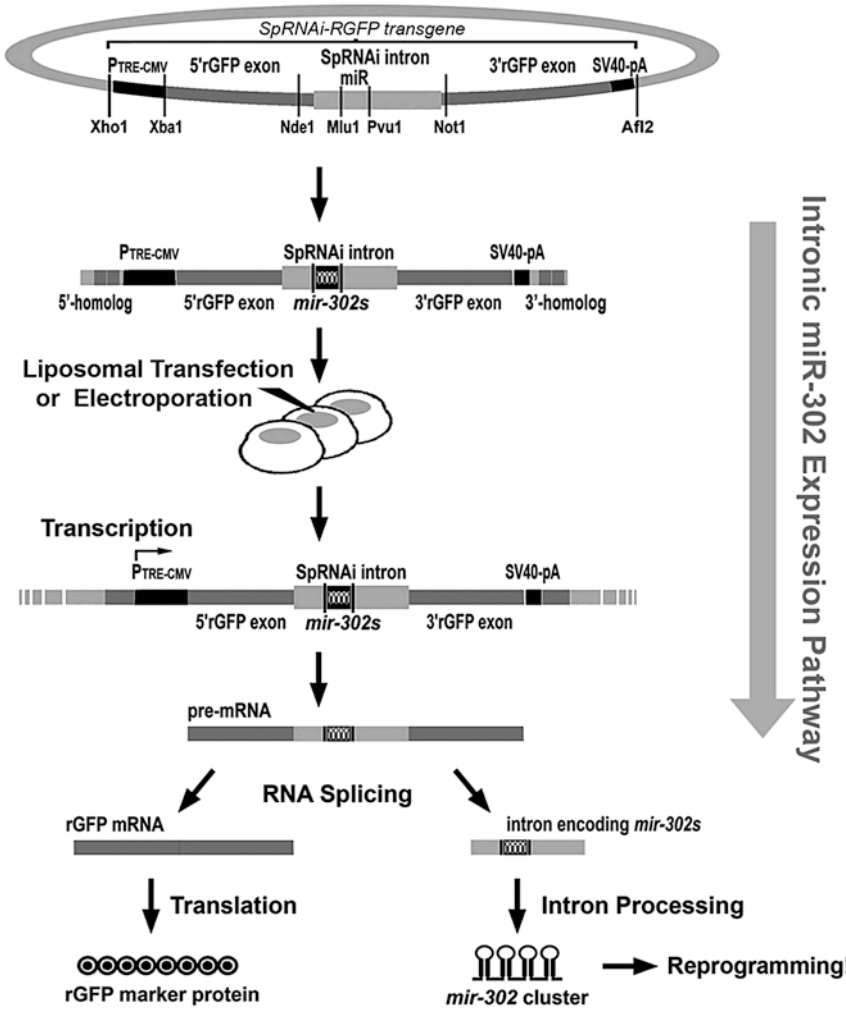

Fig. 2 Schematic procedure for iPSC generation using intronic miR-302 expression. A pre-designed miR-302-expressing *SpRNAi-RGFP* vector is transduced into human somatic cells by either electroporation or liposomal transfection. The expression of miR-302 is processed through the natural intronic miRNA biogenesis pathway, in which the miR-302 familial cluster is placed in the intron region of a red fluorescent protein (*RGFP*) gene, coexpressed with the *RGFP* gene transcripts, and then further processed into individual miR-302 molecules by RNA splicing enzymes (spliceosomal components) and RNaseIII Dicers [24]

target genes at different levels during reprogramming [2, 5]. These findings may account for the fact that 2-to-8-cell-stage embryonic cells have a relatively slower cell cycle rate (20–24 h/cycle) than that of hESCs (15–16 h/cycle) [6]. Even though both early zygotes and hESCs are known to display a short G1 phase, the G1 phase of 2-to-8-cell-stage zygotic cells is still significantly longer (4 ± 1 h) than that of hESCs. Interestingly, iPSC derivation has been reported to be either a cell-cycle-dependent (with Klf4) or a cell-cycle-independent (with Nanog) reprogramming process [7]. Since Klf4 is an

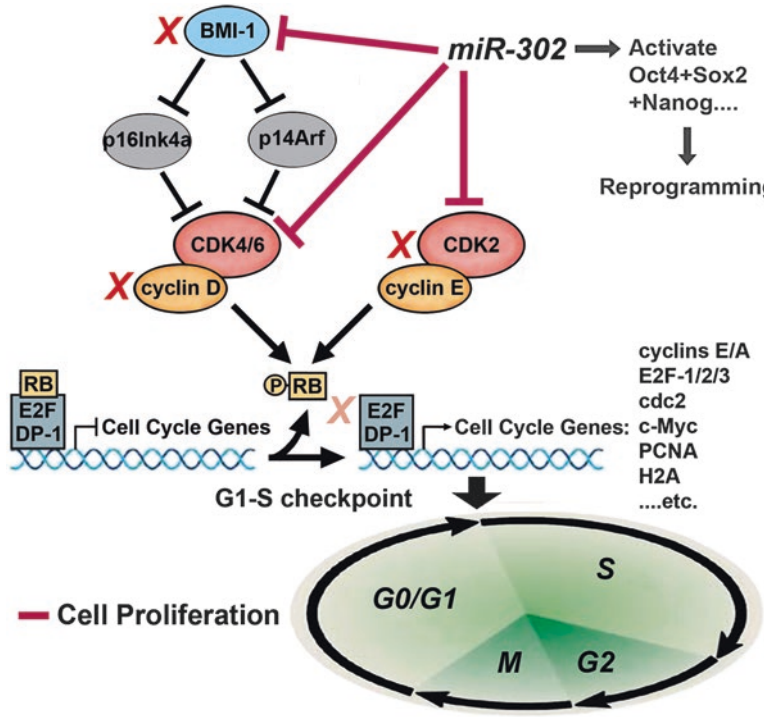

Fig. 3 Mechanism of miR-302-mediated tumor suppression in human iPSCs. MiR-302 not only concurrently suppresses several G1-phase checkpoint regulators such as CDK2, cyclin D and BMI-1 but also indirectly activates p16Ink4a and p14/p19Arf to quench most (>70%) of the cell cycle activities during reprogramming. E2F is also a predicted target of miR-302. Inducing cell cycle quiescence at the G0/G1 state prevents fast cell proliferation and tumor transformation of the reprogrammed iPSCs, leading to a more accurate and safer reprogramming process, by which all possible pre-mature cell differentiation and tumorigenicity are inhibited

upstream transcription factor of Nanog [8, 9], Klf4 may induce not only Nanog but also many other oncogenes, which promote fast cell proliferation unrelated to the function of Nanog in reprogramming [8–11]. Therefore, fast cell cycle, although can increase iPSC number, is not essential for SCR initiation to form iPSCs.

MiR-302 functions differently in normal cells versus in tumor/cancer cells. Our previous studies have shown that miR-302 triggers massive reprogrammed cell death (apoptosis) in fast proliferative tumor/cancer cells, whereas slow growing normal cells can tolerate this tumor suppression effect [1, 3]. It is conceivable that tumor/cancer cells may not survive in such a relatively slow cell cycle state due to their high metabolism and rapid consumption rates, providing a beneficial advantage in preventing tumor formation.

Based on the mechanism by which miR-302 suppresses tumor/cancer formation (Fig. 3), miR-302 not only inhibits both the

cyclin E-CDK2 and cyclin D-CDK4/6 pathways to block >70% of the G1-S cell cycle transition but also silences polycomb ring finger oncogene BMI-1 to increase the expression of two cell cycle inhibitors p16Ink4a and p14/p19Arf [3]. As a result, 16Ink4a inhibits cyclin D-dependent CDK4/6 activity via phosphorylation of retinoblastoma protein Rb and subsequently prevents Rb from releasing E2F-dependent transcription required for S phase entry [12, 13]. Furthermore, p14/p19Arf prevents HDM2, an Mdm2 p53 binding protein homolog, from binding to p53 and permits the p53-dependent transcription responsible for G1 arrest or apoptosis [14]. Through simultaneously activating multiple cell cycle attenuation and tumor suppression pathways, miR-302 induces iPSC generation while preventing stem cell tumorigenicity. In addition, since DNMT1-deficient ESCs have been observed to present a significant decrease of gene loss and mutation rates [15], miR-302 may also facilitate the genomic stability of both ESCs and iPSCs via LSD1/AOF2/KDM1-associated DNMT1 degradation [2, 3]. In view of these miR-302 functions, it is conceivable that the tumorigenicity of iPSCs and ESCs may be prevented by elevating their miR-302 expression.

Over-expression of miR-302 is not always beneficial. Human iPSCs have been reported to exhibit problems including early senescence and limited cell life expansion [16, 17]. When the miR-302 level is increased beyond 1.5–1.7-folds of that in hESCs, the degree of iPSC senescence is also increased in proportion to the concentration of miR-302. Normal somatic cells always undergo a limited number of cell divisions and then reach a quiescent state called replicative senescence. Cells that escape replicative senescence often become immortal cells; thus, replicative senescence is a cellular defense mechanism against tumor/cancer formation. Because miR-302 increases both p16Ink4a and p14/p19Arf expressions, two of the major regulators in replicative senescence, its over-expression may also cause early senescence in iPSCs. Previous studies have identified several genes encoded in the Ink4a/Arf locus, such as p16Ink4a and p14/p19Arf, which pose a barrier to the success of iPSC reprogramming [16, 18–20]. In particular, both of the p16Ink4a-RB and p14/19Arf-p53 activities are gradually enhanced and finally commit to the onset of early senescence after serial passaging of iPSCs [16, 19]. In murine iPSCs, p19Arf rather than p16Ink4a is the main factor activating senescence, whereas in humans p16Inka plays a more important role than p14Arf [16, 18]. Our recent observations have further ruled out the effect of telomerase in mirPSC senescence (Fig. 4). Due to forced miR-302 elevation, mirPSCs often present a higher degree of senescence than the iPSCs induced by the four defined factors. Under the same feeder-free conditions, the four-factor-induced iPSCs could be cultivated over 30–50 passages while mirPSCs only reach a maximum of 26 passages. However, this

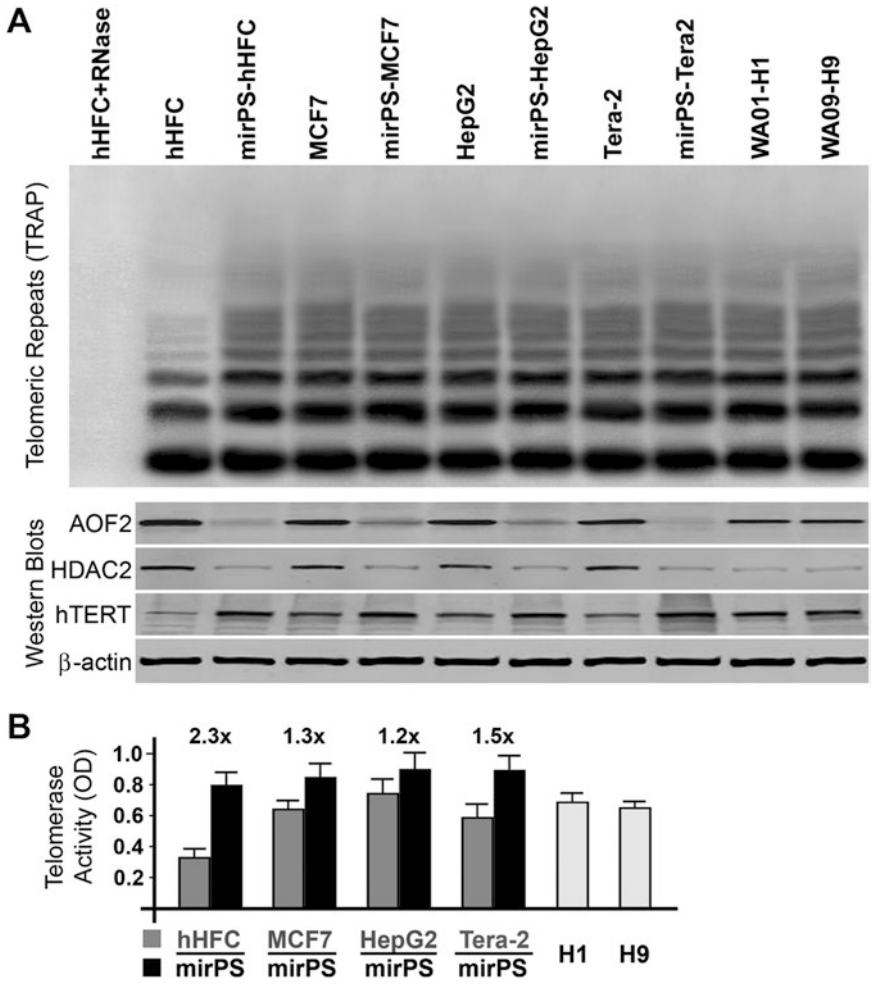

Fig. 4 Analysis of telomerase activity in various mirPSC lines in response to an elevated miR-302 level expressed over 1.3-folds of the normal miR-302 level in hESCs. (**a**) Telomerase activities shown by TRAP assays ($n = 5$, $p < 0.01$) in the upper panel. Telomerase activity is sensitive to RNase treatment (hHFC + RNase). Western blotting (lower panel) confirming the increase of hTERT and the decrease of LSD1/AOF2/KDM1 and HDAC2 expression in various mirPSC lines ($n = 5$, $p < 0.01$). (**b**) Telomerase activities measured by telomerase PCR ELISA assays (OD470–OD680; $n = 3$, $p < 0.01$)

early senescence was not due to the shortening of telomere length. It is known that LSD1/AOF2/KDM1 and histone deacetylase 2 (HDAC2) suppress the transcription of human telomerase reverse transcriptase (hTERT) and the deficiency of these epigenetic regulators has been shown to increase hTERT expression [21, 22]. Both LSD1/AOF2/KDM1 and HDAC2 are also the targets of miR-302 [2]. Using telomeric repeat amplification protocol (TRAP) and telomerase activity ELISA assays, we have confirmed that miR-302 silences both LSD1/AOF2/KDM1 and HDAC2 to enhance the hTERT activity and subsequently maintain normal or

longer telomere length in mirPSCs (Fig. 4a, b). In view of this concurrent regulation of p16Ink4a, p14/p19Arf, and hTERT activities by miR-302, mirPSCs may serve as a model for investigating the early senescence of iPSCs.

The balance between the mechanisms of tumorigenicity and senescence determines the safety and efficiency of iPSC generation. Our studies have shown that both mechanisms are regulated by the p16Ink4a-RB and p14/19Arf-p53 pathways [3]. In mirPSCs, miR-302 modulates the levels of p16Ink4a and p14/19Arf via fine-tuning the BMI-1 expression [3], providing important insight into the mechanism underlying stem cell self-renewal without the risk of tumor formation. Yet, in four-factor-induced iPSCs, the activities of Oct4, Sox2 and Klf4 were found to repress the expression of p16Ink4a and p14/19Arf, leading to fast iPSC proliferation [18]. Conceivably, the counteracting effect between miR-302 and Oct4-Sox2-Klf4 on the p16Ink4a and p14/19Arf expression may be the key for reaching the balance between tumorigenicity and senescence in iPSCs. Moreover, we also found that the expression of miR-302 and Oct4-Sox2-Nanog can form a positive feedback cycle to fulfill the full reprogramming of iPSCs [2]. In this reprogramming cycle, miR-302 and Oct4-Sox2-Nanog are reciprocally induced to constantly maintain the ESC-like pluripotent state of iPSCs. Therefore, at a certain point in the reprogramming cycle, the interaction between miR-302 and Oct4-Sox2-Nanog/Klf4 may lead to a stable iPSC state without the problem of either tumorigenicity or senescence. Based on this understanding, finding the correct combination of miR-302 and Oct4-Sox2-Nanog/Klf4 expression for generating tumor-free and senescence-free iPSCs will be a future challenge.

Through the natural mechanism of intronic miRNA biogenesis, we have identified the optimal miR-302 concentration for inducing tumor-free iPSCs [3, 23, 24]. MiR-302 is encoded in the intron region of the *La ribonucleoprotein domain family member 7* (*LARP7*, *PIP7S*) gene and expressed via an intronic miRNA biogenesis mechanism [1, 23, 25]. The miR-302 family consists of four familial sense homologues (miR-302b, c, a and d) and three distinct antisense members (miR-302b*, c* and a*), all of which are transcribed together as a polycistronic RNA cluster along with another miRNA, miR367 [26]. Many attempts were made to investigate the "miR-302" function, but no complete expression of all miR-302a–d familial members had ever achieved. Also, no studies were centered on the dose-dependent effect of miR-302, which however determines the real miR-302 function. To overcome this problem, our current study using intronic miR-302 expression was the first successful approach to display the full spectrum expression of all miR-302a-d familial members in human iPSCs, confirmed by microarray and northern blot analyses [1, 2].

We have developed a *pSpRNAi-RGFP* vector to adopt the process of intronic miRNA biogenesis [23, 24, 27]. As shown in Fig. 2, primary intronic miRNA precursors (pri-miRNAs) are transcribed by type-II RNA polymerases (Pol-II) and excised by spliceosomal components and/or Drosha to form miRNA precursors (pre-miRNAs), which are then exported out of the cell nucleus by Ran-GTP and Exportin-5 and further processed by a Dicer-like RNaseIII endoribonuclease in cytoplasm to form mature miRNAs [23, 28, 29–31]. However, the role of Drosha may be important but not required in this mechanism because the depletion of >85% Drosha with siRNA reduces less than a half of the miR-302 expression (Lin et al. unpublished), indicating that some other nuclear RNaseIII-like enzymes may replace Drosha for processing intronic pre-miRNAs [29]. Also, because mammalian intron often contains nonsense (i.e., translational stop) codons recognized by the nonsense-mediated decay (NMD) system, a cellular RNA surveillance mechanism [32, 33], the non-hairpin structures of an intron can be quickly degraded by NMD to prevent excessive RNA accumulation. RNA over-saturation has been reported to be a major problem for the direct (exonic) expression of short hairpin RNAs (shRNAs) and miRNAs in mammalian cells [34]. Under this tightly coordinated regulation by Pol-II transcription, RNA splicing, and NMD mechanisms, intronic miRNA expression presents a great advantage in the safeguard of cellular miRNA concentrations. As a result, we successfully established an effective means to express miR-302 through the cellular intronic miRNA biogenesis pathway, so as to provide a safer and more efficient approach for generating tumor-free iPSCs.

2 Materials

2.1 Synthetic Oligonucleotides

1. All synthetic oligonucleotides required for the construction of the miR-302 familial cluster are listed in Table 1 (*see* **Note 1**). Each synthetic oligonucleotide was prepared in a final concentration of 200 pmol/μL.
2. 2× hybridization buffer: 200 mM KOAc, 60 mM HEPES KOH, 4 mM MgOAc (pH 7.4 at 25 °C).
3. Incubation chambers: 94–65 °C and 4 °C.

2.2 Construction of the miR-302 Cluster

1. 10× digestion buffers for each individual restriction enzyme.
2. Restriction enzymes, such as *XhoI*, *MluI*, *BglII*, *NdeI*, *XbaI*, *PvuI*, and *BamHI*, were prepared with a stock concentration of 10 U/μL.
3. Digestion reaction mix: 10 μL of autoclaved ddH_2O, 2 μL of 10× digestion buffer, 4 μL of restriction enzyme(s), and 4 μL

Table 1
Synthetic sequences used for constructing the miR-302 familial cluster

Name	Sequence[a]
miR-302a-sense	5′-GATATCTCGA GTCACGCGTT CCCACCACTT AAACGTGGAT GTACTTGCTT TGAAACTAAA GAAGTAAGTG CTTCCATGTT TTGGTGATGG ATAGATCTCT C-3′
miR-302a-antisense	5′-GAGAGATCTA TCCATCACCA AAACATGGAA GCACTTACTT CTTTAGTTTC AAAGCAAGTA CATCCACGTT TAAGTGGTGG GAACGCGTGA CTCGAGATAT C-3′
miR-302b-sense	5′-ATAGATCTCT CGCTCCCTTC AACTTTAACA TGGAAGTGCT TTCTGTGACT TTGAAAGTAA GTGCTTCCAT GTTTTAGTAG GAGTCGTCAT ATGAC-3′
miR-302b-antisense	5′-GTCATATGAC GACTCCTACT AAAACATGGA AGCACTTACT TTCAAAGTCA CAGAAAGCAC TTCCATGTTA AAGTTGAAGG GAGCGAGAGA TCTAT-3′
miR-302c-sense	5′-GCCATATGCT ACCTTTGCTT TAACATGGAG GTACCTGCTG TGTGAAACAG AAGTAAGTGC TTCCATGTTT CAGTGGAGGC GTCTAGACAT-3′
miR-302c-antisense	5′-ATGTCTAGAC GCCTCCACTG AAACATGGAA GCACTTACTT CTGTTTCACA CAGCAGGTAC CTCCATGTTA AAGCAAAGGT AGCATATGGC-3′
miR-302d-sense	5′-CGTCTAGACA TAACACTCAA ACATGGAAGC ACTTAGCTAA GCCAGGCTAA GTGCTTCCAT GTTTGAGTGT TCGCGATCGG ATCCAC-3′
miR-302d-antisense	5′-GTGGATCCGA TCGCGAACAC TCAAACATGG AAGCACTTAG CCTGGCTTAG CTAAGTGCTT CCATGTTTGA GTGTTATGTC TAGACG-3′

[a]Red letters indicate the sequences of each individual miR-302 precursor (pre-miR302)

of each individual hybridized oligonucleotide (for example, the hybrid of miR-302a-sense and miR-302a-antisense); the reaction mix was prepared right before use.

4. 10× ligation buffer: 660 mM Tris–HCl (pH 7.5 at 20 °C), 50 mM $MgCl_2$, 50 mM dithioerythritol, and 10 mM ATP.
5. T4 DNA ligase (5 U/μL).
6. Ligation reaction mix: 6 μL of each of the digested hybridized oligonucleotides (four kinds of hybridized oligonucleotides in total 24 μL), 3 μL of 10× ligation buffer, and 3 μL of T4 ligase; the reaction mix was prepared right before use.
7. Incubation chambers: 37, 75, 10, and 4 °C.
8. 70-base-pair (bp) cut-off purification filters, such as, but not limited, QIAquick Gel Extraction Kit (Qiagen, Valencia, CA).
9. 100-bp cut-off purification filters, such as, but not limited, QIAquick PCR Purification Kit (Qiagen).
10. Microcentrifuge ≥10,000 × *g* (13,000 rpm).

2.3 Insertion of the miR-302 Cluster into an Expression Vector

1. Expression vector (0.5 μg/μL), such as *pSpRNAi-RGFP* (*see* **Note 2**; refs. 23, 27) and *pLVX-AcGFP-N1* (Clontech Laboratories, Mountain View, CA). Any expression vector containing an either *MluI/PvuI* or *XhoI/BamHI* multiple cloning site for the insertion of the miR-302 cluster in the 5′-untranslated region (5′-UTR) or in-frame intron of an reporter gene (i.e., EGFP or RGFP) can be used here.

2. 10× restriction buffer, such as *MluI* and *PvuI* for digesting *pSpRNAi-RGFP* or *XhoI* and *BamH1* for digesting *pLVX-AcGFP-N1*.
3. Restriction enzymes, such as *MluI* and *PvuI* (for *pSpRNAi-RGFP*) or *XhoI* and *BamH1* (for *pLVX-AcGFP-N1*) in a stock concentration of 10 U/μL.
4. Digestion reaction mix: 13 μL of the miR-302 cluster, 2 μL of 10× digestion buffer, 4 μL of restriction enzymes (*MluI/PvuI* or *XhoI/BamHI*), and 1 μL of the expression vector; prepare the reaction mix right before use.
5. 100-bp cut-off purification filters, such as, but not limited, QIAquick PCR Purification Kit (Qiagen).
6. Microcentrifuge ≥10,000 × *g* (13,000 rpm).
7. 10× ligation buffer: 660 mM Tris–HCl (pH 7.5 at 20 °C), 50 mM $MgCl_2$, 50 mM dithioerythritol, and 10 mM ATP.
8. T4 DNA ligase (5 U/μL).
9. Ligation reaction mix: 25 μL of the digested miR-302 cluster and expression vector mix, 3 μL of 10× ligation buffer, and 2 μL of T4 ligase; prepare the reaction mix just before use.
10. Incubation chambers: 37, 75, 10, and 4 °C.
11. Luria-Bertani (LB) agar plates containing 50 mg/mL kanamycin for *pSpRNAi-RGFP* or 100 mg/mL ampicillin for *pLVX-AcGFP-N1* clone selection.
12. Low salt LB broth containing 50 mg/mL kanamycin for *pSpRNAi-RGFP* or 100 mg/mL ampicillin for *pLVX-AcGFP-N1* clone amplification.
13. Ready-to-use transformation competent *E. coli* cells, such as, but not limited, Z-Competent *E. coli*-DH5α Kit (Zymo Research, Irvine. CA).
14. Incubation shaker: 37 °C, >180 rpm vortex.
15. Plasmid extraction kit, such as, but not limited, QIAprep Spin Miniprep Kit (Qiagen).

2.4 Transfection or Electroporation

1. Electroporator, such as, but not limited, Neon Transfection System (Invitrogen, Carlsbad, CA) or Multiporator Electroporation System (Eppendorf, Hamburg, Germany).
2. Electroporation buffer (*see* **Note 3**).
3. Polysomal or liposomal reagents, such as, but not limited, FuGENE HD Transfection Reagent (Roche Diagnostics, Indianapolis, IN).
4. Target cells (>2000 cells).
5. Cell culture medium, depending on the cell type of interest.
6. 1× trypsin/EDTA solution.

2.5 Selection and Cultivation of miR-302-Positive mirPSCs

1. Feeder-free mirPSC medium: KnockOut DMEM/F-12 medium supplemented with 10% KnockOut serum replacement (Invitrogen), 1% MEM nonessential amino acids, 100 μM β-mercaptoethanol, 1 mM GlutaMax, 1 mM sodium pyruvate, 0.1 μM A83-01, 0.1 μM valproic acid (Stemgent, San Diego, CA), 10 ng/mL bFGF, 10 ng/mL FGF-4, 5 ng/mL LIF, and a mix of 50 IU/mL penicillin and 50 μg/mL streptomycin (*see* **Note 4**).
2. G418 (a final concentration ranged from 100 to 300 μg/mL for culturing *pSpRNAi-RGFP*-transfected cells) or puromycin (a final concentration ranged from 15 to 100 μg/mL for culturing *pLVX-AcGFP-N1*-transfected cells).
3. Incubator for cell culture: 37 °C, 5% CO_2.

3 Methods

3.1 Construction of the miR-302 Cluster

The double-stranded DNA of each individual miR-302 precursor is formed by annealing the sense strand of each miR-302 familial member to its respective antisense strand; for example, miR-302a-sense to miR-302a-antisense, miR-302b-sense to miR-302b-antisense, miR-302c-sense to miR-302c-antisense, and miR-302d-sense to miR-302d-antisense (*see* Table 1). Then, the double-stranded DNAs of all four miR-302 (a, b, c and d) precursors are separately cleaved by different restriction enzymes to generate various cohesive ends. Based on these cohesive ends, all four miR-302 precursors can be sequentially ligated into one familial cluster ready for coexpression. All synthetic strands of miR-302 members must be purified by polyacrylamide gel electrophoresis (PAGE) and stored at −20 °C.

1. Hybridization: Mix the synthetic sense and antisense strands of each miR-302 member (each 1 nmol) in 10 μL of autoclaved ddH_2O; add 10 μL of 2× hybridization buffer, mix and heat to 94 °C for 3 min, and then slowly cool to 65 °C in 30 min. Stop the reaction on ice.
2. Restriction enzyme digestion: Prepare one digestion reaction mix for each hybridized miR-302 member (a, b, c, and d, respectively), containing 4 μL of the hybridized DNA, 2 μL of 10× digestion buffer, 4 μL of restriction enzymes, and 10 μL of autoclaved ddH_2O. Use 4 μL of *BglII* for miR-302a cleavage, 2 μL of *BglII* and 2 μL of *NdeI* for miR-302b cleavage, 2 μL of *NdeI* and 2 μL of *XbaI* for miR-302c cleavage, and 4 μL of *XbaI* for miR-302d cleavage. Incubate the reaction at 37 °C for 4 h and then stop at 4 °C. Purify each of the digested miR-302 member (a, b, c, and d, respectively) using a 70-bp cut-off purification filter, following the manufacturer's protocol, and recover the DNA in 30 μL of autoclaved ddH_2O.

3. Cohesive end ligation: Combine all four miR-302 members and mix well. Prepare a ligation reaction mix, containing 24 μL of the miR-302 mixture, 3 μL of 10× ligation buffer, and 3 μL of T4 ligase, and incubate the reaction at 10 °C for 16 h and then stop at 4 °C. This forms the miR-302 familial cluster containing miR-302a, b, c, and d in a 5′ to 3′ sequential order. Purify the miR-302 cluster using a 100-bp cut-off purification filter and recover it in 30 μL of autoclaved ddH_2O.

3.2 Insertion of the miR-302 Cluster into an Expression Vector

Intronic miRNA can be expressed from the 5′-UTR, 3′-UTR or in-frame intron region of a gene; hence, any expression vector containing an insertion site in these regions can be used for miR-302 expression. For example, the *pSpRNAi-RGFP* plasmid vector [23, 27] possesses an *MluI/PvuI* insertion site in its in-frame intron, while the retroviral *pLVX-AcGFP-N1* vector (Clontech) contains a *XhoI/BamHI* cloning site in the 5′-UTR of its *AcGFP* gene. Both the vectors have been tested for successfully expressing the miR-302 cluster. However, due to the low stability of the highly structured miR-302 cluster, we have noticed that during the processes of vector amplification and extraction, the transformed *E. coli* competent cells cannot be stored at 4 °C or some of the hairpin pre-miRNA structures may be lost. For storage, the vector containing the miR-302 cluster is stable at 4 °C for up to 4 months and at −80 °C for over 2 years.

1. Restriction enzyme digestion: Mix 1 μL of the expression vector to 13 μL of the miR-302 cluster and prepare one digestion reaction mix containing the 14 μL mixture, 2 μL of 10× digestion buffer, and either 2 μL of *MluI* and 2 μL of *PvuI* (for *pSpRNAi-RGFP*) or 2 μL of *XhoI* and 2 μL of *BamH1* (for *pLVX-AcGFP-N1*). Incubate the reaction at 37 °C for 4 h and then 4 °C. Purify the digested reaction using a 100-bp cut-off purification filter and recover the DNAs in 30 μL of autoclaved ddH_2O.
2. Cohesive end ligation: Prepare a ligation reaction mix, containing 25 μL of the cleaved vector and miR-302 cluster mixture, 3 μL of 10× ligation buffer, and 2 μL of T4 ligase. Incubate the reaction at 10 °C for 16 h and then 4 °C. This forms the miR-302-expressing vector.
3. Vector selection: Add 5 μL of the miR-302-expressing vector to the ready-to-use transformation competent *E. coli*-DH5α cells, mix and incubate the mixture at 4 °C for 10 min, following the manufacturer's protocol. Next, pour and smear the mixture evenly onto an antibiotic-containing LB agar plate (50 mg/mL kanamycin for *pSpRNAi-RGFP* or 100 mg/mL ampicillin for *pLVX-AcGFP-N1*) and incubate the transformed *E. coli*-DH5α cells at 37 °C, overnight.

4. Vector amplification: Pick and transfer each single-cell colony, with a sterilized platinum loop or pipet tip, from the LB agar plate into 30 mL of antibiotic-containing LB broth (50 mg/mL kanamycin for *pSpRNAi-RGFP* or 100 mg/mL ampicillin for *pLVX-AcGFP-N1*), respectively. Further incubate the cell-containing LB broth on a shaker (>180 rpm) at 37 °C, overnight.
5. Vector extraction: Isolate and recover the amplified vector in 30 μL of autoclaved ddH_2O using a plasmid extraction mini-prep filter, following the manufacturer's protocol. To confirm the insertion of the miR-302 cluster, the isolated vector can be digested with either *MluI* and *PvuI* (for *pSpRNAi-RGFP*) or *XhoI* and *BamH1* (for *pLVX-AcGFP-N1*) to generate a ~350 base-pair DNA band on 2% agarose gel electrophoresis.

3.3 Transfection or Electroporation

To express the miR-302 cluster in the cells of interest, we recommend either electroporation or liposomal/polysomal transfection. Although the *pLVX-AcGFP-N1* vector can also be used for lentiviral production, this approach must be performed with extreme care due to the unknown function of miR-302 in vivo. For miR-302-induced iPSC generation, the cell types currently tested are human skin/hair-derived somatic cells, including melanocytes, keratinocytes and fibroblasts, and neural-like HEK-293 as well as several tumor/cancerous cell lines, such as human melanoma Colo-829, breast cancer MCF7, prostate cancer PC3, hepatocellular carcinoma HepG2, and embryonal teratocarcinoma Tera-2 cells. Notably, the reprogramming efficiency may vary in different cell types; for example, using electroporation, the average iPSC formation rates are >70% for HEK-293 cells, 15–20% for keratinocytes, 7–10% for melanocytes, <1–3% for adult fibroblasts, and <1% for all tested tumor/cancerous cells, respectively. The reprogramming efficiency in other cell types remains to be determined.

1. Electroporation: Add 2000–200,000 cells and 15–40 μg of the miR-302-expressing vector in 250 μL of electroporation buffer, mix well and place into a 400 μL cuvette with aluminum electrodes. Perform electroporation tests following the manufacturer's protocol (*see* **Note 3**). After electroporation, grow the cells in the feeder-free mirPSC medium at 37 °C under 5% CO_2.
2. Liposomal/Polysomal transfection (*see* **Note 5**): Grow cells to 50% confluency in a 100 mm culture dish and replace the cell culture medium by 9 mL of serum-free cell culture medium 4 h before transfection. For transfection preparation, add 15 μg of the miR-302-expressing vector into 1 mL of serum-free cell culture medium and mix well. Next, add 50 μL of FuGENE

HD reagent into the center of the vector-medium mixture and vortex for 10 s. Place the mixture at room temperature for 15 min (*see* **Note 6**). After the incubation, add the mixture drop-wise, covering the whole 100 mm culture dish and shake the culture dish back-and-forth and right-and-left several times to evenly distribute the mixture (*see* **Note 7**). Incubate the cells at 37 °C under 5% CO_2 for 12–18 h and then replace the medium with a feeder-free mirPSC medium. Continue to grow the transfected cells in the feeder-free mirPSC medium at 37 °C under 5% CO_2.

3.4 Selection and Cultivation of miR-302-Positive mirPSCs

Since the *pSpRNAi-RGFP* and *pLVX-AcGFP-N1* vectors contain an antibiotic-resistant gene against G418 and puromycin, respectively, the positive miR-302-transfected cells can be selected by using either G418 (for *pSpRNAi-RGFP*) or puromycin (for *pLVX-AcGFP-N1*). The positive miR-302-transfected cells also express either red fluorescent RGFP (*pSpRNAi-RGFP*) or green AcGFP (*pLVX-AcGFP-N1*) for color identification under a fluorescent microscope or cell sorting by a FACS flow cytometry machine. Both antibiotic selection and color identification/sorting ensure the purity of the miR-302-transfected cell population.

1. Antibiotic selection: When the transfected cells start to express red or green fluorescent GFP, add either G418 (100–300 μg/mL for *pSpRNAi-RGFP*-transfected cells) or puromycin (15–100 μg/mL for *pLVX-AcGFP-N1*-transfected cells) to the cell culture medium and mix well. The optimal antibiotic concentration for mirPSC selection may vary dependent on the original cell types. Incubate the cells at 37 °C under 5% CO_2 for 24–48 h and then replace the medium with the fresh feeder-free mirPSC medium. Continue to grow the cells in the feeder-free mirPSC medium at 37 °C under 5% CO_2 for 3 more days and observe the purity of the fluorescent cells. If there are still many non-transfected (non-fluorescent) cells, repeat the steps of this section using a higher antibiotic concentration until the fluorescent cell population is relatively pure.
2. mirPSC culturing and passaging: Under the above feeder-free culture condition, mirPSCs tend to form large embryoid body-like colonies. When a mirPSC colony contains more than 2000 cells, divide the colony into several small pieces with a scalpel and transfer the cells to a new collagen-coating culture dish in the feeder-free mirPSC medium. Incubate the cells at 37 °C under 5% CO_2 (*see* **Note 8**).

4 Notes

1. All synthetic oligonucleotides are purified by polyacrylamide gel electrophoresis (PAGE) to ensure their highest purity and sequence integrity.
2. The detailed method for constructing the *SpRNAi-RGFP* expression vector has been described in our previous publications [23, 27].
3. Electroporation buffer varies depending on your electroporation machine. Please follow the manufacturer's suggestions.
4. The addition of A83-01, a SMAD2 inhibitor, and valproic acid, a HDAC inhibitor, is optional, depending on the cell type of interest.
5. The protocol shown here is optimized for FuGENE HD (Roche). For other liposomal/polysomal reagents, a different protocol may be adopted. Please follow the manufacturer's protocols for this section if not using FuGENE HD. Also, the transfection volume is prepared for a 100 mm culture dish containing cells at 50% confluency (in 10 mL of cell culture medium). If a smaller volume is desired, please reduce the amount of all materials and reagents in proportional to the volume of cell culture medium.
6. Maximal 30 min at room temperature.
7. Do not swirl the cell culture dish to mix the mixture. This results in an uneven distribution of the transfection mixture.
8. When the mirPSC colony grows too big (>5000 cells), the cells in the center of the colony may undergo apoptosis, which causes whole colony differentiation or death. The apoptotic mirPSC colony cannot be recovered for further passaging. Even under the best cell culture condition, the mirPSCs can maximally be passaged up to 26 generations, based on the current studies [2, 3].

References

1. Lin SL, Chang D, Chang-Lin S, Lin CH, Wu DTS, Chen DT, Ying SY (2008) Mir-302 reprograms human skin cancer cells into a pluripotent ES-cell-like state. RNA 14:2115–2124
2. Lin SL, Chang D, Lin CH, Ying SY, Leu D, Wu DTS (2011) Regulation of somatic cell reprogramming through inducible mir-302 expression. Nucleic Acids Res 39:1054–1065
3. Lin SL, Chang D, Ying SY, Leu D, Wu DTS (2010) MicroRNA miR-302 inhibits the tumorigenecity of human pluripotent stem cells by coordinate suppression of CDK2 and CDK4/6 cell cycle pathways. Cancer Res 70:9473–9482
4. Li Y, Pei J, Xia H, Ke H, Wang H, Tao W (2003) Lats2, a putative tumor suppressor, inhibits G1/S transition. Oncogene 22:4398–4405
5. Ying SY, Lin SL (2004) Intron-derived microRNAs -- fine tuning of gene functions. Gene 342:25–28
6. Becker KA, Ghule PN, Therrien JA, Lian JB, Stein JL, van Wijnen AJ, Stein GS (2006) Self-renewal of human embryonic stem cells is supported by a shortened G1 cell cycle phase. J Cell Physiol 209:883–893

7. Hanna J, Saha K, Pando B, van Zon J, Lengner CJ, Creyghton MP, van Oudenaarden A, Jaenisch R (2009) Direct cell reprogramming is a stochastic process amenable to acceleration. Nature 462:595–601
8. Rowland BD, Bernards R, Peeper DS (2005) The KLF4 tumour suppressor is a transcriptional repressor of p53 that acts as a context-dependent oncogene. Nat Cell Biol 7:1074–1082
9. Jiang J, Chan YS, Loh YH, Cai J, Tong GQ, Lim CA, Robson P, Zhong S, Ng HH (2008) A core Klf circuitry regulates self-renewal of embryonic stem cells. Nat Cell Biol 10:353–360
10. Kim J, Chu J, Shen X, Wang J, Orkin SH (2008) An extended transcriptional network for pluripotency of embryonic stem cells. Cell 132:1049–1061
11. Nandan MO, Yang VW (2009) The role of Krüppel-like factors in the reprogramming of somatic cells to induced pluripotent stem cells. Histol Histopathol 24:1343–1355
12. Parry D, Bates S, Mann DJ, Peters G (1995) Lack of cyclin D–Cdk complexes in Rb-negative cells correlated with high levels of p16INK4/MTS1 tumor suppressor gene product. EMBO J 14:503–511
13. Quelle DE, Zindy F, Ashmun RA, Sherr CJ (1995) Alternative reading frames of the NK4a tumor suppressor gene encode two unrelated proteins capable of inducing cell cycle arrest. Cell 83:993–1000
14. Kamijo T, Zindy F, Roussel MF, Quelle DE, Downing JR, Ashmun RA, Grosveld G, Sherr CJ (1997) Tumor suppression at the mouse INK4a locus mediated by the alternative reading frame product p19ARF. Cell 91:649–659
15. Chan MF, van Amerongen R, Nijjar T, Cuppen E, Jones PA, Laird PW (2001) Reduced rates of gene loss, gene silencing, and gene mutation in Dnmt1-deficient embryonic stem cells. Mol Cell Biol 21:7587–7600
16. Banito A, Rashid ST, Acosta JC, Li S, Pereira CF, Geti I, Pinho S, Silva JC, Azuara V, Walsh M, Vallier L, Gil J (2009) Senescence impairs successful reprogramming to pluripotent stem cells. Genes Dev 23:2134–2139
17. Feng Q, Lu SJ, Klimanskaya I, Gomes I, Kim D, Chung Y, Honig GR, Kim KS, Lanza R (2010) Hemangioblastic derivatives from human induced pluripotent stem cells exhibit limited expansion and early senescence. Stem Cells 28:704–712
18. Li H, Collado M, Villasante A, Strati K, Ortega S, Cañamero M, Blasco MA, Serrano M (2009) The Ink4/Arf locus is a barrier for iPS cell reprogramming. Nature 460:1136–1139
19. Utikal J, Polo JM, Stadtfeld M, Maherali N, Kulalert W, Walsh RM, Khalil A, Rheinwald JG, Hochedlinger K (2009) Immortalization eliminates a roadblock during cellular reprogramming into iPS cells. Nature 460:1145–1148
20. Marión RM, Strati K, Li H, Murga M, Blanco R, Ortega S, Fernandez-Capetillo O, Serrano M, Blasco MA (2009) A p53-mediated DNA damage response limits reprogramming to ensure iPS cell genomic integrity. Nature 460:1149–1153
21. Won J, Yim J, Kim TK (2002) Sp1 and Sp3 recruit histone deacetylase to repress transcription of human telomerase reverse transcriptase (hTERT) promoter in normal human somatic cells. J Biol Chem 277(38):230–238
22. Zhu O, Liu C, Ge Z, Fang X, Zhang X, Straat K, Bjorkholm M, Xu D (2008) Lysine-specific demethylase 1 (LSD1) is required for the transcriptional repression of the telomerase reverse transcriptase (hTERT) gene. PLoS One 3:e1446
23. Lin SL, Chang D, DY W, Ying SY (2003) A novel RNA splicing-mediated gene silencing mechanism potential for genome evolution. Biochem Biophys Res Commun 310:754–760
24. Lin SL, Kim H, Ying SY (2008) Intron-mediated RNA interference and microRNA (miRNA). Front Biosci 13:2216–2230
25. Barroso-delJesus A, Romero-López C, Lucena-Aguilar G, Melen GJ, Sanchez L, Ligero G, Berzal-Herranz A, Menendez P (2008) Embryonic stem cell-specific miR302-367 cluster: human gene structure and functional characterization of its core promoter. Mol Cell Biol 28:6609–6619
26. Suh MR, Lee Y, Kim JY, Kim SK, Moon SH, Lee JY, Cha KY, Chung HM, Yoon HS, Moon SY, Kim VN, Kim KS (2004) Human embryonic stem cells express a unique set of microRNAs. Dev Biol 270:488–498
27. Lin SL, Ying SY (2006) Gene silencing in vitro and in vivo using intronic microRNAs. In: Ying SY (ed) MicroRNA protocols. Humana, Totowa, NJ, pp 295–312
28. Lin SL, Chang D, Ying SY (2005) Asymmetry of intronic pre-microRNA structures in functional RISC assembly. Gene 356:32–38
29. Danin-Kreiselman M, Lee CY, Chanfreau G (2003) RNAse III-mediated degradation of unspliced pre-mRNAs and lariat introns. Mol Cell 11:1279–1289
30. Yi R, Qin Y, Macara IG, Cullen BR (2003) Exportin-5 mediates the nuclear export of

pre-microRNAs and short hairpin RNAs. Genes Dev 17:3011–3016

31. Lund E, Guttinger S, Calado A, Dahlberg JE, Kutay U (2004) Nuclear export of microRNA precursors. Science 303:95–98
32. Zhang G, Taneja KL, Singer RH, Green MR (1994) Localization of pre-mRNA splicing in mammalian nuclei. Nature 372:809–812
33. Lewis BP, Green RE, Brenner SE (2003) Evidence for the widespread coupling of alternative splicing and nonsense-mediated mRNA decay in humans. Proc Natl Acad Sci U S A 100:189–192
34. Grimm D, Streetz KL, Jopling CL, Storm TA, Pandey K, Davis CR, Marion P, Salazar F, Kay MA (2006) Fatality in mice due to oversaturation of cellular microRNA/short hairpin RNA pathways. Nature 441:537–541

Chapter 23

The miR-302-Mediated Induction of Pluripotent Stem Cells (iPSC): Multiple Synergistic Reprogramming Mechanisms

Shao-Yao Ying, William Fang, and Shi-Lung Lin

Abstract

Pluripotency represents a unique feature of embryonic stem cells (ESCs). To generate ESC-like-induced pluripotent stem cells (iPSCs) derived from somatic cells, the cell genome needs to be reset and reprogrammed to express the ESC-specific transcriptome. Numerous studies have shown that genomic DNA demethylation is required for epigenetic reprogramming of somatic cell nuclei to form iPSCs; yet, the mechanism remains largely unclear. In ESCs, the reprogramming process goes through two critical stages: germline and zygotic demethylation, both of which erase genomic DNA methylation sites and hence allow for different gene expression patterns to be reset into a pluripotent state. Recently, miR-302, an ESC-specific microRNA (miRNA), was found to play an essential role in four aspects of this reprogramming mechanism—(1) initiating global genomic DNA demethylation, (2) activating ESC-specific gene expression, (3) inhibiting developmental signaling, and (4) preventing stem cell tumorigenicity. In this review, we will summarize miR-302 functions in all four reprogramming aspects and further discuss how these findings may improve the efficiency and safety of the current iPSC technology.

Key words miR-302, MicroRNA, Induced pluripotent stem cell, Epigenetic reprogramming, DNA demethylation, Pluripotency

Abbreviations

3′-UTRs	The 3′-untranslated regions
5hmC	5-Hysroxymethylcytosine
Ago 1–4	Argonaute proteins 1–4
AID	Activation-induced cytidine deaminase
AOF1/2 (LSD1/2 or KMD1/1B)	Flavin-containing amine oxidase domain-containing protein ½
BER	A base excision DNA repair
BMI-1	B Lymphoma mouse Moloney leukemia virus insertion region
BMP	Bone morphogenetic protein
cMyc	c-Myelocytomatosis oncogene
CXCR4	C-X-C Chemokine receptor type 4

Shao-Yao Ying (ed.), *MicroRNA Protocols*, Methods in Molecular Biology, vol. 1733,
https://doi.org/10.1007/978-1-4939-7601-0_23,

DAZAP2	DAZ-associated protein 2
DNMT1	DNA (Cytosine-5-)-methyltransferase 1
EIF2C	Eukaryotic translation initiation factor 2C
ESC	Embryonic stem cells
GCNF or NR6A1	Germ cell nuclear factor
H3K4me2/3	Methylation of histone 3 on lysine 4
HDAC2/4	Histone deacetylase 2 and 4
HDM2	E3 ubiquitin ligase for p53
iPSCs	Induced pluripotent stem cells
Klf4	Kruppel-like factor 4
LARP7 or PIP7S	La ribonucleoprotein domain family member 7 gene
LIN28	RNA-binding protein LIN-28
mdm2	P53 E3 ubiquitin protein ligase
MEPC1/2	Methyl-CpG binding 1 and 2
miR-302	MicroRNA-302
miRNA	MicroRNA
miRNAs	MicroRNAs
mirPS cells	miR-302-mediated pluripotent stem cells
NANOG	A transcription factor critically involved with self-renewal of undifferentiated embryonic stem cells
ncRNAs	Noncoding RNAs
NR2F2	Nuclear receptor subfamily 2, group F, member 2
Oct4	Octamer-binding transcription factor 4; a protein that is critically involved in the self-renewal of undifferentiated embryonic stem cells
PCAF	p300-CBP-associated factor
PGC	Primordial germ cells
pre-miRNA	Hairpin-like miRNA precursors
pri-miRNA	Primary miRNA precursors
RAS-MAPK	Ras-mitogen-activated protein kinase
RISC	RNA-induced silencing complexes
RNA pol II	Type-II RNA polymerases
SCNT	Somatic cell nuclear transfer
SCR	Somatic cell reprogramming
SLAIN1	SLAIN motif family, member 1
Sox2	SRY (sex determining region Y)-box 2
SSEA ¾	3-Mercaptopyruvate sulfurtransferase-3 or 4
Tcf3	Transcription factor 3
Tet	Tet methylcytosine dioxygenase 1 or 2
TGFβ-SMAD	Transforming growth factorβ-mothers against DPP homolog family members
TOB2	Protein Tob2; transducer of erbB-2 2
UTF1	Undifferentiated embryonic cell transcription factor 1

1 Introduction

Stem cells are responsible for generating new cells to maintain biological function; yet, once differentiated, a stem cell usually does not revert to an earlier developmental stage. The mechanism

underlying this one-way development is DNA methylation. During stem cell differentiation, methylation of the cell genome triggers various tissue-specific gene expression patterns and hence determines the final properties of the differentiated cells. As a result, methylation and subsequently events prevent the reversion of the differentiated cells and make fate alteration impossible. However, the population of stem cells in the body is limited, and stem cells can be damaged by numerous environmental and pathogenic factors, such as pollutants, toxic materials, free radicals, stress, microbial/viral infections, and various illnesses during the life span. When the pool of stem cells becomes depleted and/or exhausted, the body grows old. For this reason, rejuvenation is almost impossible because the reversal of ageing would require generating new stem cells. It is essential to unlock and revert the properties of differentiated somatic cells to those of a stem-cell-like state if rejuvenation is to be achieved. Thus, the mechanism of stem cell generation via DNA demethylation may hold the key to slowing or even reversing the ageing process.

The global demethylation of genomic DNA normally occurs in only two stages of development. One is during the migration of primordial germ cells (PGC) into embryonic gonads (that is, germline demethylation at approximately embryonic day E10.5 to E13.5) and the other in the 2–16-cell-stage zygote after fertilization (i.e., zygotic demethylation) [1–4]. The majority of parental imprints are erased and re-established in germline PGCs but preserved in post-fertilized zygotic cells [5, 6], this suggests that the mechanisms by which demethylation occurs in germline and zygotic cells are not identical. However, the differences between these two normally occurring demethylation processes remain largely unclear. We have discovered a novel reprogramming mechanism in induced pluripotent stem cells (iPSCs) and implicated a new kind of global DNA demethylation mechanism comparable to the naturally occurring ones [7–9]. This man-made reprogramming mechanism triggers massive erasure of genomic DNA methylation sites but preserves many parental imprints similar to those affected by zygotic demethylation [9, 10]. Due to the high preservation of parental imprints associated with this new reprogramming mechanism, certain heritable properties of cells such as epigenetic memory and immunogenic compatibility have been preserved in iPSCs [11–13].

Takahashi and Yamanaka first developed the method to generate iPSC in 2006 [14]. Using retroviral delivery of four defined transcription factors (Oct4, Sox2, Klf4, and c-Myc; called OSKM) in vitro, reprogramming of somatic fibroblasts to embryonic stem cell (ESC)-like iPSCs was successfully observed [14, 15]. Subsequently, Yu et al. developed another method using a different set of four defined factors, Oct4, Sox2, Nanog, and LIN28 (OSNL) [16]. The utilization of iPSCs not only addresses the ethical concerns of using human ESCs but also may provide a patient-friendly therapy when used in conjunction

with somatic cell nuclear transfer (SCNT) technologies. Due to these advantages, iPSC-based SCNT therapy had been used to treat sickle cell anemia in a transgenic mouse model [17]. Nevertheless, the mechanism underlying the four-factor-induced iPSC transformation is still elusive, and there remain several concerns. First, oncogenic c-Myc is required to boost the success rate of iPSC formation, and the success rate is less than 0.002% when c-Myc is omitted. Second, the iPSC population is heterogeneous due to the variable delivery efficiency of the four factors. Up to this date, the best stoichiometric combination of four factors for reprogramming has not been identified. Lastly, the combined effect of the four defined factors seems to maintain merely the intrinsic network of embryonic gene expression [18, 19]; whereas the effect that leads to a global cancellation of somatic gene expression patterns remains largely unknown. Therefore, the efficiency and safety of the four-factor-induced iPSCs is questionable.

The demethylation of genomic DNA is necessary for initiating epigenetic reprogramming of somatic cell nuclei to form pluripotent stem cells [10, 20–22]. Epigenetic reprogramming involves not only global cancellation of somatic gene methylation profiles but also activation of ESC-specific gene expression. In light of zygotic demethylation during early embryogenesis, we have learned that exclusion of DNA (cytosine-5-)-methyltransferase 1 (DNMT1) from zygotic nuclei causes passive demethylation of maternal DNA in 2–16-cell-stage embryos while paternal DNA is mainly demethylated by another undefined active mechanism before the first embryonic cleavage [3–6]. As DNMT1 functions to maintain inherited CpG methylation patterns by methylating the newly replicated DNA during the S-phase of the cell cycle, the deficiency of DNMT1 activity leads to passive global DNA demethylation in the daughter cells following early zygotic cell divisions [23–25]. Yet, in this scenario, none of the previously defined reprogramming factors (either OSKM or OSNL) is involved in this critical epigenetic mechanism of reprogramming. In fact, all these defined factors are expressed after zygotic demethylation, showing no direct correlation with the epigenetic reprogramming. Hence, the activation of the defined factors described above is the result, not the cause, of the global DNA demethylation. Conceivably, factor(s) other than these defined factors may account for the epigenetic reprogramming.

Our recent studies have revealed, for the first time, that a group of noncoding RNAs (ncRNAs) rather than proteins are responsible for initiating global DNA demethylation in human iPSCs [7–9]. These ncRNAs belong to an ESC-specific microRNA (miRNA) family, miR-302, which is expressed most abundantly in human ESCs and iPSCs but not in differentiated somatic cells [25–27]. Native miR-302 consists of four familial sense homologues (miR-302b, c, a, and d) and three distinct antisense members (miR-302b*, c*, and a*), all of which are transcribed together as a polycistronic RNA cluster along with another miRNA, miR-367 [25].

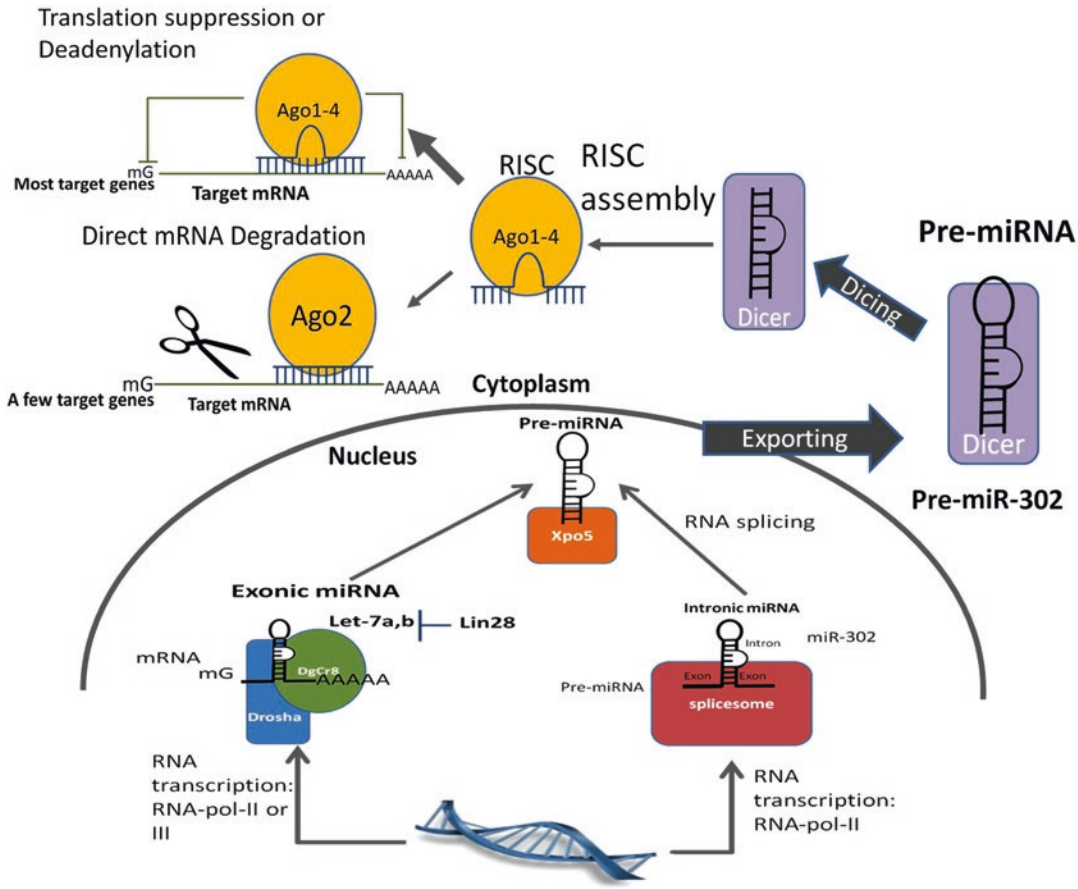

Fig. 1 The natural biogenesis mechanism of the intronic microRNA miR-302. MiR-302 is a natural intronic microRNA (miRNA), encoded in the intronic region of the *La ribonucleoprotein domain family member 7* (*LARP7* or *PIP7S*) gene. During miR-302 biogenesis, primary miRNA precursors (pri-miRNA) are first transcribed by type-II RNA polymerases (Pol-II) along with the *LARP7* gene transcripts and spliced by cellular spliceosomes to form hairpin-like miRNA precursors (pre-miRNA), which are then exported out of the nucleus by Exportin-5 (Xpo5) and further diced by Dicer-like RNaseIII endoribonucleases in cytoplasm to form mature miRNAs. Consequently, mature miR-302 molecules are assembled into RNA-induced silencing complexes (RISC) with argonaute proteins (Ago1–4) that elicit gene-specific silencing

It is noted that the elevation of miR-302 is highly coordinated with zygotic demethylation in 2–16-cell-stage embryos [25, 26]. Also, another study found that mouse iPSCs also express an elevated level of miR-291/294/295, members of the miR-302 family and the regular markers for mouse ESCs [26]. These findings suggest that the miR-302 family serves as a major reprogramming factor in both human and mouse pluripotent stem cells. However, miR-302 is a gene silencer, not an activator. As shown in Fig. 1, miR-302 functions to suppress the translation of its target genes through complementary binding and formation of RNA-induced silencing complexes (RISCs) in the 3′-untranslated regions

(3′-UTRs) of the targeted gene transcripts [28, 29]. Due to this unique function in gene silencing, miR-302 may play a role in suppressing DNMT1 to induce global DNA demethylation and hence initiate epigenetic reprogramming in both human ESCs and iPSCs.

2 Global Genomic DNA Demethylation

The somatic cell reprogramming (SCR), essential for generating iPSCs, begins with global genomic DNA demethylation. Subsequent molecular events were first reported by Lin et al. [7–9]. Furthermore, the concentration of cellular miR-302 determines the extent of genomic DNA demethylation in iPSCs [9, 10]. As shown in Fig. 2, miR-302 functions as a gene silencer to simultaneously downregulate several key epigenetic regulators, including DNMT1, lysine-specific histone demethylases 1 and 2 (AOF2/1, LSD1/2, or KDM1/1B), methyl-CpG-binding proteins 1 and 2 (MECP1/2), and histone deacetylase 2 and 4 (HDAC2/4). Concurrent silencing of these important epigenetic regulators induces global DNA demethylation, which is the first sign of the epigenetic reprogramming required for establishing stem cell pluripotency [7, 9, 10]. Given that DNA methylation often serves as a transcriptional block to repress ESC-specific gene expressions [20], miR-302 can thus induce global DNA demethylation to remove these transcriptional blocks and then re-activate a nearly full spectrum (>91–93%) of ESC-specific transcriptome expression, consequently resulting in reprogramming of somatic cells to iPSCs.

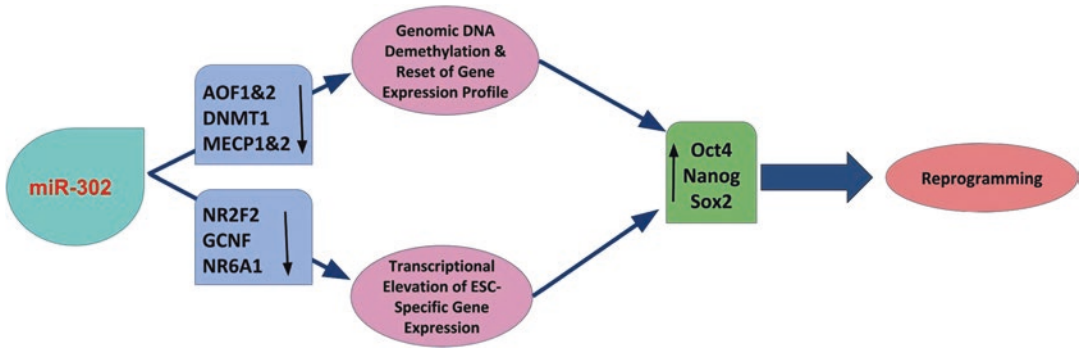

Fig. 2 A time-course comparison between zygotic and reprogramming-mediated global DNA demethylation and related ESC-specific gene activation. Both DNA demethylation events in ESCs and iPSCs occur most prevalently during the 2-to-16-cell stages when miR-302 reaches its maximal expression; however, ESCs exhibit another active demethylation mechanism which removes paternal DNA methylated sites at the one-cell stage. As a result of such global DNA demethylation, the entire cellular gene expression suite is reset and, hence, many ESC-specific genes are activated, such as Oct4, Sox2, UTF1, Nanog, Lin28, SSEA3, and SSEA4

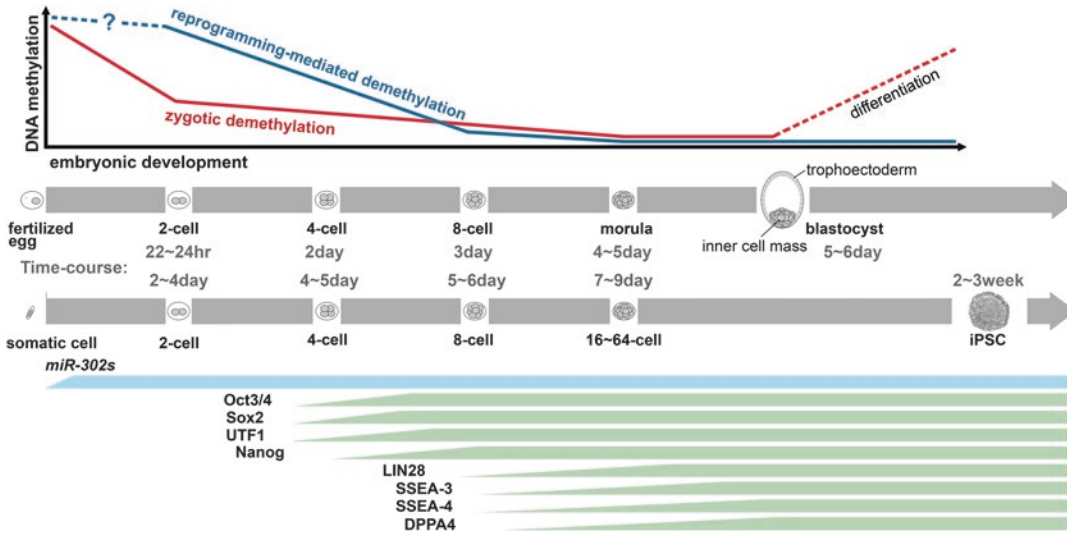

Fig. 3 The miR-302-induced epigenetic reprogramming mechanism in iPSCs. Global DNA demethylation is required for reprogramming the somatic cell genome to a pluripotent stem cell state. When the cellular miR-302 concentration is raised beyond 1.1–1.3-fold of the level found in human ESCs, miR-302 silences multiple key epigenetic regulators, such as AOF1/2, DNMT1, MBD2, and MECP1/2, to induce global DNA demethylation and, hence, allow the cell genome to be reset to a pluripotent state. On the other hand, miR-302 also silences several transcriptional repressors, such NR2F2 and GCNF/NR6A1, to promote *Oct4* and *Nanog* gene transcription, subsequently leading to a significant increase in ESC-specific gene expression

We have examined iPSC formation in a time-dependent fashion (Fig. 3) and found that the downregulation of AOF1/2, DNMT1, MECP1/2, and HDAC2 was most prominent in the first 3 days following miR-302 elevation, while the expression of Oct4, Nanog, and Sox2 was raised to a maximal level on the fifth day [7, 9]. During this time, miR-302-transfected cells rest for a few days and then 1–2 cell divisions were detected in 3–5 days. This cell-division-dependent process highly resembles the zygotic demethylation of a maternal genome, and it takes place in both parental genomes in iPSCs. Previous transgenic animal studies have shown that, in the absence of AOF1, germ cells fail to undergo de novo DNA methylation during oogenesis [30], while AOF2 deficiency leads to embryonic lethality due to a progressive loss of genomic DNA methylation and lack of cell differentiation [22]. Inhibition of either AOF1 or AOF2 also promotes methylation of histone three on lysine 4 (H3K4me2/3), a standard chromatin mark specific for ESCs and fully reprogrammed iPSCs [22, 30–32]. Therefore, silencing both AOF1 and 2 is sufficient to cause global DNA demethylation and chromatin modification required for reprogramming [9, 10]. Additionally, suppression of MECP1/2 may further enhance the AOF1/2-mediated DNA demethylation effect in iPSCs [7].

DNMT1 is another important downstream target of miR-302 because AOF2 is responsible for stabilizing DNMT1 [9, 22]. In iPSCs, miR-302 silences AOF2 to reduce DNMT1 activity [9]. Alternatively, the analytic results of a miRNA-target prediction program provided by the European Bioinformatics Institute EMBL-EBI [33] also suggest that miR-302 may directly inhibit DNMT1 translation. As a result, miR-302 strongly downregulates DNMT1 via both translational suppression and posttranslational degradation. During early embryogenesis, DNMT1 inherited from oocytes is excluded from zygotic nuclei by an undefined mechanism while zygotic DNMT1 expression is very limited due to miR-302 overexpression [4, 34–36]. The function of DNMT1 is to methylate the newly replicated DNA in daughter cells during cell divisions; hence, diminished DNMT1 activity leads to a passive global DNA demethylation in early zygotes [4, 23, 24]. Similarly, miR-302-mediated DNMT1 silencing in iPSCs also elicits passive global DNA demethylation comparable to the zygotic demethylation process. However, since passive demethylation is unable to remove the methylated sites originally left in a somatic genome before reprogramming, this reprogramming model will generate two hemi-methylated cells in every single-iPSC colony. To this, whether these hemi-methylated cells degrade via programmed cell death (apoptosis) during reprogramming or further demethylated by another active mechanism remains to be determined.

A number of active DNA demethylation mechanisms that play a role in reprogramming have been proposed. First, activation-induced cytidine deaminase (AID) initiates active DNA demethylation in early mouse embryos [3, 37, 38]. MiR-302 promotes AID expression in iPSCs [9]. AID is normally expressed in B cells, PGCs, oocytes, and early stage embryos and functions to remove 5-methylcytosine (5mC) by deaminating 5mC to thymine (T), subsequently resulting in T-guanine (G) mismatch base pairing [39, 40]. To correct such T-G mismatch pairing, a base excision DNA repair (BER) pathway was proposed for replacing the mismatched T with a C [41, 42]; yet, the enzyme required for this BER correction has not been identified in mammals. Another hypothesis involving excision repair of 5-hydroxymethylcytosine (5hmC) proposed that Tet familial enzymes, which first convert 5mC to 5hmC, can further convert it to C by spontaneous loss of its formaldehyde group [43] or by a currently undefined DNA repair system. The formation of 5hmC in ESCs and iPSCs enhances passive DNA demethylation since DNMT1 does not recognize 5hmC as a substrate for replication [44, 45]. Nevertheless, several recent studies did not support this hypothesis [45, 46]. First, Tet expression is subject to Oct4 regulation; thus, active DNA methylation cannot occur before Oct4 expression in iPSCs [45]. Second, Tet depletion has no effect on Oct4, Sox2 and Nanog expression in ESCs [45, 47]. Third, Tet depletion in mouse embryos only affects trophectoderm development and its downstream developmental signaling,

a stage much later than zygotic demethylation [46, 48]. Lastly, Tet 1 and 2 do not regulate global DNA demethylation in mouse ESCs and promordial germ cells in vitro [49]. Given these unresolved questions, the active mechanism by which genomic DNA is demethylated in iPSCs remains to be elucidated.

3 Activation of ESC-Specific Gene Expression

Emerging evidence has shown that global genomic DNA demethylation promotes Oct4–Nanog expression in early mouse embryos and mouse-human fused heterokaryons [37, 38]. Many ESC-specific genes are suppressed by DNA methylation in their promoter regions, particularly Oct4 and Nanog [20, 50, 51]. Our studies further showed that induction of iPSC formation requires a 1.1–1.3-fold higher miR-302 concentration than that found in human ESCs (>0.9–1.1 million copies per ESC) [9]. As shown in Fig. 2, such a high cellular miR-302 concentration induces both global DNA demethylation and coexpression of Oct4, Sox2, and Nanog (OSN) in iPSCs [9, 10]. The expression of Lin28 and many other ESC-specific markers was also observed 1–3 days following OSN coexpression. In human ESCs, induced miR-302 expression exceeding the normal level could increase Oct4-Nanog expression by twofold [52]. Further studies revealed that miR-302 may directly suppress the expression of nuclear receptor subfamily 2, group F, number 2 (NR2F2), a transcriptional repressor resposible for methylating Oct4 promoter, to enhance Oct4 expression [53]. Taken together, these findings strongly suggest that miR-302 triggers global DNA demethylation, and in turn, removes the transcriptional blocks on ESC-specific gene promoters, thus activating ESC-associated gene expressions.

Previous studies have also identified NR2F2 and germ cell nuclear factor (GCNF or NR6A1) as transcriptional repressors of Oct4 promoter [53, 54]. According to the online miRNA-targeting prediction programs, both NR2F2 and GCNF are direct targets of miR-302, which silences these transcriptional repressors to activate Oct4 expression in iPSCs. As OSN genes described above are involved in a feed-forward regulatory network essential for maintaining stem cell pluripotency [9, 19], the activation of Oct4 in conjunction with global DNA demethylation can thus lead to marked increases of all three OSN factors, resulting in the iPSC formation. When the miR-302 expression declines, NR2F2 and GCNF are inversely increased and thus again suppress Oct4 transcription; while corresponding levels of Sox2 and Nanog are also decreased in response to the Oct4 suppression. Interestingly, OSN had also been found to bind to the promoter regions of miR-302 and stimulate its expression [55]. Therefore, these factors are all part of a positive regulatory loop that induces a reciprocal expressions of miR-302 and

OSN for establishing and maintaining stem cell pluripotency (Fig. 2). To this, our recent studies suggest that global demethylation can be attributed to miR-302 function rather than OSN coexpression. Global demethylation in mouse embryos and mouse-human fused heterokaryons also results in elevated Oct4 and Nanog expressions [37, 38]. Further, the formation of miR-302-induced iPSC colonies takes a much shorter time (1–2 weeks) than that of iPSCs induced by either OSKM or OSNL (2–3 weeks) because OSN may need to function through miR-302-induced global demethylation to complete the full reprogramming process.

Our current understanding of miR-302-mediated reprogramming mechanisms may also provide significant insights into the mechanisms underlying the OSNL/OSKM-induced iPSC formation. Both OSNL/OSKM- and miR-302-induced reprogramming methods lead to a forced epigenetic reprogramming similar to zygotic demethylation but completely bypassing germline demethylation. When compared to SCNT-induced pluripotent stem cells, OSKM-induced iPSCs have shown less epigenomic and transcriptomic similarity to ESCs [11]. SCNT is a well-established technology for generating ESC-like pluripotent stem cells by introducing a somatic cell nucleus into the oocyte cytoplasm [56, 57]. Due to the use of oocytic ingredients, SCNT has also been proven to deliver a better reprogramming rate than OSKM-induced iPSC methods. Noteworthily, when the cytoplasm of miR-302-induced iPSCs was used in place of oocytes for SCNT, most (93%) of the hybrid cells were successfully reprogrammed to ESC-like pluripotent cells [9]. This finding resembles the previous SCNT results using oocyte cytoplasm, indicating that several oocytic miRNAs such as miR-200c and miR-371–373 may play a functional role similar to that of miR-302. Given that miR-302 is a cytoplasmic effector whereas the OSKM/OSNL are all nuclear proteins, it is obvious that miR-302 is responsible for initiating reprogramming through global DNA demethylation in the SCNT-induced pluripotent stem cells. Furthermore, miR-302 may also stimulate certain undefined factors similar to those in the oocyte cytoplasm to facilitate the completion of somatic cell reprogramming.

Thus far, the activation of ESC-specific genes and their mutual interactions have only been studied in mammalian ESCs [18, 19], not in iPSCs. iPSCs generated by different induction methods from various somatic cell types all share a highly similar epigenetic and transcriptomic profile such as that found in ESCs, implicating a similar global DNA demethylation mechanism involved in erasing and resetting different somatic epigenomes and transcriptomes into a unique ESC-like pluripotent state. In the time-course of iPSC formation (Fig. 2), we found that iPSCs take a longer time to reach the point of cell division compared to post-fertilized zygotes, probably due to the lack of germline elements such as paternal protamines and maternal oocyte transcripts. After the first cell division, the process of global

DNA demethylation is nearly identical between iPSCs and the 2–16-cell-stage zygotes up to the morula stage. During this period, the expression of OSN and undifferentiated embryonic cell transcription factor 1 (UTF1) is gradually elevated to a maximal level within 1–2 days, while Lin28 and many other ESC marker genes are expressed 1–3 days later than the OSN coexpression. Microarray analyses of genome-wide gene expression patterns in iPSCs and human ESCs have indicated that they share over 91% similarity [7, 9]. Further miRNA microarray analyses have also shown that many ESC-specific miRNAs are stimulated by miR-302 and likely function together with miR-302 to promote and/or maintain the pluripotency of iPSCs [7, 8]. As a result, the time-course of ESC-specific gene activation following miR-302 induction in iPSCs is summarized in Fig. 2.

4 Inhibition of Differentiation Signals

Like other miRNAs, miR-302 serves as a major gene silencer, but specifically in human ESCs and zygotes. Based on the analytic results of the online miRNA-target prediction programs TARGETSCAN [58] and PICTAR-VERT [59], the majority of miR302-targeted genes are transcripts of differentiation-associated genes and developmental signals, such as members of the RAS-MAPK, TGFβ-SMAD, activin/inhibitin and Nodal-Lefty signaling pathways, clearly indicating the significance of miR-302 in inhibiting stem cell differentiation [60, 61]. In vertebrates, specification of the anterior-posterior axis and left-right asymmetry depends on TGFβ-related signal proteins, such as activin/inhibin, Nodal, Lefty, and bone morphogenetic proteins (BMPs) [62]. Lefty1 and 2 are also involved in neural cell induction [63]. Additionally, Nodal signals are responsible for patterning the visceral endoderm through SMAD2-dependent pathways [64]. The silencing of Lefty1/2 by miR-302 leads to a significant delay in early ESC differentiation before germ layer specification [60], while miR-302 can also suppress BMP inhibitors TOB2, DAZAP2, and SLAIN1 to promote ESC pluripotency via preventing neural induction [61] (Figs. 4 and 5). Given that the silencing of either Lefty1/2 or BMP inhibitors results in the same inhibitory effect on neural differentiation, these findings strongly indicate that miR-302 can simultaneously target multiple parallel signaling pathways to block a specific cell lineage differentiation.

Other miRNAs are also involved in SCR. Using miRNA microarray analyses, we have observed that the expressions of other ESC-specific miRNAs, such as members of miR-17–92, miR-93, miR-367, miR-371–373, miR-374, and miR-520 families, are concurrently elevated in iPSCs [7–9]. MiR-302 shares over 440 target genes with these miRNAs, suggesting their potential roles in iPSC induction and/or formation. These conserved target genes include not only many members of the RAS-MAPK, TGFβ-SMAD, and Nodal-LEFTY

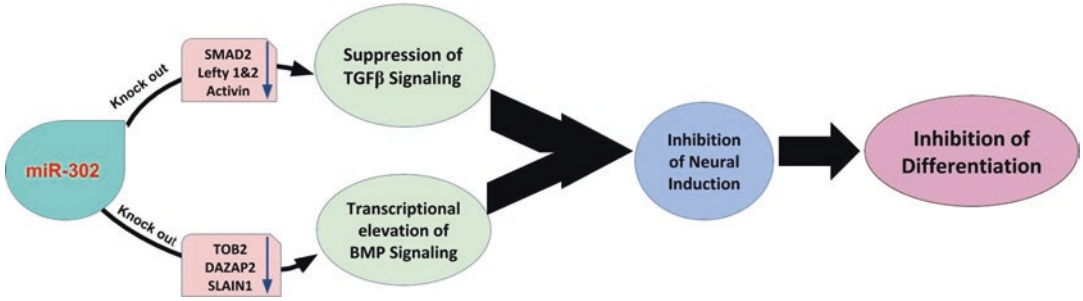

Fig. 4 The role of miR-302 in preventing stem cell differentiation. MiR-302 targets over 400 different developmental genes, including many members of the RAS-MAPK, TGFβ-SMAD, and Nodal-LEFTY signaling pathways. Current studies have shown that miR-302 silences SMAD2, Lefty1/2, and activin to inhibit certain TGFβ signaling pathways that are highly involved in early ESC differentiation. On the other hand, miR-302 suppresses several BMP inhibitors including TOB2, DAZAP2, and SLAIN1 to promote BMP signaling and thus prevent neural induction. Both downregulation of TGFβ signaling and upregulation of BMP signaling result in a strong blockade of stem cell differentiation

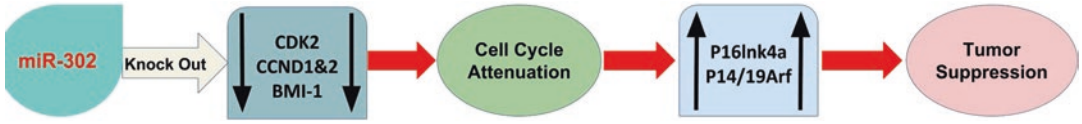

Fig. 5 The role of miR-302 in tumor suppression. MiR-302 functions as a tumor suppressor when its cellular concentration surpasses the level found in human ESCs. Occurring at nearly the same time as its reprogramming effect, miR-302 silences several key cell cycle regulators, such as CDK2, cyclin D1 and D2 (CCND1&2), and BMI-1, resulting in cell cycle attenuation at the G1-phase checkpoint. Also, silencing BMI-1 can further stimulate p16Ink4a and p14/p19Arf expression to prevent tumor formation in iPSCs

signaling pathways but also numerous transcription factors, oncogenes, and cell differentiation factors, such as E2F transcription factors, Myb-like transcription factors, HMG-box transcription factors, Sp3 transcription factors, NFkB activating protein genes, BMI-1 oncogene, Rho/Rac guanine nucleotide exchange factors, IGF receptors, protocadherins, CXCR4, EIF2C, PCAF, and many nuclear receptors and cell surface molecules. Given that these target genes are highly involved in embryonic development and/or cancer tumorigenicity, miR-302 may stimulate these homologous miRNAs to further enhance its function in preventing stem cell differentiation and tumor formation. Due to the complexity of these intricate miRNA-miRNA and miRNA-target interactions, understanding the full spectrum of these gene regulation mechanisms will be a great challenge.

MiR-302 plays a critical role in four aspects of iPSC formation, including the initiation of global DNA demethylation, activation of ESC-specific gene expression, inhibition of developmental signaling, and prevention of stem cell tumorigenicity. Because of these important functions, the present approach of miR-302-mediated iPSC

generation is simpler, safer, and more effective compared to the previous three-/four-factor induction methods. miR-302-induced pluripotent stem cells (mirPSCs) may be the best candidate for tumor-free iPSCs based on the current FDA regulations regarding concerns about tumor formation risk. Furthermore, the induced miR-302 expression can further stimulate the expression of native miR-302 and many other ESC-specific miRNAs, such as miR-92, miR-93, miR-200c, miR-367, miR-371, miR-372, miR-373, miR-374, as well as the miR-520 family. Analyses of the target genes among these miRNAs using [54] the miRBase::Sequences program [65] demonstrated that they share over 400 target genes with each other, suggesting that all these miRNAs may play critical roles in maintaining stem cell pluripotency and renewal, which in turn improve the efficiency and stability of somatic cell reprogramming to form iPSCs.

5 Prevention of Cancer Cell Tumorigenicity

The tendency to form tumors is one of the major problems inherent in stem cell therapy. Developing tumor-free ESCs/iPSCs is critical given of the current Food and Drug Administration (FDA) regulations regarding cancer stem cells. However, oncogenic transcription factors such as c-Myc and Klf4 are frequently used to boost the survival and proliferative rates of the OSK-induced iPSCs, increasing the probability of tumorigenicity in these cells. MiR-302 has been shown to induce reprogramming while preventing stem cell tumorigenicity [66]. Tumor-free pluripotency is one of the key advantages of miR-302-induced iPSCs compared to those induced by the three/four factors. However, the mechanism underlying stem cell tumorigenicity is still poorly understood. The fact that miR-302 functions in the prevention of tumors may lead to developing safer and more efficacious iPSCs or ESCs for stem cell therapy.

We have examined the mechanism by which tumor formation is prevented during normal embryogenesis. Usually, early zygotes before the morula stage (16–32 cell stage) exhibit a relatively slow cell cycle period (20–24 h/cycle), whereas cycling is faster in later blastocyst-derived ESCs (15–16 h/cycle) [67]. Embryonic cells in early zygotes possess two unique features of stemness: pluripotent differentiation into almost all cell types and unlimited self-renewal in the absence of tumor formation. Clearly, these two features are also important for the clinical applications of ESCs or iPSCs. Our study revealed for the first time that miR-302 is responsible for inhibiting human iPSC tumorigenicity through cosuppression of both cyclin E–CDK2 and cyclin D–CDK4/6 cell cycle pathways to block >70% of the G1-S phase transition [66] (Fig. 5). Furthermore, miR-302 also silences BMI-1, a cancer stem cell marker, to promote the expression of two tumor suppressor genes, p16Ink4a and

p14/p19Arf. p16Ink4a inhibits cyclin D-dependent CDK4/6 activity via phosphorylation of retinoblastoma protein Rb and subsequently prevents Rb from facilitating E2F-dependent transcription required for S phase entry [68, 69]. p14/p19Arf prevents HDM2, an Mdm2 p53-binding protein homolog, from binding to p53 and permits p53-dependent transcription responsible for G1 arrest or apoptosis [70]. Taken together, the combined effect of reducing G1-S cell cycle transition and increasing p16/p14(p19) expression results in an attenuated cell cycle period similar to that of 2–8-cell-stage embryonic cells in early zygotes (20–24 h/cycle). Hence, this longer period may reflect the time required for iPSCs to fully pass cell cycle checkpoint surveillance for preventing premature differentiation and tumor formation.

The mechanisms of miR-302-induced reprogramming and tumor suppression/prevention are parallel to each other. After induction of miR-302 expression, we found that both events occur almost simultaneously at a miR-302 concentration of 1.1–1.3-fold the level found in human ESCs, indicating that this specific concentration is the minimal threshold for reprogramming somatic cells to iPSCs while preventing iPSC tumorigenicity [7, 9, 10, 66]. Based on this understanding, many tumor-free iPSC lines have been successfully generated from human normal skin keratinocytes and melanocytes as well as cancerous melanoma Colo-829, prostate cancer PC3, breast cancer MCF7, hepatocellular carcinoma HepG2, and embryonal teratocarcinoma Tera-2 cell lines [7, 9, 66]. Notably, normal and cancerous somatic cells respond very differently to the miR-302-mediated tumor suppression effect. miR-302 overexpression often induces apoptosis in over 98% of the fast-growing cancer/tumor cells, while only a few remaining cells become iPSCs. On the contrary, the majority (>90%) of the miR-302-transfected normal cells can tolerate this inhibitory effect on cell proliferation [7, 66]. It is understandable that tumor/cancer cells may not survive with such relatively slow cell cycling due to their high metabolism and rapid substrate consumption. These results identify miR-302 as a tumor suppressor in iPSCs and hence imply a beneficial advantage in using miR-302 for not only reprogramming but also preventing cell tumorigenicity.

Furher, overexpression of miR-302 has been shown to suppress cancer progression, sensentize drug-/radio-resistant cells, and prevent metastasis, as a result of targeting gene exprssion in varuous pathways including epigenetic factors, cells cycle, and Akt and CXCR4 pathways [18, 22, 28–34, 71–88] (Table 1). These findings suggest that the SEC-specific, tumor-suppressing miR-302 can be explored for treating tumor progression and metastsis. The overall mehanisms by which miR-302 suppresses tumor formaiton still remain to be elucidated.

Table 1
Effects of miR-302 family on tumor cell growth, drug resistance, and metastasis

miR-302 family	Type of cancer	Induced by	Genes silenced	Biological manifestation	Reference
miR-302	Prostate PC3 cells	–	CDK2, CD4/6, G1-S arrest	Suppressed malignant progression	[7]
miR-302a	Prostate PC3 cells	–	Akt	Suppressed cell proliferation and tumor growth	[72]
miR-302	Tera-2 tumor	–	AOF, MRCP1-p66, MECP1/2, DNMT1, BMI-1	Global demethylation and suppressed tumor growth	[66]
miR-302	Stem cells	–	Akt1	Induced pluripotency and suppressed teratoma	[73]
miR-302a/b/c/d	MCF-7, MCF-7/MX cells	–	BCRP	Increased drug sensitivity	[74]
miR-302a	Breast cancer cell lines MDA-MB-231 and SKBR3	–	AKT1 and RAD52 (DNA repair)	Sensitizesd breast cancer cells to radiotherapy	[75]
miR-302a/b/c/d	Breast cancer	–	MEKK1 of ERK pathway	Reversing p-glycoprotein-mediated cheoresistance	[76]
miR-302 cluster	Melanoma and colon cancer	–	Epigenetic factors	Suppressed tumor progression and invasion	[77]
miR-302b	Glioms-initiating cells	–	CXCR4	Disruption of stem-like and tumorigenic properties	[78]
miR-302/367	Glioblatoma cells	–	PI3K/Akt and STAT3-	Abolished tumor and metastasis formation	[79]
miR-302	Hepatocellular carcinoma	–	Mcl-1 and DPYD	Enhanced drug sensitivity	[80]
miR-302b	Hepatocellular carcinoma	–	EGFR/Akt2/CCND1/CDK	Suppressed cell proliferation	[81]

(continued)

Table 1
(continued)

miR-302 family	Type of cancer	Induced by	Genes silenced	Biological manifestation	Reference
miR-302	Hepatocellular carcinoma	–	AOF2, H3K4 methylation, and c-Myc	Improved drug sensitivity	[82]
miR-302c	Gastric cancer	RACK1	IL8	Inhibited invasion/metastasis	[83]
miR-302	Endometrial cancer cells	–	Cyclin D1 and CDK1	Inhibited tumorigenicity	[84]
miR-302b	Malignant mesothelioma	ephrinA1	Mc1-1	Controlled cell proliferation and tumorsphere growth	[85]
miR-302/367	HeLa and SiHa cervical carcinoma	–	Cyclin D, CDK, AKT1	Blocked cell-cycle G2-M, and cell invasion	[86]
miR-302c	Chondrosarcoma	Binding of HA to CD44	PRP-1	Suppressed tumor growth	[87]
miR-302	Cancer stem cells	Binding of HA to CD44	AOF1/AOF2/DNMT1	Cancer progression	[88]

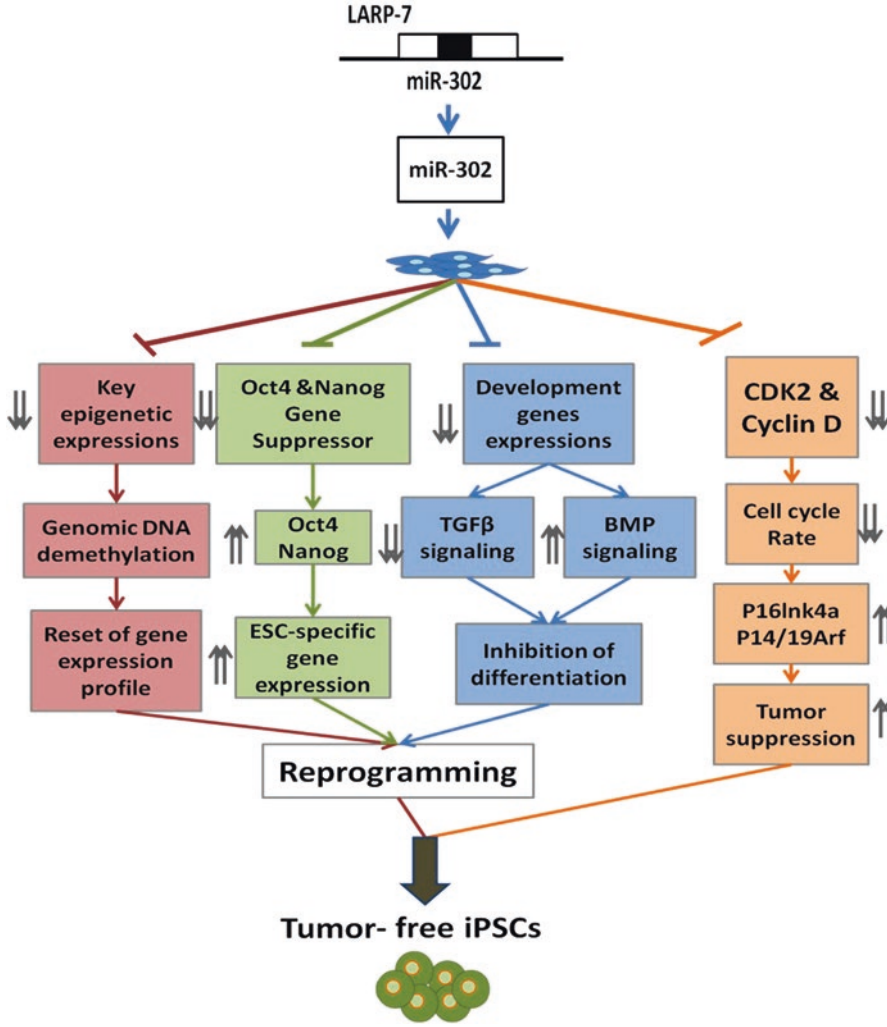

Fig. 6 Mechanistic summary underlying the induction of tumor-free pluripotent stem cells by miR-302: MiR-302, located at the intron region of the LAPR7 gene, is transcribed and processed, then functions to silence specific target genes. As a result, it induces four reprogramming effects: First, miR-302 suppresses key epigenetic gene expression, resulting in genome-wide DNA demethylation and consequently resetting different gene expression profiles into an ESC-like transcriptome state. Second, it also inhibits Oct4 & Nanog gene suppressor, leading to an increased expression of Oct4 and Nanog as well as other downstream ESC-specific gene expressions. Third, it further regulates the expression of certain developmental signaling genes, such as reducing TGFb signaling while elevating BMP expression, subsequently leading to an inhibitory effect on differentiation. Last, miR-302 concurrently knocks down both CDK2-cyclin E and CDK4/6-cyclin D pathways and hence blocks G1-S cell cycle transition as well as increases p16Ink4a and p14/19Arf expressions, all of which prevent tumor formation during reprogramming. These four mechanisms initiate and maintain the normal process of somatic cell reprogramming in order to form tumor-free iPSCs

6 Conclusion

The development of mirPSC-associated technologies holds great promises in discovering new therapies for regenerative medicine. Deciphering the mechanisms underlying mirPSC induction and prevention of stem cell tumorigenicity has led to the identification of new methods for improving the reprogramming efficiency and safety of iPSCs (Fig. 6). As a result, mirPSCs represent a new kind of tumor-free iPSCs capable of overcoming the two major problems in stem cell therapy: supply and safety. Compared to the previous three-/four-factor induction methods, these mirPSC-based technologies have prominent advantages in both reprogramming efficiency and safety. Moreover, miR-302 is a tumor suppressor in humans, whereas c-Myc, one of the four defined factors, is a well-known oncogene. In fact, it has been reported that the optimal reprogramming efficiency for miR-302 vs. the four-factor induction method is >10% vs. <1%, respectively, showing >10-fold improvement already [7, 9, 25].

References

1. Hajkova P, Erhardt S, Lane N, Haaf T, El-Maarri O, Reik W, Walter J, Surani MA (2002) Epigenetic reprogramming in mouse primordial germ cells. Mech Dev 117:15–23
2. Szabó PE, Mann JR (1999) Biallelic expression of imprinted genes in the mouse germ line: implications for erasure, establishment, and mechanisms of genomic imprinting. Genes Dev 9:1857–1868
3. Mayer W, Niveleau A, Walter J, Fundele R, Haaf T (2000) Demethylation of the zygotic paternal genome. Nature 403:501–502
4. Santos F, Hendrich B, Reik W, Dean W (2002) Dynamic reprogramming of DNA methylation in the early mouse embryo. Dev Biol 241:172–182
5. Stöger R, Kubicka P, Liu CG, Kafri T, Razin A, Cedar H, Barlow DP (1993) Maternal-specific methylation of the imprinted mouse Igf2r locus identifies the expressed locus as carrying the imprinting signal. Cell 73:61–71
6. Tremblay KD, Saam JR, Ingram RS, Tilghman SM, Bartolomei MS (1995) A paternal-specific methylation imprint marks the alleles of the mouse H19 gene. Nat Genet 9:407–413
7. Lin SL, Chang D, Chang-Lin S, Lin CH, Wu DTS, Chen DT, Ying SY (2008) Mir-302 reprograms human skin cancer cells into a pluripotent ES-cell-like state. RNA 14:2115–2124. PMID: 18755840. https://doi.org/10.1261/rna.1162708
8. Lin SL, Ying SY (2008) Role of mir-302 microRNA family in stem cell pluripotency and renewal. In: Ying SY (ed) Current perspectives in microRNAs. Springer, New York, pp 167–185
9. Lin SL, Chang D, Lin CH, Ying SY, Leu D, Wu DTS (2011) Regulation of somatic cell reprogramming through inducible mir-302 expression. Nucleic Acids Res 39:1054–1065
10. Lin SL (2011) Deciphering the mechanism behind induced pluripotent stem cell generation. Stem Cells 29:1645–1649
11. Kim K, Doi A, Wen B, Ng K, Zhao R, Cahan P, Kim J, Aryee MJ, Ji H, Ehrlich LI Yabuuchi A, Takeuchi A, Cunniff KC, Hongguang H, McKinney-Freeman S, Naveiras O, Yoon TJ, Irizarry RA, Jung N, Seita J, Hanna J, Murakami P, Jaenisch R, Weissleder R, Orkin SH, Weissman IL, Feinberg AP, Daley GQ (2010) Epigenetic memory in induced pluripotent stem cells. Nature 467:285–290
12. Zhao T, Zhang ZN, Rong Z, Xu Y (2011) Immunogenicity of induced pluripotent stem cells. Nature 474:212–215
13. Ohi Y, Qin H, Hong C, Blouin L, Polo JM, Guo T, Qi Z, Downey SL, Manos PD, Rossi DJ (2011) Incomplete DNA methylation underlies a transcriptional memory of somatic cells in human iPS cells. Nat Cell Biol 2011(13):541–549
14. Takahashi K, Yamanaka S (2006) Induction of pluripotent stem cells from mouse embryonic and adult fibroblast cultures by defined factors. Cell 126:663–676
15. Takahashi K, Tanabe K, Ohnuki M, Narita M, Ichisaka T, Tomoda K, Yamanaka S (2007) Induction of pluripotent stem cells from adult human fibroblasts by defined factors. Cell 131:861–872

16. Yu J, Vodyanik MA, Smuga-Otto K, Antosiewicz-Bourget J, Frane JL, Tian S, Nie J, Jonsdottir GA, Ruotti V, Stewart R, Slukvin II, Thomson JA (2007) Induced pluripotent stem cell lines derived from human somatic cells. Science 318:1917–1920
17. Hanna J, Wernig M, Markoulaki S, Sun CW, Meissner A, Cassady JP, Beard C, Brambrink T, Wu LC, Townes TM, Jaenisch R (2007) Treatment of sickle cell anemia mouse model with iPS cells generated from autologous skin. Science 318:1920–1923
18. Kim J, Chu J, Shen X, Wang J, Orkin SH (2008) An extended transcriptional network for pluripotency of embryonic stem cells. Cell 132:1049–1061
19. Young RA (2011) Control of the embryonic stem cell state. Cell 144:940–954
20. Simonsson S, Gurdon J (2004) DNA demethylation is necessary for the epigenetic reprogramming of somatic cell nuclei. Nat Cell Biol 6:984–990
21. Pick M, Stelzer Y, Bar-Nur O, Mayshar Y, Eden A, Benvenisty N (2009) Clone- and gene-specific aberrations of parental imprinting in human induced pluripotent stem cells. Stem Cells 27:2686–2690
22. Wang J, Hevi S, Kurash JK, Lei H, Gay F, Bajko J, Su H, Sun W, Chang H, Xu G, Gaudet F, Li E, Chen T (2009) The lysine demethylase LSD1 (KDM1) is required for maintenance of global DNA methylation. Nat Genet 41:125–129
23. Monk M, Boubelik M, Lehnert S (1987) Temporal and regional changes in DNA methylation in the embryonic, extraembryonic and germ cell lineages during mouse embryo development. Development 99:371–382
24. Hirasawa R, Chiba H, Kaneda M, Tajima S, Li E, Jaenisch R, Sasaki H (2008) Maternal and zygotic Dnmt1 are necessary and sufficient for the maintenance of DNA methylation imprints during preimplantation development. Genes Dev 22:1607–1616
25. Suh MR, Lee Y, Kim JY, Kim SK, Moon SH, Lee JY, Cha KY, Chung HM, Yoon HS, Moon SY, Kim VN, Kim KS (2004) Human embryonic stem cells express a unique set of microRNAs. Dev Biol 270:488–498
26. Barroso-delJesus A, Romero-López C, Lucena-Aguilar G, Melen GJ, Sanchez L, Ligero G, Berzal-Herranz A, Menendez P (2008) Embryonic stem cell-specific miR302-367 cluster: human gene structure and functional characterization of its core promoter. Mol Cell Biol 28:6609–6619
27. Wilson KD, Venkatasubrahmanyam S, Jia F, Sun N, Butte AJ, Wu JC (2009) MicroRNA profiling of human-induced pluripotent stem cells. Stem Cells Dev 18:749–758
28. Ying SY, Lin SL (2004) Intron-derived microRNAs -- fine tuning of gene functions. Gene 342:25–28
29. Lin SL, Kim H, Ying SY (2008) Intron-mediated RNA interference and microRNA (miRNA). Front Biosci 13:2216–2230
30. Ciccone DN, Su H, Hevi S, Gay F, Lei H, Bajko J, Xu G, Li E, Chen T (2009) KDM1B is a histone H3K4 demethylase required to establish maternal genomic imprints. Nature 461:415–418
31. Lee MG, Wynder C, Cooch N, Shiekhattar R (2005) An essential role for CoREST in nucleosomal histone 3 lysine 4 demethylation. Nature 437:432–435
32. Lee MG, Wynder C, Schmidt DM, McCafferty DG, Shiekhattar R (2006) Histone H3 lysine 4 demethylation is a target of nonselective antidepressive medications. Chem Biol 13:563–567
33. The European Bioinformatics Institute EMBL-EBI. http://www.ebi.ac.uk/enright-srv/microcosm/cgi-bin/targets/v5/detail_view.pl?transcript_id=ENST00000359526
34. Carlson LL, Page AW, Bestor TH (1992) Properties and localization of DNA methyltransferase in preimplantation mouse embryos: implications for genomic imprinting. Genes Dev 6:2536–2541
35. Bestor TH (2000) The DNA methyltransferases of mammals. Hum Mol Genet 9:2395–2340
36. Vassena R, Dee Schramm R, Latham KE (2005) Species-dependent expression patterns of DNA methyltransferase genes in mammalian oocytes and preimplantation embryos. Mol Reprod Dev 72:430–436
37. Bhutani N, Brady JJ, Damian M, Sacco A, Corbel SY, Blau HM (2010) Reprogramming towards pluripotency requires AID-dependent DNA demethylation. Nature 463:1042–1047
38. Popp C, Dean W, Feng S, Cokus SJ, Andrews S, Pellegrini M, Jacobsen SE, Reik W (2010) Genome-wide erasure of DNA methylation in mouse primordial germ cells is affected by AID deficiency. Nature 463:1101–1105
39. Conticello SG, Langlois MA, Yang Z, Neuberger MS (2007) DNA deamination in immunity: AID in the context of its APOBEC relatives. Adv Immunol 94:37–73
40. Morgan HD, Dean W, Coker HA, Reik W, Petersen-Mahrt SK (2004) Activation-induced cytidine deaminase deaminates 5-methylcytosine in DNA and is expressed in pluripotent tissues: implications for epigenetic reprogramming. J Biol Chem 279:52353–52360

41. Morgan HD, Santos F, Green K, Dean W, Reik W (2005) Epigenetic reprogramming in mammals. Hum Mol Genet 1:R47–R58
42. Rai K, Huggins IJ, James SR, Karpf AR, Jones DA, Cairns BR (2008) DNA demethylation in zebrafish involves the coupling of a deaminase, a glycosylase, and gadd45. Cell 135:1201–1212
43. Privat E, Sowers LC (1996) Photochemical deamination and demethylation of 5-methylcytosine. Chem Res Toxicol 9:745–750
44. Valinluck V, Sowers LC (2007) Endogenous cytosine damage products alter the site selectivity of human DNA maintenance methyltransferase DNMT1. Cancer Res 67:946–950
45. Koh KP, Yabuuchi A, Rao S, Huang Y, Cunniff K, Nardone J, Laiho A, Tahiliani M, Sommer CA, Mostoslavsky G, Lahesmaa R, Orkin SH, Rodig SJ, Daley GQ, Rao A (2011) Tet1 and tet2 regulate 5-hydroxymethylcytosine production and cell lineage specification in mouse embryonic stem cells. Cell Stem Cell 8:200–213
46. Ito S, D'Alessio AC, Taranova OV, Hong K, Sowers LC, Zhang Y (2010) Role of Tet proteins in 5mC to 5hmC conversion, ES-cell self-renewal and inner cell mass specification. Nature 466:1129–1133
47. Dawlaty MM, Ganz K, Powell BE, Hu YC, Markoulaki S, Cheng AW, Gao Q, Kim J, Choi SW, Page DC, Jaenisch R (2011) Tet1 is dispensable for maintaining pluripotency and its loss is compatible with embryonic and postnatal development. Cell Stem Cell 9:166–175
48. Dawlaty MM, Breiling A, Le T, Raddatz G, Barrasa MI, Cheng AW, Gao Q, Powell BE, Li Z, Xu M, Faull KF, Lyko F, Jaenisch R (2013) Combined deficiency of Tet1 and Tet2 causes epigenetic abnormalities but is compatible with postnatal development. Dev Cell 24:310–323
49. Vincent JJ, Huang Y, Chen PY, Feng S, Calvopiña JH, Nee K, Lee SA, Le T, Yoon AJ, Faull K, Fan G, Rao A, Jacobsen SE, Pellegrini M, Clark AT (2013) Stage-specific roles for tet1 and tet2 in DNA demethylation in primordial germ cells. Cell Stem Cell 12:470–478
50. Han DW, Do JT, Gentile L, Stehling M, Lee HT, Schöler HR (2008) Pluripotential reprogramming of the somatic genome in hybrid cells occurs with the first cell cycle. Stem Cells 26:445–454
51. Fouse SD, Shen Y, Pellegrini M, Cole S, Meissner A, Van Neste L, Jaenisch R, Fan G (2008) Promoter CpG methylation contributes to ES cell gene regulation in parallel with Oct4/Nanog, PcG complex, and histone H3 K4/K27 trimethylation. Cell Stem Cell 2:160–169
52. Rosa A, Spagnoli FM, Brivanlou AH (2009) The miR-430/427/302 family controls mesendodermal fate specification via species-specific target selection. Dev Cell 16:517–527
53. Rosa A, Brivanlou AH (2011) A regulatory circuitry comprised of miR-302 and the transcription factors OCT4 and NR2F2 regulates human embryonic stem cell differentiation. EMBO J 30:237–248
54. Fuhrmann G, Chung AC, Jackson KJ, Hummelke G, Baniahmad A, Sutter J, Sylvester I, Schöler HR, Cooney AJ (2001) Mouse germline restriction of Oct4 expression by germ cell nuclear factor. Dev Cell 1:377–387
55. Marson A, Levine SS, Cole MF, Frampton GM, Brambrink T, Johnstone S, Guenther MG, Johnston WK, Wernig M, Newman J, Calabrese JM, Dennis LM, Volkert TL, Gupta S, Love J, Hannett N, Sharp PA, Bartel DP, Jaenisch R, Young RA (2008) Connecting microRNA genes to the core transcriptional regulatory circuitry of embryonic stem cells. Cell 134:521–533
56. Wilmut I, Schnieke AE, McWhir J, Kind AJ, Campbell KH (1997) Viable offspring derived from fetal and adult mammalian cells. Nature 385:810–813
57. Wakayama T, Perry AC, Zuccotti M, Johnson KR, Yanagimachi R (1998) Full-term development of mice from enucleated oocytes injected with cumulus cell nuclei. Nature 394:369–374
58. TARGETSCAN. http://www.targetscan.org/
59. PICTAR-VERT. http://pictar.mdc-berlin.de/
60. Barroso-delJesus A, Lucena-Aguilar G, Sanchez L, Ligero G, Gutierrez-Aranda I, Menendez P (2011) The nodal inhibitor lefty is negatively modulated by the microRNA miR-302 in human embryonic stem cells. FASEB J 25:1497–1508
61. Lipchina I, Elkabetz Y, Hafner M, Sheridan R, Mihailovic A, Tuschl T, Sander C, Studer L, Betel D (2011) Genome-wide identification of microRNA targets in human ES cells reveals a role for miR-302 in modulating BMP response. Genes Dev 25:2173–2186
62. Constam DB, Robertson EJ (2000) SPC4/PACE4 regulates a TGFbeta signaling network during axis formation. Genes Dev 14:1146–1155
63. Meno C, Ito Y, Saijoh Y, Matsuda Y, Tashiro K, Kuhara S, Hamada H (1997) Two closely-related left-right asymmetrically expressed genes, lefty-1 and lefty-2: their distinct expression domains, chromosomal linkage and direct neuralizing activity in Xenopus embryos. Genes Cells 2:513–524
64. Brennan J, Lu CC, Norris DP, Rodriguez TA, Beddington RS, Robertson EJ (2001) Nodal signalling in the epiblast patterns the early mouse embryo. Nature 411:965–969
65. miRBase::Sequences program. http://microrna.sanger.ac.uk/
66. Lin SL, Chang D, Ying SY, Leu D, Wu DTS (2010) MicroRNA miR-302 inhibits the

tumorigenecity of human pluripotent stem cells by coordinate suppression of CDK2 and CDK4/6 cell cycle pathways. Cancer Res 70:9473–9482

67. Becker KA, Ghule PN, Therrien JA, Lian JB, Stein JL, van Wijnen AJ, Stein GS (2006) Self-renewal of human embryonic stem cells is supported by a shortened G1 cell cycle phase. J Cell Physiol 209:883–893
68. Parry D, Bates S, Mann DJ, Peters G (1995) Lack of cyclin D–Cdk complexes in Rb-negative cells correlated with high levels of p16INK4/MTS1 tumor suppressor gene product. EMBO J 14:503–511
69. Quelle DE, Zindy F, Ashmun RA, Sherr CJ (1995) Alternative reading frames of the NK4a tumor suppressor gene encode two unrelated proteins capable of inducing cell cycle arrest. Cell 83:993–1000
70. Kamijo T, Zindy F, Roussel MF, Quelle DE, Downing JR, Ashmun RA, Grosveld G, Sherr CJ (1997) Tumor suppression at the mouse INK4a locus mediated by the alternative reading frame product p19ARF. Cell 91:649–659
71. Li Z, Yang CS, Nakashima K, Rana TM (2011) Small RNA-mediated regulation of iPS cell generation. EMBO J 30:823–834
72. Zhang GM, Bao CY, Wan FN, Cao DL, Qin XJ, Zhang HL, Zhu Y, Dai B, Shi GH, Ye DW (2015) MicroRNA-302a suppresses tumor cell proliferation by inhibiting AKT in prostate cancer. PLoS One 10:e0124410. https://doi.org/10.1371/journal.pone.0124410
73. Li HL, Wei JF, Fan LY, Wang SH, Zhu L, Li TP, Lin G, Sun Y, Sun ZJ, Ding J, Liang XL, Li J, Han Q, Zhao RC. (2016) miR-302 regulates pluripotency, teratoma formation and differentiation in stem cells via an AKT1/OCT4-dependent manner. Cell Death Dis. doi: https://doi.org/10.1038/cddis.2015.383
74. Wang Y, Zhao L, Xiao Q, Jiang L, He M, Bai X, Ma M, Jiao X, Wei M (2016) miR-302a/b/c/d cooperatively inhibit BCRP expression to increase drug sensitivity in breast cancer cells. Gynecol Oncol 141:592–601. PMID: 26644266
75. Liang Z, Ahn J, Guo D, Votaw JR, Shim H (2013) MicroRNA-302 replacement therapy sensitizes breast cancer cells to ionizing radiation. Pharm Res 30:1008–1016
76. Zhao L, Wang Y, Jiang L, He M, Bai X, Yu L, Wei M (2016) MiR-302a/b/c/d cooperatively sensitizes breast cancer cells to adriamycin via suppressing P-glycoprotein(P-gp) by targeting MAP/ERK kinase kinase 1 (MEKK1). J Exp Clin Cancer Res 35:25. https://doi.org/10.1186/s13046-016-0300-8
77. Maadi H, Moshtaghian A, Taha MF, Mowla SJ, Kazeroonian A, Haass NK, Javeri A (2016) Multimodal tumor suppression by miR-302 cluster in melanoma and colon cancer. Int J Biochem Cell Biol 81(Pt A):121–132
78. Fareh M, Turchi L, Virolle V, Debruyne D, Almairac F, de-la-Forest Divonne S, Paquis P, Preynat-Seauve O, Krause KH, Chneiweiss H, Virolle T (2012) The miR 302-367 cluster drastically affects self-renewal and infiltration properties of glioma-initiating cells through CXCR4 repression and consequent disruption of the SHH-GLI-NANOG network. Cell Death Differ 19:232–244
79. Yang CM, Chiba T, Brill B, Delis N, von Manstein V, Vafaizadeh V, Oellerich T, Groner B (2015) Expression of the miR-302/367 cluster in glioblastoma cells suppresses tumorigenic gene expression patterns and abolishes transformation related phenotypes. Int J Cancer 137:2296–2309
80. Cai D, He K, Chang S, Tong D, Huang C (2015) MicroRNA-302b enhances the sensitivity of hepatocellular carcinoma cell lines to 5-FU via targeting Mcl-1 and DPYD. Int J Mol Sci 16:23668. https://doi.org/10.3390/ijms161023668
81. Wang L, Yao J, Shi X, Hu L, Li Z, Song T, Huang C (2013) MicroRNA-302b suppresses cell proliferation by targeting EGFR in human hepatocellular carcinoma SMMC-7721 cells. BMC Cancer 13. https://doi.org/10.1186/1471-2407-13-448
82. Koga C, Kobayashi S, Nagano H, Tomimaru Y, Hama N, Wada H, Kawamoto K, Eguchi H, Konno M, Ishii H, Umeshita K, Doki Y, Mori M (2014) Reprogramming using microRNA-302 improves drug sensitivity in hepatocellular carcinoma cells. Ann Surg Oncol 21(Suppl 4):S591–S600
83. Chen L, Min L, Wang X, Zhao J, Chen H, Qin J, Chen W, Shen Z, Tang Z, Gan Q, Ruan Y, Sun Y, Qin X, Gu J (2015) Loss of RACK1 promotes metastasis of gastric cancer by inducing a miR-302c/IL8 signaling loop. Cancer Res 75:3832–3841
84. Yan GJ, Yu F, Wang B, Zhou HJ, Ge QY, Su J, Hu YL, Sun HX, Ding LJ (2014) MicroRNA miR-302 inhibits the tumorigenicity of endometrial cancer cells by suppression of Cyclin D1 and CDK1. Cancer Lett 345:39–47
85. Khodayari N, Mohammed KA, Lee H, Kaye F, Nasreen N (2016) MicroRNA-302b targets Mcl-1 and inhibits cell proliferation and induces apoptosis in malignant pleural mesothelioma cells. Am J Cancer Res 6:1996–2009
86. Cai N, Wang YD, Zheng PS (2013) The microRNA-302-367 cluster suppresses the proliferation of cervical carcinoma cells through the novel target AKT1. RNA 19:85–95
87. Galoian K, Qureshi A, D'Ippolito G, Schiller PC, Molinari M, Johnstone AL, Brothers SP, Paz AC, Temple HT (2015) Epigenetic regulation of

embryonic stem cell marker miR302C in human chondrosarcoma as determinant of antiproliferative activity of proline-rich polypeptide 1. Int J Oncol 47:465–472

88. Bourguignon LY, Wong G, Earle C, Chen L (2012) Hyaluronan-CD44v3 interaction with Oct4-Sox2-Nanog promotes miR-302 expression leading to self-renewal, clonal formation, and cisplatin resistance in cancer stem cells from head and neck squamous cell carcinoma. J Biol Chem 287:32800–32824

Chapter 24

Identification and Isolation of Novel Sugar-Like RNA Protecting Materials: Glycylglycerins from Pluripotent Stem Cells

Shi-Lung Lin

Abstract

Pluripotent stem cells are a resourceful treasure box for regenerative medicine. They contain a large variety of novel materials useful for designing and developing new medicines and therapies directed against many aging-associated degenerative disorders, including Alzheimer's disease, Parkinson's disease, stroke, diabetes, osteoporosis, and cancers. Currently, identification of these novel stem cell-specific materials is one of major breakthroughs in the field of stem cell research. Particularly, since the discovery of induced pluripotent stem cells (iPSC) in year 2006, the methods of iPSC derivation further provide an unlimited resource for screening, isolating, and even producing theses novel stem cell-specific materials in vitro. Using iPSCs, we can now prepare high quality and quantity of pure stem cell-specific agents for testing their therapeutic functions in treating various illnesses. These newly found stem cell-specific agents are divided into four major categories, including proteins, saccharides, nucleic acids, and small molecules (chemicals). In this article, we herein disclose one of the methodologies for isolating and purifying glycylglycerins—a group of glycylated sugar alcohols that protect hairpin-like microRNA precursors (pre-miRNA) and some of tRNAs in pluripotent stem cells. In view of such a unique RNA-protecting feature, glycylglycerins may be used to preserve and deliver functional small RNAs, such as pre-miRNAs and small interfering RNAs (siRNA), into human cells for eliciting their specific RNA interference (RNAi) effects, which may greatly advance the use of RNAi technology for treating human diseases.

Key words Induced pluripotent stem cell (iPSC), MicroRNA (miRNA), RNA interference (RNAi), Glycylglycerin

1 Introduction

RNA is known to be a highly degradable material in nature. Due to this instability problem, RNA interference (RNAi), a Nobel Prize winning technology in year 2006, is still not applicable to any disease treatment in vivo yet. Hence, discovery of a novel RNA-protecting agent may greatly advance the use of RNAi for developing new medicines and therapies directed against a variety of human diseases. To fulfill this goal, we had devised a method to reprogram human somatic cells into tumor-risk-free induced pluripotent stem

Shao-Yao Ying (ed.), *MicroRNA Protocols*, Methods in Molecular Biology, vol. 1733,
https://doi.org/10.1007/978-1-4939-7601-0_24,

cells (iPSCs) [1–3] and then used it to generate a large number of iPSCs, which were further served as a unlimited source for screening, identifying, and isolating novel stem cell-specific materials from the iPSC lysate. As a result, we had discovered and purified a new group of world's first found RNA-protecting agents—glycylglycerins—in human iPSCs [4]. The same kind of glycylglycerins can also be found in human embryonic stem cells (ESCs) and early blastocyst-stage mouse embryos, indicating that these sugar-like glycylglycerin molecules are likely responsible for preserving ESC-specific RNAs in particular, microRNAs (miRNAs) and their precursors in pluripotent stem cells [4].

Glycylglycerins are a kind of glycylated sugar alcohols modified by a novel reaction called "glycylation." By definition, glycylation replaces the hydroxyl (HO-) groups of a sugar or sugar alcohol with glycine's glycyl (NH_2CH_2COO-) groups and thus results in the formation of an ether (R-O-R) linkage between each OH-removed carbon of the sugar/sugar alcohol and the glycyl group. This reaction involves a process of molecular condensation via dehydration. As shown in Fig. 1a, b, the majority of these glycylated sugar alcohols in iPSC lysate are glycylated glycerins (called glycylglycerins or glycylglycerols), including three major kinds of products: one is 1-, or 2-, or 3-monoglycylglycerin (MGG), another is 1,2-, or 2,3-, or 1,3-diglycylglycerin (DGG), and the other is 1,2,3-triglycylglycerin (TGG) [4]. Notably, MGG and DGG can further form ring-like structures similar to the five-member or six-member ring conformations of fructose and glucose. Also, glycylation can be a partial or completed reaction, resulting in MGG and DGG as partially glycylated products and TGG as a completely glycylated molecule. In a mixed solution of glycine, glycerin (glycerol) and L-ascorbic acid (vitamin C) at ≥37 °C, glycylation of glycerins can occur at a relatively low level (<0.54 mM) [4]; yet, the presence of a higher amount (0.73–0.95 mM) of glycylglycerins in iPSC lysate indicates that there may be another enzymatic system responsible for glycylglycerin production as well (Fig. 2a). Under a pH < 7.2 condition, MGG, DGG, and TGG are all positively charged molecules that highly interact with negatively charged materials, in particular the double helix portions of RNAs, via ionic/electrostatic affinity (Fig. 2b) [4]. Due to this unique feature, glycylglycerins have been used as an excellent RNA-protecting agent for formulating and delivering small interfering RNA (siRNA)- and miRNA-based drugs in various RNAi-associated pharmaceutical and therapeutic applications.

Glycylglycerin-formulated miRNAs and siRNAs have been tested as candidate drugs in several animal trials in vivo. The use of glycylglycerin-encapsulated miR-302 precursors (pre-miR-302s) for enhancing wound healing and tissue regeneration is one of reported proof-of-principle examples [5]. In this case, the glycylglycerin-encapsulated pre-miR-302s were further formulated

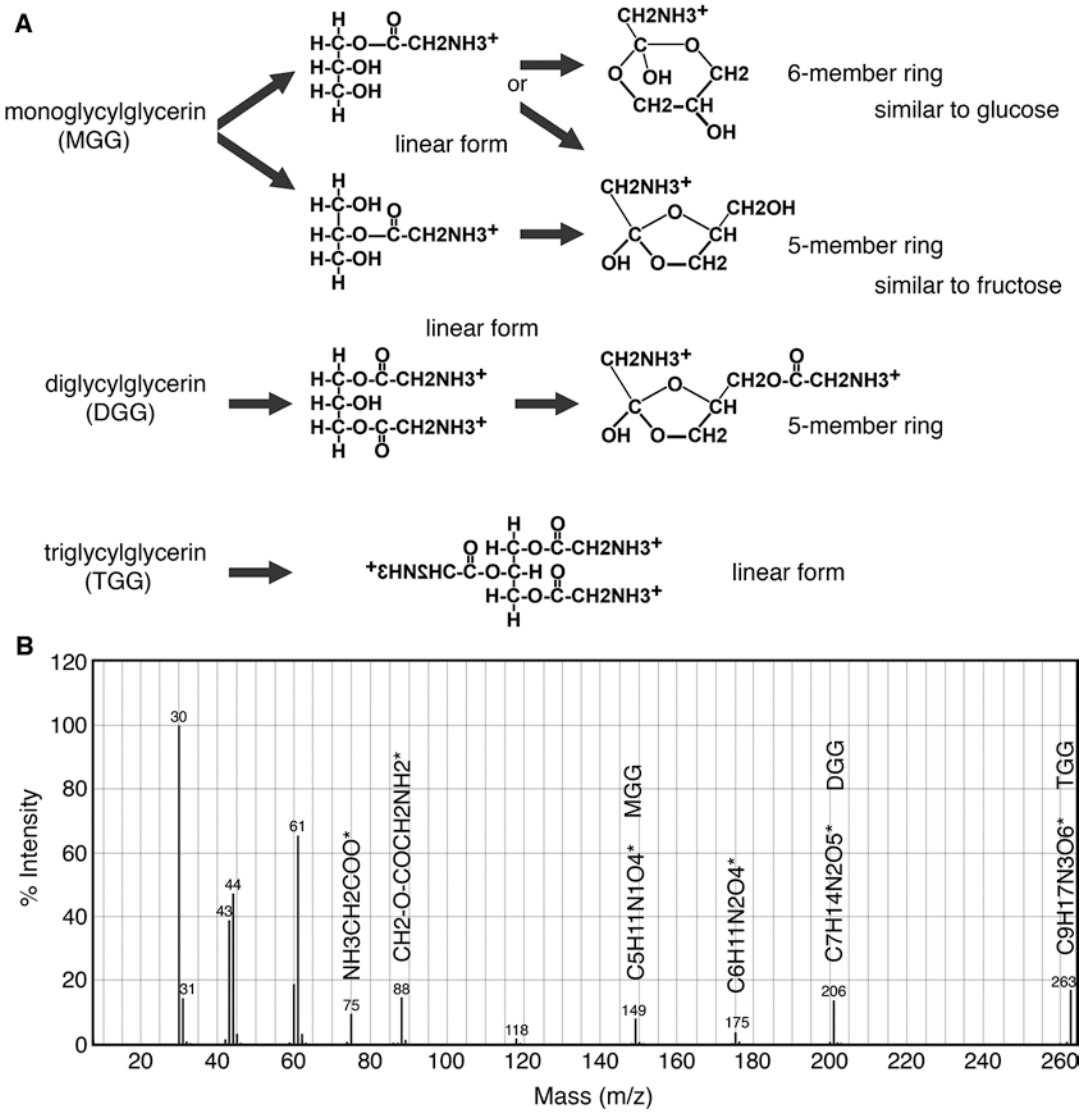

Fig. 1 Structural conformations of monoglycylglycerins (MGG), diglycylglycerins (DGG), and triglycylglycerin (TGG). (**a**) The molecular formulas for MGG, DGG, and TGG are $C_5H_{11}N_1O_4$, $C_7H_{14}N_2O_5$, and $C_9H_{17}N_3O_6$, respectively. Under a <pH 7.2 condition, all glycylglycerins form positively charged molecules due to the amino groups in the ends of their linear form structures. Notably, MGG and DGG can further form 5-member and 6-member ring structures, which highly resemble the ring conformations of fructose and glucose, respectively. (**b**) High-performance liquid chromatography–mass spectrometry (HPLC-MS) analysis detects MGG (*m/z* = 149), DGG (*m/z* = 206), and TGG (*m/z* = 263) in the spectra of iPSC cytosol extracts

with a cream-based antibiotic ointment for in-vivo treatments. As miR-302 is the most abundant ESC-specific miRNA species in human ESCs and iPSCs, it has been proposed that the somatic cell reprogramming function of miR-302 may be able to induce and/or maintain adult stem cell renewal as well, so as to facilitate the

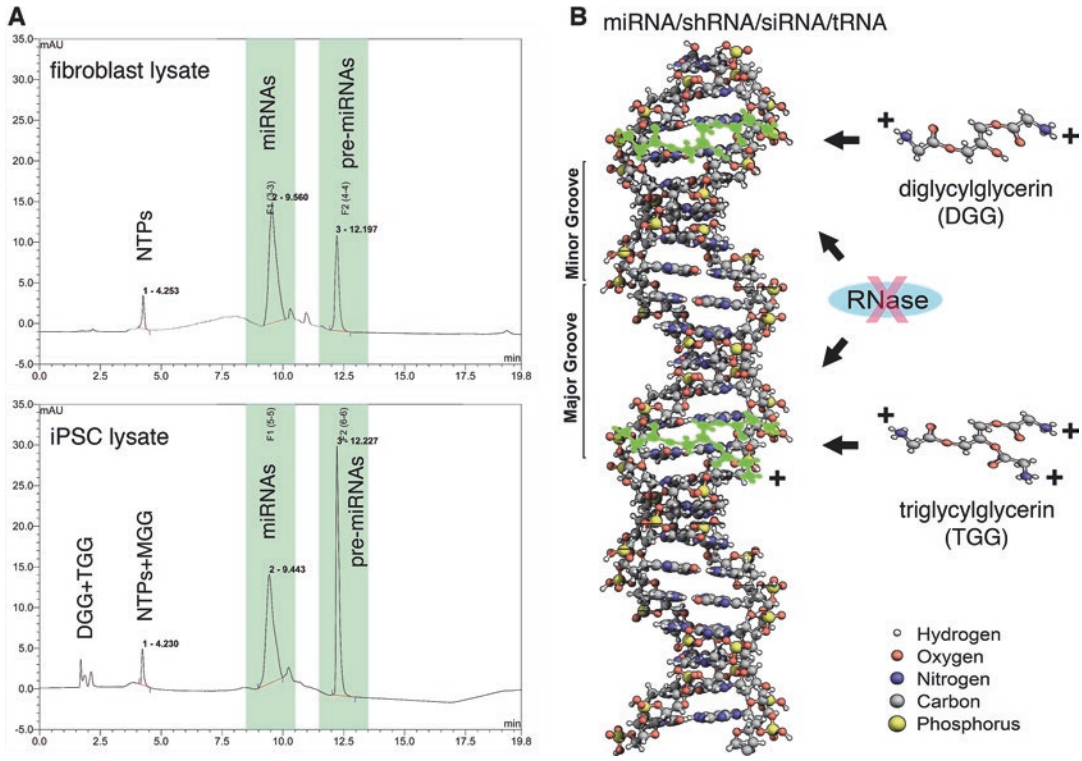

Fig. 2 Analysis of the interaction between glycylglycerins and pre-miRNAs/siRNAs using HPLC. (**a**) Comparison of glycylglycerins, miRNAs, and the related miRNA precursors (pre-miRNAs) between the cytosol extracts of human adult fibroblasts (top) and those of the fibroblast-derived iPSCs (bottom). High levels of ESC-specific DGG/TGG and pre-miRNAs were detected in iPSCs but not in adult fibroblasts. (**b**) Chemical 3-dimension modeling of electro-affinity interaction between DGG/TGG and pre-miRNA/siRNA, showing that the linear structures of 1,3-DGG and 1,2,3-TGG fit into the minor grooves of the pre-miRNA/siRNA double helixes and then the positive amino groups in the ends of DGG/TGG bind to the negatively charged phosphodiester backbones of pre-miRNA/siRNA molecules (indicated by green shadow), so as to form a layer of sugar-like coating for protecting pre-miRNA/siRNA integrity. This sugar-like coating may also facilitate pre-miRNA/siRNA delivery into cells via SGLT and GLUT transporters

processes of tissue repairing and regeneration in vivo. To test this theory, mouse skin wounds were generated by scalpel dissection and sized approximately 1 cm square. The pre-prepared ointments (0.3 mL) with or without pre-miR-302s were directly applied on the wounds, respectively, and covered the whole wounded areas, and then further sealed by liquid bandage. As shown in Fig. 3a, the results of this animal trial demonstrated that miR-302 treatments significantly enhanced the speed of wound healing over twice faster than other miR-434 treatments and blank controls. Moreover, 10 days after treatments (once per day), miR-302-treated wound areas showed normal hair regrowth and left less or almost no scar ($n = 6/6$), whereas other treatments and controls resulted in relatively large scars with no hair growth. To further measure the miRNA penetration rate in skins, we isolated total RNAs from the

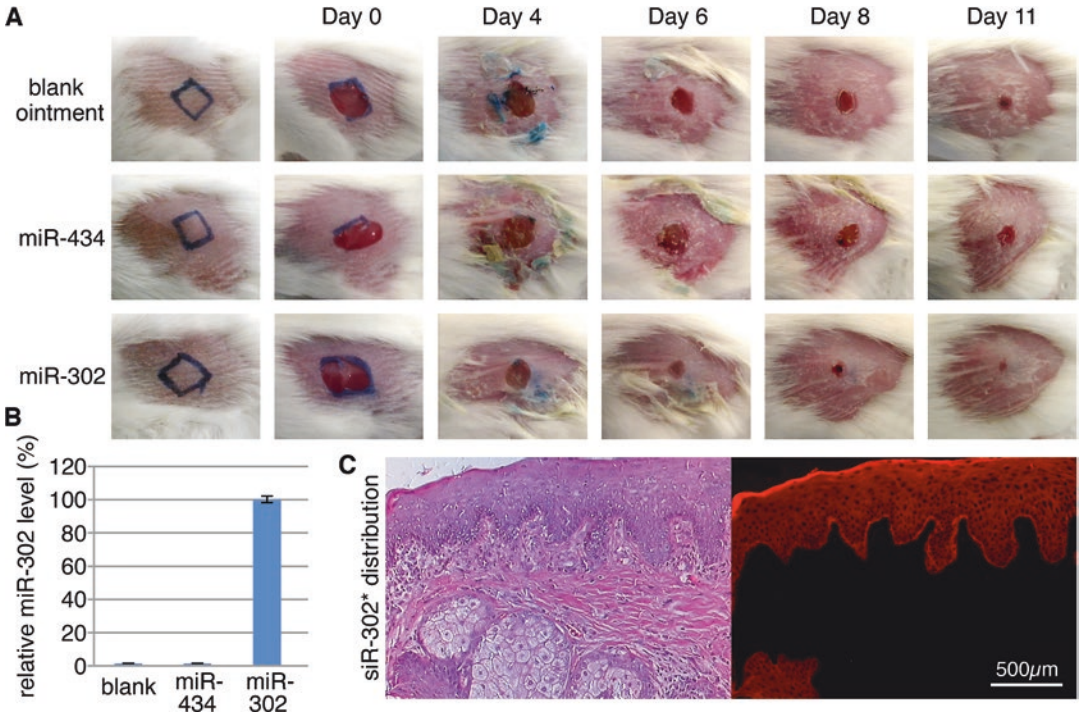

Fig. 3 The trial results of in-vivo wound healing treatments in mice using glycylglycerin-encapsulated pre-miR-302s in conjunction with a cream-based antibiotic ointment. (**a**) The trial results demonstrated that miR-302 treatments (10 μg/mL of pre-miR-302s per treatment per day, $n = 6$) significantly increased the speed of wound closure about 2–3 times faster than other miR-434 treatments (10 μg/mL of pre-miR-434 per treatment per day, $n = 6$) and blank controls (ointment only, $n = 6$). (**b**) qRT-PCR analyses of miR-302a levels in miRNA-treated and control tissues, respectively, showed that a high miR-302a concentration was detected only in miR-302-treated samples but not other treatments or controls ($n = 6$ for each group). (**c**) Fluorescent microscopic examination of the in-vivo distribution of a glycylglycerin-encapsulated Cy5.5-labeled siRNA mimic (siR-302*) further revealed that glycylglycerins protect and deliver siR-302* (labeled in red) into cells ranged from epidermis to the epidermis-dermis junction area, where skin adult stem cells reside

biopsies of the newly healed tissues and then run quantitative reverse transcription-polymerase chain reaction (qRT-PCR) assays with a set of miR-302a-specific primers to confirm that glycylglycerin-encapsulated pre-miR-302s were successfully delivered and processed into mature miR-302 in the treated tissues in vivo (Fig. 3b).

Recent trials using a glycylglycerin-encapsulated Cyanine5.5 (Cy5.5)-labeled siRNA mimic of miR-302a (siR-302*) to repeat the same wound healing experiments as aforementioned in mice further revealed that glycylglycerins can effectively deliver siR-302* deep enough to reach the epidermis-dermis junction, where skin adult stem cells are located (Fig. 3c). This evidence strongly suggests that miR-302 may function to stimulate stem cell expansion and differentiation for generating more various new tissue cells, so

as to completely repair the wounded areas and thus result in scarless wound healing. Furthermore, a more advanced in-vivo study using intravenous injection of glycylglycerin-encapsulated siR-302* into mouse tail veins showed that glycylglycerins successfully deliver siRNA into many major organs and tissues, including heart, lung, spleen, liver, blood vessels, and bone marrows (Fig. 4). Noteworthily, the success of these animal trials not only marks the first use of miRNA- and siRNA-based drugs for in-vivo treatments but also sheds light on a possible means for stimulating stem cell renewal and tissue regeneration in vivo using the renowned RNAi-associated technologies in conjunction with glycylglycerin-mediated delivery. As a result, the findings of these trials are very useful for designing and developing novel RNAi-based regenerative medicines, which may eventually lead to new treatments for many aging-related degenerative disorders, such as Alzheimer's disease, Parkinson's disease, stroke, diabetes, osteoporosis, cancers, and probably even aging itself.

The metabolism of glycylglycerins has been studied and found to go through an intracellular pathway similar to glycolysis. In this study, we used high performance liquid chromatography coupled with tandem mass spectrometry (HPLC-MS) to detect the changes of intracellular metabolites between ^{14}C-labeled MGG (1 mM)-treated and untreated human adult fibroblasts. We found that the concentrations of glycine, dihydroxyacetone phosphate (DHAP), and phosphoenolpyruvate (PEP) were significantly increased over 6–10 folds in the cell lysate of treated human fibroblasts compared to that of the untreated ones. Moreover, based on the result of a further ^{14}C-MGG metabolite tracking assay, Fig. 5 summarizes the metabolic pathway of glycylglycerins in human cells. Due to its structural similarity to monosaccharides, MGG is likely absorbed by cells through glucose and/or fructose transporter proteins, such as the Na^+-glucose cotransporters (SGLTs) and the facilitative glucose transporters (GLUTs), of which the detail uptake mechanism remains to be determined. After absorption, MGG is first processed into glycine and DHAP and then DHAP is further turned into its isomer D-glyceraldehyde-3-phosphate (GADP). After that, glyceraldehyde phosphate dehydrogenase (GAPDH) converts GADP into D-1,3-bisphosphoglycerate (1,3-BPG), which is then converted by phosphoglycerate kinase (PGK) into 3-phosphoglycerate (3-PG), by phosphoglycerate mutase (PGM) into 2-phosphoglycerate (2-PG), by enolase into phosphoenolpyruvate (PEP), and finally by a kinase (PK) into pyruvate. The end product—pyruvate—can be further utilized by the cells for generating energy (via Kreb's cycle or citric acid cycle), for producing sugars (via gluconeogenesis), and for taking part in other cellular metabolisms. In sum, the net reaction of MGG metabolism generates 1 glycine, 1 pyruvate, 2 reduced nicotinamide adenine dinucleotide (NADH), 2 adenosine triphosphate (ATP), and 1

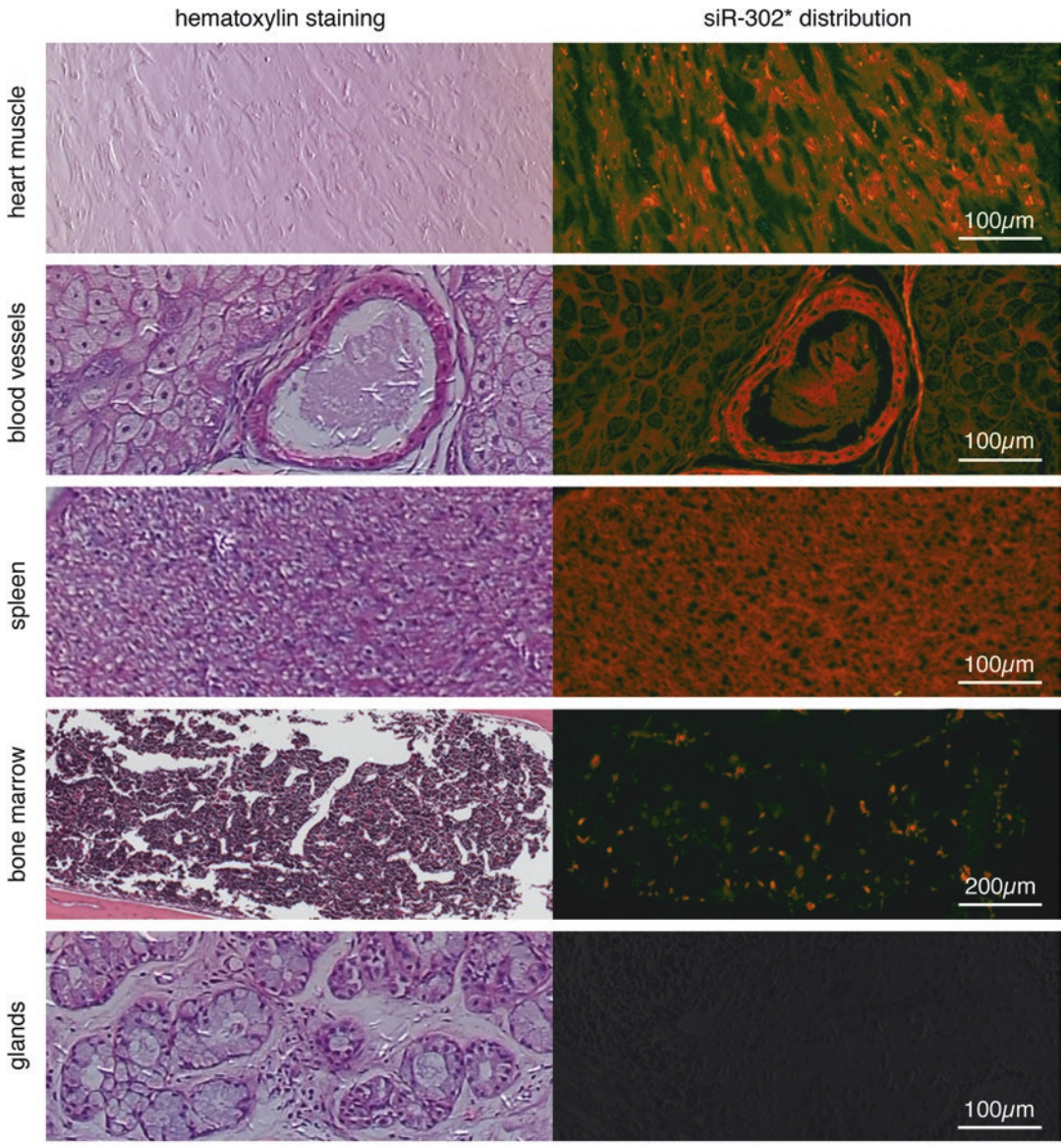

Fig. 4 Study of in-vivo siRNA distribution after intravenous injection of glycylglycerin-encapsulated siR-302* (200 μg) into the tail veins of C57BL/6J strain mice ($n = 6$). Microscopic examination confirmed that glycylglycerins are able to not only protect but also deliver siR-302* (red) into many major organs and tissues in vivo, including heart, lung, spleen, liver, blood vessels, and bone marrows, but not intestines and some gastrointestinal glands. Photos represent the in-vivo distribution of siR-302* approximately 24 h after the tail vein injection in mice

H_2O, leading to no toxic byproduct in the cells. In view of such a safety feature, glycylglycerins are not only one of the safest protecting agents for miRNA and siRNA delivery in vivo but also a potential sugar substitute for treating diabetes.

Pluripotent stem cells contain numerous novel ESC-specific materials, many of which are still not named in the current

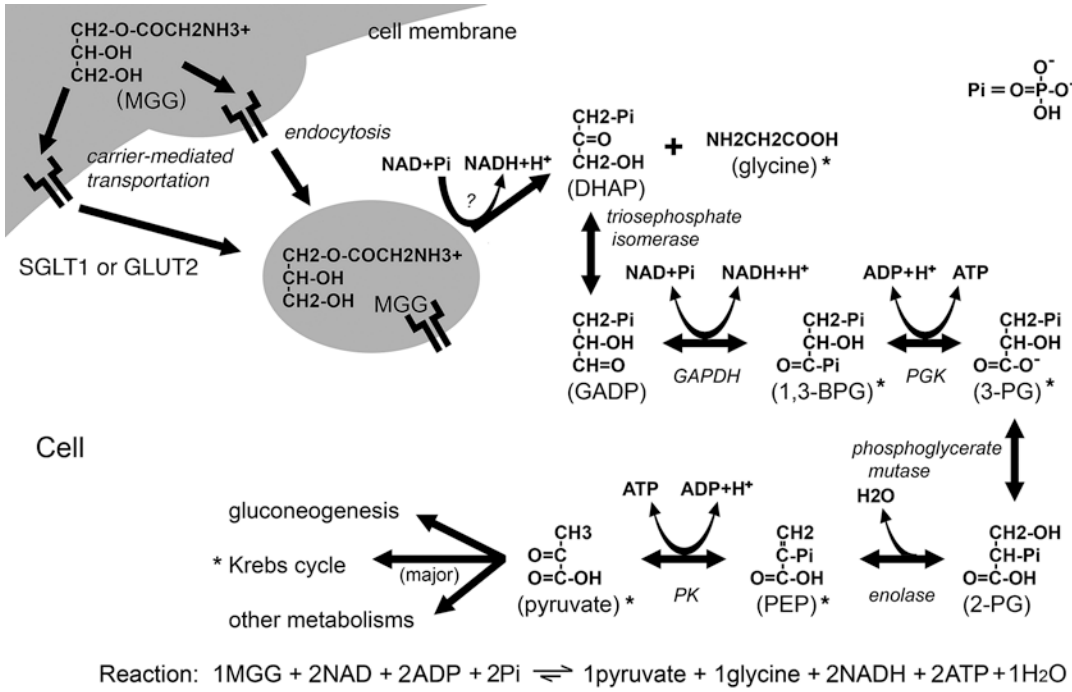

Fig. 5 The proposed metabolism pathway of glycylglycerins, such as MGG, in human cells. Due to its structural similarity to monosaccharides, MGG is absorbed via either SGLT/GLUT-mediated carrier transportation or endocytosis, or both. After uptake by the cells, MGG is processed through a mechanism similar to glycolysis into pyruvate, which is then involved in some other important biological pathways, such as Krebs cycle and gluconeogenesis

chemistry index yet. To this, our recent finding of glycylglycerins demonstrates the first practical model for the search of these novel materials in iPSCs, providing a whole new direction for the development of today's regenerative medicine. Following more and more new ESC-specific materials found, our further understandings of their functions and uses may eventually lead to great breakthroughs in novel pharmaceutical and therapeutic designs for treating a variety of human diseases. Expectedly, the application of these novel ESC-specific materials in real clinical practice is highly desirable in the near future.

2 Materials

2.1 iPSC Preparation

1. 1–1.2 billion iPSCs, which are generated using either three/four-factor induction [6–8] or miR-302 induction [1–3] methods (*see* **Note 1**).
2. Normal saline (0.9% NaCl, pH 6.5–6.9 at 37 °C) (*see* **Note 2**).

3. Sterilized cell scraper.
4. 1.5–2.5 mL high-speed centrifugation microtubes, sterilized (resistant over 22,500 × *g*).

2.2 Ultra-centrifugation andFiltration

1. Ultracentrifuge: >22,500 × *g* with temperature control (*see* **Note 3**).
2. 1 mL pipetman.
3. 0.01 μm ultrafilter column (30 kDa; Amicon Ultra-0.5 30 K, Millipore, Billerica, MA).
4. 0.001 μm nanofilter column (3 kDa; Amicon Ultra-0.5 3 K).
5. Double-autoclaved diethyl pyrocarbonate (DEPC)-treated ddH_2O (pH 5.2–5.7) (*see* **Note 2**).
6. A stainless steel, silver or platinum-based microelectrode pH meter (such as an AquaPro pH combination electrode probe, Thomas Scientific, Swedesboro, NJ) (*see* **Note 4**).

2.3 HPLC Purification

1. HPLC machine, such as an Ultimate 3000 HPLC machine (Thermo Scientific, Waltham, MA) with a DNAPac PA-100 column (BioLC Semi-Prep 9×250 mm).
2. Starting buffer: 40 mM Tris–HCl (pH 6.5–7.6) (*see* **Note 2**).
3. Mobile buffer: 40 mM Tris–HCl (pH 6.5–7.6) with 500 mM sodium perchlorate (*see* **Note 2**).

3 Methods

3.1 iPSC Preparation

Traditional cell lysate extraction methods use chemicals and buffers, which tend to destroy the natural properties of some useful ingredients inside the iPSC cytosol. To prevent this problem, we adopt a pure physical isolation method to collect iPSC cytosol for further screening, identifying, and purifying novel ESC-specific materials, which may provide significant insight into new medicines and therapies for advancing today's regenerative medicine. We herein disclose one of these methodologies for isolating glycylglycerins—one new kind of ESC-specific modified sugar alcohols—as an example to demonstrate the detail procedures.

1. Approximately 1–1.2 billion iPSCs are cultivated in 110–130 75-mL culture flasks at >50% confluency.
2. Cell washing: Remove cell culture medium and then use 10 mL of normal saline (pH 6.5–7 at 37 °C) to gently rinse and wash iPSCs two times.
3. Cell collection: Remove normal saline and then use a sterilized cell scraper to scratch down iPSCs from the surface of culture flasks. Collect all the iPSCs and the related broken cell lysate

into sterilized microtubes (maximal 1.5 mL volume for each microtube). Place the microtubes on ice and then use them in the next Subheading 3.2 immediately. Do not store the fresh iPSCs and the broken cell lysate.

3.2 Ultra-centrifugation andFiltration

Cells are broken by ultracentrifugation and then cell nucleus and large debris are precipitated to the bottom of microtubes during high-speed centrifugation. As our current studies mainly focus on small-sized iPSC ingredients (<30 kDa or <100 nucleotides), we try to remove all >30 kDa larger ingredients using 0.01 μm ultrafilter columns. After that, we further separate the remaining cell lysate into two parts, one is sized between 3 and 30 kDa and the other is less than 3 kDa. Most of the miRNA-bound glycylglycerins are located in the 3–30 kDa portion, while the free-form glycylglycerins stay in the <3 kDa portion. However, due to the fast metabolism rate of these free-form glycylglycerins, only a limited amount of glycylglycerins, particularly MGG, was detected in the <3 kDa portion of iPSC lysate. This evidence indicates that, without the mutual protection between pre-miRNAs and glycylglycerins, the free-form glycylglycerins are highly degradable in cytosol.

1. High-speed centrifugation: Place microtubes containing the iPSCs and the broken cell lysate into an ultracentrifuge and spin at a speed over 17,500 × *g* for 30 min at 4 °C.
2. Lysate collection: Use a sterilized 1 mL pipet to transfer and collect cytosol supernatants into 0.01 μm ultrafilter columns (maximal 1 mL volume for each ultrafilter column). Then, place the ultrafilter columns into a centrifuge and spin at a speed 12,000 × *g* for 30 min at 4 °C. Collect the flow-though portion for the next filtration process.
3. Lysate separation: Use a sterilized 1 mL pipet to transfer the above flow-through liquid into 0.001 μm nanofilter columns (maximal 1 mL volume for each ultrafilter column). Then, place the nanofilter columns into a centrifuge and spin at a speed 12,000 × *g* for 30 min at 4 °C. Collect both of the flow-though and filter-retained portions into two different microtubes, following the manufacturer's suggestions. Then, use the filter-retained portion for the next Subheading 3.3.
4. Sample preparation for HPLC: Redissolve the filter-retained iPSC lysate in normal saline, of which the volume is equal to the flow-through portion of the iPSC lysate.
5. pH measurement: Measure the pH value of the iPSC lysate to ensure that the range is within pH 6.2–6.9.

3.3 HPLC Purification

Due to the fast degradation rate of the free-form glycylglycerins in cytosol, we can first collect abundant miRNA/pre-miRNA-bound glycylglycerins and then further separate them using HPLC

purification methods. The final collection of either free-form or miRNA/pre-miRNA-bound glycylglycerins is dependent on the pH values of the HPLC buffers used. Buffers at ≥pH 7.2 are used for purifying free-form glycylglycerins, whereas miRNA/pre-miRNA-bound glycylglycerins are collected using buffers at ≤pH 6.7. Both of the final products are useful for developing new medicines and treatments directed against various human diseases, in particular Alzheimer's disease [9], diabetes [10], and cancers [11, 12].

1. HPLC program: Set up a 20 min HPLC program as follows—(1) 100% starting buffer for 2.5 min, (2) 85% starting buffer + 15% mobile buffer for 9.5 min, (3) 45% starting buffer + 55% mobile buffer for 3 min, (4) 25% starting buffer + 75% mobile buffer for 2.5 min, and (5) 100% starting buffer for 2.5 min.
2. HPLC condition: Set up HPLC condition as follows—(1) column temperature is 50 °C, (2) buffer flow speed is 3.6 mL/min and the resulting column pressure is less than 130 Bar, and (3) UV light detector is set at 260 nm.
3. HPLC purification: Load 50 micro-litters (μL) of the redissolved filter-retained iPSC lysate into the HPLC machine. Run the preset HPLC program under the preset HPLC condition. Then, as shown in Fig. 2a, collect the flow-through segment containing glycylglycerins at the timing around 1–5 min, of which the time variation is depending on the types of the HPLC machines used.

4 Notes

1. 1–1.2 billion iPSCs are collected from 110–130 75-mL culture flasks of iPSCs grown at >50% confluency, which provide approximately 0.8–1.0 mL of cytosol for one extraction based on the present procedure.
2. All the solutions must be made by using type 1 deionized water (ISO 3696 Grade 1). Make sure that there is no contamination of any divalent ion in the solutions, which will destabilize the interaction between glycylglycerins and miRNAs/pre-miRNAs.
3. RCF (g) = $(1.12 \times 10^{-6}) \times (\text{rpm})^2 \times r$, where r is the radius in centimeters measured from the center of the rotor to the middle of the spin column, and rpm is the speed of the rotor in revolutions per minute.
4. pH meters with a membrane-based ion-exchange electrode cannot be used for measuring the pH value of cell lysate, which may not provide accurate reading.

References

1. Lin SL, Chang DC, Chang-Lin S, Lin CH, Wu DT, Chen DT, Ying SY (2008) Mir-302 reprograms human skin cancer cells into a pluripotent ES-cell-like state. RNA 14:2115–2124
2. Lin SL, Chang DC, Lin CH, Ying SY, Leu D, Wu DT (2011) Regulation of somatic cell reprogramming through inducible mir-302 expression. Nucleic Acids Res 39:1054–1065
3. Lin SL, Ying SY (2012) Mechanism and method for generating tumor-free iPS cells using intronic microRNA miR302 induction. In: Ying SY (ed) MicroRNA Protocols, 2nd edn. Springer Publishers press, New York, pp 295–324
4. Chang-Lin S, Hung A, Chang DC, Lin YW, Ying SY, Lin SL (2016) Novel glycylated sugar alcohols protect ESC-specific microRNAs from degradation in iPS cells. Nucleic Acids Res 44:4894–4906
5. Chen SKJ, Lin SL (2013) Recent patents on microRNA-induced pluripotent stem cell generation. Recent Pat Regen Med 3:5–16
6. Takahashi K, Yamanaka S (2006) Induction of pluripotent stem cells from mouse embryonic and adult fibroblast cultures by defined factors. Cell 126:663–676
7. Yu J, Vodyanik MA, Smuga-Otto K, Antosiewicz-Bourget J, Frane JL, Tian S, Nie J, Jonsdottir GA, Ruotti V, Stewart R, Slukvin II, Thomson JA (2007) Induced pluripotent stem cell lines derived from human somatic cells. Science 318:1917–1920
8. Wernig M, Meissner A, Foreman R, Brambrink T, Ku M, Hochedlinger K, Bernstein BE, Jaenisch R (2007) In vitro reprogramming of fibroblasts into a pluripotent ES-cell-like state. Nature 448:318–324
9. Li HH, Lin SL, Huang CN, Lu FJ, Chiu PY, Huang WN, Lai TJ, Lin CL (2016) miR-302 attenuates amyloid-β-induced neurotoxicity through activation of Akt signaling. J Alzheimers Dis 50:1083–1098
10. Lin SL, Chang-Lin S, Lin YW, Chang D (2014) Use of novel monosaccharide-like glycylated sugar alcohol compositions for designing and developing anti-diabetic drugs. US patent application number 14/585978
11. Lin SL, Chang D, Ying SY, Leu D, Wu DTS (2010) MicroRNA miR-302 inhibits the tumorigenecity of human pluripotent stem cells by coordinate suppression of CDK2 and CDK4/6 cell cycle pathways. Cancer Res 70:9473–9482
12. Lin SL, Lin YW (2016) Sugar alcohol-based compositions for delivering nucleic acid-based drugs in vivo and in vitro. US patent number 9387251

INDEX

Shao-Yao Ying (ed.), *MicroRNA Protocols*, Methods in Molecular Biology, vol. 1733,
https://doi.org/10.1007/978-1-4939-7601-0, © Springer Science+Business Media, LLC 2018

K

L

M

N

O

P

Q

R

S

T

V

W

Z